Vol. 183, May 31, 1986
Complete in one issue

ISSN 0003-2670

ANALYTICA CHIMICA ACTA

International journal devoted to all branches of analytical chemistry

ELSEVIER

ANALYTICA CHIMICA ACTA

International journal devoted to all branches of analytical chemistry
Revue internationale consacrée à tous les domaines de la chimie analytique
Internationale Zeitschrift für alle Gebiete der analytischen Chemie

PUBLICATION SCHEDULE FOR 1986

	J	F	M	A	M	J	J	A	S	O	N	D
Analytica Chimica Acta	179	180	181	182 183/1	183/2 184	185	186	187	188	189	190	191

Scope. *Analytica Chimica Acta* publishes original papers, short communications, and reviews dealing with every aspect of modern chemical analysis both fundamental and applied.

Submission of Papers. Manuscripts (three copies) should be submitted as designated below for rapid and efficien handling:

Papers from the Americas to: Professor Harry L. Pardue, Department of Chemistry, Purdue University, West Lafayette IN 47907, U.S.A.

Papers from all other countries to: Dr. A. M. G. Macdonald, Department of Chemistry, The University, P.O. Box 363 Birmingham B15 2TT, England. Papers dealing particularly with computer techniques to: Professor J. T. Clerc Universität Bern, Pharmazeutisches Institut, Baltzerstrasse 5, CH-3012 Bern, Switzerland.

Submission of an article is understood to imply that the article is original and unpublished and is not being considered for publication elsewhere. Upon acceptance of an article by the journal, authors will be asked to transfer the copyrigh of the article to the publisher. This transfer will ensure the widest possible dissemination of information.

Information for Authors. Papers in English, French and German are published. There are no page charges Manuscripts should conform in layout and style to the papers published in this Volume. Authors should consul Vol. 170 for detailed information. Reprints of this information are available from the Editors or from: Elsevier Editoria Services Ltd., Mayfield House, 256 Banbury Road, Oxford OX2 7DH (Great Britain).

Reprints. Fifty reprints will be supplied free of charge. Additional reprints (minimum 100) can be ordered. An orde form containing price quotations will be sent to the authors together with the proofs of their article.

Advertisements. Advertisement rates are available from the publisher.

Subscriptions. Subscriptions should be sent to: Elsevier Science Publishers B.V., Journals Department, P.O. Bo 211, 1000 AE Amsterdam, The Netherlands. Tel: 5803 911, Telex: 18582.

Publication. *Analytica Chimica Acta* appears in 13 volumes in 1986. The subscription for 1986 (Vols. 179–191) i Dfl. 2730.00 plus Dfl. 312.00 (p.p.h.) (total approx. US $1192.94). All earlier volumes (Vols. 1–178) except Vols. 2 and 28 are available at Dfl. 231.00 (US $90.59), plus Dfl. 15.00 (US $5.88) p.p.h., per volume.

Our p.p.h. (postage, packing and handling) charge includes surface delivery of all issues, except to subscribers in th U.S.A., Canada, Japan, Australia, New Zealand, P.R. China, India, Israel, South Africa, Malaysia, Thailand, Singapore South Korea, Taiwan, Pakistan, Hong Kong, Brazil, Argentina and Mexico, who receive all issues by air deliver (S.A.L. — Surface Air Lifted) at no extra cost. For the rest of the world, airmail and S.A.L. charges are available upo request.

Claims for issues not received should be made within three months of publication of the issues. If not they cannot b honoured free of charge.

For further information, or a free sample copy of this or any other Elsevier Science Publishers journal, readers in th U.S.A. and Canada can contact the following address: Elsevier Science Publishing Co. Inc., Journal Informatio Center, 52 Vanderbilt Avenue, New York, NY 10017, U.S.A., Tel: (212) 916-1250.

0003-2670/86/$03.5

Printed in The Netherlands

Completely Revised

Instrumental Liquid Chromatography

A Practical Manual on High-Performance Liquid Chromatography Methods

Second, completely revised edition

by **N.A. PARRIS,** E.I. du Pont de Nemours & Company, Biomedical Products Department, Research and Development Division, Experimental Station Laboratory Wilmington, DE, USA

Journal of Chromatography Library 27

This extensively revised and up-to-date book is an essential tool for the HPLC user in the laboratory. It first appeared in 1976, was twice reprinted and was described in Laboratory Practice as "one of the more useful and successful texts on HPLC . . . a most readable book packed with valuable information and advice . . . strongly recommended."

Practically orientated, it is an easy-to-follow guide containing the minimum essential theoretical background. The majority of the material is based on practical experience and highlights details which may have important operational value for laboratory workers. It helps the HPLC user to select the most appropriate instrumentation, injectors, columns etc.

Applications of liquid chromatography are described with reference to the potential of the technique for qualitative, quantitative and trace analysis as well as for the preparative application. Numerous applications from the literature are tabulated and cross-referenced to sections concerned with the optimization procedures of the particular methods. The format of the original edition proved so successful that it has remained unchanged, but some 45% of the material is either new or completely revised in order to bring the column technology and applications data up-to-date.

"The style . . . is clear. The subject is placed in perspective by comparisons with other separation techniques and should provide a good reference book for all involved in practical LC," (Laboratory Practice).

"Overall the book is well written, and, because of its practical emphasis, it is highly recommended for both the aspiring and experienced chromatographer," (J. Am. Chem. Soc.).

1984 xiv + 432 pages. Price: US $ 83.25 / Dfl 225.00 (including postage).
ISBN 0-444-42061-4

ELSEVIER SCIENCE PUBLISHERS

P.O. Box 211, 1000 AE Amsterdam, The Netherlands
P.O. Box 1663, Grand Central Station, New York, NY 10163, USA

Wilson and Wilson's Comprehensive Analytical Chemistry

edited by G. Svehla

Vol. XII Thermal Analysis
Part C: Emanation Thermal Analysis and Other Radiometric Emanation Methods

by **V. BALEK**, *Rez, Czechoslovakia and* **J. TÖLGYESSY**, *Bratislava, Czechoslovakia*

This book outlines the development of the radiometric emanation methods used on the application of radioactive inert gas release from solids. It gives the theoretical basis of the method, the measuring techniques, as well as ways of evaluating results. The authors review the numerous applications of radiometric emanation methods in various branches of science and technology.

Contents: Introduction. Chapter 1. Basic principles and historical development. 2. Labelling of samples. 3. Inert gas release from solids containing corresponding parent nuclides. 4. Release of inert gas incorporated without parent in solids. 5. Measurement of inert gas release and instrumentation. 6. Applications of ETA. 7. Analytical chemistry applications. 8. Technical applications. Present state and future of radiometric emanation methods. Subject index.

1984 xvi + 304 pp. Price: US $ 70.25 / Dutch guilders 190.00. ISBN 0-444-99659-1

Vol. XII Thermal Analysis
Part D: Thermophysical Properties of Solids. Their Measurements and Theoretical Thermal Analysis

by **J. SESTÁK**, *Prague, Czechoslovakia*

The main aim of the book is to emphasize the methods of thermal analysis using a dynamic temperature regime within the framework of general thermophysical measurements. As the text is mainly based on phenomenological description it does not require any specialized knowledge of mathematics and can therefore be used by students of materials science and related branches of chemistry and physics.

Contents: Chapter 1. Introduction and preliminary remarks to individual chapters. 2. Characterization and preparation of solid samples. 3. The use of thermal analysis in the study of the behaviour of materials and substances. 4. Measurement, calibration and regulation of temperature. 5. Thermodynamic principles. 6. Thermodynamics of phase equilibria, phase diagrams. 7. The theory of phase transition. 8. Mechanism and kinetics of heterogeneous non-catalysed reactions. 9. Kinetics of processes under non-isothermal conditions. 10. The kinetic theory of glass formation in quenched melts. 11. Calorimetry: the determination of changes in thermal properties. 12. The theory and practice of differential thermal analysis. 14. Mathematical analysis of curves and the use of computers. 15. Appendix. Index.

1984 xx + 440 pp. Price: US $ 111.00 / Dutch guilders 300.00. ISBN 0-444-99653-2

Other parts of the volume include:

Vol. XIIA
Part A: Simultaneous Thermoanalytical Examinations by Means of the Derivatograph

edited by **J. Paulik** *and* **F. Paulik**

1981 xviii + 278 pp. Price: US $ 68.50 / Dutch guilders 165.00. ISBN 0-444-41949-7

Vol. XIIB
Part B: Biochemical and Clinical Applications of Thermometric and Thermal Analysis

edited by **N.D. Jespersen**

1982 xviii + 254 pp. Price: US $ 68.50 / Dutch guilders 165.00. ISBN 0-444-42062-2

ELSEVIER SCIENCE PUBLISHERS

P.O. Box 211, 1000 AE Amsterdam, The Netherlands
P.O. Box 1663, Grand Central Station, New York, NY 10163, USA

7328

ANALYTICA CHIMICA ACTA
VOL. 183 (1986)


RESPECT COPYRIGHT
BERNE
CONVENTION
100 YEARS
1886-1986
ENCOURAGE CREATIVITY

ANALYTICA CHIMICA ACTA

International journal devoted to all branches of analytical chemistry

ELSEVIER Amsterdam–Oxford–New York–Tokyo

Anal. Chim. Acta, Vol. 183 (1986)

0003-2670/86/$03.5

Printed in The Netherlands

Analytica Chimica Acta, 183 (1986) 1—46
Elsevier Science Publishers B.V., Amsterdam — Printed in The Netherlands

Review

THEORY AND APPLICATIONS OF ION-SELECTIVE ELECTRODES Part 6*

JIŘÍ KORYTA

J. Heyrovský Institute of Physical Chemistry and Electrochemistry, Czechoslovak Academy of Sciences, Opletalova 25, CS — 11000 Prague 1 (Czechoslovakia)

(Received 25th November 1985)

SUMMARY

This review of ion-selective electrodes is arranged in the same way as earlier reviews of this series. The whole subject continues to grow steadily. Considerable attention has been given to clinical analysis of body electrolytes, particularly by means of automatic devices. About 800 papers published between Spring 1983 and Spring 1985 (including several omitted in Part 5) are mentioned, covering the theory of membrane phenomena, technology, fixed-site electrodes, liquid-membrane electrodes, potentiometric biosensors and miscellaneous systems.

While the rate of publication on ion-selective electrodes increased steadily up to 1978, the period since then has seen a fairly constant output of some 400 papers per year. For the two-year period considered now, the number of publications has been fairly typical with regard to clinical methods of analysis, particularly based on automatic devices. There is still considerable interest in ion-selective field effect transistors (ISFETs) and in electrolysis at the interface of two immiscible electrolyte solutions (ITIES). The proportion between traditional subjects such as fixed-site membrane and liquid-membrane ion-selective electrodes has not undergone any conspicuous changes.

The present position of ion-selective electrodes, particularly in the field of biomedical analysis, can be compared with the history of the glass electrode as recently outlined by Czaban [2]. (As in Parts 1—5, glass pH electrodes are not considered here except in their rôle in biosensors.) From the discovery of the glass electrode by Cremer in 1906, and Haber and Klemensiewicz 1909, it took almost thirty years before Arnold Beckman introduced the first commercial pH-meter, which provided measurements with high-impedance electrode systems. While Ross and Frant's fluoride ion-selective electrode was a conspicuous success even at the end of 1960s, about fifteen years passed from the discovery of the potassium ion-selective electrode based on

*For Part 5 see ref. 1.

0003-2670/86/$16.01

valinomycin to the widespread use of Na^+/K^+-selective electrodes in clinical laboratories, where more than half of the assays are now done by these electrodes rather than by flame photometry. The installation of an ion-selective electrode system in an automatic analyzer by Technicon was a step in the correct direction. In contrast, there are still some basic problems of technology to be solved with both enzyme sensors and ion-selective field-effect transistors before they can become routine analytical devices. The most successful enzyme electrode so far, the glucose amperometric sensor, is used in only a fraction of clinical laboratories. Both these types of sensors have good prospects, which have been damaged by premature expectations evoked mostly by the popular scientific press with its claims for "biochips", etc.

Part 1 of this series on the Theory and Applications of Ion-selective Electrodes [1] covered the literature to the beginning of 1972. In addition to the general theory of membrane potentials of various types, the theory of the potential of ion-selective electrodes, and a survey of applications of non-glass ion-selective electrodes, Part 1 also included the theory of the glass electrode and dealt in some detail with the general properties of ion-carriers. About 1200 papers were covered by Part 2 [1], which was restricted to non-glass membrane systems (with the exception of chalcogenide glasses). Part 3 [1] dealt with more than 800 papers published to the end of 1978. Part 4 [1] covered about 2.5 years to the beginning of 1981 and was concerned with about 800 papers. Part 5 [1] covered about two years (to Spring 1983) and dealt with about 700 papers. The present review which is again concerned with a period of about two years (from Spring 1983 to Spring 1985) deals with about 800 papers, including several papers which were not referred to earlier. The subject is treated in an order similar to that used previously. First progress in the theory (which is not conspicuous) is dealt with, then problems of methodology are discussed, and finally new information on the basic properties of various types of electrodes, together with their analytical application, is reviewed.

Within the period of interest, there were several symposia specializing in ion-selective electrodes or including ion-selective electrodes as a major part. Besides a number of national symposia, specific mention should be made of the First Meeting of the European Working Group on Ion-Selective Electrodes (Oslo, June, 1983) [3], International Meeting on Chemical Sensors (Tokyo, 1983) [4], International Symposium on the Theory and Application of Ion-selective Electrodes in Physiology and Medicine (Rabenstein, F.R.G., September, 1983), Symposium on Electrochemical Sensors (Rome, June, 1984), Fourth Scientific Session on Ion-Selective Electrodes (Mátrafüred, Hungary, October, 1984) and International Symposium on Ion-selective Electrodes (Shanghai, June, 1985) [5].

Two bibliographies of recent titles on ion-selective electrodes were published [6, 7].

Books and reviews

Numerous books and reviews have been published [1—4, 8—71]. Two important conference proceedings were published, one dealing with clinical

analysis of ionized calcium, sodium and potassium [3], and the other with the progress of chemical sensors [4]. A chapter on ion-selective electrodes appeared in the Comprehensive Treatise of Electrochemistry [14]. A Czech monograph on ion-selective electrodes was issued [39]. Sensors based on biological principles were the subject of the book by Schindler and Schindler [58]. A special issue of the Scandinavian Journal of Clinical Laboratory Investigations was devoted to ionized calcium determination by means of ion-selective electrodes [21].

The reviews on ion-selective electrodes published in journals and specialized monographs are listed in Table 1. Progress on ion-selective electrode investigations in China up to 1979 was reviewed [71].

TABLE 1

Reviews on ion-selective electrodes

Subject	Reference
General review	10, 11, 13, 18, 24, 27, 28, 29, 34, 41, 59, 67—69
Clinical analysis	2, 17, 35a, 40, 56, 60
Biosensors,	8, 9, 25, 26, 35, 64
—, based on immobilized enzymes	43, 65
—, based on immobilized bacteria	36
Fluoride ion-selective electrode	12
Coated-wire electrodes	15
Drug analysis	16
Analytical applications	19
Intracellular measurements	20, 66
Solid-state ion-selective electrodes	22, 33
Ion-selective field-effect transistors	23, 32
—, in vivo applications	45
H.p.l.c. detectors	30, 31
Cell membrane potential monitoring	37
Electrolysis at ITIES	38
Water analysis	42, 50, 52
Liquid-membrane anion-selective electrodes	44
Detection limits	46
Carbon substrate ion-selective electrodes	47
Solid contact problem	48
Soil analysis	49
Process analysis	51
Applications in physiology, medicine and pharmacy	53, 62
Flow analysis	54, 63
Non-aqueous solvents	55
Automatic analyzer testing	57
Neutral-carrier ion-selective electrodes	61
Titrations based on ion-pairs	70

THEORY OF MEMBRANE PHENOMENA AT ION-SELECTIVE ELECTRODES

In the period concerned, progress in the theory has not been particularly conspicuous, as is clear from the small number of papers [72—82]. Kornyshev and Volkov [77] worked out the theory for standard Gibbs solvation energies of individual ions on the basis of which they predicted the values of standard Gibbs transfer energies between organic solvents and water. These data have fundamental importance for selectivity coefficients of ion-selective electrodes, based on ionized ion-exchangers, as well as for half-wave potentials in electrolysis at ITIES.

Hung's theory of distribution potentials (Part 5, p. 4) has been extended to selectivity coefficients of ion-selective electrodes with nitrobenzene as membrane solvent [75]. A similar approach [79] was applied to the problem of membranes with mixed solvents. A theory of liquid ion-exchanger membrane ion-selective electrodes [76] has been based on the idea of counter-transport of the ion to be determined and the interferent (cf. Part 3, pp. 10—13; Part 5, pp. 5, 6). The complicated situation arising in measurement of the impedance spectrum of a valinomycin-based membrane electrode with a Milipore filter or PVC support has been discussed [72—74].

The theory of solid-membrane ion-selective electrodes has been improved in the time-dependent model [80]. The solution transport of ions participating in the ion-exchange reactions at the membrane/solution interface must be taken into account (cf. Part 5, ref. 181).

A theory of the response characteristics of potentiometric gas sensors based on internal polymer membrane electrodes has been described [78]. The theory is based on the following five assumptions (see Fig. 1): (1) the rate of species exchange between the bulk reservoir of internal electrolyte buffer and the thin electrolyte film in contact with the membrane is very slow relative to the rate of gas diffusion into the thin film and the rates associated with equilibrium reactions in that layer; (2) the partial pressure of the gas is equal on both sides of the membrane; (3) diffusion of water vapour

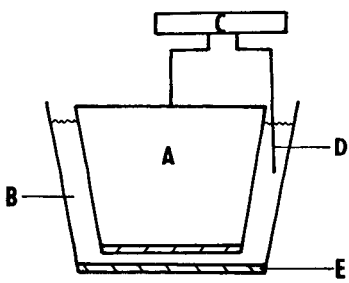

Fig. 1. Schematic diagram of a potentiometric gas sensor based on a polymer-membrane electrode: (A) internal polymer-membrane ion-selective electrode; (B) reservoir of internal electrolyte buffer; (C) pH meter; (D) Ag/AgCl reference electrode; (E) outer gas-permeable membrane (silicone rubber for CO_2 sensor, polytetrafluoroethylene for NH_3 sensor). (According to Meyerhoff et al. [78].)

across the gas-permeable membrane does not change the ionic strength of the internal electrolyte buffer film because the osmolarities of the sample and of the internal buffer solutions are similar; (4) the thin film of buffer has an extremely small volume relative to the possible sample volumes, and so the concentration of gas in the thin film is exactly the same as in the sample; and (5) the equilibration of the gas with the thin film does not significantly alter the ionic strength of the latter. The theory based on these assumptions is in good coincidence with the experiments. It predicts, for example, that the gas probe with a nonactin-based ammonium ion-selective electrode can be used for ammonia concentrations up to 10^{-3} mol dm^{-3}. In the case of the CO_2 sensor, the sort (Tris or Bis-Tris) and concentration of the buffer and the internal carbonate or hydrogen-carbonate ion-selective electrode must be chosen depending on the concentration range of the CO_2 to be determined.

On the same principles as in the theory of the time-dependent model of a solid-membrane ion-selective electrode [80], Morf et al. [81] worked out a theory for the time response of potentiometric gas sensors to the species determined and the interferents.

The theory of enzyme electrodes has been reviewed in Chinese [82].

TECHNOLOGY OF ION-SELECTIVE ELECTRODES

The technology of ion-selective electrodes has received considerable attention [15, 17, 23, 30—32, 38, 45—48, 55, 57, 60, 83—281].

Construction of ion-selective electrodes

Many papers have dealt with the construction of ion-selective electrodes [15, 47, 48, 89, 97, 103, 107, 126, 144, 153, 154, 165, 175, 182, 185, 186, 200, 203, 211, 216, 254, 269, 275].

Solid contact problem. In their review, Nikolskii and Materova [48] discussed the problem of ion-selective electrodes with solid contacts in great detail. The necessiry of a common charge-carrier in the contact and in the membrane is emphasized (cf. Part 1, p. 354; and Part 5, ref. 6, p. 64). Glass electrodes with internal metallic contact and the coated-wire electrodes were critically examined. Introduction of a redox system into the glass or liquid membrane was suggested (see also [79, 252, 254]). A reversible solid-state contact was found useful in a fluoride ion-selective electrode used in clinical analysis [126].

One type of solid-contact ion-selective electrode, the carbon-substrate electrode [47], was reviewed with particular attention to Růžička's Selectrodes. Carbon-filled polymer paste ion-selective electrodes functioning as sensors for silver, copper, lead, cadmium, halides and nitrate ions, pH and redox systems have been described [154]. The pH-response of a platinum or vitreous carbon electrode modified by a 1,2-diaminobenzene polymer film has been discussed [103], as has an ion-selective electrode consisting of graphite modified with an acrylic acid film containing quaternary ammonium

or thiocyanate ions [185]. Coated-wire ion-selective electrodes have been reviewed [15].

Polymer membrane materials. Calcium ion-selective electrodes with covalently-bound organophosphate sensor groups (Part 5, p. 7) have been reviewed [107] and a further study on this subject has been published [153].

An improved dynamic response of potentiometric ammonia gas sensors was expected with pure teflon membranes [89]. The membrane materials for the carbon-dioxide gas sensor have been discussed [175]. A procedure for coupling enzymes with nylon net improved the response of enzyme electrodes [200]. Alkyd resin paint (Glasstone No. 1000, Clear) was used to incorporate silver iodide for an iodide ion-selective electrode [165].

Electrode-system structure. The membrane composition for the neutral carrier system for magnesium (ETH 1692) in *o*-nitrophenyl octyl ether with various additions of potassium-tetrakis(*p*-chlorophenyl)borate has been studied [203]. The best additive/carrier molar ratio found was 0.2 (for a 1:2 cation/carrier complex). A hydrogen ion-selective electrode based on tridodecylamine incorporated in a plasticized poly(vinyl chloride) membrane showed good performance in both the CO_2 and NH_3 gas sensors on either the static or continuous-flow arrangement [211]. Under appropriate conditions, the static sensor exhibited slopes of the potential/log (analyte concentration) plots in the range 48—62 mV with potentials reproducible to less than ±1.5 mV at gas concentrations higher than 10^{-3} mol dm^{-3}.

Several sensors with incorporated electronics have been described [182, 186, 269]. Several electronic circuits were tested for use in the body of ion-selective electrodes (fluoride and pH-glass electrode) to convert the high-impedance output signal to a low-impedance signal, in order to improve the signal-to-noise ratio. These systems were suitable for applications in which the signal had to be transmitted over long distances [182]. The ion-selective membrane has also been linked to a monolithic chip using hybrid technology [186].

Other systems. Fabrication of inexpensive ion-selective electrodes has been described [144, 216]. A combination ion-selective electrode for the analysis of body electrolytes has been suggested [275].

Calibration, selectivity and detection limit

Numerous papers have been concerned with this group of problems [46, 91, 92, 99, 108, 112, 119a, 120, 125a, 130, 134, 141, 170, 171, 184, 191, 219, 225, 243, 244, 261, 264, 265, 278].

Calibration and standards. The Clinical Chemistry Division of IUPAC in conjunction with International Federation of Clinical Chemistry has worked out recommendations on physicochemical quantities and units in clinical chemistry, with particular emphasis on activities and activity coefficients [243]. This very useful document, which is consistent with similar recommendations of other IUPAC Divisions, particularly concerned with physical chemistry, should be made more widely available in an abridged form which could be easily understood by clinical chemists with biomedical background.

Five standard reference solutions for calibration of ion-selective electrodes and ISFETs used in clinical chemistry have been proposed [108]. In order to simulate various compositions of blood electrolytes, they contain varying concentrations of Ca^{2+}, Na^+, K^+ and Cl^- and compositions of zwitterionic buffers. These standards may help to achieve uniform calibration of potentiometric clinical analyzers. The activity coefficient of sodium ion has been determined in relation to the apparent ionic strength of normal blood plasma [244]. The problems of standards for clinical chemistry have been outlined [130].

Particular attention has been paid to the standardization of ionized calcium determination in serum [99, 112, 141, 261]. Reference intervals for ionized calcium in patients were determined [99, 112, 141, 261] and reference materials and calibration solutions suggested [99, 112, 141]. A more exact definition of ionized calcium has been suggested [261]: "ionized calcium" in human serum is the concentration of calcium ions that are solvated with water. There is at present no completely satisfactory resolution to the different modes of reporting calcium results in molar concentration, molal concentration or activity. It was suggested that calcium concentrations should be reported in units of mmol dm^{-3}, the numerical value of which is obtained by dividing the experimentally found calcium activity by the conventionally accepted activity coefficient 0.3. Although the activity coefficient may vary between samples, only one activity coefficient should be used because its purpose is simply to convert ion activity to more conventional units of concentration (from the report of American Association of Clinical Chemists Working Group on Ionized Calcium [261]). Similar problems arise with K^+ and Na^+ determinations in blood [190]. A quality assessment of the determination of calcium on national [264] and international [184] scales has been reported. The necessity of simultaneous pH measurement with ionized calcium determination in newborns has been stressed [128] (cf. [102]).

More precise methods of determining mean activity coefficients with sodium, potassium, calcium and nitrate ion-selective electrodes have been described [91, 225]. The pH glass electrode and sodium ion-selective electrode in a cell without liquid junction have been applied to the determination of the acidity constants of five deuterated bases, tris(hydroxymethyl)aminomethane (Tris), hydrazine, morpholine, ammonia and cyclohexylamine in D_2O in the temperature range 15—45°C [125a].

A computer-controlled calibration of ion-selective electrodes has been suggested; a non-linear regression technique in the region close to the detection limit is of advantage [92]. Calibration characteristics of ion-selective electrodes used for water analysis has been determined by the standard addition method [170].

Selectivity coefficients. An automated method for determining selectivity coefficients has been suggested [119a, 171]. Selectivity coefficients have been determined by means of a linearized multiple-standard-addition technique [191]. In a "matched-potential" technique [134], the change in

ion-selective electrode potential was measured upon changing the analyte concentration; the interferent was then added to an identical reference solution until the same potential change was obtained and the selectivity coefficient was obtained as the ratio of the analyte to interferent concentrations. No advantage with respect to conventional methods is obvious. The conditions for the breakdown of the correlation between ion-exchange constants and electrode selectivity coefficients have been examined [120]. An approach based on the theory of experiments design has been applied to the determination of selectivity coefficients [219].

Detection limit. The detection limit problem has been reviewed briefly [46]. An automated method for evaluating detection limits has been described [119a]. The need to consider adsorption effects in the assessment of the detection limit of precipitate-based ion-selective electrodes has been indicated [265].

Response time

Several papers have dealt with the response time [100, 102, 104, 113, 115, 164, 187a, 224, 240, 278]. A unified model for transient potentials of ion-selective electrodes, accounting for "overshoot" and oscillating behaviour, has been proposed [240]. The response times of the electrochemical cell and of the ion-selective electrode alone should be distinguished [224]. A definition of the response time based on the differential quotient of the electrode potential with respect to time has been discussed [187a]. The response time of neutral-carrier ion-selective electrodes has been studied for a tubular-shape electrode [115]; the results were fitted to three equations describing the dynamic behaviour of the electrode. Film diffusion was shown to be the rate-determining step for the initial part of the E/t dependence [114, 115]. A charge-pulse technique has been used to shorten the response time [164].

In a study of the kinetic parameters of the enzyme electrode for adenosine, it was shown that enzyme immobilization by bovine serum albumin cross-linking significantly affected the kinetic properties [100]. Other reports have dealt with the response times of the Ag_2S membrane ion-selective electrode in aqueous and mixed solvents [113], and the dynamic properties of various ion-selective electrodes [114], also from the standpoint of metrology [278].

Measuring procedures

Various methods have been discussed [30, 31, 86, 101, 106, 119, 129, 131, 132, 156, 159, 161, 169, 172, 187, 189, 193, 202, 205, 215, 217, 221, 229, 238, 239, 245, 246, 248, 252, 255, 256, 258, 259, 263, 270, 273, 279–281].

Standard addition methods. Several papers have dealt with single [156, 159, 202, 229, 238], double [207, 217, 229] and multiple [119, 187, 189] standard-addition methods in ion-selective electrode potentiometry. The precision of the double standard-addition method has been analyzed and its

limitations pointed out [156]. The errors originating in the measurement of the addition process have been discussed with respect to the measurement noise [202]. A more detailed analysis on the basis of Monte Carlo simulations [202] has been described [187]. Computerized data-processing in ion-selective electrode potentiometry has been the subject of several papers [119, 238, 239, 270, 280, 281].

Flow analysis. A flow-through tubular PVC matrix membrane with an internal metal contact for flow-injection analysis has been described [86]. The applications of flow-through detectors have been reviewed [263], particularly for clinical analysis [205].

Chromatographic detectors. Ion-selective electrode detectors for high-performance liquid chromatography have been reviewed [30, 31, cf. 119].

A chloride ion-selective electrode was used as a detector for inorganic anions separated by ion-pair chromatography [161]. Anions [256] and monovalent cations [255] were determined with an ion-selective electrode detector in ion-exchange chromatography. Figure 2 shows the ion-chromatograms obtained with valinomycin and nonactin ion-selective electrodes as detectors. A detector for open-tubular column liquid chromatography has been described [192]; the anion-selective microelectrode with a tip diameter of approximately 1 μm was directly inserted into the downstream end of 25-μm and 10-μm inner diameter columns. An analogous system for alkali metal and quaternary ammonium ions has been reported [193].

Liquid-junction potential. The effects of the liquid-junction potential on measurements with ion-selective electrodes, particularly in body fluids, have been discussed in several papers [101, 106, 246, 258, 259, 293]. The suspension or Pallmann effect on the liquid-junction potential observed in the presence of charged colloids, e.g., biopolymers, was satisfactorily explained by Overbeck [215] (cf. [248]) as a Donnan potential where the colloidal

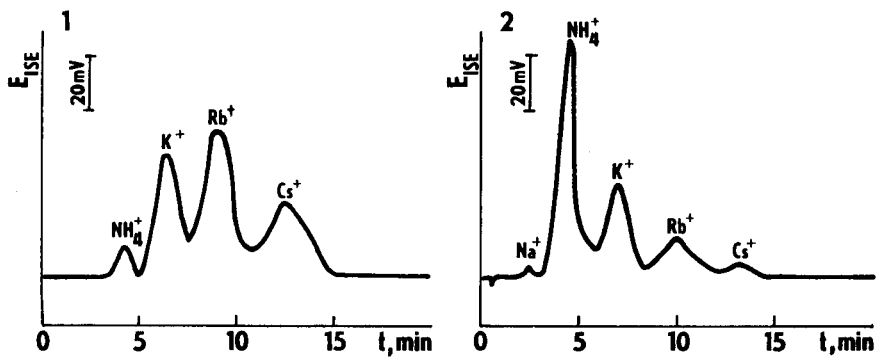

Fig. 2. Ion chromatograms of monovalent ions obtained with ion-selective electrodes: (1) liquid membrane based on valinomycin; (2) liquid membrane based on nonactin. Column, Wescan Cation 269-004; eluent, HNO_3 (pH 2.5) at 1.5 ml min^{-1}; sample, 1 × 10^{-4} M each cation (Li^+, Na^+, NH_4^+, K^+, Rb^+, Cs^+); injection volume, 100 ml; injection time t = 0. (According to Suzuki et al. [255].)

ions function as non-diffusible ions. In this way, the findings of higher or lower activities of ions present in blood electrolyte were explained [106, 245, 246, 258, 259, 273]. Replacement of KCl by sodium formate in the liquid bridge has been suggested [245].

Other problems. Analysis with ion-selective electrodes having inadequate calibration characteristics [172] and in the low-level non-Nernstian response region [131] has been described. Use of an ion-selective electrode as reference electrode has been suggested [270]. The effects of impurities present in liquid membranes have been discussed [221].

Besides e.m.f. measurements, Volta (contact) potential measurements can also be used in potentiometry but this generally complicates the measuring system. In two recent papers [129, 169], an ionized air reference electrode of this type based on americium-241 was suggested and its good performance described. However, it is doubtful whether anybody would willingly introduce a radioactive device into the laboratory when the same function can be achieved with conventional reference electrodes.

Automatic procedures

The general interest in automatic devices involving ion-selective electrodes is steadily increasing, mainly in the clinical field [17, 57, 60, 83, 85, 87, 94, 96, 97, 109—111, 117, 118, 121, 123—125, 127, 133, 142, 143, 147, 151, 157, 160, 176, 177, 181, 183, 188, 190, 197—199, 207, 209, 218, 230, 232, 237, 241, 242, 251, 257, 260, 262, 271, 272, 274].

Evaluation of automatic analyzers. Some discussion on the performance of various automatic analyzers for clinical use (see Part 5, pp. 10—12, 22—23) has clarified the differences in the results between various systems. The principles for comparative evaluation of various systems have been summarized [17, 57, 125, 230, 232]. Sachs et al. [232] proposed a questionnaire on the basis of which parallel evaluation of Na-K analyzer is obtained; the results of such evaluations can be obtained from the authors. Russel [230] changed the reference electrode and the calibration buffers on a Corning M902 Na-K analyzer in order to illustrate how instruments from different manufacturers can give varying results on the same serum sample. Various analyzer evaluations, which are a continuation of the discussions reviewed in Part 5, are listed in Table 2. The SMAC, ASTRA-8, AMT-721 and IL-343 electolyte analyzers have been compared [143]. The Kodak Ektochem ion-selective analyzer has been described [111].

Construction of new automatic systems for biomedical analysis. An ISFET-based analyzer for blood electrolyte cations (hydrogen, sodium, potassium and calcium) has been developed; indwelling cannula sampling was used in an ex vivo approach [110, 242]. A microprocessor-controlled system based on liquid-membrane ion-selective electrodes was suitable for automatic measurements of Na^+ and K^+ concentrations in urine [118]. Another automatic system for measurement of Na^+, K^+, Ca^{2+} and H_3O^+ activities was based on catheter ion-selective electrodes in abdominal aorta [60]. Calcium

TABLE 2

Evaluations of automatic analyzers for electrolyte concentration in plasma, serum and whole blood (and urine)

Analyzer	Analytes	Ref.
Hitachi 705	Na^+, K^+, Cl^-	83
Beckman E-2	Na^+, K^+	272
Corning 902	Na^+, K^+	94, 230
Technicon Ra-100	Na^+, K^+, CO_2	117
IL 502	Na^+, K^+	121
Microlyte (KONE)	Na^+, K^+	127
KNA 1 (Radiometer)	Na^+, K^+	127
NOVA-1	Na^+, K^+	133, 181
NOVA-2	Ca^{2+}	192, 237
NOVA-4	Na^+, K^+, Cl^-, CO_2	218
NOVA-6	Na^+, K^+, Ca^{2+}	251
NOVA-7	Ca^{2+}	199
ASTRA-8	Na^+, K^+	143, 147, 151, 207
AMT-721	Na^+, K^+	143, 271
Bectin Dickinson QEA	Na^+, K^+	160
Dupont aca	Na^+, K^+	176
Radiometer	Ca^{2+}	188

ion-selective electrode measurements were simulated in order to elucidate the differences in the results obtained with various commercially available analyzers [96]. An analyzer for Na^+, K^+ and Cl^- in serum has been described [85]. An automatic system for measurement of Ca^{2+} release after stepwise acidification has been developed [198].

Measuring conditions and errors. The conditions for treatment of blood and serum [123, 124, 260], and particularly the effects of silicone-separator tubes and storage time and temperature [183, 262] before Ca^{2+} determination have been discussed. Errors in the determination of sodium and potassium in blood, previously ascribed to the binding to hydrogencarbonate [142], were shown to be due to a liquid-junction effect [109]. Errors in potassium determination in physiological fluids were explained as an anion interference [177]; unfortunately, the authors did not indicate which anions interfered (anion interference is connected with their hydrophobicity, see Part 2, p. 13).

Other automated systems. An automatic system for copper(II) monitoring with an ion-selective electrode in a purification plant electrolyte has been described [97]; the copper ion was in the range $0.5—10^{-4}$ mol dm^{-3} and interference by iron(III) ions was removed by addition of ascorbic acid. An automatic device for determination of stability constants from solubility data was based on monitoring the solid-phase dissolution with an ion-selective electrode [209]. An automatic analyzer for chloride and fluoride determinations has been described [257]. An automatic recording apparatus has been used for catalytic kinetic analysis with ion-selective electrodes [157].

Ion-selective electrodes in non-aqueous media

The behaviour of ion-selective electrodes in non-aqueous media has been the subject of several papers [55, 105, 113, 116, 129, 163, 166a]. A report to the IUPAC Commission of Electroanalytical Chemistry deals with this topic [55]. A method for the determination of trace amounts of alkaline impurities in non-aqueous solvents with ion-selective electrodes has been described [105] (see also [116]). Standard Gibbs energies of transfer between water and acetone/water mixtures were measured with cation-selective electrodes [129]. Stability constants of the copper-acetate complex in alcohol/water mixtures were evaluated with a copper ion-selective electrode [163]. Fluoride was determined in aqueous and aqueous organic solvents [166a]. The response time of a silver sulphide ion-selective electrode in aqueous organic media was examined [113].

Ion-selective field-effect transistors (ISFETs)

Considerable attention has been given to the construction and application of ISFETs [23, 32, 45, 84, 88, 90, 93, 95, 98, 110, 146, 150, 152, 166, 173, 174, 180, 201, 204, 208, 210, 236, 242, 247, 266, 269]. The properties and applications of ISFETs have been reviewed [23, 32, 174].

Theory. The role of buried hydroxide sites in the response mechanism of inorganic gate pH-ISFETs has been discussed [98]. Equilibrium noise in ISFETs has been described [146].

Construction. A suspended mesh ISFET can improve the adhesion of the ion-selective membrane to the insulator layer [95]. Methods of encapsulation of polymeric membrane-based ISFETs have been described [152]. For a K^+-ISFET, valinomycin-doped photoresist membranes were satisfactory [166]. A pH ISFET with a Ta_2O_5 layer was viable [173, 210]. The system of two ISFETs with different sensitivities did not require an additional reference electrode [180]. A polymer-gate ISFET was characterized [201]. Potassium and sodium micro-ISFETs with tip diameters of 30 μm were based on aluminosilicates as the outer ion-sensing layer [208]. A sodium ISFET was obtained by ion implantation into alumina-based gates [236]. Damage by electric charge during handling of an ISFET can be prevented [247]. A multi-species microprobe for potentiometric measurements has been described [266]; with an appropriate patterning technique, a multispecies electrode of IrO_2 for H_3O^+, AgCl for Cl^-, LaF_3 for F^- and Ag can be prepared. A potassium ISFET with an urushi-based membrane [269] and well known ISFETs with Si_3N_4 [84] and SiO_2 [90] insulator layers have been described.

Applications. A four-function ISFET integrated-circuit sensor for blood K^+, Na^+, Ca^{2+} and pH has been developed [110, 242]. A pH ISFET has been used as the detector in a microprocessor-based coulometric pH-stat [93]. A urea sensor can be made from a pH ISFET coated with a cross-linked urease-albumin membrane [88]. A microsize ISFET-based urea sensor has been described [204]. A bioelectrode with two pH ISFETs and a Pt pseudo-reference electrode has been described [150].

Electrolysis at the interface of two immiscible electrolyte solutions (ITIES)

Electrolysis at ITIES (for a recent progress review, see [38]), which is a mostly voltammetric alternative to ion-selective electrode potentiometry, has been dealt with in an increasing number of papers [135, 136–140, 148, 149, 155, 158, 162, 168, 178, 194–197, 212–214, 226–228, 231, 233–235, 249, 250, 267, 268, 276, 277]. The subjects studied are listed in Table 3. A method for evaluation of ohmic potential drop arising in electrolysis at ITIES by means of a galvanostatic pulse has been described [194].

Miscellaneous problems

The effects of γ-radiation fields on the behaviour of ion-selective electrodes have been described [145]. Two more papers appeared on bipolar pulse-conductometric monitoring of ion-selective electrodes [222, 223] (see Part 5, p. 6). A conditioning buffer for regeneration of gas-sensing ion-selective electrodes has been suggested [167]. An alternative method for silanization of the surface of ion-selective microelectrodes has been reported [206]. Connection of four or even eight ion-selective electrodes in series was claimed to give enhanced sensitivity of measurement [220, 253].

TABLE 3

Electrolysis at the inferface of two immiscible electrolyte solutions (ITIES)

Subject	Ref.
Ion-transfer across water/1,2-dichloroethane interface	135, 136
Ion-transfer across ITIES with adsorbed phospholipid monolayer	137
Zero-charge potential of ITIES	138
Adsorption of phospholipids at ITIES	139
Interfacial tension of ITIES	140
Electric double-layer structure at ITIES	148, 149, 155, 235
Ion-transfer across ITIES studied by a.c. polarography	158, 213
Electrocapillarity of ITIES	167
Ion-selective electrode potential interpreted by voltammetric study at ITIES	168
Monensin-mediated alkali metal and hydrogen ions transfer across ITIES	178
Determination of calcium, barium and strontium by differential pulse stripping voltammetry at ITIES	195
Chronopotentiometry at ITIES	196, 197, 226
Determination of standard Gibbs energies of ion transfer	212, 249, 250
Ion-transfer between polymer-electrolyte gel and electrolyte solution	214
Differential capacity of ITIES	194, 227, 228, 234
Determiantion of aniline traces in nitrobenzene	231
Kinetics of choline and acetylcholine transfer across ITIES	232
Mediation of ITIES by molecules of biological importance	267, 268
Transfer of 1,10-phenanthroline and derivatives across ITIES	276
Valinomycin-mediated potassium ion-transfer across ITIES	277

FIXED-SITE ION-SELECTIVE ELECTRODES

As in earlier parts [1], all fixed-site systems except the silicate glass electrodes and electrodes with obscure properties are included in this section. The fixed-site ion-selective electrodes have been the subject of numerous papers [12, 113, 126, 163, 166, 282–458].

Silver halide electrodes and similar systems

The silver halide ion-selective electrodes have been applied to halide determination in electroplating baths [442] and geothermal brines [448]. The effect of pH on the behaviour of these electrodes has been studied [328]. These electrodes are useful for determinations of halide salts of cationic surfactants [335]. Zinc(II) bromide, iodide and thiocyanate complexes can be studied in methanol by means of the respective ion-selective electrodes [318]. Errors connected with the drift of bromide and iodide ion-selective electrodes can be avoided [427].

Chloride ion-selective electrodes. Various applications of these electrodes are listed in Table 4. A HgCl/HgS chloride ion-selective electrode has been studied [412]. Drug interferences with chloride determination in serum with the chloride ion-selective electrode have been reported [360]. A flow-injection potentiometric determination was used for residual chlorine in water [429]. For the determination of the chlorine content of rocks, the sample was decomposed with hydrofluoric acid, chloride was oxidized to chlorine which was separated and reduced by sulphite in a gas-diffusion cell, and the resulting chloride was finally determined with an ion-selective electrode [286]. A commercial chloride ion-selective electrode has been evaluated [369].

TABLE 4

Applications of chloride ion-selective electrodes

Use	Ref.
Chloride determinations	
—, in milk	291, 324
—, in wine	292
—, in aromatic polyamide fibre production solutions	300
—, in titanium	309
—, in waste water	316, 350, 359
—, in biochemical preparations	317
—, at low concentration ranges	345, 387
—, in environmental samples, after pretreatment	351
—, in plant tissues	356, 408, 409
—, in European infant formulae	397
—, in drugs	407
—, in salt brines	419
—, in oxidizing media	423
—, in water with flow injection	428

Bromide ion-selective electrode. A potentiometric cell consisting of a bromide ion-selective electrode and a platinum electrode is sensitive to free residual chlorine (at pH 5 and 0.1 M bromide) [378].

Iodide ion-selective electrode. Various applications of this electrode are listed in Table 5. The iodide ion-selective electrode has been suggested as reference electrode in an iodide-buffered solution [384]. The properties of an Ag_3SI single-crystal iodide ion-selective electrode have been investigated [413]. A silver-iodide carbon-paste electrode has been described [326]. Iodide ion-selective electrodes of three different shapes have been designed [368].

Cyanide ion-selective electrodes. The surface properties of a precipitate-based cyanide ion-selective electrode have been studied [338, 401]. Because of the dissolution mechanism of the most widely used cyanide electrode (see Part 1, p. 365), the main interferent is iodide and the other interferents are those interfering with the iodide electrode. Thus, a merely empirical study of the selectivity coefficients of the cyanide electrode [432] without consideration of this aspect is of little value.

The cyanide ion-selective electrode has been used for cyanide determination in waters [347, 349, 367] and in waste-waters [367, 391, 451]. A flow-injection method has been applied [382]. Trace gold was determined with this electrode by means of a catalytic process [373]. A cyanide electrode based on an $AgCN/Ag_2S$ mixture was used for total cyanide determination in thiocyanate-containing waste-waters [314].

Silver sulphide-ion-selective electrodes

The applications of the sulphide ion-selective electrode are listed in Table 6. This electrode was also used for successive determinations of S^{2-} and

TABLE 5

Applications of iodide ion-selective electrodes

Use	Ref.
Iodide determinations	
—, in organic compounds	308
—, in drugs	310
—, in urine	313
—, by flow injection	382
Determination with iodide electrode	
—, of mercury(II), titrimetric	290
—, of iodine after ion-exchange chromatographic separation	299
—, of thiosulphate, thiourea and ascorbic acid, titrimetric	301
—, of thallium	307
—, of W(VI), catalytic	361, 382
—, of Mo(VI), catalytic	362, 424, 382
—, of stability constants of Hg(II) thiosemicarbazonate	366
—, of sulphides	455

TABLE 6

Applications of sulphide ion-selective electrodes

Use	Ref.
Determination of sulphide	
—, in bacterial cultures	282—284
—, in waste waters	298, 375
—, by flow-injection analysis	333
—, in waters	341, 385, 401a, 426, 438
—, at low concentration range	344
Determination with sulphide electrode	
—, of hydrogen sulphide in coke oven gas	295, 296
—, of hydrogen sulphide in atmosphere	383
—, of Ag^+	431
—, of thiols	399
—, of thiols in natural gas	329
—, of sulphite	376
—, of chloride in waters	342
—, of ovalbumin	363, 364
—, of nicotinamide adenine dinucleotide phosphate (enzymatic)	346

SH^- by potentiometric titration [352], and in evaluation of the ionization constants of H_2S [340]. Various sulphur forms were determined simultaneously in alkaline solution [337]. The sulphide ion-selective electrode was used in an aqueous/organic solvent mixture [113]. The stability of a sulphide antioxidant buffer was assessed [334]. Chemical pretreatment of a copper-containing silver wire for preparation of a silver/silver sulphide ion-selective electrode has been described [404]. A hydrogen sulphide gas sensor based on an Ag_2S internal sensor with a solid-state LaF_3 electrode as reference was used to determine sulphide in printing and dyeing waste-waters in the concentration range from 5×10^{-8} to 10^{-2} mol dm^{-3} [457]. Electrodes based on hydrophobized graphite rods covered with mercury(II) chalcogenides or their mixtures with silver chalcogenides or mercury were used for titrations with EDTA [32].

Divalent chalcogenide electrodes

Copper ion-selective electrodes. The applications of the copper ion-selective electrode are listed in Table 7. A ternary copper-silver-selenium compound was used for a copper(II) ion-selective electrode membrane [386]. Adsorption of copper ions on the surface of a precipitate-based Cu(II) ion-selective electrode as well as the dissolution of the membrane were shown to affect the detection limit [343]. Chelating ligands affected the response of a chalcocite ion-selective electrode [352]. In the case when the substrate of an enzymatic reaction binds metal ions more or less than the products of this

TABLE 7

Applications of copper ion-selective electrodes

Use	Ref.
General study	336, 370, 395, 435
Determination of copper	
—, in organic compounds	306
—, in technical Zn electrolyte	330
Sequential complexiметric titration of Cu(II), Zn and Fe(III)	421
Complexiметric titration of aluminium	371, 416
Complexiметric titration of zinc	355
Potentiometric determination,	
—, of amino acids	287
—, of citrate	393
—, of thorium	394a
Kinetic determination of Fe(III)	403
Determination of stability constants	
—, of copper-acetate complex	163
—, of copper and cadmium iminodiacetate complexes	420
Cu(II) hydrolysis study	339
Copper/serum albumin interaction study	380

reaction, monitoring of the activity of the metal ion with an ion-selective electrode can be used for assessment of the rate of the reaction [289]. In another version (metal-stat), the substrate can be added automatically to keep the potential of the ion-selective electrode constant. The copper ion-selective electrode was used for assay of inorganic pyrophosphatase and carboxypeptidase A by means of these methods [289]. Selectivity coefficients of a copper ion-selective electrode have been reported [430].

Lead ion-selective electrode. Applications of the lead ion-selective electrode are listed in Table 8. The surface morphology of this electrode has been studied [400].

Cadmium ion-selective electrode. The cadmium ion-selective electrode has been used for indirect determination of cadmium in waters [456] and of sulphide [302], for potentiometric titrations of cadmium, calcium and magnesium mixtures [381] and for assessment of the stability constants of cadmium complexes [456].

Fluoride ion-selective electrode

The applications of the fluoride ion-selective electrode are listed in Table 9. Regeneration of badly responding electrodes has been studied [297, 331]. Introduction of a silver fluoride layer into the internal contact of a commercial electrode has been recommended [297] (cf. Part 4, p. 9). The connection between the statistical detection limit and different working conditions has been studied [414]. The hydroxide interference with the fluoride electrode has been explained by formation of soluble $LaOH^{2+}$ and $La(OH)_2^+$ complexes [325].

TABLE 8

Applications of lead ion-selective electrode

Use	Ref.
Determination of Pb^{2+}	
—, in white spirits	311
—, in cystine	453
—, in waste waters	379, 458
Determination of sulphate	
—, in rare earth sulphoxides	374
—, in natural waters	410, 411, 450
—, in glauberite	452
Analysis of sulphate, sulphite and dithionate mixtures	415
Determination of bile phosphate	303
Determination of polyphosphates	425

TABLE 9

Applications of fluoride ion-selective electrode

Use	Ref.
Determination of fluoride	
—, general papers	288, 305, 427, 434
—, in dental surgery	12, 433
—, in serum	126, 417
—, in spinal fluid	126
—, in aqueous organic solvents	166a, 327
—, in waters	285, 293, 392, 447, 449
—, in the environment	294
—, in food	304, 357, 406
—, in pharmaceuticals	312, 377
—, in glass ceramics	315
—, in hydrofluoric acid solutions	319
—, in breast milk	321
—, in soils	322
—, in fertilizers	323, 354
—, in organic compounds	332, 454
—, at low concentrations	365
—, in fluoroacetate	372
—, in plant tissues	394, 437
—, in body fluids and organs	417, 418
—, in plating baths	422
—, in flow streams	436
Determination of tellurium	396
Determination of solubility products of rare earth fluorides	358
Determination of stability constants of fluoride complexes	348

Other systems

For the determination of the hydrogen ion concentration in hydrofluoric acid solutions, a glass with the composition 10% Ag_2O, 20% Li_2O, 50% P_2O_5, 10% MgO and 10% WO_2 (all % by weight) was suggested [389]. A nitrate sensor was based on an alkali-free magnesium phosphate glass; the most suitable one contained 10% CuO, 55% P_2O_2, 15% MgO, 10% Al_2O_3 and 10% SiO_2 (all % by weight) [390]. A polymeric sulphur nitride electrode gave a response towards Ag^+ ions; although the potential was not reproducible, this electrode was suitable for titrations [405]. A fluoride glass membrane was suggested for a fluoride ion-selective electrode [407]. Iron-doped chalcogenide glasses of the composition $Fe_x(Ge_{28}Sb_{12}Se_{60})_{100-x}$ (x = 0—2.2) were used for electrodes selective to Fe^{3+} and Cu^{2+} [439, 440]. For Ag^+ determinations in strongly acidic media, silver selenoarsenate glasses provided suitable materials for the electrode membranes [441]. The proton and ion conductivity of $(NH_4)_3PMo_{12}O_4 \cdot nH_2O$ has been studied and an ammonium ion-selective heterogeneous membrane suggested [442, 443]. Copper ion-selective electrodes based on β-vanadium oxide bronzes have been described [444, 445] (cf. Part 5, p. 21). The high-temperature zirconia pH sensor has been compared with the glass electrode [388] (cf. Part 4, p. 20). More experience is needed for evaluation of sulphate-selective electrodes based on lead sulphate or an anion-exchanger membrane [398].

LIQUID-MEMBRANE ELECTRODES

A high proportion of the papers has dealt with liquid-membrane ion-selective electrodes [37, 70, 73, 74, 122, 211, 289, 409, 459—744].

Calcium and magnesium ion-selective electrodes

At present, the calcium ion-selective electrodes are still the most studied of all liquid-membrane ion-selective electrodes. The effect of variation of hydrodynamic conditions on the response of a macrocyclic carrier-based calcium ion-selective electrode has been studied [654]. A calcium ion-selective electrode was based on bicyclic polyether amide derivatives and seemed to have reasonable prospects for determination of Ca^{2+} in undiluted blood sera [583]. Effects of polar additives on the selectivity of tri-octoxybenzene sulphonic acid-based electrodes towards Ca^{2+} and Mg^{2+} were reported [503]. A divalent cation-selective electrode was used for enzyme assessment [289]. The effects of pH and NaCl on the measurement of ionized calcium in matrices of serum and human albumin with a calcium ion-selective electrode were studied [652]. The transport of calcium through the membrane of an ion-selective electrode was confirmed [628]. Anionic surfactants were found to interfere with the calcium ion-selective electrode [517—519].

Applications of the calcium ion-selective electrode are listed in Table 10. Many clinical applications were mentioned above in the section on automatic procedures. Calcium ion-selective microelectrodes were applied to intracellular

TABLE 10

Applications of calcium and divalent cation-selective electrodes

Use	Ref.
General papers	471, 484, 497, 573a, 704
Determination of calcium	
—, in human milk	461
—, in plasma	498, 702
—, in blood	702
—, in blood, in extracorporeal circulation	464, 563
—, in saliva	498
—, in bile	505, 696
—, in serum,	620, 634, 702, 716, 725
effect of blood pressure	514, 624
indicator of hypercalcemia	603, 611
—, in urine	552
—, in presence of biochemical materials	577, 578
—, in pancreatic juice	604
—, in phosphate ores	643
Determination of both calcium and magnesium	
—, general papers	546, 695, 705
—, in determination of stability constants of gallate complexes	661
—, in ion-association study in substituted hydroxybenzoate solutions	504

calcium determination in rabbit papillary muscles [489], in squid giant axons [499], in *Aplysia* neurons [536], in frog skeletal muscle fibres [614] and in cleaving embryonic cells of *Oryzias latipes* [666]. Intracellular free magnesium was measured with a magnesium ion-selective microelectrode in neurons of *Helix aspersa* [462] and in frog skeletal muscle [615].

Nitrate ion-selective electrode

Applications of the nitrate ion-selective electrode are listed in Table 11.

Potassium ion-selective electrodes

The mechanism of the response of the valinomycin-based potassium ion-selective electrode has been studied [72—74]. Lipophilic bis(crown ether) derivatives were examined for potassium ion-selective membranes [558, 560, 580—582]. A silicone rubber-based membrane containing valinomycin was found to give better performance than a PVC-based membrane for potassium determinations in undiluted urine samples [465]. The long-term stability of the valinomycin-based membranes was studied [539]. The valinomycin-based electrode was applied to ion solvation study [122] and for the determination of monopotassium glycyrrhizate [726].

TABLE 11

Applications of nitrate ion-selective electrodes

Use	Ref.
General studies	572, 594
Determination of nitrates	
—, in plants	409, 585, 659, 660, 687
—, in waters	459, 554, 630, 647
effect of surfactants	548
—, in vegetable and melon crops	473
—, in barley plants	492, 493
—, in environment	544, 692
—, in soil	544, 554, 585, 610, 658, 659, 686
—, in milk	554, 646
—, in animal feed	568
—, in waste water	596

Applications of potassium ion-selective electrodes are listed in Table 12. Many clinical applications of this electrode were mentioned in the section on automatic analysers. Applications of potassium ion-selective microelectrodes are listed in Table 13. Since the Corning Company withdrew its ion-exchanger for potassium ion-selective microelectrodes (Corning K^+-LIX 477317) from the market, the only remaining ion-exchanger solution is Orion K^+-LIX which has inferior properties to the Corning solution with respect to selectivity to K^+ over Na^+ [601]. It would be better, in any case, to use a valinomycin solution with a proper concentration of tetrakis(*p*-chloro)phenylborate.

Sodium and lithium ion-selective electrodes

Various ionophores for sodium ion-selective electrodes have been suggested showing selectivities towards sodium with respect to potassium upto 20 [708]. The conductivity of sodium-selective membranes with electroneutral ionophores was determined [681]. A Na^+-selective electrode with solid contact was described [667]. Applications of the sodium ion-selective electrodes are listed in Table 14, including charged carrier, neutral carrier and glass sodium ion-selective electrodes.

Crown polyethers with small internal cavity were studied for lithium ion-selective electrodes [587, 588] (see also [522, 523]). New neutral ionophores for Li^+ based on *cis*-cyclohexane-1,2-dicarboxamide [622] and substituted diphenylmaleimide [709] were reported. The effect of addition of organophosphorus compounds to Li^+-selective electrode based on dibenzo-14-crown-4 was studied [565].

Other systems based on ionized ion-exchangers

The general remarks concerning many of these systems remain the same as in Part 5, p. 26. However, a rewarding tendency may be found in more

TABLE 12

Applications of potassium ion-selective electrodes

Use	Ref.
General studies	538, 599, 609, 619, 625, 633, 723, 727, 736, 743
Determination of potassium	
—, in blood	516, 608, 744
—, in plasma	500, 516, 690, 744
—, in serum	500, 516, 623, 698, 703, 744
—, with a tube-mounted electrode	507
—, in grape juice	540
—, with a disc with immobilized valinomycin	599
—, in beryllium oxide	616
—, in food	627, 651
—, in herb injections	631
—, in soil	641
—, in electrolyte infusion solutions	642
—, in urine	465, 698
—, in fertilizers	712

TABLE 13

Applications of potassium ion-selective microelectrode

Use	Ref.
Determination of potassium	
—, general study	691
—, in tight epithelia	494, 495
—, in *Stentor coeruleus*	506
—, in brain slices	555
—, in canine cardiac Purkinje fibres	589
—, in proximal tubule of *Necturus* kidney	598
—, of interstitial myocardial K^+	656
—, in plant roots	722, 724

systematic studies concerned with relationships between the ion-exchanger or analyte structure and the selectivity of the electrode [525, 526, 533, 551, 553, 669—671, 683—685, 715, 739].

Applications of well proven systems have continued. These include the tetrafluoroborate ion-selective electrode for determination of boron in wastewaters [602], in ascharite [644] and in steels [706] (for microanalysis, see [714]). Several papers have been concerned with perchlorate [502, 632, 668, 697], periodate [547, 737, 738] and cesium [485] ion-selective electrodes. The carbonate ion-selective electrode was used in the Technicon RA-1000 instrument for determination of total CO_2 in blood [486]. A

TABLE 14

Applications of sodium ion-selective electrodes

Use	Ref.
Determination of sodium	
—, in blood	475, 516, 608
—, in serum	466, 500, 516, 537
—, in plasma	468, 500, 515, 516, 690
—, in urine	466, 703
—, in foods	469, 651
—, in brush border membrane[a]	470
—, in bacterial culture	474
—, at low concentration	520
—, in meat products	521
—, in kidney muscle[a]	573
—, in cheese	584
—, at rat small intestine	618
—, in brine streams	687
—, in waters	719
—, near mechanoreceptor cells of *Patinopecten yessoensis*[a]	740

[a]Microelectrode study.

hydrogencarbonate electrode was applied in the evaluation of the CO_2 dissociation constant [574]. Tubular potentiometric polymeric pH and NH_4^+ ion-selective electrodes were compared as detectors in the automated determination of ammonia [607] (see also [211]). An improved liquid-membrane chloride ion-selective electrode with reduced salicylate interference was used for direct determination of chloride in undiluted urine samples [718]. The chloride-selective microelectrodes, which have been reviewed [479], were applied to the study of chloride absorption by *Amphiuma* small intestine [717] and of chloride activity in stripped frog skin [527]. A H_3O^+-selective microelectrode based on tri-n-dodecylamine in *o*-nitrophenyl octyl ether was used for measurement of vacuolar pH of plant cells in suspension culture [600]. Acetylcholine and choline ion-selective microelectrodes were developed [571]. Nitrite in animal feed was determined with a commercial ion-selective electrode [568]. Direct potentiometry with a NH_4^+-selective electrode was used to determine ammonium ion in fertilizers [712]. Surfactant electrodes (see Part 5, p. 26) have been studied extensively [556, 557, 597, 650, 655, 662, 664]. Lipophilic-cation selective electrodes have been used for assessment of cell membrane potentials [37, 463, 576] (see Part 5, p. 26).

Anion-selective electrodes based on ionized ion-exchangers have been reported for tetrachloroaurate(III) [481, 531, 699, 700], cholate [482, 483], picrate [496, 639, 640], hexafluorotantalate [510, 741], chromate [511], tetrachlorogallate(III) [512], perrhenate [513, 636, 637], molybdenum(IV) chelates [524], copper 8-quinoline dithiocarboxylate [530],

dicyanoaurate(I) [532, 534], tetrachloroferrate [535], niobium(V) anionic complexes [559, 742], cobalt(II) and zinc(II) tetrathiocyanate complexes [562], tungstate [566], dicyanoargentate [569, 570, 734], permanganate [575], flufenamate [586], hexafluoroarsenate [590], hexafluorophosphate [591], tetrachlorothallate(III) [592, 593], various 2- and 8-quinolinedithiocarboxylates of *d*-elements [605], lactate [621], salicylate [621, 626], tetrabromothallate(III) [634, 638], dichloroacetate [645], trinitrobenzenesulphonate [663], molybdenum(VI) anionic complexes [680], bismuth(III) complex with 5-mercapto-3-(naphthyl-2-)-1,3,4-thidiazol-2-thione (Bismuthiol III) [693, 694], copper(II) alkylthiophosphate complex [707], thiocyanate [721], tetrachloroindate(III) [731]. In some cases, possible applications were mentioned. Two types of internal reference electrodes for these systems were suggested [508].

Cation-selective electrodes based on ionized ion-exchangers include systems with some degree of selectivity for quinine [467], chloramine-B [472], cinchonine [487], berberine [488], succinylcholine [491], hexamethonium [491], decamethonium [491], caffeine [549], atropine [550], scopolamine [567], copper(I)-methylphenanthroline complex [579], uranyl ion [509, 617], methyltrialkylammonium ions [649], 2-aminoperidinium [657], ethidium [665], diphenhydramine [674], levamisole [675], amethocaine [676], strychnine [677], berberine [678], chloramine-T [701], moroxydine [728], promethazine [729], tetrahydropalmatine [730], thiamine [732], phenytoin [733] and alizarin [736].

New ion-exchanging ions include triphenylstilbenylborate [491] and trialkylcyclotetrasiloxanylammonium [501]. Selectivity coefficients for an ion-selective electrode based on Crystal Violet dissolved in nitrobenzene have been reported for 48 anions [672]. Various potentiometric titrations based on ion-pair formation with an ion-selective indicator electrode has been described [70, 541—543, 545, 710, 711, 713].

Other systems based on neutral ligands

Among the electrodes based on crown polyethers (coronands) sensors for guanidinium [476], dicubain and hexylcain [679] have been described. Direct potentiometric determination of the enantiomeric excess of 1-phenylethylammonium ion is possible with an electrode based on a chiral ligand of the tetracarboxamide-substituted 18-crown-6 type [480, 629]. Bis(crown polyether)-based ion-selective electrodes for thallium(I) [561] and rubidium ion [564] have been reported. A general study of the crown polyether systems is available [528].

Electrodes based on macrocyclic lactone ionophores include a tetranactin-based ammonium ion-selective electrode [529]. The tubular polymeric ammonium and hydrogen ion-selective electrodes were compared as detectors in automated determination of ammonia [607] (cf. [211]). The ammonium-selective electrode was used for determinations of ammonia in plasma [490] and of ammonium ion in fertilizers [712]. The cation selectivity of

liquid-membrane electrodes based on macrocyclic lactones and lactone lactams has been studied [477, 478].

Electrodes based on ligands of the poly(oxyethylene) type were examined for sulphate titration [595] and non-ionic surfactant determinations [688, 689]. The liquid-liquid extraction of complexes formed with these ligands has been studied in connnection with their electrochemical response [460].

Other electrodes based on neutral carriers include a Pb^{2+}-selective electrode with *N,N*-dioctadecyl-*N,N'*-dipropyl-3,6-dioxaoctanediamide as active substance; this electrode actually responds to monovalent cationic complexes of the type PbX^+ (X = OH^-, Cl^-, NO_3^-, CH_3COO^-) [612]. Anion-selective electrodes based on trioctyltin [720] also respond to hydrogencarbonate [653]. Uranyl ion-selective electrodes are based on tri-n-octylphosphine [613] or substituted diphenylmaleimide [709] ligands. The H_3O^+-selective microelectrode based on tri-n-dodecylamine in *o*-nitrophenyl octyl ether is useful for measurement of vacuolar pH of plant cells in a suspension culture [600].

POTENTIOMETRIC BIOSENSORS

Several reviews of this field [8, 9, 25, 26, 35, 36, 43, 64, 65, 82] have been published as well as descriptions of new sensors and improvements of known sensors [200, 745—767].

Enzyme electrodes

A β-glucose oxidase membrane system with an iodide-selective electrode has been suggested for determining β-glucose [745]. Another glucose sensor is based on the fluoride-selective electrode [751, 752]. An enzyme electrode for butylthiocholine iodide depends on immobilized cholinesterase [746]. In an enzyme electrode for salicylate, immobilized salicylate hydroxylase is used [748]. In the method for determination of creatinine in plasma with an enzyme electrode, excess of ammonia can be removed in an automated flow arrangement [749]. New versions of the creatinine [750, 757] and urea [765] enzyme electrodes have been suggested. A miniature enzyme electrode for urea was designed [753]. A urea enzyme electrode was used for urea determination in whole blood [766]. A histidine-sensitive electrode was described [754]. A method for determination of serum ornithine carbonyl transferase was developed [756]. With the help of an immobilized asparaginase sensor, asparagine and asparaginase in human serum were determined [758]. An arginine enzyme electrode was based on immobilized arginase and urease [759]. An *N*-acetyl-L-methionine sensor was applied to acylase determinations [760]. A bound cofactor/dual enzyme electrode system for L-alanine was designed [761]. Immobilized lysine decarboxylase was used in an L-lysine enzyme electrode [762]. A dual-enzyme electrode proved suitable for determination of flavin adenine dinucleotide in the presence of riboflavin and flavin mononucleotide [767]. Enzyme electrode functions could be improved by a new procedure for coupling enzymes with fine-mesh nylon net [200].

Immunoelectrodes and bacterial electrodes

A sensor for immunoassay is based on a tetraalkylammonium ion-selective electrode placed in a suspension of liposomes that are loaded with a salt of the tetraalkylammonium cation and contain lipid antigens on their surface. By action of an antibody and a protein complement, a lysis reaction of the liposomes is started. The concentration of released tetraalkylammonium ions depends on the antibody concentration and is determined with the ion-selective electrode [763]. This method can be used for assessment of anti-cardiolipin antibodies in syphilis serology [764].

A microbial sensor for uric acid has been described [755]. The presence of azide in the working buffer and cold storage of the electrode improved the selectivity of the arginine bacterial sensor [747].

MISCELLANEOUS SYSTEMS

The bilayer lipid membrane (BLM) model is widely used in membrane biology and biophysics. An ammonia sensor is based on BLM modified with nonactin. Under an applied electric potential difference, the transmembrane current is a function of the ammonia concentration in the bathing solution [768]. This sort of sensor (see also [768a, 768b]) shows high promise after some technological problems have been overcome.

Manganese(IV) oxide [769] and the lead(IV) oxide [770] electrodes can act as sensors for Mn^{2+} and Pb^{2+}. A tungstate-selective electrode based on lead tungstate [771] and a molybdate-selective electrode [772] have also been mentioned.

The author is at a loss whether or not to include an aged nitrate-selective electrode recommended as a sensor for halide titrations [773]. The same doubts arise in reading the papers dealing with inselective sensors recommended for titrations [774—776].

Recently, numerous papers have appeared which are concerned with various precipitate-based electrodes which show problematic reproducibility and dubious selectivity [777—794]. Many of these systems had been investigated in the past and rejected. More self-criticism should be required from authors before such contributions enter the literature.

The assistance of the Technical and Economic Research Institute of Chemical Industry, Prague, who supplied computerized Chemical Abstract Condensates dealing with ion-selective electrodes, is highly appreciated. The author is obliged to Mrs. M. Kozlová of the Heyrovský Institute, for her help with arranging the material for this review. Colleagues from all over the world who send reprints and reports in the field of ion-selective electrodes provide invaluable assistance for these reviews. Their continued help will be much appreciated.

REFERENCES

1 J. Koryta, Anal. Chim. Acta, 61 (1972) 329; 91 (1977) 1; 111 (1979) 1; 139 (1982) 1; 159 (1984) 1. (Parts 1—5).
2 J. D. Czaban, Anal. Chem., 57 (1985) A345.
3 A. H. J. Maas, J. Kofstad, O. Siggaard-Andersen and G. Kokholm (Eds.), Ionized Calcium, Sodium and Potassium by Ion Selective Electrodes, Vol. 5, Private Press, Copenhagen, 1984.
4 T. Seiyama, K. Fueki, J. Shiokawa and S. Suzuki (Eds.), Proceedings of the International Meeting in Chemical Sensors, Kodansha, Tokyo, 1983.
5 Z. R. Zhang (Ed.), International Symposium on Ion-Selective Electrodes, Shanghai Normal University, Shanghai, June, 1985.
6 G. J. Moody and J. D. R. Thomas, Ion Sel. Electr. Rev., 5 (1983) 243.
7 G. J. Moody and J. D. R. Thomas, Ion Sel. Electr. Rev., 6 (1984) 209.
8 M. Aizawa, Kagaku Sosetsu, 45 (1984) 148.
9 M. Aizawa, Kagaku (Kyoto), 39 (1984) 490.
10 M. A. Arnold, Am. Lab., 15 (1983) 34.
11 M. A. Arnold and M. E. Meyerhoff, Anal. Chem., 56 (1984) 20R.
12 M. Borysewicz-Lewicka, M. Chmielnik, A. Rydzewska and F. Cyplik, Czas. Stomatol., 36 (1983) 9.
13 R. P. Buck, in R. A. Minear and L. H. Keith (Eds.), Electrochemical Methods: Ion-Selective Electrodes in Water Analysis, Vol. 2, Academic Press, Orlando, 1984, p. 249.
14 R. P. Buck, Electrochemistry of Ion-Selective Electrodes, in R. E. White, J. O. Bockris, B. E. Conway and E. Yeager (Eds.), Comprehensive Treatise of Electrochemistry, Vol. 8, Plenum, New York, 1984, p. 137.
15 R. W. Cattrall and I. C. Hamilton, Ion Sel. Electr. Rev., 6 (1984) 125.
16 V. V. Cosofret and R. P. Buck, Ion Sel. Electr. Rev., 6 (1984) 59.
17 A. K. Covington, Med. Lab. World, July (1982) 11, 13, 17.
18 A. K. Covington, Ion Exchange and Ion-selective Electrodes, in D. S. Flett (Ed.), Ion Exchange Membranes, Horwood, Chichester, 1983, p. 75.
19 U. P. Decker and R. Geyer, Acta Hydrochim. Hydrobiol., 12 (1984) 19.
20 M. B. A. Djamgoz and P. J. Laming, Trends Neurosci., 4 (1981) 280.
21 K. Engel, K. Redersen, S. P. Nielsen and O. S. Andersen (Eds.), Ionized Calcium Workshop No. 1, Scand. J. Clin. Lab. Invest., 43, Suppl. 165 (1983).
(a) J. N. Fang and G. X. Zhou (Eds.), Li Zu Ze Xing Dian Ji Qe Liang Yi Qi (Guide for ion-selective electrode measurement), Jingsu Keji, Nanjing, P.R.C., 1984, 180 pp.
22 T. A. Fjeldly, Analusis, 11 (1983) 479.
23 A. Fog, Dan. Kemi, 64 (1983) 56.
24 H. Fong, Clin. Biochem. Rev., 4 (1983) 4.
25 M. Gronow, Trends Biochem. Sci., 9 (1984) 336.
26 G. G. Guilbault, Anal. Proc. (London), 20 (1983) 550.
27 K. Hiiro, Bunseki, 2 (1984) 115.
28 F. Honold, MTA-J., 6 (1984) 54.
29 N. Ishibashi, Anal. Proc. (London), 21 (1984) 361.
30 N. Ishibashi, A. Jyo and T. Imato, Kagaku No Ryoiki, Zokan, 138 (1983) 107.
31 N. Ishibashi, A. Jyo and T. Imato, Anal. Chem. Symp. Ser., 17 (1983) 570.
32 J. Janata, Sens. Actuators, 4 (1983) 255.
33 M. S. Jovanović, Glas. Chem. Drus. Beogr., 48 (1983) 477.
34 G. Kandemir, Kim. Sanayi, 27 (1984) 85, 137.
35 I. Karube and S. Suzuki, Ion Sel. Electr. Rev., 6 (1984) 15.
(a) M. Kessler, J. Höfer and D. K. Harrison (Eds.), Ion Measurement in Physiology and Medicine, Springer-Verlag, Berlin, 1985.
36 R. K. Kobos, Trends Anal. Chem., 2 (1983) 154.
37 Y. Kobotake, Med. Philos., 3 (1984) 507.

38 J. Koryta, Electrochim. Acta, 29 (1984) 445.
39 J. Koryta and K. Štulík, Iontově Selektivní Elektrody, Academia, Prague, 1984.
40 J. H. Ladenson, Anal. Proc. (London), 20 (1983) 554.
41 C. C. Liu and F. W. Klink, Am. Inst. Chem. Eng. Symp. Ser., 79 (1983) 46.
42 M. Mascini and A. Liberti, Sci. Total Environ., 37 (1984) 121.
43 M. Mascini, G. Palleschi and D. Moscone, Cosmet. News, 31 (1983) 270.
44 E. A. Materova and T. Ya. Bart, Ion. Obmen i Ionometriya, Leningrad, 4 (1984) 92.
45 B. A. McKinley, B. A. Houtchens and J. Janata, Ion Sel. Electr. Rev., 6 (1984) 173.
46 D. Midgley, Anal. Proc., 21 (1984) 284.
47 D. Midgley and D. E. Mulcahy, Ion Sel. Electr. Rev., 5 (1983) 165.
48 B. P. Nikolskii and E. A. Materova, Ion Sel. Electr. Rev., 7 (1985) 3.
49 M. Oda, Y. Suzuki and K. Shimura, Yasai Shikenjo Hokoku, 11 (1983) 161.
50 R. Perez Olmos, Quim. Ind. (Madrid), 29 (1983) 583.
51 R. Perez Olmos, Ing. Quim. (Madrid), 16 (1984) 35.
52 A. T. Pilipenko and F. M. Tulyupa, Khim. Tekhnol. Vod., 5 (1983) 426.
53 V. A. Popkov and V. Yu. Reshetnyak, Farmatsiya (Moscow), 32 (1983) 79.
54 E. Pungor, K. Tóth and A. Hrabeczy-Páll, Trends Anal. Chem., 3 (1984) 11.
55 E. Pungor, K. Tóth, P. G. Klatsmányi and K. Izutsu, Pure Appl. Chem., 55 (1983) 2023.
56 W. C. Purdy, Chem. Int., 4 (1984) 13.
57 Ch. Sachs, Ion Sel. Electr. Rev., 6 (1984) 3.
58 J. G. Schindler and M. M. Schindler, Bioelektrochemische Membran-Elektroden, W. de Gruyter, Berlin, 1983.
59 S. Scholle and S. Scholle, Jr., Chem. Prum., 32 (1982) 148.
60 W. Simon, D. Ammann, P. Anker, U. Oesch and D. M. Band, Ann. N.Y. Acad. Sci., 428 (1984) 279.
61 W. Simon, E. Pretsch, W. E. Morf, D. Ammann, U. Oesch and O. Dinten, Analyst (London), 109 (1984) 207.
62 Y. Su, Shengwu Huaxue, 50 (1983) 2.
63 J. D. R. Thomas, Anal. Chem. Symp. Ser., 18 (1984) 141.
64 M. Thompson and U. J. Krull, Trends Anal. Chem., 3 (1984) 173.
65 C. Tran-Minh, Ion Sel. Electr. Rev., 7 (1985) 41.
66 R. Y. Tsien, Ann. Rev. Biophys. Bioeng., 12 (1983) 91.
67 Y. Umezawa, Gendai Kagaku, 146 (1983) 50.
68 Y. Umezawa, Kagaku (Kyoto), 38 (1983) 805.
69 F. Van Lente, Lab. Med., 15 (1984) 165.
70 K. Vytřas, Ion Sel. Electr. Rev., 7 (1985) 77.
71 H. Wang, Rev. Anal. Chem., 7 (1983) 76.
72 R. D. Armstrong, A. K. Covington and G. P. Evans, Anal. Chim. Acta, 166 (1984) 103.
73 R. D. Armstrong, A. K. Covington and G. P. Evans, J. Electroanal. Chem., 159 (1983) 33.
74 R. D. Armstrong, A. K. Covington, G. P. Evans and T. Handyside, Electrochim. Acta, 29 (1984) 1127.
75 B. Hundhammer, J. Seidlitz, S. Becker, S. K. Dhawan and T. Solomon, J. Electroanal. Chem., 180 (1984) 355.
76 T. Kakiuchi and M. Senda, Bull. Chem. Soc. Jpn., 57 (1984) 1801.
77 A. A. Kornyshev and A. G. Volkov, J. Electroanal. Chem., 180 (1984) 363.
78 M. E. Meyerhoff, Y. M. Fraticelli, W. N. Opdycke, C. G. Bachus and A. D. Gordus, Anal. Chim. Acta, 154 (1983) 12.
79 K. M. Mikhelson, V. M. Lutov, A. L. Grekovich, E. A. Materova and L. P. Dement'eva, Elektrokhimiya, 20 (1984) 1457.
80 W. E. Morf, Anal. Chem., 55 (1983) 1165.
81 W. E. Morf, I. A. Mostert and W. Simon, Anal. Chem., 57 (1985) 1122.
82 S. Yao, Hunan Daxue Xuebao, 10 (1983) 98.
83 A. Adam, J. Boulanger, P. Ers and M. Parmantier, Clin. Chem., 30 (1984) 1720.

84 E. G. Akhalkatsi, I. D. Borinets, V. A. Dolidze, G. I. Darchiani, L. I. Dzhakobaya, I. L. Korin, I. L. Korin, Z. I. Taliashvili and G. P. Chichua, Soobshch. Akad. Nauk Gruz. SSR, 112 (1983) 329.
85 K. Akita, T. Hirai, Y. Kurosawa, E. Mizuno, H. Kiyose and H. Naka, Eisei Kensa, 33 (1984) 688.
86 S. Alegreti, J. Alonso, J. Bartroli, J. M. Paulis, J. L. F. C. Lima and A. A. S. C. Machado, Anal. Chim. Acta, 164 (1984) 147.
87 A. Ansari and C. R. Drew, Clin. Chem., 28 (1982) 1630.
88 J. Anzai, T. Kusano, T. Osa, H. Nakajima and T. Matsuo, Bunseki Kagaku, 33 (1984) E131.
89 M. A. Arnold, Anal. Chim. Acta, 154 (1983) 33.
90 V. M. Autyunyan, R. A. Bagdasaryan and A. S. Pogosyan, Elektrokhimiya, 19 (1983) 1521.
91 R. G. Bates, A. G. Dickson, M. Gratzl, A. Hrabeczy-Pall, E. Lindner and E. Pungor, Anal. Chem., 55 (1983) 1275.
92 U. Becht, S. Ebel and B. Reyer, Fresenius Z. Anal. Chem., 319 (1984) 371.
93 P. Bergvelt, B. H. Van der Schoot and J. H. L. Onakiewicz, Anal. Chim. Acta, 151 (1983) 143.
94 P. Bijster, H. L. Vader and C. J. J. Vink, J. Autom. Chem., 4 (1982) 125.
95 G. Blackburn and J. Janata, J. Electrochem. Soc., 129 (1982) 2580.
96 A. B. T. J. Boink and A. H. J. Maas, Computer Simulation of Calcium Ion-selective Electrode Measurement, in A. H. J. Maas, J. Kofstad, O. Siggaard-Andersen and G. Kokholm (Eds.), Ionized Calcium, Sodium and Potassium by Ion Selective Electrodes, Vol. 5, Private Press, Copenhagen, 1984, p. 123.
97 A. M. Bond, H. A. Hudson, P. A. Vandenboock, F. L. Walter and H. R. A. Exelby, Anal. Chem., 55 (1983) 2071.
98 L. Bousse and P. Bergveld, Sens. Actuators, 6 (1984) 65.
99 G. N. Bowers, Jr., Towards an Ionized Calcium Reference System. Activities of the American Working Group, in A. H. J. Maas, J. Kofstad, O. Siggaard-Andersen and G. Kokholm (Eds.), Ionised Calcium, Sodium and Potassium by Ion Selective Electrodes, Vol. 5, Private Press, Copenhagen, 1984, p. 81.
100 C. R. Bradley and G. A. Rechnitz, Anal. Chem., 56 (1984) 664.
101 D. P. Brezinski, Talanta, 30 (1983) 347.
102 B. H. Buckley and S. C. H. Smith, Some Factors Influencing the Quality of Ionized Calcium Measurements, in A. H. J. Maas, J. Kofstad, O. Siggaard-Andersen and G. Kokholm (Eds.), Ionised Calcium, Sodium and Potassium by Ion Selective Electrodes, Vol. 5, Private Press, Copenhagen, 1984, p. 173.
103 G. Cheek, C. P. Wales and R. J. Nowak, Anal. Chem., 55 (1983) 380.
104 A. N. Khutsishvili, Z. Sh. Asatiani, E. I. Bondarenko and G. I. Orlova, Elektrokhimiya, 21 (1985) 308.
105 J. F. Coetzee and B. K. Deshmukh, Anal. Chem., 55 (1983) 2422.
106 A. D. Cornier, J. D. Czaban and A. M. Fejes, Whole Blood-plasma Bias Introduced at the Liquid Junction in Direct Potentiometry, in A. H. J. Maas, J. Kofstad, O. Siggaard-Andersen and G. Kokholm (Eds.), Ionised Calcium, Sodium and Potassium by Ion Selective Electrodes, Vol. 5, Private Press, Copenhagen, 1984, p. 139.
107 G. C. Corfield, L. Ebdon and A. T. Ellis, Calcium Ion-selective Electrodes with Covalently-bound Organophosphate Sensor Groups, in Polymer Science and Technology, Vol. 21, Plenum Press, New York, 1983, p. 341.
108 A. K. Covington, A. B. T. Boink and A. H. J. Haas, Standard Reference Solutions for Blood Electrolyte Determinations, in A. H. J. Maas, J. Kofstad, O. Siggaard-Andersen and G. Kokholm (Eds.), Ionised Calcium, Sodium and Potassium by Ion Selective Electrodes, Vol. 5, Private Press, Copenhagen, 1984, p. 229.
109 A. K. Covington, C. T. G. Flear and R. Lockie, Errors in Analysis of Sodium and Potassium in Blood Electrolytes with Variable Bicarbonate, in A. H. J. Maas,

J. Kofstad, O. Siggaard-Andersen and G. Kokholm (Eds.), Ionised Calcium, Sodium and Potassium by Ion Selective Electrodes, Vol. 5, Private Press, Copenhagen, 1984, p. 205.
110 A. K. Covington and A. Sibbald, Microelectronic Chemical Sensors for Clinical Analysis of Blood Electrolyte Cations, in A. H. J. Maas, J. Kofstad, O. Siggaard-Andersen and G. Kokholm (Eds.), Ionised Calcium, Sodium and Potassium by Ion Selective Electrodes, Vol. 5, Private Press, Copenhagen, 1984, p. 225.
111 J. C. Crawhall and W. C. Purdy, Trends Anal. Chem., 1 (1982) 184.
112 J. A. Crowell, R. E. Moore and G. N. Bowers, Clin. Chem., 29 (1983) 1187.
113 U. P. Decker and R. Brott, Z. Chem., 24 (1984) 77.
114 H. Degawa, N. Shinozuka and S. Hayano, Chem. Lett., 1 (1983) 25.
115 H. Degawa, N. Shinozuka and S. Hayano, Bull. Chem. Soc. Jpn., 57 (1984) 706.
116 B. K. Deshmukh and J. F. Coetzee, Anal. Chem., 56 (1984) 2373.
117 H. Dickler, H. Adler, D. Svenjak, R. Johnson, H. Lanzu and R. Herron, Clin. Chem., 29 (1983) 1193.
118 S. Dütsch, H. B. Jenny, K. J. Schlatter, P. M. J. Perisset, G. Wolff, J. T. Clerc, E. Pretsch and W. Simon, Anal. Chem., 57 (1985) 578.
119 S. Ebel and U. Becht, Fresenius' Z. Anal. Chem., 320 (1985) 117.
(a) C. E. Efstathiou, Anal. Chim. Acta, 154 (1983) 41.
120 V. V. Egorov, E. M. Rakhmanko, G. L. Starobinets, V. A. Repin and Ya. F. Lushchik, Vestsi Akad. Nauk BSSR, 5 (1984) 42.
121 M. T. Everitt, M. A. Kenny and C. J. Delaney, Clin. Chem., 28 (1982) 1630.
122 D. Feakins, M. Knox and B. E. Hickey, J. Chem. Soc., Faraday Trans. I, 80 (1983) 961.
123 C. C. Feistel, G. Boehm and C. Kuo, Effects of Sample Handling Procedures on Free Ionized Calcium Concentration in Whole Blood and Serum, in A. H. J. Maas, J. Kofstad, O. Siggaard-Andersen and G. Kokholm (Eds.), Ionised Calcium, Sodium and Potassium by Ion Selective Electrodes, Vol. 5, Private Press, Copenhagen, 1984, p. 115.
124 C. C. Feistel and G. Matsuyama, Clin. Chem., 28 (1982) 1631.
125 C. C. Feistel, N. D. Vaziri and R. Y. Darwish, Evaluation of In-line Sensors for Continuous Measurement of Potassium Concentration, in A. H. J. Maas, J. Kofstad, O. Siggaard-Andersen and G. Kokholm (Eds.), Ionised Calcium, Sodium and Potassium by Ion Selective Electrodes, Vol. 5, Private Press, Copenhagen, 1984, p. 239.
(a) R. Fernandez Prini, C. Rozenberg de Pattin, K. Tanaka and R. G. Bates, J. Electroanal. Chem. Interfacial Electrochem., 144 (1983) 415.
126 T. A. Fjeldly, K. Nagy and B. Stark, Sens. Actuators, 3 (1983) 111.
127 N. Fogh-Andersen, Direct Potentiometry of Sodium and Potassium in Whole Blood, Plasma and Serum, in A. H. J. Maas, J. Kofstad, O. Siggaard-Andersen and G. Kokholm (Eds.), Ionised Calcium, Sodium and Potassium by Ion Selective Electrodes, Vol. 5, Private Press, Copenhagen, 1984, p. 197.
128 N. Fogh-Andersen, P. S. Frederiksen, E. A. Andersen and J. Thode, Influence of pH on Ionized Calcium in Newborns, in A. H. J. Maas, J. Kofstad, O. Siggaard-Andersen and G. Kokholm (Eds.), Ionised Calcium, Sodium and Potassium by Ion Selective Electrodes, Vol. 5, Private Press, Copenhagen, 1984, p. 49.
129 F. R. Foulkes, W. F. Graydon and M. Garamszeghy, J. Electrochem. Soc., 131 (1984) 1325.
130 C. G. Fraser, Desirable Performance Standards for Clinical Chemistry Tests, in A. L. Latner and M. K. Schwatz (Eds.), Advances in Clinical Chemistry, Vol. 23, Academic Press, Orlando, 1983, p. 299.
131 J. W. Frazer, D. J. Balaban, H. R. Brand, G. A. Robinson and S. M. Lanning, Anal. Chem., 55 (1983) 855.
132 Z. Froebe, K. Richon and W. Simon, Chromatographia, 17 (1983) 467.
133 C. Fuchs, D. Dorn and V. W. Armstrong, Laboratoriumsmedizin, 7 (1983) 208.
134 V. P. Y. Gadzekpo and G. D. Christian, Anal. Chim. Acta, 164 (1984) 279.

135 G. Geblewicz and Z. Koczorowski, J. Electroanal. Chem., 158 (1983) 37.
136 G. Geblewicz, Z. Figaszewski and Z. Koczorowski, J. Electroanal. Chem., 177 (1984) 1.
137 H. H. J. Girault and D. J. Schiffrin, Proc. Int. Symp. Bioelectrochem. Bioenerg., Nottingham, 1983.
138 H. H. J. Girault and D. J. Schiffrin, J. Electroanal. Chem., 161 (1984) 415.
139 H. H. J. Girault and D. J. Schiffrin, J. Electroanal. Chem., 179 (1984) 277.
140 H. H. J. Girault, D. J. Schiffrin and B. D. V. Smith, J. Electroanal. Chem., 137 (1982) 207.
141 G. Graham and M. Burritt, Clin. Chem., 29 (1983) 1187.
142 S. W. Graves, M. L. Lando, C. H. Smith, R. Compton and J. H. Ladenson, Clin. Chem., 29 (1983) 1272.
143 S. E. Gross and H. Khayam-Bashi, Clin. Chem., 28 (1982) 1629.
144 H. Gruber, GIT Fachz. Lab., 28 (1984) 429.
145 J. Gulens, S. J. West and J. W. Ross, Anal. Chem., 56 (1984) 2367.
146 A. Haemmerli, J. Janata and J. J. Brophy, J. Electrochem. Soc., 129 (1982) 2306.
147 G. S. Hall, T. D. O'Leary and A. P. Prior, Clin. Chem., 28 (1982) 1248.
148 P. Hájková, D. Homolka, V. Mareček and Z. Samec, J. Electroanal. Chem., 151 (1983) 277.
149 P. Hájková, D. Homolka, V. Mareček, A. G. Volkov and Z. Samec, Elektrokhimiya, 21 (1985) 209.
150 Y. Hanazato and S. Shiono, Anal. Chem. Symp. Ser., 17 (1983) 513.
151 T. M. Happe, Clin. Chem., 29 (1983) 1310.
152 N. J. Ho, J. Kratochvíl, G. F. Blackburn and J. Janata, Sens. Actuators, 4 (1983) 413.
153 P. C. Hobby, G. J. Moody and J. D. R. Thomas, Analyst (London), 108 (1983) 581.
154 C. R. Hoffmann, M. R. Haskard and D. E. Mulcahy, Anal. Lett., A17 (1984) 1499.
155 D. Homolka, P. Hájková, V. Mareček and Z. Samec, J. Electroanal. Chem., 159 (1983) 233.
156 G. Horvai and E. Pungor, Anal. Chem., 55 (1983) 1988.
157 J. F. Huang, X. J. Chen, P. G. Dai and D. W. Yuan, Fenxi Huaxue, 12 (1984) 148.
158 B. Hundhammer, T. Solomon and H. Alemu, J. Electroanal. Chem., 149 (1983) 179.
159 L. Ilcheva, M. Polianova, J. Dalukov and B. R. Chapman, Analyst (London), 110 (1984) 359.
160 P. Jalandara and T. T. Ho, Clin. Chem., 28 (1982) 1631.
161 A. Jyo, K. Mori and N. Ishibashi, Bull. Chem. Soc. Jpn., 56 (1983) 3507.
162 T. Kakiuchi and M. Senda, Bull. Chem. Soc. Jpn., 56 (1983) 2912.
163 S. Kamata and M. Toyohara, Nippon Kagaku Kaishi, 2 (1985) 185.
164 K. Kanno, T. Gatayama and M. Koyama, Anal. Chem. Symp. Ser., 17 (1983) 545.
165 T. Katsu, K. Togawa and Y. Fujita, Bull. Chem. Soc. Jpn., 56 (1983) 3446.
166 S. Kawakami, T. Akiyama and Y. Ujihira, Fresenius' Z. Anal. Chem., 318 (1984) 349. (a) M. Kawamura, Y. Kida , Y. Koide and T. Kashima, Kyoritsu Yakka Daigaku Kenkyu Nempo, 27 (1982) 7.
167 D. F. Keeley and F. H. Walters, Anal. Lett., A16 (1983) 1581.
168 S. Kihara and Z. Yoshida, Talanta, 31 (1984) 789.
169 D. W. Kirk and F. R. Foulkes, J. Electrochem. Soc., 131 (1984) 1332.
170 G. G. Kiselev, R. P. Lichko and T. A. Mezhburd, Gidrokhim. Mater, 88 (1983) 56.
171 G. G. Kiselev, T. A. Mezhburd, O. M. Petrukhin, E.N. Avdeeva and E. V. Trofimova, Zh. Anal. Khim., 40 (1985) 88.
172 G. G. Kiselev and V. N. Nikonov, Zavod. Lab., 49 (1983) 7.
173 M. von Klein and M. Kuisl, VDI Ber., 509 (1984) 275.
174 M. von Klein, M. Kuisl and Th. Ricker, Technisch. Mess., 50 (1983) 381.
175 R. K. Kobos, J. J. Parks and M. E. Meyerhoff, Anal. Chem., 54 (1982) 1976.
176 D. D. Koch, D. Parrish and J. H. Ladenson, Clin. Chem., 29 (1983) 1090.
177 D. D. Koch and J. H. Ladenson, Anal. Chem., 55 (1983) 1807.
178 J. Koryta, Guo Du, W. Ruth and P. Vanýsek, Faraday Discuss. Chem. Soc., 77 (1984) 9.

179 A. M. Krstulovic and H. Colin, Analusis, 11 (1983) 111.
180 M. Kuisl and M. Klein, NTG-Fachber, 79 (1982) 289.
181 E. Langhoff and F. Steiness, Clin. Chem., 28 (1982) 170.
182 J. Langmaier, K. Štulík and R. Kalvoda, Anal. Chim. Acta, 148 (1983) 19.
183 L. Larsson and S. Öhman, Clin. Chem., 31 (1985) 169.
184 L. Larsson and S. Öhman, Experiences with Internal Quality Controls for Serum Ionized Calcium, in A. H. J. Maas, J. Kofstad, O. Siggard-Anderson and G. Kokholm (Eds.), Ionised Calcium, Sodium and Potassium by Ion Selective Electrodes, Vol. 5, Private Press, Copenhagen, 1984, p. 155.
185 R. S. Lawton and A. M. Yacynych, Anal. Chim. Acta, 160 (1984) 149.
186 S. I. Lappävuori and P. S. Romppainen, Electrocomponent Sci. Technol., 10 (1983) 129.
187 L. Li and X. Zhao, Jisuanji Yu Yingyong Huaxue, 1 (1984) 217.
(a) E. Lindner, K. Toth, E. Pungor and Y. Umezawa, Anal. Chem., 56 (1984) 808.
188 C. A. Loshoo and G. N. Bowers, Clin. Chem., 28 (1982) 1577.
189 Ch. S. Luo and F. Ch. Chang, Hua Hsueh, 42 (1984) 69.
190 A. H. J. Maas, O. Siggard-Anderson, H. F. Weisberg and W. G. Zijlstra, Clin. Chem., 31 (1985) 482.
191 C. Macca and M. Čakrt, Anal. Chim. Acta, 154 (1983) 51.
192 A. F. Malekpour, D. Taylor and M. E. King, Clin. Chem., 28 (1982) 1576.
193 A. F. Manz and W. Simon, J. Chromatogr. Sci., 21 (1983) 326.
194 V. Mareček and Z. Samec, J. Electroanal. Chem., 149 (1983) 185.
195 V. Mareček and Z. Samec, Anal. Chim. Acta, 151 (1983) 265.
196 O. R. Melroy and R. P. Buck, J. Electroanal. Chem., 151 (1983) 1.
197 O. R. Melroy, W. E. Bronner and R. P. Buck, J. Electrochem. Soc., 130 (1983) 373.
198 H. J. Marsoner, C. Ritter and W. Odar, Indirect Potentiometric Determination of Total Calcium in Plasma, in A. H. J. Maas, J. Kofstad, O. Siggaard-Andersen and G. Kokholm (Eds.), Ionised Calcium, Sodium and Potassium by Ion Selective Electrodes, Vol. 5, Private Press, Copenhagen, 1984, p. 105.
199 R. Martin, C. Jones, K. Letievre, D. Maymanti, L. Mulholland, M. Pelosi, J. St. Andre and C. C. Young, Clin. Chem., 29 (1983) 1188.
200 M. Mascini, M. Iannello and G. Palleschi, Anal. Chim. Acta, 146 (1983) 135.
201 T. Matsuo and N. Nakajima, Sens. Actuators, 5 (1984) 293.
202 P. C. Meier, Anal. Chem., 57 (1985) 373.
203 P. C. Meier, W. E. Morf, M. Läuble and W. Simon, Anal. Chim. Acta, 156 (1984) 1.
204 Y. Miyahara, T. Moriizumi, S. Shiokawa, H. Matsuoka, I. Karube and S. Suzuki, Nippon Kagaku Kaishi, 6 (1983) 823.
205 W. E. Morf and W. Simon, Anal. Chem. Symp. Ser., 18 (1984) 33.
206 J. L. Munoz, F. Deyhimi and J. A. Coles, J. Neurosci. Methods, 8 (1983) 231.
207 J. W. North, Clin. Chem., 28 (1982) 1248.
208 Y. Ohta, S. Shoji, M. Esashi and T. Matsuo, Sens. Actuators, 2 (1982) 387.
209 A. Olin and G. Wikmark, Anal. Chem., 55 (1983) 1402.
210 A. R. Olszyna, W. K. Wladyslaw, D. Sobczynska and W. Torbicz, Mater. Elektron., 2 (1982) 28.
211 W. N. Opdycke, S. J. Parks and M. E. Meyerhoff, Anal. Chim. Acta, 155 (1983) 11.
212 T. Osakai, T. Kakutani, Y. Nishiwaki and M. Senda, Bunseki Kagaku, 32 (1983) E81.
213 T. Osakai, T. Kakutani and M. Senda, Bull. Chem. Soc. Jpn., 57 (1984) 370.
214 T. Osakai, T. Kakutani and M. Senda, Bunseki Kagaku, 33 (1984) E371.
215 J. Th. G. Overbeck, The Donnan Equilibrium, in Progress in Biophysics and Biophysical Chemistry, Vol. 6, Pergamon Press, London, 1956, p. 57.
216 A. Palanivel and P. Riyazuddin, J. Chem. Educ., 61 (1984) 920.
217 Z. Pan, Fenxi Huaxue, 11 (1983) 364.
218 M. Panteghini, M. Calarco, A. Malchiodi and R. Bonora, G. Ital. Chim. Clin., 7 (1982) 361.

219 A. Parczewski and A. Madej, Chem. Anal. (Warsaw), 27 (1983) 133.
220 A. Parczewski and R. Stepak, Z. Anal. Chem., 316 (1983) 29.
221 J. Petr and J. Šenkýř, Scr. Fac. Mat. Univ. Purkynianae Brun., 13 (1983) 161.
222 C. R. Powley and T. A. Nieman, Anal. Chim. Acta, 152 (1983) 173.
223 C. R. Powley and T. A. Nieman, Anal. Chim. Acta, 166 (1983) 1.
224 E. Pungor and Y. Umezawa, Anal. Chem., 55 (1983) 1432.
225 E. Pungor, A. Hrabeczy-Pall, E. Lindner, M. Gratzland and R. G. Bates, Magy. Kem. Foly., 84 (1983) 337.
226 J. D. Reid, O. R. Melroy and R. P. Buck, J. Electroanal. Chem., 147 (1983) 71.
227 J. D. Reid, P. Vanýsek and R. P. Buck, J. Electroanal. Chem., 161 (1984) 1.
228 J. D. Reid, P. Vanýsek and R. P. Buck, J. Electroanal. Chem., 170 (1984) 109.
229 T. D. Rice, Anal. Chim. Acta, 151 (1983) 383.
230 L. J. Russel, A Practical Approach to Understanding Flame Photometry and ISE Differences and Some Implications for Ionized Calcium Measurements, in A. H. J. Maas, J. Kofstad, O. Siggaard-Andersen and G. Kokholm (Eds.), Ionised Calcium, Sodium and Potassium by Ion Selective Electrodes, Vol. 5, Private Press, Copenhagen, 1984, p. 187.
231 W. Ruth and P. Vanýsek, Microchem. J., 29 (1984) 162.
232 Ch. Sachs, A. Truchand and M. Boigne, Comparative Evaluation of Na-K Electrometric Analyzers, in A. H. J. Maas, J. Kofstad, O. Siggaard-Andersen and G. Kokholm (Eds.), Ionised Calcium, Sodium and Potassium by Ion Selective Electrodes, Vol. 5, Private Press, Copenhagen, 1984, p. 213.
233 Z. Samec, V. Mareček and D. Homolka, J. Electroanal. Chem., 158 (1983) 25.
234 Z. Samec, V. Mareček and D. Homolka, J. Electroanal. Chem., 170 (1984) 383.
235 Z. Samec, V. Mareček and D. Homolka, Faraday Discuss. Chem. Soc., 77 (1984) 10.
236 Y. Sanada, T. Akiyama, Y. Ujihira and E. Niki, Fresenius' Z. Anal. Chem., 312 (1982) 526.
237 R. S. Sandhu and S. J. Fischman, Clin. Chem., 28 (1982) 409.
238 S. Scholle and S. Scholle, Jr., Chem. Prum., 33 (1983) 661.
239 P. Schuler and R. Degner, GIT Fachz. Lab., 28 (1984) 785, 790.
240 A. Shatkay and S. Hayano, Anal. Chem., 57 (1985) 364.
241 J. E. Sherwin, B. B. Bruegger, T. Beliste and O. Flores, Clin. Chem., 28 (1982) 1630.
242 A. Sibbald, A. K. Covington and R. F. Carter, Clin. Chem., 30 (1984) 135.
243 O. Siggaard-Andersen, R. A. Durst and A. H. J. Mass, Pure Appl. Chem., 56 (1984) 567.
244 O. Siggaard-Andersen and N. Fogh-Andersen, The Activity Coefficient of Na^+ and the Apparent Ionic Strength of Normal Blood Plasma, in A. H. J. Maas, J. Kofstad, O. Siggaard-Andersen and G. Kokholm (Eds.), Ionised Calcium, Sodium and Potassium by Ion Selective Electrodes, Vol. 5, Private Press, Copenhagen, 1984, p. 199.
245 O. Siggard-Anderson, N. Fogh-Andersen, J. Thode and T. Christiansen, Elimination of the Erythrocyte Effect on the Liquid Junction Potential in Potentiometric Measurements on Whole Blood using Unconventional Salt Bridge Solutions, in A. H. J. Maas, J. Kofstad, O. Siggaard-Andersen and G. Kokholm (Eds.), Ionised Calcium, Sodium and Potassium by Ion Selective Electrodes, Vol. 5, Private Press, Copenhagen, 1984, p. 149.
246 O. Siggaard-Andersen, N. Fogh-Andersen and J. Thode, Scand. J. Clin. Lab. Invest., 43(165) (1983) 43.
247 R. Smith, R. J. Huber and J. Janata, Sens. Actuators, 5 (1983) 127.
248 K. Sollner, J. Colloid Sci., 8 (1953) 179.
249 T. Solomon, H. Alemu and B. Hundhammer, J. Electroanal. Chem., 169 (1984) 303.
250 T. Solomon, H. Alemu and B. Hundhammer, J. Electroanal. Chem., 169 (1984) 311.
251 J. St. Andre, C. Jones, K. Le Lievre, D. Magnanti, R. Martin, L. Mulholland, M. Pelosi and C. C. Young, Clin. Chem., 29 (1983) 1188.
252 O. K. Stefanova, M. V. Rozhdestvenskaya and B. F. Gorshkova, Elektrokhimiya, 19 (1983) 1225.

253 R. Stefak, Z. Anal. Chem., 315 (1983) 629.
254 G. I. Shumilova, Z. S. Alagova, E. A. Materova and O. K. Suvorova, Elektrokhimiya, 20 (1984) 711.
255 K. Suzuki, H. Aruga and T. Shirai, Anal. Chem., 55 (1983) 2011.
256 K. Suzuki, H. Aruga, H. Ishiwada, T. Oshima, H. Inoue and T. Shirai, Bunseki Kagaku, 32 (1983) 585.
257 K. X. Tan, Z. Wang and G. L. Zhang, Fenxi Huaxue, 11 (1984) 942.
258 J. Thode, N. Fogh-Andersen and O. Siggaard-Andersen, Clin. Chem., 29 (1983) 1554.
259 J. Thode, N. Fogh-Andersen, M. Siggaard-Andersen and O. Siggaard-Andersen, Ann. Clin. Biochem., 20 (1983) 271.
260 J. Thode, N. Fogh-Andersen and O. Siggaard-Andersen, New Procedures for the Measurement of Ionized Calcium, in A. H. J. Maas, J. Kofstad, O. Siggaard-Andersen and G. Kokholm (Eds.), Ionised Calcium, Sodium and Potassium by Ion Selective Electrodes, Vol. 5, Private Press, Copenhagen, 1984, p. 71.
261 J. Toffaletti, Report from the American Association of Clinical Chemists, Working Group on Ionized Calcium, in A. H. J. Maas, J. Kofstad, O. Siggaard-Andersen and G. Kokholm (Eds.), Ionised Calcium, Sodium and Potassium by Ion Selective Electrodes, Vol. 5, Private Press, Copenhagen, 1984, p. 17.
262 J. Toffaletti, N. Blosser and K. Kirvan, Clin. Chem., 30 (1984) 553.
263 M. Trojanowicz, in Electrochemical Detection in Flow Analysis, Conference Proceedings, Mátrafüred, 1982, p. 189.
264 A. Uldall, N. Fogh-Andersen, J. Thode, A. B. T. J. Boink, J. Kofstad, L. Larsson, S. Närvänen, K. O. Pedersen and T. Weber, Quality Assessment of the Determination of Ionized Calcium with Ion-selective Electrode, in A. H. J. Maas, J. Kofstad, O. Siggaard-Andersen and G. Kokholm (Eds.), Ionised Calcium, Sodium and Potassium by Ion Selective Electrodes, Vol. 5, Private Press, Copenhagen, 1984, p. 165.
265 Y. Umezawa, E. G. Harsányi, K. Tóth, S. Fujiwara and E. Pungor, Lower Detection Limit of Some Precipitate-based Ion-selective Electrodes, in A. H. J. Maas, J. Kofstad, O. Siggaard-Andersen and G. Kokholm (Eds.), Ionised Calcium, Sodium and Potassium by Ion Selective Electrodes, Vol. 5, Private Press, Coepnhagen, 1984, p. 539.
266 J. Van der Spiegel, I. Lauke, P. Chan and D. Babic, Sens. Actuators, 4 (1983) 291.
267 P. Vanýsek and R. P. Buck, J. Electrochem. Soc., 131 (1984) 1792.
268 P. Vanýsek, J. D. Reid, M. A. Craven and R. P. Buck, J. Electrochem. Soc., 131 (1984) 1788.
269 S. I. Wakida, T. Tanaka, A. Kawahara and K. Hiiro, Bunseki Kagaku, 33 (1984) 556.
270 P. Wall, E. G. Bellinger and T. Brown, Lab. Pract., 32 (1983) 88.
271 P. West, J. Autom. Chem., 5 (1983) 182.
272 J. K. White and D. W. Chan, J. Clin. Lab. Autom., 4 (1984) 23.
273 J. W. Winkelmann, C. Merritt, W. J. Scott, A. Kumar and G. Baune, Clin. Chem., 30 (1984) 482.
274 B. Wolf, S. Ishii and O. Flores, Clin. Chem., 28 (1982) 1630.
275 X. Xue, C. Lu, S. Gao and G. Wu, Fenxi Huaxue, 11 (1983) 548.
276 Z. Yoshida and H. Freiser, J. Electroanal. Chem., 162 (1984) 307.
277 Z. Yoshida and H. Freiser, J. Electroanal. Chem., 179 (1984) 31.
278 I. A. Zaidenman and L. G. Golovko, Elektrokhimiya, 21 (1985) 57.
279 B. Zeng, Zhongnan Kuangye Xueyuan Xuebao, 3 (1983) 89.
280 Y. Zeng and S. Lin, Jisuanji Yu Yingyong Huaxue, 1 (1984) 222.
281 Y. Zhuang and D. Qi Deyno, Chem. J. Chin. Univ., 4 (1983) 708.
282 I. K. Al-Hitti, G. J. Moody and J. D. R. Thomas, Analyst (London), 108 (1983) 43.
283 I. K. Al-Hitti, G. J. Moody and J. D. R. Thomas, Analyst (London), 108 (1983) 1209.
284 I. K. Al-Hitti, G. J. Moody and J. D. R. Thomas, Anal. Proc. (London), 20 (1983) 119.
285 K. Ariga, Kankyo Gijutsu, 12 (1983) 697.
286 P. J. Aruscavage and E. Y. Campbell, Talanta, 30 (1983) 745.
287 E. M. Athanasiou-Malaki and M. A. Kouparris, Anal. Chim. Acta, 161 (1984) 349.

288 R. J. Barnhard, J. Chem. Educ., 60 (1983) 679.
289 A. A. Baykov and E. B. Kostenko, Anal. Biochem., 134 (1983) 330.
290 J. L. Bernal, R. Pardo and M. J. Del Nozal, An. Quím., Ser. B, 79 (1983) 305.
291 J. L. Bernal, M. J. Del Nozal, A. J. Aller and L. Deban, An. Bromatol., 33 (1983) 219.
292 J. L. Bernal, M. J. Del Nozal, A. J. Aller and L. Deban, Rev. Agroquím. Tecnol. Aliment., 23 (1983) 137.
293 A. Betti, F. Fagioli and M. C. Pietrogrande, Hung. Sci. Instrum., 53 (1982) 23.
294 M. Betinelli, Analyst (London), 108 (1983) 404.
295 O. P. Bhargava and M. Gmitro, Am. Lab., 15 (1983) 28.
296 O. P. Bhargava and M. Gmitro, Int. Lab., 13 (1983) 62.
297 J. W. Bixler and L. S. Solomon, Anal. Chem., 56 (1984) 3004.
298 K. Brunt, Anal. Chim. Acta, 163 (1984) 293.
299 E. C. V. Batler and R. M. Gershey, Anal. Chim. Acta, 164 (1984) 153.
300 L. N. Bykova and N. N. Gridina, Zavod. Lab., 50 (1984) 9.
301 A. C. Calokerinos and T. P. Hadjiioannou, Microchem. J., 28 (1983) 464.
302 A. C. Calokerinos, M. Timotheou-Potamia, E. Sarentonis and T. P. Hadjiioannou, Anal. Chim. Acta, 151 (1983) 85.
303 L. Campanella, M. Tomassetti, G. D'Ascenzo, G. De Angelis, R. Morabito and L. Sorrentino, J. Pharm. Biomed. Anal., 1 (1983) 163.
304 A. D. Campbell and P. A. Dawson, Mikrochim. Acta, I (1983) 489.
305 A. D. Campbell and P. B. Graham, N.Z. J. Sci., 26 (1983) 433.
306 A. Campiglio, Mikrochim. Acta, I (1983) 443.
307 F. C. Chang, Hua Hsueh, 40 (1982) 66.
308 F. C. Chang and W. L. Chang, J. Chin. Chem. Soc. (Taipei), 29 (1982) 163.
309 C. Chen and D. Feng, Fenxi Huaxue, 11 (1983) 360.
310 W. J. Chen, C. J. Dong, Z. F. Qiu and Z. Z. Chen, Yaowu Fenxi Zazhi, 4 (1984) 134.
311 Y. Z. Chen, D. Cao, S. Wei, R. Wang and G. Ding, Shipin Yu Fajiao Gongye, 1 (1984) 11.
312 P. A. Compagnon, Sci. Tech. Pharm., 12 (1983) 495.
313 G. J. S. Cooper and M. S. Croxson, Clin. Chem., 29 (1983) 1320.
314 N. J. Csikai and A. J. Barnard, Anal. Chem., 55 (1983) 1677.
315 T. I. Danilovich, V. V. Abramov and P. A. Andreev, Zavod. Lab., 49 (1983) 23.
316 U. P. Decker, Wiss. Z. Tech. Hochsch. Carl Schorlemmer, 25 (1983) 464.
317 A. Dimante and A. Veveris, Latv. PSR Zinat. Akad. Vestis, Kim. Ser., 3 (1983) 360.
318 H. Doe, A. Shibagaki and T. Kitagawa, Inorg. Chem., 22 (1983) 1639.
319 E. K. Dzerzhko, A. A. Ennan and L. A. Grigorenko, Izv. Vyssh. Uchebn. Zaved., 28 (1985) 44.
320 G. A. East and I. A. Da Silva, Anal. Chim. Acta, 149 (1983) 227.
321 S. Esala, E. Vuori and L. Niisto, Mikrochim. Acta, I (1983) 155.
322 B. Eyde, Fresenius' Z. Anal. Chem., 316 (1983) 299.
323 B. Eyde, Fresenius' Z. Anal. Chem., 320 (1985) 41.
324 C. L. V. A. Fernandes, J. L. F. C. Lima and A. A. S. C. Machado, Rev. Port. Quim., 24 (1982) 213.
325 D. Ferry, M. Machtinger and D. Bauer, Analusis, 12 (1984) 90.
326 A. T. Filipenko, E. M. Skobets, O. P. Ryabushko and Yu. S. Savin, Ukr. Khim. Zh., 50 (1984) 490.
327 T. N. Fotina and K. I. Frolov, Zavod. Lab., 50 (1984) 13.
328 S. Furuta, M. Okada and H. Matsushita, Denki Kagaku Oyobi Kogyo Butsuri Kagaku, 51 (1983) 488.
329 T. Garai, I. Dároczy, F. Nádudvari, D. Vasonits and M. Szücs, Acta Chim. Hung., 115 (1984) 173.
330 M. Geissler and R. Kunze, Fresenius' Z. Anal. Chem., 318 (1984) 15.
331 M. Geissler and R. Kunze, Z. Chem., 24 (1984) 269.
332 N. E. Gel'man, L. V. Chervina, Z. G. Barakovskaya and M. M. Buzlanova, Zh. Anal. Khim., 39 (1984) 876.

333 M. G. Glaister, G. J. Moody and J. D. R. Thomas, Analyst (London), 110 (1985) 113.
334 M. G. Glaister, G. J. Moody, T. Nash and J. D. R. Thomas, Anal. Chim. Acta, 165 (1984) 281.
335 H. Gomathi, G. Subramanian, N. Chandra and G. P. Rao, Talanta, 30 (1983) 861.
336 M. I. Gomez del Rio, M. C. Barbas Arribas and P. Sanchez Batunero, Analusis, 11 (1983) 131.
337 T. D. Gornostaeva, V. A. Pronin and V. Ya. Semenov, Zavod. Lab., 49 (1983) 14.
338 M. Gratzl, L. Polos, K. Tóth, E. Pungor, M. F. Ebel, G. Zuba and J. Wernink, Magy. Kém. Foly., 90 (1984) 481.
339 J. Gulens, P. K. Leeson and L. Séguin, Anal. Chim. Acta, 156 (1984) 19.
340 D. L. Guo and H. B. Cui, Huaxue Tongbao, 1 (1984) 19.
341 H. Guterman, S. Ben-Yaakov and A. Abeliovici, Anal. Chem., 55 (1983) 1731.
342 H. Hara and S. Okazaki, Analyst (London), 109 (1984) 1317.
343 E. G. Harsányi, K. Tóth and E. Pungor, Anal. Chim. Acta, 152 (1983) 163.
344 E. G. Harsányi, K. Tóth and E. Pungor, Anal. Chim. Acta, 161 (1984) 333.
345 E. G. Harsányi, K. Tóth, E. Pungor, Y. Umezawa and S. Fujiwara, Talanta, 31 (1984) 579.
346 S. S. M. Hassan and G. A. Rechnitz, Anal. Chim. Acta, 151 (1983) 473.
347 G. T. Hefter and R. A. Longmore, Int. J. Environ. Anal. Chem., 16 (1984) 315.
348 G. T. Hefter, C. B. Chan and N. H. Tioh, Anal. Chem., 56 (1984) 749.
349 H. Hirawa, Kankyo Gijutsu, 12 (1983) 687.
350 M. Hori and Y. Kobayashi, Bunseki Kagaku, 32 (1983) 75.
351 M. Hori, M. Hirako, K. Ishii and Y. Kobayashi, Bunseki Kagaku, 33 (1984) 203.
352 A. Hulanicki, T. K. V. Krawczyk and A. Lewenstam, Anal. Chim. Acta, 158 (1984) 343.
353 S. Ikeda, H. Satake and H. Legawa, Bunseki Kagaku, 34 (1985) 60.
354 L. Ilcheva, A. Urumova, E. Lalova, K. Nauzhagu and S. Ruseva, Khim. Ind. (Sofia), 10 (1982) 452.
355 L. Ilcheva, M. Polianova, V. Adewuyi and P. Bozadziev, J. Indian Chem. Soc., 59 (1982) 1352.
356 A. K. M. S. Islam, G. L. Kerven and C. J. Asher, Commun. Soil Sci. Plant Anal., 14 (1983) 645.
357 M. Itoh, R. Demura, S. Tsukada and I. Yamamoto, Eisei Kagaku, 29 (1983) 167.
358 H. Itoh, H. Hachiya, M. Tsuchiya, Y. Suzuki and Y. Asano, Bull. Chem. Soc. Jpn., 57 (1984) 1689.
359 Ch. L. Ji, Pige Keji, 3 (1984) 30.
360 E. Kaneko, Y. Nagata, S. Kagawa, K. Mimura and A. Matsuoka, Rinsho Byori, 31 (1983) 1345.
361 M. Kataoka, K. Nishimura and T. Kambara, Bunseki Kagaku, 32 (1983) 516.
362 M. Kataoka, K. Nishimura and T. Kambara, Talanta, 30 (1983) 941.
363 K. Kawano, T. Yoshinaga and T. Tanimura, Bunseki Kagaku, 32 (1983) 308.
364 K. Kawano, T. Yoshinaga and T. Tanimura, Bunseki Kagaku, 32 (1983) 347.
365 E. Kissa, Anal. Chem., 55 (1983) 1445.
366 F. Lazaro, M. D. Luque de Castro and M. Válcarcel, Microchem. J., 30 (1984) 358.
367 A. Leszczynski, Gaz, Woda Tech. Sanit., 57 (1983) 186.
368 J. Li, Y. Gu and S. Duan, Fenxi Huaxue, 12 (1984) 1009.
369 J. L. F. C. Lima and A. A. S. C. Machado, Rev. Port. Quim., 24 (1982) 61.
370 J. L. F. C. Lima and A. A. S. C. Machado, Rev. Port. Quim., 24 (1982) 156.
371 W. Lin, J. Mo and L. Shen, Zhongshan Daxue Xuebao, 4 (1982) 125.
372 G. Livanos and P. J. Milham, J. Assoc. Off. Anal. Chem., 67 (1984) 10.
373 Ch. M. Lu and Z. F. Zhao, Fenxi Huaxue, 12 (1984) 17.
374 W. Lu, Z. Zhu and Y. Zhang, Fenxi Huaxue, 11 (1983) 765.
375 M. Luo, Y. Li, X. Cheng and B. Gou, Pige Keji, 1 (1983) 8.
376 G. B. Marshall and D. Midgley, Analyst (London), 108 (1983) 701.

377 J. R. Marzilli, J. Assoc. Off. Anal. Chem., 67 (1984) 682.
378 D. Midgley, Talanta, 30 (1983) 547.
379 J. Y. Mo, Ch. W. Ou, F. Q. Tang, G. F. Fu and N. S. Zeng, Huaxue Shijie, 23 (1982) 350.
380 P. Mohanakrishnan and C. F. Chignell, J. Pharm. Sci., 71 (1982) 1180.
381 J. Motonaka, S. Ikeda and N. Tanaka, Bunseki Kagaku, 33 (1984) 551.
382 H. Müller, Anal. Chem. Symp. Ser., 18 (1984) 353.
383 K. Nagashima, M. Matsumoto and S. Suzuki, Bunseki Kagaku, 32 (1983) 717.
384 K. Nagy and J. Ekstand, Fresenius' Z. Anal. Chem., 315 (1983) 138.
385 H. J. Neidhardt and H. D. Steinleitner, Acta Hydrochim. Hydrobiol., 12 (1984) 247.
386 M. Neshkova and J. Havas, Anal. Lett, A16 (1983) 1567.
387 L. Neupert, Acta Hydrochim. Hydrobiol., 10 (1983) 557.
388 L. W. Niedrach, Anal. Chem., 55 (1983) 2426.
389 T. Nomura and G. Nakagawa, Bull. Chem. Soc. Jpn., 56 (1983) 3632.
390 T. Nomura and G. Nakagawa, Bull. Chem. Soc. Jpn., 57 (1984) 1491.
391 Ch. Okumoto, M. Nagashima, S. Mizoiri, M. Kazama and N. Akiyama, Eisei Kagaku, 30 (1984) 7.
392 T. Okutani, Bunseki Kagaku, 33 (1984) 443.
393 Å. Olin and B. Wallén, Anal. Chim. Acta, 151 (1983) 65.
394 M. Ottaviani, P. Magnatti and G. D. di Delupis, Mikrochim. Acta, III (1984) 313.
(a) R. Ouyang, Ch. Yuan and Q. Li, He Huaxue Yu Fangshe Huaxue, 5 (1983) 186.
395 A. Palanivel and P. Riyazuddin, Indian J. Chem., 23A (1984) 1051.
396 R. Pardo, J. L. Bernal and E. Barrado, Anal. Chim. Acta, 142 (1982) 285.
397 R. Perez Olmos and J. Echevarria, Quím. Ind. (Madrid), 29 (1983) 275.
398 F. Persin and G. Durand, Analusis, 12 (1984) 312.
399 S. Pinzanti, G. Popeschi and E. La Porta, J. Pharm. Biomed. Anal., 1 (1983) 47.
400 E. Pungor, K. Tóth, G. Nagy, L. Polos, M. F. Ebel and I. Wernisch, Anal. Chim. Acta, 147 (1983) 23.
401 E. Pungor, M. Gratzl, L. Pólos, K. Tóth, M. F. Ebel, G. Zuba and J. Wernisch, Anal. Chim. Acta, 156 (1984) 9.
(a) W. Qian, Y. Gu, J. Li, D. Sun and X. Zhu, Shandong Haiyang Xueyuan Xuebao, 14 (1984) 47.
402 Z. F. Qiu and Z. Z. Chen, Yaowu Fenxi Zazhi, 4 (1984) 159.
403 N. Radić and M. Vudrag, J. Electroanal. Chem., 178 (1984) 321.
404 N. Radić, K. J. Mulligan and H. B. Mark, Anal. Chem., 56 (1984) 297.
405 N. Radić, K. J. Mulligan and H. B. Mark, Analyst (London), 104 (1984) 963.
406 G. S. Rao, Ann. Rev. Nutr., 4 (1984) 115.
407 D. Ravaine, G. Perera and Z. Hanane, Anal. Chem. Symp. Ser., 17 (1983) 521.
408 M. Rosol and J. Supuka, Biologia (Bratislava), 39 (1984) 41.
409 S. G. Samokhvalov, A. A. Shaimukhametova and V. G. Prizhukova, Agrokhimiya, 5 (1983) 118.
410 R. Sarin, J. Indian Inst. Sci., 64 (1983) 121.
411 J. Seabra e Barros and M. de J. Iavares, Bol. Mus. Lab. Mineral. Geol., Fac. Cienc. Univ. Lisboa, 16 (1981) 35.
412 Yu. A. Serikov and V. I. Komova, Zavod. Lab., 49 (1983) 8.
413 D. S. Shin and S. Ch. Lee, Taehan Hwahakhoe Chi, 28 (1984) 86.
414 V. Simeonov, A. Voulgaropoulos, M. Sofoniou and G. Vasilikiotis, Fresenius' Z. Anal. Chem., 319 (1984) 376.
415 P. A. Siskos, E. P. Diamandis, E. Gillieron and J. C. Colbert, Talanta, 30 (1983) 980.
416 H. F. Steger, Talanta, 30 (1983) 717.
417 H. Steinecke and W. Fischer, Z. Med. Laboratoriumsdiagn., 24 (1983) 304.
418 H. Steinecke and R. Scharper, Kriminalistik Forens. Wiss., 49 (1983) 98.
419 L. Steinhauser and J. Šikola, Vet. Med. (Praha), 28 (1983) 693.
420 R. Stella and M. T. G. Valentini, Anal. Chim. Acta, 152 (1983) 191.

421 R. Stella, M. T. G. Valentini and P. A. Borroni, Anal. Lett., 17 (1984) 433.
422 G. Subramanian, N. Chandra and G. P. Rao, Met. Finish., 81 (1983) 53.
423 G. Subramanian, N. Chandra and G. P. Rao, Talanta, 31 (1984) 79.
424 K. Tan, Fenxi Huaxue, 11 (1983) 433.
425 T. Tanaka, Fresenius' Z. Anal. Chem., 320 (1985) 278.
426 J. Tauchnitz, M. Hanrieder, G. Kiesel, R. Mahrwald and H. Hennig, Acta Hydrochim. Hydrobiol., 12 (1984) 315.
427 Y. Tomida, N. Kato and T. Ando, Bunseki Kagaku, 33 (1984) 420.
428 M. Trojanowicz and W. Matuszewski, Anal. Chim. Acta, 151 (1983) 77.
429 M. Trojanowicz, W. Matuszewski and A. Hulanicki, Anal. Chim. Acta, 136 (1982) 85.
430 R. D. Tsingarelli and I. P. Nikolenko, Zh. Anal. Khim., 39 (1985) 2027.
431 S. D. Tsingarelli, O. M. Tabakova and I. P. Nikolenko, Zh. Anal. Khim., 39 (1984) 622.
432 D. Tuhtar, Anal. Chem., 55 (1983) 2205.
433 J. E. Tyler and J. E. A. Comer, Analyst (London), 110 (1985) 15.
434 V. Tymáň, Chem. Listy, 78 (1984) 992.
435 I. Uemasu and Y. Umezawa, Denki Kagaku, 51 (1983) 99.
436 W. J. van Oort and E. J. J. M. van Eerd, Anal. Chim. Acta, 155 (1983) 21.
437 P. N. Vijan and B. Alder, Am. Lab., 16 (1984) 16, 19—22, 24.
438 D. V. Vivit, J. W. Ball and E. A. Jehme, Environ. Geol. Water Sci., 6 (1984) 79.
439 Yu. G. Vlasov and E. A. Bychkov, Hung. Sci. Instrum., 53 (1982) 35.
440 Yu. G. Vlasov and E. A. Bychkov, Ion. Obmen i Ionometriya, Leningrad, 4 (1984) 142.
441 Yu. G. Vlasov, E. A. Bychkov, E. A. Kazakova and Z. U. Borisova, Zh. Anal. Khim., 39 (1984) 452.
442 Yu. G. Vlasov, M. S. Miloshova, P. P. Antonov, E. A. Bychkov and A. Ya. Efa, Elektrokhimiya, 19 (1983) 1049.
443 Yu. G. Vlasov, M. S. Miloshova, P. P. Antonov, A. Ya. Efa and E. A. Bychkov, Elektrokhimiya, 19 (1983) 1173.
444 V. L. Volkov and L. I. Manakova, Zh. Anal. Khim., 38 (1983) 793.
445 V. L. Volkov and L. I. Manakova, Zh. Anal. Khim., 39 (1984) 2035.
446 K. Vytřas and M. Horčicová, Sb. Věd. Pr., Vys. Šk. Chemickotechnol., Pardubice, 45 (1982) 187.
447 R. Wagner and T. Richter, Z. Wasser Abwasser Forsch., 15 (1982) 296.
448 F. H. Walters, Anal. Lett., A 17 (1984) 1681.
449 F. H. Walters and D. F. Keeley, Anal. Lett., A16 (1983) 847.
450 W. Wang and D. Li, Fenxi Huaxue, 10 (1982) 614.
451 G. S. Wang, Q. Z. Shi, K. Weng and Z. Xiang, Hangzhou Daxue, Ziran Kexueban, 10 (1983) 495.
452 X. Xue and J. Chen, Huaxue Shijie, 25 (1984) 416.
453 X. Xue and J. Zhou, Huaxue Shijie, 25 (1984) 331.
454 G. Yao and Y. Shi, Yaowu Fenxi Zazhi, 4 (1984) 242.
455 X. F. Yin and X. N. Xiu, Huanjing Kexue, 5 (1984) 47.
456 A. Yuchi, H. Wada and G. Nakagawa, Anal. Chim. Acta, 149 (1983) 209.
457 Y. Zhu, H. Gong, Z. Zeng and X. Zhou, Chem. J. Chin. Univ., 4 (1983) 575.
458 Y. Zhu, R. Yu, Y. Lin and T. Jin, Fenxi Huaxue, 10 (1982) 548.
459 R. Z. Akhmetov, A. T. Dzhagiparova and E. Yu. Dmitrieva, Teploenergetika (Moscow), 9 (1983) 63.
460 P. H. V. Alexander, G. J. Moody and J. D. R. Thomas, Anal. Proc. (London), 22 (1985) 13.
461 J. C. Allen and M. C. Neville, Clin. Chem., 29 (1983) 858.
462 F. J. Alvarez-Leefmans, S. M. Gamino and T. J. Rink, J. Physiol. (London), 354 (1984) 303.
463 P. Amoroso, L. Campanella, G. De Angelis, T. Ferri and R. Morabito, J. Membr. Sci., 16 (1983) 259.

464 P. Anker, D. Ammann, P. C. Meier and W. Simon, Clin. Chem., 30 (1984) 454.
465 P. Anker, J. Hans-Beat, U. Wuthier, R. Asper, D. Ammann and W. Simon, Clin. Chem., 29 (1983) 1447.
466 P. Anker, H.-B. Jenny, U. Wuthier, R. Asper, D. Ammann and W. Simon, Clin. Chem., 29 (1983) 1508.
467 J. Anzai, C. Isomura and T. Osa, Chem. Pharm. Bull., 33 (1985) 236.
468 J. Assaily, J.-D. Monet, Y. Goureau and J.-L. Bagot, Clin. Chim. Acta, 143 (1984) 37.
469 W. F. Averill, Food Technol. (Chicago), 37 (1983) 44, 46, 56.
470 H. Baerentsen, F. Giraldez and T. Zeuthen, J. Membr. Biol., 75 (1983) 205.
471 G. Bains, A. Reymond and G. Lesgards, Ann. Falsif. Expert. Chim., 77 (1984) 215.
472 Yu. K. Barkauskas and Z. Ramanauskas, Zavod. Lab., 49 (1983) 22.
473 V. V. Berezhnova and M. A. Arustamyan, Agrokhimiya, 7 (1984) 110.
474 O. V. Bibik, G. I. Ruzal, L. M. Zorina and N. V. Tremasov, Khim.-Farm. Zh., 19 (1985) 113.
475 P. Bijster and K. L. J. Vink, Clin. Chem., 30 (1984) 6.
476 M. Bochenska and J. F. Biernat, Anal. Chim. Acta, 162 (1984) 369.
477 A. V. Bogatskii, N. G. Lukyanenko, Yu. P. Popkov, N. Yu. Nazarova, M. U. Mamina and Z. A. Chernotkach, Dokl. Akad. Nauk SSSR, 271 (1983) 630.
478 A. V. Bogatsky, N. G. Lukyanenko, V. N. Golubev, N. Yu. Nazarova, L. P. Karpenko, Yu. A. Popkov and V. A. Shapkin, Anal. Chim. Acta, 157 (1984) 151.
479 W. F. Baron, J. Membr. Biol., 72 (1983) 1.
480 W. Bussmann, W. E. Morf, J.-D. Vigneron, J.-M. Lelin and W. Simon, Helv. Chim. Acta, 67 (1984) 1439.
481 L. Z. Cai, S. Q. Lu and Z. L. Lu, Huaxue Tongbao, 12 (1983) 23.
482 L. Campanella, L. Sorrentino and M. Tomassetti, Analyst (London), 108 (1983) 1490.
483 L. Campanella, L. Sorrentino and M. Tomassetti, Ann. Chim. (Rome), 74 (1984) 483.
484 R. W. Cattrall, M. J. Newlands and M. F. Mackay, Anal. Chim. Acta, 155 (1983) 235.
485 F. C. Chang, S. C. Wu and C. H. Huang, J. Chin. Chem. Soc. (Taipei), 30 (1983) 91.
486 E. Chapoteau and W. James Smith, Clin. Chem., 29 (1983) 1187.
487 H. Chi and T. Zhou, Yaowu Fenxi Zazhi, 2 (1982) 321.
488 H. Chi and T. Zhou, Yaoxue Xuebao, 18 (1983) 278.
489 S. I. Cho, D. Y. Uhm and S. D. Rhee, Chungang Uidaechi, 7 (1982) 281.
490 R. J. Cooke and R. L. Jensen, Clin. Chem., 29 (1983) 1563.
491 V. V. Cosofret and R. P. Buck, Anal. Chim. Acta, 162 (1984) 357.
492 C. E. Deane-Drummond and A. D. M. Glass, Plant. Physiol., 73 (1983) 100.
493 C. E. Deane-Drummond and A. D. M. Glass, Plant Physiol., 73 (1983) 105.
494 J. Delong and M. M. Civan, J. Membr. Biol., 74 (1983) 155.
495 J. Delong and M. M. Civan, J. Membr. Biol., 72 (1983) 183.
496 E. P. Diamandis and T. P. Hadjiioannou, Microchem. J., 28 (1983) 399.
497 S. E. Didina, A. L. Grekovich, E. A. Materova and A. S. Bychkov, Zh. Anal. Khim., 39 (1985) 2031.
498 B. A. Dilena, R. N. Walmsley and G. G. Fraser, Clin. Chem., 29 (1983) 1856.
499 R. Dipolo, H. Rojas, J. Vergara, R. Lopez and C. Caputo, Biochim. Biophys. Acta, 728 (1983) 311.
500 B. A. Dobrolyubova, Gig. Sanit., 8 (1984) 68.
501 V. A. Drozdov, N. P. Kolbyagin and Yu. Urusov, Zh. Anal. Khim., 38 (1983) 2143.
502 C. E. Eftasthiou and T. P. Hadjiioannou, Talanta, 30 (1983) 145.
503 V. V. Egorov, G. L. Starobinets, A. M. Zvonok, Ya. F. Lushchik and L. V. Koleshko, Vestsi Akad. Nauk SSSR, 4 (1984) 40.
504 M. M. Emara, N. A. Farid, A. M. Wasti, M. M. Bahr and H. M. Abd-Elbary, J. Phys. Chem., 88 (1984) 3345.
505 X. Fa, X. Zhou, W. Zhang, H. Hua and Z. Jiang, Beijing Daxue Xuebso, Ziran Kexueban, 3 (1982) 63.
506 S. Fabczak, Acta Protozool., 22 (1983) 175.

507 R. E. Farrell and A. D. Scott, Talanta, 31 (1984) 1005.
508 D. Feng, Fenxi Huaxue, 12 (1984) 251.
509 D. Feng, Huaxue Tongbao, 3 (1984) 119.
510 D. Feng and Ch. Chen, Fenxi Huaxue, 10 (1982) 676.
511 D. Feng and Ch. Chen, Huaxue Xuebao, 41 (1983) 371.
512 D. Feng and J. H. Chen, Fenxi Huaxue, 11 (1983) 822.
513 D. Feng and Z. Xie, Huaxue Tongbao, 6 (1982) 22.
514 N. Fogh-Andersen, L. Hedegaard, J. Thode and O. Siggaard-Andersen, Clin. Chem., 30 (1984) 116.
515 N. Fogh-Andersen and O. Siggaard-Andersen, Clin. Chem., 30 (1984) 1843.
516 N. Fogh-Andersen, P. D. Wimberley, J. Thode and O. Siggaard-Andersen, Clin. Chem., 30 (1984) 433.
517 A. J. Frend, G. J. Moody, J. D. R. Thomas and B. J. Birch, Anal. Proc. (London), 20 (1983) 122.
518 A. J. Frend, G. J. Moody, J. D. R. Thomas and B. J. Birch, Analyst (London), 108 (1983) 1072.
519 A. J. Frend, G. J. Moody, J. D. R. Thomas and B. J. Birch, Analyst (London), 108 (1983) 1357.
520 N. Fukushi, Gunma Daigaku Kyoyobu Kiyo, 17 (1983) 29.
521 B. A. Fulton, C. E. Meloan, M. D. Wichman and R. C. Fry, Anal. Chem., 56 (1984) 2919.
522 V. P. Y. Gadzekpo and G. D. Christian, Anal. Lett., A16 (1983) 1371.
523 V. P. Y. Gadzekpo, J. M. Hungerford, A. M. Kadry, Y. A. Ibrahim and G. D. Christian, Anal. Chem., 57 (1985) 493.
524 Z. A. Gallai, L. K. Shpigun, E. N. Abanina and N. M. Sheina, Zh. Anal. Khim., 39 (1984) 1067.
525 Z. Gao and H. Sheng, Youji Huaxue, 3 (1983) 187, 199.
526 Z. Gao, Q. Yuan, J. Luo and H. Shen, Huaxue Xuebao, 41 (1983) 139.
527 F. Giraldez and K. T. G. Ferreira, Biochim. Biophys. Acta, 769 (1984) 625.
528 V. N. Golubev and A. D. Gutsol, Elektrokhimiya, 19 (1983) 1588.
529 V. N. Golubev and A. D. Gutsol, Latv. PSR Zinat. Akad. Vestis., Kim. Ser., 6 (1982) 666.
530 V. N. Golubev and V. V. Ramkovich, Elektrokhimiya, 19 (1983) 1443.
531 V. N. Golubev and S. K. Timofeeva, Zh. Anal. Khim., 38 (1983) 1998.
532 V. N. Golubev and S. K. Timofeeva, Latv. PSR Zinat. Akad. Vestis., Kim. Ser., 1 (1983) 45.
533 H. Gong, C. Wang and D. Xiao, Chem. J. Chin. Univ., 5 (1984) 266.
534 H. Z. Gong, D. Xiao and C. Wang, Gaodeng Xuexiao Huaxue Xuebao, 5 (1984) 45.
535 H. Gong, Y. Zhu, Y. Zeng and Y. Ou, Gaodeng Xuexiao Huaxue Xuebao, 4 (1983) 529.
536 A. L. F. Gorman, S. Levi, E. Nasi and D. Tillotson, J. Physiol. (London), 353 (1984) 127.
537 Y. Gourmelin, A. Truchand, J. Hersant, G. Glikmanas and B. Bigorie, Clin. Chem., 29 (1983) 1193.
538 A. L. Grekovich and T. A. Shuina, Ionnyi Obmen Ionometriya, 4 (1984) 128.
539 J. J. Griffin and G. D. Christian, Talanta, 30 (1983) 201.
540 N. Kh. Grinberg and E. I. Kessel'brener, Konservn. Ovoshchesush. Prom., 3 (1984) 37.
541 I. A. Gurev, A. K. Chueva, G. M. Lizunova and I. A. Sbitneva, Farmatsiya (Moscow), 32 (1983) 60.
542 I. A. Gurev and M. I. Drofa, Zh. Anal. Khim., 38 (1983) 1659.
543 I. A. Gurev and Z. M. Gureva, Zh. Anal. Khim., 38 (1983) 1289.
544 I. A. Gurev, N. N. Kalachev, V. V. Kutsovskaya, M. A. Buslaeva and E. A. Gushchina, Agrokhimiya, 6 (1984) 105.

545 I. A. Gurev, S. A. Tumanov and A. B. Usov, Izv. Vyssh. Uchebn. Zaved., Khim. Khim. Tekhnol., 26 (1983) 1064.
546 A. D. Gutsol and V. N. Golubev, Zh. Anal. Khim., 38 (1983) 970.
547 F. Hao, L. Cai, J. Pan, S. Chen and F. Bian, Fenxi Huaxue, 11 (1983) 857.
548 H. Hara and S. Okazaki, Analyst (London), 110 (1985) 11.
549 S. S. M. Hassan, M. A. Ahmed and M. M. Saoudi, Anal. Chem., 57 (1985) 1126.
550 S. S. M. Hassan and F. S. Tadros, Anal. Chem., 56 (1984) 542.
551 M. He, J. Pan and Y. Liu, Fenxi Huaxue, 11 (1983) 81.
552 X. G. He, H. W. Wu, Z. H. Yin and H. Q. Huang, Hunan Yixueyuan Xuibao, 9 (1984) 191.
553 M. W. He, J. H. Pan, M. An, Q. G. Liu, Z. S. Sun and Q. Quo, Shanxi Daxue Xuebao, Ziran Kexueban, 20 (1983) 58.
554 E. Hopirtean and E. Stefaniga, Rev. Chim. (Bucharest), 35 (1984) 945.
555 J. Hounsgard and C. Nicholson, Probing the Extracellular Space of Brain Slices with Ion-selective Microelectrodes, in R. Dingledine (Ed.), Brain Slices, Plenum, New York, 1984, p. 263.
556 Z. Y. Hu, X. X. Qian and J. Chen, Fenxi Huaxue, 12 (1984) 145.
557 Z. Hu, X. Qian, J. Chen and Q. Yuan, Fenxi Huaxue, 11 (1983) 746.
558 D. Huan, Ch. Zhu, J. Zhang, D. Wang and H. Hu, Gaodeng Xuaxiao Huaxue Xuebao, 5 (1984) 641.
559 S. Huang, Y. Zhu and G. Yan, Gaodeng Xuexiao, Huaxue Xuebao, 5 (1984) 646.
560 D. Huang, J. Zhang, Ch. Zhu, D. Wang, H. Hu, T. Fu, H. Ou, Z. Shen and Z. Yu, Huaxue Xuebao, 42 (1984) 101.
561 D. Huang, Ch. Zhu, J. Zhang, H. Lei, D. Wang, H. Hu, T. Fu, H. Ou, Z. Shen and Z. Yu, Fenxi Huaxue, 12 (1984) 89.
562 T. Hui and H. Hang, Chem. J. Chin. Univ., 4 (1983) 666.
563 E. S. Hysing, J. Kofstad, P. Lilleaasen and O. Stokke, Influence of Different Priming Solutions on Ionized Calcium During Heart Operation, in A. H. J. Maas, J. Kofstad, O. Siggaard-Andersen and G. Kokholm (Eds.), Ionized Calcium, Sodium and Potassium by Ion Selective Electrodes, Vol. 5, Private Press, Copenhagen, 1984, p. 53.
564 T. Ikeda, A. Abe, K. Kikukawa and T. Matsuda, Chem. Lett., (1983) 369.
565 T. Imato, M. Katahira and N. Ishibashi, Anal. Chim. Acta, 165 (1984) 285.
566 J. F. P. M. Inacio, J. L. F. C. Lima and A. A. S. C. Machado, Rev. Port. Quim., 23 (1981) 133.
567 M. S. Ionescu, D. Negoin and V. V. Cosofret, Anal. Lett., B16 (1983) 553.
568 H. J. Issaq, G. M. Muschik and N. H. Risser, Anal. Chim. Acta, 154 (1983) 335.
569 V. Jankauskas, E. N. Avdeeva, R. Kazlauskas and O. M. Petrukhin, Zavod. Lab., 49 (1983) 15.
570 V. Jankauskas, E. N. Avdeeva, P. Kazlauskas and O. M. Petrukhin, Zh. Anal. Khim., 38 (1983) 636.
571 A. Jaramillo, S. Lopez, J. B. Justice, J. D. Salamone and D. B. Neill, Anal. Chim. Acta, 146 (1983) 149.
572 A. Jyo, T. Imato, H. Kohno and N. Ishibashi, Bull. Chem. Soc. Jpn., 56 (1983) 3177.
573 K. Kajimo and M. Fujimoto, Jpn. J. Physiol., 32 (1982) 997.
(a) J. Kalous, K. Vytřas and A. Terberová, Collect. Czech. Chem. Commun., 48 (1983) 1137.
574 K. Kajino, Y. Matsumura and M. Fujimoto, Nippon Seirigaku Zasshi, 44 (1982) 663.
575 M. Kataoka, N. Unjyo and T. Kambara, Talanta, 30 (1983) 741.
576 C. W. Keevil and I. R. Hamilton, Anal. Biochem., 139 (1984) 228.
577 S. A. H. Khalil, G. J. Moody and J. D. R. Thomas, Analyst (London), 110 (1985) 353.
578 S. A. H. Khalil, G. J. Moody, X. G. De Oliveira Neto and J. D. R. Thomas, Anal. Proc. (London), 22 (1985) 10.
579 Yu. P. Kholmovoi, O. M. Petrukhin, L. M. Rub and V. D. Anapolskii, Zavod. Lab., 49 (1983) 1.

580 K. Kimura, H. Tamura and T. Shono, J. Chem. Soc., Chem. Commun., 9 (1983) 492.
581 K. Kimura, A. Ishikawa, H. Tamura and T. Shono, Bull. Chem. Soc. Jpn., 56 (1983) 1859.
582 K. Kimura, A. Ishikawa, H. Tamura and T. Shono, J. Chem. Soc., Perkin Trans., 2 (1984) 447.
583 K. Kimura, K. Kumani, S. Kitazawa and T. Shono, Anal. Chem., 56 (1984) 2369.
584 P. S. Kindstedt, L. R. Mattick and F. V. Kosikowski, J. Dairy Sci., 66 (1983) 988.
585 J. Kinkeldei, Laborprax., 7 (1983) 268, 271.
586 S. Kiryu, Y. Oda and M. Sasaki, Chem. Pharm. Bull., 31 (1983) 1089.
587 S. Kitazawa, K. Kimura, H. Yano and T. Shono, J. Am. Chem. Soc., 106 (1984) 6978.
588 S. Kitazawa, K. Kimura, H. Yano and T. Shono, Analyst (London), 110 (1985) 295.
589 R. P. Kline and I. S. Cohen, Biophys. J., 46 (1984) 663.
590 A. V. Kopityin, P. Gábor-Klatsmáyni and E. Pungor, Magy. Kem. Foly., 89 (1983) 561.
591 A. V. Kopytin, P. Gábor-Klatsmányi, V. P. Izvekov, E. Pungor and E. G. Ilyin, Anal. Chim. Acta, 162 (1984) 133.
592 A. V. Kopytin, P. Gábor-Klatsmányi, V. P. Izvekov, E. Pungor and G. A. Yagodin, Anal. Chim. Acta, 162 (1984) 123.
593 A. V. Kopytin, P. Gábor-Klatsmányi, E. Pungor and G. A. Yagodin, Magy. Kem. Foly., 89 (1983) 42.
594 J. Kotek, Chem. Prum., 34 (1984) 23.
595 J. Kotek, Chem. Prum., 34 (1984) 519.
596 J. Kotek and M. Bareš, Chem. Prum., 33 (1983) 254.
597 G. C. Kresheck and I. Constantinidis, Anal. Chem., 56 (1984) 152.
598 T. Kubota, B. A. Biagi and G. Giebisch, J. Membr. Biol., 73 (1983) 51, 61.
599 M. Kumakura, I. Kaetsu and S. Adachi, J. Electrochem. Soc., 131 (1984) 1272.
600 A. C. Kurkdjian and H. Barbier-Brygoo, Anal. Biochem., 132 (1983) 96.
601 P. J. Laming and M. B. A. Djamgoz, J. Neurosci. Methods, 8 (1983) 399.
602 P. Lanza and G. Mortera, Ann. Chim. (Rome), 73 (1983) 371.
603 L. Larsson, B. Kågedal and G. Toss, Ionized Calcium as Indicator of Hypercalcemia, in A. H. J. Maas, J. Kofstad, O. Siggaard-Andersen and G. Kokholm (Eds.), Ionized Calcium, Sodium and Potassium by Ion Selective Electrodes, Vol. 5, Private Press, Copenhagen, 1984, p. 31.
604 P. Layer, J. Holtz, D. Maruhn and H. Goebell, Clin. Chem., 29 (1983) 745.
605 O. A. Lebedeva, O. Striks and E. Jansons, Latv. PSR Zinat. Akad. Vestis, Kim. Ser., 6 (1983) 696.
606 Ch. O. Lee and W. B. Im, KROC Found. Ser., 17 (1984) 157.
607 H. L. Lee and M. E. Meyerhoff, Analyst (London), 110 (1985) 371.
608 V. G. Leontev, M. M. Sokolova and G. P. Tsayun, Fiziol. Zh. SSSR, 69 (1983) 563.
609 S. Li and J. Gong, Fenxi Huaxue, 12 (1984) 738.
610 S. Li and K. A. Smith, Commun. Soil Sci. Plant Anal., 15 (1984) 1437.
611 K. Lindeman and O. Müller-Plathe, Ionized Calcium for the Detection and Treatment of Osteolytic Processes, in A. H. J. Maas, J. Kofstad, O. Siggaard-Andersen and G. Kokholm (Eds.), Ionized Calcium, Sodium and Potassium by Ion Selective Electrodes, Vol. 5, Private Press, Copenhagen, 1984, p. 63.
612 E. Lindner, K. Tóth, E. Pungor, F. Behm, P. Oggenfuss, D. H. Welti, D. Ammann, W. E. Morf, E. Pretsch and W. Simon, Anal. Chem., 56 (1984) 1127.
613 C. S. Luo, E. C. Chang and Y. C. Yeh, Anal. Chem., 54 (1982) 2333.
614 J. R. López, L. Alamo, C. Caputo, R. DiPolo and J. Vergara, Biophys. J., 43 (1983) 1.
615 J. R. López, L. Alamo, C. Caputo, J. Vergara and R. DiPolo, Biochim. Biophys. Acta, 804 (1984) 1.
616 B. Lu, H. Han and R. Wang, Fenxi Huaxue, 11 (1983) 165.
617 J. X. Lu, L. M. Zhang and L. P. Yang, He Huaxue Yu Fangshe Huaxue, 6 (1984) 113.
618 M. L. Lucas and M. J. Cannon, Biochim. Biophys. Acta, 730 (1983) 41.

619 Ya. F. Lushchik, V. V. Egorov, E. M. Rakhmanko, G. L. Starobinets and L. M. Berkus, Vestsi Akad. Nauk BSSR, 5 (1983) 28.
620 V. Lustig, Clin. Chem., 30 (1984) 1417.
621 E. A. Materova, T. Ya. Bart, V. S. Karavan and V. Yu. Andreev, Ion. Obmen Ionometriya (Leningrad), 4 (1984) 120.
622 E. Metzger, D. Ammann, U. Schafer, E. Pretsch and W. Simon, Chimia, 38 (1984) 440.
623 M. E. Meyerhoff and P. M. Kovach, J. Chem. Educ., 60 (1983) 766.
624 K. Midtbo, O. Hals and O. P. Foss, Serum Ionized Calcium in Hypertensive Patients Before and After Calcium-gluconate Injection, in A. H. J. Maas, J. Kofstad, O. Siggaard-Andersen and G. Kokholm (Eds.), Ionized Calcium, Sodium and Potassium by Ion Selective Electrodes, Vol. 5, Private Press, Copenhagen, 1984, p. 39.
625 K. N. Mikhelson, A. L. Grekovich and E. A. Materova, Elektrokhimiya, 19 (1983) 249.
626 M. Mitsana-Papazoglou, E. P. Diamandis and T. P. Hadjiioannou, Anal. Chim. Acta, 159 (1984) 393.
627 T. Miyazaki and T. Aomi, Denki Kagaku Oyobi Kogyo Butsuri Kagaku, 52 (1984) 521.
628 G. J. Moody and J. D. R. Thomas, J. Power Sources, 9 (1983) 137, 146.
629 W. E. Morf, W. Bussmann and W. Simon, Helv. Chim. Acta, 67 (1984) 1427.
630 S. Nakashima, M. Yagi, M. Zenki, A. Takahashi and K. Toei, Fresenius' Z. Anal. Chem., 319 (1984) 506.
631 M. Ni, Yaowu Fenxi Zazhi, 3 (1983) 48.
632 P. Ni, X. Du and G. Wu, Fenxi Huaxue, 10 (1982) 750.
633 Sh. K. Norov, L. M. Mamadzhanov, A. K. Tashmukhamedova, N. Zh. Saifullina and B. A. Tashmukhamedov, Zh. Anal. Khim., 39 (1984) 613.
634 G. A. Ortolano, R. C. Stuart, K. R. Wunschel, E. A. Kaiser, R. P. Hammond and A. K. Swonger, Microchem. J., 28 (1983) 409.
635 J. Pan, L. Cai, F. Hao, C. Li and Y. Li, Gaodeng Xuexiao Huaxue Xuebao, 5 (1984) 473.
636 J. Pan, F. Hao, L. Cai, H. Wang and W. Wang, Shanxi Daxue Xuebao, 18 (1982) 71.
637 J. Pan, F. Hao, W. Wang and H. Wang, Gaodeng Xuexiao Huaxue Xuebao, 5 (1984) 473.
638 J. Pan, M. He, L. Cai, Q. Guo, Y. Li, Z. Sun and Ch. Li, Huaxue Xuebao, 42 (1984) 1094.
639 J. Pan, M. He and Y. Liu, Fenxi Huaxue, 11 (1983) 518, 521.
640 J. Pan, Y. Liu, F. Ma and A. Chen, J. Shanxi Univ., 48 (1983) 48.
641 M. A. Parra and J. Torrent, Soil Sci. Soc. Am. J., 47 (1983) 335.
642 G. Peinhardt and J. Siemroth, Pharmazie, 38 (1983) 33.
643 L. S. Peng, Fenxi Huaxue, 12 (1984) 477.
644 L. Peng and P. Xin, Yanshi Kuangwu Ji Deshi, 3 (1984) 173.
645 J. G. Pentari and C. E. Eftasthiou, Anal. Chim. Acta, 153 (1983) 161.
646 R. Perez-Olmos and J. Echevarria, Alimentaria, 142 (1983) 51.
647 R. Perez-Olmos, J. Echevarria and B. Uribe, Ing. Quím. (Madrid), 15 (1983) 49.
648 O. M. Petrukhin and Yu. P. Kholmovoi, Zh. Anal. Khim., 38 (1983) 1992.
649 L. Ping, Huaxue Shiji, 4 (1982) 346, 384.
650 X. X. Qian, J. Z. Chen and Z. Y. Hu, Huanjing Huaxue, 3 (1984) 17.
651 E. Rabe, Z. Lebensm.-Unters.-Forsch., 176 (1983) 270.
652 S. J. Rehfeld, J. Barkeley and H. F. Loken, Clin. Chem., 30 (1984) 304.
653 H. Ruprecht, P. Oggenfress, U. Oesch, D. Ammann and W. E. Morf, Inorg. Chem., 79 (1983) 67.
654 O. Ryba and J. Petránek, Collect. Czech. Chem. Commun., 49 (1984) 2371.
655 K. Ryu, J. M. Lowery, D. F. Evans and E. L. Cussler, J. Phys. Chem., 87 (1983) 5015.
656 T. Saito, S. Saito, I. Watanabe, K. Hibiya, E. Tokutake, Y. Tamura, Y. Ozawa and M. Hatano, Kokyu To Junkan, 31 (1983) 309.
657 T. Sakuhara, M. Kataoka and T. Kambara, Denki Kagaku, 51 (1983) 905.
658 S. G. Samokhvalov, V. G. Prizhukova, M. N. Arsene'va and T. S. Gruzdeva, Pochvovedenie, 3 (1984) 142.

659 S. G. Samokhvalov, V. G. Prizhukova, M. N. Arseneva, A. M. Kapustin, G. M. Sorokina and A. I. Golubtsov, Agrokhimiya, 12 (1984) 105.
660 S. G. Samokhvalov, V. G. Prizhukova, L. I. Molkanova, A. M. Kapustin, A. I. Golubtsov and T. N. Toroptseva, Agrokhimiya, 4 (1983) 106.
661 B. J. Sandmann, M. H. Chien and R. A. Sandmann, Anal. Lett., A18 (1985) 149.
662 P. U. Sap, D. F. Angel and C. Luca, Rev. Roum. Chim., 28 (1983) 883.
663 E. G. Sarantonis and M. I. Karayannis, Anal. Biochem., 130 (1983) 172.
664 I. Satake, S. Noda and T. Maeda, Bull. Chem. Soc. Jpn., 56 (1983) 2581.
665 B. B. Sauer, R. A. Flint, J. B. Justice and C. G. Trowbridge, Arch. Biochem. Biophys., 234 (1984) 580.
666 A. Q. Schantz, J. Cell Biol., 100 (1985) 947, 954.
667 J. G. Schindler and M. M. Schindler, Fresenius' Z. Anal. Chem., 320 (1985) 258.
668 W. Selig, Mikrochim. Acta (Wien), I (1983) 333.
669 K. Selinger, Chem. Anal. (Warsaw), 27 (1982) 51.
670 K. Selinger, Chem. Anal. (Warsaw), 27 (1982) 383.
671 K. Selinger and R. Starościk, Chem. Anal. (Warsaw), 27 (1982) 223.
672 J. Šenkýř and K. Kouřil, J. Electroanal. Chem., 180 (1984) 383.
673 Yu. V. Shavnya, O. M. Petrukhin, A. S. Bobrova and Yu. M. Chikin, Zh. Anal. Khim., 39 (1984) 275.
674 G. Shen and X. Li, Hunan Daxue Xuebao, 11 (1984) 86.
675 G. Shen and D. Liao, Yaowu Fenxi Zazhi, 4 (1984) 200.
676 G. Shen, S. Yao and X. Liu, Yaowu Fenxi Zazhi, 3 (1983) 257.
677 G. Shen, S. Yao and S. Sun, Chem. J. Chin. Univ., 5 (1984) 138.
678 G. Shen, S. Yao, X. Jiang and W. Wu, Fenxi Huaxue, 11 (1983) 481.
679 K. Shiranama, H. Kamaya and I. Ueda, Anal. Lett., B16 (1983) 1485.
680 L. K. Shpigun and E. N. Abanina, Zh. Anal. Khim., 39 (1984) 1829.
681 G. I. Shumilova, Z. S. Alagova and E. A. Materova, Elektrokhimiya, 20 (1984) 1140.
682 Yu. A. Sirikov, D. Bilinkis, V. I. Komova, Z. I. Gurova and Yu. A. Belov, Zavod. Lab., 50 (1984) 3.
683 B. S. Smolyakov and V. V. Kokovkin, Izv. Sib. Otd. Akad. Nauk SSSR, 1 (1983) 16.
684 B. S. Smolyakov and V. V. Kokovkin, Izv. Sib. Otd. Akad. Nauk SSSR, 1 (1983) 24.
685 B. S. Smolyakov and V. V. Kokovkin, Izv. Sib. Otd. Akad. Nauk SSSR, 4 (1984) 11.
686 J. Staňa, Agrochémia, 22 (1982) 119.
687 J. Sucharová, Rostl. Výroba, 29 (1983) 951.
688 M. Sugawara, S. Nagasawa and N. Ohashi, J. Electroanal. Chem., 176 (1984) 183.
689 M. Sugawara, N. Ohashi, M. Saruhashi and T. Kambara, Denki Kagaku, 51 (1983) 97.
690 A. V. Svyatkovskii, M. A. Svyatkovskii, I. V. Kudryashova, E. A. Materova and E. B. Nikolskaya, Ionnyi Obmen Ionometriya, 4 (1984) 173.
691 E. Syková, Prog. Biophys. Molec. Biol., 42 (1983) 135.
692 J. C. Synnott, S. J. West and J. W. Ross, Stud. Environ. Sci., 23 (1984) 143.
693 W. Szczepaniak and M. Ren, Talanta, 30 (1983) 945.
694 W. Szczepaniak and M. Ren, Talanta, 31 (1984) 212.
695 B. Taboryska and J. Dojlido, Chem. Anal. (Warsaw), 28 (1983) 633.
696 H. Takahashi, Arch. Jpn. Chir. (Nihon Geka Hokan), 53 (1984) 3.
697 T. Tamura and M. Kataoka, Bunseki Kagaku, 33 (1984) 591.
698 H. Tamura, K. Kumami, K. Kimura and T. Shono, Mikrochim. Acta, II (1983) 287.
699 X. Tan, G. Lai and Z. Peng, Fenxi Huaxue, 12 (1984) 479.
700 X. Tan, Z. Peng and G. Lai, Fenxi Huaxue, 12 (1984) 169.
701 M. M. Timotheou-Potamia, M. A. Koupparis and T. P. Hadjiioannou, Microchem. J., 28 (1983) 392.
702 P. Urban, B. Buchmann and D. Scheidegger, Clin. Chem., 31 (1985) 264.
703 C. Van Leeuwen and G. A. Harff, Tijdschr. Med. Ver. Klin. Chem., 8 (1983) 154.
704 F. J. Vanstabel and W. D. Likens, Ann. Clin. Biochem., 21 (1984) 339.
705 O. G. Vartanova, Sh. K. Norov and N. A. Parpiev, Zh. Anal. Khim., 39 (1984) 813.

706 B. Vialatte, J. Aléveque, H. Quinot and A. Taupe, Analusis, 11 (1983) 446.
707 G. E. Vlasova, Yu. A. Zolotov, E. V. Rybakova, V. A. Zarinskii, L. K. Shpigun and I. V. Volobueva, Zh. Anal. Khim., 38 (1983) 631.
708 F. Voegtle, T. Kleiner, R. Leppkes, M. W. Laeubli, D. Ammann and W. Simon, Chem. Ber., 116 (1983) 2028.
709 A. Villiger, W. E. Morf and W. Simon, Helv. Chim. Acta, 66 (1983) 1078.
710 K. Vytřas, T. Čapoun and J. Kalous, Anal. Chim. Acta, 162 (1984) 373.
711 K. Vytřas, J. Kalous and T. Čapoun, Anal. Chim. Acta, 162 (1984) 141.
712 K. Vytřas, J. Kalous and L. Černá, Agrochémia, 23 (1983) 176.
713 K. Vytřas, J. Symerský, C. Dogru and A. Onur, Anal. Chim. Acta, 149 (1983) 217.
714 C. Wang and X. Chen, Chem. J. Chin. Univ., 5 (1984) 267.
715 D. Wegmann, H. Weiss, D. Ammann, W. E. Morf, E. Pretsch, K. Sugahara and W. Simon, Mikrochim. Acta, 3 (1984) 1.
716 P. West, Clin. Chem., 29 (1983) 1315.
717 J. F. White, D. Ellingson and K. Burnup, J. Membr. Biol., 78 (1984) 223.
718 J. P. Willis, C. C. Young, R. Martin, P. Stearns, H. Pelosi and D. Magnanti, Clin. Chem., 29 (1983) 1193.
719 G. Wu, C. Lu, S. Gao, X. Xue, X. Du, G. Tan, J. Xu, Z. Yao, F. Zhang and Z. Yan, Fenxi Huaxue, 11 (1983) 515.
720 U. Wuthier, H. V. Pham, R. Zünd, D. Welti, R. J. J. Funck, A. Bezegh, D. Ammann, E. Pretsch and W. Simon, Anal. Chem., 56 (1984) 535.
721 X. Xu, Fenxi Huaxue, 11 (1983) 41.
722 M. Xu and Z. Liu, Turang Xuebao (Nanjing), 19 (1983) 367.
723 V. E. Yurinskaya, O. K. Stefanova and E. A. Materova, Elektrokhimiya, 17 (1981) 1628.
724 J. Xuan, Turang Xuebao (Nanjing), 14 (1982) 196.
725 X. Xue, Fenxi Huaxue, 11 (1983) 51.
726 X. X. Xue and S. F. Su, Zhong Cao Yao, 15 (1984) 200.
727 Y. S. Yang and S. H. Cai, Huaxue Shiji, 6 (1984) 133.
728 S. Yao and G. Gao, Yaoxue Xuebao, 19 (1984) 550.
729 S. Yao, G. Shen and H. Chen, Yaowu Fenxi Zazhi, 4 (1984) 100.
730 S. Yao, G. Shen and Z. F. Ruo, Yaowu Fenxi Zazhi, 4 (1984) 103.
731 S. Yao, G. Shen and H. Wang, Fenxi Huaxue, 11 (1983) 405.
732 S. Yao, X. Xu and G. Shen, Yaoxue Xuebao, 18 (1983) 612.
733 S. Yao and Y. Tang, Yaoxue Xuebao, 19 (1984) 455.
734 R. Q. Yu and S. S. Huang, Talanta, 30 (1983) 427.
735 Z. Yu, Z. Huang, M. Zhang and X. Zhou, Huaxue Xuebao, 40 (1982) 1076.
736 W. Yu, G. Zhang and H. Wang, Huaxue Xuebao, 41 (1983) 228.
737 R. Yu, Y. Feng, W. W. Huang and Z. G. Guo, Gaodeng Xuexiao Huaxue Xuebao, 5 (1984) 169.
738 R. Yu, Y. Feng, W. Huang and Z. Guo, Chem. J. Chin. Univ., 5 (1984) 174.
739 Q. Yuan, Ch. L. Liu and J. Z. Luo, Fenxi Huaxue, 12 (1984) 412.
740 P. M. Zhadan and P. A. Doroshenko, Fiziol. Zh. (Kiev), 29 (1983) 741.
741 G. X. Zhang, S. F. Wang and H. J. Wang, Acta Chim. Sinica, 41 (1983) 90.
742 G. Zhang, S. Wang and H. Wang, Fenxi Huaxue, 12 (1984) 665.
743 G. Zhang, X. Yin and H. Wang, Fenxi Huaxue, 11 (1983) 532.
744 L. Zhao and H. Wang, Tianjin Yiyao, 12 (1984) 372.
745 I. K. Al-Hitti, G. J. Moody and J. D. R. Thomas, Analyst (London), 109 (1984) 1205.
746 G. K. Budnikov, E. P. Medyaniseva, A. V. Volkov and S. S. Aronzon, Zh. Anal. Khim., 38 (1983) 1283.
747 C. A. Corcoran and R. K. Kobos, Anal. Lett., 16 (1983) 1291.
748 T. Fonong and G. A. Rechnitz, Anal. Chim. Acta, 158 (1984) 357.
749 Y. M. Fraticelli and M. E. Meyerhoff, Anal. Chem., 55 (1983) 359.
750 G. G. Guilbault and P. R. Coulet, Anal. Chim. Acta, 152 (1983) 223.

751 M. H. Ho, Biomed. Sci. Instrum., 20 (1984) 85.
752 M. H. Ho and T. G. Wu, Ann. N.Y. Acad. Sci., Enzyme Eng., 434 (1984) 523.
753 J. P. Joseph, Mikrochim. Acta, II (1984) 473.
754 P. M. Kovach and M. E. Meyerhoff, Anal. Chem., 54 (1982) 1991.
755 T. Kawashima, K. Tomida, N. Tominaga, T. Kobayashi and H. Onoshi, Chem. Lett., (1984) 653.
756 M. Y. Keating and G. A. Rechnitz, Anal. Lett., B17 (1984) 349.
757 M. Mascini, G. Palleschi, D. D'Ottavio and G. Mazzella, Ann. Chim., 73 (1983) 29.
758 D. P. Nikolelis, Anal. Chim. Acta, 161 (1984) 343.
759 D. P. Nikolelis and T. P. Hadjiioannou, Anal. Chim. Acta, 147 (1983) 33.
760 D. P. Nikolelis and T. P. Hadjiioannou, Anal. Lett., B16 (1983) 401.
761 C. P. Pau and G. A. Rechnitz, Anal. Chim. Acta, 160 (1984) 141.
762 N. D. Tran, J. L. Romette and D. Thomas, Biotechnol. Bioeng., 25 (1983) 329.
763 Y. Umezawa, Ion-Selective Immunoelectrodes, in T. Seiyama, K. Fueki, J. Shiokawa and S. Suzuki (Eds.), Proc. Int. Meet. Chem. Sens., Kodansha, Tokyo, 1983, p. 705.
764 Y. Umezawa, S. Sofue and Y. Takamoto, Talanta, 31 (1984) 375.
765 P. M. Vadgama, K. G. M. Alberti and A. K. Covington, Anal. Chim. Acta, 136 (1982) 403.
766 K. Yasuda, H. Miyagi, Y. Hamada and Y. Takata, Analyst (London), 109 (1984) 61.
767 A. R. M. Yatim and T. L. Riechel, Anal. Lett., 17B (1984) 835.
768 M. Thompson, U. J. Krull and L. I. Bendell-Young, Talanta, 30 (1983) 919.
(a) M. Thompson and U. J. Krull, Anal. Chim. Acta, 141 (1982) 33.
(b) M. Thompson and U. J. Krull, Anal. Chim. Acta, 147 (1983) 1.
769 D. Midgley and D. E. Mulcahy, Talanta, 32 (1985) 7.
770 D. Midgley, Anal. Chim. Acta, 159 (1984) 63.
771 G. S. Ihn, J. H. Lee and R. P. Buck, Taehan Hwahakhoe Chi, 27 (1983) 111.
772 G. S. Ihn, J. H. Lee and T. W. Min, Taehan Hwahakhoe Chi, 28 (1984) 238.
773 E. Barrado and R. Pardo, Rev. Roum. Chim., 29 (1984) 693.
774 W. S. Selig, Ind. Eng. Chem. Proc. Res. Dev., 23 (1984) 140.
775 W. S. Selig, Int. Lab., 4 (1984) 50.
776 W. S. Selig, Am. Lab., 16 (1984) 36, 38.
777 S. Agrawal and M. Abe, Analyst (London), 108 (1983) 712.
778 A. K. Jain and Ch. Bala, Fresenius Z. Anal. Chem., 319 (1984) 307.
779 A. K. Jain and Ch. Bala, Ann. Chim. (Rome), 75 (1985) 101.
780 A. K. Jain, R. P. Singh and Ch. Bala, Anal. Lett., 15 (1982) 1557.
781 A. K. Jain, R. P. Singh and Ch. Bala, J. Chem. Technol. Biotechnol., 34A (1984) 363.
782 J. Jeng and J. S. Shin, Analyst (London), 109 (1984) 641.
783 U. S. Lal, M. C. Chattopadhyaya, K. Choah and A. K. Dey, Indian Agric., (1982) 139.
784 W. U. Malik, S. K. Srivastava and A. Banzal, Indian J. Chem., 22A (1983) 221.
785 S. D. Pandey and P. Tripathi, Electrochim. Acta, 27 (1982) 1715.
786 S. K. Srivastava and C. K. Jain, Talanta, 31 (1984) 1021.
787 S. K. Srivastava and C. K. Jain, Bunseki Kagaku, 33 (1984) E525.
788 S. K. Srivastava and C. K. Jain, Mikrochim. Acta, 3 (1984) 53.
789 S. K. Srivastava and C. K. Jain, Water Res., 19 (1985) 53.
790 S. K. Srivastava, S. Kumar and C. K. Jain, Analyst (London), 109 (1984) 667.
791 S. K. Srivastava, S. Kumar and S. Kumar, J. Electroanal. Chem. Interfacial Electrochem., 161 (1984) 345.
792 S. K. Srivastava, A. K. Sharma and C. K. Jain, Talanta, 30 (1983) 285.
793 S. K. Srivastava, S. Kumar, N. Pal and R. Agrawal, Fresenius' Z. Anal. Chem., 315 (1983) 353.
794 S. K. Srivastava, N. Pal, R. P. Singh and S. Agrawal, Indian J. Chem., 22A (1983) 1033.

Analytica Chimica Acta, 183 (1986) 47—57
Elsevier Science Publishers B.V., Amsterdam — Printed in The Netherlands

THE ANALYTICAL APPLICATION OF SQUARE-WAVE VOLTAMMETRY

EDWARD J. ZACHOWSKI[a], MAREK WOJCIECHOWSKI[b] and JANET OSTERYOUNG*

Department of Chemistry, State University of New York at Buffalo, Buffalo, NY 14214 (U.S.A.)

(Received 17th September 1985)

SUMMARY

The effects of changing certain parameters of the applied potential waveform at a dropping mercury electrode (DME) in square-wave voltammetry (s.w.v.) were investigated and compared with theory. Optimum parameters of the waveform are determined for a reversible system, lead(II) in 0.10 M perchloric acid. Current sensitivities for Pb(II) at a static mercury drop electrode by both the integrating and instantaneous current-measurement schemes available in a laboratory computer-based system are compared to those obtained from a commercial instrument suitable for s.w.v. An irreversible system, Ni(II) in 0.10 M HCl, was investigated at the static mercury drop electrode and optimum parameters determined as for Pb(II).

Square-wave voltammetry (s.w.v.) is one of the newer pulse voltammetric techniques and has received increasing attention in recent years [1]. From an analytical point of view, the major advantages of s.w.v. lie in its ability to complete an entire potential scan on only one drop of a dropping mercury electrode, which greatly reduces the time needed relative to other pulse techniques. It also gives the analyst the option of reducing the signal-to-noise ratio by repetitive scanning and signal averaging. In the recording of a square-wave voltammogram, the currents on both the forward and reverse pulses are measured, so that kinetic information similar to that obtained in cyclic voltammetry is available; such information of similar quality cannot be obtained from other pulse techniques such as differential pulse polarography (d.p.p.). Currents for s.w.v. are calculated to be significantly greater than those predicted for d.p.p. [2]. This increased sensitivity depends on reversibility and arises because the signal is the difference between the forward and reverse currents. This difference current yields a peak value which is greater in magnitude than either the forward or reverse currents, provided the two are opposite in sign.

---

[a]Present address: Carter-Wallace, Inc., Cranbury, NJ 08512, U.S.A.
[b]Present address: Department of Chemistry, University of Maryland, Baltimore County, Catonsville, MD 21228, U.S.A.

0003-2670/86/$03.50

The current literature in s.w.v. lacks experimental results concerning quantitative applications. Square-wave voltammetry has been used for the determination of chelating agents [3], some biochemical and pharmaceutical compounds [4—7], and for anodic stripping voltammetry [8, 9]. However, with the exception of an early paper testing theory [10], studies investigating how changing certain parameters of the applied potential waveform in s.w.v. influences the signal have not been published. This work deals systematically with three aspects of the quantitative application of square-wave voltammetry. First, the dropping mercury electrode provides a clean, reproducible surface and therefore is attractive for quantitative purposes. A reversible system, Pb(II) in 0.10 M perchloric acid, was examined at the DME to identify any unexpected effects of the complex hydrodynamics on the square-wave signal and to establish the optimum values of square wave parameters. Second, irreversible systems are, in general, less attractive than reversible ones for voltammetric methods that depend on peak currents because of diminished sensitivity and resolution. The importance of these effects and their dependence on square-wave parameters were examined for reduction of nickel(II) in 0.10 M hydrochloric acid at a stationary (static drop) mercury electrode. Third, technical requirements often result in commercial implementation of techniques which give parametric dependence of the signal other than that predicted by theory. This can be important particularly in method development. The s.w.v. mode of a new commercial instrument, the EG&G PARC 384B Polarographic Analyzer, was examined to compare the signal with predictions of theory [11] and with our own experimental system.

THEORETICAL CONSIDERATIONS

The applied potential waveform at the DME is shown in Fig. 1. The complete potential range of interest is scanned during the lifetime of a single drop. The drop is permitted to grow for a specified length of time (delay time, t_d) before the waveform is applied. The waveform itself, which is a square wave superimposed on a staircase potential, is then applied with some selected values of potential step (E_s), square-wave amplitude (E_{sw}), and frequency ($f = 1/\tau$). (Note that the amplitude of the square wave is one half the peak-to-peak value.) Current is sampled at the end of the forward pulse (forward current, i_f) and the reverse pulse (reverse current, i_r). The signal, which is termed the difference current, is defined as: $i = i_f - i_r$. Provided that the square-wave amplitude is large enough ($nE_{sw} > 15$ mV, [11]) to reverse the electrode reaction that occurred on the forward pulse (in the vicinity of $E_{1/2}$), a current that is opposite in sign will be obtained on the reverse pulse. Thus, the difference current is greater in magnitude than either the forward or reverse currents. The gain in sensitivity that s.w.v. offers over other differential-pulse techniques might be lost if the pulse amplitude is too small or if slow electron transfer kinetics become important.

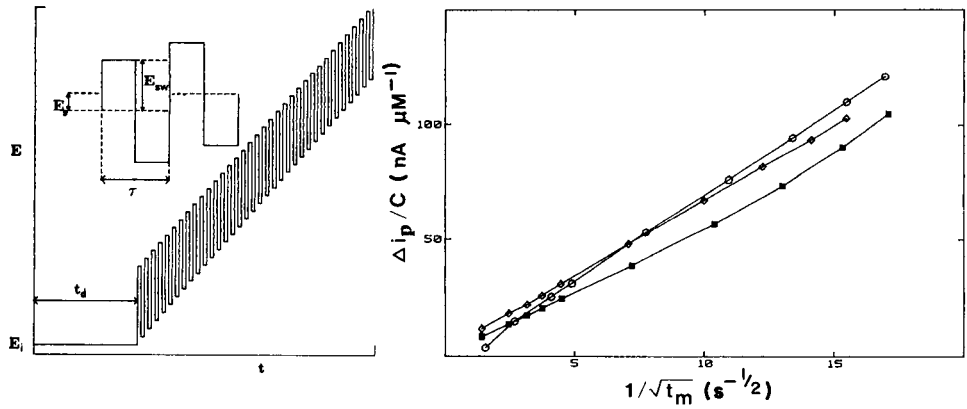

Fig. 1. Potential waveform for square-wave voltammetry at the dropping mercury electrode. E_s, step height; E_{sw}, square-wave amplitude; τ, square-wave period; t_d, delay time at initial potential, E_i.

Fig. 2. Sensitivity as a function of the actual time of current measurement, t_m: (○) computer-based instrument in q-mode; (◇) i-mode; (▪) the PARC 384B.

A factor to consider when s.w.v. is done at a DME is that the entire scan must be completed within the natural drop time of the DME (t_{nd}). Therefore, the sum of the delay time (t_d), i.e., the age of the drop when the scan is initiated, and the time required to complete the scan of desired potential range (E_R), must be less than t_{nd}: $t_{nd} > t_d + E_R/E_s f$. Because the area of the drop increases with time, each measurement of the current corresponds to a different surface area of the electrode. Varying the parameters of the waveform, such as delay time, initial potential (E_{IN}), step height, and frequency, changes the time of each current measurement (t_m), i.e., the age of the drop when the waveform reaches potential E is

$$t_m = t_d + (E_{IN} - E)/E_s f$$

(Note that E corresponds to the hypothetical potential of the staircase waveform step on which a square wave is superimposed. It is the potential against which the s.w.v. currents are customarily plotted. The actual potential is $E + E_{sw}$ on the forward pulse and $E - E_{sw}$ on the reverse pulse.) Therefore to compare s.w.v. curves obtained at the DME with different waveform parameters, individual currents should be normalized to the same drop area. For example, $i_{norm} = i/t_m^{2/3}$ provides normalization to the area of a 1-s drop. This treatment of data assumes that the only effect of drop growth is increase in area, and can indicate deviations from diffusional control of the electrode process.

For diffusion-controlled reversible processes [11], the forward, reverse, and difference peak currents should be proportional to $f^{1/2}$. The same is true for the forward and difference peak currents for totally irreversible systems.

In the former case, increasing the value of E_s increases both the forward and reverse currents by about the same amount (equal in both magnitude and sign) thus leaving the difference current almost unchanged. This should hold also for experiments with the DME if the currents are normalized to a constant drop area.

Square-wave voltammetry is inherently a digital technique. However, one can define the effective scan rate: $v = E_s f$. On the basis of the discussion above, it is important to emphasize that in s.w.v. the scan rate is not a meaningful parameter of the experiment, as it is in linear scan or cyclic voltammetry, for example.

EXPERIMENTAL

Perchloric acid and hydrochloric acid (Baker Ultrex, analyzed reagent) were used as received. Stock solutions of lead(II) nitrate (Fisher) and nickel(II) nitrate (Mallinkrodt) were standardized by potentiometric titration with EDTA using a Metrohm 636 Titroprocessor.

The DME used consisted of a Sargent-Welch capillary with a mercury flow rate of 1.56 mg s^{-1} and t_{nd} = 5.0 s at a mercury column height of 39 cm at open circuit in water. The drop time was controlled by an EG&G PARC model 1746 drop knocker.

An EG&G PARC model 303 static mercury drop electrode (SMDE) was used for the experiments comparing current sensitivities offered by the different instrumental systems. The drop size used was large (A = 0.025 cm^2) for the experiments with Pb(II) and medium (A = 0.016 cm^2) for experiments using Ni(II).

A saturated calomel electrode was used as reference and was separated from the solution by a salt bridge containing the supporting electrolyte. The counter electrode was a platinum helix. Solutions were deaerated by passing argon at a flow rate of 80 ml min^{-1}. The argon was purified from residual oxygen using a BASF R3-11 catalyst, and was then saturated with water. The cell temperature was maintained at 25°C by means of a circulating bath.

Square-wave voltammetry was done via a computer-controlled pulse voltammetric system based on a Digital Equipment Corporation PDP 8/e with homemade electronics and interface [12, 13]. All voltammograms presented here are the ensemble average of ten repetitive scans, each obtained on a fresh mercury drop in the same solution. Data-processing programs were used to subtract background current, normalize currents to a 1-s drop time, and eliminate high-frequency noise using a Fourier Transform.

The system has two modes of current measurement, i-mode and q-mode. The former measures the current instantaneously by sampling the output of an A/D converter 7.5 μs before the end of each forward and reverse pulse. In the q-mode, the current flowing during the last one third of the pulse is collected on the capacitor of an integrating operational amplifier and the resulting output voltage is converted to an instanteous current corresponding to

the midpoint of the sampling time. In the q-mode, the upper frequency limit of the hardware was 800 Hz. This integrating mode of current measurement was used for all experiments done at a DME.

A Digital Equipment Corporation PDP 8/f computer equipped with dual RX01 floppy disk drives, Tektronix 4105 display, LA50 printer, and ADM 3-A terminal was interfaced with an EG&G PARC model 384B Polarographic Analyzer via the RS-232 port, so that experimental parameters could be entered at the ADM-3A terminal and communicated to the instrument. Data obtained by the PARC 384B were transferred back to the DEC PDP 8/f and displayed on the Tektronix 4105. This made it possible to process data obtained with the DEC PDP 8/e and by the PARC 384B in exactly the same way. However, data processing was possible only for the difference currents because on the PARC instrument the forward and reverse current components are not available to the user.

Experiments comparing the DEC PDP 8/e and the PARC 384B/DEC PDP 8/f combination were done in batch fashion using the same solutions in the same experimental runs.

RESULTS AND DISCUSSION

Reversible lead(II) system

The purpose of the first series of experiments was to compare the instrumental response of the reversible lead(II) system under quantitatively significant conditions at the DME with that expected from theory for a stationary planar electrode. Data obtained for five different step heights, E_s, while holding other parameters of the waveform constant are presented in Table 1. These data demonstrate that, as the magnitude of the step is increased, the magnitude of the forward current is increased because of the larger increment of potential applied. However, the reverse reaction (oxidation of lead out of the mercury drop) occurs at a slower rate. Because these changes are roughly

TABLE 1

Dependence of the forward, reverse and difference current peaks on potential step in s.w.v. with the DME[a]

E_s (mV)	Current (μA)		
	Forward peak	Reverse peak	Difference peak
1	0.463	−0.303	0.758
2	0.482	−0.275	0.730
5	0.526	−0.272	0.774
10	0.576	−0.203	0.777
20	0.659	−0.144	0.768

[a]10 μM Pb(II) in 0.10 M $HClO_4$; E_{sw} = 25 mV; f = 150 Hz; currents (μA) were normalized to a 1-s drop area and the peaks were measured from the zero current line.

equal in magnitude, no significant change in the difference peak current is observed. In general, i_p is not a strong function of E_s.

Normalization to constant area. The method of normalizing current for different drop areas was examined for experiments involving two delay times, 0.5 and 1.0 s, and five different step heights at constant square-wave amplitude and frequency. These conditions provide a very stringent test of normalization, because the rates of change of area are large. Results are provided in Table 2. The currents before normalization differ by a maximum of 50%, but after normalization the values are similar with an average deviation of 2.0%. Deviations can be attributed to the problems that arise from shielding and stirring of the mercury and solution at the small delay times used. At the largest potential steps, stirring effects might be especially important. The results show that the normalization of current for change in drop area works well in routine work. If the drop area is very small (i.e., for short delay times) or the potential step is very large, this normalization may present problems for highly accurate intercomparison of data. It should be noted, however, that in routine applications of s.w.v. at the DME, the drop growth will not affect the quality of results if the delay time and all the waveform parameters are held constant. Under these conditions normalization of the current is not required. These experiments showed that longer delay times (at least 1 s) improve the precision of results.

Dependence on frequency. The peak current should vary linearly with $t^{-1/2}$. Frequencies ranging from 8 to 800 Hz were used for experiments with five different potential steps and five different square-wave amplitudes. Plots of the different peak current vs. $f^{1/2}$ yielded the expected linear result, with only small deviations occurring at the higher frequencies ($\geqslant$450 Hz) [14].

Calibration graphs for Pb(II) were generated at seven different square-wave frequencies; three separate dilutions were used at each concentration. The slopes of the lines and relevant data are in Table 3. A statistical treatment

TABLE 2

The effect of drop growth on the difference current peak (μA) in s.w.v. with DME[a]

Delay time (s)	Current peak (μA) at E_s = 1—20 mV				
	1	2	5	10	20
Without normalization					
0.50	0.826	0.659	0.596	0.577	0.588
1.00	1.125	0.963	0.919	0.917	0.938
After normalization to a 1-s drop[b]					
0.50	0.873	0.830	0.847	0.847	0.861
1.00	0.899	0.857	0.868	0.871	0.877

[a] E_{sw} = 20 mV, f = 250 Hz; 10 μM Pb(II) in 0.1 M $HClO_4$. [b] Also normalized to E_s = 5 mV [14].

TABLE 3

Calibration results for the determination of Pb(II) by square-wave voltammetry

Frequency (Hz)	Slope (nA μM^{-1})	Intercept (nA)	Std. dev. of slope (nA μM^{-1})	Std. dev. of intercept (nA)	Correlation coefficient
32	31	1.4	1.5	3.8	0.985
80	52	7.9	0.8	2.0	0.998
150	73	1.2	0.7	1.8	0.999
250	97	3.8	0.9	2.3	0.999
450	138	0.1	2.4	5.6	0.998
650	173	31.6	3.2	7.8	0.998
800	207	55.3	2.9	7.2	0.999

showed that at the 95% confidence level, the standard deviation of the current measurements is not a function of concentration, but is a function of frequency for all concentrations used.

The optimum parameters of the waveform for quantitative purposes were established from values of the peak width at half height, $W_{1/2}$ (Table 4), and from values of σ/m, where σ is the standard deviation of the background and m is the slope of the calibration line (Table 5). The minimum values of σ/m lie in the frequency range 150—450 Hz. The points at low frequencies are shifted upwards because of the lower slopes, while the points obtained at higher frequencies suffer from increased random noise of the background measurements. It appears that best results are obtained for a small value of E_s (1—5 mV) and a square-wave frequency of approximately 450 Hz. In this range, peak width does not increase unacceptably with increasing E_s. In order to obtain significantly faster scan rates and larger faradaic currents, it would be desirable to use E_s = 5 mV. Theory for a reversible system [15] predicts that the value nE_{sw} = 50 mV maximizes the ratio $i_p/W_{1/2}$, independent of frequency.

TABLE 4

Difference current peak widths ($W_{1/2}$, mV) for 10 μM Pb(II) in 0.10 M $HClO_4$[a]

E_s (mV)	Peak widths (mV) at f = 32—800 Hz						
	32	80	150	250	450	650	800
1	—	—	62.9	63.1	62.9	62.7	61.8
2	—	63.2	63.6	63.2	63.1	64.9	63.7
5	62.9	62.0	62.4	66.8	62.9	64.1	62.9
10	58.6	66.5	62.5	64.8	65.0	65.2	62.5
20	64.5	72.7	67.5	70.1	71.2	66.4	69.9

[a] t_d = 1 s (DME); E_{sw} = 25 mV.

TABLE 5

Calculated values of σ/m (μM) for s.w.v. determination of Pb(II) at the DME (t_d = 1 s)[a]

E_s (mV)	σ/m (μM) for f = 32—800 Hz						
	32	80	150	250	450	650	800
1	—	—	0.03	0.03	0.03	0.07	0.2
2	—	0.07	0.03	0.07	0.03	0.07	0.2
5	0.2	0.1	0.07	0.07	0.03	0.1	0.1
10	0.2	0.1	0.1	0.07	0.1	0.1	0.1
20	0.4	0.3	0.07	0.07	0.2	0.1	0.2

[a] E_{sw} = 25 mV. σ = standard deviation of background current measured in supporting electrolyte alone; m = slope of calibration graph (see Table 3).

It should be emphasized that the experimental design used here, chosen to permit wide systematic parametric variation with the same conditions for the DME, does not provide optimum performance. At f = 450 Hz, E_s = 5 mV, E_{sw} = 25 mV, detection limits, estimated as $3\sigma/m$, are ca. 0.1 μM. This value could be improved substantially by using longer delay times and slower flow rates [3] and by optimizing the procedure for subtracting the background current [8].

Comparison of instrumental systems. The next experiments were done in order to compare the current sensitivities offered by the different current-measurement techniques and instrumental systems (i.e., the computer-controlled voltammetric instrument and the PARC 384B). Experiments were done on the same solutions and calibration graphs for Pb(II) were obtained by measuring i_p for four different concentrations at each frequency. The frequency range 1—120 Hz, which corresponds to the frequency limits of the 384B, was examined. The slopes of these calibration plots (i.e., the sensitivity in nA μM^{-1}) are plotted in Fig. 2 as a function of $t_m^{-1/2}$.

The theoretical sensitivity of square-wave voltammetry is defined as $nFA(Df)^{1/2}\ \Delta\psi(2\pi)^{-1/2}$, where $\Delta\psi$ is the dimensionless difference peak-current parameter [11]. For a reversible, diffusion-controlled process under the experimental parameters used here (i.e., nE_s = 8 mV and nE_{sw} = 48 mV) $\Delta\psi$ has the value 1.271 for the i-mode [14]. Thus for n = 2, $D = 0.94 \times 10^{-5}$ cm^{-2} s^{-1} [16] and A = 0.025 cm^2, the predicted value of the slope in Fig. 2 is 7.51 nA s$^{1/2}$ μM^{-1}.

Each of the different modes of current measurement has a different t_m associated with it for a certain frequency. The relation between frequency and t_m for these three modes is: (1) i-mode, $t_m = 1/2\ f$; (2) q-mode, t_m = 5/12 f; (3) PARC 384B, $t_m = (1/2\ f - 0.75)$ ms (see operating manual for PARC 384B instrument).

Figure 2 shows that the PARC 384B produces difference peak currents which are less than those predicted by theory and which deviate somewhat from the predicted linear dependence of i_p on $t_m^{-1/2}$. These features should

not cause problems in routine use but need to be considered for intercomparison of results obtained with different equipment and in method development. (This treatment ignores the fact that the predicted dependence of i_p on t_m is not precisely an inverse square-root dependence. The difference should be negligible [11].)

Irreversible systems: nickel(II)

Nickel(II) in 0.10 M hydrochloric acid was chosen for studying an irreversible system. In this medium stock solutions are readily prepared and are stable for months. At pH as low as 1, hydrogen evolution does not interfere with the determination of Ni(II) in this medium; E_p for the Ni(II) reduction ranged from −0.627 V (1 Hz) to −0.686 V (120 Hz) vs. SCE. The polarographic behavior of Ni(II) in various aqueous supporting electrolytes has been investigated repeatedly [17–22]. Apparently the only electrochemical reduction of Ni(II) that can occur in aqueous media is $Ni^{2+} + 2e^- \rightarrow Ni$ and some mechanisms have been suggested to explain results obtained in complexing and noncomplexing media [23]. The polarographic wave for the reduction of Ni(II) in noncomplexing electrolytes is about 0.5 V more negative than that which is predicted for the reversible Ni(II)/Ni couple, which is about −0.50 V vs. SCE [16]. This can be attributed to the irreversibility of the reduction (caused by a preceding slow dehydration step) of the $Ni(H_2O)_6^{2+}$ ion. In the presence of some complexing agents such as thiocyanate, pyridine, or halides, the half-wave potential shifts to values considerably more positive than those for the reduction of the hydrated species. Under the experimental conditions used here, the Ni(II) species present in bulk solution are $Ni(OH_2)_6^{2+}$ and $NiCl(OH_2)_5^+$ [24].

The DEC PDP 8/e system was used to examine the individual forward and reverse currents in s.w.v. (Fig. 3). The absence of any anodic reverse currents indicates that the reaction is totally irreversible within the time scales for these experiments. This irreversibility can be attributed to the very low solubility of nickel in mercury [22]. Difference current voltammograms in the range of frequencies from 5 to 120 Hz are shown in Fig. 4 (without background subtraction). It can be seen that E_p shifts to more negative values and the width at half height increases as the time scale of the experiment is decreased. The peak potential depends linearly on log f. The slope of $\partial E_p / \partial \log f = -29.7$ mV is that predicted for a totally irreversible electrode reaction with $n = 2$ [15].

Voltammograms for three different concentrations were collected at eleven different square-wave frequencies with the SMDE. Other experimental parameters were $E_s = 4$ mV, $E_{sw} = 24$ mV and $t_d = 1$ s. The peak currents obtained were used to generate calibration curves for the frequencies examined. A tangent baseline correction was used in measuring i_p, because the current at negative potentials was not zero after subtraction of the background current. The linear working range extended up to 7.0×10^{-4} M. For a square-wave frequency of 75 Hz ($E_s = 4$ mV, $E_{sw} = 24$ mV) the sensitivity was 12.8 nA μM^{-1}. The comparable measured value for Pb(II) was 73.3 nA μM^{-1}, or a ratio

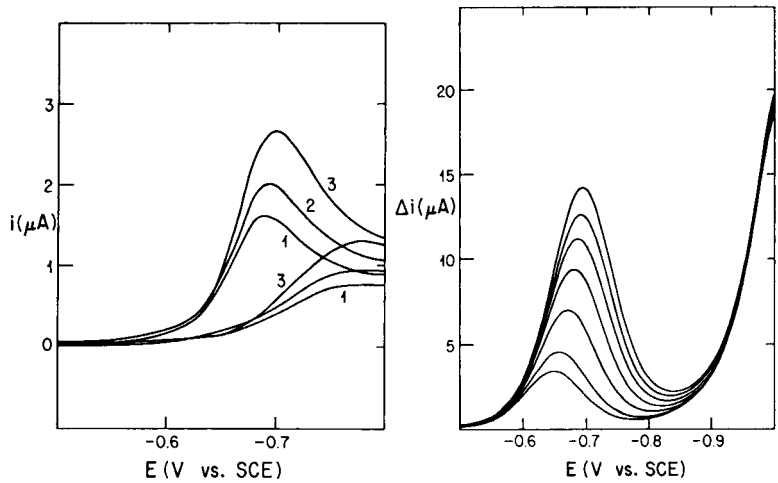

Fig. 3. Forward and reverse current voltammograms for 0.073 mM Ni(II) in 0.10 M HCl. DME with t_d = 1 s; E_s = 5 mV; E_{sw} = 25 mV; computer-based system; the currents were normalized to a 1-s drop area. Frequency (Hz): (1) 30; (2) 50; (3) 100.

Fig. 4. Square-wave voltammograms for 0.92 mM Ni(II) in 0.10 M HCl. SMDE with t_d = 1 s; E_s = 4 mV; E_{sw} = 24 mV. Frequency in order of increasing current: 5, 10, 25, 50, 75, 100, 120 Hz.

of 0.17. For this two-electron reduction, the first step is slow, so the apparent number of electrons (n_a) is unity, and for αn_a = 0.50 the predicted ratio is about 0.2 [15]. Any advantage gained in current sensitivity at higher frequency is offset by the sloping baseline caused by hydrogen reduction (due to uncatalysed reduction).

Conclusions

Square-wave voltammetry at the DME works well for analytical purposes. The normalization of current response to unit time is accurate within a few percent even under demanding conditions and therefore is a useful procedure for obtaining results normalized to constant drop area. Normalized results for both reversible and irreversible systems agree with theory for a stationary electrode. Under the optimal conditions (E_s = 5 mV, f = 450 Hz) for a model reversible system, the effective scan rate is 2.25 V s^{-1}, so that an entire range can be scanned in less than 1 s. Operation at longer delay times (e.g., 6 s) would increase sensitivity by about 3-fold and decrease the background capacity current caused by drop growth, which is proportional to $t^{-1/3}$. Practical instrumental implementations cause a dependence of current on frequency; this deviates slightly from theoretical predictions, but does not present problems for quantitative applications. The reduction of Ni(II), an irreversible reaction, behaves as expected theoretically and yields peak currents suitable for quantitative purposes.

This work was supported by the loan of equipment from EG&G PARC and by financial support by the National Science Foundation under grant no. CHE-8305748.

REFERENCES

1 J. Osteryoung and R. A. Osteryoung, Anal. Chem., 57 (1985) 101A.
2 S. Borman, Anal. Chem., 54 (1982) 698A.
3 Z. Stojek and J. Osteryoung, Anal. Chem., 53 (1981) 847.
4 M. Shah and J. G. Osteryoung, Anal. Chem., 54 (1982) 586.
5 A. Webber, M. Shah and J. G. Osteryoung, Anal. Chim. Acta, 157 (1984) 1.
6 A. Webber, M. Shah and J. G. Osteryoung, Anal. Chim. Acta, 154 (1983) 105.
7 A. Webber and J. G. Osteryoung, Anal. Chim. Acta, 157 (1984) 17.
8 M. Wojciechowski, W. Go and J. Osteryoung, Anal. Chem., 57 (1985) 155.
9 C. Wechter, N. Sleszynski, J. J. O'Dea and J. Osteryoung, Anal. Chim. Acta, 175 (1985) 45.
10 J. A. Turner, J. H. Christie, M. Vukovic and R. A. Osteryoung, Anal. Chem., 49 (1977) 1904.
11 J. H. Christie, J. A. Turner and R. A. Osteryoung, Anal. Chem., 49 (1977) 1899.
12 T. R. Brumleve, J. J. O'Dea, J. G. Osteryoung and R. A. Osteryoung, Anal. Chem., 53 (1981) 702.
13 H. Keller and R. A. Osteryoung, Anal. Chem., 43 (1971) 342.
14 E. J. Zachowski, M. A. Dissertation, SUNY at Buffalo, September, 1984.
15 J. J. O'Dea, J. G. Osteryoung and R. A. Osteryoung, Anal. Chem., 53 (1981) 695.
16 I. M. Kolthoff and J. J. Lingane, Polarography, Interscience, New York, 1941.
17 G. F. Reynolds, H. I. Shalgosky and T. J. Webber, Anal. Chim. Acta, 8 (1953) 564.
18 R. H. Jones, Analyst (London), 71 (1946) 60.
19 J. J. Lingane, Ind. Eng. Chem., Anal. Ed., 18 (1946) 7.
20 I. M. Kolthoff and G. Matsuyama, Ind. Eng. Chem., Anal. Ed., 17 (1945) 10.
21 J. J. Lingane and H. Kerlinger, Ind. Eng. Chem., Anal. Ed., 13 (1941) 2.
22 A. Baranski and Z. Galus, J. Electroanal. Chem., 46 (1973) 289.
23 A. J. Bard, Encyclopedia of the Electrochemistry of the Elements, M. Dekker, New York, 1976.
24 R. H. Herber and J. W. Irvine, Jr., J. Am. Chem. Soc., 78 (1956) 905.

Analytica Chimica Acta, 183 (1986) 59—66
Elsevier Science Publishers B.V., Amsterdam — Printed in The Netherlands

GLUCOSE ENZYME ELECTRODE WITH EXTENDED LINEARITY
Application to Undiluted Blood Measurements

WILLIAM H. MULLEN*, FIONA H. KEEDY and STEPHEN J. CHURCHOUSE

Department of Physical Chemistry, The University, Newcastle upon Tyne NE1 7RU (Great Britain)

PANKAJ M. VADGAMA

Department of Clinical Biochemistry and Metabolic Medicine, The Medical School, Framlington Place, Newcastle upon Tyne, NE2 4HH (Great Britain)

(Received 18th September 1985)

SUMMARY

An enzyme electrode is described for glucose determination in unstirred, undiluted whole blood. The system comprises an H_2O_2-detecting electrode upon which is placed a membrane laminate incorporating glucose oxidase. The external membrane was pretreated with methyltrichlorosilane. The electrode response was linearly dependent on glucose concentration up to 50 mmol l^{-1} glucose, it had a decreased dependence on dissolved oxygen concentrations and gave response times of 30—90 s. Whole blood glucose measurements correlated well with a routine spectrophotometric method.

The high demand for blood glucose measurements in routine clinical laboratories has given rise to a variety of analytical systems for large batches. Although the enzymatic methods used offer high accuracy and precision, the need for sample dilution, separation of red cells and temperature control inevitably makes for cumbersome instrumentation. For simplified home glucose monitoring in diabetic patients, reagent-impregnated strips are available. These enable measurement on drops of whole, undiluted blood and give a colour reaction which may be read by eye or with a reflectometer. Accurate timing of the reaction is essential, and during routine monitoring such reagent strips have often shown a poor correlation with standard assays [1, 2].

The linear ranges of enzymatic methods are normally limited by the Michaelis constant of the enzyme (K_m), and sample dilution is usually necessary for clinical assays. This applies to enzyme electrode techniques [3] as well as to more conventional spectrometric methods. Measurement of undiluted samples would simplify instrumentation and eliminate any volume errors caused by the presence of cellular elements in blood. The needle-type enzyme electrode, devised by Shichiri et al. [4] for in vivo glucose monitoring, achieves this requirement. The device includes an outer polyurethane membrane with low permeability to restrict diffusion of glucose to the underlying glucose oxidase layer. A linear range of up to 28 mmol l^{-1} glucose is

0003-2670/86/$03.50

obtained and direct, invasive monitoring of diabetics is possible. Attempts have been made to extend the range of more conventional glucose enzyme electrodes by the use of external nylon [5] and porous PTFE [6] membranes to restrict diffusion; however, in the former case linearity was achieved only up to 15 mmol l^{-1}, whilst for the latter a sigmoidal response was obtained over the range 0—40 mmol l^{-1}. Whereas the above electrodes used either oxygen or hydrogen peroxide detection to measure the enzymatic reaction, an alternative has been to use ferrocene as an electron mediator between glucose oxidase and the working electrode [7]; this approach has given linearity up to 30 mmol l^{-1} glucose.

This paper describes the application of the concept of diffusional limitation to the design of a reagentless glucose enzyme electrode suitable for bedside and home glucose monitoring [8]. In addition to the ability to measure undiluted samples, the major aims were pH- and temperature-independence and a stable output in unstirred solutions. To this end, enzyme layers covered with organosilane-treated membranes were used.

EXPERIMENTAL

Apparatus and reagents

A Rank oxygen electrode system (Rank Brothers, Bottisham, Cambridge) was used. The electrode was polarized at +650 mV for hydrogen peroxide detection, the meter was linked to a chart recorder. The electrode comprised a central 2-mm diameter platinum working electrode with an outer 12-mm diameter silver ring as the reference (Fig. 1). A similar electrode polarized at

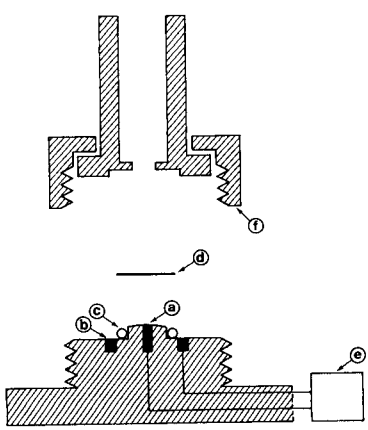

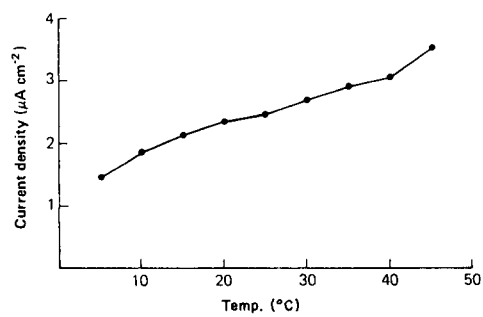

Fig. 1. Diagram of the Rank system: (a) platinum working electrode; (b) Ag/AgCl reference electrode; (c) sealing "O" ring; (d) membrane laminate; (e) meter; (f) screw-fit top with sample chamber.

Fig. 2. Effect of temperature on electrode response to 10 mmol l^{-1} glucose.

−650 mV was used for oxygen measurements, with 1 mol l^{-1} potassium chloride as the electrolyte and a PTFE covering membrane.

Glucose oxidase (EC 1.1.3.4, from *Aspergillus niger*; 210 IU mg^{-1} protein) was obtained from Boehringer Mannheim. Dimethyldichlorosilane, methyltrichlorosilane, methyldichlorosilane, 3-aminopropyltriethoxysilane, cellulose acetate and glutaraldehyde (aqueous 25% solution) were obtained from Aldrich Chemical Co., and phenyltrichlorosilane and 1,1,1-trichloroethane (AristaR) from BDH Chemicals. Polycarbonate membranes (0.05-μm pore) were supplied by Nuclepore, Pleasanton, California. Bovine serum albumin (fraction V) was from Sigma Chemical Co.

Preparation of membranes

Silanization of polycarbonate membranes. Membranes were treated with 3-aminopropyltriethoxysilane as previously described [9], using an aqueous 10% solution of the reagent. For organochlorosilane application, solutions in 1,1,1-trichloroethane were freshly prepared. For treatment with methyltrichlorosilane or phenyltrichlorosilane, a 2 × 4-cm polycarbonate membrane was immersed for 30 s in the appropriate solution (2—5% v/v) and then immediately transferred to a glass slide. A second slide was placed over the membrane and light pressure applied to remove any trapped air bubbles. The two slides were separated, allowing the film of solution on the membrane to evaporate. Dimethyldichlorosilane and methyldichlorosilane solutions (2% v/v) were applied dropwise to similar membranes placed on glass slides and the solvent was allowed to evaporate; this procedure was repeated as required to achieve the desired linear calibration range. Before use, the silane-treated membranes were rinsed for 1 min under a jet of distilled water and allowed to dry at room temperature.

Preparation of cellulose acetate membranes. A 5 × 5-cm glass plate was treated with dimethyldichlorosilane (2% v/v in 1,1,1-trichloroethane) to provide a hydrophobic surface; 1.2 ml of cellulose acetate solution (1.2% w/v in acetone) was applied evenly to the plate and allowed to evaporate. Care was taken to ensure that evaporation was uniform. The resulting membrane was left to dry in air for at least 1 h before use. This method of fabrication is a simplified version of that used by Tsuchida and Yoda [10] to obtain asymmetric permselective membranes for screening out electroactive organic species in solution.

Preparation of enzymatically active membranes

A solution (10 μl) containing 30 mg ml^{-1} glucose oxidase and 200 mg ml^{-1} serum albumin was mixed with an aqueous 5% (w/v) solution of glutaraldehyde (5 μl), to cross-link the enzyme chemically. The mixture was left to become viscous before applying it to one side of a silane-treated polycarbonate membrane. The membrane was pressed between two silanized (hydrophobic) glass slides in a vice for 5 min. The slides were then prised apart and the membrane left in air to dry for at least 5 min prior to use.

Procedure for glucose determination

An isotonic buffer containing 52.8 mmol l^{-1} Na_2HPO_4, 15.6 mmol l^{-1} NaH_2PO_4, 5.1 mmol l^{-1} NaCl and 0.15 mmol l^{-1} EDTA (pH 7.4) was used for aqueous samples. The surface of the Rank hydrogen peroxide sensor was moistened with buffer to allow electrical contact between working and reference electrodes. A 1-cm^2 piece of cellulose acetate membrane was held against the enzyme-covered side of a similar-sized piece of silanized polycarbonate membrane. This laminate was positioned over the electrode with the cellulose acetate membrane towards the electrode surface, and was held in position by the screw-fit top of the electrode body (Fig. 1). Measurements were made on 0.5-ml samples added dropwise onto the membrane laminate.

Whole blood samples, stored in fluoride/oxalate tubes, were obtained from a routine clinical laboratory. A calibration check, with 10 mmol l^{-1} glucose, was made prior to each blood analysis.

RESULTS

Membrane silanization

The linear range of the enzyme electrode increased with increasing membrane exposure to the organochlorosilane, up to the limits shown in Table 1. Only the organochlorosilanes were found to affect the response to glucose. The response time following organotrichlorosilane treatment was unrelated to the calibration linearity obtained, whereas use of organodichlorosilanes gave an increasing response time with increasing linearity. Thus with dimethyldichlorosilane, linearity up to 20 mmol l^{-1} was associated with a response time of 1—2 min, whereas membranes giving responses linear up to 50 mmol l^{-1} gave response times of 3–5 min. For membranes with linear calibration ranges between 15 and 80 mmol l^{-1}, the sensitivity to glucose was inversely proportional to the linearity. For blood glucose analysis, an optimized system with 2% methyltrichlorosilane was used; this gave membranes with linearity up to 50 mmol l^{-1} glucose, response times (to 98% of final reading) of 30—90 s and resolution to ±0.05 mmol l^{-1} glucose.

TABLE 1

Effect of organosilane treatment on glucose enzyme electrode response

Reagent	Maximum linear range achieved (mmol l^{-1})	Response time[a]
None	5	12—30 s
Methyltrichlorosilane	500	30—90 s
Phenyltrichlorosilane	500	30—90 s
Methyldichlorosilane	50	2–5 min
Dimethyldichlorosilane	70	2–5 min
3-Aminopropyltriethoxysilane	5	12—30 s

[a]Time to reach 98% of maximum response.

The effect of interposing a cellulose acetate membrane between the enzyme layer and the electrode surface is shown in Table 2. Interference from electroactive species found in blood on the response to a 1 mmol l^{-1} glucose standard was substantially decreased, so that they had little effect on the glucose signal.

Dependence on variables

With a methyltrichlorosilane-treated outer membrane, the electrochemical signal in quiescent blood or a 10 mmol l^{-1} glucose solution reached a plateau within 2 min, and was stable thereafter for at least 1 h. Variation in sample volume between 20 μl and 4 ml had no effect. Changing between unstirred and stirred conditions had no effect on the magnitude or time of response, nor on the stability of the signal.

Response to 5 mmol l^{-1} glucose solution varied by less than 10% over the pH range 6—8. The sensitivity to temperature was $<2\%\ ^{\circ}C^{-1}$ between 15 and 30° C (Fig.2), allowing the use of an unthermostatted electrode. The dissolved oxygen concentration did not significantly affect the magnitude or linear range of the response above a partial pressure of 30 mm Hg; linearity was decreased to 28 mmol l^{-1} at 20 mm Hg (Fig. 3).

Stability and use

Initial exposure of the membranes to blood had no detectable effect on the response to a 10 mmol l^{-1} glucose standard. However, after 5—10 measurements there was a small increase in the size of response, with an associated decrease in the linear range. This occurred on exposure to either blood or standards and was minimised by decreasing any mechanical disturbance of the membranes. Membrane stability was checked between samples by using an aqueous 10 mmol l^{-1} glucose standard. After 15 samples, the response had increased by 15—30% with a reduction in the upper linear limit from 50 to 35 mmol l^{-1} glucose.

There was no effect on sensitivity or dynamic response on storing membrane laminates at 4° C for 1 month.

TABLE 2

Effects of interfering species on the response to a 1.0 mmol l^{-1} glucose standard with and without cellulose acetate membrane

Species added	Amount (mmol l^{-1})	Response (μA cm^{-2})	
		Without membrane	With membrane
None	—	9.0	8.3
Ascorbic acid	0.2	14.5	9.1
Cysteine	0.1	9.9	8.3
Glutathione	1.0	11.5	8.3
Uric acid	0.5	26.0	8.4
All of the above	1.8	33.0	9.3

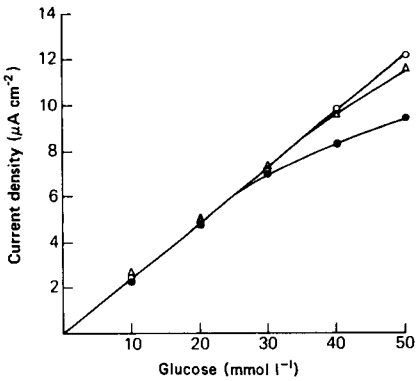

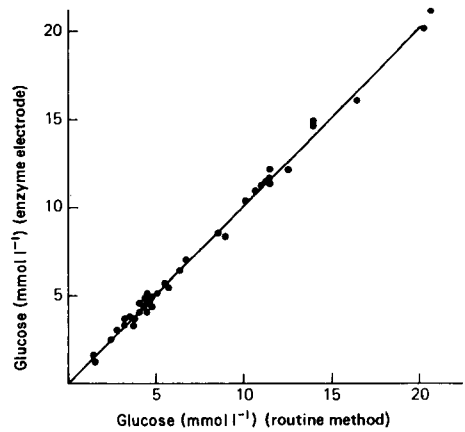

Fig. 3. Effect of oxygen partial pressure in sample on enzyme electrode calibration: (○) 30 mm Hg/160 mm Hg; (△) 25 mm Hg; (●) 20 mm Hg.

Fig. 4. Correlation between results for whole blood by the enzyme electrode and routine spectrophotometric assays.

Correlation of the results of glucose measurements on whole blood samples (y) with the results from a routine spectrophotometric method based on glucose oxidase [11] (x), gave a linear regression of $y = 1.002x + 0.24$ ($r = 0.998$, $n = 44$, Fig. 4).

DISCUSSION

Electrochemical techniques have an important advantage over spectrophotometric methods for clinical analysis in that they permit direct measurement in turbid biological fluids. Most notably this allows measurements in whole blood without prior separation of plasma or serum. This is exemplified by the widely-used YSI glucose electrode (Yellow Springs Instruments Co., Ohio), although the restricted linear range of this device necessitates sample dilution.

Enzyme electrode response may be limited by the rate of enzyme reaction or by the rate of substrate diffusion to the enzyme [3, 12]. In a diffusion-controlled system there is a decreased substrate concentration within the enzyme layer; this leads to diminished sensitivity and frequently an increase in the apparent K_m [13]. For a two-substrate enzyme such as glucose oxidase the apparent K_m for glucose is also affected by the concentration of co-substrate (oxygen), which if rate-limiting will tend to decrease the linear response range for glucose. Such factors may explain the variations in linearity found between different designs of glucose enzyme electrode [14, 15]. Theoretical treatments of diffusional effects on two-substrate enzyme reactions have been given [12, 16], and these emphasize the importance of the concentration of the co-substrate.

In the present system, exposure of the porous polycarbonate membrane to an organosilane monomer such as methyltrichlorosilane, in the presence of atmospheric water vapour, has the effect of decreasing membrane permeability, by the in situ formation of a silicone polymer:

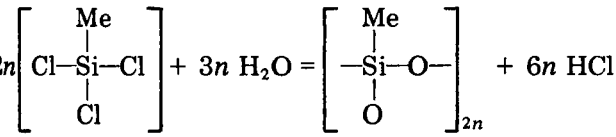

This diminishes glucose diffusion through the membrane, producing a smaller glucose signal and an increased apparent K_m. That membrane diffusion is the rate-limiting process is indicated by the independence of response from external stirring effects. Furthermore, the smaller signal of the diffusion-limited system implies the existence of a catalytic reserve in the enzyme layer. This may account for the relative insensitivity of the system to pH variation, compared to other glucose electrodes which show significant pH dependence over the pH range 5—8 [10]. Of undoubted importance to the extension of linearity is the maintenance of relatively free diffusion of oxygen through the silane-treated membrane; while glucose diffusion is markedly decreased, the effect on oxygen diffusion following silanization is minimised by the high oxygen permeability of silicone rubber [17]. A possible additional factor is the regeneration of oxygen at the platinum working electrode by electrochemical oxidation of hydrogen peroxide: $H_2O_2 = O_2 + 2H^+ + 2e^-$. This would tend further to minimise oxygen depletion, and may be an advantage of using a hydrogen peroxide-based system rather than one requiring oxygen detection.

A further possible consequence of silane treatment is the improved blood compatibility of the resulting membranes. Organosilanes are widely used to improve the blood compatibility of glass, and silicone rubber has been used for the manufacture of prostheses such as replacement heart valves [18].

The methodology described here is likely to be readily translated to other hydrogen peroxide-producing oxidases to give a family of dilution-free analytical systems. The final system would appear to be suitable for bedside measurements, and with pre-calibrated, replaceable membranes would furnish single-use devices for home glucose monitoring.

The authors acknowledge financial support from the SERC and Imperial Chemical Industries plc.

REFERENCES

1 G. Petranyi, M. Petranyi, I. N. Scobie, P. H. Sonksen, R. Crane, J. Roberts and I. S. Menzies, Br. Med. J., 288 (1984) 757.
2 R. K. Bernstein, Diabetes Care, 8 (1985) 101.

3 P. W. Carr and L. D. Bowers, Immobilized Enzymes in Analytical and Clinical Chemistry, Academic Press, New York, 1980.
4 M. Shichiri, R. Kawamori, Y. Goriya, Y. Yamasaki, M. Nomura, N. Hakui and H. Abe, Diabetologia, 24 (1983) 179.
5 S. J. Updike, M. Shults and B. Ekman, Diabetes Care, 5 (1982) 207.
6 Kureha, Kagaku, Kogyo (Assignees), UK Patent Application GB 2124545A, 1984.
7 A. E. G. Cass, G. Davis, G. D. Francis, H. A. O. Hill, W. J. Aston, I. J. Higgins, E. V. Plotkin, L. D. L. Scott and A. P. F. Turner, Anal. Chem., 56 (1984) 667.
8 P. M. Vadgama, U.K. Pending Pat. Appl. 8514176, 1985.
9 H. H. Weetall, Methods Enzymol., 44 (1976) 134.
10 T. Tsuchida and K. Yoda, Enzyme Microbiol. Technol., 3 (1981) 326.
11 P. Trinder, Ann. Clin. Biochem., 6 (1969) 24.
12 J.-C. Engasser and P. Hisland, J. Theor. Biol., 77 (1979) 427.
13 D. A. Gough, J. K. Leypoldt and J. C. Armour, Diabetes Care, 5 (1982) 190.
14 E. Lobel and J. Rishpon, Anal. Chem., 53 (1981) 51.
15 T. Yao, Anal. Chim. Acta, 148 (1983) 27.
16 J. K. Leypoldt and D. A. Gough, Anal. Chem., 56 (1984) 2896.
17 W. J. Roff and J. R. Scott, Fibres, Films, Plastics and Rubbers, Butterworths, London, 1971, p. 463.
18 J. W. Boretos, Concise Guide to Biomedical Polymers, Charles C. Thomas, Springfield, IL, 1973, p. 11.

Analytica Chimica Acta, 183 (1986) 67—74
Elsevier Science Publishers B.V., Amsterdam — Printed in The Netherlands

UTILISATION D'UN "BLANC INTERFERENCES" DANS LA DETERMINATION DES NITRATES PAR POTENTIOMETRIE SELECTIVE

B. BERLIOZ et J. J. VALLON*

Laboratoire Pharmaceutique de Biochimie, Toxicologie et Analyse des Traces, Hôpital Edouard Herriot, et Laboratoire de Chimie Analytique III et Bromatologie, Faculté de Pharmacie, 8 Avenue Rockefeller, Lyon (France)

(Reçu le 29 Juillet 1985)

SUMMARY

(*Use of an interference blank in the determination of nitrate by ion-selective potentiometry.*) During selective potentiometry of nitrate in meat product additives, a new interference originating from polyphosphate ions was encountered. The selectivity coefficients measured were 5×10^{-2} for tripolyphosphate, 10^{-2} for chloride, 8×10^{-4} for pentapolyphosphate and 6×10^{-4} for pyrophosphate. An "interference blank" technique is proposed; nitrate is destroyed in the medium to be studied, so that calibration is possible in the presence of interfering substances regardless of their identity or concentration. The method is successfully applied to monitoring of meat product additives.

RESUME

Au cours de la potentiométrie sélective des nitrates appliquée aux mélanges d'additifs pour charcuterie, une nouvelle interférence a été constantée: celle des polyphosphates. Son étude et celle des chlorure et nitrite a conduit à mesurer les coefficients potentiométriques de sélectivité de l'électrode à nitrate. Une technique dite "blanc interférences" a été mise au point: elle permet, par destruction des nitrates dans le milieu à étudier, d'effectuer un étalonnage en présence de toute substance interférente même de nature et de concentration inconnues. Elle a été appliquée avec succès au contrôle des additifs pour charcuterie.

Le dosage des nitrates dans les produits alimentaires et en particulier dans les mélanges d'additifs pour charcuterie est un problème analytique encore mal résolu. Les méthodes disponibles, chimiques ou physicochimiques, sont nombreuses: colorimétrie directe [1, 2] ou après réduction en nitrite sur colonne de cadmium [3, 4], spectrophotométrie dans l'U.V. [5] et polarographie [6, 7]. Toutes ces méthodes souffrent d'un manque de fiabilité dû à des interférences diverses, en particulier dans les milieux complexes.

La recherche d'une méthode simple et rapide de dosage des nitrates nous a orienté vers la potentiométrie par électrode à membrane sélective. La technique a déjà fait l'objet de nombreux travaux pour le dosage des nitrates dans le sol [8, 9], les extraits végétaux [9, 10, 11], les eaux [9, 12], certains aliments [13], etc. Pour éliminer l'interférence des chlorures, nous utilisons

0003-2670/86/$03.50

l'addition de sulfate d'argent solide avec surveillance de la concentration des chlorures grâce à l'électrode Ag/AgCl [9, 10, 13].

L'étude des interférences rencontrées avec la potentiométrie sélective des nitrates dans les mélanges d'additifs pour charcuterie nous a permis de mettre en évidence celle des polyphosphates, constamment présents dans ces mélanges. Nous avons également étudié l'interférence des chlorures et des nitrites en mesurant les coefficients potentiométriques de sélectivité.

La deuxième étape du travail a consisté à éliminer ces interférences par divers procédés: les chlorures sont facilement précipités par l'oxyde d'argent solide; pour les polyphosphates, des tentatives d'hydrolyse acide ou alcaline ou de neutralisation par complexation des ions Ca^{2+} se sont révélées infructueuses. Ces échecs nous ont conduits à constituer un "blanc interférences", dans lequel les nitrates ont été sélectivement détruits, et qui sert de milieu de dilution pour établir une droite étalon de nitrate.

PARTIE EXPERIMENTALE

Matériel et réactifs

La mesure des potentiels ou du pH est faite à l'aide d'un potentiomètre pH-mètre Tacussel ISIS 20 000. L'électrode de référence utilisée est une électrode Tacussel type C4, au calomel à KCl saturé avec allonge de protection contenant le tampon de force ionique.

L'électrode sélective aux nitrates est une électrode Tacussel, type PNO_3-1. Nous avons utilisé une électrode de verre Tacussel, type TB-10, pour la mesure du pH; une électrode d'argent Tacussel, type Ag-3 a été utilisée pour suivre la concentration de chlorure.

Les réactifs utilisés sont tous de qualité analytique (Prolabo, Normapur); l'étalonnage est réalisé à l'aide de nitrate de sodium; l'ajustement du pH est fait par de l'acide acétique. Pour l'étude des interférences, nous avons recours à du nitrite de sodium, du chlorure de potassium, du pyrophosphate de sodium, et du pentapolyphosphate de sodium. Pour précipter les chlorures, nous avons utilisé de l'oxyde d'argent solide.

L'acétate de potassium, le sulfate d'aluminium et l'acide sulfamique entrent dans la constitution du tampon de force ionique. Nous avons utilisé du sulfate de cadmium et des baguettes de zinc pour la préparation du cadmium métal.

Etude des interférences

Nous avons déterminé les coefficients de sélectivité de la membrane pour les nitrates en présence d'acétate, de chlorure, de nitrite, de pyrophosphate, de tripolyphosphate et de pentapolyphosphate. Pour cela, nous avons tracé les variations de potentiel de la membrane en fonction de concentrations croissantes en nitrate (10^{-5}—10^{-2} M) en présence de différents ions interférents: acétate 10^{-2} et 10^{-1} M; chlorure 10^{-2} et 10^{-1} M dans l'acétate de potassium 10^{-2} M; nitrate 10^{-3}, 10^{-2} et 10^{-1} M dans l'acétate de potassium

10^{-2} M; pyrophosphate 10^{-2}, 10^{-1} et 1 M dans l'acétate de potassium 10^{-2} M; tripolyphosphate 10^{-3}, 10^{-2} et 10^{-1} M dans l'acétate de potassium 10^{-2} M; et pentapolyphosphate 10^{-2}, 10^{-1} et 1 M dans l'acétate de potassium 10^{-2} M. Les courbes sont tracées sur papier semi-logarithmique. Le pH des solutions est ajusté à 5,5 avant les mesures, à l'aide d'acide acétique.

La Fig. 1 donne un exemple des courbes en présence de chlorure. La présence d'ions interférents (chlorure, nitrite, tripolyphosphate, etc. . . .) diminue le domaine de réponse nernstienne de la membrane.

Elimination contrôlée des chlorures. L'élimination des chlorures préalablement au dosage des nitrates est indispensable pour les mélanges d'additifs contenant du chlorure de sodium.

Nous avons précipité les chlorures par l'oxyde d'argent solide. La variation de concentration en chlorure est suivie grâce à une électrode d'argent. Un saut de potentiel d'environ 300 mV signale le point final de la précipitation. Le dosage des nitrates est ensuite effectué après la filtration du chlorure d'argent et ajustement du pH à 5,5 au pH-mètre. La Fig. 2 montre l'influence de concentrations croissantes en chlorures sur la concentration apparente, $[NO_3^-]_{app}$, en nitrates avant et après action de Ag_2O. Les chlorures entraînent une erreur par excès sur la concentration en nitrates. L'oxyde d'argent supprime cette interférence.

Mise au point de la méthode du "blanc interférences"

Le principe est d'éliminer les nitrates d'une solution inconnue contenant des nitrates et des polyphosphates. Le milieu ainsi obtenu ("blanc interférences") sert alors de milieu de dilution pour la fabrication d'une gamme étalon de nitrate. L'élimination des nitrates est réalisée en deux étapes: (1) réduction en nitrite par addition de cadmium fraîchement préparé jusqu'à stabilisation du potentiel de l'électrode à nitrate; et (2) destruction des

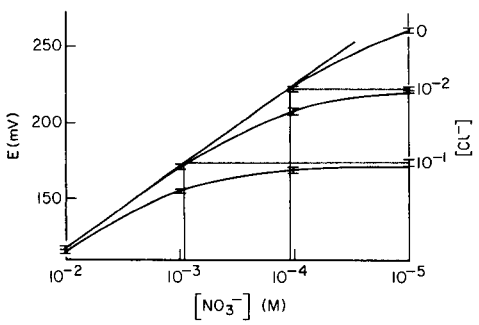

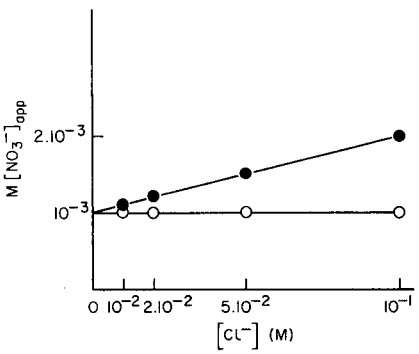

Fig. 1. Interférence des chlorures; détermination de $K^{pot}_{NO_3^-,Cl^-}$.

Fig. 2. Suppression de l'Interférence des chlorures par addition de Ag_2O: (•) avant Ag_2O; (○) après Ag_2O. Concentration initiale de nitrate, 10^{-3} M. Concentrations de nitrate mesurées, $[NO^{-3}]_{app}$.

nitrites par l'acide sulfamique ajouté dans un tampon de pH et de force ionique et agitation 15 min.

Le tampon de force ionique et de pH, utilisé lors de la deuxième étape, contient du sulfate d'aluminium 0,0132 M et de l'acide sulfamique 0,02 M; il tamponne les solutions finales à pH $\approx$ 3,4.

Les concentrations des étalons sont choisies de manière à encadrer étroitement x, la réponse de l'électrode risquant de ne pas être Nernstienne (linéaire) en cas de forte interférence.

Méthode proposée

Préparation de l'étalon 1 de nitrate (Et_1). A 40 ml d'une solution A de concentration en nitrate inconnue, on ajoute 2—3 g de cadmium métallique après ajustement du pH à 5,5; la solution est agitée (agitateur magnétique): la réduction des nitrates en nitrites donne la solution B.

A 10 ml de cette solution B, sont ajoutés 10 ml de tampon (sulfate d'aluminium 0,0132 M/acide sulfamique 0,02 M) pour la destruction du nitrite et 1 ml d'une solution de nitrate de concentration connue. Le mélange est agité (agitateur magnétique).

Préparation de l'étalon 2 de nitrate (Et_2). A 10 ml de solution B sont ajoutés 10 ml de tampon et 1 ml d'une solution de nitrate de concentration connue.

Préparation de l'essai (x). A 10 ml de la solution A sont ajoutés 10 ml du tampon et 1 ml d'eau distillée; il s'agit de la solution x de concentration en nitrate inconnue.

Mesure des potentiels et résultats. Les potentiels de Et_1, Et_2 et x sont mesurés: une courbe d'étalonnage, à partir des potentiels de Et_1 et Et_2, permet de déduire la concentration en nitrates de la solution A par mesure du potentiel de x.

RESULTATS

Coefficients potentiométriques de sélectivité

La réponse de l'électrode en présence d'un anion interférent i de concentration C_i et de valence n, et d'acétate de potassium 10^{-2} M (utilisé comme tampon de force ionique) s'écrit:

$$E = E_0 - S \log [[NO_3^-] + (K^{pot}_{NO_3^-,i}[C_i]^{1/n}) + (K^{pot}_{NO_3^-,CH_3COO^-} \times 10^{-2})]$$

où E désigne le potentiel mesuré (en V), E_0 le potentiel "standard" (V), S la pente (V) et où $K^{pot}_{NO_3^-,i}$ et $K^{pot}_{NO_3^-,CH_3COO^-}$ représentent respectivement les coefficients de sélectivité de la membrane vis à vis du nitrate en présence d'un anion interférent i ou d'acétate.

Dans le Tableau 1, sont rassemblés les coefficients de sélectivité trouvés à pH 5,5. Les coefficients de sélectivité, pour les polyphosphates, varient selon le pH. A pH 3,5, K pour le tripolyphosphate est sensiblement égal à 10^{-2}. A pH 5,5, le tripolyphosphate se comporte comme un ion monovalent, tandis

TABLEAU 1

Coefficients de sélectivité

i	NO_2^-	TPP[a]	Cl^-	CH_3COO^-	Penta-P[b]	PP[c]
$K^{pot}_{NO_3^-,i}$	$1,5 \cdot 10^{-1}$	$5 \cdot 10^{-2}$	10^{-2}	$1,2 \cdot 10^{-3}$	$8 \cdot 10^{-4}$	$6 \cdot 10^{-4}$

[a]Tripolyphosphate. [b]Pentapolyphosphate. [c]Pyrophosphate.

que le pentapolyphosphate et le pyrophosphate se comportent comme des ions divalents. Ainsi, ces derniers interfèrent plus que l'acétate; les interférences peuvent être classées selon l'ordre décroissant: $NO_3^- > NO_2^- >$ TPP > Cl^- > Penta-P ≈ PP > CH_3COO^-.

Etude de la validité de la méthode

Sensibilité. La sensibilité (pente de la droite étalon) diminue quand les concentrations en tripolyphosphate augmentent (Tableau 2). Elle a été mesurée, après étalonnage en deux points ($[Et_1] = 5 \cdot 10^{-3}$ M et $[Et_2] = 10^{-3}$ M), pour des concentrations croissantes de tripolyphosphate et après élimination préalable du nitrate à la concentration initiale unique de $2,5 \cdot 10^{-3}$ M. Compte-tenu de l'incertitude sur la mesure du potentiel (±0,5 mV), l'erreur entraînée sur la détermination de la teuneur en nitrate augmente quand la pente diminue c'est-à-dire quand le tripolyphosphate augmente.

Limite de détection. Nous l'avons calculée de façon théorique à partir de l'incertitude et de l'équation de la réponse en solution pure, $E = E_0 - \log([NO_3^-] + 1,2 \cdot 10^{-3}[CH_3COO^-])$. Elle est égale à $5 \cdot 10^{-6}$ M quand $[CH_3COO^-] = 10^{-2}$ M (force ionique μ = 0,01 M), et $5 \cdot 10^{-5}$ M quand $[CH_3COO^-] = 10^{-1}$ M (μ = 0,1 M). A force ionique égale (10^{-2} ou 10^{-1} M), elle est moins bonne en présence d'ions interférents.

Répétabilité. Nous l'avons étudiée en appliquant la méthode à une solution contenant $10^{-3} \cdot 10^{-3}$ M nitrate et 10^{-2} M TPP, en effectuant cinq déterminations; les concentrations des étalons étant $2 \cdot 10^{-3}$ M (Et_1) et $5 \cdot 10^{-4}$ M (Et_2). La moyenne trouvée $\bar{x}$ est égale à $0,99 \cdot 10^{-3}$ M pour cinq déterminations. L'écart-type est égal à s = 0,042 et le coefficient de variation s_r = 4,2%.

Application au dosage des nitrates dans des mélanges d'additifs pour charcuterie

Dans le tableau 3 sont rassemblées les teneurs en nitrates de quelques mélanges d'additifs: teneur annoncée par le fabricant, teneur trouvée par colorimétrie (après réduction du nitrate en nitrite par passage sur colonne de cadmium) et par potentiométrie (méthode des ajouts dosés et méthode utilisant un blanc interférences).

TABLEAU 2

Influence des concentrations de TPP sur la pente de la droite d'étalonnage

TPP (M)	0	$1 \cdot 10^{-2}$	$2{,}5 \cdot 10^{-2}$	$5 \cdot 10^{-2}$	$1 \cdot 10^{-1}$
Pente (mV)	53	44	33	27	20

TABLEAU 3

Teneurs en nitrate de mélanges d'additifs mesurées par différentes méthodes

Mélange	Teneur en nitrate (%)			
	Annoncée	Colorimétrie	Potentiométrie	
			Ajouts dosés	Blanc interférences
1	0,30	0,34	0,48	0,36
2	0,30	0,28	0,39	0,30
3	0,63	0,87	1,05	0,84
4	1	1,05	1,35	1,1
5	1	0,73	0,94	0,69
6	0,83	1,1	1,2	1,15
7	3	2,3	2,6	2,5
8	0,5	0,44	0,58	0,45
9	0,63	0,57	0,65	0,55

DISCUSSION

L'étude des interférences montre que la réponse de l'électrode peut ne plus être Nernstienne en présence d'ions interférents; elle l'est d'autant moins que le rapport du nitrate aux ions parasites est plus petit. Les interférences peuvent être classées selon l'ordre décroissant: $NO_3^- > NO_2^- >$ TPP $> Cl^- >$ Penta-P $\approx$ PP $> CH_3COO^-$.

Les principales interférences rencontrées dans la détermination de la teneur en nitrate des mélanges d'additifs sont celle des chlorures, pas toujours présents, et surtout celle des polyphosphates. L'interférence du nitrite sera problématique essentiellement pour la détermination dans les produits de charcuterie. En effet, les mélanges d'additifs n'en contiennent pas.

Les corrections des interférences pourraient être calculées en introduisant les valeurs des concentrations et des coefficients de sélectivité des anions interférents dans l'équation de réponse de l'électrode. Les corrections calculées seraient ensuite appliquées à l'activité des nitrates mesurée. Pourtant l'application de cette technique n'est pas possible car les valeurs des coefficients de sélectivité dépendent de l'environnement ionique qui, le plus souvent, n'est pas connu, et surtout, le coefficient de sélectivité des polyphosphates ne peut être déterminé car il s'agit de mélanges de polyphosphates de poids moléculaires différents dont on ne connaît pas les proportions dans les

produits commerciaux. Ils contiennent essentiellement du pyrophosphate et du tripolyphosphate; le pourcentage de chaque type n'est pas connu.

Avec les chlorures, une concentration de 10^{-1} M limite la linéarité de la réponse à 10^{-2} M et un rapport de concentrations $[Cl^-]/[NO_3^-] = 100$ entraîne une erreur de 100% sur la détermination du nitrate par la technique classique des ajouts dosés. L'élimination contrôlée du chlorure par l'oxyde d'argent solide fait disparaître l'interférence.

La méthode du blanc interférences est intéressante pour plusieurs raisons: elle ne nécessite pas de connaître la composition qualitative et quantitative du milieu; elle ne nécessite donc pas de déterminer les valeurs des coefficients potentiométriques de sélectivité; et elle limite l'erreur faite sur la détermination à l'erreur due à l'incertitude sur le potentiel et ceci même lorsque la réponse n'est pas Nernstienne. Cela est intéressant car la méthode des ajouts dosés n'est pas applicable quand la réponse n'est pas linéaire.

Les étalons et la solution à doser sont amenés à une même force ionique par un tampon. Nous avons choisi le sulfate d'aluminium comme tampon car, son rapport force ionique/concentration étant de 15, il permet d'obtenir une force ionique de 0,1 M pour une concentration de 0,0066 M; d'autre part, il permet de tamponner le pH du milieu à 3,4.

Il est intéressant de travailler à pH bas car l'ionisation des polyphosphates y est faible et l'interférence qu'ils provoquent est moindre.

Pour un rapport de concentration TPP/NO_3^- de 20 (qui n'est jamais aussi élevé dans les mélanges d'additifs), l'erreur sur la détermination de nitrate par la méthode du blanc interférences est de 5%, tandis qu'elle serait de 100% avec la méthode des ajouts dosés.

L'application de la méthode au dosage du nitrate de 9 mélanges d'additifs pour charcuterie a été très concluante. Les résultats sont comparables à ceux fournis par la méthode colorimétrique (colorimétrie du nitrite après passage sur colonne de cadmium), alors que la méthode classique des ajouts dosés entraîne toujours des erreurs par excès.

Conclusion

La méthode du blanc interférences proposée pour la détermination potentiométrique du nitrate à l'aide d'une électrode sélective a l'avantage de ne pas nécessiter de connaître la composition du milieu et d'être applicable dans le cas des mélanges d'additifs pour charcuterie contenant des polyphosphates, espèce interférente difficile à éliminer.

Elle présente une spécificité et une sensibilité voisine de celle des méthodes colorimétriques habituellement utilisées. Elle devrait pouvoir s'appliquer au dosage des nitrates dans les milieux protéiques tels que les viandes de charcuterie.

Les auteurs tiennent a remercier le Professeur J. A. Berger de nous avoir aimablement procuré les échantillons d'additifs commérciaux.

BIBLIOGRAPHIE

1 A. S. Baker, J. Agric. Food Chem., 15 (1967) 802.
2 H. G. Wiseman et W. C. Jacobson, J. Agric. Food Chem., 13 (1965) 36.
3 R. De Borger et A. Jennen, Rev. Agric., 3 (1968) 453.
4 W. E. Eipeson, M. Mahadevian, R. V. Gowramma et L. V. L. Sastry, J. Food Sci. Technol., 11 (1974) 209.
5 F. A. J. Armstrong, Anal. Chem., 35 (1963) 1292.
6 D. N. Willett, H. P. Peterson et R. J. Moubry, J. Assoc. Off. Anal. Chem., 51 (1968) 658.
7 I. Montenegro, J. Cruz et L. Matias, Rev. Port. Quim., 13 (1971) 217.
8 A. R. Mack and R. B. Sanderson, Can. J. Soil. Sci., 51 (1971) 95.
9 P. J. Milham, A. S. Awad, R. E. Pavll et J. H. Bull, Analyst (London), 95 (1970) 751.
10 J. L. Paul et R. M. Carlson, J. Agric. Food Chem., 16 (1968) 766.
11 A. S. Baker et R. Smith, J. Agric. Food Chem., 17 (1969) 1284.
12 A. Hulanicki, R. Lewandowski et M. Maj, Anal. Chim. Acta, 69 (1974) 409.
13 C. Mergey et J. M. Bonnoît, Analusis, 6 (1978) 164.

Analytica Chimica Acta, 183 (1986) 75—80
Elsevier Science Publishers B.V., Amsterdam — Printed in The Netherlands

DETERMINATION OF CREATININE WITH A SENSOR BASED ON IMMOBILIZED GLUTAMATE DEHYDROGENASE AND CREATININE DEIMINASE

KUNIO KIHARA* and EIKA YASUKAWA

Central Research Laboratory, Mitsubishi Petrochemical Company Ltd., Wakaguri, Ami, Inashiki-gun, Ibaraki 300-03 (Japan)

(Received 30th September 1985)

SUMMARY

Glutamate dehydrogenase and creatinine deiminase are immobilized by adsorption on wet poly(vinyl chloride) membranes. Creatinine is determined by a sensor consisting of the two membranes placed over an ammonia-sensing electrode. Endogenous ammonia is removed as it passes through the glutamate dehydrogenase layer. Creatinine (1—50 mg dl^{-1}) is converted to ammonia in the inner creatinine deiminase layer and is detected by the ammonia electrode. The assay requires 3 min, the minimum detectable concentration is 1 mg dl^{-1} at pH 8.5, and the precision is ca. 5%. Endogenous ammonia can be tolerated up to 2×10^{-4} M.

Determination of creatinine in biological fluids is of significant value for the diagnosis of renal, muscular and thyroid functions. The chemical methods most widely used for creatinine determination are based on the reaction between creatinine and picrate, the well-known Jaffe reaction [1]. As this method is time-consuming, complicated and inselective, an enzyme sensor based on creatinine deiminase (E.C. 3.5.4.21) with an ammonia-sensing electrode [2, 3] and a biosensor based on immobilized creatinine deiminase and nitrifying bacteria with an oxygen electrode [4] have been investigated to improve analysis. However, these methods require a blank correction for endogenous ammonia and are not very sensitive.

A new hybrid enzyme sensor consisting of two immobilized-enzyme membranes and an ammonia-sensing electrode is described here for the simple, sensitive and selective determination of creatinine without interference from endogenous ammonia. The double membrane is composed of an ammonia-eliminating layer preceding the layer that reacts with creatinine; the former membrane holds immobilized glutamate dehydrogenase (GlDH) (E.C. 1.4.1.4) and the latter immobilized creatinine deiminase. Both are PVC membranes, as used for other enzymes [5—7]. Endogenous ammonia in the sample first penetrates the immobilized GlDH layer where it is enzymatically converted to non-responsive product:

$$NH_4^+ + \alpha\text{-ketoglutarate} + NADH \rightarrow \text{glutamate} + NAD^+ + H_2O$$

0003-2670/86/$03.50

Creatinine does not react in the first layer and reaches the immobilized creatinine deiminase layer where it is enzymatically converted to ammonia:

Creatinine + H_2O → *N*-methylhydantoin + NH_3

The ammonia produced is detected by the ammonia electrode.

EXPERIMENTAL

Materials

The enzymes used were glutamate dehydrogenase (GlDH) (E.C. 1.4.1.4, from Proteus sp., 30 IU mg^{-1} solid, protein content 28%; Oriental Yeast Co., Tokyo) and creatinine deiminase (E.C. 3.5.4.21, from Coryme-bacterium lilium, 38 IU mg^{-1} protein; Kyowa Hakko Kogyo Co., Tokyo). Creatinine, α-ketoglutarate, NADH, tris(hydroxymethyl)aminomethane (Tris), *N,N*-bis-(2-hydroxyethyl)glycine (Bicine), 1,3-bis[tris(hydroxymethyl)methylamino]-propane (Bis-tris propane) and cyclohexylaminopropanesulfonic acid (CAPS) were purchased from Nakarai Chemical Co. (Kyoto). Creatinine test kits were from Wako Pure Chemical Industries (Osaka). Poly(vinyl chloride) (PVC, m.w. 48400) was from Kanegafuchi Kagaku Co. (Tokyo). Deionized water was used for all procedures.

Procedures

Enzyme assay. The GlDH activity was determined by measuring the decrease in absorbance of NADH at 340 nm [8]. Creatinine deiminase activity [9] was based on the determination of the amount of ammonia released from creatinine by the method of Berthelot [10].

Immobilization of the enzymes on wet membranes. Immobilization of the enzyme was done as reported previously [6, 7]. A PVC/dimethylformamide solution (8%, w/w) was cast on a glass plate (10 × 7 cm) and immediately immersed in methanol at room temperature for 4 h. The wet membrane (ca. 40 μm thick, 8 mm diameter) obtained was washed with distilled water. Immobilization of GlDH was done by the absorption method as follows: the wet membrane was added to 0.6 ml of an enzyme solution (400 mg dl^{-1} GlDH, 10 mM phosphate buffer, pH 7.0, 20 mM disodium EDTA) and incubated for 24 h at 4°C. The GlDH/PVC membrane obtained was washed with a large volume of phosphate buffer and stored in phosphate buffer containing 20 mM disodium EDTA. The creatinine deiminase/PVC membrane was prepared similarly, using a solution of creatinine deiminase (200 mg dl^{-1}, 50 mM phosphate buffer, pH 7.5). The activities of the GlDH and creatinine deiminase membranes were 0.45 and 1.1 IU cm^{-2} and the activity recoveries of the immobilized enzymes were 4.2% and 28.9%, respectively.

Assembly of the sensor. Figure 1 is a schematic diagram of the system. The GlDH/PVC membrane and the creatinine deiminase/PVC membrane were attached to the tip of the ammonia electrode (Orion Research, model 95-12). The membranes and the ammonia electrode were separated by a teflon mem-

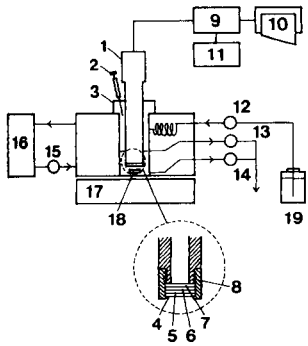

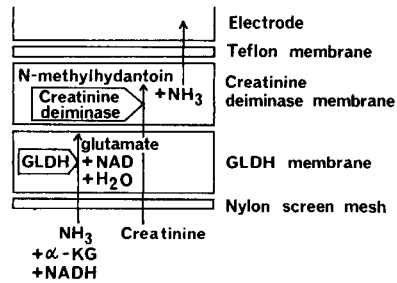

Fig. 1. Schematic diagram of the creatinine sensor system (not to scale): (1) ammonia electrode; (2) microsyringe; (3) cell; (4) nylon screen mesh; (5) GlDH/PVC membrane; (6) creatinine deiminase/PVC membrane; (7) gas-permeable teflon membrane; (8) bottom cap; (9) digital mV meter; (10) recorder; (11) digital printer; (12—15) peristaltic pumps; (16) water bath; (17) magnetic stirrer; (18) stirrer; (19) buffer solution.

Fig. 2. Cross-section of the immobilized enzyme membranes.

brane to prevent penetration of contaminants into the electrode. The enzyme electrode was inserted in a 2.0-ml cell which was filled with solution that was magnetically stirred. Readings of the ammonia electrode potential were taken on an Orion digital pH meter (model 701) and recorded with a digital printer (model 751) and a recorder (Yokogawa Electric Works, Tokyo, type 3066). The temperature of the buffer solution and the cell was maintained at 30 ± 0.5°C.

Recommended method. Buffer solution (50 mM Tris, pH 8.5, 1 ml) containing α-ketoglutarate (5 mM) and NADH (0.6 mM) was fed into the cell by the peristaltic pump 12 (Fig. 1), and pump 13 was operated to remove the overflow. After the potential had reached a steady state, 100 μl of sample solution was injected into the cell, after which the potential gradually increased and reached a steady state. The buffer solution including the sample solution was completely discarded by pump 14 and the cell was washed with buffer solution and the potential returned to the initial level. The potential difference between the two steady states was used as a measure of the creatinine concentration. The electrode potential differences obtained from various concentrations of creatinine standard solutions were plotted against the creatinine activities determined by the modified Jaffe method, using a creatinine test kit, to provide a calibration graph.

RESULTS AND DISCUSSION

Principle of the multilayer creatinine electrode

Figure 2 shows a cross-section of the immobilized membrane layers. Ammonia in the sample is converted to water in the first layer. Creatinine in

the sample does not react in the first layer, and reaches the second layer where it is converted to ammonia. In order to measure the creatinine concentration, the response of the sensor was measured. After the potential became constant when the buffer solution (50 mM Bis-tris propane, pH 9.5 and 50 mM Tris, pH 8.5) was fed into the cell, the standard creatinine solution (100 μl, 5 mg dl^{-1}) was injected into the cell. As shown in Fig. 3, initially the potential changed with reaction time and reached a steady state in 3 min. This indicates that creatinine penetrated the first layer and was decomposed rapidly to ammonia in the second layer, showing rapid diffusion of substrate and high specific activity of the immobilized creatinine deiminase when the wet PVC membrane was used as the enzyme carrier. From this response curve, the potential was measured 3 min after sample injection in further experiments.

Calibration

The calibration curves for creatinine at various pH values are shown in Fig. 4. The optimum pH for the determination of creatinine was 8.5—9.5. This could be explained on the basis that the optimum pH for creatinine deiminase is 7—9 [9] and the sensitivity of the ammonia electrode increases with increasing pH because of the ammonium-ammonia equilibrium [11]. The minimum detectable concentration of creatinine with this sensor was 0.5 mg dl^{-1} at pH 9.5 and 1.0 mg dl^{-1} at pH 8.5. Below pH 8.0 the sensitivity decreased significantly with decreasing pH (Fig. 4).

Effect of endogenous ammonia

The optimum pH for GlDH-catalyzed amination of α-ketoglutarate is in the range 7.5—8.5; above pH 9, the GlDH activity is relatively low [8].

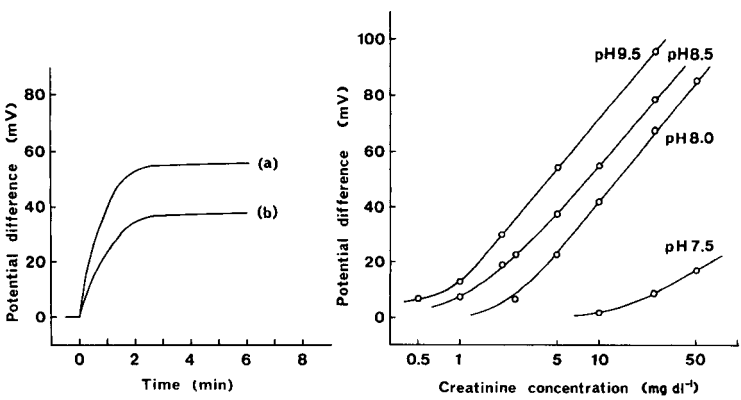

Fig. 3. Response curve of the sensor for a 5 mg dl^{-1} creatinine solution in different buffers: (a) 50 mM Bis-tris propane, pH 9.5; (b) 50 mM Tris, pH 8.5.

Fig. 4. Calibration curves for creatinine at different pH values. Buffers: pH 7.5, 8.0 (50 mM Tris); pH 8.5 (30 mM Bicine); pH 9.5 (50 mM Bis-tris propane). Each buffer contained α-ketoglutarate (5 mM) and NADH (0.6 mM). Sample solution: 100 μl.

Creatinine, however, could be determined at pH 8.5 (Fig. 4). Thus creatinine solutions including endogenous ammonia were measured at pH 8.5 in order to eliminate the effects of endogenous ammonia. Table 1 shows the effects of ammonia when the creatinine solution contained various concentrations of ammonium chloride. The potential differences increased with increasing ammonia concentration when the creatinine deiminase monolayer membrane sensor was used, but the double membrane enzyme sensor eliminated the effect of ammonia below 2×10^{-4} M. The normal concentration of ammonia in blood serum is $<5 \times 10^{-5}$ M, and for a patient with hepatic coma the level is as high as 2×10^{-4} M, so this enzyme sensor has the ability to determine creatinine in blood serum directly without correction for endogenous ammonia.

The reproducibility of creatinine measurements was examined by making ten determinations of a 5 mg dl^{-1} solution. The relative standard deviation was 4.8% for within-day measurements. The sensor was useful only for 10 days, after which the sensitivity decreased owing to the leaching out of

TABLE 1

Effect of ammonium chloride on creatinine determination

Membrane[a]	Creatinine concn. (mg dl^{-1})	NH_4Cl concn. (mM)	Potential difference (mV)	Creatinine found[b] (mg dl^{-1})	Error (%)
A	5	0.00	37.5	5.04	+1
A	5	0.10	37.5	5.04	+1
A	5	0.20	38.5	5.24	+5
A	5	0.40	47.5	7.46	+49
A	5	1.00	54.1	9.64	+93
B	5	0.00	38.0	5.15	+3
B	5	0.10	41.7	5.94	+19
B	5	0.20	46.8	7.24	+45
B	5	0.40	52.1	8.89	+78
B	5	1.00	62.6	13.4	+168
A	10	0.00	54.3	9.71	−3
A	10	0.10	54.3	9.71	−3
A	10	0.20	55.1	10.0	0
A	10	0.40	60.4	12.3	+23
A	10	1.00	64.3	14.3	+43
B	10	0.00	55.1	10.0	0
B	10	0.10	59.1	11.7	+17
B	10	0.20	61.6	12.9	+29
B	10	0.40	64.6	14.5	+45
B	10	1.00	71.8	19.2	+92

[a]Membrane A is the double membrane system; B is the single layer of immobilized creatinine deiminase. [b]Evaluated from Fig. 4.

the internal electrolyte from the ammonia electrode. This aspect needs further attention.

The immobilized GlDH membrane retained 80% of its initial activity after storage in 10 mM phosphate buffer (pH 7.0) containing 20 mM disodium EDTA for 6 months at 4°C and the immobilized creatinine deiminase membrane retained 85% after storage in 50 mM phosphate buffer (pH 7.5) for 6 months at 4°C.

The authors thank Kyowa Hakko Company, Tokyo, for the supply of creatinine deiminase.

REFERENCES

1 M. Jaffe, Z. Physiol. Chem., 10 (1886) 391.
2 H. Thompson and G. A. Rechnitz, Anal. Chem., 46 (1974) 246.
3 M. Mascini and G. Palleshi, Anal. Chim. Acta, 136 (1982) 69.
4 I. Kubo, I. Karube and S. Suzuki, Anal. Chim. Acta, 15 (1983) 371.
5 S. Hirose, E. Yasukawa, M. Hayashi and W. R. Vieth, J. Memb. Sci., 11 (1982) 177.
6 K. Kihara, E. Yasukawa, M. Hayashi and S. Hirose, Anal. Chim. Acta, 159 (1984) 81.
7 K. Kihara, E. Yasukawa and S. Hirose, Anal. Chem., 56 (1984) 1876.
8 H. Shimuzu, T. Kuratsu and F. Hirata, J. Ferment. Technol., 57 (1979) 428.
9 T. Uwajima and O. Terada, Agr. Biol. Chem., 41 (1977) 339.
10 J. Berthelot, Rep. Chem. Appl., 1 (1859) 284.
11 Instruction Manual for Ammonia Electrode, Orion Research Inc., Cambridge, MA, U.S.A., 1983.

Analytica Chimica Acta, 183 (1986) 81—88
Elsevier Science Publishers B.V., Amsterdam — Printed in The Netherlands

APPLICATION D'UN REACTIF SULFOVANADIQUE EN MILIEU ACETIQUE ANHYDRE A L'ETUDE ANALYTIQUE DE QUELQUES ACIDES α-CARBONYLES OU α-HYDROXYLES

D. PRADEAU et M. HAMON*

Faculté des Sciences Pharmaceutiques et Biologiques de Paris-Sud, 3 rue J. B. Clément, 92290 Chatenay Malabry (France)

M. ARNOULD

Pharmacie Centrale des Hôpitaux de Paris, 7 rue du Fer à Moulin, 75221 Paris Cedex 05 (France)

(Reçu le 16 Juillet 1985)

RÉSUMÉ

L'obtention d'un réactif sulfovanadique en milieu acétique anhydre a permis d'étudier les cinétiques d'oxydation d'acides α-carbonylés (glyoxylique, pyruvique, phénylglyoxylique) et d'acides α-alcools (glycolique, lactique, mandélique, gluconique). L'étude de reproductibilité montre la possibilité d'une réaction immédiate pouvant être utilisée pour un dosage. Seul l'acide lactique, qui s'oxyde selon une cinétique lente, ne se prête pas à un dosage instantané.

SUMMARY

(*Application of a vanadium(V) reagent in anhydrous acetic acid to the determination of some α-carbonyl or α-hydroxyl carboxylic acids*). The reagent is prepared from vanadium pentoxide and sulfuric acid in anhydrous acetic acid medium. The oxidation kinetics of various α-carbonyl (glyoxylic, pyruvic, phenylglyoxylic) and α-hydroxyl (glycolic, lactic, mandelic, gluconic) acids are described. A study of the reaction stoichiometry shows that the immediate reaction, corresponding to the consumption of 2—9 mol V(V) mol^{-1} of acid, depending on the acid, is useful quantitatively, except for lactic acid which gives a slow non-stoichiometric reaction.

Les solutions de pentoxyde de vanadium en milieu sulfurique aqueux présentent un pouvoir oxydant élevé [1, 2]. L'intérêt majeur de ce type d'oxydant réside dans la consommation d'une quantité importante de réactif par de nombreuses molécules organiques multifonctionnelles. C'est le cas, en particulier, pour des substances appartenant à des séries intéressantes au plan thérapeutique, telles que les dérivés, le plus souvent méthoxylés, de l'isoquinoléine [3—10] ou du chromanne [11, 12] et même des polyéthylèneglycols [13, 14]. L'action oxydante du vanadium(V) n'est obtenue qu'en présence d'une concentration suffisante en acide. C'est ainsi que, pour obtenir des résultats analytiques convenables, il est nécessaire d'opérer en milieu

0003-2670/86/$03.50

sulfurique 2,5 ou 5 M. Toutefois, il n'y a pas, en phase aqueuse, formation de complexes sulfovanadiques dans ces conditions, puisque ceux-ci n'existent qu'avec une concentration en acide sulfurique de l'ordre de 10 M correspondant à un milieu de manipulation difficile. Les réactions sont rarement instantanées, même en milieu très acide, et il est souvent nécessaire d'opérer à chaud, soit à la température du bain-marie bouillant, soit même, dans le cas des polyoxyéthylèneglycols de poids moléculaire élevé, à la température d'ébullition du mélange.

Les complexes sulfovanadiques présentent, dans l'eau, un potentiel oxydo-réducteur supérieur à celui des ions vanadyle VO_2^+ ou $V(OH)_4^+$ [1]. C'est pourquoi nous avons étudié la possibilité d'en préparer des solutions dans des solvants moins dissociants que l'eau. Les alcools, et même les cétones, sont oxydés plus ou moins lentement par des solutions de pentoxyde de vanadium en milieu sulfurique concentré. Aussi avons-nous envisagé l'emploi d'un solvant à groupement fonctionnel carboxylique, dont il était possible d'espérer une absence de réactivité. L'acide acétique, dont la constante diélectrique (ϵ = 6,2) est très faible, a ainsi été choisi. Outre l'amélioration de la stabilité des complexes sulfovanadiques, ce caractère peu dissociant peut favoriser la formation de complexes initiaux entre la molécule organique et le vanadium pentavalent, accélérant ainsi la réaction d'oxydation. Nous indiquons, dans ce mémoire, la préparation d'une telle solution. Nous présentons ensuite les résultats obtenus pour une série de molécules bifonctionnelles de structure relativement simple: les acides α-carbonylés et α-hydroxylés. En effet, leur réactivité en milieu aqueux s'est avérée assez faible et leur consommation de réactif évolue au cours du temps, de telle sorte que la mise en oeuvre d'un dosage en est rendue difficile. Cette étude présente, en outre, l'avantage de permettre une première approche des mécanismes réactionnels.

PARTIE EXPERIMENTALE

Réactifs

Solution vanadique 0,05 M (exprimée en ion vanadyle VO_2^+) en milieu sulfurique dans l'acide acétique anhydre. Introduire le pentoxyde de vanadium (1,137 g) dans une fiole jaugée de 250 ml, ajouter l'acide sulfurique concentré p.a. (70 ml). Faire dissoudre en chauffant légèrement pendant 1 h à une température de 70°C, sous agitation constante. Refroidir après dissolution. Placer la fiole dans un bain d'eau glacée et compléter peu à peu avec l'acide acétique anhydre QSP (250 ml), en évitant tout élévation importante de température. Attendre le retour à la température du laboratoire pour compléter au volume nominal.

Solution étalon 0,125 M de sulfate de fer(II) et d'ammonium. Peser exactement 12,254 g de sel de Mohr et les introduire dans une fiole de 250 ml. Dissoudre et compléter au volume avec une solution diluée (1 + 9) d'acide sulfurique. Titrer par une solution de permanganate de potassium 0,1 N.

Mode opératoire

Pour préparer la solution "témoin", dans un bécher de 100 ml, introduire 20 ml de la solution vanadique 0,05 M. Diluer à 50 ml avec une solution aqueuse d'acide sulfurique 5 M.

Pour préparer la solution "essai", peser une prise d'essai correspondant à la réduction attendue d'environ 0,2—0,5 mmol de réactif vanadique. Si cette masse est trop faible pour obtenir une pesée exacte, préparer une solution mère dans l'acide acétique et en prélever une partie aliquote correspondant à ces indications. Introduire cette prise d'essai dans un bécher de 100 ml. Ajouter 20 ml de solution vanadique 0,05 M. Diluer à 50 ml avec une solution aqueuse d'acide sulfurique 5 M.

Laisser réagir la solution "témoin" et la solution "essai" pendant le temps prescrit. Au bout de ce temps, doser les deux solutions "témoin" et "essai" par la solution étalon de fer(II) en utilisant une indication potentiométrique (platine: électrode indicatrice, calomel: électrode de référence).

RESULTATS

Elaboration du réactif oxydant

Le choix du solvant non-aqueux s'étant porté sur l'acide acétique, il convenait d'étudier la possibilité d'obtenir des solutions utilisables dans ce milieu. En effet, dans le cas de l'eau, qui est, à notre connaissance, le seul solvant a avoir été étudié jusqu'à maintenant, le pentoxyde de vanadium, s'il est presque insoluble en milieu neutre, donne des solutions de concentrations acceptables en milieu acide. Il était donc possible d'espérer que le caractère prototropique plus faible de l'acide acétique permettrait, à l'instar d'une solution aqueuse acide, la mise en solution directe du pentoxyde de vanadium, cependant l'acide acétique ne dissout aucune trace de réactif.

Une autre possibilité consistait à dissoudre dans ce solvant des complexes sulfovanadiques préalablement formés. Ceux-ci sont obtenus par dissolution du pentoxyde de vanadium dans l'acide sulfurique concentré (environ 18 M). Il apparait une coloration rouge orangé foncée, signe probable de la formation de tels complexes [15]. En effet, la dilution de cette solution sulfurique par l'eau conduit à la disparition de la teinte rouge qui passe au jaune puis à l'incolore. Au contraire, la dilution dans l'acide acétique permet d'obtenir une solution fortement colorée en orangé, laissant prévoir le maintien de la complexation.

Oxydation de divers acides α-carbonylés et α-hydroxylés

Pour comparer le comportement de cet oxydant, en phases aqueuse et acétique, nous avons choisi des molécules à groupement fonctionnel acide possédant en α un autre groupement oxygéné, alcoolique ou carbonylé et dont le dosage présente un intérêt pratique au plan pharmaceutique. En effet, toutes les observations qui ont pu être réalisées montrent une grande affinité de cet oxydant vis à vis du groupement carboxylique. Les travaux

de Vinh-Chon-Thanh [16], qui ont porté sur plusieurs de ces composés, nous permettront de faire la comparaison avec nos propres résultats.

Trois acides α-carbonylés et leur trois homologues α-hydroxylés ont été étudiés. Ils diffèrent par la présence ou non d'un substituant hydrocarboné sur le carbone porteur du groupement oxygéné non acide. Ce choix a pour but de préciser l'importance de la présence de ce radical sur le mécanisme réactionnel. En outre, en raison de son intérêt en contrôle de médicaments, un acide polyhydroxylé, l'acide gluconique, a été également oxydé. Les résultats sont regroupés dans le Tableau 1. L'examen de ce tableau montre tout d'abord que les acides α-carbonylés réagissent d'une façon instantanée en consommant dans tous les cas une quantité d'oxydant de 2 mol (exprimées en vanadium(V)) par mole d'acide. Il est donc possible d'envisager la formation parallèle de dioxyde de carbone et d'acide formique, acétique ou benzoïque. La vérification de l'absence de réactivité de ces trois acides dans le milieu a été réalisée.

En revanche, le comportement des acides α-hydroxylés est beaucoup plus variable. Si l'acide mandélique réagit d'une manière attendue et comparable à l'acide cétonique correspondant en consommant instantanément quatre moles d'oxydant par mole, l'acide lactique et surtout l'acide glycolique présentent des cinétiques d'oxydation fort différentes. Une mole du premier réduit progressivement jusqu'à 5,5 mol de vanadium(V) (Fig. 1) alors qu'en milieu aqueux, il ne consomme que les quatre moles attendues. Au contraire, dans le cas de l'acide glycolique, les consommations initiale et finale sont bien de l'ordre de 4 mol mol^{-1} d'acide. Mais un phénomène paradoxal se produit. Une diminution de la quantité de vanadium(V) consommé est observée. Ce phénomène a été vérifié à plusieurs reprises (Fig. 1).

Dans le cas de l'acide gluconique, une consommation un peu supérieure à 9 mol mol^{-1} est obtenue immédiatement. Mais ici encore, on observe au cours du temps un recul léger de cette consommation suivi d'un retour à la valeur initiale.

Afin de préciser le mécanisme de ces réactions et de tenter de leur donner une explication, le dosage des produits réactionnels gazeux a été réalisé. Les résultats en sont donnés dans le Tableau 2.

TABLEAU 1

Cinétique de quelques acides α-hydroxylés ou α-carbonylés en milieu acétique

Acide	Formule	Nombre de mole de VO_2^+ consommées par mole au temps (h)									
		0	0,25	0,5	1	2	3	4	5	14	24
Glyoxylique	CHOCOOH	2,10		2,16		2,12	2,20		2,10		2,10
Pyruvique	$CH_3COCOOH$	1,90		2,05	2,20	2,20		2,26	2,15		2,30
Phénylglyoxylique	$C_6H_5COCOOH$	2,00		2,10	2,19	2,20	1,90		2,10		2,10
Glycolique	$CH_2OHCOOH$	4,20	3,38	3,18	3,13	2,78	2,52	2,67	3,29	3,45	3,84
Lactique	$CH_3CHOHCOOH$	2,27	2,47	2,66	2,77	2,83	3,40	3,76	4,08	4,81	5,24
Mandélique	$C_6H_5CHOHCOOH$	3,75		4,10	3,85	3,90	3,71	4,01	4,00		4,00
Gluconique	$CH_2OH(CHOH)_4COOH$	9,15		8,60		9,15	9,40				9,25

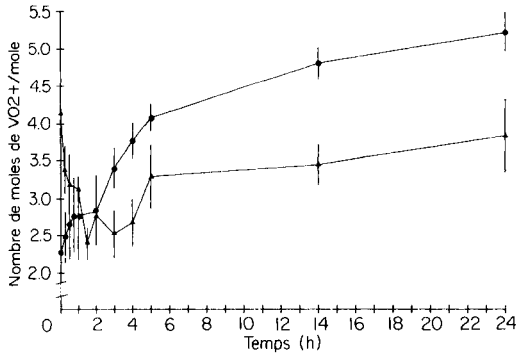

Fig. 1. Cinétique d'oxydation de l'acide lactique (•) et glycolique (▲).

TABLEAU 2

Produits réactionnels gazeux dégagés

Acide	CO_2 dégagé (mol mol^{-1})	CO dégagé (mol mol^{-1})	Acide	CO_2 dégagé (mol mol^{-1})	CO dégagé (mol mol^{-1})
Glyoxylique	0,5	0	Phénylglyoxylique	0,75	0
Glycolique	0,86	0	Mandélique	1,33	0
Pyruvique	0,96	0	Gluconique	0,99	0,48
Lactique	1,27	0,245			

Dosage des acides α-carbonylés et des acides glycolique, mandélique et gluconique

Il a paru intéressant d'établir une méthode de dosage de ces composés dont la plupart présente un intérêt dans le domaine du contrôle de médicaments. Les résultats de l'étude de reproductibilité du dosage de quantités de l'ordre de 0,1—0,2 mmol sont regroupés dans le Tableau 3. La précision de ces dosages est bonne, même si, pour l'acide gluconique, les résultats en sont un peu plus dispersés.

TABLEAU 3

Etude de la reproductibilité de l'oxydation instantanée de quelques acides α-hydroxylés ou α-carbonylés

Acide	VO_2^+ consommée[a] (mol mol^{-1})		Acide	VO_2^+ consommée[a] (mol mol^{-1})	
	Moyenne	Ecart type[b]		Moyenne	Ecart type[b]
Glyoxylique	2,12	0,027	Phenylglyoxylique	2,04	0,017
Glycolique	4,20	0,05	Mandélique	4,03	0,046
Pyruvique	2,14	0,049	Gluconique	9,605	0,595

[a]Le dosage du réactif oxydant (témoin négatif) était 4,49 ± 0,011 g l^{-1}. [b]n = 10.

Dérivés carbonylés

Le cas des dérivés carbonylés ne présente aucune difficulté. La réaction générale d'oxydation est la suivante:

$$RCOCOOH + 2VO_2^+ + 2H^+ \rightarrow RCOOH + CO_2 + H_2O + 2VO^{2+}$$

où R = H, CH_3 ou C_6H_5. La seule différence avec l'oxydation en milieu aqueux réside dans une nette accélération de la vitesse de réaction qui permet ici la réalisation d'un dosage instantané.

Enfin il est important de souligner que, si l'absence d'oxydabilité de l'acide acétique, utilisé comme solvant de la réaction, était attendue, il n'en est pas de même pour l'acide formique dont le caractère réducteur vis à vis d'oxydant présentant un potentiel redox élevé est bien connu.

Dérivés hydroxylés

Logiquement, il était possible de s'attendre à une consommation de quatre moles d'ion vanadyle par mole d'acide mandélique, puisque la seule différence avec les composés précédents réside dans le groupement fonctionnel alcoolique. L'acide mandélique est le seul à se comporter ainsi et réagit selon

$$C_6H_5CHOHCOOH + 4VO_2^+ + 4H^+ \rightarrow C_6H_5COOH + CO_2 + 3H_2O + 4VO^{2+}$$

L'augmentation de la consommation d'oxydant par rapport à ce qui était prévisible et qui est observé en milieu aqueux pour l'acide lactique (Tableau 1) est éclairée par l'isolement de 1,25 mol de dioxyde de carbone par mole d'acide (correspondant à un excès de 0,25 mol) et de 0,25 mol de monoxyde de carbone. Ces deux valeurs correspondent, en effet, à l'oxydation d'un quart des ions CH_3CO^+ éventuellement formés lors de l'oxydation en monoxyde et dioxyde de carbone. L'oxydation parait donc réalisée selon les équations suivantes:

$$CH_3CHOHCOOH + 4VO_2^+ + 5H^+ \rightarrow CH_3CO^+ + CO_2 + 4H_2O + 4VO^{2+}$$

puis pour trois-quarts des molécules, le radical acétyle réagit selon

$$CH_3CO^+ + H_2O \rightarrow CH_3COOH + H^+$$

et pour le dernier quart selon

$$CH_3CO^+ + 4VO_2^+ + H^+ \rightarrow CO + CO_2 + 2H_2O + 4VO^{2+}$$

En milieu aqueux, le radical acétyle se trouve en contact avec de nombreuses molécules d'eau susceptibles de réagir pour former l'acide acétique et éviter ainsi toute nouvelle oxydation. Dans le cas étudié ici, le plus faible nombre de ces molécules d'eau permet peut-être une première explication du phénomène observé, sans pour autant pouvoir élucider les raisons de la proportion de radical acétyle subissant l'oxydation. La consommation théorique de réactif oxydant par mole d'acide lactique est donc de 5 mol. Cette valeur est sensiblement en accord avec les résultats expérimentaux.

Pour l'acide glycolique, la diminution de la quantité d'oxydant consommé est surprenante au premier abord. Nous avons cherché à étudier le comportement du formaldéhyde susceptible de se former dans ces conditions. Celui-ci consomme 1,75 mol de vanadium(V) par mole en 1 h environ. La mise en évidence de complexes entre le dioxyde de carbone ou l'acide formique et le pentoxyde de vanadium nous fait émettre l'hypothèse de la formation d'un complexe entre le formaldéhyde ou l'un de ses précurseurs et le vanadium(V) [17] qui se dissocierait ensuite en libérant puis en oxydant peu à peu cet aldéhyde.

L'hypothèse précédente trouve, peut-être, un début de confirmation dans le phénomène analogue, mais moins net, qui apparaît dans le cas de l'acide gluconique où une molécule de formaldéhyde peut également se former. Le cas de cette dernière molécule est toutefois plus difficile à analyser.

Conclusion

La réalisation de solutions sulfovanadiques en milieu acétique anhydre permet l'extension de dosages oxydimétriques par le vanadium(V) à ce milieu non aqueux. Les résultats de l'étude cinétique de l'oxydation de sept acides α-carbonylés ou α-hydroxylés montrent la possibilité d'une réaction immédiate et reproductible, applicable au dosage dans le cas des acides glyoxylique, pyruvique, phénylglyoxylique, glycolique et mandélique.

Cette réaction est beaucoup plus sélective et souvent plus profonde que l'oxydation permanganique. Ainsi ce dernier ne réagit pas sur un acide α-cétonique comme l'acide phénylglyoxylique. Pour l'acide gluconique, la méthode nous parait également applicable au contrôle des matières premières pharmaceutiques, même si les résultats sont un peu plus dispersés.

Il a été possible de constater que les résultats analytiques ne sont pas toujours identiques à ceux observés en milieu aqueux. Cette observation pose la question de mécanismes réactionnels différents que nous avons tenté d'expliciter. La rapidité de réactions nous fait envisager d'étendre cette étude à des molécules d'intérêt thérapeutique insolubles dans l'eau et d'en réaliser le dosage éventuel.

BIBLIOGRAPHIE

1 P. Malangeau et M. Guernet, 21ème série des Actualités de Chimie Analytique Organique Pharmaceutiques et Bromatologiques, Masson, Paris, 1972, p. 43—72.
2 E. Randrianjohany, Thèse de Doctorat d'Etat des sciences pharmaceutiques Série E no. 184 (1969), Université de Paris.
3 S. Klein, M. J. Waechter et M. Hamon, Analusis, 10 (1982) 120.
4 E. Postaire, M. Tsitini Tsami, C. Viel et M. Hamon, Talanta, 30 (1983) 193.
5 M. Tsitini Tsami et M. Hamon, Pharm. Delt., Epistem. Ekdosis, 4 (1978) 67.
6 M. Tsitini Tsami, M. Chaigneau, J. Likforman et M. Hamon, Analusis, 8 (1980) 428.
7 M. Tsitini Tsami, M. J. Waechter, M. Chaigneau et M. Hamon, Analusis, 7 (1979) 42.
8 M. Tsitini Tsami, M. J. Waechter, J. Likforman, J. Delcroix et M. Hamon, Analusis, 9 (1981) 283.
9 M. J. Waechter et M. Hamon, Ann. Pharm. Fr., 34 (1976) 281.

10 M. J. Waechter, J. Likforman et M. Hamon, Analusis, 5 (1977) 34.
11 J. E. Hila, M. Chastagnier, M. Tsitini Tsami, H. Souliau et M. Hamon, Talanta, 3 (1984) 655.
12 J. E. Hila, M. Tsitini Tsami, M. Hamon et J. P. Delcroix, Analusis, 10 (1982) 220.
13 C. Dauphin, C. Bahsoun, M. Hamon et J. Likforman, Anal. Chim. Acta, 149 (1983) 313.
14 C. Dauphin, A. Dauphin et M. Hamon, Analusis, 7 (1979) 73.
15 P. Pascal, Nouveau traité de chimie minérale, Tome XII, Masson, Paris, 1958, p. 177.
16 Vinh-Chon-Thanh, Thèse de Doctorat d'Etat es sciences pharmaceutiques, série E no. 7 (1973), Université de Paris XI.
17 C. Dauphin, Thèse de Doctorat d'Etat des sciences pharmaceutiques, série E 224 (1985), Université de Paris XI.

Analytica Chimica Acta, 183 (1986) 89—96
Elsevier Science Publishers B.V., Amsterdam — Printed in The Netherlands

LEACHING BEHAVIOR OF METAL-CONTAINING SPECIES IN RESIDUAL OILS WITH DIFFERENT ORGANIC SOLVENTS

TOSHIYUKI TSUKADA, KOICHI SAITOH and NOBUO SUZUKI*
Department of Chemistry, Faculty of Science, Tohoku University, Sendai 980 (Japan)
(Received 20th August 1985)

SUMMARY

The leaching behavior of two different residual oils is investigated with 24 organic solvents including alkanes, aromatics, esters, ethers, ketones, alcohols and nitrogen compounds. A 2-g portion of sample oil is shaken with 20 ml of the organic solvent. The leaching of the organic matrix of the oil is determined by weighing the dissolved organic matrix after removal of solvent. The leaching of vanadium, iron and nickel was determined by flame atomic absorption spectrophotometry after ashing of the dissolved fraction. The leaching of those metals depends strongly on the solvent used; for example, vanadium is almost completely leached into toluene, but only slightly into methanol. The leaching of iron is poor compared with that of vanadium or nickel. In most solvents, leaching of those metal-containing species is poorer than that of organic material. Exceptionally, *N,N*-dimethylformamide is more efficient in leaching vanadium species than organic material.

The presence of metals in petroleum is well established. Heavy crude oil, for example, generally contains vanadium, nickel, sodium and iron at mg l^{-1} levels or more [1, 2]. Various analytical methods have been used to determine metals in petroleum samples. For example, vanadium has been determined by flame atomic absorption spectrometry (a.a.s.) [3, 4], graphite-furnace a.a.s. [5, 6], inductively-coupled plasma (i.c.p.) emission spectrometry [7], spectrophotometry with [8] and without [9] prior ashing, and neutron activation analysis [10]. These analytical methods are effective in determining the total concentration of the metal of interest. When more detailed information about a chemical species involving metal in petroleum is desired, some separation technique such as adsorption chromatography [11], gel-permeation chromatography [12] or gas chromatography [13] must be introduced.

Metals in petroleum are present in various chemical species and these metal species exist together with large amounts of a very complicated organic matrix in oil samples. Accordingly, an appropriate preliminary separation is required in connection with highly sensitive methods such as mass spectrometry [14].

Liquid-liquid extraction is one of the most widely used techniques for separation. A typical example is the fractionation of crude oil into maltene

0003-2670/86/$03.50

and asphaltene by use of an alkane, such as hexane. The selection of an organic solvent is obviously important for extractive separations. Dunning et al. [15] examined the use of several solvents including water, alcohol, hexane, iso-octane, cyclohexane and benzene for fractionation of oil prior to detection of porphyrins. The solvent dependency of the leaching of metal as well as organic matrix must be a useful guide for selection of the solvent to be used.

This paper describes the leaching of vanadium, iron and nickel from two kinds of residual oil into many different organic solvents.

EXPERIMENTAL

Materials and apparatus

Two residual oil samples prepared from two different Middle Eastern heavy crude oils were kindly supplied by the Idemitsu Petrochemical Co., Tokyo, Japan.

Twenty-four organic solvents including alkanes, aromatics, esters, ethers, ketones, alcohols and nitrogen compounds were used after distillation.

The standard solutions used for a.a.s. were prepared from 99.9% vanadium, 99.99% iron and nickel metals. Nitric and sulfuric acids (Wako Pure Chemicals, Osaka) and sodium chloride (Merck, Darmstadt) were of analytical grade. Water was double-distilled in glass apparatus.

A flame atomic absorption spectrometer (Nippon Jarrell-Ash, Model AA-1) was used with a burner for nitrous oxide/acetylene flames (with a 50-mm slot) or for air/acetylene flames (with a 100-mm slot). For the determination of vanadium, the conditions were 7.0 l min^{-1} nitrous oxide, 4.9 l min^{-1} acetylene, 318.4-nm wavelength and optical path height 8 mm; for iron, 7.7 l min^{-1} air, 1.4 l min^{-1} acetylene, 248.3 nm, 7-mm optical path height; and for nickel, 7.7 l min^{-1} air, 1.5 l min^{-1} acetylene, 232.0 nm, 15-mm optical path height.

Procedure

A 2-g portion of the residual oil was shaken with a 20-ml aliquot of the selected solvent for 5 h at 25°C. After centrifugation, the supernatant liquid was isolated from the insoluble residue (A), and then passed through a 0.45-μm membrane filter. The filtrate was heated, in order to eliminate the solvent, at near the boiling temperature of the solvent for 1 h in a quartz crucible placed on a hot plate and under an infrared lamp. After additional heating at 150°C for 1 h, the non-volatile residue obtained was cooled in a desiccator. From the weight of this residue was calculated the percent soluble fraction of the sample oil, which is regarded as the percent leaching of the total organic matrix of the oil. The insoluble residue (A) of the oil obtained after the initial leaching procedure was dissolved in benzene, and transferred to a quartz crucible. After evaporation of benzene in a way similar to that used for the soluble fraction the non-volatile material was weighed; this is regarded as the insoluble fraction of oil in the solvent tested.

Both the soluble and insoluble fractions of the sample oil were digested with concentrated sulfuric acid at 250°C until the fuming no longer occurred. This coked material was ashed in a furnace with a temperature program from 200°C to 520°C at a rate of 180°C h^{-1} and then held at 520°C for at least 12 h. The ash was treated with a 5-ml aliquot of diluted nitric acid (7 mol l^{-1}) on a hot plate until dissolution was completed. After evaporation to dryness, the ash was dissolved in 0.5 ml of concentrated nitric acid and the solution was made up to 25 ml with water. In this step, an aqueous solution of sodium chloride was also added so that the final concentration of sodium ion was 100 μg ml^{-1} in the solution. This solution was used for the atomic absorption spectrometry of vanadium, iron and nickel.

For the determination of the total metal content of the residual oil, a 2-g portion of the oil sample was directly ashed and then treated as above to give 25 ml of aqueous solution.

RESULTS AND DISCUSSION

The vanadium, iron and nickel contents of the residual oil samples

Before the present analytical procedure was applied to oil samples, its reliability was examined for a NBS (U.S. National Bureau of Standards) reference material GM-5. The a.a.s. data for vanadium, iron and nickel were evaluated by the absolute calibration and standard addition methods. The results obtained by these two methods are compared with those assigned by NBS in Table 1. The present values for vanadium and nickel obtained by either method are compatible with the certified values within 95% confidence limits. The iron content of GM-5 is not given by NBS.

The vanadium, iron and nickel contents were determined for two kinds of practical residual oil samples by the calibration method. These two samples are referred hereafter as Oil A and Oil B for the sake of convenience. The results are summarized in Table 1.

TABLE 1

Determination of vanadium, iron and nickel in residual oil samples

Sample	Method[a]	N[b]	Metal content (mg kg^{-1})		
			V	Fe	Ni
NBS GM-5[c]	I	7	77.2 ± 5.5	35.2 ± 1.8	96.1 ± 6.4
NBS GM-5	II	8	78.7 ± 3.9	34.8 ± 1.7	101.2 ± 8.1
Oil A	I	11	164 ± 11	2.5 ± 0.2	53.4 ± 0.4
Oil B	I	5	38.6 ± 0.5	6.8 ± 0.1	10.7 ± 0.2

[a]I, absolute calibration method; II, standard addition method. [b]Number of determinations. [c]NBS values: V, 79.0 ± 1.2 mg kg^{-1}; Ni, 93.0 ± 1.2 mg kg^{-1}.

Leaching of organic matrix

The quantity of soluble fraction of each residual oil depends on the solvent used. The percent leachings of organic matrix into the soluble fraction are summarized in column 5 in Tables 2 and 3. Hildebrand's solubility parameter (δ) [16] was used as a convenient measure of the nature of the solvent, and a relationship between the percent leaching of matrix and δ of the solvent was plotted for oil A, as shown in Fig. 1. A considerable amount of organic components is dissolved in solvents such as alkanes, ethers and aromatic hydrocarbons having δ values smaller than about 10 $cal^{1/2}$ $cm^{-3/2}$. According to the solubility parameter concept [16], the solubility of a non-electrolyte is governed by the difference between δ of the solute and δ of the organic solvent, and reaches a maximum when these δ values are the same. Figure 1 suggests that the major components of the sample oil seem to be organics with δ values smaller than about 10 $cal^{1/2}$ $cm^{-3/2}$.

The solvent dependence of the soluble percentage for Oil B is quite similar to that for Oil A. Figure 2 shows the correlation between the percentages of soluble matrix of these two oils.

Leaching of vanadium, iron and nickel

The leaching of these metals is expressed in terms of percentage of the metal content in the soluble fraction of the oil sample relative to the total metal content in the oil sample. The results for Oil A and Oil B with various solvents are summarized on columns 6—8 in Tables 2 and 3, respectively.

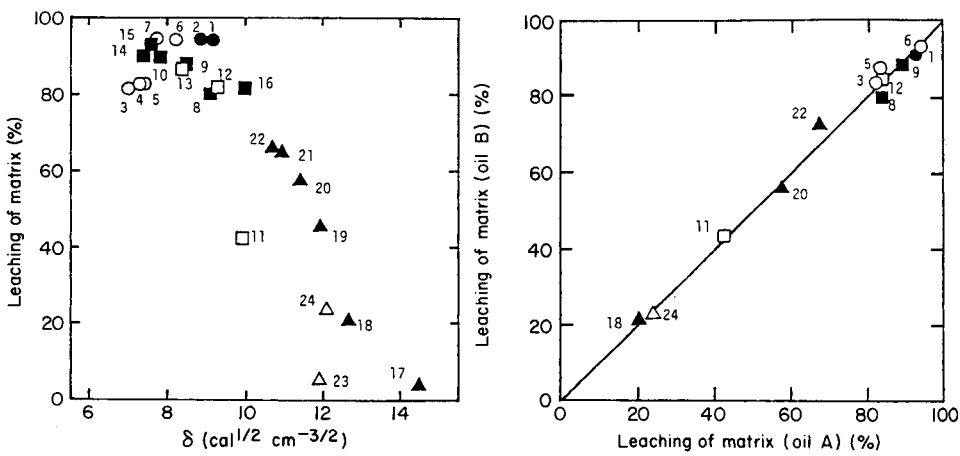

Fig. 1. Percent leaching of the organic matrix of Oil A plotted against the solubility parameter (δ) of the solvent used. The numbers 1—24 correspond to the solvent numbered in Table 2. Solvent symbols: (●) aromatic; (○) alkane; (■) ester or ether; (□) ketone; (▲) alcohol; (△) nitrogen compound.

Fig. 2. Percent leaching of organic matrix of Oil A (abscissa) and Oil B (ordinate) in the same solvent. Numbers and symbols as in Fig. 1.

TABLE 2

Percent leaching of organic matrix, vanadium, iron and nickel from Oil A

Solvent No.	Name	δ [b]	N [a]	Organic matrix (%)	V (%)	Fe (%)	Ni (%)
1	Benzene	9.2	4	92.7 ± 2.9[c]	98.2 ± 4.9	36 ± 12	97.4 ± 1.9
2	Toluene	8.9	3	93.7 ± 5.4	100 ± 3	36 ± 12	99.3 ± 2.8
3	Pentane	7.0	3	81.6 ± 3.2	37.1 ± 1.4	12 ± 8	40.8 ± 0.6
4	Hexane	7.3	3	82.8 ± 2.2	48.6 ± 2.1	12 ± 8	50.4 ± 0.6
5	Heptane	7.4	3	83.0 ± 1.2	53.0 ± 1.4	12 ± 4	54.9 ± 0.7
6	Cyclohexane	8.2	3	93.1 ± 2.5	100 ± 3	36 ± 4	96.4 ± 1.9
7	Methylcyclohexane	7.8	3	92.8 ± 3.5	98.8 ± 2.4	40 ± 16	96.4 ± 1.9
8	Ethyl acetate	9.1	3	80.0 ± 1.8	40.5 ± 0.5	8 ± 4	40.4 ± 0.7
9	Butyl acetate	8.5	3	88.3 ± 1.1	79.9 ± 1.2	20 ± 4	77.7 ± 0.9
10	Isoamyl acetate	7.8	3	89.6 ± 0.7	82.3 ± 0.6	24 ± 4	79.4 ± 1.8
11	Acetone	9.9	4	42.0 ± 0.6	25.3 ± 0.5	8 ± 4	18.4 ± 0.6
12	Methyl ethyl ketone	9.3	3	82.1 ± 2.1	58.2 ± 1.1	12 ± 4	53.6 ± 0.4
13	Methyl isobutyl ketone	8.4	3	86.8 ± 3.3	79.3 ± 3.7	16 ± 8	78.7 ± 1.7
14	Diethyl ether	7.4	1	90.3	71.3	16	80.0
15	Dibutyl ether	7.6	1	93.0	82.3	16	86.5
16	1,4-Dioxane	10.0	1	81.6	65.2	24	59.4
17	Methanol	14.5	1	40.0	0.5	ND	0.5
18	Ethanol	14.5	3	20.7 ± 1.0	2.9 ± 0.7	4 ± 4	1.9 ± 0.6
19	1-Propanol	11.9	3	45.7 ± 4.1	7.3 ± 0.8	ND	6.2 ± 0.9
20	1-Butanol	11.4	3	57.6 ± 2.4	9.9 ± 1.2	4 ± 4	11.2 ± 0.7
21	1-Pentanol	11.0	2	65.4 ± 5.3	21.8 ± 1.1	8 ± 4	22.5 ± 0.9
22	1-Hexanol	10.7	2	66.5 ± 5.8	32.8 ± 1.5	12 ± 8	32.9 ± 0.2
23	Acetonitrile	11.9	3	5.2 ± 0.2	5.2 ± 0.5	4 ± 4	1.9 ± 0.2
24	*N,N*-Dimethylformamide	12.1	3	23.9 ± 0.3	37.6 ± 0.9	12 ± 8	24.9 ± 0.4

[a]Number of measurement. [b]Hildebrand's solubility parameter in $cal^{1/2}$ $cm^{-3/2}$ [16]. [c]95% confidence limit for $N > 2$, and range for $N = 2$.

There is a considerable solvent dependence in the leaching of vanadium as well as nickel; the percent leachings of both metals range from less than 1% (in methanol) to nearly 100% (in toluene). A good correlation between the percent leachings of vanadium and nickel is clearly observed in Oil A as shown in Fig. 3. A similar good correlation was also obtained for Oil B.

The percent leaching of vanadium in Oil A is plotted, as an example, against Hildebrand's solubility parameter (δ) in Fig. 4. Despite the scatter, it is clear that large values of percent leaching of vanadium predominate for solvents having δ values in the range 8—9 $cal^{1/2}$ $cm^{-3/2}$. The same trends were obtained in the percent leaching of nickel in Oil A and also of both vanadium and nickel in Oil B. These results indicate that both vanadium and nickel in these oils are predominantly present in organic species which are easily soluble in relatively less polar solvents.

The leaching of iron is generally poor in comparison with those of vanadium and nickel. A plot of the percent leaching of iron vs. that of vanadium for

TABLE 3

Percent leaching of organic matrix, vanadium, iron and nickel from Oil B

Solvent No.	Name	δ [b]	N [a]	Organic matrix (%)	V (%)	Fe (%)	Ni (%)
1	Benzene	9.2	3	92.2 ± 0.3[c]	92.2 ± 4.7	15 ± 3	98.1 ± 1.9
3	Pentane	7.0	2	82.4 ± 1.3	40.9 ± 2.1	3 ± 2	40.2 ± 0.9
5	Heptane	7.4	2	88.3 ± 2.2	62.2 ± 1.3	4 ± 2	61.7 ± 0.9
6	Cyclohexane	8.2	3	92.4 ± 1.4	93.5 ± 3.4	13 ± 2	100 ± 1
8	Ethyl acetate	9.1	2	83.5 ± 0.8	32.0 ± 0.5	3 ± 2	29.9 ± 0.9
9	Butyl acetate	8.5	2	88.2 ± 1.0	79.3 ± 3.4	7 ± 2	81.3 ± 1.9
11	Acetone	9.9	2	43.7 ± 0.4	18.7 ± 0.8	2 ± 2	10.3 ± 1.9
12	Methyl ethyl ketone	9.3	2	83.2 ± 0.1	49.2 ± 1.8	4 ± 0	43.9 ± 1.9
18	Ethanol	14.5	2	20.9 ± 0.9	ND	ND	0.9 ± 0.9
20	1-Butanol	11.4	2	60.5 ± 3.5	8.0 ± 3.9	3 ± 1	6.5 ± 0.0
22	1-Hexanol	10.7	2	73.0 ± 2.5	23.3 ± 0.3	3 ± 0	23.4 ± 0.9
24	*N,N*-Dimethylformamide	12.1	2	23.5 ± 1.1	26.4 ± 0.3	4 ± 1	14.0 ± 0.0

[a—c] As in Table 2.

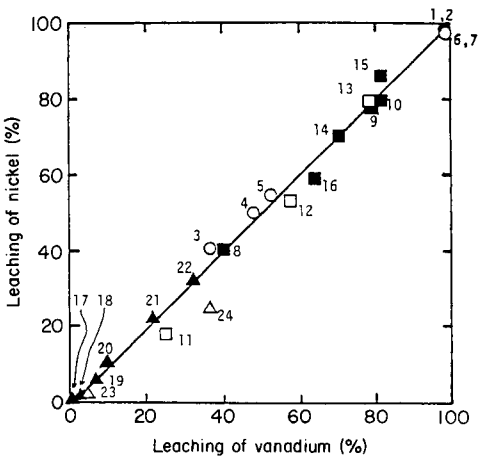

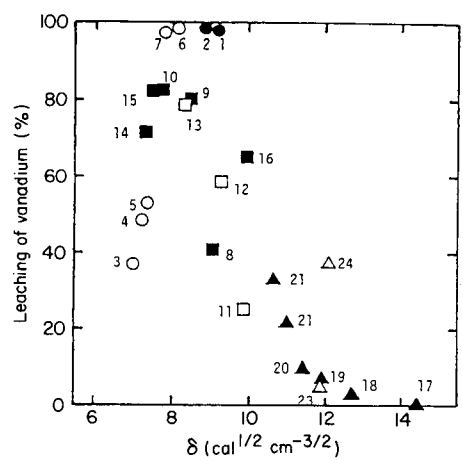

Fig. 3. Percent leaching of nickel (ordinate) and vanadium (abscissa) from Oil A. Numbers and symbols as in Fig. 1.

Fig. 4. Percent leaching of vanadium from Oil A as a function of the solubility parameter (δ) of the solvent used. Numbers and symbols as in Fig. 1.

Oil A is shown in Fig. 5. The percent leaching of iron did not exceed 40% with the variety of solvents tested. A similar plot was obtained for Oil B. Obviously, the types of iron species in these oil samples are quite different from those of vanadium and nickel.

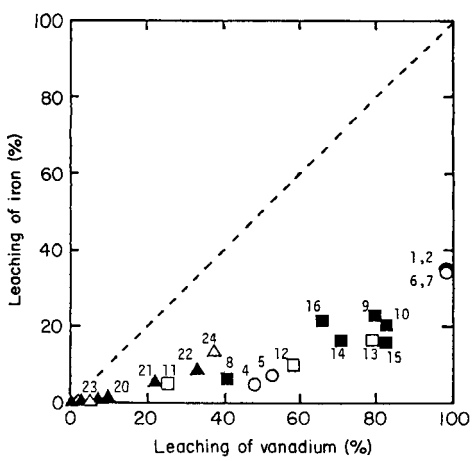

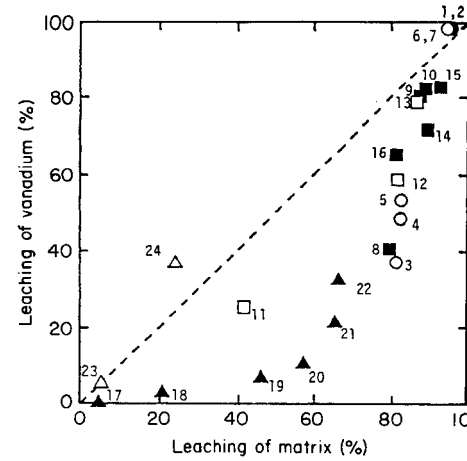

Fig. 5. Percent leaching of iron (ordinate) and vanadium (abscissa) from Oil A. Numbers and symbols as in Fig. 1.

Fig. 6. Percent leaching of vanadium plotted against that of organic matrix for Oil A. Numbers and symbols as in Fig. 1.

Selectivity in the leaching

Figure 3 shows that a few solvents, e.g., dimethylformamide (solvent no. 24) and acetone (no. 11), are slightly selective for vanadium rather than nickel in the leaching. The leaching behavior of vanadium is compared with that of soluble organics in Fig. 6. The percent leaching of vanadium obtained with most of the solvents is less than that of the soluble organic matrix. One obvious exception is found in the case of dimethylformamide (no. 24) in which the leaching of vanadium species occurs in preference to soluble organic substances. This selectivity of dimethylformamide for the leaching of vanadium species was also found in the case of Oil B. It is interesting that dimethylformamide is a reasonably selective solvent for vanadium rather than for organic substances. This solvent should be useful for isolation or concentration of the vanadium species contained in residual or heavy crude oil.

No clear-cut evidence is available as yet to show how the chemical species in the leaching fraction depend on the solvent used. This subject will be dealt with in subsequent papers.

The authors thank Idemitsu Petrochemical Co., Tokyo, Japan, for providing the residual oil samples.

REFERENCES

1 R. H. Hofstader, O. I. Milner and J. H. Runnels (Eds.), Analysis of Petroleum for Trace Metals, Am. Chem. Soc., Washington DC, 1976.
2 K. R. Shar, R. H. Filby and W. A. Haller, J. Radioanal. Chem., 6 (1970) 413.

3 R. E. Kauffman, C. S. Seba and W. E. Rhine, Anal. Chem., 54 (1982) 975.
4 J. Wieckowska, Mikrochim. Acta, 1 (1982) 195.
5 T. Sasaki, S. Hagi and H. Yamamoto, J. Jpn. Petrol. Inst., 23 (1980) 210.
6 R. H. Fish and J. J. Komlenic, Anal. Chem., 56 (1984) 510.
7 K. Fujimatsu, T. Iino, H. Uchida, K. Iwasaki, T. Kogane and Y. Matano, Bunseki Kagaku, 30 (1981) T11.
8 JPI Standard Method of Test for Vanadium in Fuel Oil, JPI-5S-11-79, The Japan Petrol. Inst., Tokyo, 1979.
9 T. Yamashige, Y. Ohmoto and Y. Shigetomi, Bunseki Kagaku, 29 (1980) 537.
10 C. Bergerioux and L. Zikovsky, J. Radioanal. Chem., 57 (1980) 97.
11 M. Blumer and M. Rudrum, J. Inst. Pet., London, 56 (1970) 99.
12 D. H. Hausler and L. T. Taylor, Anal. Chem., 53 (1981) 1227.
13 S. Dilli and E. Potsalides, Anal. Chim. Acta, 128 (1981) 109.
14 E. Baker, T. F. Yen, J. P. Dickie, R. E. Rhodes and L. F. Clark, J. Am. Chem. Soc., 89 (1967) 3631.
15 H. N. Dunning, J. W. Moore and A. T. Myers, Ind. Eng. Chem., 46 (1954) 2000.
16 A. F. M. Barton, Chem. Rev., 75 (1975) 731.

Analytica Chimica Acta, 183 (1986) 97—104
Elsevier Science Publishers B.V., Amsterdam — Printed in The Netherlands

MOLECULAR EXCLUSION CHROMATOGRAPHY IN STUDIES OF THE VANADIUM- AND NICKEL-CONTAINING SPECIES IN RESIDUAL OIL

TOSHIYUKI TSUKADA, KOICHI SAITOH and NOBUO SUZUKI*
Department of Chemistry, Faculty of Science, Tohoku University, Sendai 980 (Japan)
(Received 9th September 1985)

SUMMARY

A residual oil sample prepared from a crude oil is chromatographed on a column having a molecular-weight exclusion limit at about 5000. Three-dimensional chromatograms (absorbance/wavelength/time) are recorded with a u.v.-visible rapid-scanning detector. The elution profiles of vanadium- or nickel-containing species are obtained by applying atomic absorption spectrophotometry to fractions of the column effluents. Both vanadium- and nickel-containing species are detected over the whole molecular-weight range available with the column. The elution profiles of vanadium and nickel differ; the major elution peak for vanadium appears at a slightly lower molecular-weight region of the chromatogram than that for nickel. By reference to the real-time recorded absorption spectra of the effluents, it is suggested that at least some of the metals are present as metalloporphyrins.

The presence of vanadium and nickel in heavy crude oil has been dealt with by many investigators [1—3]. The abundance of each metal has been determined by various methods, for example, by atomic absorption spectrometry [4—6]. In most instances, the total concentration of a metal has been determined. When more detailed information about chemical species involving metals in petroleum is needed, some separation techniques must be introduced, because metals in petroleum are considered to be present as various chemical species and also present together with large amounts of organic matrix.

In the preceding paper [7], the leaching behavior of vanadium, nickel and iron from residual oils was investigated with many organic solvents. The leaching of each metal depended greatly on the solvent used. Some solvents showed considerable selectivity for leaching of vanadium-containing substances. These facts suggested that these metals were present as a mixture of different metal complexes.

In the present approach to the problems of studying metals in petroleum, molecular exclusion chromatography (m.e.c.) is used as the separation method. The notable advantages of m.e.c. are its applicability to a variety of compounds with a wide range of molecular weights and the close relationship found between the retention time (or retention volume) and the molecular

0003-2670/86/$03.50

size (or molecular weight) of a solute. The method has proved valuable not only in polymer chemistry but also in other fields. Molecular exclusion (gel permeation) chromatography is widely used in the analysis of petroleum samples. Especially, the preparative m.e.c. technique is effective as the first separation for a complicated sample in preference to complementary separations. Although the interpretation of the chromatograms is less straightforward for fossil fuels than for polymers, the method allows at least relative determinations of molecular size and, with certain provisions, molecular weight [8]. Most applications of m.e.c. to petroleum samples have been used to obtain information about their organic components, and the method has rarely been used to obtain information about the metal-containing species in petroleums. However, extensive experience of the m.e.c. behavior of metal complexes [9—13] suggested that m.e.c. should be useful for separations of metal-containing species in petroleum.

The elution profiles of vanadium and nickel species as well as that of the total organics are investigated in the present work. In order to facilitate qualitative information about the eluting species, the absorption spectra of the column effluent were monitored continuously by an ultraviolet-visible multiwavelength detector.

EXPERIMENTAL

Materials

The residual oil sample from a Middle East heavy crude oil was kindly supplied by Idemitsu Petrochemical Co., Tokyo. The vanadium and nickel contents of this sample were previously found to be 164 ± 11 and 53.4 ± 0.4 mg kg^{-1}, respectively [7].

The standard solutions used for atomic absorption spectrometry were prepared from 99.9% vanadium and 99.99% nickel metals. Vanadyl and nickel etioporphyrins (VOEtio and NiEtio, respectively) were prepared as described earlier [14]. The standards used for the preparation of a m.e.c. calibration curve were monodisperse polystyrenes of molecular weight (m.w.) 200 000, 10 000, 4000, 2300, 900 and 500, mesitylene (m.w. 120) and acetone (m.w. 58).

Benzene and methanol were of reagent grade; nitric and sulfuric acids were analytical-grade materials (Wako Pure Chemicals, Osaka). Water was double-distilled in glass apparatus.

Instrumentation

Determination of vanadium and nickel. A flame atomic absorption spectrometer (Nippon Jarrell-Ash, Model AA-1) was used; the instrumental conditions were as described previously [7].

Chromatographic system. The column was packed in a pyrex tube (52 cm × 17.5-mm i.d.) with Shodex 801 gel which was kindly supplied by the maker (Showa Denko, Tokyo). The benzene/methanol eluent (95:5, v/v) was

delivered to the column by a Kusano KP-6S pump (Tokyo) at a flow rate of 1.22 ml min^{-1}. A rapid-scanning ultraviolet-visible multiwavelength detector (MWD) [15] was used for the experiments on the residual oil sample. This detector sweeps the spectral range from 200 to 800 nm in 750 ms, with a repetition rate of 1 Hz. The absorption spectrum of the column effluent was displayed at each optical scan and also recorded at rapid intervals, so that three-dimensional chromatograms could be obtained.

In the calibration procedure for the chromatographic column, a refractive index detector (LDC Model 1107L) was used instead of the MWD.

Procedure

A 2-g portion of the residual oil sample was dissolved in 20 ml of benzene. After passing through a 0.45-μm membrane filter, the solution was diluted to 40 ml with benzene. A 0.40-ml portion of this solution was injected into the m.e.c. column. The eluent flow rate was 1.22 ml min^{-1}. The chromatograms were recorded simultaneously at detector wavelengths of 370 and 405 nm. Real-time monitoring of the absorption spectra of the column effluent was also done with the MWD as described above. The column effluent was collected in fractions every 3 min.

The same chromatographic treatment was repeated ten times in order to collect enough of the desired fractions of the column effluent. All the m.e.c. experiments were done at 25°C.

The separate 3-min fractions of the ten effluents were combined appropriately and heated at about 80°C for 1 h in a quartz crucible placed on a hot plate under an infrared lamp. After additional heating at 150°C for 1 h, the non-volatile residue obtained was cooled in a desiccator and then weighed. The residue was regarded as the total organic material eluted in the relevant fraction of column effluent.

The non-volatile organic material obtained in the above-mentioned procedure was digested with concentrated sulfuric acid at 250°C until no fumes were evolved. This material was ashed with temperature programming from 200 to 520°C and then held at 520°C for 12 h. The ash was dissolved in diluted nitric acid, evaporated to dryness, redissolved in 0.5 ml of concentrated nitric acid, and finally diluted to 25 ml with water, as described previously [7]. This aqueous solution was used for atomic absorption spectrometry. Vanadium and nickel were evaluated from calibration graphs [7].

RESULTS AND DISCUSSION

Calibration of the chromatographic column

Benzene was used initially as the solvent for m.e.c. of the present oil sample, but undesirable adsorption of some colored materials on the column was observed. When the solvent contained methanol at 5% (v/v), the colored material migrated through the column. So, 95:5 benzene/methanol was used as the eluent.

The column was characterized, in the usual way, by the molecular weight range suitable for separation on the basis of size-exclusion. In order to obtain accurate determinations of molecular weight, the column has to be calibrated by using the compound to be tested and its homologues, because the retention is not always the same for various types of compounds even if they have the same molecular size [11, 12]. When the present type of column was calibrated for the sake of convenience with polystyrene standards of molecular weight 500—200 000, mesitylene and acetone, the exclusion limit of the column was found to occur at m.w. ≈ 5000. All test compounds (polystyrene) with m.w. >5000 were eluted in the column void volume (V_o = 19 ml); the column hold-up time (t_o) was 15.5 min at the eluent flow rate of 1.22 ml min^{-1}. For compounds with m.w. <5000, the retention volume (V_r) and retention time (t_r) increased as the molecular weight of the compound decreased. Thus, the available molecular weight range for the size-exclusive separation was measured to be up to 5000 on this column.

Because residual oil is not a simple mixture of homologous compounds, the calibration graph prepared with polystyrene is not valid for accurate determination of the molecular weights of components of the oil. However, it is useful for discussing the relative molecular weight or size of the components. The molecular weight of some components of the residual oil were estimated in this work on the basis of the column calibration with polystyrene standards for the sake of convenience, unless otherwise noted.

Multiwavelength detection of the chromatogram

There is no particular wavelength at which the chromatogram has to be recorded in the analysis of residual oil. Because the oil is a very complex mixture, monitoring at a fixed wavelength cannot be effective for detection. Real-time monitoring of the absorption spectrum, however, is powerful in obtaining qualitative information about the eluting species.

The rapid-scanning u.v.-visible detector (MWD) was designed [15] so that the spectra of the eluting species could be recorded in the 200—800-nm range without interruption of the elution, and also to record simultaneously the chromatograms at at least two wavelengths. The MWD was used effectively in m.e.c. studies on metal complexes of β-diketones [13, 15] and in h.p.l.c. studies on metal tetraphenylporphyrin complexes [16] to confirm the elution of these complexes without degradation on the columns.

Figure 1 shows the molecular exclusion chromatograms of the present residual oil recorded simultaneously at 370 and 405 nm. The elution of sample components is detected over the whole range of retention times available for the chromatographic separation, which means that the oil consists of various components with molecular weights up to at least about 5000. Both chromatograms in Fig. 1 show elution peaks at a retention time (t_r) of about 21 min (corresponding to $V_r \approx 26$ ml). The shoulder peak found at about 29 min ($V_r \approx 35$ ml) appears more clearly on the chromatogram recorded at 405 nm than on that obtained at 370 nm. This phenomenon is easily ex-

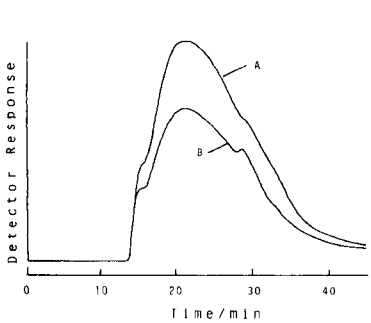

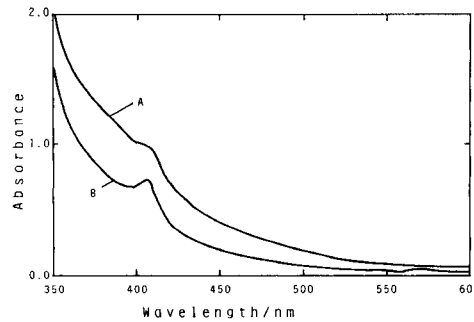

Fig. 1. Chromatograms of the residual oil recorded at different wavelengths: (A) 370 nm; (B) 405 nm. Conditions: Shodex 801 column (52 cm × 17.5-mm i.d.), benzene/methanol (95:5) eluent at 1.22 ml min^{-1}, 25°C.

Fig. 2. Absorption spectra of the column effluent at different retention times: (A) 21 min; (B) 29 min.

plained from the spectrum recorded at 29 min. The eluting species at 29 min show characteristic absorption around 400 nm but not around 370 nm (Fig. 2); similar but fainter characteristic absorption around 400 nm is exhibited by the species eluting at 21 min (cf. Fig. 1). It is clear that the spectra of eluting species should be recorded at short time intervals and then compared.

Figure 3 is a three-dimensional representation of the chromatogram, i.e., a plot of the absorbance vs. wavelength vs. time. In all experiments, the absorption spectra in the range 200—800 nm were monitored every second during

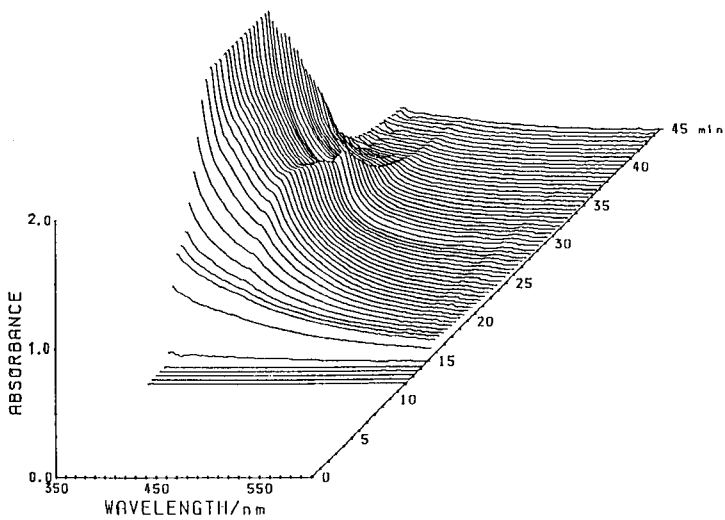

Fig. 3. Three-dimensional chromatogram for the separation of the residual oil sample. Chromatographic conditions as in Fig. 1.

the elution, but for clarity only the spectra over 350—600 nm at 32-s intervals are shown in Fig. 3. It is obvious from this chromatogram that most components of the residual oil absorb strongly in the ultraviolet region. It is notable that components with absorption maxima around 400 nm are eluted from the column over a wide range of elution times.

Elution profile of organic components

The elution profile of the residual oil with respect to the organic components is shown as a histogram in Fig. 4. The amount of non-volatile organic substances per unit volume of column effluent is represented as a function of V_r. Obviously, the residual oil contains organic components of a wide range of molecular weights and the predominant species have molecular weights in the range of several hundreds to nearly 2000. The chromatogram recorded at 405 nm is superimposed on the histogram in Fig. 4; there is considerable correspondence between the profiles.

Elution profile of vanadium- or nickel-containing species

The vanadium and nickel contents of each fraction of the column effluent were determined by atomic absorption spectrometry. The elution profiles of vanadium and nickel are shown as histograms in Fig. 5. Both vanadium and nickel were eluted over the full molecular-weight range available with the column (i.e., up to about 5000 in the case of polystyrene). This indicates

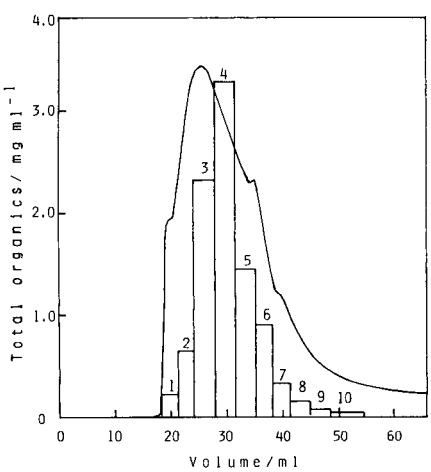

Fig. 4. The elution profile of total organic components of the residual oil (histogram) and the chromatogram obtained by detection at 405 nm (curve). Chromatographic conditions as in Fig. 1.

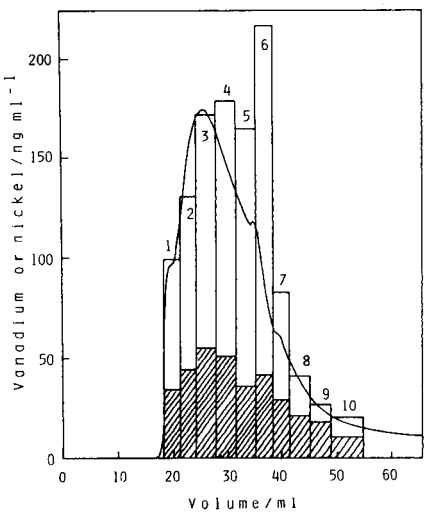

Fig. 5. The elution profiles of vanadium (open histogram) and of nickel (shaded histogram), and the chromatogram obtained by detection at 405 nm (curve). Chromatographic conditions as in Fig. 1.

that both vanadium and nickel are present in various chemical species of different molecular weights. The elution profiles of the two metals differ (Fig. 5); vanadium shows its highest elution peak in fraction 6 (V_r = 35.4—38.4 ml; t_r = 29.0—31.5 min), whereas nickel has its elution peak in fraction 3 (V_r = 24.4—28.1 ml; t_r = 20.0—23.0 min). Fraction 6 is assigned to lower molecular weights than fraction 3. This means that the predominant chemical species of vanadium and nickel in the residual oil are somewhat different.

The chromatogram obtained by detection at 405 nm is superimposed on the elution profiles for vanadium and nickel in Fig. 5. This chromatogram is similar to the elution profile for nickel rather than that for vanadium. However, the shoulder peak appears in the region of the highest vanadium elution ($V_r \approx 35$ ml; $t_r \approx 29$ min). The contributions of nickel-containing species to the absorption profile cannot be neglected but the dominant contribution of vanadium-containing species having a characteristic absorption at around 405 nm is clearly observed. Promising candidates for such compounds are porphyrins. The presence of metalloporphyrins, especially vanadium porphyrins, in fossil oil has been suggested [17, 18] and the characteristic intense absorption bands of porphyrin compounds around 400 nm are well known as the "Soret band" [19].

In order to examine the validity of the above idea, the same chromatographic examination was applied to the residual oil containing added vanadium and nickel etioporphyrins (VOEtio, NiEtio) which were chosen as model compounds of petroporphyrin. The VOEtio and NiEtio were eluted at 27 min (V_r = 32 ml) and 28 min (V_r = 34 ml), respectively. As shown in Fig. 6, the distinct absorption maximum related to VOEtio is observed at 27 min.

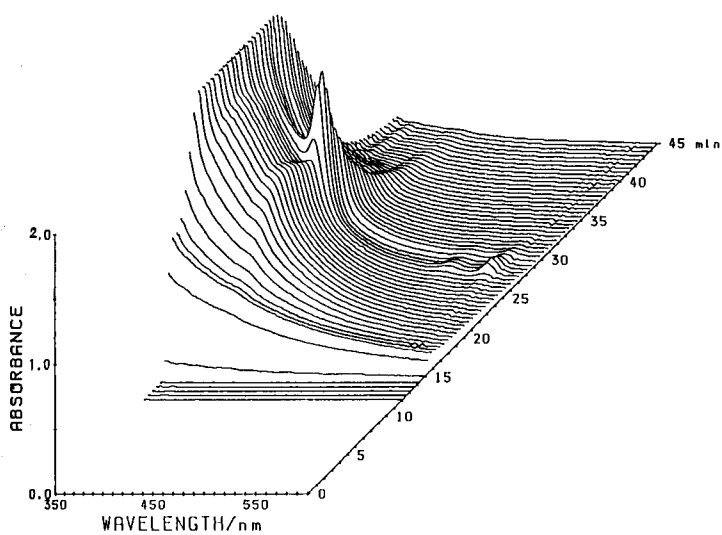

Fig. 6. Three-dimensional chromatogram for the separation of the residual oil containing added VOEtio at a concentration of 24 μmol l^{-1}. Chromatographic conditions as in Fig. 1.

The situation is, of course, more complicated because components having absorption maxima at around 400 nm appear over a wide range of elution times (see Fig. 3). Although the evidence is not yet sufficiently clear-cut for definite identification, these components are considered to be some sort of porphyrin compounds or their aggregates. It is expected that more detailed information about metal species in petroleum will be obtained by coupling the present approach with the leaching procedures with various solvents [7]. This will be dealt with in a subsequent paper.

The authors thank Idemitsu Petrochemical Co., Tokyo, and Showa Denko, Tokyo, for providing the residual oil sample and the column packing material, respectively.

REFERENCES

1 R. H. Hofstader, O. I. Milner and J. H. Runnels (Eds.), Analysis of Petroleum for Trace Metals, Am. Chem. Soc., Washington DC, 1976.
2 K. R. Shar, R. H. Filby and W. A. Haller, J. Radioanal. Chem., 6 (1970) 413.
3 F. E. Dickson, C. J. Cunesh, E. L. McGinnis and L. Petrakis, Anal. Chem., 44 (1972) 978.
4 T. Sasaki, S. Hagi and H. Yamamoto, Sekiyu Gakkai Shi, 23 (1980) 210.
5 R. E. Kauffman, C. S. Seba and W. E. Rhine, Anal. Chem., 54 (1982) 975.
6 J. Wieckowska, Mikrochim. Acta, 1 (1982) 195.
7 T. Tsukada, K. Saitoh and N. Suzuki, Anal. Chim. Acta, 183 (1986) 89.
8 K. H. Altgelt, in K. H. Altgelt and T. H. Gouw (Eds.), Chromatography in Petroleum Analysis, M. Dekker, New York, 1979, p. 287.
9 N. Suzuki and K. Saitoh, Bull. Chem. Soc. Jpn., 50 (1977) 2907.
10 N. Suzuki, K. Saitoh and M. Shibukawa, J. Chromatogr., 138 (1977) 79.
11 K. Saitoh and N. Suzuki, Bull. Chem. Soc. Jpn., 51 (1978) 116.
12 H. Noda, K. Saitoh and N. Suzuki, J. Chromatogr., 168 (1979) 250.
13 K. Saitoh and N. Suzuki, Anal. Chem., 52 (1980) 30.
14 S. Miyake, K. Sitoh and N. Suzuki, Chromatographia, 20 (1985) 417.
15 K. Saitoh and N. Suzuki, Anal. Chem., 51 (1979) 1683.
16 N. Suzuki and K. Saitoh, in H. Hatano (Ed.), High Resolution Chromatography, Nankodo, Tokyo, 1983, p. 134.
17 H. N. Dunning, J. W. Moore and A. T. Myers, Ind. Eng. Chem., 46 (1954) 2000.
18 T. F. Yen, L. J. Boucher, J. P. Dickie, E. C. Tynan and G. B. Vaughan, J. Inst. Pet., London, 55 (1969) 87.
19 K. M. Smith, in K. M. Smith (Ed.), Porphyrins and Metalloporphyrins, Elsevier, Amsterdam, 1975, p. 19.

Analytica Chimica Acta, 183 (1986) 105—128
Elsevier Science Publishers B.V., Amsterdam — Printed in The Netherlands

THE INFLUENCE OF OPERATING CONDITIONS ON THE EVALUATION OF BIOLOGICAL MARKER COMPOUND DISTRIBUTIONS IN PETROLEUM GEOCHEMISTRY BY GAS CHROMATOGRAPHY AND GAS CHROMATOGRAPHY/MASS SPECTROMETRY

STEPHEN D. KILLOPS[a]

Masspec Analytical, Wallbridge, Stroud, Gloucestershire (Great Britain)

(Received 3rd July 1985)

SUMMARY

The effects of the operating conditions for gas chromatography and gas chromatography/mass spectrometry (g.c./m.s.) on the observed distributions of biological marker compounds in petroleum are considered. Resolution and the accuracy and precision of quantification were investigated for components of geochemical significance. Methylsilicone stationary phases were generally suitable for aliphatic biomarker analysis, although some components co-eluted on these phases. The inclusion of ca. 5% phenyl groups into methylsilicone phases provided improved resolution of certain alkane biomarkers, and also allowed satisfactory analysis of classes of aromatic biomarker compounds. Vaporising and non-vaporising injection techniques in g.c./m.s. were compared for accuracy and reproducibility of relative component quantification. Cooled on-column injection was found to be the most suitable technique in biomarker analysis. The effect of long-term variation in the operating conditions for the spectrometer on the reproducibility of quantification data was found to be at least as significant as the effect of the sample injection technique.

A small proportion (<5%) of the organic constituents of sediments is readily solvent-extractable and comprises components which can be directly attributed to compounds found in plants, animals and bacteria. These compounds are commonly termed "biological markers" (or "biomarkers") and have recognisable molecular skeletons, which can remain virtually unchanged in sediments for long periods of time. The alterations that do occur in the molecular structures follow a systematic pattern. Molecular maturation occurs as a result of increasing temperature, sediment depth, pressure and time. During the diagenetic processes, biologically derived molecules are changed into thermodynamically more stable forms by a combination of reduction, defunctionalisation, rearrangement, aromatisation and stereochemical isomerisation, which can be dependent upon the sedimentary environment.

[a]Present address: 52 Lypiatt View, Bussage, Stroud, Gloucs., Great Britain.

0003-2670/86/$03.50

Analysis of biological marker compounds in oils and sediments can give much useful information, such as thermal history from the extent of molecular maturation, oil/oil and oil/source rock correlation, sedimentation conditions and the effects of migration and biodegradation (the applications of biological markers in petroleum geochemistry have been reviewed [1]). Among the compound types frequently studied are isoprenoidal acyclic alkanes, terpenoidal alkanes, steroidal alkanes and aromatic steroidal hydrocarbons.

Several molecular maturity parameters have been developed [1] which can provide numerical evaluation of the relative degree to which various thermally-mediated, molecular alterations have progressed. Among these processes are the degree of configurational isomerisation at an acyclic centre in steranes and hopanes, and aromatisation of C-ring monoaromatic steroidal hydrocarbons (see Fig. 1).

A typical analysis involves obtaining a total neutrals fraction from the extractable lipids, which can be further fractionated into aliphatic and aromatic fractions. Both of these fractions are usually complex mixtures, requiring high-resolution (i.e., capillary column) gas-liquid chromatography (g.c.) to provide adequate resolution of components. Normal and isoprenoidal alkanes can be present in sufficiently large amounts to be analysed by high-resolution g.c. with a flame ionisation detector (where extensive biodegradation has not preferentially removed these components [2]). However, steroidal

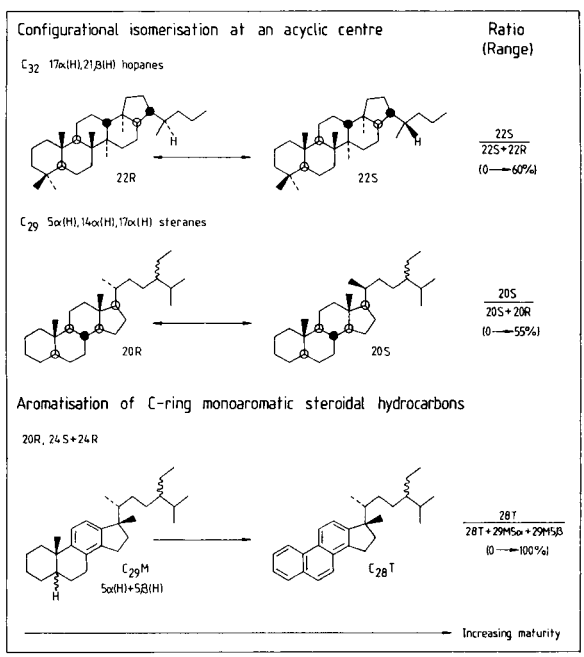

Fig. 1. Three major biomarker reactions used to assess maturity of oils, and their numerical evaluation. (See ref. 1 and references therein.)

and terpenoidal hydrocarbons are often present in minor abundances, which, in conjunction with the complexity of hydrocarbon fractions, makes gas chromatography/mass spectrometry (g.c./m.s.) necessary to elucidate component distributions.

The importance of biomarker analysis in petroleum geochemistry has grown in recent years; this places increasing emphasis on the optimisation of the chromatographic techniques used and on the efficient use of analysis time. The major requirements for g.c./m.s. analysis of biomarker compound distributions are that: (i) adequate resolution of components can be achieved to allow precise identification of compounds; (ii) results are reproducible, permitting meaningful comparison of samples over long periods of time; (iii) quantification of components is accurate in order to allow accurate evaluation of geochemical parameters. While these requirements apply quite generally, they have not always been adequately considered in biomarker analysis. Some specific problems encountered in petroleum geochemistry are investigated in this paper.

EXPERIMENTAL

Comparison of OV-1 and SE-52 for alkane biomarker analysis

A Carlo Erba 4160 gas chromatograph fitted with a Grob split/splitless injector [3] and a cooled, on-column injector [4] was used with helium carrier gas (1.0 kg cm^{-2}, ca. 3 cm^3 min^{-1}). Samples were injected in toluene solution (0.5 μl) via the cooled, on-column injector. Fused silica columns were used: 25 m × 0.32 mm i.d., 0.17-μm WCOT, bonded-phase OV-1 or SE-52 (Hewlett-Packard). The temperature programme was 1 min at 100° C, 100—150° C at 10° min^{-1} and 150—300° C at 6° min^{-1}.

The columns were taken directly through to the ion source of a Finnigan 3200 quadrupole mass spectrometer. The spectrometer was operated in the electron ionisation mode, with the following typical conditions: analyser temperature ca. 70° C; transfer-line temperature ca. 250° C; filament current 300 μA; electron energy 30 eV. Data acquisition and processing were controlled by an INCOS 2015 (Nova 4) computer. Multiple ion detection (MID) with a total scan time of 1 s was used (seven ions with a dwell time of 135 ms/ion). Data acquisition commenced at 150° C.

Comparison of stationary phases for aromatic steroidal hydrocarbon analysis

The g.c./m.s. analysis was conducted with three ion MID (270 ms/ion dwell time) and a total scan time of 1 s. Helium carrier-gas flows of ca. 3 cm^3 min^{-1} were used with the following four columns. Column (a) was a 25 m × 0.32 mm i.d., 0.15-μm WCOT bonded OV-1, fused silica column (Erba Science, Mega), with a carrier-gas inlet pressure of 1.0 kg cm^{-2}. Cooled, on-column injection (0.5 μl toluene solution) was used. The column was taken directly through to the m.s. ion source. Column (b) was a 25 m × 0.3 mm i.d. persilylated [5], 0.3-μm WCOT OV-73, soda-glass column, with a carrier-gas

inlet pressure of 1.2 kg cm^{-2}. The sample (1 μl of toluene solution) was injected via the splitless, vaporising injector (injector temperature 300°C), using an "in-barrel", hot needle technique (see below). Column eluate was taken through to the m.s. ion source via a short length of deactivated (uncoated) fused silica (ca. 50 cm × 0.25 mm i.d., SGE), butt-jointed to the glass capillary column with a low dead-volume, glass lined union (SGE). Column (c) was a 12 m × 0.33 mm i.d., 0.5-μm WCOT bonded OV-1701 (BP-10, SGE), fused silica column, with a carrier-gas inlet pressure of 0.2 kg cm^{-2}. Cooled, on-column injection (0.5 μl of toluene solution) was used, and the column was taken directly through to the m.s. ion source. Column (d) was a 10 m × 0.23 mm i.d., ca. 0.2-μm WCOT OV-17, glass column (SGE), with a carrier-gas inlet pressure of 0.3 kg cm^{-2}. Splitless, "in-barrel", hot needle injection (1 μl of toluene solution) was used (see below), with an injector temperature of 300°C. Column eluate was taken through to the m.s. ion source via a short length of fused silica column, as for column (b) above.

For all analyses, the temperature programme was 1 min at 100°C, 100°C to upper temperature limit (UTL) at 6° min^{-1}, and an isothermal period (as necessary) at the UTL. For OV-1 and OV-73, the UTL was 300°C, and for OV-1701 and OV-17 the UTL was 250°C. Other g.c./m.s. conditions were as described above for alkanes.

Comparison of stationary phases for g.c. of methylphenanthrenes

Carlo Erba 5360 (with Grob split/splitless [3] and on-column [4] injectors) and 4130 (with Grob split/splitless injector [3]) chromatographs were used with flame ionisation detection. Samples were injected in hexane solution, and the temperature programme was 1 min at 60°C, then 60°C to UTL at 6° min^{-1} (UTLs were the same as indicated immediately above).

A helium carrier-gas flow rate of ca. 3 cm^3 min^{-1} was used with the following five columns. Column (a) was a 10 m × 0.23 mm i.d., ca. 0.2-μm WCOT OV-17, glass column (SGE), with a carrier gas pressure of 0.5 kg cm^{-2}, and splitless, "in-barrel", hot needle injection (1 μl, see below). Column (b) was a 20 m × 0.25 mm i.d., persilylated [5], 0.25-μm WCOT OV-73, Pyrex glass column, with a carrier-gas pressure of 1.8 kg cm^{-2}, and splitless, "in-barrel", hot needle injection (1 μl, see below). Column (c) was a 25 m × 0.32 mm i.d., 0.17-μm WCOT bonded OV-1 ("new"), fused silica column (Hewlett-Packard), with a carrier-gas pressure of 1.2 kg cm^{-2}, and cooled, on-column injection (0.5 μl). Column (d) was a 20 m × 0.32 mm i.d., 0.15-μm WCOT bonded OV-1 ("old"), fused silica column (Erba Science, Mega), with a carrier-gas pressure of 1.0 kg cm^{-2}, and cooled, on-column injection (0.5 μl). Column (e) was a 25 m × 0.32 mm i.d., 0.17-μm WCOT bonded SE-52, fused silica column (Hewlett-Packard), with a carrier-gas pressure of 1.2 kg cm^{-2}, and cooled, on-column injection (0.5 μl).

Comparison of splitless, vaporising injection techniques

A Finnigan 4300 gas chromatograph with Grob splitless injector [3] (ca. 1 cm^3 volume), and an injector temperature of 300°C, was used with a

20 m × 0.25 mm i.d., ca. 0.3-μm WCOT OV-1, glass column (Jaeggi) and helium carrier gas (ca. 1.2 kg cm^{-2}, ca. 3 cm^3 min^{-1}). Samples were injected in hexane solution (1 μl), with the split closed 30 s before injection and opened 30 s after injection. The column eluate was taken through to the ion source of a Finnigan 3200 quadrupole mass spectrometer via a platinum/iridium capillary. A temperature programme of 1 min at 50°C, then 50 to 120°C at 20° min^{-1} and 120 to 300°C at 6° min^{-1} was used for aliphatic fractions (oil 1), with data acquisition commencing at 120°C. For aromatic fractions (oil 2) the temperature programme was 1 min at 50°C, then 50—160°C at 20° min^{-1} and 160—300°C at 6° min^{-1} (data acquisition commenced at 160°C). Other g.c./m.s. conditions were as given above for the comparison of OV-1 and SE-52 columns.

For the "in-needle" technique, sample was injected immediately after introduction of the syringe needle into the injector, using a plunger-in-needle syringe (1 μl, SGE), and the needle was left in the injector for ca. 20 s after injection. For the "in-barrel" technique, a plunger-in-barrel syringe was used (10 μl, SGE); the syringe needle was allowed to warm in the injector for ca. 3 s prior to rapid injection and was removed immediately after injection.

Comparison of splitless, vaporising and cooled, on-column injection techniques

General g.c./m.s. conditions were as described above. The split/splitless injector [3] of the Carlo Erba 4160 chromatograph was operated at 300°C, and had a volume of ca. 1 cm^3 (the glass liner dimensions were: length 79.5 mm, o.d. 5.5 mm, i.d. 4 mm). Helium carrier gas was used at 1.0 kg cm^{-2} inlet pressure (ca. 3 cm^3 min^{-1}) for both splitless and cooled, on-column injection. A 25 m × 0.32 mm i.d., 0.15-μm WCOT bonded OV-1, fused silica column (Erba Science, Mega) was used for aliphatic fractions (oil 3), with a temperature programme of 1 min at 120°C and 120—300°C at 6° min^{-1} (data acquisition commenced at 150°C). A 25 m × 0.32 mm i.d., 0.17-μm WCOT bonded SE-52, fused silica column (Hewlett-Packard) was used for aromatic fractions (oil 4), with a temperature programme of 1 min at 120°C, 120—180°C at 10° min^{-1} and 180—300°C at 6° min^{-1} (data acquisition commenced at 160°C). The columns were taken directly through to the m.s. ion source.

Samples were injected in toluene solution. For the splitless injection, a 1-μl "in-barrel", hot needle method was used (as above); for the cooled, on-column injection, 0.5 μl of sample was injected rapidly, from a syringe designed for use with the Carlo Erba injector (5 μl, plunger-in-barrel, 7.5-cm needle, SGE).

RESULTS AND DISCUSSION

Adequate resolution of components, accurate quantification and reproducible results are prerequisites of biomarker compound analysis by g.c./m.s. Various factors can affect these requirements, such as choice of stationary phase, sample injection method and m.s. operating conditions. The effects of

these factors are examined and discussed for typical oil and sediment samples in the following sections.

Selection of stationary phase for aliphatic hydrocarbons

Methyl polysiloxane stationary phases (e.g., OV-1, OV-101, SE-30) are the commonest choice for the analysis of biomarker alkanes, a major reason being that identification of a wide range of sterane and terpane biomarkers has been established by relative retention times in single ion chromatograms using OV-1 stationary phase [6–11]. Given this choice of stationary phase, it should be remembered that other column parameters (such as the residual acidity/basicity and deactivation of the glass surface, the degree of polymerisation and cross-linking of the phase, and the phase thickness) can significantly affect column performance [12, 13], in addition to the effects of g.c. operating conditions (e.g., carrier-gas flow and temperature programme). While OV-1 generally provides adequate resolution of biomarker alkanes from oils, there are occasions when improved resolution of certain components would be desirable. In order to investigate the effects of changing the stationary phase on resolution of components, a comparison was made of the relative elution orders of biomarker alkanes on OV-1 and SE-52 (5% phenyl methylsilicone).

It can be seen in the *m/z* 191 single-ion chromatogram (Fig. 2) that component Ts (a C_{27} pentacyclic terpane; structure 5, Fig. 3) co-elutes with a C_{29} tricyclic terpane and that gammacerane (Gam, a pentacyclic terpane of terrigenous, higher plant origin; structure 8, Fig. 3) co-elutes with C_{31} 17α, 21β, 22R hopane on OV-1 stationary phase. On SE-52 stationary phase, both these pairs of components are resolved. However, there may be a co-eluant in the Tm peak on SE-52, shown by comparison of the Tm relative responses on both phases. In this example, multiple ion detection was used, as the biomarker concentrations were insufficient to permit adequate analysis by data collection over a wide mass range. Thus, on OV-1 it would not be possible to establish positively the presence of the terrigenous indicator, gammacerane (without including its molecular ion in the MID scan), or to quantify accurately component Ts (the ratio Ts/Tm for a suite of related samples appears to increase with increasing maturity [6]). In contrast to the observed behaviour of terpanes, the elution order of steranes (*m/z* 217 ion chromatogram, Fig. 2) on SE-52 appeared to be nearly identical to that on OV-1 stationary phase.

Differences were observed in the relative retention patterns of acyclic alkanes on OV-1 and SE-52. Baseline resolution of n-heptadecane and pristane (Pr) is possible on OV-1, but not on SE-52 (Fig. 2, *m/z* 183 ion chromatograms) and similar stationary phases for a 25-m column and helium carrier gas. Resolution of isoprenoidal from normal alkanes is necessary if the ratio Ph/Pr is to be used to assess anoxicity in sediments [14]. It should also be noted that, while the resolution of the component pairs n-heptadecane/pristane and n-octadecane/phytane was greater on OV-1 than SE-52, n-nonadecane

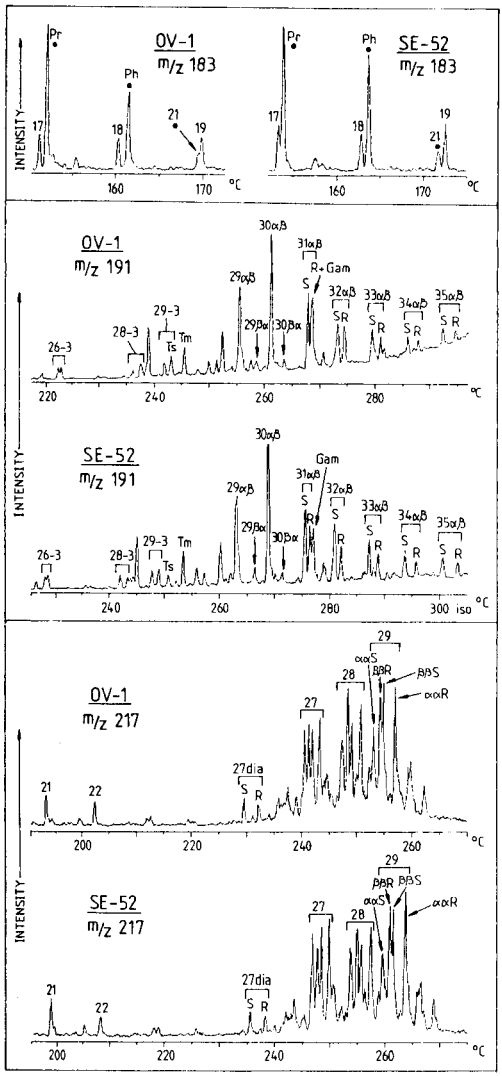

Fig. 2. Partial single-ion chromatograms (g.c./m.s. with multiple-ion detection) comparing the effects of changing stationary phase on the observed relative elution orders of acyclic alkanes (*m/z* 183), terpanes (*m/z* 191) and steranes (*m/z* 217) from an oil. (In *m/z* 183 on chromatograms, numerals represent n-alkane carbon numbers and • represents isoprenoidal alkanes. See Table 1 and Fig. 3 for component identifications.)

and a C_{21} isoprenoidal alkane were resolved on SE-52, but not on OV-1 (Fig. 2, *m/z* 183 ion chromatograms).

While both columns were nominally identical, apart from the stationary phase formulation (i.e., 25 m × 0.32 mm i.d. 0.17 μm WCOT bonded phase, fused silica columns from Hewlett-Packard), under the same analytical

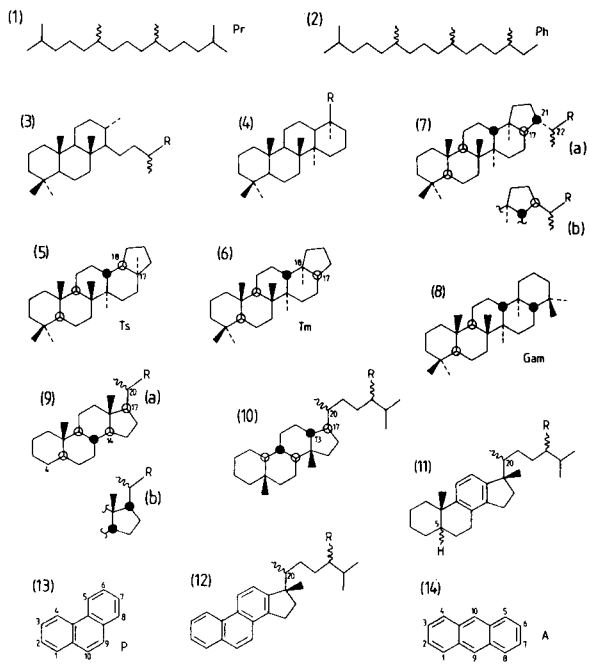

Fig. 3. Representative structures of biomarker compounds. (See Table 1 for identifications.)

conditions (including identical carrier gas pressure), alkanes appeared to be retained on the SE-52 column for a longer period than on the OV-1 column (e.g., the C_{35} 17α, 21β, 22S/R hopanes eluted prior to 300°C on OV-1, but eluted in the isothermal period at 300°C on SE-52). Further, the tricyclic terpanes seemed relatively less well retained than the pentacyclic terpanes on SE-52 than on OV-1.

It seems that, while it is possible to obtain most of the necessary biomarker compound data upon OV-1 stationary phase, SE-52 can provide useful, additional data, where the acquisition of such data justifies the extra time involved. It is debatable whether alkane biomarker analysis using SE-52 stationary phase alone would provide more useful data than those obtained from OV-1.

Selection of stationary phase for aromatic hydrocarbons

The analysis of aromatic biomarkers by g.c./m.s. has become of interest relatively recently and is probably less often applied than that of aliphatic biomarkers. Because frequent changing of capillary columns in g.c./m.s. systems can be inconvenient, aromatic hydrocarbons have been analysed on the same OV-1 columns used for alkanes (see e.g. [15]), as well as on the theoretically more suitable SE-52 and SE-54 (5% phenyl, 1% vinyl methylsilicone) phases. It would be expected that a stationary phase containing

TABLE 1

Identification of biomarkers referred to in text and figures (see Fig. 3 for structures)

Abbreviation	Identification	Structure (see Fig. 3)
Isoprenoidal alkanes		
Pr	pristane	1
Ph	phytane	2
Terpanes		
23-3, 24-3, 25-3, 26-3, 28-3, 29-3	C_{23}-C_{29} tricyclic terpanes	3 R=H to C_5H_{11}
24-4	C_{24} tetracyclic terpane	4
Ts	18α(H)-22,29,30-trisnorhopane II	5
Tm	17α(H)-22,29,30-trisnorhopane	6
29αβ	17α(H),21β(H)-30-norhopane	7a R=H
29βα	17β(H),21α(H)-30-norhopane	7b R=H
30αβ	17α(H),21β(H)-hopane	7a R=CH_3
30βα	17β(H),21α(H)-hopane	7b R=CH_3
31αβS/R	22S and 22R isomers of 17α(H),21β(H) C_{31}-C_{35} hopanes	7a R=C_2H_5
32αβS/R		7a R=C_3H_7
33αβS/R		7a R=C_4H_9
34αβS/R		7a R=C_5H_{11}
35αβS/R		7a R=C_6H_{13}
Gam	gammacerane	8
Steranes		
21	4α(H),5α(H),17α(H) C_{21} and C_{22} steranes	9a R=H
22		9a R=CH_3
22-4Me	4-methyl 4α(H),5α(H),17α(H) C_{22} and C_{23} steranes	As for 21 and 22 + CH_3 at C4
23-4Me		
27diaS/R	20S and 20R isomers of C_{27} 13β(H), 17α(H)diasterane	10 R=H
27	cholestanes	9 R=C_6H_{13} [a]
28	24-methylcholestanes	9 R=C_7H_{15} [a]
29ααR/S	20R and 20S isomers of 5α(H), 14α(H),17α(H)-24-ethylcholestane	9a R=C_7H_{15} [a]
29ββR/S	20R and 20S isomers of 5α(H), 14β(H),17β(H)-24-ethylcholestane	9a R=C_8H_{17} [a]
Monoaromatic steroidal hydrocarbons		
21	C_{21} and C_{22} monoaromatics	11 [b]
22		11 [b]
27βS/R, 27αS/R, 28βS/R, 28αS/R, 29βS/R, 29αS/R	20S and 20R, 5β(H) and 5α(H) isomers of C_{27}-C_{29} monoaromatics	11 R=H
		11 R=H
		11 R=CH_3
		11 R=CH_3
		11 R=C_2H_5
		11 R=C_2H_5

TABLE 1 (continued)

Abbreviation	Identification	Structure (see Fig. 3)
Triaromatic steroidal hydrocarbons		
20	C_{20} and C_{21} triaromatics	12[c]
21		12[c]
26S/R	20S and 20R isomers of C_{26}-C_{28} triaromatics	12 R=H
27S/R		12 R=CH_3
28S/R		12 R=C_2H_5
Polynuclear aromatic hydrocarbons		
P	phenanthrene	13[d]
A	anthracene	14[d]

[a]Side-chain configuration as in structure **10**, where R=H, CH_3 and C_2H_5 for C_{27}, C_{28} and C_{29}, respectively. [b]Nuclear structure as in structure **11**, but with alkyl side-chain as for steranes **21** and **22**. [c]Nuclear structure as in structure **12**, but with alkyl side-chain as for steranes **21** and **22**. [d]Ring numbering convention for position of substituents is given in structures **13** and **14**.

phenyl groups would provide greater resolution and capacity factor for aromatic hydrocarbons than OV-1 [12, 13].

The degree of aromatisation of biomarkers is known to increase with maturity, and so the extent of conversion of mono- to tri-aromatic steroidal hydrocarbons can provide maturity information [16]. The postulated aromatisation process is shown in Fig. 1. Aromatic steroidal hydrocarbons are generally present in such low abundance that g.c./m.s. with multiple ion detection is necessary. Separation of these compounds on four different columns was studied to establish the effects of selectivity/polarity of the stationary phase on resolution. The apolar methylsilicone phase OV-1 was compared with the apolar phenyl group-containing phases OV-73 (5.5% phenyl methylsilicone) and OV-17 (50% phenyl methylsilicone), and with the more polar OV-1701 (7% phenyl, 7% cyanopropyl methylsilicone).

As could be expected, the monoaromatic components with long alkyl chains (which are essentially aliphatic in nature) were generally well resolved on OV-1 (Fig. 4). Overall resolution of monoaromatics on OV-73 did not appear to be as good as that on OV-1 (Fig. 4). However, the monoaromatic components used in maturity calculations (29αR and 29βR, Fig. 4; see also Fig. 1) seemed to be resolved on OV-73, but not on OV-1, upon which 28αR co-eluted with 29βR [17]. In addition, chromatography of triaromatic components was improved on OV-73. Therefore, in assessing maturity from aromatic steroidal hydrocarbons, OV-73 is to be preferred to OV-1, but distributions of individual monoaromatics can be assessed better on OV-1 than on OV-73, should this be required.

On the OV-1701 column used here, chromatography of steroidal aromatic hydrocarbons was generally poorer than on OV-1 or OV-73 (Fig. 4). A 12-m column was used rather than the more usual 25-m OV-1 or OV-73 column in

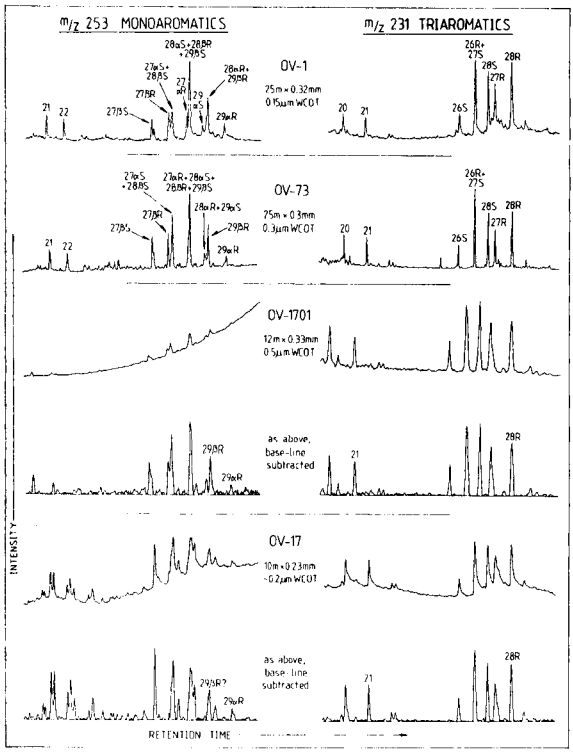

Fig. 4. Partial single-ion chromatograms (g.c./m.s. with multiple ion detection) comparing the effects of changing stationary phase on the observed relative elution orders of monoaromatic (*m/z* 253) and triaromatic (*m/z* 231) steroidal hydrocarbons from an oil. (See Table 1 and Fig. 3 for component identifications.)

order to ensure elution of all components within the temperature programme, as for the OV-1 and OV-73 columns (although the effects of the greater OV-1701 film thickness on retention times should be noted). Elution of components during the isothermal period at the upper temperature limit (UTL) resulted in undesirable peak broadening. The 250°C UTL of OV-1701 was a disadvantage in this analysis. Further, phase bleed was pronounced in the *m/z* 253 ion chromatogram, and so baseline-subtracted ion chromatograms are shown in Fig. 4 to aid comparison with chromatograms from other stationary phases. The pronounced bleed for the OV-1701 column primarily resulted from the thick (0.5 μm) coating, and demonstrates a possible disadvantage of thick-film capillary columns in g.c./m.s.

Disadvantages were observed for OV-17 (Fig. 4), which were similar to those noted for OV-1701. Column length had to be reduced to 10 m to reduce peak broadening of triaromatic components eluting well into the isothermal period at 250°C, and phase bleed interfered with the *m/z* 253 ion chromatogram (Fig. 4) (the 250°C UTL and the phase bleed are related to Carbowax deactivation of the glass surface).

Methylsilicone stationary phases containing ca. 5% phenyl groups (e.g., SE-52, SE-54, OV-73) seem most suitable for analysis of aromatic steroidal hydrocarbons, possibly in conjunction with an OV-1 analysis where more complete assessment of monoaromatic distributions is required. These observations reflect the expected effects of stationary phase selectivity (i.e., the affinity of the stationary phase for a particular class of compounds).

A further molecular maturity parameter based on aromatic hydrocarbons is the methylphenanthrene index (MPI) [18—20]. Evaluation of this maturity parameter requires quantification of phenanthrene and four of its methyl homologues (1-, 2-, 3- and 9-methylphenanthrene). The relative abundance of these compounds generally allows their quantification by g.c. with flame ionisation detection (provided that isolation from co-eluant methyldibenzothiophenes can be achieved [17, 18]). Figure 5 compares the g.c. analysis of an alkylphenanthrene fraction from a sediment on three stationary phases, OV-1, OV-73 and OV-17. As expected from selectivity considerations, resolution of methylphenanthrenes (MPs) appeared to increase with increasing phenyl group content of the methylsilicone stationary phase (even when a 10-m OV-17 column is compared with OV-1 and OV-73 columns of twice the length in Fig. 5). Baseline resolution of 3MP and 2MP and of 9MP and

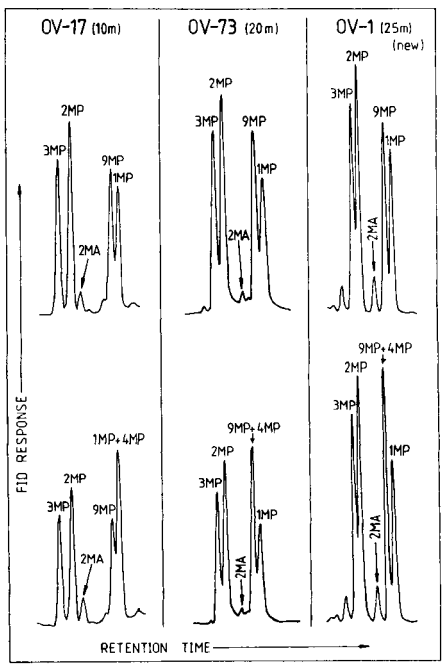

Fig. 5. Partial gas chromatograms comparing the effects of changing stationary phase on the observed relative elution order of methylphenanthrenes from a sediment. (MP, methylphenanthrene; MA, methylanthracene. See Fig. 3, structures 13 and 14, for ring-numbering conventions.)

1MP has been reported on a 50-m SE-52 column [21]. However, on methylsilicone phases containing up to ca. 5% phenyl groups, co-elution of 4MP and 9MP occurs (see Fig. 5). Although the relative abundance of 4MP has been reported to be low compared with the other MP isomers in oils [19—21], higher relative levels have been reported in Recent sediments [22], hence it is desirable to resolve all five MP isomers. Resolution of 4MP and 9MP has been reported on a free fatty-acid phase, but this phase gave poor resolution of 9MP and 1MP [21]. On OV-17 (Fig. 5) it was observed that the relative retention time of 4MP compared with 1MP and 9MP was greater than on both OV-1 and OV-73. On this OV-17 column, 4MP co-eluted with 1MP.

The possibility of complete resolution of all five MP isomers on a stationary phase containing a greater proportion of phenyl groups (such as OV-25) was not investigated. It has recently been shown that a slight improvement in resolution of dimethyldibenzothiophenes can be obtained on a 25% biphenylmethylpolysiloxane stationary phase rather than OV-17 [23], and it is possible that improved resolution of methylphenanthrenes could also be obtained with the biphenyl phase. However, a combination of chromatograms from OV-73 (or SE-52) and OV-17 should permit accurate relative quantification of all MP isomers.

While it can be seen from Fig. 5 that a new OV-1 column provided resolution of MP isomers comparable to an OV-73 column, OV-1 columns become surface-active towards any but the most apolar components (i.e., alkanes) after repeated use in the analysis of aromatic fractions. This activity develops much more rapidly with OV-1 than with phases containing ca. 5% phenyl groups, and the resulting peak tailing and loss of resolution after about 50 runs with aromatics can be seen in Fig. 6. A further disadvantage of using OV-1 in the analysis of MPs is the incomplete resolution of MPs from other components, 2-methylanthracene (2MA) and 4,5-methylenephenanthrene (MeeP), commonly present in alkylphenanthrene fractions of sediments. The relative elution positions of these components on SE-52 are shown in Fig. 6.

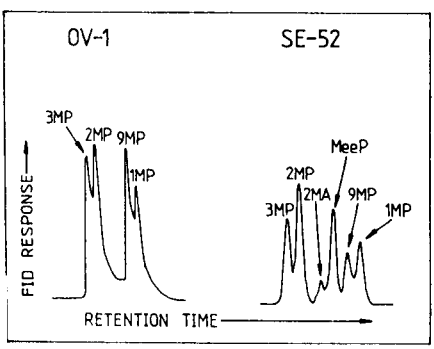

Fig. 6. Partial gas chromatograms comparing the effects of repeated use in the analysis of aromatics OV-1 (20 m column) and SE-52 (25 m column) stationary phases on observed peak shapes of methylphenanthrenes. (MP, methylphenanthrene; MA, methylanthracene; MeeP, 4,5-methylenephenanthrene. See Fig. 3 for ring-numbering conventions.)

Resolution of 2MA, MeeP and 9MP was poorer on OV-1 than on SE-52, as would be expected from the poorer resolution of 2MA and 9MP observed on OV-1 (see Fig. 5).

Effect of the injection technique in g.c./m.s. analysis

Biomarkers are generally present in oils at very low levels, and so split, vaporising injection with high splitting ratios is not a suitable technique to use in the g.c./m.s. of these compounds [24]. The amount of material entering the column can be increased by reducing the split ratio, and splitless injection is commonly used; the relative merits of split and splitless injection, and the necessary g.c. operating conditions, have been considered elsewhere [24—26]. Several comparisons of various injection methods for vaporising injectors have been reported, but these have chiefly been confined to the study of n-alkane standard mixtures by g.c. with flame ionisation detection, and were done over relatively short periods of time [24, 27—30]. A study of vaporising injection techniques with splitless injection was undertaken to examine possible discrimination against the less volatile components and also data reproducibility from g.c./m.s. analysis of biomarkers in oils. One method involved an "in-needle" technique, where the sample was retained in the needle of a plunger-in-needle syringe and injected rapidly after introduction of the needle into the injector. The other method was an "in-barrel" hot-needle technique, in which the sample was retained in the barrel of a plunger-in-barrel syringe, and the needle was allowed to warm in the injector for ca. 3 s prior to rapid injection.

Figure 7 illustrates typical discrimination effects of the "in-needle" technique compared with the "in-barrel" technique for a range of steranes (*m/z* 217 ion chromatograms) and terpanes (*m/z* 191 ion chromatograms) for a representative oil. The "in-needle" method shows a relative decrease in the ratio of amounts of pentacyclic to tricyclic terpanes and of C_{33}—C_{35} to other pentacyclic terpanes compared with "in-barrel" injection. These observations are consistent with discrimination against high-boiling components arising from their incomplete transfer from syringe to column [29]. This effect can also be observed in the relative quantities of C_{21} and C_{22} steranes compared with the C_{27}—C_{29} steranes (*m/z* 217 single ion chromatograms, Fig. 7).

For the g.c./m.s. analysis represented in Fig. 7, full data collection (over a mass range of *m/z* 50—450) was used, with 2 s/scan and a temperature programme rate of 4° min^{-1} for the "in-needle" method, and 1 s/scan with a temperature programme rate of 6° min^{-1} for the "in-barrel" method. Inspection of the peak labelled 31αβ22R + Gam in the *m/z* 191 single-ion chromatograms (Fig. 7) suggests that, at the relatively slow 4° min^{-1} programming rate, peak tops can be missed with a 2-s scan. While the statistical significance of this behaviour was not investigated over a series of analyses, it would appear that peak-area quantification is to be preferred to peak-height quantification. Also, the important visual comparison of chromatograms is hampered by the absence of peak tops. It should be noted that some mass spectrometers (e.g., old magnetic sector instruments) are not able to scan faster than 2 s/scan

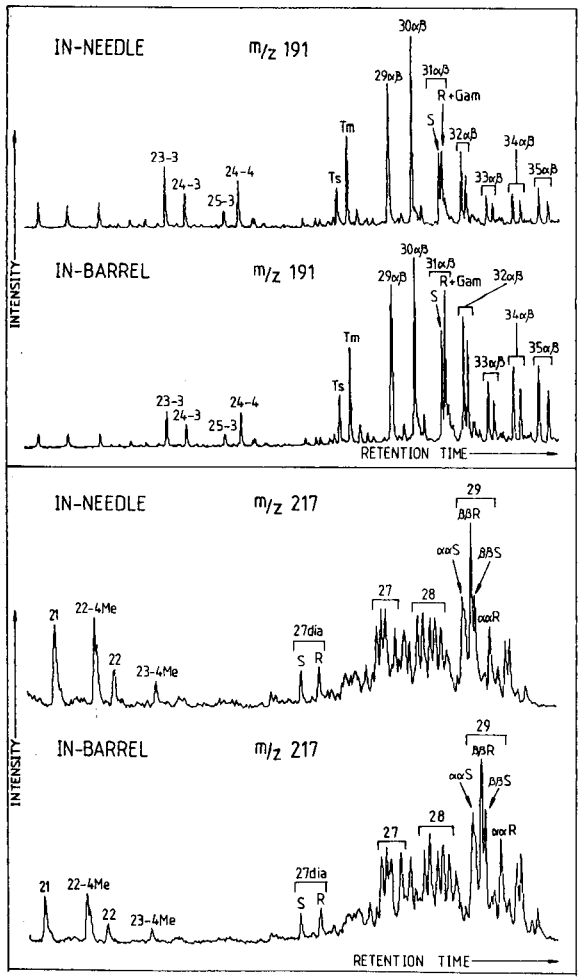

Fig. 7. Partial single-ion charomatograms comparing the effects of different vaporising, splitless injection techniques on the observed distribution of terpanes (*m/z* 191) and steranes (*m/z* 217) from an oil. (See Table 1 and Fig. 3 for component identification.) The "in-needle" analyses were done at 4° min^{-1} and 2 s/scan; "in-barrel" analyses were done at 4° min^{-1} and 1 s/scan.

in full data mode, and it would seem that care must be taken in selecting temperature-programming rates if an adequate number of data sampling points are to be obtained across a peak.

The effects of vaporising injection methods on the reproducibility and discrimination of g.c./m.s. data were analysed statistically. Multiple ion detection was used to increase signal/noise ratios and residence time for the ions of interest, minimising variability from the data processing. The two injection techniques used were as described above, and all other conditions for each analysis were identical (including a total scan time of 1 s, see

Experimental section). Ratios of geochemical significance were chosen, using the aliphatic biomarkers C_{23} tricyclic terpane (23-3, Table 1), C_{30} 17α(H), 21β(H) hopane (30αβ, Table 1) and C_{33} 17α(H),21β(H),22S pentacyclic terpane (33αβS, Table 1) (approximate relative n-alkane elution positions C_{23}, C_{31} and C_{34}, respectively), as well as the aromatic biomarkers C_{21} and C_{28} 20R triaromatic steroidal hydrocarbons (21 and 28R, respectively, Table 1) (approximate relative n-alkane elution positions C_{25} and C_{31}, respectively). The terpane ratio 23-3/30αβ (and also 23-3/33αβS) can be used as a correlation parameter, and the triaromatic steroidal hydrocarbon ratio 21/28R can be used as a maturity indicator [1]. Results from g.c./m.s. conducted over a period of ca. 2 months (for each injection technique and each oil) are represented by mean, standard deviation (SD) and relative standard deviation (RSD) values in Table 2. Values were calculated from peak heights (in parentheses) as well as peak areas. Ratios of the form B/A and B/(A + B) are presented in Table 2. It has been suggested [1] that the use of ratios of the form B/(A + B) is preferable, as minor variations in A or B, when one value is much greater than the other, are exaggerated by the ratio B/A. Lower RSD values can be seen to result from using ratios of the form B/(A + B) in Table 2.

TABLE 2

Comparison of discrimination and reproducibility in biomarker analysis by g.c./m.s. (multiple ion detection) with different splitless, vaporising injection techniques

[Ratios for terpanes (23-3, 30αβ and 33αβS) were calculated from *m/z* 191 ion chromatogram peak areas, and ratios for triaromatic steroidal hydrocarbons (21 and 28R) were calculated from *m/z* 231 ion chromatogram peak areas; values in parentheses are based on peak-height measurements. See Experimental section for g.c./m.s. conditions and Table 1 for component identifications.]

Biomarker ratios	Splitless "in-barrel"				Splitless "in-needle"			
	Mean	No. of samples	SD ($n-1$)	RSD (%)	Mean	No. of samples	SD ($n-1$)	RSD (%)
Oil 1								
23-3% / 30αβ	47.91	9	5.29	11.1	86.85	7	37.55	43.2
23-3% / 23-3 + 30αβ	32.31 (34.91)	9 (9)	2.42 (2.89)	7.5 (8.3)	44.85 (43.41)	7 (7)	9.58 (10.09)	21.4 (23.2)
23-3% / 23-3 + 33αβS	57.08 (64.39)	9 (9)	2.72 (3.65)	4.8 (5.7)	76.23 (77.23)	7 (7)	8.01 (8.37)	10.5 (10.8)
Oil 2								
21% / 28R	28.86	11	5.68	19.7	45.87	12	11.08	24.2
21% / 21 + 28R	22.25 (17.68)	11 (9)	3.52 (3.28)	15.8 (18.6)	31.08 (22.20)	12 (12)	5.24 (3.54)	16.9 (15.9)

In comparison with the "in-barrel" injection technique, the "in-needle" method resulted in significant discrimination against the less volatile components, as indicated by the higher mean ratio values (Table 2) for the "in-needle" technique. Furthermore, RSD values were significantly greater for the "in-needle" than the "in-barrel" injection method (Table 2), indicating poorer reproducibility for the former method. While RSD values were similar for peak-height and peak-area data, differences were noted in mean ratio values, which were more pronounced where relatively small peaks were involved (i.e., 33$\alpha\beta$S terpane and 21 triaromatic steroidal hydrocarbon). This again suggests that peak-area measurements are to be preferred, particularly where small peaks are concerned; the approximation that peak height is proportional to component concentration is not sufficiently accurate at low concentrations.

It is apparent that the "in-needle", splitless injection technique can provide a misleading representation of the relative distribution of components across the volatility range encountered. "In-barrel" splitless injection with a cold needle (i.e., rapid injection of sample immediately after insertion of the needle) has been reported to produce similar results to the "in-needle" method [29].

Although "in-barrel", hot-needle, splitless injection appears to provide a more accurate representation of biomarker compound distributions than the corresponding "in-needle" technique, it too has been found not to give a completely accurate account of relative component quantities, resulting from a degree of discrimination [27, 28]. On-column injection, with secondary cooling of the part of the column into which the syringe needle is introduced, has been found to provide freedom from discrimination and improved reproducibility of quantification for standard mixtures in g.c. with flame ionisation detection [4, 26—28, 31—34].

A comparison of splitless "in-barrel" and cooled on-column injection was made in the g.c./m.s. analysis of biomarkers. The relative effects of on-column and "in-barrel" injection on observed aliphatic biomarker distributions for a representative oil are shown in Fig. 8. Discrimination effects during "in-barrel" injection can be seen from the relative quantities of pristane and phytane in m/z 183 ion chromatograms, of tri- and tetra-cyclic terpanes in m/z 191 ion chromatograms, and of short-chain steranes in m/z 217 ion chromatograms (Fig. 8).

Discrimination and reproducibility were statistically examined using the same terpanes and triaromatic steroidal hydrocarbons as in the comparison between "in-needle" and "in-barrel" injection techniques reported above. The results are presented in Table 3; each of the four sets of data (oil 3 splitless, oil 3 on-column; oil 4 splitless, oil 4 on-column) was obtained over a period of ca. 2 months. Mean ratio values (Table 3) indicated that the "in-barrel" injection technique suffered from a small degree of discrimination against the less volatile components. In addition, on-column injection appeared to provide better reproducibility, as RSD values for on-column injection were lower than those for "in-barrel" injection.

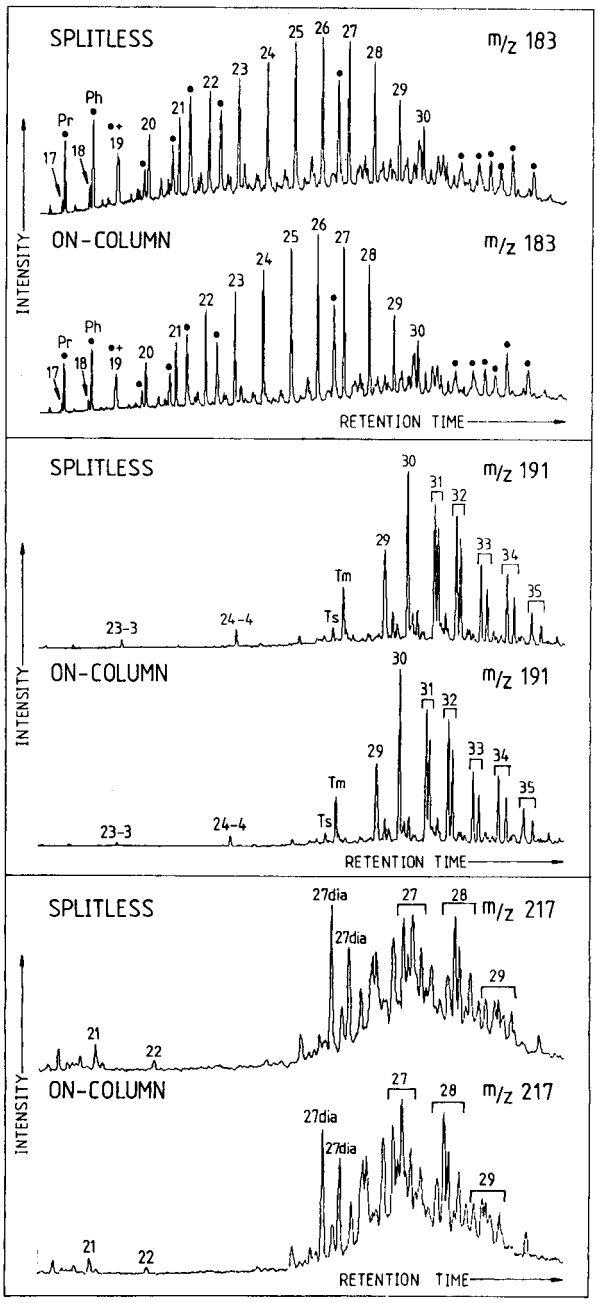

Fig. 8. Partial single-ion chromatograms (g.c./m.s., multiple ion detection) comparing the effects of vaporising, splitless and non-vaporising, on-column injection techniques on the observed distribution of acyclic alkanes (*m/z* 183), terpanes (*m/z* 191) and steranes (*m/z* 217) from an oil. (In *m/z* 183 ion chromatograms, numerals represent n-alkane carbon numbers and • represents isoprenoidal alkanes. See Table 1 and Fig. 3 for other component identifications.)

TABLE 3

Comparison of discrimination and reproducibility in biomarker analysis by g.c./m.s. (multiple ion detection) with splitless, vaporising injection and cooled, on-column injection (see notes to Table 2)

Biomarker ratios	Cooled "on-column"				Splitless "in-barrel"			
	Mean	No. of samples	SD ($n-1$)	RSD (%)	Mean	No. of samples	SD ($n-1$)	RSD (%)
Oil 3								
23-3% / 30αβ	60.56	5	11.56	19.1	67.74	5	16.73	24.7
23-3% / 23-3 + 30αβ	37.47 (39.69)	5 (5)	4.45 (7.60)	11.9 (19.1)	39.92 (41.79)	5 (5)	5.79 (4.88)	14.5 (11.7)
23-3% / 23-3 + 33αβS	68.84 (74.25)	5 (5)	4.00 (3.77)	5.8 (5.1)	68.89 (76.00)	5 (5)	5.61 (6.03)	8.2 (7.9)
Oil 4								
21% / 28R	38.13	5	6.91	18.1	47.79	6	14.92	31.2
21% / 21 + 28R	27.42 (30.36)	5 (5)	3.68 (3.57)	13.4 (11.8)	31.72 (34.96)	6 (6)	7.39 (8.24)	23.3 (23.6)

The RSD values for cooled, on-column injection in Table 3 are larger than those commonly reported for g.c. (flame ionisation detection) of n-alkane standards, which are typically $<2\%$ [4, 26, 31, 32]. These higher RSD values may be partly attributed to errors in quantification of small peaks. When some ratios were calculated from major peaks in ion chromatograms (i.e., 29αβ and 30αβ terpanes, and 28R and 26R + 27S triaromatic steroidal hydrocarbons; the 26R and 27S components co-elute), RSD values (Table 4) were found to approach those previously reported for on-column injection. Furthermore, when, for example, data for oil 4 (Table 3) were treated statistically in smaller sets, corresponding to g.c./m.s. analyses done over periods of a few days, the RSD values improved to $\leqslant 3.5\%$ for on-column and $<8.0\%$ for "in-barrel" injection for the triaromatic steroidal hydrocarbon ratio 21/(21 + 28R).

The results reported in Tables 2 and 3 provide a measure of long-term reproducibility. It appears that RSD values of ca. $\geqslant 5\%$ probably reflect variations in m.s. operating conditions (which depend on both instrument and operator) as much as errors introduced by on-column injection. This may be partly attributed to the influence of m.s. tuning on the proportion of the ion current carried by the characteristic fragment ion (i.e., the relative degree of fragmentation of the parent molecule) for each component of a class of compounds.

The above results suggest that there are limitations to the accuracy of quantification of components using a vaporising, splitless injector, particularly

TABLE 4

Reproducibility of ratios based on major components in *m/z* 191 and *m/z* 231 ion chromatograms

[Ratios are based on peak-area measurements from *m/z* 191 ion chromatograms for terpanes 29αβ and 30αβ, and from *m/z* 231 ion chromatograms for triaromatic steroidal hydrocarbons 28R and 26R + 27S (26R and 27S co-elute on OV-1 and SE-52 stationary phases). See Table 1 for component identification.]

Biomarker ratios	RSD (%)		Biomarker ratios	RSD (%)	
	Splitless "in-barrel"	Splitless "in-needle"		Cooled "on-column"	Splitless "in-barr
Oil 1 $\frac{30\alpha\beta\%}{30\alpha\beta + 29\alpha\beta}$	1.0	4.3	*Oil 3* $\frac{30\alpha\beta\%}{30\alpha\beta + 29\alpha\beta}$	3.5	3.8
Oil 2 $\frac{28R\%}{28R + (26R + 27S)}$	2.3	4.3	*Oil 4* $\frac{28R\%}{28R + (26R + 27S)}$	2.3	5.5

with regard to both the long-term comparison of maturity data and the comparison of data obtained by different injection techniques. Furthermore, the accuracy of quantification can be reduced by peak tailing arising from activity in the injector system, which is known to increase with increasing contamination of the glass liner in the vaporising injector [28]. Although it is possible to make some allowance for discrimination by the inclusion of internal standards spanning the volatility range encountered in samples, with the complexity of the mixtures in question the additional problem of co-elution of components with standards can then arise. The use of cooled, on-column injection is preferable [26, 33—35], but not all g.c./m.s. systems are equipped with such an injector.

Quantification by mass spectrometry

Accurate relative quantification of components during g.c./m.s. analysis requires that equal proportions of all components are transferred to the column. From the above results it is apparent that cooled, on-column injection is the most suitable sample introduction technique for the analysis of biomarkers. Adsorption losses can be minimised by placing the column outlet adjacent to the ion source, which often requires the flexibility of fused silica columns. However, the range of stationary phases available on such columns (particularly the more polar varieties [36]) is limited compared with those on standard glass columns. Glass columns can be interfaced to the ion source of the spectrometer by a short length of deactivated (uncoated) fused silica column [37], as used in some aspects of the work reported here. A further necessity for accurate quantification is the acquisition of an adequate number

of data samples for a component (i.e., the interrelationship of m.s. scan and g.c. temperature programme rates requires consideration).

The evaluation of most maturity parameters from single-ion chromatograms for terpanes and steranes requires only relative quantification and not absolute quantification of components [38]. This requirement removes problems associated with the addition of known amounts of internal standards to samples, with the relative ionisation efficiency of each component, with the proportion of the total ion current carried by the characteristic fragment ion for each component, and, where two masses are being compared, with the relative sensitivity of the spectrometer to each mass (which can depend on instrument tuning and the degree of contamination of the ion source) [38]. However, a problem that can affect both relative and absolute quantification by g.c./m.s. with multiple ion detection is the possibility of non-linearity in the response at low eluate concentrations. Figure 9 demonstrates this effect for varying concentrations of component A [butyl(4-chloro-2-methylphenoxy)acetate] with a constant concentration of component B (perdeuteroanthracene); for quantification, the *m/z* 200 peak-area response was used for A and the *m/z* 188 peak-area response for B. Cooled, on-column injection on to a fused silica column was used, with the column exiting directly into the ion source of the spectrometer. At least ten data scans/peak were recorded, and components A and B eluted within 5° C of each other. All these conditions were calculated to minimise their contribution to non-linearity of response, and the internal standard, component B,

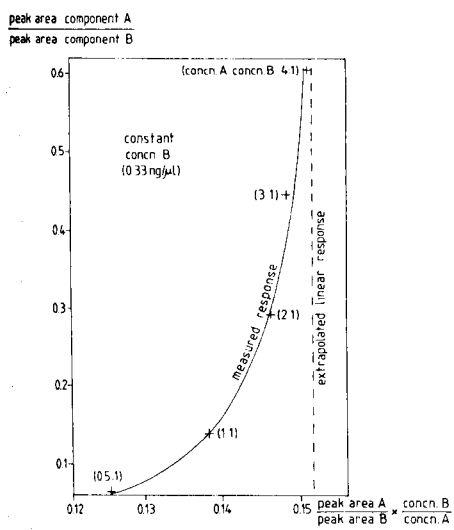

Fig. 9. Calibration plot of g.c./m.s. (multiple ion detection) response illustrating the possibility of non-linear m.s. response at low substrate concentrations. Data were obtained from solutions containing constant concentrations of internal standard B, perdeuteroanthracene, with varying concentrations of component A, butyl(4-chloro-2-methylphenoxy)acetate. (See text for details.)

allowed for any variation in the amount of sample reaching the ion source. For a linear m.s. response, ratios of (peak area)/(concentration) for component A should be constant, and so a vertical line (broken line in Fig. 9) would be expected in Fig. 9. However, the response for component A can be seen to be non-linear below a concentration of ca. 0.5 ng μl^{-1} (an injection volume of 0.5 μl was used).

Variations in the limit of linear response depend on a number of factors, such as the compound and fragment ion monitored, and the m.s. scanning and tuning conditions. Although component A was a chloroaromatic pesticide, the inferences from its quantification as described above apply to all classes of compound, including biomarkers. It can be expected that non-linear m.s. response would affect the accuracy/reproducibility of geochemical ratios from g.c./m.s. (multiple ion detection) analysis where one or more of the components under consideration is present at sufficiently low concentration. Such effects become significant with variations in both long-term m.s. sensitivity (arising from tuning effects, degree of source contamination, etc.) and absolute quantities of analyte (which depends, inter alia, on the accuracy of syringes). Aromatic steroidal hydrocarbons are generally present at very low levels in oils, and so errors arising from non-linear m.s. response may be reflected in the higher RSD values for the ratio 21/(21 + 28R) than those for ratios based on terpanes in Tables 2 and 3.

CONCLUSIONS

The analysis of biomarkers in oils and sediments by high-resolution g.c. or g.c./m.s. requires consideration of a number of factors if accurate and reproducible results are to be obtained. One such factor is the choice of stationary phase necessary to obtain adequate resolution of components. Because of the complexity of the total aliphatic and total aromatic fractions from oils, one stationary phase is unlikely to provide the required resolution of all biomarkers. Selectivity towards a particular group of compounds (rather than a general polarity description) is a major factor in the choice of a stationary phase. For the evaluation of geochemically significant ratios, an OV-1 (or equivalent) stationary phase is suitable for alkane biomarkers, and SE-52 (or equivalent) is suitable for aromatic hydrocarbons. Co-elution of some components inevitably occurs with the use of any one stationary phase, and it is possible to obtain useful additional information by using another stationary phase for each biomarker application (such as SE-52 for alkanes and OV-1 for aromatic steroidal hydrocarbons). However, the value of the additional information obtained from duplicate analyses on different stationary phases must be sufficient to compensate for the increased time required.

Further considerations affecting the choice of capillary column in g.c./m.s. are an upper temperature limit allowing elution of all components without an excessive final isothermal period (which causes peak broadening) and low levels of bleed from the stationary phase. Where possible, the capillary

column should exit in the ion source, and unions (where selective adsorption can occur) are best avoided. Flexible, fused silica columns are often the most suitable choice.

The accuracy and reproducibility of quantification of relative amounts of biomarkers from single-ion chromatograms depend upon both the g.c. and m.s. operating conditions. Cooled, on-column injection appears to be the most appropriate sample introduction method for the analysis of biomarkers. It avoids the discrimination against the less volatile components experienced with splitless, vaporising injection (which may not be recognised without comparison of techniques), and also provides superior reproducibility of quantification data.

Evaluation of the reproducibility of geochemical ratios derived from ion-chromatogram peak areas over a period of several weeks suggested that variations in m.s. response can be more significant than errors introduced by the on-column injection technique. Reproducibility was poorer for ratios derived from components that were present in oils at very low levels, such as aromatic steroidal hydrocarbons. Quantification of such components may be affected by non-linearity of m.s. response, which can be significant at sufficiently low concentrations of the component. Addition of internal standards does not necessarily permit accurate quantification if the m.s. response is non-linear. To ensure the maximum accuracy in peak-area determinations, consideration must be given to the m.s. scan rate and the g.c. temperature programme rate, which together determine the number of data points recorded for a peak.

With the growing number of biomarker compound groups being used for evaluation of the maturity of oils etc., it is apparent that the need for improved resolution of components, greater accuracy in component quantification and long-term reproducibility of data will increase.

The author thanks Vanessa Howell for helpful comments and suggestions during the preparation of this paper. The use of facilities at Masspec Analytical is gratefully acknowledged.

REFERENCES

1 A. S. Mackenzie, in J. Brooks and D. Welte (Eds.), Advances in Petroleum Geochemistry, Vol. 1, Academic Press, London, 1984, pp. 115—214.
2 J. Connan, in J. Brooks and D. Welte (Eds.), Advances in Petroleum Geochemistry, Vol. 1, Academic Press, London, 1984, pp. 299—336.
3 K. Grob and K. Grob, Jr., J. High Resolut. Chromatogr., Chromatogr. Commun., (1978) 57.
4 M. Galli, S. Trestianu and K. Grob Jr., J. High Resolut. Chromatogr., Chromatogr. Commun., 2 (1979) 366.
5 K. Grob, G. Grob and K. Grob, Jr., J. High Resolut. Chromatogr., Chromatogr. Commun., 2 (1979) 677.
6 W. K. Seifert and J. M. Moldowan, Geochim. Cosmochim. Acta, 42 (1978) 77.
7 F. R. Aquino Neto, J. M. Trendel, A. Restle, J. Connan and P. A. Albrecht, in

M. Bjorøy et al. (Eds.), Advances in Organic Geochemistry 1981, Wiley, New York, 1983, pp. 659—667.
8 J. K. Volkman, R. Alexander and R. I. Kagi, Geochim. Cosmochim. Acta, 47 (1983) 1033.
9 J. K. Volkman, R. Alexander, R. I. Kagi and G. W. Woodhouse, Geochim. Cosmochim. Acta, 47 (1983) 785.
10 V. J. Howell, J. Connan and A. K. Aldridge, in P. A. Schenck, J. W. De Leeuw and G. W. M. Lijmbach (Eds.), Advances in Organic Geochemistry 1983, Pergamon, Oxford, 1984, pp. 83—92.
11 J. M. Moldowan, Geochim. Cosmochim. Acta, 48 (1984) 2767.
12 M. L. Lee, D. L. Vassilaros, C. M. White and M. Novotny, Anal. Chem., 51 (1979) 768 and references therein.
13 G. Schomburg, J. High Resolut. Chromatogr., Chromatogr. Commun., 2 (1979) 461.
14 B. M. Didyk, B. R. T. Simoneit, S. C. Brassell and G. Eglinton, Nature (London), 272 (1978) 216.
15 M. Bjorøy, P. W. Brooks and K. Hall, in M. Bjorøy et al. (Eds.), Advances in Organic Geochemistry 1981, Wiley, New York, 1983, pp. 87—93.
16 A. S. Mackenzie, C. F. Hoffman and J. R. Maxwell, Geochim. Cosmochim. Acta, 45 (1981) 1345.
17 S. D. Killops and J. W. Readman, Org. Geochem., 8 (1985) 247.
18 M. Radke and D. H. Welte, in M. Bjorøy et al. (Eds.), Advances in Organic Geochemistry 1981, Wiley, New York, 1983, pp. 504—512.
19 M. Radke, D. H. Welte and H. Willsch, Geochim. Cosmochim. Acta, 46 (1982) 1.
20 M. Radke, H. Willsch, D. Leythaeuser and M. Teichmuller, Geochim. Cosmochim. Acta, 46 (1982) 1831.
21 M. Ewald, M. Lamotte, P. Garrigues, J. Rima, A. Veyres, R. Lapouyade and G. Bourgeois, in M. Bjorøy et al. (Eds.), Advances in Organic Geochemistry 1981, Wiley, New York, 1983, pp. 705—709.
22 P. Garrigues and M. Ewald, Org. Geochem., 5 (1983) 53.
23 M. L. Lee, J. C. Kuei, N. W. Adam, B. J. Tarbet, M. Nishioka, B. A. Jones and J. S. Bradshaw, J. Chromatogr., 302 (1984) 303.
24 G. Schomburg, H. Behlau, R. Dielmann, F. Weeke and H. Husmann, J. Chromatogr., 142 (1977) 87.
25 K. Grob, Jr. and A. Romann, J. Chromatogr., 214 (1981) 118.
26 G. Schomburg, H. Husmann and R. Rittmann, J. Chromatogr., 204 (1981) 85.
27 K. Grob, Jr. and H. P. Neukom, J. High Resolut. Chromatogr., Chromatogr. Commun., (1979) 15.
28 K. Grob and G. Grob, J. High Resolut. Chromatogr., Chromatogr. Commun., (1979) 109.
29 K. Grob, Jr. and S. Rennhard, J. High Resolut. Chromatogr., Chromatogr. Commun., 3 (1980) 627.
30 R. R. Freeman (Ed.), High Resolution Gas Chromatography, 2nd edn., Hewlett-Packard, 1981, pp. 54—73.
31 M. Galli and S. Trestianu, J. Chromatogr., 203 (1981) 193.
32 K. Grob and K. Grob, Jr., J. Chromatogr., 151 (1978) 311.
33 D. H. McMahon, J. Chromatogr. Sci., 23 (1985) 137.
34 F. I. Onuska, R. J. Kominar and K. Terry, J. Chromatogr. Sci., 21 (1983) 512.
35 K. Knauss, J. Fullemann and M. P. Turner, J. High Resolut. Chromatogr., Chromatogr. Commun., 4 (1980) 641.
36 S. R. Lipsky and W. C. McMurray, J. Chromatogr., 217 (1981) 3.
37 P. Sandra, M. Schelfaut and M. Verzele, J. High Resolut. Chromatogr., Chromatogr. Commun., 5 (1982) 50.
38 J. Rullkötter, A. S. Mackenzie, D. H. Welte, D. H. Leythaeuser and M. Radke, in P. A. Schenck, J. W. De Leeuw and G. W. M. Lijmbach (Eds.), Advances in Organic Geochemistry 1983, Pergamon, Oxford, 1984, pp. 817—827.

Analytica Chimica Acta, 183 (1986) 129—140
Elsevier Science Publishers B.V., Amsterdam — Printed in The Netherlands

TRACE DETERMINATION OF α-KETO ACIDS IN NATURAL WATERS

DAVID J. KIEBER* and KENNETH MOPPER

University of Miami, Rosenstiel School of Marine and Atmospheric Science, Division of Marine and Atmospheric Chemistry, 4600 Rickenbacker Causeway, Miami, FL 33149-1098 (U.S.A.)

(Received 15th July 1985)

SUMMARY

Numerous chromatographic methods have been developed to detect α-keto acids in physiological or sea-water samples. These methods generally involve derivatization in a strongly acidic medium with elevated temperatures, desalting, preconcentration, and liquid-liquid extraction procedures prior to chromatographic analysis. These procedures may introduce significant errors because of adsorption losses, contamination, or decomposition of the α-keto acids. To avoid these potential problems, a chemically mild method to detect α-keto acids in sea water was developed. The method is based on the reaction of α-keto acids with 2,4-dinitrophenylhydrazine in sea water to form stable hydrazone derivatives. Desalting of the reaction mixture and preconcentration of the hydrazone derivatives is accomplished by a column-switching technique. The derivatives are separated by reversed-phase, high-performance liquid chromatography and detected by absorption spectrometry. Quantification of α-keto acids in the nM to μM concentration range shows complete recovery in sea water, excellent precision at 10—20 pmol (<5% relative standard deviation), and absorbances that are linearly related to α-keto acid concentrations. The detection limit of this method is 1—5 pmol for a 2-ml injection. Applications of this method to the detection of α-keto acids in marine sediment and sea-water samples are illustrated, and the first shipboard results are presented.

There is an increasing awareness of the interplay between dissolved organic matter (DOM) in sea-water and many biogeochemical phenomena including particle-organic interactions, sea-air interactions, light absorption, trace metal complexation, and food web dynamics [1, 2]. Measurements of specific components of DOM such as amino acids [3], flavins [4], and aldehydes and ketones [5] have provided valuable insights into these interactions. α-Keto acids represent a potentially important component of DOM. These compounds are key biochemical intermediates in metabolic pathways including glycolysis, photorespiration, and amino acid and carbohydrate metabolism [6]. In addition, α-keto acids readily undergo abiotic decarboxylation, substitution, and condensation reactions that may be important in organic-rich environments such as the sea-surface microlayer or particle surfaces. In the sea, apart from biological sources, α-keto acids are produced through the photochemical oxidation of dissolved organic matter [7]. Despite their probable importance, the biological and chemical behavior of this class of compounds in the marine environment is poorly understood.

0003-2670/86/$03.50

Information concerning the α-keto acid content of sea water has been difficult to obtain primarily because of difficulties associated with detection of trace quantities of these hydrophilic compounds in a concentrated salt water solution. Numerous chromatographic methods have been developed to detect α-keto acids in physiological samples [8] or sea-water samples [9, 10]. The basic approach to quantifying α-keto acids generally involves the reaction of these compounds with a chromophore or fluorophore that enables their detection at low concentrations. The derivatives that are formed are concentrated and separated from absorbing or fluorescing interferences before they are injected into the chromatograph. Such procedures are chemically harsh (requiring evaporation, strongly acidic conditions, or elevated temperatures) and usually involve transfer steps (liquid-liquid extraction) prior to sample injection. It is well documented that this type of multi-step procedure introduces significant errors caused by adsorption losses, contamination, or decomposition of the components of interest when applied to the detection of organic constituents in sea water [11]. In addition, vacuum filtration may cause nonsystematic cell lysis or stress-induced release of organic compounds by plankton or bacteria in sea water [12].

In the present study, a more compatible method to detect α-keto acids in sea water was developed. The method is based on the pre-column reaction of α-keto acids with 2,4-dinitrophenylhydrazine (DNPH). This reaction proceeds directly in sea water. Desalting of the reaction mixture and preconcentration of the hydrazone derivatives are accomplished by a column-switching technique. The derivatives are separated by reversed-phase, high-performance liquid chromatography (RPHPLC), and detected by absorption spectrometry. Optimization of reaction and chromatographic conditions is described. Applications of this method to the determination of α-keto acids in marine sediment and sea-water samples, and the first shipboard results are presented.

EXPERIMENTAL

Apparatus

The pumping system consisted of an Eldex Model Chromat-A-Trol gradient controller and an Eldex Model 100A single-piston pump (Eldex Laboratories, Menlow Park, CA). The mobile phase composition was programmed by low-pressure ratioing valves activated by the controller. Complete mixing of the solvents was accomplished with a Beckman Model 400 two-stage, dynamic mixer (Beckman Instrument Co., Atlanta, GA) that was placed between the pump and the Valco Model CV-6-UHPa-N60 injection valve (Valco Instrument Co., Houston, TX). Samples were injected into either a 100-μl sample loop or an 0.2 × 5.5-cm RP-18 (40 μm) enrichment column. Chromatographic separations were done with a 100 × 4.6-mm stainless steel Adsorbosphere C_{18} reversed-phase (RP-18) column containing 3-μm packing (Applied

Science, State Park, PA). A guard column containing 40-μm RP-18 packing (Applied Science) was attached directly to the analytical column. Detection was accomplished with an ISCO Model V[4] variable-wavelength detector set at 360 or 370 ± 3 nm with a 5-μl thermostated flow cell (ISCO, Lincoln, NE). Results were recorded on a Hewlett-Packard Model 3390A reporting integrator.

Standards and reagents

Chromatographic-grade organic solvents (Burdick and Jackson) and buffer salts (Baker Chemical Co.) were used without further purification. Sodium pyruvate, α-ketoglutaric acid, sodium glyoxylate, and oxaloacetic acid, were purchased from Sigma Chemical Co. Water was obtained by passing tap water through both a Milli-RO and a Milli-Q system containing an Organex-Q attachment (Millipore). The 2,4-dinitrophenylhydrazine (DNPH; Fluka Chemical Co.) was recrystallized once from acetonitrile that was freshly distilled from acidified DNPH [13]. The reagent was made by dissolving 20 mg of recrystallized DNPH in 10 ml of acetonitrile.

Stock solutions of standards (1 mM) were prepared in water and stored at 4°C. All standards, except α-ketoglutarate and oxaloacetate, were stable for at least one week. Solutions of the unstable standards were prepared just prior to their use. Mixed standards were prepared from stock solutions and diluted with water just prior to the addition of the reagent.

Procedures

Derivatization procedure. Sea water was generally not filtered prior to derivatization because filtration contaminated samples. Samples that were filtered were done by gravity filtration through a precombusted (400°C, 4 h) Whatman GF/C filter with a Gelman polycarbonate support.

A sea-water sample (5 ml) was acidified with 40 μl of 1 M hydrochloric acid, then 40 μl of the reagent was added. After a 1-h derivatization reaction at room temperature, a column-switching technique was used to inject an aliquot of the sample into the chromatogram. A 2-ml aliquot of the sample was injected into an enrichment column (refer to Apparatus) that was preconditioned by washing it with 10 ml of methanol followed by 10 ml of water. The injector was then switched from the load position to the inject position for 1 min. In this position, the mobile phase flowed through the enrichment column and backflushed the sample onto the analytical column. After a 1-min injection, the injector was switched back to the load position and reconditioned. No column-switching technique was used when α-keto acids were detected at micromolar concentrations; the sample was injected from a 100-μl sample loop.

Blanks. Three types of blanks were routinely used to correct for absorbing interferences. A reagent blank was done by adding the reagent and 1 M HCl to water and immediately injecting this mixture into the chromatograph. Alternatively, the reagent and 1 M HCl were added to Gulf Stream sea-water (containing no α-keto acids). After a 1-h derivatization reaction, an aliquot

of this mixture was injected into the chromatograph. In the third type of blank, the DNPH reagent was not added to the sea-water sample. Instead, the sea water was injected into the chromatograph to correct for naturally occurring absorbing interferences.

Conditions for HPLC. All chromatographic separations were done at room temperature and at a mobile phase flow rate of 0.7 ml min^{-1}. The mobile phases were filtered through a 0.22-μm Nylon-66 membrane filter (MicronSep, Honeoye Falls, NY).

The mobile phases used in the chromatographic system to separate the hydrazone derivatives were 30% methanol in an aqueous phosphate buffer (10 mM, pH 6.8), and methanol alone. The compounds of interest eluted from the column within 10 min when they were separated by isocratic elution at 0% methanol. However, some strongly retained substances did not elute from the analytical column at 0% methanol. Therefore, it was necessary to perform the following gradient to elute these compounds: 0% methanol for 10 min, 0—100% methanol in 4 min, isocratic at 100% methanol for 5 min, 100—0% methanol in 4 min, then isocratic at 0% methanol for 7 min to equilibrate the analytical column with the starting mobile phase.

Hydrazone absorption spectra. Concentrated solutions of hydrazones were prepared by adding 800 μl of reagent to 5 ml of an aqueous 1 mM standard (α-ketoglutarate, pyruvate, or glyoxylate). After a 1-h reaction at room temperature, the derivatized standard was loaded onto a SepPak C-18 cartridge (Waters Associates) that was preconditioned with 10 ml of methanol and then 10 ml of water. The SepPak cartridge was subsequently rinsed with 20 ml of 20% methanol in pH 2 water; the hydrazones were eluted from the SepPak with 1 ml of methanol. The eluate was diluted with water to a final volume of 20 ml, and an absorption spectrum was obtained from 250 to 500 nm (against 5% methanol in water as a reference) with a Hewlett-Packard Model 8450A UV/VIS scanning spectrophotometer.

Absorption spectra were also obtained for pyruvate and glyoxylate hydrazones as they eluted from the chromatograph using a Hewlett-Packard (HP) Model 1040A diode-array detector interfaced to an HP Model 85 personal computer.

RESULTS AND DISCUSSION

Optimization of reaction conditions

Reagent concentration. The concentration of DNPH was varied from 10 to 500 μM in the reaction mixture. The pH was held constant at 2.3, and the total α-keto acid concentration was held constant at 10 μM in the first experiment and 100 nM in the second experiment. With a 1-h reaction at room temperature, the highest yields of hydrazone for oxaloacetate, α-ketoglutarate, pyruvate, and glyoxylate were observed when the concentration of reagent in the reaction mixture was at least 100 μM. This corresponded to at least a ten-fold molar excess of reagent when the total α-keto acid concentra-

tion was 10 μM, and a thousand-fold molar excess when the total α-keto acid concentration was 100 nM.

Effect of pH. The effect of pH on the reactivity of DNPH towards α-keto acids in sea water was examined. The pH of the reaction mixture was varied from 0 to 5 by the addition of 12 M HCl. Throughout this experiment, the reagent and the total α-keto acid concentrations were held constant at 100 and 5 μM, respectively. With a 1-h reaction at room temperature, the recovery of hydrazones was highest within the pH range 1—3 (Fig. 1). Therefore, the derivatization of α-keto acids at trace concentrations does not require the strongly acidic conditions (>0.5 M) that are normally used [14].

Reaction time. The reaction of α-keto acids with DNPH was allowed to vary from 1 min to 7 h prior to injection into the chromatograph. The reagent concentration, pH, and total α-keto acid concentration were held constant at 100 μM, 2.3 nM, and 50 nM, respectively. At room temperature, the reaction was complete for all α-keto acids tested in 45 min (Fig. 2). After 45 min, the concentration of the α-ketoglutarate, pyruvate, and glyoxylate hydrazones remained constant with time; the concentration of the oxaloacetate hydrazone, in contrast, decreased rapidly after 45 min. This decrease probably resulted from decarboxylation of the oxaloacetate hydrazone [8, 15].

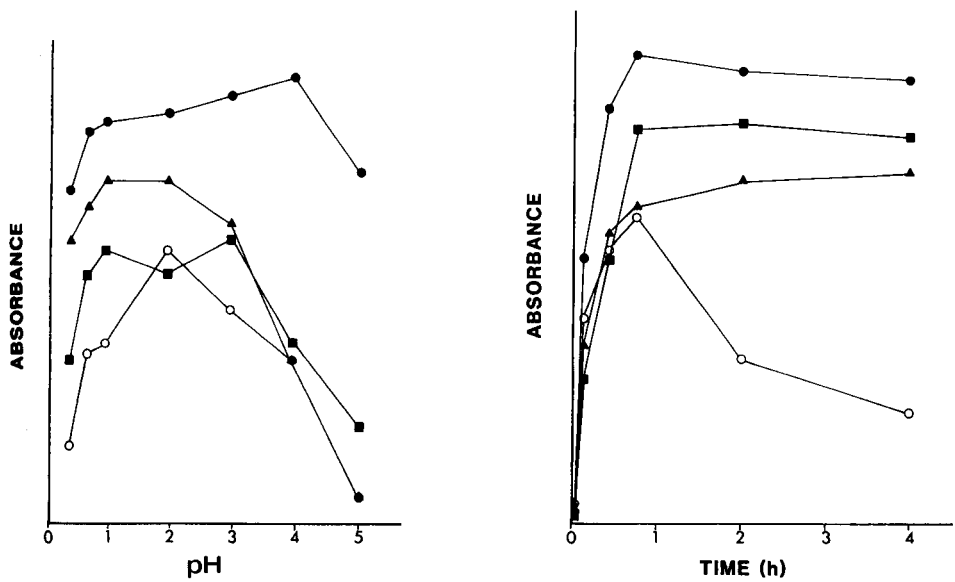

Fig. 1. Effect of pH on the reactivity of DNPH towards α-keto acids. Reaction time, 1 h at room temperature. Chromatographic conditions as in the text. Hydrazone: (●) glyoxylate, (▲) pyruvate, (○) oxaloacetate, (■) α-ketoglutarate.

Fig. 2. Effect of the time of reaction on the derivatization of α-keto acids with 100 μM DNPH at pH 2.3. Symbols as in Fig. 1.

Optimization of the chromatographic separation

The pH of the mobile phase should dramatically affect the chromatographic retention of α-keto acid hydrazones because these derivatives contain a weakly acidic carboxyl moiety. This effect was examined by altering the pH of the aqueous phase, a 0.05 M sodium acetate buffer, from 3.2 to 6.8. During this experiment, chromatographic separation of the hydrazones was done isocratically with a mobile phase that consisted of a 35% methanol/65% buffer solution. Results demonstrated that the pH of the mobile phase dramatically affected the retention time (capacity factor) of the hydrazones and the chromatographic selectivity (Fig. 3). The best resolution in the shortest time was achieved when the pH of the mobile phase was greater than 4.9. A phosphate buffer with a pH of 6.8 was generally used during the analysis of sea-water samples; at a lower mobile phase pH, the pyruvate hydrazone coeluted with the reagent.

On-line enrichment of hydrazone derivatives

Because α-keto acids were generally detected in sea water at nanomolar concentrations, it was necessary to concentrate the α-keto acid hydrazones to allow their detection. Hydrazones could effectively be concentrated in the injector by using a 40-μm packed C-18 column in place of an injector loop. At a pH near 2, the α-keto acid hydrazones were strongly retained by the

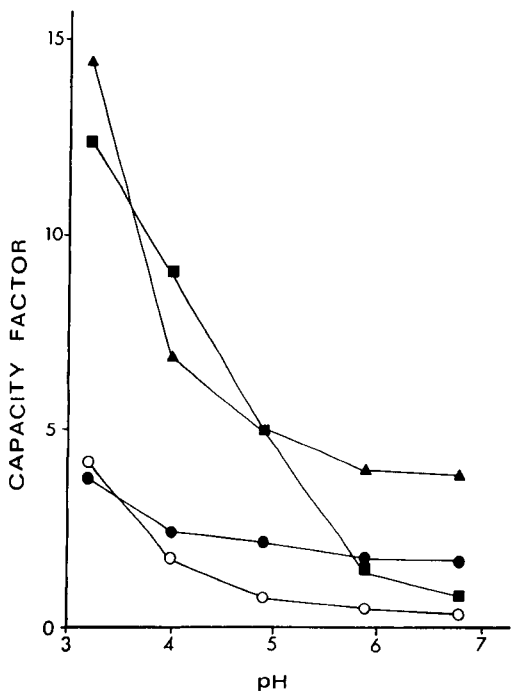

Fig. 3. Effect of the pH of the acetate buffer used in the mobile phase on the relative chromatographic retention of α-keto acid hydrazones. Symbols as in Fig. 1.

column. It was possible to inject a large volume of derivatized sample (1—7 ml) onto the enrichment column because the hydrazones formed a concentrated, narrow band at the top of this column. Once the sample had been injected and rinsed with 5 ml of pH 2 water, the injector was switched from the load to the inject position. The enrichment column was then exposed to the pH 6.8 mobile phase for a minimum of 1 min. At this pH, the α-keto acid hydrazones are backflushed from the enrichment column onto the analytical column. Some of the reagent and relatively hydrophobic derivatives (e.g., formaldehyde hydrazone) were also eluted from the enrichment column. The pH of the reaction mixture should be greater than 2 when this technique is used; a pH below 2 causes rapid deterioration of the reversed-phase packing in the enrichment column.

Hydrazone absorption spectra

Ultraviolet-visible absorption spectra were taken for separate solutions of DNPH and DNP hydrazones of α-ketoglutarate, pyruvate, and glyoxylate in 5% methanol/95% water; absorption maxima were observed at 353, 378, 366, and 365 ± 1 nm, respectively. Absorption spectra were also obtained for pyruvate and glyoxylate hydrazones as they eluted from the chromatograph using the diode-array detector; both hydrazones had an absorption maximum at 363 ± 2 nm. The purity of the pyruvate hydrazone that eluted from the chromatogram was examined by comparing the absorption spectra that were obtained for the leading edge, the apex, and tailing edge of the eluting peak (Fig. 4A). When these absorption spectra are overlaid, it is evident that the spectra are identical, thereby demonstrating that the eluting peak represented a single compound (Fig. 4C). Comparison of the absorption spectra of eluting peaks was also used to identify hydrazones present in derivatized sea water that was collected from Biscayne Bay. The two peaks present in the chromatogram of a Biscayne Bay sample representing the glyoxylate and pyruvate hydrazones (Fig. 4B) had identical absorption spectra to the external pyruvate and glyoxylate hydrazone standards (Fig. 4C).

Linearity, precision, recovery, and detection limit

The linearity of response was determined for pyruvate and glyoxylate over the concentration range 5—100 nM (6 dilutions) in sea water using standard additions. When the column-switching technique was used, responses were found to be linearly related to the α-keto acid concentration of the sample (Table 1).

The precision of the derivatization and chromatographic procedure was determined at both the nM- and μM-concentration range for pyruvate and glyoxylate. In general, the relative standard deviation for 10 pmol of hydrazone injected was less than 5%.

The recovery of pyruvate and glyoxylate (10 nM each) added to Gulf Stream water was determined relative to an aqueous solution of these acids. The recovery of these acids was greater than 98% (n = 5) in sea water.

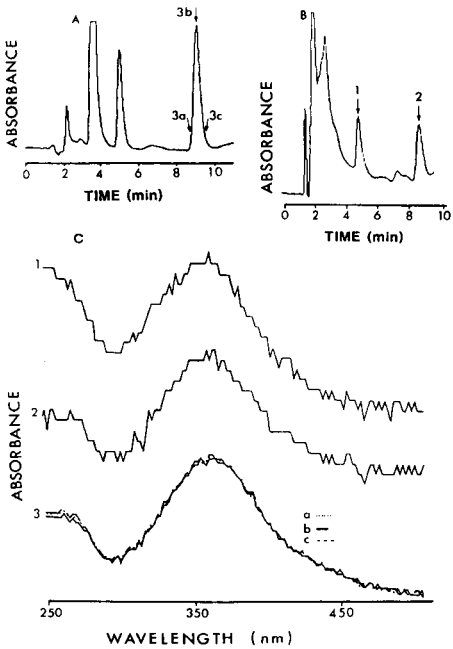

Fig. 4. (A) Chromatogram of a 25 nM standard (2 ml injected); derivatization and chromatographic conditions as in text; detection at 380 ± 10 nm; spectral scans from 250 to 500 nm were taken at 3a (leading edge), 3b (apex) and 3c (tailing edge) for the pyruvate hydrazone peak. (B) Chromatogram of a derivatized sea-water sample (7 ml injected); detection at 380 ± 10 nm; spectral scans from 250 to 500 nm were taken at the apex of peak 1 (glyoxylate) and peak 2 (pyruvate). (C) Spectra of peaks 1, 2, 3a, 3b and 3c as described above.

The detection limit of the method for the quantification of α-keto acids in sea water is approximately 1 pmol per injected α-keto acid with a signal-to-noise ratio of four. This corresponds to an injection of 2 ml of sea water with a concentration of pyruvate or glyoxylate of 0.5 nM. The detection limit may vary depending on the presence of absorbing interferences in the sample (e.g., fulvic substances). In general, though, the detection limit of this

TABLE 1

Linear regression of peak area vs. concentration of pyruvate or glyoxylate hydrazone ($n = 6$)

	Pyruvate	Glyoxylate
y-Intercept ± SD (mm^2)	0.43 ± 0.97	−0.07 ± 1.01
Slope ± SD ($mm^2\ nM^{-1}$)	1.50 ± 0.11	2.66 ± 0.11
Standard Error $_y$(mm^2)	0.58	0.58
r^2	0.98	0.99

method is only limited by the detector noise and not by the presence of absorbing interferences.

Samples

The DNPH method was developed to quantify α-keto acids in sea-water and marine-sediment samples. However, this method could easily be adapted for the detection of these compounds in other types of natural samples (e.g., lake water, rain water) or in physiological fluids.

Sea water and sediment. The application of the DNPH method to sea water and sediment-pore water is shown in Fig. 5. Sea-water was generally not filtered prior to the derivatization reaction. Vacuum or gravity filtration generally resulted in an increase in the α-keto acid concentration of a sample, probably as a result of stress-induced release of these compounds by organisms [12]. Sea-water was collected from a variety of coastal and offshore stations. Pyruvate and glyoxylate were the major α-keto acids that were detected and these acids were generally present in the low nanomolar range.

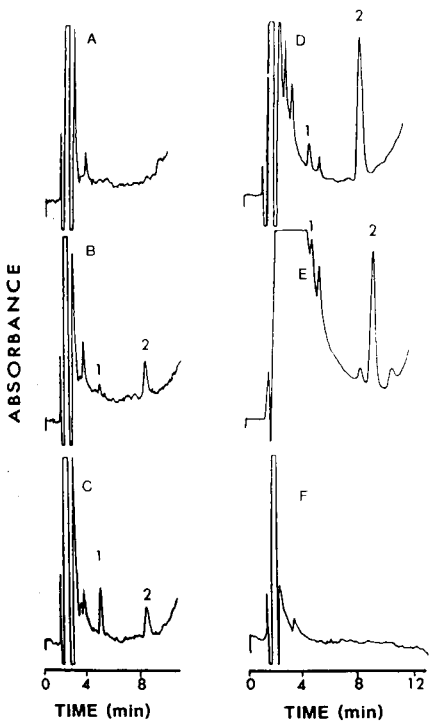

Fig. 5. Typical chromatograms of derivatized sea-water samples and blanks. Chromatographic conditions and derivatization procedure as in text; 2 ml injected. Peaks: (1) glyoxylate; (2) pyruvate. (A) Reagent blank in sea water (reaction 1 h) collected at 180 m in the Gulf Stream; (B) Gulf Stream water collected at 25 m; (C) Gulf Stream water collected at 180 m with glyoxylate and pyruvate added to a final concentration of 5 nM; (D) sea water from Biscayne Bay, Florida; (E) anaerobic sediment pore water from Biscayne Bay; (F) underivatized Biscayne Bay sea water.

The HPLC system was mounted in a portable cabinet and taken out to sea during a research cruise (R/V Cape Florida, June, 1985) off the eastern coast of Florida. Samples were collected in the Gulf Stream using 10-l teflon-lined Go-Flo samplers (General Oceanics, Miami, FL). The DNPH reagent and 1 M HCl were added to samples within 15 min after their collection. Pyruvate and glyoxylate were detected in low concentrations ($\leqslant$16 nM) as shown in Fig. 6.

Concentrations of α-keto acids in sea water are relatively low compared to other components of the dissolved organic pool such as amino acids or sugars [16]. This finding is in agreement with the results obtained in an earlier study by Kieber [15], who reported concentrations of pyruvate and glyoxylate in the 1—5 nM range in the Delaware Bay using a different HPLC technique that is based on the derivatization reaction of α-keto acids with *o*-phenylenediamine (OPD). However, the concentrations that are reported in the present study are approximately two orders of magnitude lower than those reported by Steinberg and Bada [9, 17] in the eastern Pacific ocean. These investigators also used the OPD technique but in conjunction with a multi-step procedure involving sample filtration, liquid-liquid extraction, and sample concentration. Similar inconsistencies have been observed in the determination of amino acids in sea water with harsh, multi-step procedures

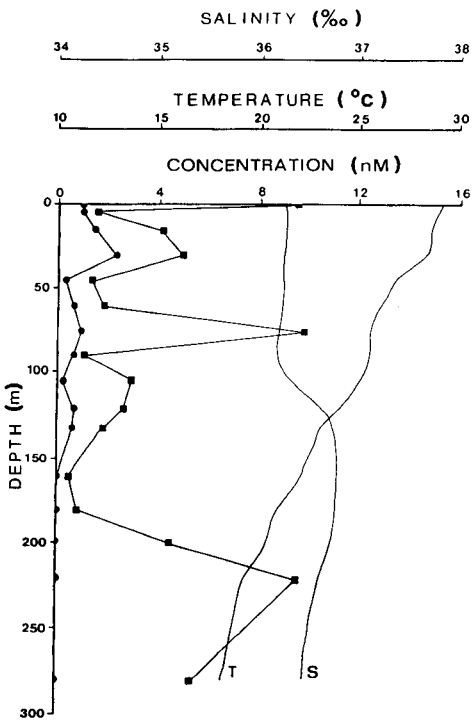

Fig. 6. Depth profile of glyoxylate (•), pyruvate (▪), temperature (T), and salinity (S) in the Gulf Stream.

(for a review, refer to [11]) yielding amino acids concentrations orders of magnitude greater than those reported using the mild, single-step procedure of Lindroth and Mopper [18].

Surface sediment was collected from Biscayne Bay along the edge of a mangrove stand. The pore water was extracted by gravity filtration through a Whatman GF/C glass fiber filter with a Gelman polycarbonate support. Pyruvate was detected in the μM concentration range and was the predominant α-keto acid that was detected although other unidentified compounds were also present (Fig. 5E). Pyruvate was also the major α-keto acid detected in pore water collected in the Great Marsh (Lewes, Delaware) using the quinoxalinol method [15]. The high concentration of pyruvate in various pore waters (μM) is noteworthy, because it was thought previously that pyruvate should not be present in the sediment within the sulfate-reducing zone [19].

Conclusions

The classical carbonyl reagent, 2,4-dinitrophenylhydrazine, has been adapted to the determination of trace amounts of α-keto acids in natural waters. The mild, single-step derivatization procedure has been developed to overcome the major problems inherent in harsh, multi-step procedures, especially stress-induced release of organic matter by organisms which may result in substantial overestimation of actual concentration levels. This may be an important consideration for key biochemical intermediates such as pyruvate which is only present at nano- to low-micromolar concentrations in natural waters.

In sediment interstitial waters, there are significantly higher concentrations of α-keto acids, particularly pyruvate. This suggests that pyruvate may play a previously unrecognized role as an important intermediate in organic turnover in sulfate-reducing sediments.

The authors wish to thank the United States Office of Naval Research for their generous support of this project (N 00014-85-C-0020). Thanks are also extended to the captain and crew of the R/V Cape Florida for their assistance. We would also like to thank Richard Sikorski for operating the HP diode-array computer interface.

REFERENCES

1 K. Mopper and E. T. Degens, in B. Bolin, E. T. Degens, S. Kempe and P. Ketner (Eds.), The Global Carbon Cycle, Wiley, New York, 1979, p. 293.
2 R. B. Gagosian and C. Lee, in E. K. Duursma and R. Dawson (Eds.), Marine Organic Chemistry, Elsevier/North Holland, Amsterdam, 1981, p. 91.
3 K. Mopper and P. Lindroth, Limnol. Oceanogr., 27 (1982) 336.
4 S. Vastano, P. Milne, K. Mopper and R. Zika, Trans. Am. Geophys. Union, 66 (1985) 1257.
5 K. Mopper, Trans. Am. Geophys. Union, 66 (1985) 1258.
6 A. L. Lehninger, Biochemistry, Worth, New York, 1975.
7 D. J. Kieber and K. Mopper, Trans. Am. Geophys. Union, 66 (1985) 1266.

8 A. J. L. Cooper, J. Z. Ginos and A. Meister, Chem. Rev., 83 (1983) 321.
9 S. M. Steinberg and J. L. Bada, Mar. Chem., 11 (1982) 299.
10 D. J. Kieber and K. Mopper, J. Chromatogr., 281 (1983) 135.
11 R. Dawson and G. Liebezeit, in E. K. Duursma and R. Dawson (Eds.), Marine Organic Chemistry, Elsevier/North Holland, Amsterdam, 1981, p. 445.
12 B. D. Johnson and P. J. Wangersky, Limnol. Oceanogr., 30 (1985) 966.
13 E. Sawicki and C. R. Sawicki, Aldehydes:Photometric Analysis, Vol. 1, Academic Press, New York, 1975, p. 57.
14 B. Buslig, J. Chromatogr., 247 (1982) 193.
15 D. J. Kieber, M.Sc. Thesis, University of Delaware, 1983.
16 E. K. Duursma and R. Dawson, Marine Organic Chemistry, Elsevier/North-Holland, Amsterdam, 1981.
17 S. M. Steinberg and J. L. Bada, J. Mar. Res., 42 (1984) 697.
18 P. Lindroth and K. Mopper, Anal. Chem., 51 (1979) 1667.
19 D. B. Nedwell and C. M. Brown, Sediment Microbiology, Academic Press, New York, 1982, p. 82.

Analytica Chimica Acta, 183 (1986) 141—154
Elsevier Science Publishers B.V., Amsterdam — Printed in The Netherlands

BASELINE CORRECTION METHOD FOR SECOND-HARMONIC DETECTION WITH TUNABLE DIODE LASERS

H. ABBINK SPAINK, T. T. LUB* and R. P. OTJES

Netherlands Energy Research Foundation ECN, Westerduinweg 3, P.O. Box 1, 1755 ZG Petten (The Netherlands)

H. C. SMIT

Laboratory for Analytical Chemistry, University of Amsterdam, Nieuwe Achtergracht 166, 1018 WV Amsterdam (The Netherlands)

(Received 17th September 1985)

SUMMARY

To measure small absorbances in tunable diode laser infrared spectrometry, second-harmonic detection is often used. The spectrum obtained is the sum of the desired molecular line profile, a contribution of the laser emission profile and various types of noise. It is shown that the undesired contributions can be reduced significantly by subtracting a least-squares fitted low-degree polynomial from the spectrum, followed by applying a digital low-pass filter to the remainder. A theory is developed for estimating the systematic error introduced by this procedure. The method is applied in a calibration experiment for nitrogen dioxide in air at low part-per-billion by volume levels.

In the past decade, semiconductor lasers have become an important tool in infrared spectroscopy because of their special features of tunability, low spectral bandwidth (in general less than 0.001 cm^{-1}), fast response and relatively high spectral radiance. Their main applications include high-resolution spectroscopy and trace gas analysis (usually in relation to environmental studies) [1—3].

The smallest absorbances measured with diode lasers (for low-pressure gas mixtures) reported in the literature vary from 10^{-7} to 10^{-5} m^{-1} [2, 3], depending mostly on the quality of the laser used. In practical situations, however, these limits will seldom be reached because many parameters need to be optimized. First, the alignment of the optical system is generally time-consuming. In daily operation, the alignment requires adjustment of five interdependent settings (see Fig. 1). Mathematically, this is a six-dimensional problem and is thus hard to cope with. Secondly, it takes a large amount of time to find a good absorption line. This depends not only on the spectrum itself but also on the characteristics of the laser; a strong absorption line can be used only if it coincides with a strong laser mode.

For measuring small absorptions, second-harmonic detection (2f-detection) is often used. The basic principle of this technique is to modulate the laser

0003-2670/86/$03.50

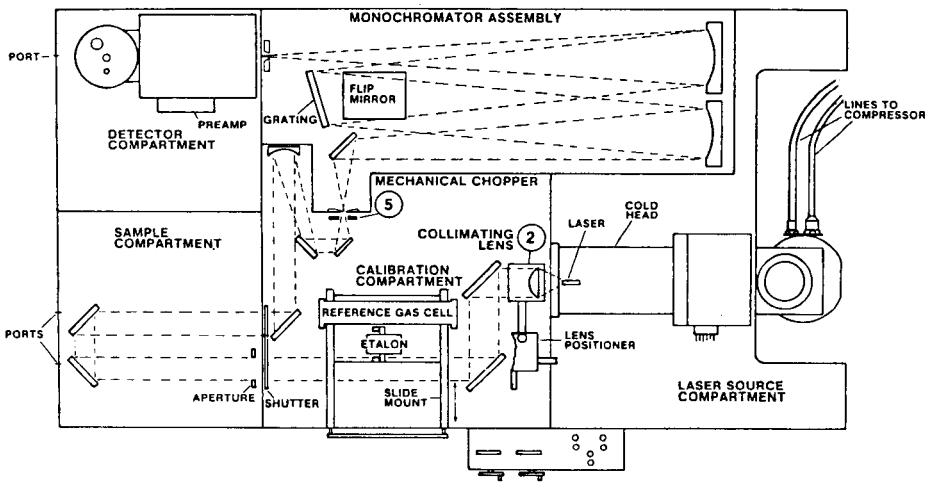

Fig. 1. Scheme of a commercial LS-3 spectrometer (courtesy Spectra Physics). The collimating lens (2) is also used for laser beam alignment. It can be displaced in three directions.

wavelength (at frequency f) and to demodulate at twice the modulation frequency. The resulting signal resembles the second derivative of the original signal (Fig. 2) and thus reduces contributions that vary slowly with wavelength, e.g., most of the laser emission profile. A detailed discussion on 2f-detection is available [4]. Nevertheless, when very small absorptions are measured, there is usually a contribution of the laser profile which eventually dominates the signal. This introduces another restriction on the choice of the absorption line: the emission profile should be smooth in the neighbourhood of the wavelength of the peak maximum.

Computerizing the system offers the possibility to solve many of these problems. First, the optical alignment procedure can be speeded up and improved greatly with the aid of a numerical optimization procedure; secondly, the laser contribution to the 2f-signal can be reduced by using suitable numerical baseline-correction techniques. In the present paper only the second point will be discussed. In another paper, the results obtained with the automatic alignment will be discussed.

Baseline contributions can be reduced in many ways, e.g., by subtracting the empty-cell spectrum or by applying non-linear fitting techniques. During the present measurements, it appeared that very satisfactory results can be obtained with a much simpler method involving estimation of the baseline by making a least-squares fit of the entire signal (baseline + absorption) with a low-degree polynomial. In fact, this method turned out to work better than subtraction of the empty-cell spectrum, for in the latter case the noise of the blank measurement is added to the signal and, moreover, matching of the two spectra may cause problems because of laser instabilities. Non-linear fitting techniques might give better results, but they have the practical

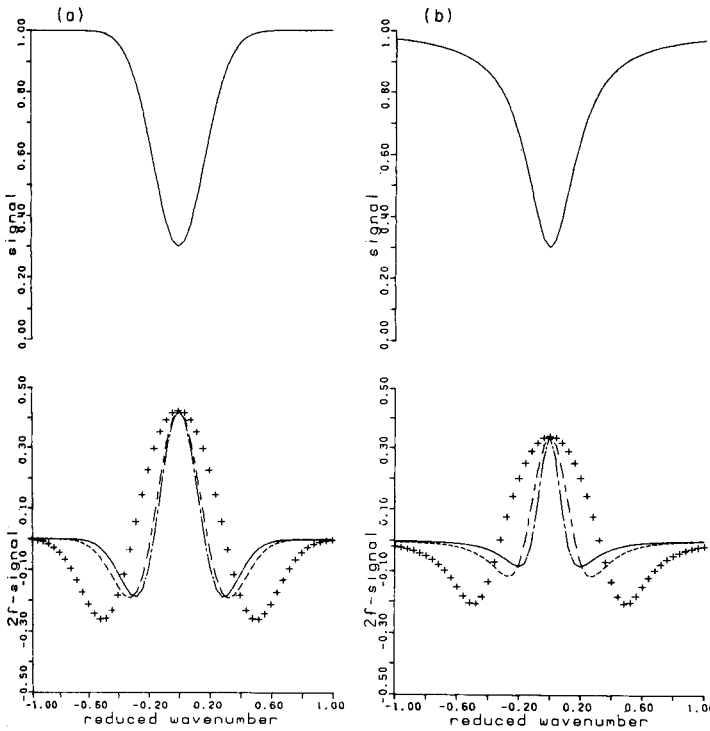

Fig. 2. Difference between second-derivative and second-harmonic spectra. For small modulation amplitudes ($\ll\sigma$), both signals coincide (centre lines). For larger modulation amplitudes, $1\sigma_{1/2}$ (dashed line) and $2.5\sigma_{1/2}$ (+) the two differ significantly. Signals are given in arbitrary units. For ease of comparison, all figures are scaled to an equal value at $x = 0$.

disadvantages of requiring more computer memory, much more computation time and more prior knowledge about the number of absorption lines, the approximate position of each individual line and a mathematical model for describing the profile (which make this method less versatile).

The aim of the present paper is to give a theoretical and experimental justification for the simple polynomial subtraction technique.

THEORY

The baseline subtraction method introduced here makes use of two important assumptions: (1) the baseline can indeed be approximated by a polynomial of degree n (i.e., this polynomial is a good fitting function); (2) the presence of the absorption signal does not influence the baseline estimate significantly. In theory, the first assumption need not introduce any problem if n is made large enough. However, one is restricted in the choice of the value of n by the second assumption; if n is too large not only

the baseline but also a significant part of the signal will be fitted. Furthermore, because computers have a finite precision, and computation time increases quadratically with n, it is not really practicable to fit any function with a high-degree polynomial ($n > 8$). In the case of slowly varying background signals, however, a polynomial with degree $n < 7$ generally will give a satisfactory description of the baseline. The second assumption cannot be accepted without an evaluation of the magnitude of the error. This will be done in the next section.

For estimating this error, two types of absorption profiles are considered: (1) collision-broadened lines (pressure > 60 Torr), with a Lorentzian shape; (2) Doppler-broadened lines (pressure < 1 Torr) with a Gaussian shape. For the intermediate cases (Voigt profiles), it is reasonable to assume that the error has a value somewhere between the values of the extreme cases. To simplify the problem a few additional assumptions are needed: (1) only one absorption is present and it is centered in the middle of the recorded spectrum; (2) noise contributions may be neglected; (3) the second-harmonic signal may be replaced by a second derivative. The acceptability of the last assumption is demonstrated in Figs. 2 and 3. For large modulation amplitudes

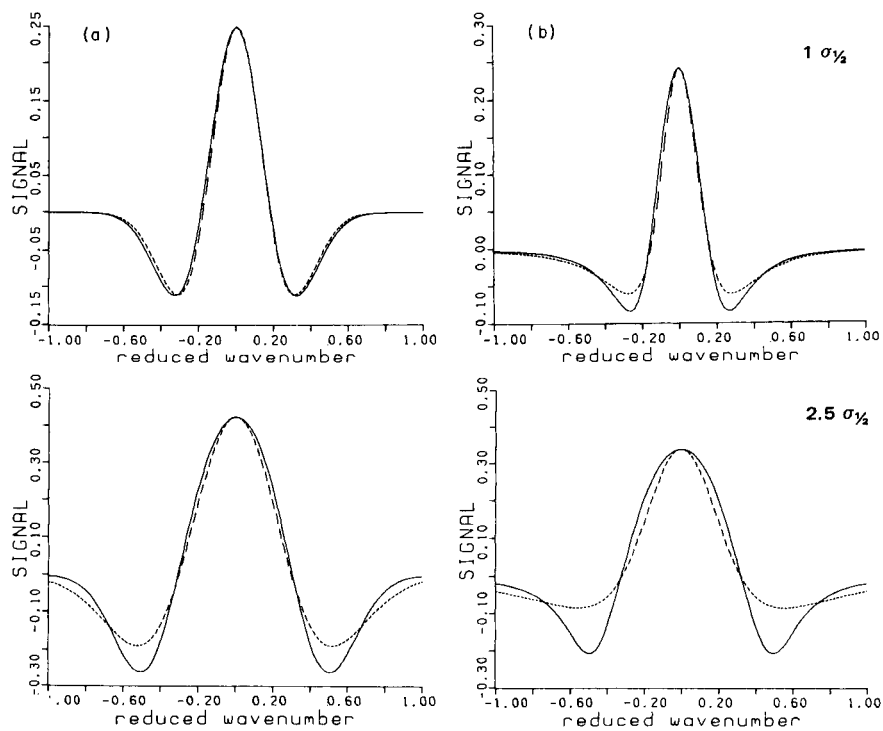

Fig. 3. Fit of second-harmonic signals with the second derivative of a Gaussian (a) and Lorentzian (b) shape that has identical zero crossings for two different modulation amplitudes (dashed curves).

(≥absorption halfwidth), the second-harmonic signal differs significantly from the true second derivative of the original Gaussian peak. However, if one is not concerned with the exact relation between the direct absorption and the second-harmonic signal, the broadened second-harmonic signal may be interpreted as the second derivative of a Gaussian absorption with a larger width. The linewidth of this (imaginary) absorption can be determined from the zero crossings of the second harmonic signal. If now the second derivative of a Gaussian profile with that linewidth is calculated, a line shape is obtained that resembles the original second-harmonic signal (apart from a constant multiplier). Two examples are demonstrated in Fig. 3(a) (dashed curves); the upper trace corresponds to a modulation amplitude of $1\sigma_{1/2}$ and the lower trace to $2.5\sigma_{1/2}$. Figure 3(b) shows the results of similar calculations for two Lorentzian line shapes. For large modulation amplitudes, the "second derivative" shows a slightly smoother behaviour than the second-harmonic signal, so the former will be more susceptible to error when a polynomial fit is applied for estimating the baseline. Thus it may be concluded that the replacement of a second-harmonic shape by a second derivative will cause a slight over-estimate of the error introduced by the baseline correction method.

The least-squares fit of the baseline with the fitting function $b_i = b(x_i)$,

$$b_i = \sum_{k=0}^{n} \beta_k x_i^k \tag{1}$$

where x_i is the x value of the ith measuring point, is obtained when the sum χ^2,

$$\chi^2 = \sum_{i=1}^{N} (b_i - y_i)^2 \tag{2}$$

where y_i is the measured value at x_i, and N is the number of measurements, is minimized by adapting the parameters β_k of the estimation function $b(x)$. For computational reasons, the x values are transformed to the interval $[-1, +1]$, so x_i is given by

$$x_i = -1 + (i-1)\Delta x \tag{3}$$

where $\Delta x = 2/(N-1)$. Without loss of generality N is assumed to be an odd number. The minimum of χ^2 is obtained by zeroing all derivatives with respect to the parameters (β_k). This results in a set of $n+1$ simultaneous equations:

$$\begin{aligned}
&S_0\beta_0 + S_1\beta_1 + S_2\beta_2 + \ldots\ldots\ldots + S_n\beta_n &&= S_Y(0)\\
&S_1\beta_0 + S_2\beta_1 + S_3\beta_2 + \ldots\ldots\ldots + S_{n+1}\beta_n &&= S_Y(1)\\
&\qquad\qquad\qquad\qquad\qquad\qquad\qquad\vdots &&\quad\vdots\\
&S_n\beta_0 + S_{n+1}\beta_1 + S_{n+2}\beta_2 + \ldots\ldots + S_{2n}\beta_n &&= S_Y(n)
\end{aligned} \tag{4}$$

where $S_k = \Sigma_{i=1}^{N} x_i^k$ and $S_Y(k) = \Sigma_{i=1}^{N} y_i x_i^k$. These equations can be written in matrix form,

$$\sigma\bar{\beta} = \bar{S}_Y \tag{5}$$

$$\sigma = \begin{pmatrix} S_0 & S_1 & S_2 \ldots\ldots\ldots S_n \\ S_1 & S_2 & S_3 \ldots\ldots\ldots S_{n+1} \\ \vdots & & \vdots \\ S_n & S_{n+1} & S_{n+2} \ldots\ldots\ldots S_{2n} \end{pmatrix}$$

$$\bar{\beta} = \begin{pmatrix} \beta_0 \\ \beta_1 \\ \vdots \\ \beta_n \end{pmatrix} \quad \text{and} \quad \bar{S}_Y = \begin{pmatrix} S_Y(0) \\ S_Y(1) \\ \vdots \\ S_Y(n) \end{pmatrix}$$

The solution is given by

$$\bar{\beta} = \sigma^{-1}\bar{S}_Y \tag{6}$$

As a consequence of the choice of the X-interval, sums S_k are 0 for odd values of k. The sums of even powers of x can be calculated by using the formulae for sums of powers of natural numbers [5]:

$$S_k = \frac{2\Delta x^{-1}}{k+1} + 1 + \frac{1}{6}\binom{k}{1}\Delta x^k + \ldots = \frac{N-1}{k+1} + 1 + \frac{k}{6(N-1)} + \ldots \tag{7}$$

For large N, these sums may be approximated by

$$S_k = [(N-1)/(k+1)] + 1 \tag{8}$$

The relative error in this approximation is of the order of $(k+1)/(N-1)$.

Clearly the elements of σ and σ^{-1} do not depend on the signal strength. If it is assumed that the signal consists only of a 2f-absorption signal, $s(x)$, and a baseline contribution, $b(x)$ [so $y(x) = s(x) + b(x)$] then the mixed sums $S_Y(k)$ are composed of two sums: one of the absorption signal itself, $S_S(k)$, and one of the baseline, $S_B(k)$. The sum $S_S(k)$ is responsible for the error in the baseline estimation. Equation 5 can now be written as

$$\bar{\beta} + \delta\bar{\beta} = \sigma^{-1}(\bar{S}_B + \bar{S}_S) = \sigma^{-1}\bar{S}_B + \sigma^{-1}\bar{S}_S \tag{9}$$

The magnitude of $S_S(k)$ can be estimated by replacing the sum by an integral:

$$S_Y(k) = \sum_{i=1}^{N} y_i x_i^k = (1/\Delta x) \sum_{i=1}^{N} y_i x_i^k \Delta x \approx (1/\Delta x) \int_{-1}^{+1} y x^k \mathrm{d}x$$

If the Gaussian function is expressed by $G(x) = I_0 \exp(-x^2/2\sigma_D^2)$, where I_0 is the peak height, and σ_D is the Doppler width (after transformation to [−1, 1]), then the second derivative has the form

$$s(x) = (-1/\sigma_D^2)[(x/\sigma_D)^2 - 1]G(x) \tag{10}$$

In the case of a Lorentzian lineshape, $L(x) = I_0\,\sigma_l^2/(x^2 + \sigma_l^2)$, where σ_l is the Lorentz halfwidth (HWHM), $s(x)$ is given by

$$s(x) = I_0\,[2\sigma_l^2(3x^2 - \sigma_l^2)/(x^2 + \sigma_l^2)^3] \tag{11}$$

With these expressions the sums $S_S(k)$ can be calculated. Results are given in Table 1. Note that $s(x)$ is an even function in both cases, so that sums with odd powers of x are 0.

In most measurements the absorption halfwidth is small in comparison to the total spectrum length (in the spectra shown in Fig. 7 for example, the halfwidth is 0.24 in reduced units), thus the results given in Table 1 may be simplified in the following manner: all terms with powers of σ higher than 2 can be neglected; all terms with $G(1)$ (Gaussian profile) can be neglected; and arctan$(1/\sigma)$ (Lorentzian absorption) can be replaced by $\pi/2$. The simplified expressions are summarized in Table 2.

With these results the error vector $\delta\bar{\beta}$ can be calculated. Because matrix-elements σ_{ij}^{-1} are 0 for $i + j$ odd, the vector elements $\delta\beta_i$ are zero for odd values of i. Further, it should be noted that the concentration information is obtained by measuring the difference between the minimum $s(0)$ and the maximum $s(x_{max})$. This means that an error in the estimate of β_0 does not cause an error in the final result, so that only the values of $\delta\beta_2, \delta\beta_4, \ldots$ are

TABLE 1

Mixed sums for a Gaussian and Lorentzian profiles

(A) Mixed sums for a Gaussian absorption function ($\sigma = \sigma_D$)

k	$S_S(k)$
0	$[-(N-1)/\sigma^2]G(1)$
2	$[-(N-1)/\sigma^2]G(1)(1 + 2\sigma^2) + (N-1)2\int_0^1 G(x)\mathrm{d}x$
k	$[-(N-1)/\sigma^2]G(1)[1 + k\sigma^2 + k(k-1)\sigma^4 + k(k-1)(k-3)\sigma^6 + \ldots + k(k-1)\ldots 5\cdot 3\sigma^k] + (N-1)k(k-1)(k-3)\ldots 5\cdot 3\sigma^{k-2}\int_0^1 G(x)\mathrm{d}x$

(B) Mixed sums for a Lorentzian profile ($\sigma = \sigma_l$)

k	$S_S(k)$
0	$-(N-1)I_0\,2\sigma^2/(1 + \sigma^2)^2$
2	$-(N-1)I_0[2\sigma^2/(1 + \sigma^2)^2 + 2\sigma^2/(1 + \sigma^2) - 2\sigma \arctan(1/\sigma)]$
k	$-(N-1)I_0[[2\sigma^2/(1 + \sigma^2)^2] + [k\sigma^2/(1 + \sigma^2)] - k(k-1)(-1)^{k/2}\{\sum_{i=0}^{k/2-2}[(-1)^i/(2i + 1)]\sigma^{k-2-2i} - \sigma^{k-1}\arctan(1/\sigma)\}]$

TABLE 2

Approximations of the mixed sums

(A) Gaussian function

k	$S_S(k)$
0	0
2	$(N-1)I_0 2\sigma(\pi/2)^{1/2}$
k	$(N-1)I_0 k(k-1)(k-3)\ldots 5\cdot 3\sigma^{k-1}(\pi/2)^{1/2}$

(B) Lorentzian function

k	$S_S(k)$
0	$-(N-1)I_0 2\sigma^2$
2	$-(N-1)I_0(4\sigma^2 - 2\sigma\pi/2)$
$k \geqslant 4$	$-(N-1)I_0\{[-6\sigma^2/(k-3)] + (-1)^{k/2}k(k-1)\sigma^{k-1}\pi/2\}$

important. It can be concluded that the relative error in the measurement of $s(x_{max}) - s(0)$ merely depends on the ratio between the absorption halfwidth and the length of the total spectrum and the degree n of the polynomial.

Figure 4 shows the relations between the absorption halfwidth and the relative error calculated for different values of n (2, 4, 6 and 8) for Gaussian and Lorentzian absorption profiles. At first glance it seems that Gaussian absorptions are more susceptible to error than Lorentzians. This, however, is merely a consequence of the choice of the absorption halfwidth as a parameter. The halfwidth can be a useful quantity in direct detection, but in the case of second-harmonic signals it loses its meaning. A more natural parameter for second-harmonic functions would be the distance between the minimum and the maximum ($\sigma_{min-max}$). When this parameter is used the situation is reversed, as shown in Fig. 4(c).

The baseline subtraction procedure can be summarized in the following algorithm:

(1) sample spectrum at N equidistant data-points: $y_1, y_2, \ldots, y_N$;
(2) calculate step size for the x-values: $\Delta x = 2/(N-1)$;
(3) select degree polynomial (n);
(4) calculate all non-zero elements of the $(n+1) \times (n+1)$ — matrix σ:

$$\sigma_{ij} = S_{i+j-2} = \sum_{k=1}^{N} x_k^{i+j-2} = \sigma_{ji} \quad (i = 1, 2, \ldots, n+1; j = 1, 2, \ldots, n+1; i+j \text{ even})$$

$$(x_k = -1 + (k-1)\Delta x)$$

(5) calculate mixed sums $S_Y(j)$ from $S_Y(j) = \Sigma_{k=1}^{N} y_k x_k^j$ (see Eqn. 4);

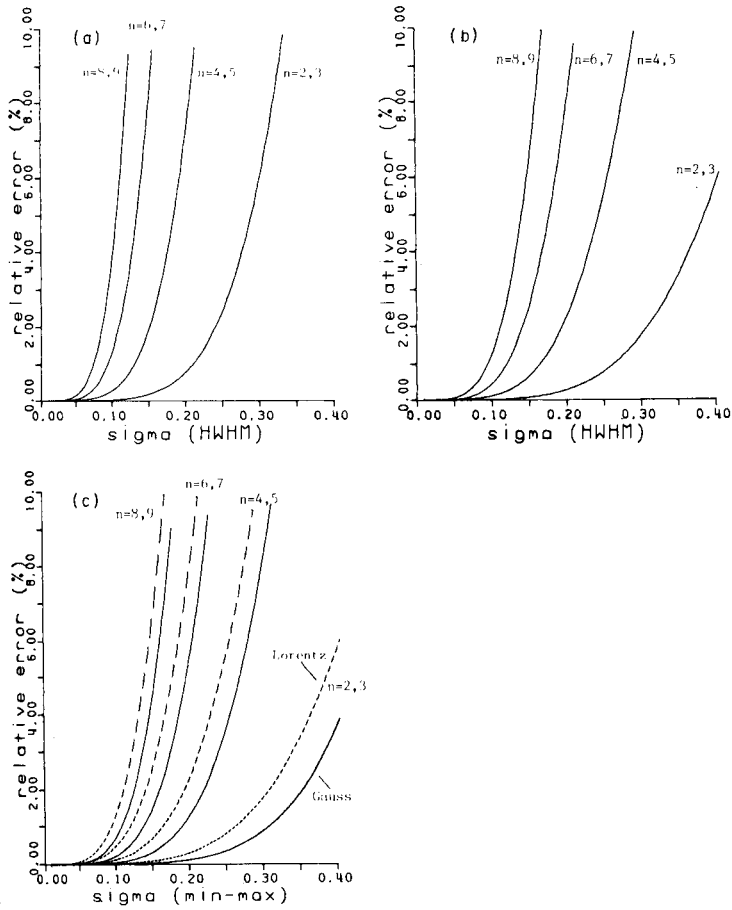

Fig. 4. (a) Diagram showing relation between the relative systematic error in the signal value and the reduced halfwidth of the absorption line (HWHM) for baseline estimations with polynomials of degree n = 2, 4, 6 and 8 for a Gaussian absorption profile; (b) the same relation for a Lorentzian profile. (c) Error as a function of the distance between the minimum and the maximum in the second-harmonic spectrum.

(6) invert matrix σ;
(7) calculate polynomial coefficients $\beta_0, \beta_1, \ldots, \beta_n$ (Eqn. 6);
(8) calculate value polynomial at data points: $P(x_k) = \beta_0 + \beta_1 x_k + \beta_2 x_k^2 + \ldots + \beta_n x_k^n$;
(9) subtract polynomial $y'_k = y_k - P(x_k)$ $(k = 1, 2, \ldots, N)$.

For errors greater than approximately 10%, the above calculation is no longer valid because in such cases other effects such as a shift in the position of the maximum of the absorption profile must be considered. The method could be improved by introducing the following iterative procedure: (1) calculate sums; (2) subtract estimated baseline; (3) calculate linewidth and $s(0)$

from resulting signal; (4) calculate signal contribution to the sums; (5) subtract signal contribution from sums; (6) repeat procedure (starting with step 2) until the change in the final signal is negligible. However, at low concentration/signal levels, noise contributions (which have been neglected so far) will cause a larger error in the final result, and in most practical situations the iterative procedure will not be useful.

EXPERIMENTAL

Instrumentation

A complete diode laser spectroscopy system (Spectra-Physics LS-3; Fig. 1), which incorporates all necessary cryogenics, electronics, optics, etc. is used at ECN to study the behaviour of pollutants in the atmosphere. The system is equipped with a 1-m multiple reflection sample cell (White cell) for measuring small absorptions. During the measurements described here, the White cell was set at a moderate pathlength of 40 m. For reasons outlined above, the LS-3 was interfaced with a LSI 11/23 computer. All important manual functions (laser current settings, temperature setting, and the positioning of the collimation lens, the monochromator grating and the White cell D-mirror) were made computer-controllable. Basically no new functions were added. Figure 5 gives an overview of the computerized spectrometer. All interface units were developed at ECN.

Data acquisition

Data acquisition is done by a slow 12-bit analog/digital converter (ADC; Digital ADV11-A). The minimum sampling time is 20 ms. Spectra of small absorptions are obtained by scanning the laser repetitively over a range about eight times the width (HWHM) of the absorption line studied. The maximum sampling rate of the ADC imposes an upper limit on the scanning rate, for Shannon's theorem must be obeyed. The minimum sampling rate for a 2f-signal of a Gaussian absorption was found by calculating its power spectrum.

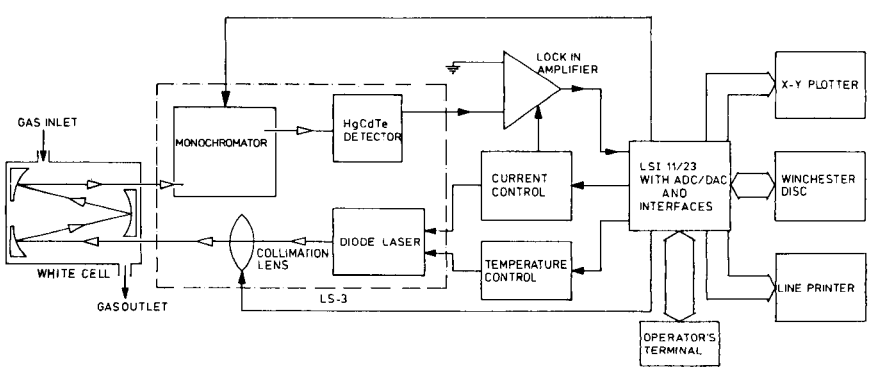

Fig. 5. Scheme of the automated LS-3 spectrometer.

The number of samples necessary for a complete reconstruction of the original signal turned out to be at least 3.5 per linewidth. So at a fixed sampling rate Δt, the maximum scan rate is given by the equation $(d\sigma/dt)_{max} = \sigma_{1/2}/3.5\Delta t$, where $\sigma_{1/2}$ is the absorption halfwidth (HWHM).

The final spectrum is obtained by subtracting (the least squares estimate of) the baseline from each spectrum, averaging the corrected spectra, and filtering the resulting spectrum digitally with a low-pass filter. The low-pass filter was designed with the aid of the IEEE software package Programs for Digital Signal Processing [6]. Several types of low-pass filters present in this package were tested. It was found that a filter that was designed by using a Czebyshev window [6] gave very satisfactory results in terms of sharpness of the cutoff. The filter has a fixed transition width of 0.1 normalized frequency units and a peak stop-band ripple of 1% (the normalized frequency is defined as the ratio of the actual frequency to the sample frequency). The degree of the polynomial and the filter cut-off frequency are supplied by the user.

Gas calibration system

For calibrating the laser absorption measurements (and other types of measurements involving trace gas detection), a permeation system was designed and developed at ECN. It is capable of generating calibrated flows of several gases of interest. In the case of nitrogen dioxide, which was used in these experiments, the system generates a primary flow of 10 SLM 206 mm^3 m^{-3} (ppb (v)) nitrogen dioxide in air. This concentration is checked regularly by means of wet-chemical methods. The primary flow is diluted with filtered laboratory air with the aid of critical capillaries, as shown in Fig. 6. The total error in the concentration calibration is less than 10%.

The gas flow in the White cell is ca. 3.3 SLM at a pressure varying from 10 to 18 Torr. Because the cell volume is ca. 14 l, the White cell content is renewed every 6 s.

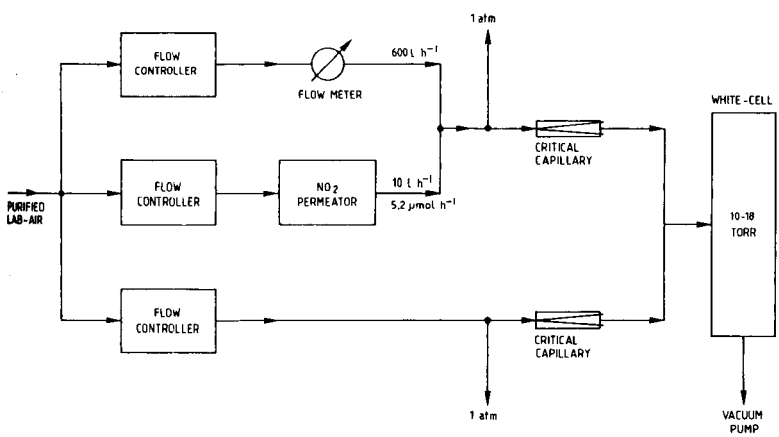

Fig. 6. Scheme of the calibration system.

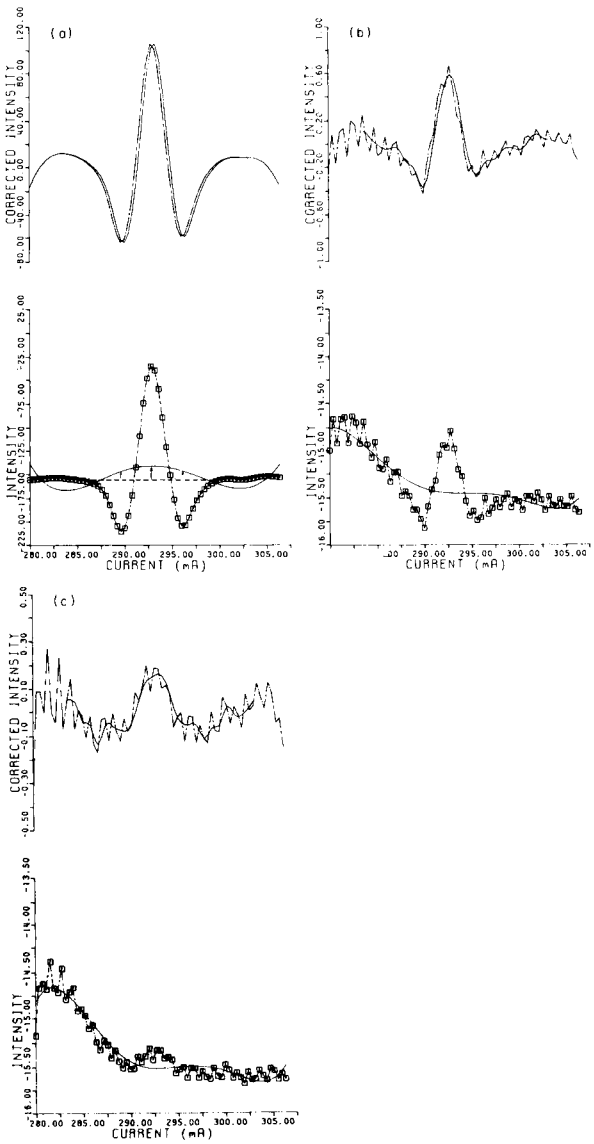

Fig. 7. Spectra of nitrogen dioxide at ca. 1578 cm^{-1}. (Because the spectra were obtained by sweeping the laser current the unit used on the abscissa is mA; intensities are in arbitrary units.) In each set, the lower traces show the original spectrum (□) and the estimated baseline (——). The upper traces show the spectra obtained after baseline subtraction (———) and low-pass filtering (——). (a) Pure nitrogen dioxide at ca. 1 Torr; the arrows indicate the errors caused by the baseline estimation procedure at points $x = 0$ and $x = \pm x_{max}$ (see main text); the errors carry the same sign, so that partial cancellation will occur. (b) 60 ppb(v) NO_2 in air (15 Torr, pathlength 40 m). (c) 8.5 ppb(v) NO_2 in air.

RESULTS AND DISCUSSION

For testing the present theory, calibration measurements were done with nitrogen dioxide at low pressure (10—20 Torr). Because a well-isolated absorption line was required for this purpose, a line at ca. 1578 cm^{-1} was selected, even though this line is nearly ten times weaker than many absorption lines in the region 1620—1630 cm^{-1} [6]. Results are given in Fig. 7. The lower traces show the measured spectra and the baseline estimate, while the upper traces show the spectra after baseline correction and filtering with a low-pass filter with a normalized cutoff frequency of 0.26.

The lower trace of Fig. 7(a) shows the 2f-absorption spectrum of pure nitrogen dioxide at a pressure of ca. 1 Torr. The baseline estimate was obtained by using a fifth-degree polynomial. Because the baseline contribution in the spectrum of Fig. 7(a) is small, the error in the baseline estimate can be calculated directly from the figure. This results in a value of ca. 3%, which is in excellent agreement with the theoretically predicted error for a Gaussian profile with a halfwidth of 0.165 (the halfwidth can be calculated from the zero-crossings in Fig. 7a). The dashed curves in Fig. 7(b) and (c) are spectra of 60 and 8.5 ppb (v) nitrogen dioxide in laboratory air. Each spectrum is the average of 10 successively recorded spectra. The total measuring time is ca. 3 min. In Fig. 7(c) the signal is dominated by the laser emission profile, so that nitrogen dioxide concentrations cannot be measured in this range without correction for the laser profile. Application of the baseline subtraction procedure (with a fifth-degree polynomial) followed by filtering with a low-pass digital filter produces the upper traces. Clearly, this spectrum resembles the pure spectrum well, although it is slightly distorted by low-frequency noise, probably caused by laser instabilities. At lower concentrations ($\leqslant$4 ppb) this noise appeared to exceed the signal magnitude, thus determining the detection limit.

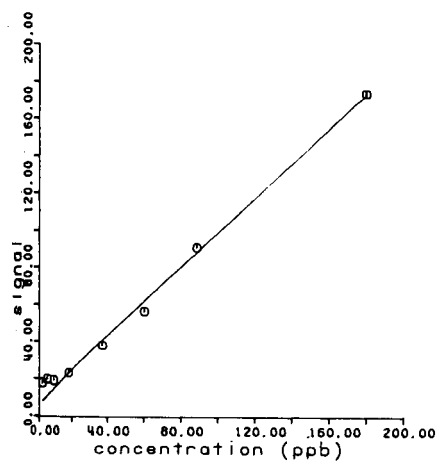

Fig. 8. Calibration curve for nitrogen dioxide in air.

Figure 8 shows the calibration curve obtained from these measurements. A linear relationship between the concentration of nitrogen dioxide and the corrected second-harmonic signal is found down to a level where low-frequency noise becomes dominant. Because the difference between the minimum and the maximum is taken as the analytical signal, the 1/f-noise causes a zero offset in the calibration curve. For a further reduction of the detection limit, it is necessary to reduce the 1/f-noise contribution. This can be done by increasing the sweep repetition rate to a level well above the highest frequency occurring in the noise spectrum. Preliminary measurements have shown that, in the system used, most important noise sources have frequencies below 400 Hz, so that the sweep repetition frequency should be at least 1 kHz. Hence the system will be extended with a fast ADC so that the detector signal can be processed directly.

We thank Mr. P. J. Kaandorp for designing and building all computer interfaces. We also thank Prof. J. Strackee, Laboratory of Medical Physics, University of Amsterdam, for valuable discussions on digital filtering and baseline correction procedures.

REFERENCES

1 K. J. Linden and A. W. Mantz, S.P.I.E. (The International Society for Optical Engineering), Vol. 320, Advances in Infrared Fibers II, 1982, p. 109.
2 J. Reid, M. El-Sherbiny, B. K. Garside and E. A. Ballik, Appl. Opt., 19 (1980) 3349.
3 H. I. Schiff, D. R. Hastie, G. I. Mackay, T. Iguchi and B. A. Ridley, Environ. Sci. Technol., 17 (1983) 352A.
4 J. Reid and D. Labrie, Appl. Phys., B26 (1981) 203.
5 I. S. Gradshteyn and I. M. Ryzhik, Tables of Integrals, Series and Products, Academic Press, New York/London, 1965.
6 Programs for digital signal processing, IEEE Press, New York, 1979.
7 L. S. Rothman and L. G. Hanscom, Air Force Geophysics Laboratory trace gas compilation, 1982 version; available from National Climatic Center of NOAA, Environmental Data Service, Federal Building, Asheville, NC 28801, U.S.A.

Analytica Chimica Acta, 183 (1986) 155—161
Elsevier Science Publishers B.V., Amsterdam — Printed in The Netherlands

SEPARATION OF NICKEL FROM OTHER ELEMENTS BY CATION-EXCHANGE CHROMATOGRAPHY IN DIMETHYLGLYOXIME/ HYDROCHLORIC ACID/ACETONE MEDIA

A. H. VICTOR

National Chemical Research Laboratory, Council for Scientific and Industrial Research, P.O. Box 395, Pretoria 0001 (South Africa)

(Received 19th August 1985)

SUMMARY

Nickel can be separated from Zn, Co, Cu(II), Mn(II), Fe(III), U(VI) and other elements which readily form chloro complex ions, by eluting them with 0.5 M HCl/93% acetone from AG50W-X4 resin. Nickel is then eluted selectively with 0.5 M HCl/95% acetone containing 0.1 M dimethylglyoxime, while the alkali and alkaline-earth elements, Al, Ti(IV), Sc, Y, La, lanthanides, Zr, Hf and Th are still retained. Separations are sharp and quantitative.

Ion-exchange chromatography has frequently been used for the separation of nickel from solutions containing one or a few other elements but little information seems to be available for its selective separation from most other elements in a single-column operation. This is not surprising, because nickel does not form reasonably stable complexes with the simple ions (e.g., chloride, bromide, nitrate or sulphate) which are often used for ion-exchange separations. Ligands which form complexes with nickel, such as amines, have been used for its separation from some elements [1—3]. Anion-exchange distribution coefficients of elements in hydrochloric acid/oxalate medium [4] suggest that in this medium nickel can probably be separated from most other elements, except Be, Pb, Cd and Zn. Such a separation, however, has not yet been investigated in detail.

A useful approach is offered by cation-exchange chromatography in hydrochloric acid/acetone medium. The cation-exchange distribution coefficients of elements in hydrochloric acid/acetone [5] show that those elements which have relatively strong tendencies to chloride complex formation such as Zn, Cd, Cu(II), Co, Pb, Hg(II), Bi, Fe(III), Ga, U(VI), Au(III), the platinum metals as well as Mn(II), should be eluted ahead of nickel with a suitable hydrochloric acid/acetone solution, while nickel together with the alkali and alkaline-earth metals, Al, Ti(IV), Sc, Y, the rare earths, Zr, Hf and Th should be retained. Thereafter, however, it is difficult to separate nickel from K, Be, Mg, Ca and Al with any of the common mineral acids, because of the small separation factors. The problem was solved by Wahlgren et al. [6] who used

0003-2670/86/$03.50

0.6 M hydrochloric acid/90% acetone containing 0.25 M dimethylglyoxime (DMG) as complexing agent to elute nickel selectively and separate it from the other elements which were more strongly retained; 0.6 M hydrochloric acid/90% acetone was used to elute elements forming chloride complexes from Dowex AG50W-X8 resin before nickel was eluted. In this earlier work, quantitative separations, elution curves or values of distribution coefficients were not described; only a 1-g resin column was used, which meant that only limited amounts of retained elements could be handled. This method [6] seemed promising, however, and it was decided to investigate it in more detail.

For the development of a more widely applicable method, a larger column is required. However, when 1 mmol of nickel was eluted from a column containing 20 g of AG50W-X8 resin with 0.6 M hydrochloric acid/90% acetone/0.25 M DMG as eluent, tailing of nickel at a very low concentration level was observed. This tailing effect was not observed when the 4% cross-linked AG50W resin was used. For this reason, as well as to investigate the possibility of eluting nickel with less DMG, the AG50W-X4 resin was chosen for further work on the selective and quantitative separation of nickel.

EXPERIMENTAL

Reagents, solutions and apparatus

Analytical reagent-grade chemicals were used throughout. Water was distilled and passed through an Elgastat deionizer.

The eluents were 5% 10 M hydrochloric acid/93% acetone/2% water (v/v) (eluent I), and 5% 10 M hydrochloric acid/95% acetone (v/v) containing 0.1 M dimethylglyoxime (eluent II).

A Varian-Techtron AA5 spectrometer and a Zeiss PMQ-II spectrophotometer were used for atomic absorption spectrometric (a.a.s.) and spectrophotometric measurements, respectively.

Ion-exchange resin and columns. The AG50W-X4 strongly-acid sulphonated polystyrene cation-exchanger was used. Resin of 100—200 mesh particle size was used for equilibrium studies and resin of 200—400 mesh for column work. The borosilicate glass columns (20 mm bore, 45 cm long) had a porosity-2 sintered-glass plate and a tap at the bottom and a B-19 joint at the top.

Procedures

Determination of distribution coefficients. Solutions (250 ml) of 0.2, 0.5 and 1.0 M hydrochloric acid containing 80, 90 or 95% of acetone and 0.1 or 0.2 M DMG as well as 1 mmol amounts of nickel were equilibrated for 16 h with 2.5 g of AG50W-X4 (H^+) resin which had been dried at 60° C in a vacuum pistol. After equilibration, the resin was collected on a sintered-glass plate in a short (20 cm) column and washed with 80% acetone and then with water. Adsorbed nickel was eluted with 50 ml of 3 M hydrochloric acid and determined by the method outlined in Table 1.

TABLE 1

Analytical methods used

Element	Method
Ni	Titration with EDTA in ammoniacal solution, murexide indicator. Small amounts by a.a.s. (232.0-nm line, air/acetylene flame).
Mn(II), Ca	Titration with EDTA in ammoniacal solution, methylthymol blue indicator, hydroxylammonium chloride present for Mn. Small amounts of Mn by a.a.s. (279.5-nm line, air/acetylene flame).
U(VI)	Gravimetrically as U_3O_8 after precipitation with CO_2-free ammonia. Small amounts spectrophotometrically with chlorophosphonazo-III at 672 nm in presence of DTPA at pH 1 [7].
Li, Na, K	Gravimetrically as sulphates (evaporation to dryness with H_2SO_4 in Pt crucible and ignition at 600°C for 15 min).
Co	Titration with EDTA at pH 6, pyridine buffer, naphthylazoxine S indicator.
Cu(II)	Titration with EDTA in the presence of 1,10-phenanthroline, methylthymol blue indicator.
Zn	Titration with EDTA at pH 5.5, xylenol orange indicator.
Fe(III), Al	Titration with excess of DCTA and back-titration with $ZnSO_4$, pH 5.5, xylenol orange indicator.
Mg	Titration with EDTA at pH 10, eriochrome blue-black B indicator.
NH_3OH^+	Addition of excess of $KBrO_3$ followed by HCl (~2 M HCl overall), and iodimetric titration of excess after 15 min.

To determine nickel in the filtrates, the solutions were diluted with water and acetone was added when necessary to give final solutions which contained about 70% acetone and $\leqslant$0.35 M hydrochloric acid. These solutions were passed through columns containing 21.7 ml (5 g dry weight) of AG50W-X4 resin (200—400 mesh). The columns were washed with 80% acetone and water and the strongly adsorbed nickel was eluted with 100 ml of 3 M hydrochloric acid. After evaporation, nickel was determined (Table 1).

The distribution coefficients [5] calculated (Table 2) indicate that nickel can be eluted with appropriate hydrochloric acid/acetone solutions containing only 0.1 M DMG instead of the 0.25 M DMG used by Wahlgren et al. [6]. The quantitative aspects of using 0.5 M hydrochloric acid/95% acetone/0.1 M DMG as eluent were investigated in more detail.

Elution curves. A column (45 × 2.0 cm) containing 65 ml (15 g dry weight) of AG50W-X4 resin was used. A solution (50 ml) of 0.2 M hydrochloric acid/85% acetone, containing 1 mmol each of uranium(VI), manganese(II) and nickel and 2 mmol of lithium, was passed through the column, previously equilibrated with 0.2 M hydrochloric acid/85% acetone. The ions were washed onto the column with 3 × 5 ml portions of 0.5 M hydrochloric acid/93%

TABLE 2

Distribution coefficients of nickel in HCl/acetone containing dimethylglyoxime (DMG) on AG50W-X4 resin

HCl (M)	Acetone (%)	Distribution coefficient	
		0.1 M DMG	0.2 M DMG
0.20	80	1081	833
	90	244	108
	95	13.7	8.8
0.50	80	143	96.3
	90	17.8	9.1
	95	4.3	3.6
1.0	80	23.6	13.8
	90	3.4	3.3

acetone (eluent I), and uranium(VI) and manganese(II) were eluted with 350 ml of eluent I. Fractions (25 ml) were taken from the start of the sorption step at a flow rate of about 3.0 ± 0.5 ml min^{-1} with an automatic fraction collector. Nickel was eluted with 0.5 M hydrochloric acid/95% acetone/0.1 M DMG (eluent II) and the elution continued until 500 ml of the eluent had been passed through. The fractions were evaporated and the elements were determined as outlined in Table 1. After evaporation of the nickel fractions, accompanying hydroxylammonium ions which originated from the decomposition of DMG on heating with hydrochloric acid [8, 9] were oxidized with hydrogen peroxide in the presence of a little hydrobromic acid, before nickel was determined. The elution curve is presented in Fig. 1.

Figure 2 shows an elution curve for the separation of nickel from the constituents present in the eluate after its initial separation on the 65-ml resin column. For this purpose, 1 mmol of nickel in 50 ml of eluent I was adsorbed on an equilibrated 65-ml resin column. Adsorbed nickel was then eluted with 250 ml of eluent II. The eluate was collected, via a 15-cm delivery tube from the column, under 100 ml of water in a 500-ml separatory funnel; this was necessary to avoid possible losses of the nickel-DMG complex in the medium used (see below). The collected eluate/water mixture (ca. 350 ml), which was about 0.36 M in hydrochloric acid, 68% in acetone and 0.071 M in DMG, was passed through a second column containing 21.7 ml (5 g) of AG50W-X4 resin, previously equilibrated with 0.1 M hydrochloric acid/70% acetone, at about 4.5 ± 0.5 ml min^{-1}. Nickel was adsorbed at the top of the column, the effluent was discarded, and the column was rinsed with 50 ml of 80% acetone to remove residual DMG and small amounts of diacetyl. Co-adsorbed hydroxylammonium ions which were formed to some extent, even at room temperature, during the contact time of DMG with hydrochloric acid after nickel had been eluted from the first column, were eluted with 130 ml of 0.5 M

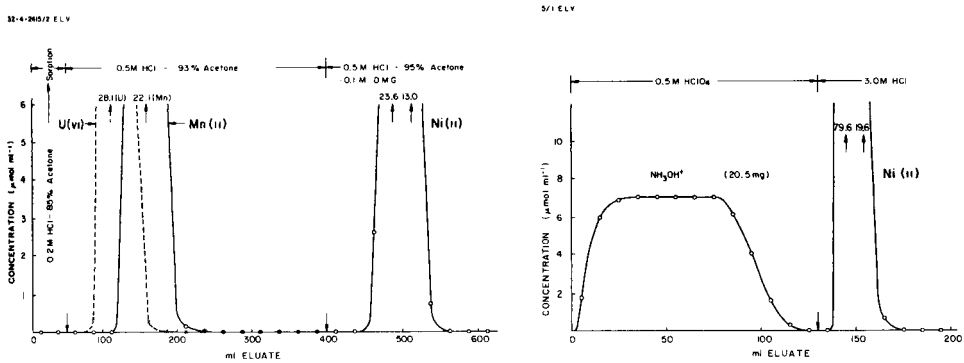

Fig. 1. Elution curve for 1 mmol each of Mn(II), U(VI) and Ni(II) and 2 mmol of Li; column (19.5 × 2.0 cm) of 65 ml (15 g) AG50W-X4 resin, 200—400 mesh; flow rate 3.0 ± 0.5 ml min^{-1}. Lithium was not eluted in 500 ml of eluent II.

Fig. 2. Elution curve for the separation of 1 mmol of Ni(II) from excess of DMG and about 20.5 mg of NH_3OH^+; column (6.5 × 2.0 cm) of 21.7 ml (5 g) AG50W-X4 resin, 200—400 mesh; flow rate 3.0 ± 0.5 ml min^{-1}.

perchloric acid at about 3.0 ± 0.5 ml min^{-1}. Nickel was then eluted with 100 ml of 3 M hydrochloric acid. Hydroxylammonium ions and nickel were determined in the fractions (10 ml).

Quantitative separation of ternary synthetic mixtures. Appropriate volumes of standard solutions of nickel and two other elements, one which formed a stable chloride complex and the other not, were accurately measured out in triplicate, mixed, and taken to dryness. The salts were dissolved and adsorbed from 50 ml of 0.2 M hydrochloric acid/85% acetone on 65-ml resin columns, previously equilibrated with the same medium. After sorption, elements less strongly adsorbed than nickel, such as Cu(II), Co, Mn(II), Fe(III), U(VI), etc, were eluted with 350 ml of eluent I; nickel was then eluted with 250 ml of eluent II, the eluate being collected beneath the surface of about 100 ml of water as already described. After elution from the first column, nickel in the eluates was separated from acetone, DMG and the decomposition products of the latter on secondary columns containing 21.7 ml of resin as previously described. Nickel was finally eluted with 100 ml of 3 M hydrochloric acid. The DMG remaining on the 65-ml resin columns, was washed out with 100 ml of 80% acetone and the latter washed out with 50 ml of water. Elements which still remained on these columns (Li, Na, K, Mg, Ca and Al) were eluted with 300 ml of 3 M hydrochloric acid. After evaporation of all the eluates, the elements were determined (Table 1). Results for these synthetic mixtures are presented in Table 3.

TABLE 3

Results for quantitative separations of ternary synthetic mixtures

Elements	Amounts taken (mg)	Amounts found[a] (mg)	Elements	Amounts taken (mg)	Amounts found[a] (mg)
Mn(II)	54.82	54.80 ± 0.04	Fe(III)	55.61	55.63 ± 0.04
Ni	59.04	59.04 ± 0.03	Ni	0.590	0.589 ± 0.003
Li	14.10	14.11 ± 0.02	Mg	24.17	24.16 ± 0.02
Co	59.13	59.12 ± 0.04	U(VI)	239.1	239.0 ± 0.1
Ni	59.04	59.03 ± 0.04	Ni	5.90	5.90 ± 0.02
Al	26.92	26.93 ± 0.02	K	40.10	40.11 ± 0.05
Cu(II)	63.64	63.64 ± 0.04	Zn	65.57	65.58 ± 0.05
Ni	59.04	59.05 ± 0.04	Ni	59.04	59.03 ± 0.04
Ca	38.68	38.70 ± 0.03	Na	23.05	23.07 ± 0.04

[a]Means of triplicate determinations with calculated standard deviation.

RESULTS AND DISCUSSION

The described method is satisfactory for the selective and quantitative separation of nickel from other elements (Table 3). By using the AG50W-X4 resin, at least up to 1 mmol amounts of nickel can be eluted selectively from relatively large resin columns without tailing and with a lower concentration of DMG. Of those elements which have relatively strong tendencies to chloride complex formation, manganese(II) has the largest value for its distribution coefficient in hydrochloric acid/acetone [5, 6, 10]. A volume of 350 ml of eluent I provides a considerable safety margin to ensure quantitative elution and separation of manganese(II), as well as other elements forming chloride complex ions. Another advantage of using the X4 resin is that uranium(VI) shows considerably less tailing than on the X8 resin [5, 10].

After elution of the elements forming chloride complexes, including those which are also complexed by DMG [Pd(II), Pt(II), Cu(II), Co, Pb, Bi, etc.], at least up to 1 mmol of nickel can be eluted quantitatively with 250 ml of eluent II. The distribution coefficients (Table 2) show that, at a fixed DMG concentration, nickel is more easily eluted as the hydrochloric acid and acetone concentrations are increased. This does not agree with the findings of Wahlgren et al. [6].

An unexpected phenomenon which appeared during this work, is that nickel is somewhat volatile in hydrochloric acid solutions containing DMG and high acetone concentrations. Even during the determination of distribution coefficients, some nickel ($\leqslant$0.1 mg) in the aqueous phase volatilized during the filtration. For the preparation of the first elution curve, fractions containing nickel were immediately diluted with water after elution in order to minimize this volatilization. Further experiments showed that when 250-ml portions of eluent II containing about 1 mmol of nickel were left in 600-ml beakers at room temperature in a fume cupboard for 1, 2 and 4 h,

about 2.9, 4.1 and 5.0%, respectively, of the original amount of nickel volatilized. No volatilization of nickel was detected when the nickel eluate was collected beneath the surface of about 100 ml of water. Table 3 shows that quantitative recoveries of nickel were then obtained. A convenient means of recovering the nickel in the eluate is to include another cation-exchange separation on a smaller column; nickel is thus separated from DMG and its decomposition products and can finally be recovered in 100 ml of 3 M hydrochloric acid (Fig. 2). The rate of decomposition of DMG to form hydroxylammonium ions was too slow to have any significant effect on the elution of nickel during the first column operation. It was found, by determining the adsorbed hydroxylammonium ion, that about 1.7% and 1.4% of the DMG decomposed during the first and second column operations, respectively. It is advisable, therefore, to use freshly prepared eluents.

Elements which remain on the first column after the elution of nickel, can be eluted, together with hydroxylammonium ions, by using 3 M hydrochloric acid. Hydrogen peroxide in the presence of a little hydrobromic acid, which serves as an indicator by forming bromine with excess of hydrogen peroxide, proved effective for oxidation of hydroxylammonium ions. Of the group of strongly retained elements, lithium has the lowest distribution coefficient. No lithium could be detected in the eluate after 500 ml of eluent II passed through the column (Fig. 1). The separation of nickel from the alkali and alkaline-earth metals as well as aluminium is clearly effective.

REFERENCES

1 J. Inczedy, Hung. Acta Chim., 62 (1969) 1.
2 F. Hilgeman, K. Shimomura and H. F. Walton, Sep. Sci., 4 (1969) 111.
3 J. Inczedy, P. Klatsmanyi-Gabor and L. Erdey, Hung. Acta Chim., 69 (1971) 137.
4 F. W. E. Strelow, C. H. S. W. Weinert and C. Eloff, Anal. Chem., 44 (1972) 2352.
5 F. W. E. Strelow, A. H. Victor, C. R. van Zyl and C. Eloff, Anal. Chem., 43 (1971) 870.
6 M. Wahlgren, K. A. Orlandini and J. Korkisch, Anal. Chim. Acta, 52 (1970) 551.
7 F. W. E. Strelow and T. N. van der Walt, S. Afr. J. Chem., 32 (1979) 169.
8 A. Tougarinoff, Ann. Soc. Sci. Bruxelles, 54B (1934) 314.
9 F. J. Welcher, Organic Analytical Reagents, Vol. 3, van Nostrand, New York, 1947, p. 197.
10 A. H. Victor, S. Afr. J. Chem., 36 (1983) 76.

Analytica Chimica Acta, 183 (1986) 163—177
Elsevier Science Publishers B.V., Amsterdam — Printed in The Netherlands

AN ION-EXCHANGE PROCEDURE FOR QUANTIFYING BIOLOGICALLY ACTIVE COPPER IN SEA WATER

N. G. ZORKIN

Envirocon Pacific Limited, #205-2250 Boundary Rd., Burnaby, B.C. V5M 3Z3 (Canada)

E. V. GRILL and A. G. LEWIS*

Department of Oceanography, The University of British Columbia, 6270 University Boulevard, Vancouver, British Columbia V6T 1W5 (Canada)

(Received 31st January 1985)

SUMMARY

An ion-exchange column method is described for determining the dissolved inorganic copper concentration and copper(II) ion activity in sea water. The method is based on the assumption that the amount of copper sorbed by a sulfonic-acid cation exchanger is related to the activities of the cationic forms of copper in solution. This assumption was tested in artificial sea water containing copper and the organic ligands EDTA, NTA, histidine and glutamic acid. A correlation was also observed between the inorganic copper fraction determined by the ion-exchange procedure and the toxic fraction of copper quantified by a diatom bioassay (*Thalassiosira pseudonana*). These results demonstrate the potential of such a technique for determining the concentration of biologically active trace metals in marine and estuarine environments.

Copper is an environmental constituent of considerable importance to marine phytoplankton. It is not only necessary for the proper functioning of many physiological processes but is also potentially toxic at concentrations observed in some coastal waters [1, 2]. The toxicity of copper is profoundly influenced by its chemical speciation. Complexation with organic ligands or adsorption to colloidal material has been shown to reduce the toxicity [3—5]. The results of algal assays combined with computer model/speciation calculations indicate that the copper(II) ion is the most toxic species [6—10]. Although hydroxy complexes [11], and some amino acid [12] and lipid-soluble metal complexes [13] have also been reported to exhibit toxicity toward certain organisms, it is still unclear how important such complexes are in the natural environment.

At present, no reliable method is available to quantify the concentration of copper(II) ion in sea water. Although direct activity measurements have been attempted with ion-selective electrodes [14, 15], the concentration range of copper in sea water is well below that for which the electrodes currently available display a Nernstian response, a factor that severely complicates data interpretation [16]. Furthermore, responses of these electrodes

0003-2670/86/$03.50

in sea water are adversely affected by interferences from chloride [17, 18]. Computer-modeling techniques have also been used to calculate free metal ion activities in sea water, but have limited application because the nature and concentration of the organic complexing agents present in natural waters are generally unknown.

Techniques such as anodic stripping voltammetry (a.s.v.) [19—22], ultrafiltration or dialysis [23—27], and sorption by chelating resins [28, 29] have been used in speciation studies and, in some cases, have provided data that can be related to bioassay results. For example, Young et al. [30] correlated mortality of larval coon-stripe shrimp to labile copper as quantified by differential-pulse a.s.v., and Srna et al. [31] found a correlation between complexing capacity values determined by a technique using a.s.v. and a biological technique using a marine diatom. However, because such techniques only quantify operationally defined classes of metal species based on their behavior during the measurement step and not a particular metal form, one would not expect the results to be related to the concentration of biologically active metal under all circumstances. This is best illustrated by the observations of Florence et al. [32], who attempted to estimate biologically active copper using a.s.v. at different plating potentials in the presence of various organic ligands. Although the a.s.v.-labile copper could be related to the toxic metal fraction in the presence of certain natural ligands, in most cases the instrumental and algal results could not be correlated.

This report describes a method for estimating the amount of biologically active copper in sea water that is based on the assumption that copper(II) ion is the most toxic species and its concentration can be related to the amount of metal sorbed by a sulfonic-acid cation exchanger. The procedure is similar to that used previously to determine cation activities in complex media such as milk [33, 34], and to that used by Cantwell et al. [35] to estimate free nickel concentrations in sewage solutions.

THEORY

When a cation-exchange resin is placed in contact with a solution containing a divalent transition metal ion such as Cu^{2+}, an exchange reaction occurs that, assuming that the resin is initially loaded with Na^+ ions, can be represented by the equation $Cu^{2+} + 2\ \overline{Na}^+ \rightleftharpoons 2\ Na^+ + \overline{Cu}^{2+}$, where the overbar indicates ions bound in the resin phase. Application of the law of mass action to this reaction gives

$$K_{Cu,Na} = \{Na^+\}^2\{\overline{Cu}^{2+}\}/\{\overline{Na}^+\}^2\{Cu^{2+}\} = ([Na^+]^2[\overline{Cu}^{2+}]/[\overline{Na}^+]^2[Cu^{2+}]) \times (f_{Cu}\gamma_{Na}^2/f_{Na}^2\gamma_{Cu}) \quad (1)$$

where the braces and square brackets represent, respectively, activities and concentrations, and f and γ are the activity coefficients of the ions in, respectively, the resin and solution phases. All applications considered here assume that the resin used is of the sulfonic acid type and does not display high selectivity for transition metal cations. Also, it is assumed that the resin is used in a column and that the test solution is passed through the column until the two phases achieve equilibrium and the composition of the effluent is identical with that of the influent.

Sea water essentially has a constant relative composition, i.e., the concentration of each of the major constituents varies with the sample salinity, the latter representing the total amount of dissolved solids in solution. In sea water having an average salinity of 35 g kg^{-1}, the summed concentration of the major cations is about 0.6 eq kg^{-1} (Table 1) whereas that of trace metals such as Cu^{2+} is less than 1 μeq kg^{-1}. Hence, after equilibration of a resin column with sea water as indicated above, the number of exchange sites occupied by the major cations greatly exceeds that occupied by the trace metal cations, and any exchange of Cu^{2+} for major cations caused by a change in dissolved copper concentration will not significantly alter the bulk composition of the resin phase. As a result, the activity coefficients of the ions in the resin phase will remain constant as long as the sample salinity, which controls the concentration of major ions, and the pH, which controls the concentration of complex-forming bases such as hydroxides and carbonate, remain constant. If Eqn. 1 is rewritten in the form

$$\lambda_0 = [\overline{Cu}^{2+}]/[Cu^{2+}] = K_{Cu,Na}([\overline{Na}^{+}]^2/[Na^{+}]^2)(f^2_{\overline{Na}}\gamma_{Cu}/f_{\overline{Cu}}\gamma^2_{Na}) \quad (2)$$

then because equivalent expressions can be written for the exchange of Cu^{2+} with the other major cations (K^+, Mg^{2+} and Ca^{2+}), it is evident that λ_0, the distribution coefficient of the free Cu^{2+} ions, will have a constant value for a given pH and salinity.

In sea water, Cu^{2+} occurs not only as free ions but also in various complexes. These include positively charged (e.g., $CuCl^+$, $Cu(OH)^+$), neutral (e.g., $CuCl_2$, $CuCO_3$), and negatively charged (e.g., $Cu(CO_3)_2^{2-}$) species. Because a cation-exchange resin sorbs all cationic species, the total concentration

TABLE 1

Major ion concentrations of standard ocean water (SOW)

Component	Concentration (M)	Component	Concentration (M)
Sodium	4.80×10^{-1}	Chloride	5.59×10^{-1}
Magnesium	5.46×10^{-2}	Sulfate	2.88×10^{-2}
Calcium	1.05×10^{-2}	Carbonate	2.38×10^{-3}
Potassium	1.03×10^{-2}	Bromide	8.40×10^{-4}
Strontium	6.38×10^{-5}	Borate	4.85×10^{-4}
		Fluoride	7.14×10^{-5}

of copper in the resin phase will be

$$[\overline{Cu}] = [\overline{Cu^{2+}}] + \sum_{i=1}^{n(+)} [\overline{CuL_{i,n}}] \quad (3)$$

where $[\overline{CuL_{i,n}}]$ represents the concentration of complexes formed between Cu^{2+} and n molecules of the ith ligand and $\Sigma_{i=1}^{n(+)}$ is used to indicate that the summation includes only values of n resulting in positively charged complexes. Substituting in terms of the distribution coefficients and solution concentrations of the various species, Eqn. 3 becomes

$$\lambda[Cu] = \lambda_0[Cu^{2+}] + \sum_{i=1}^{n(+)} \lambda_{i,n}[CuL_{i,n}] = (\lambda_0 + \sum_{i=1}^{n(+)} \lambda_{i,n}\beta_{i,n}[L_i]^n)[Cu^{2+}] \quad (4)$$

where λ is an overall distribution coefficient for all (cationic) forms of copper, [Cu] is the total dissolved concentration, and $\beta_{i,n}$ the stability constant of the dissolved complexes. Thus, on substituting for [Cu] using the relationship

$$[Cu] = (1 + \sum_{i=1}^{n} \beta_{i,n}[L_i]^n)[Cu^{2+}] \quad (5)$$

and solving for λ, it is evident that

$$\lambda = (\lambda_0 + \sum_{i=1}^{n(+)} \lambda_{i,n}\beta_{i,n}[L_i]^n)/(1 + \sum_{i=1}^{n} \beta_{i,n}[L_i]^n) \quad (6)$$

The distribution of copper between the resin and solution phases will therefore be determined by the pH and salinity of the sea water and by the ligand composition.

In artificial sea water free from organic ligands, the concentration of inorganic ligands is fixed by pH and salinity. Calculations using the MINEQL [36] program indicate that the only cationic copper complexes present in significant amounts in artificial sea water are the monochloro and monohydroxo species, suggesting that these will also occur in the resin phase.

In natural sea waters, part of the dissolved copper will be complexed by organic ligands or be bound to colloidal matter. Assuming that none of these forms of copper bears a positive charge and thus the cationic metal concentration is directly proportional to the inorganic metal concentration, the amount of copper sorbed by the resin will be determined solely by the inorganic copper fraction present in true solution. Thus the amount of inorganic copper, Cu_i, can be calculated from the relationship $[Cu_i] = [\overline{Cu}]_x/\lambda_i$, where $[\overline{Cu}]_x$ is the experimentally determined sorbed copper value for the natural sea-water sample and λ_i is the value of the distribution coefficient of copper derived from measurements on artificial sea water of the same pH and salinity.

The activity of the Cu^{2+} ion in sea-water samples is related to Cu_i through the relationship $\{Cu\} = \gamma_{Cu}\alpha[Cu_i]$, where α is the fraction of Cu_i present as free ions. The values of γ can be estimated from relationships such as the Davies equation [37] while α can be calculated from computer models such as MINEQL. Hence, ion exchange-based methods can, in principle, be used to estimate the activity of Cu^{2+} in natural sea-water solutions.

The values of α and γ derived from existing models are at best only crude estimates; consequently, the accuracy of the activities based on their use is rather doubtful. Inorganic copper, which is closely related to the activity, is by contrast experimentally well defined, suggesting its use as an alternative parameter for assessing the toxicity of copper to organisms in natural sea waters. Because Cu_i values will differentiate copper bound to organic ligands and colloidal matter from that present in inorganic species in true solution, they provide a measure of the biologically effective copper concentration (ECC) of the solution. The ECC value (i.e., Cu_i) of a sample should be useful in studying the effect of organic matter on the toxicity of copper.

EXPERIMENTAL

Reagents and apparatus

All chemicals were reagent grade except for hydrochloric acid which was purified before use by isothermal distillation of the concentrated reagent-grade acid. Copper standard solutions were prepared by dissolving copper metal in nitric acid. Artificial sea water was prepared using the formula for Standard Ocean Water (SOW) of Morel et al. [38] and then passed through a column of Chelex-100 resin to reduce trace metal contamination. The copper content of the purified SOW, as determined by a.s.v., was less than 5 nM. The artificial sea water was preferred to natural sea water as the test medium because its composition is well defined.

All glass and plasticware were initially cleaned by soaking for several hours in 6 M HCl, two days in 0.5 M HCl, and finally rinsing thoroughly with water distilled in glass. All pH measurements were made with a Corning Model 130 pH meter equipped with a Corning semimicro combination electrode.

Column preparation and operation

The resin columns were prepared with Bio-Rad 1 × 5-cm Econocolumns and Bio-Rad Ag50W-X12 (200—400 mesh, hydrogen form) analytical-grade cation-exchanger. A 1-g portion of the resin (weighed as received) was suspended in water, poured into a column, successively eluted with methanol, water and SOW made 0.1 M in hydrochloric acid, and finally equilibrated with SOW having a pH of 8.0. The columns were used repeatedly and were regenerated by the method given above except that the methanol rinse was omitted. Column flow rates were controlled by pumping the samples with a Technicon Autoanalyzer pump (Model II) equipped with Lancer manifold pump tubing (Lancer, St. Louis, MO). All column manipulations were done

in a laminar flow hood in which polypropylene had been substituted for all replaceable metal parts.

The column equilibration procedure involved pumping the sample solution through the columns until the metal concentration in the effluent was identical with that in the influent. The feed was then stopped and any excess of solution remaining in the interstitial spaces of the resin column was displaced by applying a slight positive air pressure with the pump. The resin was then eluted with 25 ml of SOW, 0.1 M in hydrochloric acid and the copper concentration in the column eluate was quantified by a.s.v.

Determination of copper

For a.s.v. measurements, a Princeton Applied Research Model 300 polarographic analyzer was used in the differential pulse stripping mode (d.p.a.s.v.) with a mercury film on a glassy carbon electrode. The electrode was preplated with mercury and subjected to 3—4 plating/stripping cycles before use.

Pyrex sample cells (PAR Model K60) were used. Samples were acidified with 6 M HCl to a pH of 2.0. After the solution had been purged with nitrogen for 5 min, copper was plated at a potential of —0.7 V (vs. SCE) with magnetic stirring. Because the detection limit of the method is dependent on the length of time used for plating, the plating time was varied according to the concentration of metal in solution. After a predetermined time, stirring was stopped and the solution was allowed to come to rest for 15 s. Copper was then stripped by scanning anodically to a potential of —0.15 V (pulse height 50 mV, scan rate 5 mV s^{-1}). Two successive plating/stripping cycles were normally done for each sample, with the first being used to condition the electrode and the second to measure the peak current. Concentrations were evaluated by reference to calibration curves prepared in SOW.

Algal assays

The diatom *Thalassiosira pseudonana* (Hustedt) Hasle and Heimdal (WHOI clone 3H) was initially obtained from axenic cultures maintained in the artificial sea-water medium of Harrison et al. [39]. Stock cultures were grown aseptically in 250 ml of Aquil [38] modified by reducing the ethylenediaminetetraacetate (EDTA) concentration to 0.5 μM. All stock and experimental cultures were grown in 500-ml polycarbonate Erlenmeyer flasks at 15 ± 1°C and an in-flask light intensity of 95 μEin m^2 s^{-1} on a 16/8-h light-dark cycle.

All algal experiments were run in modified Aquil without EDTA. The medium was prepared with distilled water. As with SOW, the major nutrient stock solutions were passed through Chelex-100 resin to reduce trace metal contamination. To prevent precipitation during autoclaving, acid-cleaned (6 M sulfuric acid), filtered (0.4-μm Nucleopore) carbon dioxide was bubbled through the Aquil until the pH reached 5.5. The medium was then autoclaved (30 min, 121°C, 15 psi) and cooled in a 4-l glass aspirator bottle. If necessary,

the pH was adjusted to 8.0 ± 0.05 by bubbling with acid-cleaned, filtered air. Copper and ligand additions were made after autoclaving.

Algal assays were done with 250 ml of culture medium and an initial cell density of $1-2 \times 10^{-3}$ cells ml^{-1}. Cell concentrations were determined with a model Zf Coulter counter (Coulter Electronics) immediately after inoculation and on four subsequent days. Growth rate was evaluated over the exponential phase of growth by averaging daily growth rates. Each test was run in triplicate.

RESULTS

Resin characterization

It is essential that the ion-exchange resin attains complete equilibrium with the input solution before the amount of sorbed metal is determined. The volume of sea water needed to equilibrate 1 g of resin was measured by pumping 300 ml of SOW that contained 79 nM copper through a resin column and monitoring the copper concentration in the effluent. As shown in Fig. 1, the effluent concentration increased to an apparently constant level that was not significantly different from that of the influent after passage of about 200 ml. To establish the appropriate flow rate, aliquots of SOW containing 79 nM copper were pumped through resin columns at flow rates ranging from 0.8 to

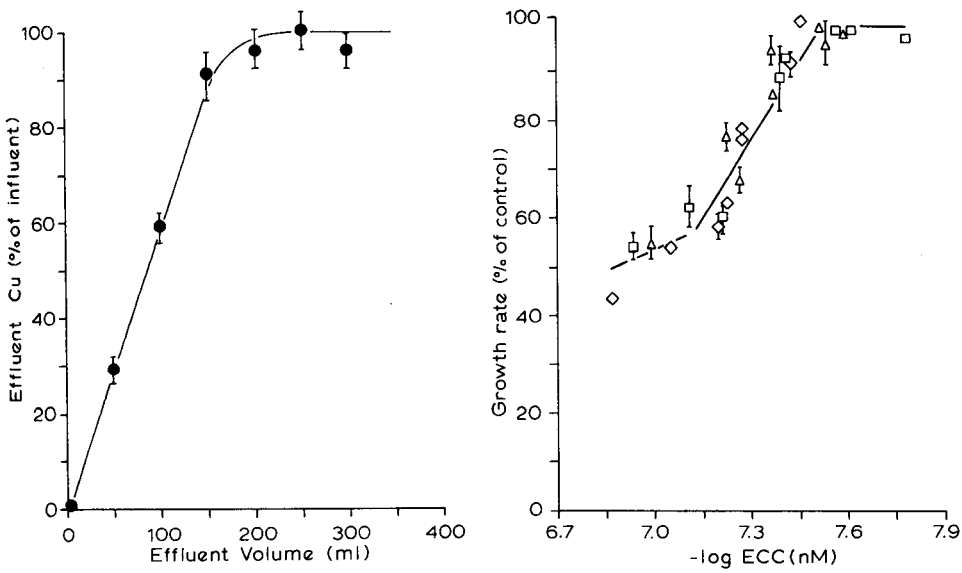

Fig. 1. Volume of sea water needed to equilibrate 1 g of resin, vertical bars represent ± 1 standard deviation. For details see text.

Fig. 2. Growth rate of *Thalassiosira pseudonana* versus the ECC value of the sample estimated by the ion exchange technique. EDTA (□), glutamic acid (△), NTA (◇) were added to modified AQUIL at various copper-ligand concentration ratios. For the concentration of metals and ligands used, refer to Table 3. Vertical bars represent ± 1 standard deviation, $N = 3$.

2.9 ml min^{-1}. The amount of copper sorbed was similar for all flow rates between 1.7 and 2.9 ml min^{-1}. Based on these results, a sample volume of 250 ml and a pumping rate of ca. 2.0 ml min^{-1} were adopted as standard conditions for all subsequent work.

The precision of the copper sorption measurements was evaluated by pumping SOW containing 79 nM copper through a set of eight resin columns and quantifying copper in the eluates by d.p.a.s.v. The mean of the copper concentration in the eluates (25 ml) was 224 nM and the relative standard deviation (RSD) of the observations was 7%. However, the RSD of the a.s.v. procedure used to quantify the sorbed copper, evaluated from ten replicate samples of SOW containing approximately the same copper concentration as the column eluates (236 nM), was 8%, suggesting that the overall precision of the method was in effect controlled by that of the d.p.a.s.v. procedure.

To ensure that the overall distribution coefficient of copper remained constant over a concentration range that could be considered environmentally realistic, the amount of copper sorbed to the resin from SOW was determined as a function of the total dissolved inorganic copper concentration up to a maximum value of 157 nM. The relationship between the concentration of sorbed and solution copper was linear (r = 0.9993) with a distribution coefficient value of 0.076 l g^{-1}.

To establish if the sorption of copper would be affected by the addition of Aquil phytoplankton nutrients to SOW, an experiment was done using SOW that had been enriched with phosphate, nitrate, dissolved silica, and Co, Mo, Zn and Fe. The iron stock was prepared at 0.45 mM and allowed to precipitate and form a colloidal suspension before being added to the samples. The results, shown in Table 2, indicate that the sorption of copper was not measurably affected provided that iron was absent. However, the addition of iron at a concentration level of 0.45 μM increased the amount of copper sorbed by about 30%. Doubling the iron concentration to 0.9 μM produced a small additional increase, but further increases up to a concentration of

TABLE 2

Effects of Aquil nutrients on the sorption of copper

Treatment[a]	Eluate Cu (nmol g^{-1})	Total Cu concentration[b] (nM)
Control (no nutrients)	6.5	71
All nutrients except Fe	6.9	71
0.45 μM Fe only[c]	8.2	69
0.90 μM Fe only	8.5	80
1.35 μM Fe only	8.8	69
1.80 μM Fe only	8.5	69

[a]SOW containing 79 nM Cu and Aquil nutrients passed through a set of resin columns. [b]Samples were acidified to pH 2.0 with ultrapure 6 M HCl and analyzed by d.p.a.s.v., after nutrient addition. [c]Iron(III) chloride stock of 0.45 mM.

1.8 μM had no obvious effect. The d.p.a.s.v. measurements made on aliquots of the iron-containing test solutions indicated that their dissolved copper concentration was, with one exception, similar to the iron-free control (Table 2). The increased sorption observed in the case of the iron-containing solutions was therefore not due to contaminant copper derived from the iron stock solution.

Further tests showed a decrease in flow rates as the iron concentration in solution was increased to >1 μM, suggesting that the oxide particles tend to become trapped in the interstices of the resin (Kazumi and Zorkin, unpublished work). Thus the increased retention of copper by the columns appears to be due more to its sorption by oxide particles trapped between the resin beads than to increased sorption by the resin phase.

Sorption of copper in the presence of organic complexing agents

In theory, the amount of copper sorbed to the resin depends on the activity of copper(II) ions and not on the total copper concentration in solution. To verify this, a series of experiments was conducted with the model organic ligands, ethylenediaminetetraacetic acid (EDTA), nitrilotriacetic acid (NTA), L-glutamic acid, and histidine. These ligands were used to vary the cationic metal concentration of the solution while a constant total metal concentration was maintained.

Duplicate samples containing copper plus one of the model ligands were prepared in SOW (pH 8.0) and allowed to stand for 12 h to permit the copper to equilibrate with the ligand. Because hydrated iron(III) oxide was the only Aquil nutrient to affect the ion-exchange procedure, it was added at the Aquil concentration to all copper/ligand mixtures to simulate conditions in the culture medium used for the algal assays. The samples were pumped through a set of columns together with standards (SOW containing copper but with no added organic ligand). The ratio of the amount of copper sorbed from the standards to the amount of copper sorbed from the test solution was then used to calculate the ECC (i.e., Cu_i) of the samples containing organic ligands (see above). The ECC value is proportional to the cationic metal concentration and the copper(II) ion concentration of the sample, provided that the inorganic ligand composition of the test and standard solutions are similar.

The metal speciation of the copper/ligand solutions was also determined by calculation with the MINEQL program. This model is supplied with a data file consisting of stability constants selected mainly from the collections of Sillen and Martell [40]. The pK values used in the model, corrected for the ionic strength of the medium (I = 0.7), were as follows: EDTA, 18.06; NTA, 12.61; histidine, 10.47; and glutamic acid, 6.61.

In the case of the samples containing EDTA, NTA and glutamic acid, the amount of copper sorbed, as would be expected, decreased as the concentration of the complexing ligand increased. This is reflected in the ECC values of the samples being lower than the total amount of copper added to the

samples (Table 3). Moreover, the ligand concentration needed to reduce the ECC to a given value increased in the order EDTA < NTA < glutamic acid, which is also the order in which the stability constants of the copper/ligand complexes decrease.

The resin sorption procedure gave anomalous results when histidine was used as the model ligand (Table 3). In this case, the amount of copper sorbed by the resin was greater than that sorbed from the organic ligand-free standards, resulting in ECC values greater than the total copper content of the solution. This increase is consistent with the fact that the charge on the Cu/histidine complex will range between +1 and +2, in the pH range of the samples. Hence, although complexation by histidine decreased the activity of

TABLE 3

Results of the resin column experiments with model organic ligands in SOW

Ligand[a]	Ligand conc. (μM)	Total Cu added (nM)	ECC values (nM)	Calc.[a] inorg. Cu conc. (nM)
L-Glutamic acid	10	79	61	62
	25	79	44	38
	50	79	32	16
	75	79	27	9
	10	157	107	126
	25	157	57	74
	50	157	44	32
	75	157	27	17
NTA	0.10	79	66	47
	0.25	79	55	26
	0.50	79	38	14
	0.75	79	36	10
	0.10	157	142	105
	0.25	157	92	60
	0.50	157	61	32
	0.75	157	55	21
EDTA	0.05	39	25	4
	0.10	39	17	0.9
	0.05	79	41	32
	0.10	79	28	4
	0.05	118	80	71
	0.10	118	39	25
	0.05	157	123	112
	0.10	157	65	64
Histidine	0.25	39	50	—
		79	87	0.9
		118	121	—
		157	154	6.6

[a]Calculated by MINEQL (I = 0.7, pH 8.0).

the copper(II) ion in solution, sorption of the Cu/histidine complex increased the amount of copper sorbed.

The ECC values were then compared to the inorganic copper concentrations of the solutions as determined by MINEQL (Table 3). Except for three values with glutamic acid, all calculated inorganic metal concentrations were lower than the corresponding ECC values, suggesting that the ion-exchange method was over-estimating the concentration of inorganic copper. However, it is likely that some of the discrepancy in the data is due to the chemical model. As the stability constants used to drive the model are derived in solutions unlike that of sea water and are determined at a different ionic strength, the extrapolation of these stability constants to a sea-water matrix and the concurrent ionic strength corrections needed may lead to inaccurate results. Furthermore, it is possible that certain assumptions associated with the amount of free ligand in the sample were not valid. For example, in the computer model it was assumed that over 99% of the iron added to the sample would bind to hydroxide and only a very small fraction would bind to the ligand. However, if a large fraction of iron did bind to the ligand, the amount of ligand available for complexation with copper would be reduced and this would cause the amount of inorganic copper in the sample to be greater than predicted by the model.

In conclusion, although the ion-exchange method could be used to make a semiquantitative estimate of the organic complexation of copper, the discrepancy between the predicted and measured values of inorganic copper did not allow verification of the quantitative nature of the method. Further work is presently being conducted in this area.

Algal assays

To determine the biological significance of the ion-exchange procedure, algal assays were done on solutions having the organic ligands, EDTA, NTA, histidine and glutamic acid, added to modified Aquil at copper/ligand concentration ratios similar to those used in the ion-exchange experiments. At each dissolved copper concentration tested, the addition of these ligands reduced the toxicity of copper, as indicated by an increase in growth rate, and the extent of reduction was related to the stability of the copper/ligand complex and the concentration of the ligand. The lowest concentrations of each ligand that allowed full growth (equal to the growth of the controls) in the presence of 79 nM copper were 50 nM EDTA, 100 nM histidine, 750 nM NTA and 250 nM glutamic acid (Table 4). The ability of histidine to reduce copper toxicity was greater than that of NTA even though the stability of the copper/histidine complex is lower. This occurred because the actual free ligand concentration available for complexation with copper is greater for histidine than for NTA because a larger percentage of NTA is bound to calcium and magnesium ions. For example, in SOW of 35‰ salinity and at a ligand concentration of 100 μM, MINEQL predicts that 66% of the NTA will be bound to calcium and 33% bound to magnesium, while over 97% of histidine will still be in the uncomplexed form.

TABLE 4

Growth rate data from bioassays using model organic ligands in modified Aquil

Ligand	Ligand conc. (μM)	Total Cu added (nM)	Growth rate (div./day)	Growth rate (% of control)
Glutamic acid	10	1[a]	1.76 ± 0.03	
	10	79	1.37 ± 0.05	78 ± 3[b]
	10	157	0.99 ± 0.05	56 ± 3
	10	236	0.88 ± 0.05	50 ± 0
	10	315	0.81 ± 0.01	46 ± 1
	25	1[a]	1.86 ± 0.09	
	25	78	1.79 ± 0.05	96 ± 3
	25	157	1.29 ± 0.04	69 ± 2
	25	236	1.03 ± 0.01	55 ± 1
	25	315	0.93 ± 0.05	50 ± 3
	50	1[a]	2.00 ± 0.04	
	50	79	2.02 ± 0.04	101 ± 2
	50	157	1.75 ± 0.02	87 ± 1
	75	1[a]	1.98 ± 0.01	
	75	79	1.97 ± 0.02	100 ± 1
	75	157	1.91 ± 0.09	97 ± 5
	75	236	1.62 ± 0.10	82 ± 5
	75	315	1.52 ± 0.05	77 ± 2
NTA	0.10	1[a]	1.97 ± 0.01	
	0.10	79	1.17 ± 0.04	59 ± 2
	0.10	157	0.87 ± 0.01	44 ± 1
	0.10	236	0.86 ± 0.05	44 ± 3
	0.10	315	0.70 ± 0.02	35 ± 1
	0.25	1[a]	1.89 ± 0.02	
	0.25	79	1.50 ± 0.05	79 ± 3
	0.25	157	1.05 ± 0.01	55 ± 1
	0.25	236	0.88 ± 0.02	47 ± 1
	0.25	315	0.84 ± 0.04	45 ± 2
	0.50	1[a]	2.04 ± 0.03	
	0.50	79	1.89 ± 0.04	93 ± 2
	0.50	157	1.31 ± 0.03	64 ± 1
	0.50	236	1.09 ± 0.08	54 ± 4
	0.50	315	1.07 ± 0.04	52 ± 2
	0.75	1[a]	1.81 ± 0.04	
	0.75	79	1.84 ± 0.03	102 ± 1
	0.75	157	1.40 ± 0.02	77 ± 1
	0.75	236	1.13 ± 0.03	63 ± 2
	0.75	315	0.97 ± 0.02	54 ± 1
EDTA	0.05	1[a]	1.52 ± 0.05	
	0.05	39	1.61 ± 0.03	100 ± 2
	0.05	79	1.45 ± 0.10	95 ± 7
	0.05	118	1.02 ± 0.06	67 ± 4
	0.05	157	0.88 ± 0.03	58 ± 2
	0.10	1[a]	1.80 ± 0.00	
	0.10	39	1.82 ± 0.03	101 ± 1

TABLE 4 (continued)

Ligand	Ligand conc. (μM)	Total Cu added (nM)	Growth rate (div./day)	Growth rate (% of control)
	0.10	79	1.86 ± 0.01	104 ± 1
	0.10	118	1.74 ± 0.04	97 ± 2
	0.10	157	1.13 ± 0.05	63 ± 2
Histidine	0.10	1[a]	1.90 ± 0.01	
	0.10	79	1.87 ± 0.03	99 ± 2
	0.10	157	0.89 ± 0.02	47 ± 1
	0.10	236	0.52 ± 0.01	27 ± 1
	0.10	315	0.27 ± 0.07	14 ± 3
	0.25	1[a]	2.10 ± 0.01	
	0.25	79	2.11 ± 0.04	100 ± 2
	0.25	157	2.14 ± 0.04	102 ± 2
	0.25	236	1.47 ± 0.06	70 ± 3
	0.25	315	1.02 ± 0.06	49 ± 3
	0.50	1[a]	1.96 ± 0.01	
	0.50	157	1.98 ± 0.01	101 ± 0
	0.50	315	2.05 ± 0.04	105 ± 2
	0.50	472	1.98 ± 0.01	101 ± 1
	0.50	630	1.93 ± 0.03	99 ± 2

[a]Control. [b]Mean ±s.d. of 3 replicates.

These results demonstrated that copper complexed to these organic ligands was not toxic and that the toxicity of the metal was related to the inorganic copper fraction. This is consistent with the results of other workers [6—10] who have found that free copper(II) ion, which is proportional to the inorganic copper fraction, is the species most toxic to phytoplankton and that it is the activity of the metal that controls toxicity.

Algal growth rates were then compared to the ECC values determined for solutions having similar copper and ligand concentrations. A plot of algal growth rates and ECC values for samples having EDTA, NTA, or glutamic acid added showed a correlated relationship (Fig. 2). Although the ion-exchange and algal procedures used in preparing Fig. 2 were done at different times, the comparison should be valid in view of the reproducible composition of the Aquil medium. Histidine, however, showed a poor relationship between the ECC values and the algal growth rates. This was attributed to sorption of the positively-charged copper/histidine complex by the resin.

DISCUSSION

Although the ion-exchange technique described here appears to be suitable for estimating the fraction of metal that is toxic to marine phytoplankton in artificial sea water, it is potentially subject to interferences when applied to real systems. The most serious of these is due to ligands such as histidine which, because they lack sufficient negative charge to neutralize the positive charge on the Cu^{2+} ion, form cationic complexes which are sorbed by the

resin. Ammonia, which occurs at a maximum concentration of about 3.5 μM in oxygenated sea waters, is the most abundant ligand of this type. However, the low stability of copper/ammonia complexes ensures that their concentration will normally be less than 1% of the free Cu^{2+} ion. Thus, unless the distribution constant of the copper/ammonia complexes is exceptionally large relative to that of the other cationic species, ammonia complexation should not significantly affect the amount of copper sorbed except, possibly, in anoxic waters or the interstitial waters of sediments.

Copper also forms cationic complexes with amino acids such as histidine. Moreover, the total concentration of dissolved free amino acids in oceanic surface waters has been reported to be as high as 100 nM [40], an amount approximating the histidine concentrations that produced anomalous results in the application tests. However, the stability constant of the copper/histidine complex is about 2 orders of magnitude larger than that of glycine, alanine and serine, the predominant dissolved free amino acids in sea water. Consequently, the concentration of copper/amino acid complexes should be less than 1% of that of the free copper(II) ion, and amino acid interference, as in the case of ammonia, should be negligible. Nevertheless, total dissolved free amino acid concentrations exceeding 1000 nM, including histidine concentrations as high as 100 nM, have been observed in the vicinity of submarine sewer outfalls along the California coast [41], suggesting that the ion-exchange method would have limited use in such waters. However, free amino acids must compete for copper with various other ligands present in sea water such as humic and fulvic acids. As the latter can constitute a major part of the dissolved organic matter [42], only a small proportion of the copper should be bound to amino acids even when their concentrations are high. Because humic and fulvic acids appear to carry a strong negative charge, their copper complexes, in contrast with those of amino acids, should not be sorbed by the resin. The ratio between the amount of copper in amino acid complexes and the ECC is unaffected by this competition and thus the relative magnitude of the resulting error in the ECC value should remain the same.

This research received support from the International Copper Research Association, Inc. and from the Natural Science and Engineering Research Council, Canada.

REFERENCES

1 E. Steeman Nielsen and L. Kamp-Nielsen, Physiol. Plant., 23 (1970) 828.
2 S. J. Erickson, J. Phycol., 8 (1972) 318.
3 P. H. Whitfield and A. G. Lewis, Estuarine Coastal Mar. Sci., 4 (1976) 255.
4 T. M. Florence and G. E. Batley, Talanta, 24 (1977) 151.
5 D. M. McKnight and F. M. Morel, Limnol. Oceanogr., 25 (1980) 62.
6 W. Sunda and R. L. Guillard, J. Mar. Res., 34 (1976) 511.
7 D. M. Anderson and F. M. M. Morel, Limnol. Oceanogr., 23 (1978) 283.

8 G. A. Jackson and J. J. Morgan, Limnol. Oceanogr., 23 (1978) 268.
9 G. S. Canterford and D. R. Canterford, J. Mar. Biol. Ass. U.K., 60 (1980) 227.
10 J. Gavis, R. R. L. Guillard and B. L. Woodward, J. Mar. Res., 39 (1981) 315.
11 R. Wagermann and J. Barica, Water Res., 13 (1979) 515.
12 H. Borgman and K. M. Ralph, Water Res., 17 (1983) 1697.
13 T. M. Florence, Anal. Chim. Acta, 141 (1982) 73.
14 P. M. Williams and R. J. Baldwin, Mar. Sci. Commun., 2 (1976) 162.
15 W. Rosen and P. M. Williams, Geochem. J., 12 (1978) 21.
16 R. J. Simpson, in A. K. Covington (Ed.), Ion-Selective Electrode Methodology, Vol. 1, CRC Press, Boca Raton, Florida, 1979, p. 43.
17 G. B. Oglesby, W. W. Duer and F. J. Millero, Anal. Chem., 49 (1977) 877.
18 J. C. Westall, F. M. M. Morel and D. N. Hume, Anal. Chem., 51 (1979) 1792.
19 H. E. Allen, W. R. Matson and K. N. Mancy, J. Water Pollut. Control. Fed., 42 (1970) 573.
20 M. I. Abdullah, B. Reusch Berg and R. Klimek, Anal. Chim. Acta, 84 (1976) 307.
21 J. C. Duinker and C. J. M. Kramer, Mar. Chem., 5 (1977) 207.
22 T. M. Florence and G. E. Batley, J. Electroanal. Chem., 75 (1977) 791.
23 J. E. Schindler, J. J. Alberts and K. R. Honick, Limnol. Oceanogr., 17 (1972) 952.
24 A. W. Andren and R. C. Harris, Geochim. Cosmochim. Acta, 39 (1975) 1253.
25 R. G. Smith, Anal. Chem., 48 (1976) 74.
26 B. T. Hart and S. H. R. Davies, Austr. Water Res. Council Tech. Rep. No. 35. Austr. Govt. Publish. Service, Canberra, 1978.
27 P. Benes and V. Majer, Trace Chemistry of Aqueous Solutions, Elsevier, Amsterdam, 1980.
28 T. M. Florence and G. E. Batley, Talanta, 23 (1976) 179.
29 P. M. Figura and B. McDuffie, Anal. Chem., 52 (1980) 1433.
30 J. S. Young, J. M. Gurtisen, C. W. Apts and E. A. Crecelius, Mar. Environ. Res., 2 (1979) 265.
31 R. F. Srna, K. S. Garrett, S. M. Miller and A. B. Thum, Environ. Sci. Tech., 14 (1980) 1482.
32 T. M. Florence, B. G. Lumsden and J. J. Fardy, Anal. Chim. Acta, 151 (1983) 281.
33 G. Christianson, R. Jennes and S. T. Coulter, Anal. Chem., 26 (1954) 1923.
34 K. N. Pearce and L. K. Creamer, Anal. Chem., 46 (1974) 457.
35 F. F. Cantwell, J. S. Nielsen and S. E. Hrudey, Anal. Chem., 54 (1982) 1498.
36 J. C. Westall, J. L. Zachary and F. M. Morel, Technical Note No. 18, Water Quality Lab., Dept. of Civil Eng., MIT, Cambridge, MA, 1976.
37 C. W. Davies, Ion Association, Butterworth, London, 1962.
38 F. M. M. Morel, J. G. Rueter, D. M. Anderson and R. R. L. Guillard, J. Phycol., 15 (1979) 135.
39 P. J. Harrison, R. E. Waters and F. J. R. Taylor, J. Phycol., 16 (1980) 281.
40 L. G. Sillen and A. E. Martell, Stability Constants of Metal-ion Complexes, Chemical Society, Special Publications No. 17 and 25, 1964 and 1974.
41 C. Lee and J. L. Bada, Earth Plan. Sci. Lett., 26 (1975) 61.
42 C. Lee and J. L. Bada, Limnol. Oceanogr., 22 (1979) 502.

Analytica Chimica Acta, 183 (1986) 179—185
Elsevier Science Publishers B.V., Amsterdam — Printed in The Netherlands

THE USE OF MICROEMULSIONS IN FLOW INJECTION ANALYSIS
Spectrofluorimetric Determination of Primary Amines

M. HANIF MEMON and PAUL J. WORSFOLD*
Department of Chemistry, University of Hull, Hull HU6 7RX (Great Britain)
(Received 12th November 1985)

SUMMARY

The use of microemulsions in flow-injection systems is considered, with particular reference to the determination of C_6—C_{10} primary amines by derivatization with *o*-phthalaldehyde and 2-mercaptoethanol. Microemulsions provide an ideal interface for reactions between a water-soluble reagent and a non-aqueous sample. The effect of reaction conditions (*R* value, droplet concentration, pH and flow rate) on the fluorescence signal is discussed and calibration data for three primary alkylamines are given.

Organized molecular assemblies (e.g., micelles, reversed micelles and microemulsions) are formed when amphiphilic surfactant molecules are dissolved in water and/or oil environments at concentrations above their critical micelle concentration. Reversed micelles and water-in-oil (w/o) microemulsions are formed when a suitable surfactant, such as 1,2-bis(2-ethylhexyloxycarbonyl)-1-ethane sulphonate (dioctyl sulphosuccinate (Sigma); AOT), is dissolved in a hydrophobic solvent such as heptane. When the water/AOT mole ratio (*R*) is less than 7, the term reversed micelle is used [1], and when *R* is greater than 7 the term microemulsion is used. The mean radius of the aggregates varies with the *R* value according to the equation: radius (nm) = $0.175R + 1.5$ [2]. Although there is no clear dividing line between reversed micelles and microemulsions, as the "water pool" increases the amount of "free" water relative to "bound" water increases and the properties of the hydrophilic core tend towards the properties of bulk water [3].

The analytical applications of organized molecular assemblies have recently been reviewed by Pelizzetti and Pramauro [3]. The major attractions of such systems are their ability to solubilize and concentrate certain ions and molecules and the possibility of modifying chemical equilibria, reaction rates and reaction pathways [4]. Applications extend to a variety of electrochemical, spectrometric and chromatographic procedures, but the area of molecular luminescence is a particularly interesting one.

The enhancement of fluorescence measurements by the use of micelles has been reported by Hinze et al. [5]. In such systems, sensitivity can be increased by decreasing quenching effects and increasing the microviscosity of the solvent, interference effects can be minimized by shielding and the experimental arrangement is often simplified.

0003-2670/86/$03.50

Because of the heterogeneous nature of oil/water systems, it is essential for quantitative procedures that the reaction conditions are as reproducible as possible. The technique of flow injection analysis (f.i.a.), which involves controlled mixing of sample and reagent within an enclosed system, is therefore a useful tool for studying the analytical potential of microemulsions.

The fluorimetric determination of primary amines in aqueous media, by derivatization with *o*-phthalaldehyde (OPA) and 2-mercaptoethanol, was first reported by Roth [6]; the method has subsequently been adapted to f.i.a. [7, 8] for aqueous samples. This paper describes the use of a water-in-oil (w/o) microemulsion in a flow-injection manifold for the determination of long-chain primary amines in heptane by OPA/2-mercaptoethanol derivatization with fluorescence detection. The effect of various microemulsion parameters is also considered.

EXPERIMENTAL

Reagents

A stock *o*-phthalaldehyde (OPA; Sigma) solution (0.5 M) was prepared by dissolving OPA (0.6705 g) in absolute ethanol (10 cm^3). A stock solution (0.5 M) of 2-mercaptoethanol (2-ME; BDH Chemicals) was prepared by dissolving 2-ME (0.35 cm^3) in absolute ethanol (10 cm^3). A stock AOT (Sigma) solution (0.45 M) was prepared by dissolving AOT (50.02 g) in heptane (250 cm^3; Fisons h.p.l.c. grade), and working solutions were prepared by dilution with heptane. Primary amine stock solutions (0.01 M) were prepared by dissolving hexylamine (133 mm^3), octylamine (166 mm^3) or decylamine (199 mm^3) in heptane (100 cm^3), and standards covering the range 0—5.0 $\times$ 10^{-5} M were prepared by serial dilution in heptane. An adjustable pipette (Gilson P200) was used to dispense the amines. A series of aqueous buffer solutions (0.025 M) was prepared by dissolving disodium tetraborate decahydrate (pH 8—11) or disodium hydrogenphosphate (pH 11—12) in water and adjusting the pH with hydrochloric acid or sodium hydroxide. Potassium chloride (0.025 M) was used for pH 12—13.

Effect of variables

To study the effect of aggregate size on the maximum fluorescence emission wavelength the water/AOT mole ratio (R) was varied as follows. Stock OPA (1.0 cm^3) and stock 2-ME (2.0 cm^3) solutions were diluted to 5.0 cm^3 with phosphate buffer (pH 12.0). A 100-mm^3 aliquot of this solution was mixed with various volumes of phosphate buffer, diluted to 10 cm^3 with 0.15 M AOT and shaken vigorously for 2 min to obtain clear microemulsions with R values ranging from 4 to 45. All microemulsions containing more than 0.5 cm^3 of phosphate buffer were kept in a water bath at 30°C. A 0.5-cm^3 aliquot of 5.0 $\times$ 10^{-5} M hexylamine was added to each microemulsion and shaken, and the wavelength of maximum fluorescence emission was measured.

To investigate the effect of R value on the fluorescence emission intensity, stock OPA (1.0 cm^3) and stock 2-ME (2.0 cm^3) solutions were diluted to 5.0 cm^3 with phosphate buffer (pH 12.0). A 0.25-cm^3 aliquot of this solution was mixed with various volumes of phosphate buffer, diluted to 25 cm^3 with 0.15 M AOT and shaken vigorously for 2 min to provide a series of microemulsions with R values in the range 4—45. Microemulsions containing more than 1.25 cm^3 of buffer were kept at 30°C. Similarly, the effect of droplet concentration was investigated by keeping the reagent concentration constant (1 mM OPA and 2 mM 2-ME) and the R value constant at 18.5 and varying the volume of buffer and the concentration of AOT (0.05—0.45 M) simultaneously.

To monitor the effect of pH on the derivatization reaction, stock OPA (100 mm^3) and stock 2-ME (200 mm^3) solutions were diluted to 5 cm^3 with the appropriate buffer, further diluted to 100 cm^3 with 0.15 M AOT and shaken vigorously for 2 min. To optimize the concentration of OPA for the derivatization reaction, microemulsions were prepared as immediately above using phosphate buffer (pH 12.0) and OPA solutions of 0.05, 0.10, 0.25, 0.50, 1.00 and 2.00 mM. Hexylamine (5.0×10^{-5} M in heptane) was the primary amine used in all the above experiments.

For calibration, the reagent stream was prepared daily by mixing stock OPA (100 mm^3) and stock 2-ME (200 mm^3), diluting to 5 cm^3 with phosphate buffer (pH 12.0), further diluting to 100 cm^3 with 0.15 M AOT and shaking vigorously for 2 min. For comparative purposes, the reaction in heptane was studied using stock OPA (100 mm^3) and stock 2-ME (200 mm^3) in heptane (100 cm^3) as the reagent stream.

Instrumentation and procedures

A spectrofluorimeter (Perkin-Elmer 3000) with a 1.0-cm^2 cross-section cuvette and an excitation wavelength of 340 nm was used to establish the maximum fluorescence emission wavelength at different R values. For all other experiments, a single-channel flow-injection manifold with a 50-cm mixing coil was used. The microemulsion reagent stream was pumped at 1.1 $cm^3\ min^{-1}$ by a peristaltic pump (Gilson Minipuls-2) equipped with solvent-resistant isoversinic pump tubing (Anachem). The primary amine sample (20 mm^3) was introduced into the reagent stream via a rotary teflon valve (Rheodyne 5020). Teflon tubing (0.5 mm, i.d.) was used throughout the remainder of the system. The detector was a filter fluorimeter (Perkin-Elmer LS-2) equipped with an 8-mm^3 flow-through cell and connected to a strip-chart recorder (Chessell BD 4040). A 340-nm excitation filter was used and the emission wavelength was set at 432 nm, except for the R value experiments, where the maximum emission wavelength for each R value was used.

RESULTS AND DISCUSSION

Effect of microemulsion parameters on the fluorescence signal

Figure 1 shows that as the R value increases there is a red shift in the wavelength of maximum fluorescence emission. The excitation wavelength maximum remains unchanged at 340 nm. A similar shift has been reported for the OPA/2-ME reaction in micellar systems [9]. The red shift observed in microemulsions arises from an increasing interaction between solvent water molecules and the excited singlet state of the fluorophore as the R value increases, and may be related to the corresponding increase in micropolarity and decrease in viscosity. The sharper decrease in the wavelength of maximum fluorescence emission for $R < 8$ may be explained by the fact that the water molecules are tightly bound in the sodium ion hydration shell, and, to a lesser extent, involved in binding to sulphonate or carboxyl groups in the microemulsion by ion-dipole interactions or hydrogen bonding [10], and therefore are not free to interact with the excited state of the fluorophore.

A concomitant increase in the fluorescence intensity at lower R values might be expected, for the reasons outlined above, but in fact the opposite effect is observed, as shown in Fig. 2. A possible explanation for the decrease in fluorescence intensity at $R < 18.5$ is that the rate of the derivatization reaction is significantly decreased by steric and mobility constraints within the microemulsion. The results for variation in droplet "concentration" at constant reagent concentration and constant R value (18.5), shown in Fig. 3, support this explanation. The droplet "concentration" is the concentration of AOT divided by the aggregation number for AOT microemulsions at a

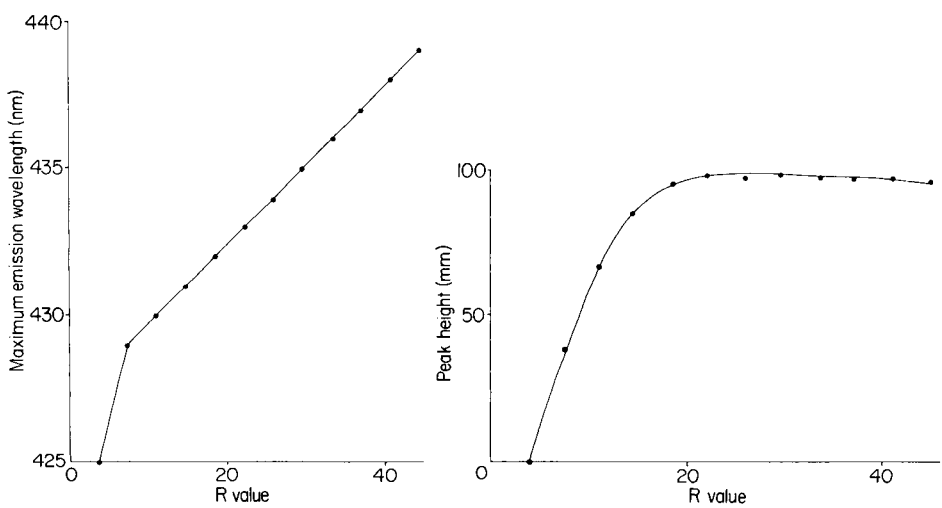

Fig. 1. The relationship between R value ([water]/[AOT]) and the wavelength of maximum fluorescence emission of the OPA adduct. (Excitation at 340 nm, 5×10^{-5} M hexylamine.)

Fig. 2. The relationship between R value and maximum fluorescence emission intensity.

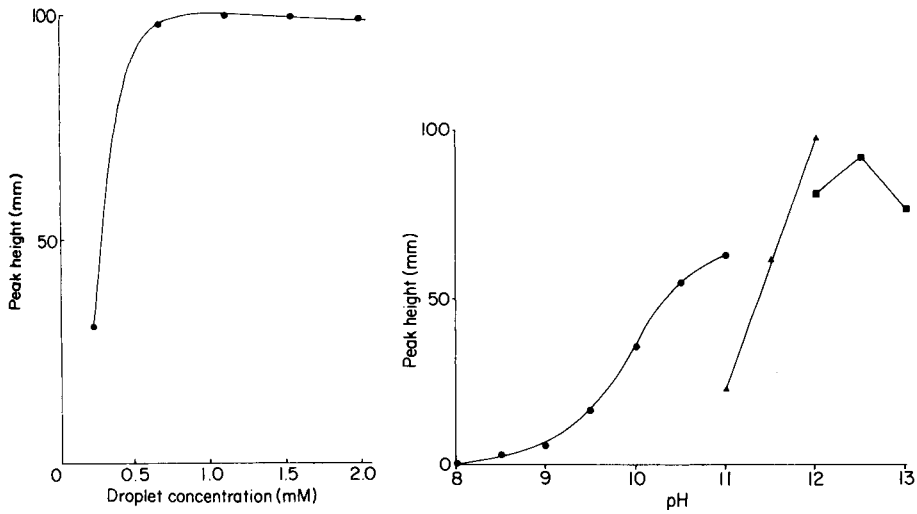

Fig. 3. The relationship between droplet concentration and fluorescence intensity at constant total reagent concentration and constant R value (18.5) assuming an aggregation number of 220. The points represent AOT concentrations of 0.05, 0.15, 0.25, 0.35 and 0.45 M.

Fig. 4. The effect of pH on the fluorescence intensity: (•) borate buffer; (▲) phosphate buffer; (■) chloride solution.

given R value. Therefore, as the AOT concentration increases from 0.05 to 0.45 M, and assuming an aggregation number (the number of AOT molecules in each aggregate) of 220 [11], the droplet concentration increases from 0.2 mM to 2.0 mM. Maximum sensitivity occurs in the range 0.15—0.25 M AOT, which corresponds to a droplet concentration of 0.7—1.1 mM, as compared to an OPA concentration of 1.0 mM. Hence the sharp decrease in response below an AOT concentration of 0.15 M could be due to steric and mobility constraints as described above. The small decrease in response at higher AOT concentrations is due to a decrease in the number of droplets containing OPA and 2-ME.

Optimization of reaction conditions

Because of the different properties of the water pool in the microemulsion and the bulk water phase, the pK_a values of solutes in the two phases will also be different. For pH-sensitive reactions, such as the OPA/2-ME derivatization reaction, the pH of the buffer used must be adjusted to allow for this difference [12]. The composition and concentration of the buffer system, as well as the R value, will have some bearing on the effective pH within the microemulsion, and this can be determined theoretically [13]. The purity of AOT and its hydrolysis at high pH will also affect the pH in the microemulsion [14].

The effect of pH on the fluorescence signal obtained with the OPA/2-ME reaction is shown in Fig. 4; the pH shift from the bulk-phase optimum (pH 6—8 for primary amines [15]) is apparent. Phosphate buffer (pH 12.0) was therefore used for all subsequent work, in spite of its quenching effect on the fluorescence of the OPA adduct [15]. The completeness of the reaction at pH 12 and the subsequent decomposition of the fluorophore were clearly demonstrated by using the stopped-flow technique. The concentration of OPA giving maximum response was found to be $\geqslant 0.5$ mM and the concentration of 2-ME was kept in excess at a mole ratio of 2:1 to OPA [16].

The effect of flow rate on the fluorescence signal, when the optimized microemulsion composition and experimental conditions given above were used with a 50-cm mixing coil, is shown in Fig. 5. The highest flow rate commensurate with maximum extent of reaction was 1.1 ml min^{-1}, giving a possible sample throughput of 120 h^{-1}. Increasing the coil length to increase sample residence time resulted in decreased sensitivity owing to decomposition of the OPA adduct [16].

Calibration for primary amines

Calibration graphs for hexylamine, octylamine and decylamine, covering the range 0—5.0 × 10^{-5} M, are shown in Fig. 5. The correlation coefficients over this range are 0.9999, 0.9999 and 0.9993, respectively. The sensitivity

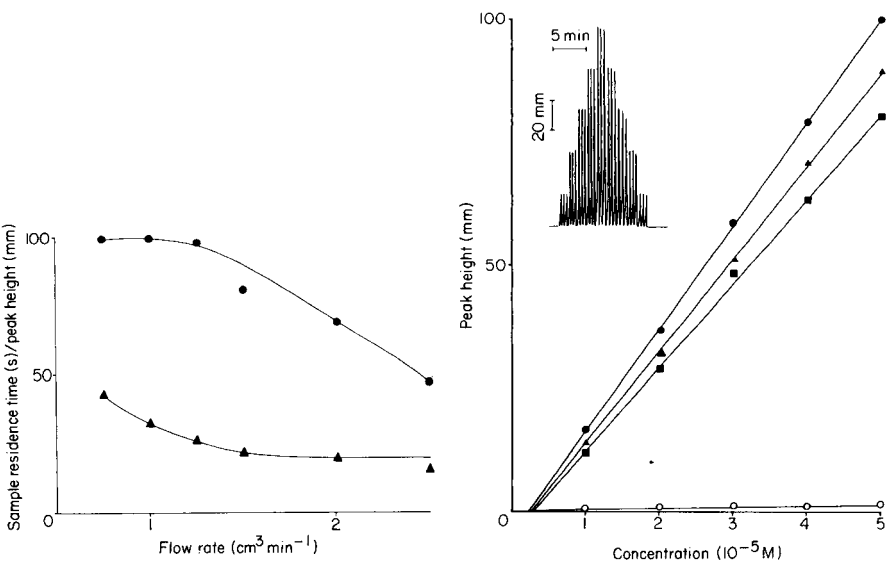

Fig. 5. The effect of flow rate: (▲) on sample residence time; (●) on fluorescence intensity.

Fig. 6. Calibration graphs: (●) hexylamine; (▲) octylamine; (■) decylamine. A calibration curve for hexylamine in a totally non-aqueous system is also shown (○). The inset shows a typical recorder trace for hexylamine over the range 0—5.0 × 10^{-5} M.

increases with decreasing amine chain length as a result of increased partitioning into the microemulsion droplets as the chain length decreases. The fact that the calibration graphs for the microemulsion system do not pass through the origin arises from dilution of the reagent by the sample, thus decreasing the background fluorescence in the carrier stream. Also shown in Fig. 6 is the response obtained for hexylamine when the OPA/2-ME reagent is dissolved directly in heptane. The relative responses indicate the efficiency of the microemulsion system for the determination of primary amines in non-aqueous solution by derivatization with OPA/2-ME.

Conclusions

This work demonstrates that f.i.a. is a suitable technique for investigating the analytical potential of microemulsions. The results show that reactions involving a non-aqueous sample and an aqueous reagent (and probably vice versa) can be quantitatively investigated using the f.i.a./microemulsion combination and that reaction rates and fluorescence signals can be modified by changing basic experimental variables.

The combination of f.i.a. with microemulsions can also be used with other detection processes (e.g., u.v./visible spectrophotometry and chemiluminescence) and provides a unique system for the study of aqueous/non-aqueous interaction as in, e.g., liquid/liquid extraction, and for the manipulation of the spectral and kinetic parameters in reacting systems.

The authors thank Dr. Paul Fletcher for several helpful discussions. One of us (M. H. M.) thanks the Ministry of Education, Government of Pakistan, for a Research Grant and the University of Sind for study leave.

REFERENCES

1 P. L. Luisi, Angew. Chem., 24 (1985) 439.
2 J. D. Nicholson and J. H. R. Clarke, in K. Mittal and B. Lindman (Eds.), Surfactants in Solution, Plenum Press, New York, 1984, p. 1663.
3 E. Pelizzetti and E. Pramauro, Anal. Chim. Acta, 169 (1985) 1.
4 L. J. Cline Love, J. G. Habarta and J. G. Dorsey, Anal. Chem., 56 (1984) 1132A.
5 W. L. Hinze, H. N. Singh, Y. Buba and N. G. Harvey, Trends Anal. Chem. 3 (1984) 193.
6 M. Roth, Anal. Chem., 43 (1971) 880.
7 J. I. Braithwaite and J. N. Miller, Anal. Chim. Acta, 106 (1979) 395.
8 R. L. Petty, W. C. Michel, J. P. Snow and K. S. Johnson, Anal. Chim. Acta, 142 (1982) 299.
9 H. N. Singh and W. L. Hinze, Analyst (London), 107 (1982) 1073.
10 M. Wong, J. K. Thomas and M. Gratzel, J. Am. Chem. Soc., 98 (1976) 2391.
11 N. J. Bridge and P. D. I. Fletcher, J. Chem. Soc., Faraday Trans. 1, 79 (1983) 2161.
12 O. A. El Seoud, in P. L. Luisi and B. E. Straub (Eds.), Reverse Micelles, Plenum Press, New York, 1984, p. 81.
13 O. A. El Seoud and R. C. Vieira, J. Colloid. Interface Sci., 93 (1983) 289.
14 P. D. I. Fletcher, N. M. Perrins, B. H. Robinson and C. Toprakcioglu, in P. L. Luisi and B. E. Straub (Eds.), Reverse Micelles, Plenum Press, New York, 1984, p. 69.
15 K. Imai, T. Toyo'oka and H. Miyano, Analyst (London), 109 (1984) 1365.
16 R. F. Chen, C. Scott and E. Trepman, Biochim. Biophys. Acta, 576 (1979) 440.

Analytica Chimica Acta, 183 (1986) 187—196
Elsevier Science Publishers B.V., Amsterdam — Printed in The Netherlands

A SENSITIVE CONTINUOUS-FLOW BIOLUMINESCENT SYSTEM FOR DETERMINING ETHANOL IN SERUM AND SALIVA

S. GIROTTI*, A. RODA, S. GHINI and A. L. PIACENTINI

Istituto di Scienze Chimiche, Università di Bologna, Via S. Donato, 15 - 40127 Bologna (Italy)

G. CARREA and R. BOVARA

Istituto di Chimica degli Ormoni, C.N.R., Via M. Bianco, 9 - 20131 Milano (Italy)

(Received 29th July 1985)

SUMMARY

A continuous-flow system, based on NAD(P)H:FMN oxidoreductase and bacterial luciferase co-immobilized on a nylon coil placed in front of a photomultiplier, and alcohol dehydrogenase separately immobilized on a second nylon coil, is described for the assay of ethanol in serum and saliva. The flow is air-segmented and 5—50-μl samples are required. The sample throughput is 25—30 h^{-1} with no carryover. The detection limit is 1 μmol l^{-1} ethanol (50 pmol injected) and the response is linear between 50 and 2500 pmol of ethanol. The relative standard deviation is 3—10% for both within-day and between-day assays, and serum and saliva can be analyzed directly. The immobilized enzymes are satisfactorily stable and up to 900 samples can be analyzed with one enzyme reactor.

Many studies have been reported on the properties of immobilized enzymes and their use for analytical purposes [1]. The stability of immobilized enzymes, which generally exceeds that of their soluble counterparts, and their re-usability, makes immobilization valuable for the determination of substrates, activators, inhibitors and enzymes. Analysis for metabolites in biological systems requires sensitive and selective methods, because analytes are present at low concentration and also because further dilution of biological samples is often needed to avoid matrix interferences.

Luminescent bacteria contain enzymes which catalyze the following reactions [2]:

$$NAD(P)H + H^+ + FMN \rightleftharpoons NAD(P)^+ + FMNH_2 \quad (1)$$

$$FMNH_2 + O_2 + RCHO \rightarrow FMN + RCOOH + H_2O + light \quad (2)$$

Reaction 1 is catalyzed by NAD(P)H:flavin mononucleotide (FMN) oxidoreductase and reaction 2, which produces light in the presence of oxygen and a long-chain aldehyde (RCHO), is catalyzed by bacterial luciferase. If NAD(P)H is the limiting substrate, the light intensity is proportional to the NAD(P)H concentration. The components of any reaction that specifically

0003-2670/86/$03.50

produces or consumes NADH or NADPH can be monitored by means of this bioluminescent system. With immobilized enzymes, the sensitivity is very high; NADH concentrations as low as 1×10^{-10} M can be measured [3]. Furthermore, the easier handling and decreased costs have prompted the development of several sensitive analytical methods for metabolite and enzyme determination [4—6], based on immobilized enzymes.

Attempts have been made to automate these bioluminescent assays by immobilization of these enzymes on Sepharose [3, 7, 8] or glass-bead [9] columns, and by use of a luminometer as a sensitive detector or by photographic detection [10]. To overcome some problems related to Sepharose columns (carryover, packing or disruption of gel matrix, bacterial contamination), a highly sensitive continuous-flow system was recently developed for the determination of NADH and bile acids in serum and saliva [11–13]; a nylon tube was used as a solid support for the bioluminescence-producing enzymes and for the specific hydroxysteroid dehydrogenase. The bioluminescent enzymes were covalently linked to the interior of the nylon coil, which was inserted directly into a luminometer. The system fulfilled all the requirements of specificity, stability and sensitivity and was suitable for clinical application.

In the present paper, the development of a continuous-flow bioluminescent assay for ethanol is described. The method is based on the coupling of reactions 1 and 2 with the alcohol dehydrogenase (ADH)-catalyzed reaction [9, 14—18]:

$$CH_3CH_2OH + NAD^+ \rightleftharpoons NADH + H^+ + CH_3CHO$$

The ADH is immobilized on a nylon coil separately from the bioluminescent enzymes so that they can be used at their pH optimum in the continuous-flow system. The effects of immobilization conditions on enzyme properties such as activity, stability, K_m and the choice of the coupling conditions (spacer, chemical methods) are discussed.

EXPERIMENTAL

Reagents

Luciferase from *Photobacterium fischeri* (E.C. 1.14.14.3; 15 mU mg^{-1} protein), NAD(P)H:FMN oxidoreductase from *Photobacterium fischeri* (E.C. 1.6.8.1; 100 U mg^{-1} protein), alcohol dehydrogenase (E.C. 1.1.1.1; 400 U mg^{-1} protein) from yeast, NAD (lithium salt) and FMN were purchased from Boehringer Mannheim. n-Decylaldehyde (decanal) and dithiothreitol (DTT) were obtained from Sigma Chemical Co., and glutaraldehyde (aqueous 25% solution) was from Merck.

All solutions were made with apyrogenic reagent-grade water prepared with a Milli-Q System (Millipore). Nylon-6 tubes (1-mm internal diameter) were obtained from Snia Viscosa. All other reagents and compounds were of analytical grade.

Solutions

The working bioluminescent solution was 0.1 M potassium phosphate buffer, pH 6.9, 10 μM in FMN, 27 μM in decanal and 0.5 mM in DTT. The solution was prepared 20—30 min before it was needed. Decanal was previously dissolved in isopropanol (0.05%, v/v) and was stable for several weeks at 4°C. The working bioluminescent solution showed no significant alteration after 8—10 h at room temperature in the dark. The NAD (lithium salt) was dissolved in water to obtain a 1 mM solution and made daily.

Enzyme assay

The activity of free oxidoreductases was measured in a 3-ml cuvette by monitoring the formation or consumption of NADH spectrophotometrically at 340 nm.

The conditions for the various assays were as follows: NAD(P)H:FMN oxidoreductase in 0.1 M potassium phosphate buffer, pH 7.0, which was 0.15 mM in NADH, 0.2 mM in FMN and 1 mM in DTT; ADH in 0.1 M potassium phosphate buffer, pH 9.0, 2 mM in NAD and 0.1 M in ethanol. The composition of the assay buffers was identical to that used with free enzymes.

The activity of the immobilized enzymes was determined by monitoring the eluate from the nylon tubes spectrophotometrically; 20—100 ml h^{-1} flow rates and 25—100-cm long tubes were used [19].

Enzyme immobilization

Nylon coils (1 cm diameter) were formed by heating tubes at 100°C for 15 min. The nylon coils (4—5 m) were treated with triethyloxonium tetrafluoroborate [11] for 10 min at 25°C, before one of the following procedures.

In procedure A, the *O*-alkylated tubes were washed with dichloromethane, filled immediately with a solution of 1,6-diaminohexane in methanol (10% w/v) and incubated for 1 h at 30°C. After extensive washing with water, the tubes were activated, within 48 h, by perfusion with 5% (w/v) glutaraldehyde in 0.1 M borate buffer, pH 8.5, for 15 min at 20°C and then washed with 0.1 M potassium phosphate buffer, pH 8.0.

In procedure B, after treatment with 1,6-diaminohexane and washing with methanol, the tubes were filled with a 2.5% (w/v) solution of dimethyl pimelimidate in 20% (v/v) *N*-ethylmorpholine in methanol and incubated for 1 h at 25°C. The tubes were washed with methanol and 0.1 M potassium phosphate buffer, pH 8.0.

In procedure C, adipic acid dihydrazide was used as a spacer instead of 1,6-diaminohexane. The *O*-alkylated tubes were filled with a 3% (w/v) solution of adipic acid dihydrazide in formamide and incubated for 3 h at room temperature before being activated with glutaraldehyde.

Procedure D was the same as C but with dimethyl pimelimidate in place of glutaraldehyde.

The activated tubes (1-m portions) were filled with solutions of enzyme (NAD(P)H:FMN oxidoreductase, 10 kU l^{-1}; luciferase, 12 U l^{-1}; ADH, 185 kU l^{-1}) in 0.1 M potassium phosphate buffer, pH 8.0, which was 0.2 mM in DTT and 0.5 mM in NAD, and left overnight at 4° C. After removal of the enzyme solutions, the tubes were washed thoroughly with 0.1 M potassium phosphate buffer, pH 7.0, to remove protein that was not covalently linked. The proportion of enzyme immobilized was calculated by subtracting the unbound enzyme activity from the total added activity. The immobilized enzymes were stored in 0.1 M potassium phosphate buffer, pH 7.0, which was 1% in bovine serum albumin, 1 mM in DTT and 0.02% in sodium azide, at 4° C.

Apparatus

The manifold developed for the continuous-flow assay is shown in Fig. 1. For analyses by means of separately immobilized enzymes, the flow system involved four streams: the first supplied the bioluminescent enzymes with the working bioluminescent solution, the second and third supplied the immobilized ADH (1-m coil), placed outside the luminometer, with 1 mM aqueous NAD^+ solution and 0.02 M sodium pyrophosphate buffer, pH 9.0. The fourth was a continuous flow of air into which a known volume of sample was intermittently added. A multichannel peristaltic pump (Minipuls HP4, Gilson) and calibrated tubes of different diameters were used to produce different flow rates. The bioluminescent reactor, a 0.5—1 m coil of nylon tubing containing co-immobilized luciferase and NAD(P)H:FMN oxidoreductase, was wound around a plexiglas support and positioned inside the luminometer in front of the photomultiplier tube (PMT) window. The diameter (1.0—1.6 cm) and the height of the coil (1.2—3.0 cm, corresponding to 0.5—1.0 m of nylon tube) were appropriately selected so that most of the light could reach the PMT. Moreover, a piece of white cardboard was placed

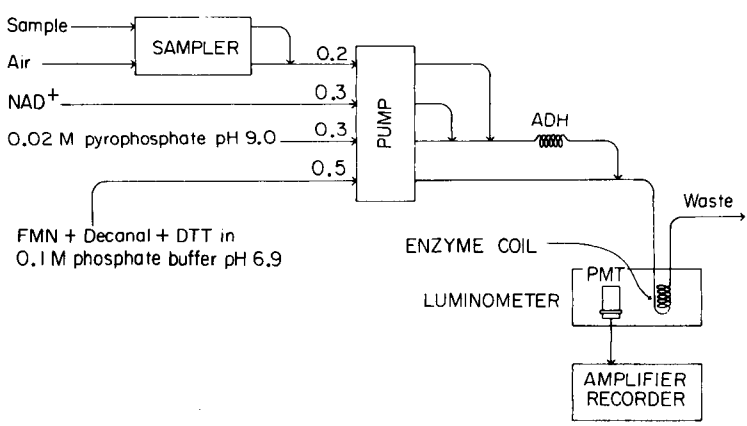

Fig. 1. Manifold for the bioluminescent continuous-flow assay of ethanol. Flow rates are given in ml min^{-1}.

behind the transparent coil, thus reflecting more light on to the PMT. Before reaching the reactor, the stream passed through a stainless-steel coil (0.8 mm i.d.) which not only provided mixing but prevented a possible light-piping effect [11]; a similar steel coil was also inserted after the reactor. A model 1250 luminometer (LKB) was used; it required only slight modifications to the original light-monitoring system. The sample (5—100 μl) was aspirated uniformly without fragmentation [11, 12]. Operational steady-state (stable background) was reached in about 5 min after preliminary washing with 0.1 M potassium phosphate buffer, pH 6.9, 0.5 mM in DTT.

Samples

Blood samples were collected by venous puncture, before and after intake of alcoholic beverages (mainly wine). The sera collected were stored at −20°C. Before injection, they were diluted (1 + 99) with 0.02 M sodium pyrophosphate buffer, pH 9.0, and vortex-mixed for 15 s; 10—25 μl was injected.

Saliva (1 ml) was collected before and 1—2 h after intake of 15—33 ml of wine or beer, and frozen at −20°C until required. Once thawed, it was vortex-mixed and centrifuged at 1200*g* for 10 min. The supernatant liquid was carefully collected, diluted (1 + 99) with 0.02 M sodium pyrophosphate buffer, pH 9.0, and analyzed.

Ethanol was determined in plasma and saliva by standard addition; ethanol solutions were added to samples to give a final concentration range of 1×10^{-4}—1×10^{-5} M. Diluted samples and standards were kept in stoppered vessels and analyzed within 36 h in order to prevent bacterial growth and alteration of ethanol content [15].

RESULTS

Properties of the immobilized enzymes

The effect of the immobilization procedure on the activity recovery of NAD(P)H: FMN oxidoreductase and the response of the luminescent reactor are shown in Table 1. Regarding the oxidoreductase, the highest recovery was obtained with 1,6-diaminohexane and dimethyl pimelimidate, whereas the use of adipic acid dihydrazide as a spacer gave very low activities. This suggests that the positive charge conferred to the matrix by the diamine is favourable for the activity of the oxidoreductase. The highest response of the luminescent reactor, which is a function of the activity of both oxidoreductase and luciferase, was obtained with procedure A. This indirectly indicates that glutaraldehyde increases the activity recovery of luciferase. It should be emphasized that it was not possible to determine the activity of the singly immobilized luciferase because, to our knowledge, no reliable method is available for the flow assay of the enzyme.

With alcohol dehydrogenase (ADH), the immobilization procedure scarcely influenced the activity recovery of the immobilized enzyme, which was

TABLE 1

Effect of the immobilization procedure on the activity of immobilized bioluminescent enzymes

Procedure	Activity recovery of NAD(P)H:FMN oxidoreductase[a] (%)	Relative response of the luminescent reactor[b] (%)
(A) 1,6-diaminohexane/glutaraldehyde	1.3	100
(B) 1,6-diaminohexane/dimethyl pimelimidate	2.5	62
(C) Adipic acid dihydrazide/glutaraldehyde	0.1	8
(D) Adipic acid dihydrazide/dimethyl pimelimidate	0.2	6

[a]7 U of NAD(P)H:FMN oxidoreductase and 8 mU of luciferase were added per metre of nylon tube. In all cases, more than 90% of the enzyme present in the coupling solution was immobilized onto the nylon tube. [b]Response of immobilized NAD(P)H:FMN oxidoreductase to 50 pmol of NADH; peak height expressed as a percentage of the highest value.

relatively low in all cases. For instance, with procedure A, which was routinely used for the luminescent enzymes and ADH, the activity recovery of immobilized ADH was 1.5% of the free enzyme. In this case, 120 U of ADH was added per metre of nylon, and 75% of the enzyme present in the coupling solution was covalently linked to the matrix. Dithiothreitol, which has a stabilizing effect on the luminescent enzymes and ADH, did not interfere with the immobilization of the enzymes on nylon [20, 21]. The $K_{m,app.}$ values for substrates and coenzymes of immobilized enzymes were similar to those of the free enzymes, except for ADH with NAD^+ as substrate (Table 2). The higher K_m value of the immobilized enzyme should be due to diffusional limitations, frequently present in immobilized enzyme systems [1, 21].

Immobilized ADH had a half-life of 80 days for the whole range of alcohol concentrations; NAD(P)H:FMN oxidoreductase had a half-life of 20 days when incubated in 0.1 M potassium phosphate buffer, pH 7.0, which was 1 mM in DTT and 0.02 in sodium azide, at room temperature. Therefore, both immobilized enzymes showed satisfactory stability.

Assay

Details on the influence of flow rate, sample volume, FMN and decanal concentrations on the response to NADH of immobilized bioluminescent enzymes have been reported elsewhere [19]. Here, the performance of the bioluminescent assay of ethanol is mainly considered. The pH and ionic strength of solutions are important parameters in the continuous-flow system. The ADH reaction was conducted at pH 9.0 to achieve the highest activity. The ionic strength of the buffer was kept low so that the optimum

TABLE 2

Michaelis constants of free and immobilized enzymes obtained from Lineweaver-Burk plots

Enzyme	Substrate or coenzyme	K_m of free enzyme (M)	$K_{m,app.}$ of immobilized enzyme (M)
NAD(P)H:FMN oxidoreductase	FMN	4.2×10^{-5}	3.9×10^{-5}
	NADH	2.0×10^{-4}	4.0×10^{-4}
Alcohol dehydrogenase	Ethanol	1.3×10^{-2}	1.1×10^{-2}
	NAD^+	7.4×10^{-5}	1.0×10^{-3}

pH for bioluminescent enzymes, which have a narrow maximum around pH 7.0 [2], was achieved by mixing with the working bioluminescent buffer. The assay was only slightly temperature-dependent in the range 20—30° C, so that no thermostatting was necessary. Dithiothreitol was not added to the pyrophosphate buffer, in spite of its stabilizing effect on ADH, because it gave rise to somewhat erratic responses.

The detection limit of the assay (3 σ) was 1 μmol ethanol per litre of sample, corresponding to 50 pmol determined, but such low values normally were not encountered because the ethanol content of the saliva and serum samples was higher than 250 pmol per injection. With buffered ethanol solutions the response was linear between 50 and 2500 pmol (slope = 0.042 ± 0.002 mV $pmol^{-1}$, intercept = 0.399 ± 0.210 mV, standard error = 0.273, n = 8) and a similar linear range (250—2500 pmol) was achieved by serial dilution of saliva (1.38 g l^{-1} ethanol) and serum (0.87 g l^{-1} ethanol). Table 3 shows the results of a within-day and between-day reproducibility study. The relative standard deviation (RSD) was always less than 10% both at high and low concentrations of ethanol (1.50 g l^{-1} and 0.25 g l^{-1}) in serum and saliva. The recovery was between 94 and 103% when these ethanol standards were added to ethanol-free saliva and serum samples. A similar recovery (96—105%) was obtained when standards were added to samples already containing 0.60—1.0 g l^{-1} ethanol. Therefore, no systematic difference was detected between the biological media and buffered ethanol solutions.

Typical time courses of light emission from the continuous-flow system are shown in Fig. 2 for saliva samples and Fig. 3 for serum samples. The alcohol concentration determined in saliva and serum (0.08—3.3 g l^{-1}) was in good agreement with previously observed values [15]. About 25—30 measurements per hour were possible. Washing between samples is advisable to avoid carryover. The lifetime and operational stability of immobilized enzymes were satisfactory. More than 900 measurements were done with an immobilized enzyme reactor (bioluminescent or ADH) before the sensitivity or accuracy was seriously affected. The residual activity of the enzymatic system after 2 months of use with analysis of more than 50 samples per day,

TABLE 3

Within-day and between-day reproducibility (n = 10) of bioluminescent assay of ethanol

Sample	Mean content ($g\ l^{-1}$)	Within-day		Between-day	
		SD ($g\ l^{-1}$)	RSD (%)	SD ($g\ l^{-1}$)	RSD (%)
Saliva[a]	1.38	0.04	3.2	0.07	4.7
Saliva[b]	0.11	0.01	5.2	0.01	9.1
Serum[b]	0.24	0.02	8.3	0.02	9.4
Serum[a]	1.52	0.09	5.7	0.11	7.3

[a]High pool. [b]Low pool.

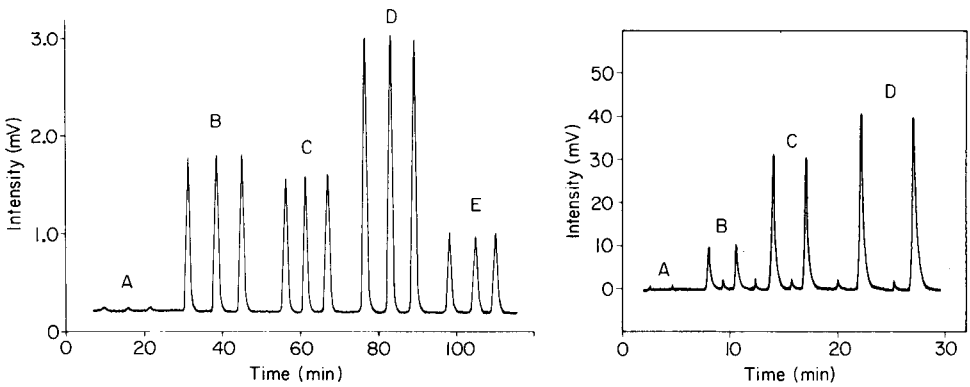

Fig. 2. Representative traces obtained for bioluminescent ethanol assay in saliva samples: (A) saliva sample before ethanol intake; (B) standard ethanol (100 pmol); (C) saliva sample 1 h after ethanol intake; (D) saliva in (C) plus standard ethanol (100 pmol); (E) saliva sample 2 h after ethanol intake.

Fig. 3. Representative traces obtained for bioluminescent ethanol assay in serum samples: (A) serum sample before ethanol intake; (B) serum sample after ethanol intake; (C) standard ethanol (1.5 nmol); (D) serum sample in (B) plus standard ethanol (1.5 nmol).

was about 20% of the initial activity, when the coils were used at room temperature and stored at 4° C.

DISCUSSION

The bioluminescent continuous-flow system for ethanol determination in serum and saliva is sensitive, simple and reliable. In contrast to the flow system based on enzymes immobilized on arylamine glass [9], the present method does not require a time-consuming separation step and reaction with ADH before injection into the flow system. The selectivity was high; alcohols such as methanol, isopropanol, isobutanol, isoamyl alcohol, benzyl alcohol

and glycerol did not react in the system. Propan-1-ol and butan-1-ol reacted but, because their affinity for ADH is low as is their concentration in serum and saliva [15], they can be neglected. When samples with a high concentration of ethanol are diluted for assay, some ethanol can be lost because of its volatility. Therefore, very careful treatment of such samples is necessary. With the use of separately immobilized enzymes (bioluminescent and ADH), interferences by contaminating enzymes and compounds [2, 9] were avoided and the background light emission was more stable and low. The operational stability is similar to, or better than, that of other flow systems [3, 7–9], and is much better than that obtained with soluble enzymes. With the nylon-immobilized enzymes, at least 10 times more determinations are possible than with the same amount of free enzymes. This system is also cheaper than other flow methods that use soluble ADH and spectrophotometric detectors [18].

The reagents did not require very constant temperature or refrigeration, and only the working bioluminescent solution had to be shielded from light. Unlike Sepharose column reactors [3, 7, 8], nylon reactors presented no problems with packing or disruption of gel matrix or with bacterial growth, which markedly enhances the background light level. This, together with their handiness, makes nylon tubes a very suitable enzyme support for continuous-flow analysis, in spite of the relatively low activity recovery of immobilized enzymes, which is still sufficient to achieve high sensitivity. The bioluminescent system required only minor modifications to a commercial detector, and allowed ethanol to be determined directly in serum and saliva at low cost and with good reproducibility. This method is also promising for the study of ethanol effects in local cancer treatment.

The financial support of Tecnobiomedica s.p.a. and the excellent technical assistance of Miss M. A. Angellotti are gratefully acknowledged.

REFERENCES

1 L. Goldstein, in K. Mosbach (Ed.), Methods in Enzymology, Immobilized Enzymes, Vol. 44, Academic Press, New York, 1976, p. 397.
2 E. Jablonski and M. DeLuca, Clin. Chem., 25 (1979) 1622.
3 D. Vellom, J. Hinkley, A. Loucks, H. Egghart and M. DeLuca, in L. J. Kricka, P. E. Stanley, G. H. G. Thorpe and T. P. Whitehead (Eds.), Analytical Applications of Bioluminescence and Chemiluminescence, Academic Press, London, 1984, p. 133.
4 A. Roda, L. J. Kricka, M. DeLuca and A. F. Hofmann, J. Lipid Res., 23 (1982) 1354.
5 G. Wienhausen and M. DeLuca, Anal. Biochem., 127 (1982) 380.
6 L. J. Blum and P. R. Coulet, Anal. Chim. Acta, 161 (1984) 355.
7 K. Kurkijarvi, R. Raunio and T. Korpela, Anal. Biochem., 125 (1982) 415.
8 L. J. Kricka, G. Wienhausen, J. E. Kinkley and M. DeLuca, Anal. Biochem., 129 (1983) 392.
9 K. Oda, S. Yoshida, S. Hirose and T. Takeda, Chem. Pharm. Bull., 32 (1984) 185.
10 K. Green, L. J. Kricka, G. H. G. Thorpe and T. P. Whitehead, Talanta, 31 (1984) 173.
11 S. Girotti, A. Roda, S. Ghini, B. Grigolo, G. Carrea and R. Bovara, Anal. Lett., 17 (1984) 1.

12 A. Roda, S. Girotti, S. Ghini, B. Grigolo, G. Carrea and R. Bovara, Clin. Chem., 30 (1984) 206.
13 A. Roda, S. Girotti, S. Ghini, B. Grigolo, G. Carrea and R. Bovara, in L. J. Kricka, P. E. Stanley, G. H. G. Thorpe and T. P. Whitehead (Eds.), Analytical Applications of Bioluminescence and Chemiluminescence, Academic Press, London, 1984, p. 129.
14 E. Jablonsky and M. DeLuca, in M. DeLuca (Ed.), Methods in Enzymology, Bioluminescence and Chemiluminescence, Vol. 57, Academic Press, New York, 1978, p. 202.
15 H. O. Beutler, in H. U. Bergmeyer (Ed.), Method of Enzymatic Analysis, Vol. 6, VCH, Weinheim, 1984, p. 598.
16 G. Jung and G. Ferard, Clin. Chem., 24 (1978) 873.
17 T. Lovgren, A. Thore, J. T. Lavi, I. Styrelius and R. Raunio, J. Appl. Biochem., 4 (1982) 103.
18 P. J. Worsfold, J. Růžička and E. H. Hansen, Analyst (London), 106 (1981) 1309.
19 A. Roda, S. Girotti, S. Ghini and G. Carrea, Methods in Enzymology, in Immobilized Enzymes and Cells, K. Mosbach (Ed.), Academic Press, London, 1985.
20 W. E. Hornby and L. Goldstein, in K. Mosbach (Ed.), Methods in Enzymology, Vol. 44, Academic Press, London, 1976, p. 118.
21 G. Carrea, R. Bovara and P. Cremonesi, Anal. Biochem., 136 (1984) 328.

Analytica Chimica Acta, 183 (1986) 197—205
Elsevier Science Publishers B.V., Amsterdam — Printed in The Netherlands

SPECTROPHOTOMETRIC DETERMINATIONS OF TRACES OF SELENIUM BY CATALYTIC REDUCTION OF TETRANITRO BLUE TETRAZOLIUM

WAYNE C. HAWKES*

Western Human Nutrition Research Center, Agricultural Research Service, U.S. Department of Agriculture, P.O. Box 29997, Presidio of San Francisco, CA 94129 (U.S.A.)

(Received 27th August 1985)

SUMMARY

The method is based on the catalytic effect of selenium on the reduction of tetranitro blue tetrazolium by dithiothreitol; it is simple, rapid and effective with several forms of selenium. With this catalytic assay, 1.2 ng of Se as selenite, 21 ng of Se as selenocysteine or 150 ng of Se as selenocystine can be detected (3 × SD). The relative standard deviations of the method are 2.7%, 5.4%, and 9.1% for the determinations of 0.2 μg, 2 μg, and 5 μg Se as selenite, selenocysteine, and selenocystine, respectively. The method is free of interferences from common ions and most of the interfering cations can be masked with organic acids. Data are included on the effects of pH, temperature, and reagent concentrations.

The method most commonly used to quantify trace levels of selenium is based on measurement of the fluorescent piazselenol formed by the reaction of selenite with diaminonaphthalene [1]. This fluorescence method is very sensitive and selective but requires careful control of pH [2] and a lengthy extraction step. Catalytic assays, which offer simple, sensitive, and selective methods for many elements [3, 4], have also been applied. A spot test for selenium has been based on its catalytic effect on the bleaching of methylene blue by sodium sulfide [5]. The quantitative method based on the reciprocal of the bleaching time had a detection limit of 0.05 μg [6]. Although the methylene blue method was quite selective for selenium, the time-based measurements made it difficult to apply to large numbers of samples or to automated systems. Another catalytic determination of selenium was based on the reduction of 1,4,6,11-tetraazanaphthacene by glyoxal and hypophosphorous acid and had a detection limit of 0.03 μg Se [7]; this method suffered from non-linear calibration and the use of a reagent that is not commercially available.

The present paper describes the development of a new method for the determination of selenium based on its catalytic effect on the reduction of tetranitro blue tetrazolium (2,2′,5,5′-tetra-(*p*-nitrophenyl)-3,3′-(3,3′-dimethoxy-4,4′-diphenylene)ditetrazolium chloride, TNBT) [8] by dithiothreitol

0003-2670/86/$03.50

(DTT). The method is rapid and simple, uses only readily available reagents, and is free of interferences from most common ions.

EXPERIMENTAL

Reagents

Selenite standard solutions were prepared by dilution in water of a 1000 mg l^{-1} atomic absorption standard in dilute nitric acid (Sigma Chemical Co.). Selenocystine (Sigma) was dissolved in 1 M HCl and diluted with water and 0.01 M HCl to give standard solutions in 0.01 M HCl. Selenocysteine was prepared fresh each day by reduction of solid selenocystine with sodium tetrahydroborate; the standards were prepared in 1 mM DTT and kept on ice.

The TNBT solution was prepared by dissolving 1 mg ml^{-1} in water and filtering through a 0.22-μm filter. The 1 M DTT was prepared fresh each day by dissolving 0.772 g of DTT in 3.5 ml of water plus 0.75 ml of 2 M sodium hydroxide and was kept on ice until used. The formaldehyde was a standard 37% reagent-grade solution in water. The iron reagent was prepared by dissolving 0.04 g of iron(III) chloride hexahydrate, 2.5 g of disodium-EDTA, and 5 ml of triethanolamine in 92.5 ml of water.

Recommended procedure

Place 0.5 ml of sample, containing 0.001–0.5 μg Se (as selenite) in a small test tube; add 0.5 ml of formaldehyde solution, 0.5 ml of iron reagent, and 0.1 ml of DTT to the tube and allow to stand for 4—5 min at room temperature. To start the reaction, add 0.2 ml of TNBT, mix, and transfer to a spectrophotometer cell controlled at 30°C. The final concentrations of reactants are 56.6 mM DTT and 122 μM TNBT. Record the change in absorbance at 600 nm for 4 min against a water reference. Repeat the measurement in the absence of added selenium and subtract this blank value to obtain the net absorbance change in 4 min. Disposable, semi-micro, plastic cuvettes are recommended because the colored product tends to accumulate on the surfaces.

Statistical methods. Unless otherwise stated, the results of linear regressions are presented as estimate ± standard error. Significance levels were calculated from the associated t values using a one-tailed test.

RESULTS AND DISCUSSION

Effects of reagents

Tetrazolium dyes were selected as indicators because they have the relatively rare property of becoming intensely colored upon reduction [9]. This property had several important consequences: (1) it allowed the accurate measurement of initial rates; (2) it improved the detection limits because the blanks were essentially colorless; and (3) it caused the rate of absorbance change to be more constant. Of the three tetrazolium compounds tested

(TNBT, nitro blue tetrazolium, and tetrazolium blue), TNBT was chosen for its greater solubility in water and corresponding wider dynamic range. The molar absorptivity of the formazan product was determined at 600 nm by reducing 0.01 ml of the TNBT solution under standard conditions in the presence of 1 μg Se as selenite, giving a value of 29,700 ± 300 cm^{-1} M^{-1}. Because of the limited solubility of the formazan, the rate of absorbance increase declined above absorbance of 0.5.

Four sulfur-containing compounds were tested as reductants: sodium sulfide, β-mercaptoethanol, dithioerythritol, and DTT. Although sodium sulfide and mercaptoethanol reacted readily and gave reasonable blank values, they were not used because of the sigmoidal shapes of their absorbance vs. time curves; DTT was preferred to dithioerythritol because it gave lower blanks and was more soluble in water.

As reported for the methylene blue/sodium sulfide catalytic assay [6], the presence of 10% formaldehyde in the reaction mixture caused a marked stabilization of the blank with little or no effect on the catalyzed reaction rate. As was also reported for the methylene blue assay, the presence of approximately 40 μg of iron(III) caused a considerable increase in the rate of the catalyzed reaction without any measurable effect on the formaldehyde-suppressed blank rate.

Effect of pH and temperature

The blank reaction rate was unaffected by increasing pH up to pH 8.9, where a rapid increase was observed (Fig. 1). The pH profile of the blank reaction resembled the titration curve of a thiol and reflected the enhanced reducing power of thiolate anions compared to thiols. The catalyzed reaction rate increased with increasing pH with inflection points at approximately pH 8.3 and pH 10.2 and a plateau between pH 8.6 and pH 9.6 (Fig. 1). A pH

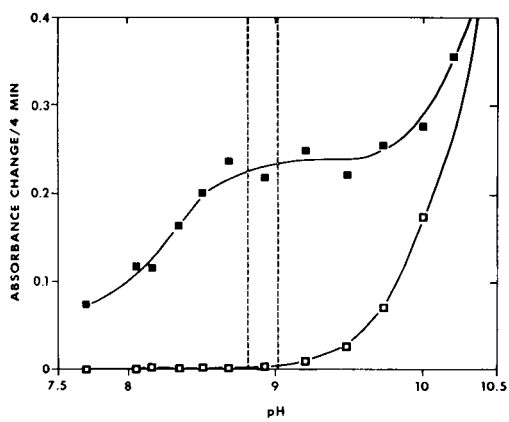

Fig. 1. pH dependence of reaction as in the recommended procedure: (□) without Se; (■) with 0.2 μg Se as selenite. The pH was adjusted by addition of 0—0.075 ml of 1 M HCl or 1 M NaOH. The dashed lines indicate the normal working pH range.

of 8.9 was chosen for the standard reaction conditions because the catalyzed reaction was insensitive to small pH differences and the blank had an acceptably low reaction rate.

Increasing the temperature caused an increase in the rate of the catalyzed reaction (1.8-fold per 10°C). However, the rate of the blank reaction increased much faster with increasing temperature (2.8-fold per 10°C), causing a net decrease in the signal-to-blank ratio and a concomitant increase in the detection limits. A temperature of 30°C was chosen because it was the lowest temperature that could be maintained in the sample compartment without cooling.

Precision

Five selenium-containing compounds were tested in this system and were found to have the following relative catalytic activities (per μg Se): selenite ⩾ selenocysteine ≈ glutathione peroxidase > selenocystine >>> selenomethionine ≈ 0. Because of the large amount of glutathione peroxidase required for these determinations and the negligible activity of selenomethionine, these forms of Se were not further investigated. Selenite, selenocysteine, and selenocystine gave linear calibration plots over a 250 to 500-fold concentration range (Table 1). Both the sensitivity (Table 1) and the precision (Table 2) were best with selenite. The detection limits with selenite, calculated either as twice the blank (3.5 ng Se) or as three times the standard deviation at the lowest standard tested (1.2 ng), were nearly as low as those reported for fluorescence using diaminonaphthalene (1 ng and 0.5 ng, respectively) [1], but the imprecision with fluorescence was slightly better (3.1% vs. 3.5% relative standard deviation for determinations of 0.02 μg Se).

TABLE 1

Standard calibration graphs[a]

Compound	Sensitivity[b] (ΔA vs. μg Se)	Detection limit[c] (μg)	Range (μg)	Correlation coefficient
Selenite	1.211 ± 0.016	0.0012	0.001—0.5	0.999
Selenocysteine	0.076 ± 0.003	0.021	0.02—5	0.994
Selenocystine	0.028 ± 0.001	0.150	0.02—5	0.993

[a]In these regressions the intercepts were not significantly different from zero ($p > 0.10$). Data are based on 10 levels of standards. [b]Slope of calibration graphs with standard errors, from linear regressions of the change in absorbance at 600 nm per 4 min (minus the blank rate) against the total amount of selenium in 0.5-ml samples. [c]Amount of selenium corresponding to a net reaction rate equal to three times the standard deviation at the lowest standard tested (see Table 2).

TABLE 2

Precision of the recommended procedure

Form of Se	Mass of Se (μg)			Relative standard deviation[a] (%)
	Taken	Found (mean)	Standard deviation[a]	
Selenite	0.005	0.0054	0.0004	7.4
	0.02	0.0209	0.0007	3.5
	0.2	0.1960	0.0053	2.7
Selenocysteine	0.05	0.0409	0.007	18
	0.5	0.486	0.023	4.6
	2.0	1.92	0.104	5.4
Selenocystine	0.2	0.208	0.05	24
	1.0	1.09	0.14	13
	5.0	4.70	0.43	9.1

[a] $n = 6$.

Interferences

Thirty-eight compounds were tested for interference in the standard procedure using 0.5-ml solutions that contained 0.14 μg Se as selenite (3.55 μM) and 4.6 mM of the test compound (1280/1 molar ratio). The following compounds caused no significant interference under these conditions: $AlCl_3$, $BaCl_2$, $CaCl_2$, $CdCl_2$, KF, KI, $LaCl_3$, LiCl, $MgCl_2$, NaBr, $Na_2B_4O_7$, $NaHCO_3$, Na_2HPO_4, $NaMoO_4$, $NaNO_2$, $NaWO_4$, $NiCl_2$, $Pb(CH_3CO_2)_2$, $SrCl_2$, and $ZnCl_2$. Those compounds which interfered at 4.6 mM were re-tested at decreasing concentrations in 0.5-ml samples containing 50 mM sodium citrate, sodium tartrate, or sodium oxalate as masking agents. Because the masking agents caused an approximate 25% decrease in the sensitivity, it was necessary to compare these samples to standard graphs obtained in the presence of the appropriate masking agents. Nine of the test compounds caused significant interferences at molar ratios below 50:1 in the presence of masking agents (Table 3). Because all of the interferents except permanganate and arsenite are cationic, they can be effectively removed by pretreatment of the samples with a strong cation-exchanger such as Dowex 50W-X8. Alternatively, samples containing substances that cause an increased or partial recovery can be evaluated by the method of standard additions.

Because selenium is most often determined as selenite after digestion in perchloric acid, a special sample matrix was formulated that approximated the products from the perchloric acid and nitric acid digestion procedure described by Watkinson [1]. Selenite standard solutions were prepared in 1.2 M $HClO_4$/0.2 M HCl/0.2 M triethanolamine, adjusted to pH 8.9 with sodium hydroxide. This sample matrix completely inhibited the catalyzed reaction under the standard conditions. At least part of this effect was due to precipitation of the TNBT as a perchlorate salt [9]. Work is underway in

TABLE 3

Interference studies

(Conditions were as described in the Recommended Procedure with 0.14 μg Se as selenite (3.55 μM) and up to 4600 μM test substance in 0.5 ml of solutions containing the indicated masking agent (50 mM as sodium salt).)

Compound	Maximum tolerated amount[a]		Masking agent	Compound	Maximum tolerated amount[a]		Masking agent
	μM	Molar ratio			μM	Molar ratio	
Inhibitors				*Accelerators*			
$CeSO_4$	4600	1280	Oxalate	$BeSO_4$	4600	1280	Citrate
$MnSO_4$	4600	1280	Tartrate	NaCN	4600	1280	Citrate
$ZrCl_4$	2800	770	Oxalate	$CoSO_4$	800	225	Oxalate
$Cr(CH_3CO_2)_3$	1800	500	Citrate	$FeCl_3$	400	110	Citrate
$TiCL_4$	200	56	Citrate	$CuSO_4$	40	11	Citrate
Na_2AsO_3	80	22	Tartrate	$SnCl_2$	9	2.5	Oxalate
$KMnO_4$	40	11	Tartrate	$TeCl_4$	0.4	0.13	Citrate
$BiCl_3$	10	2.8	Oxalate				
$SbCl_3$	4	1.3	Citrate				
$PdCl_2$	3	0.8	Citrate				
$AuCl_3$	2	0.5	Citrate				

[a]Highest level of interferent that caused less than a 5% change in the observed rate of the catalyzed reaction. Molar ratio is given with respect to Se.

this laboratory to find conditions suitable for the catalytic determination of selenite in perchloric acid digests.

Inhibition by iodoacetic acid

The catalytic effects of selenite, selenocysteine, and selenocystine were inhibited by iodoacetic acid in a concentration-dependent manner (Fig. 2). Because the inhibition was complete at iodoacetate concentrations below 0.5 mM, the inhibition must have been due to interaction with the selenium catalysts and not with the DTT, which was present at a concentration of 56.6 mM. The reactivities with iodoacetate suggest that all three of the selenium catalysts form an ionized moiety ($R\text{-}Se^-$) at some point in the catalytic cycle, as proposed for the methylene blue catalytic assay [5]. That such a moiety is required for catalytic activity is suggested by the lack of detectable activity in selenomethionine, which cannot form a selenium anion.

Activation energies

Linear regression analysis of Arrhenius plots of the temperature dependence of the reactions (Fig. 3) showed an activation energy for the uncatalyzed (blank) reaction of 20.7 ± 0.8 kcal mol^{-1}. The Arrhenius plots for the reactions catalyzed by selenite, selenocysteine, and selenocystine showed activation

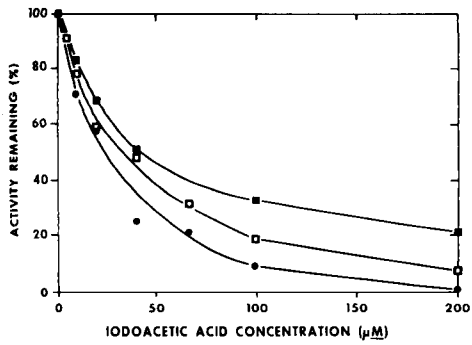

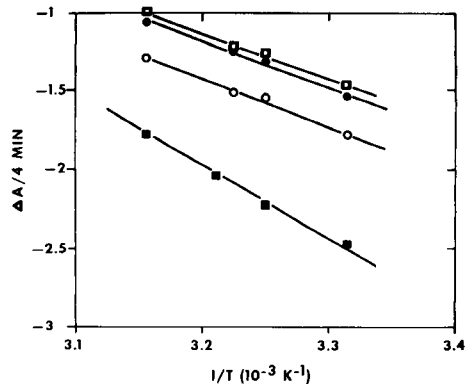

Fig. 2. Inhibition by iodoacetic acid on reaction: (■) 0.16 μg Se as selenite; (●) 0.8 μg Se as selenocysteine; (□) 2.5 μg Se as selenocystine. The iodoacetic acid was added to the samples 4—5 min before the start of the reactions, as in the recommended procedure, to give the indicated final concentrations.

Fig. 3. Temperature-dependence of reaction. Recommended procedure except that the temperature of the reactions was varied from 30 to 44°C. Catalysts: (■) none; (□) 0.02 μg Se as selenite; (○) 0.2 μg Se as selenocysteine; (●) 1 μg Se as selenocystine.

energies of 13.0 ± 0.8, 13.7 ± 1.0, and 13.0 ± 0.5 kcal mol^{-1}, respectively, indicating efficient catalysis.

Kinetic quantitation

The stoichiometry of the reaction between DTT and TNBT is

$$2\,DTT_{(red)} + TNBT \rightarrow 2\,DTT_{(ox)} + \text{TNB-diformazan}_{(blue)}$$

Figures 4 and 5 show the dependence of the catalyzed reaction rates on the concentrations of TNBT and DTT, respectively. Regression of the logarithm of the catalyzed reaction rate against the logarithm of the concentration of each reactant at five concentrations of the other reactant gave mean reaction orders of 0.91 ± 0.21 for TNBT and 1.80 ± 0.22 for DTT. A similar analysis of the blank reaction rate data gave mean reaction orders of 0.85 ± 0.11 for TNBT and 1.80 ± 0.70 for DTT. Because of the symmetry of the TNBT molecule and the distance between the reactive tetrazolium centers, this reaction most probably proceeds via a competitive, consecutive, second-order mechanism:

$$DTT_{(red)} + TNBT \xrightarrow{k_1} DTT_{(ox)} + \text{TNB-monoformazan}$$

$$DTT_{(red)} + \text{TNB-monoformazan} \xrightarrow{k_2} DTT_{(ox)} + \text{TNB-diformazan}$$

In such reactions, the apparent reaction orders are determined by the ratio of k_1 to k_2 [10]. Because the apparent reaction orders were essentially the

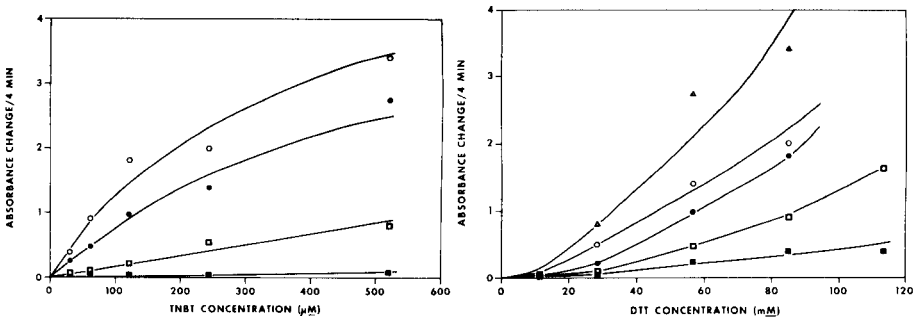

Fig. 4. Effect of tetranitro blue tetrazolium concentration. Recommended procedure except that the concentration of TNBT was varied while the DTT concentration was held constant at: (▪) 11.3 mM; (□) 28.3 mM; (●) 56.6 mM; (○) 84.8 mM, or 113.1 mM (not shown). The catalyst was 0.04 μg Se as selenite.

Fig. 5. Effect of dithiothreitol. Recommended procedure except that the concentration of DTT was varied while the TNBT concentration was held constant at: (▪) 30.6 μM (□) 61.2 μM; (●) 122 μM; (○) 244 μM; (▲) 520 μM. The catalyst was 0.04 μg Se as selenite

same in the catalyzed and blank reactions, catalysis must increase both k_1 and k_2 by about the same amounts. This would be expected if an adduct of DTT and selenium replaced DTT as the actual reducing agent in both steps. This interpretation is consistent with the observed inhibition by iodoacetic acid and with the reaction mechanism proposed for selenium catalysis of methylene blue reduction by sodium sulfide, wherein selenosulfide replaces sulfide as the reducing agent [5].

Because the rate equations for competitive, consecutive second-order reactions are very complex and, in general, cannot be solved analytically, an attempt was made to fit the data to the empirical rate expression: $d(TNBT)/dt = k(TNBT)^{0.9}(DTT)^{1.8}$. Regression of the apparent 0.9th-order TNBT rate constants against the DTT concentrations raised to the 1.8th power and of the apparent 1.8th-order DTT rate constants against the TNBT concentrations raised to the 0.9th power, gave apparent rate constants of 5.11 ± 0.42 $M^{-1.7}$ min^{-1} for the blank reaction and 2.37 ± 0.44 $M^{-1.7}$ min^{-1} for the catalyzed reaction. Dividing the rate constant for the catalyzed reaction by the selenium concentration (2.81×10^{-7} M) yielded an overall rate constant for the catalyzed reaction of $8.43 \pm 1.57 \times 10^6$ $M^{-2.7}$ min^{-1}. These empirical rate expressions fit the experimental data within ±25% in the range of 28.3–84.8 mM DTT and 30.6–122 μM TNBT with a tendency to underestimate the rates at lower or higher concentrations.

Although these rate expressions are not an adequate description of the kinetics of this reaction, they do indicate the catalytic effectiveness of selenite in this reaction. The ratio of the rate constant for the catalyzed reaction to the rate constant for the blank reaction, or $1.65 \pm 0.31 \times 10^6$ M^{-1}, is a measure of the increase in the reaction rate per molar concentration of

selenite. The complete kinetic analysis of these complex reactions is a very difficult mathematical problem and is beyond the scope of this work.

REFERENCES

1 See, e.g., J. H. Watkinson, Anal. Chem., 38 (1966) 92.
2 R. F. Bayfield and L. F. Romalis, Anal. Biochem., 144 (1985) 569.
3 K. B. Yatsimirskii, Kinetic Methods of Analysis, Pergamon Press, Oxford, 1966.
4 P. W. West, Anal. Chem., 23 (1951) 176.
5 F. Feigl and P. W. West, Anal. Chem., 19 (1947) 351.
6 P. W. West and T. V. Ramakrishna, Anal. Chem., 40 (1968) 966.
7 T. Kawashima and M. Tanaka, Anal. Chim. Acta, 40 (1968) 137.
8 G. Michal, H. Mollerung and J. Siedel, in H. U. Bergmeyer (Ed.), Methods of Enzymatic Analysis, 3rd edn., Verlag Chemie, Deerfield Beach, Florida, 1983.
9 J. W. Nineham, Chem. Rev., 55 (1955) 355.
10 A. A. Frost and R. G. Pearson, Kinetics and Mechanism, Wiley, New York, 1961.

Analytica Chimica Acta, 183 (1986) 207—215
Elsevier Science Publishers B.V., Amsterdam — Printed in The Netherlands

QUANTITATION OF ENZYMATICALLY GENERATED HYDROGEN PEROXIDE BASED ON AQUEOUS PEROXYOXALATE CHEMILUMINESCENCE

M. L. GRAYESKI*, E. J. WOOLF and P. J. HELLY
Chemistry Department, Seton Hall University, South Orange, NJ 07079 (U.S.A.)
(Received 10th June 1985)

SUMMARY

The method involves the reaction of 4,4'-{oxalyl bis[(trifluoromethylsulfonyl)imino]-ethylene}bis(4-methylmorpholinium trifluoromethanesulfonate) with hydrogen peroxide in the presence of rhodamine-B. Precise measurements, with 1—3% relative standard deviation, can be made in both static and flow systems. In the flow system, the response to hydrogen peroxide is linear from 10^{-3} M hydrogen peroxide down to the limit of detection of 7×10^{-6} M.

Since the first report of the quantitation of enzymatically generated hydrogen peroxide by chemiluminescence in 1974 [1], several chemiluminescent and bioluminescent systems have been found suitable for this assay. However, application of these methods based on luminol [1—5], or Cypridina [6] or earthworm [7] bioluminescence, or nonaqueous peroxyoxalate [8—12], or acridinium [13] chemiluminescence have several limitations. Luminol luminesces most efficiently above pH 9 [2], whereas many enzymes are active over the narrow pH range 5—7. Biological reductants, such as uric acid, are known to interfere with enzymatic assays of glucose based on luminol [3]. The bioluminescence methods require expensive and perishable reagents and these reactions are also most efficient near pH 7 or above. Although acridinium compounds luminesce over a wide pH range, the reaction products of acridinium esters are only slightly soluble in water [14], which leads to precipitation problems in flow systems. Among the most promising of the methods is peroxyoxalate chemiluminescence; a suitable oxalate reacts with hydrogen peroxide to form a proposed intermediate, 1,2-dioxetane-dione, which then reacts with an appropriate fluorophore. This reaction has been demonstrated to be suitable for measurements over a wide pH range, has fewer interferences than some other reactions, and produces minimal blank signals [8]. In addition, wavelength selection of emitted light is possible through the use of different fluorophores.

A major disadvantage of peroxyoxalate chemiluminescence is that the most efficient oxalate derivatives typically used, 2,4-dinitrophenyl oxalate and 2,4,6-trichlorophenyl oxalate, are insoluble in water. Because these

0003-2670/86/$03.50

oxalates are stable and efficient in esters such as ethyl acetate, cosolvents are needed to assure the miscibility of all reactants. Besides being unsuitable for enzymatic reactions, the use of organic/aqueous solvent systems results in mixing variations, leading to measurements with low precision [15].

A packed-column peroxyoxalate reactor has recently been developed in an effort to eliminate mixing irregularities [16]. While this system allows better precision (<2% RSD), it cannot tolerate more than 20% water in the carrier stream. The imprecision of peroxyoxalate chemiluminescence measurements, along with the need for high concentrations of organic solvents, restricts the potential automation of such assays.

Recently, a new class of water-soluble chemiluminescent oxalic acid derivatives has been developed [17]. Among the most efficient of these derivatives is 4,4′-{oxalyl bis[(trifluoromethylsulfonyl)imino]ethylene}bis-(4-methylmorpholinium trifluoromethanesulfonate) (METQ). In this paper, an evaluation of peroxyoxalate chemiluminescence for quantifying enzymatically generated hydrogen peroxide is reported.

EXPERIMENTAL

Reagents

The METQ was prepared by the method of Tseng and Rauhut [17]. *N*-(2-Aminoethyl)morpholine is treated with trifluoromethane sulfonic acid anhydride to produce an amide which is treated with oxalyl chloride. The product, *N*,*N*′-bis(2-morpholinoethyl)-*N*,*N*′-bis(trifluoromethylsulfonyl)oxamide is treated with methyl trifluoromethanesulfonate in dichloromethane to yield the final product, METQ. After recrystallization from acetone/dichloromethane, the product had a melting point of 195—197°C; the overall yield was about 20%.

Rhodamine-B (laser grade) and *N*-methylacridone were from Aldrich Chemical Co. Aminopyrene sulfonic acid (mixed isomers) was prepared by the method of Arient et al. [18]. Buffers were prepared from reagent-grade sodium acetate or dipotassium hydrogen phosphate. β-D(+)-Glucose, uric acid, and glucose oxidase (type VII, from *Asperigillus niger*) were from Sigma Chemical Co. Hydrogen peroxide standard solutions were prepared by diluting a 30% stock solution (Aldrich). All solvents used were HPLC grade from either Fisher Scientific or J. T. Baker.

Instrumentation

Experiments in a static system were done with a Turner Designs (Mountain View, CA) model 20 photometer equipped with a Turner model 20-010 pipet injector system, and attached to a Heath/Zenith model SR-204 strip-chart recorder. Peak intensities and peak areas were measured with the built-in microprocessor.

The flow system consisted of either a Sage model 351 syringe pump (Sage Inst. Co., Cambridge, MA) equipped with two 50-ml gas-tight syringes (Hamilton Co.) or a gas-propulsion solvent delivery system (Control Equipment Corp., Lowell, MA), two Rheodyne (Conti, CA) type-50, sample-

injection valves, a Kel-F mixing T-joint (Rainin Inst. Co., Woburn, MA), and a flow cell consisting of a 40-cm coil of 0.8-mm i.d. teflon tubing sandwiched between two glass plates. The distance between the T-joint and the entry to the coil was 5 cm. All connections between components were made with 0.8-mm i.d. teflon tubing. The flow cell was positioned in front of a Hamamatsu type R1104 photomultiplier tube (PMT), which in turn was housed in a Pacific Instruments (Concord, CA) model 3262 housing, equipped with a wideband linear amplifier model 2A35. The PMT and amplifier were powered by a Pacific Instruments model 204-03L high voltage power supply. Voltage for the PMT was maintained at 1000 V. The output from the amplifier was recorded on a Laboratory Data Control model 3301-M-R recorder equipped with inputs of 1, 2, 5, 10, 20, 50, and 100 mV full scale.

Procedures

Static system. A portion (100 μl) of hydrogen peroxide solution and 50 μl of 10^{-4} M rhodamine-B in 0.025 M acetate pH 5 buffer, which was also 10^{-3} M in Deceresol NI surfactant, were pipeted into a 1.6 ml-polypropylene cuvette (Evergreen Scientific, Los Angeles, CA). The cuvette was placed in the photometer, and 100 μl of 2.0×10^{-3} M METQ in acetonitrile was injected from the pipet delivery system. Injection of the METQ initiated the electronic integrator of the photometer. The chemiluminescence intensity/time curve was then integrated for 60 s after a delay time of 2 s to allow for mixing.

Flow system. A block diagram of the flow system is shown in Fig. 1. Solvent reservoirs A and B were filled with fluorophore solution at the pH of interest. The flow rates of the carrier streams were controlled by the syringe-pump setting or by adjusting the pressure of the gas-propulsion system. The METQ was injected from injector A while the hydrogen peroxide solution was injected from injector B. Injectors A and B were turned simultaneously to the inject position, and the resulting chemiluminescence signal was recorded.

Assay of glucose. For calibration, standard solutions of glucose were prepared in 1 mM phosphate pH 6 buffer; 3 ml of each standard was transferred to a 12 × 50-mm polypropylene culture tube and 100 μl of a solution (150 U ml^{-1}) of glucose oxidase in 1 mM phosphate pH 6 buffer was added to each

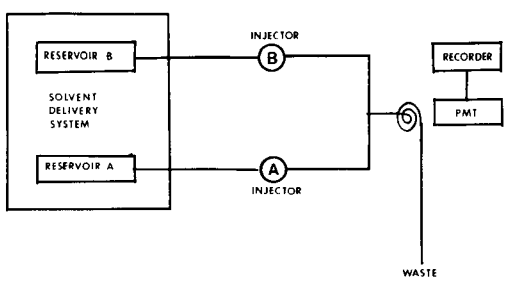

Fig. 1. Flow system. Reservoirs A and B contain fluorophore in buffer; METQ is injected at A and sample at B.

tube. These solutions were incubated for 15 min at room temperature, and then injected into the flow system. The recommended conditions for the flow system are 10^{-4} M rhodamine-B in 1 mM phosphate pH 6 buffer, 2 ml min^{-1} flow rates (each stream), 6.25 g l^{-1} (6.9 mM) METQ solution in acetonitrile, and 27-μl loops on each injector.

Glucose in urine. Urine (15 μl) was pipeted into a polypropylene culture tube containing 3 ml of 1 mM phosphate pH 6 buffer. The resulting solution was then treated as stated above for the glucose standards. For the standard additions, 1 ml of urine was spiked with 0–100 μl of a 2×10^{-2} M glucose solution. The resulting "spiked" urine was then processed as described above.

RESULTS AND DISCUSSION

Static system

All imprecision data are reported as relative standard deviations (RSD) unless noted otherwise.

Solvent system for METQ. Initial experiments with aqueous solutions of METQ demonstrated that while METQ is quite soluble in water, it undergoes rapid hydrolysis, with a half-life of ca. 8 min. Although solid METQ can be weighed, and the other reactants can be dissolved in water before being added to the solid in order to provide a totally aqueous system, this approach is inconvenient and imprecise. Instead, solvents completely miscible with water were investigated with regard to METQ stability, signal intensity, and precision of measurement. It was found that METQ is unstable in methanol and ethanol, insoluble in tetrahydrofuran, and fairly soluble in acetone and acetonitrile. Under identical conditions, METQ dissolved in acetonitrile produced approximately 3-fold more light than when it was dissolved in acetone. Precision in both solvents was similar (3–4% RSD). Further experiments showed that METQ was stable for at least 48 h when dissolved in HPLC-grade acetonitrile. Thus, stock solutions of METQ in acetonitrile were used.

pH Dependence. Unlike many other reactions that produce chemiluminescence, peroxylate chemiluminescence in nonaqueous solvents produces significant emission over a wide pH range for certain oxalate derivatives [19]. Therefore, the effect of pH on peak height and area was investigated to establish the useful pH range of METQ.

The effect of pH was investigated by changing the pH of the hydrogen peroxide solution and by measuring peak height and integrating peak area for 1 min (after a 2-s delay). At alkaline pH, the reaction is so fast that most of the light is emitted within a few seconds, while at pH 5 the reaction is slowed sufficiently that light is still being emitted after 1 min, but maximum intensity still occurs within the first few seconds (Fig. 2A). This effect is observable over the pH range 4–11 (Fig. 2B). Such a rate increase is expected for a base-catalyzed reaction and the proposed mechanism involves deprotonation of the hydrogen peroxide by the base. Because the reaction is so

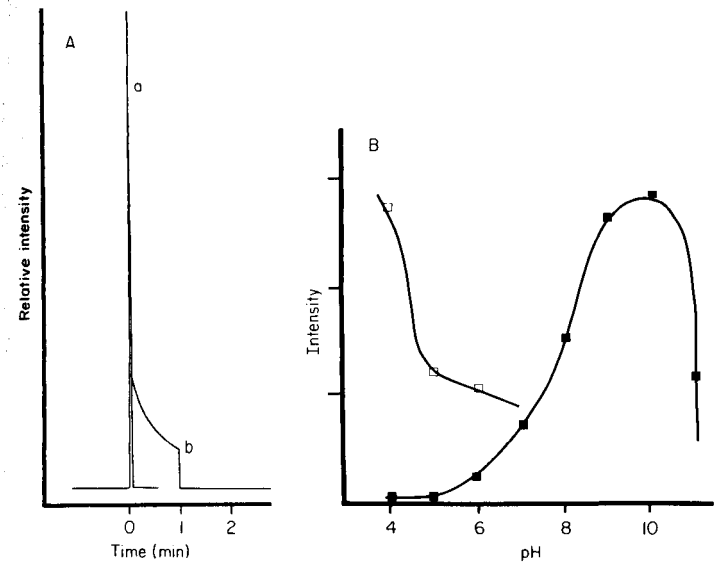

Fig. 2. Effects of pH in static system. (A) Responses: (a) at pH 9; (b) at pH 5. (B) Response to 10^{-4} M H_2O_2 with 0.025 M phosphate buffers: (□) integrated area; (■) maximum intensity. Other conditions as in text.

fast in alkaline solution, a significant amount of emission is probably not measured during the initial part of the reaction due to instrumental response limitations. However, the decrease in measured area may also indicate decreased chemiluminescence efficiency, i.e., competing reactions in alkaline solution that do not produce light. Although maximum intensities (measured by peak height) are larger for pH > 8, the reaction is fast enough at pH 4 to allow significant emission within a 2-min time period. Therefore, quantitation with aqueous peroxyoxalate is possible over the pH range of 4—8.

Precision. For the quantitation of 2×10^{-5} M hydrogen peroxide in the static system, the relative standard deviation for six replicates was 1.3% for peak area and 2.17% for peak height. These results represent a significant improvement of precision relative to systems in which mixtures of ethyl acetate, acetonitrile, and water were present. In these mixed solvent systems, imprecisions of 5–21% RSD resulted because of solvent immiscibility and/or micro precipitation [15]. In addition, the use of acetonitrile allows easier adaptation of the measurement system to flow systems, which in turn allows for ease of automation.

Flow system

The flow system (Fig. 1) utilizes the merging-zones design [20]; small volumes of analyte and METQ reagent are simultaneously injected into carrier streams that contain fluorophore before mixing downstream. The advantage of this design is that only small volumes (<100 μl) of sample and

reagent solution are required. The response can be optimized through several variables.

Choice of fluorophore. An advantage of peroxyoxalate chemiluminescence is that the emission wavelength of the reaction can be varied by using different fluorophores. Thus, background interference can be eliminated by choosing a fluorophore which emits in a desirable wavelength region. However, while different fluorophores can be excited via peroxyoxalate chemiluminescence, the overall luminescence efficiency of the reaction is known to be fluorophore-dependent [21]. For this application, the fluorophore used must be efficiently excited during the energy-transfer step, it must have a high fluorescence efficiency, and it must be water-soluble. Few fluorophores satisfy all these requirements.

The fluorophores tested here were rhodamine-B, aminopyrene sulfonic acid, and *N*-methylacridone (Table 1). Rhodamine-B and aminopyrene were chosen because they are reported to be very efficient in the peroxyoxalate system [15, 22]. Although sulfonation tends to lower fluorescence efficiency, aminopyrene was sulfonated prior to use in order to improve water solubility. *N*-Methylacridone was evaluated because it has a fluorescence efficiency close to unity in water [14]; however, although chemiluminescence was observed here with high concentrations of hydrogen peroxide, 10^{-5} M peroxide could not be detected when *N*-methylacridone was used at a concentration near its solubility limit [14] in each carrier stream. Chemiluminescence was readily observed at 10^{-5} M hydrogen peroxide with rhodamine-B or aminopyrene sulfonic acid. The intensities were equivalent for both these fluorophores but rhodamine-B has several advantages, including long wavelength emission, relatively low cost, and commercial availability in high purity.

Effects of pH and flow rate. When a flow system is used, the rate of the peroxyoxalate reaction, primarily controlled by pH, and the flow rate must be adjusted to allow for maximum emission of light during the short period of time that the analyte is monitored by the PMT. The pH and flow-rate effects are convoluted, because flow rate affects the dispersion of the sample zone. The effect of varying flow rates (Fig. 3) can be explained by considering

TABLE 1

Effect of fluorophore on response to hydrogen peroxide

Fluorophore	Concentration[a] (M)	Response[b]
N-Methylacridone	2×10^{-5}	—
Rhodamine-B	1×10^{-4}	8.0 ± 0.1
Aminopyrene sulfonic acid	1×10^{-4}	7.1 ± 0.3

[a]Concentration of fluorophore present in each carrier stream (1 mM phosphate pH 5.5 at 3 ml min^{-1}). [b]Blank-corrected response to 10^{-5} M H_2O_2 for 8.3 mM METQ; 27-μl loops on both injectors.

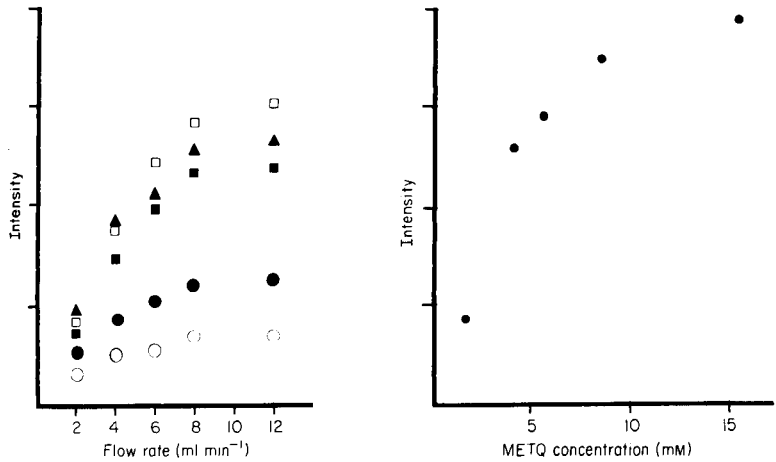

Fig. 3. Effect of pH and total flow rate on response of flow system. pH: (○) 5; (●) 5.5; (▲) 6.0; (□) 6.5; (■) 7. Conditions: 10^{-4} M rhodamine-B in carrier streams containing 1 mM buffer; 10^{-5} M H_2O_2 and 8.3 mM METQ in acetonitrile injected with 27-μl loops.

Fig. 4. Effect of METQ concentration. Total flow rate 4 ml min^{-1}; other conditions as for Fig. 3.

the fast rate ($t_{1/2} \approx 5$ s at pH 6) of the chemiluminescence reaction. At 2 ml min^{-1}, there is a dead time of 0.75 s in the flow system which corresponds to the time from injection of the sample to its reaching the detector. The dead time decreases with higher flow rates to as low as 0.023 s at 12 ml min^{-1}. At low flow rates, most of the emission occurs before reaching the detector, and higher flow rates lead to increased signals. However, to avoid excessive use of reagent, total flow rates above 12 ml min^{-1} were not investigated.

The decrease in signal above pH 6.5 (Fig. 3) is also a result of the rate of the chemiluminescence reaction. At higher pH, most of the emission is produced before the sample zone reaches the detector. Because the residence time in front of the detector also decreases at higher flow rates (from 7.6 s at 2 ml min^{-1} to 0.24 s at 12 ml min^{-1}), the intensity eventually reaches a maximum, in this case, at pH 6.5. For the conditions investigated, maximum emission for the injection of 10^{-5} M hydrogen peroxide was observed at pH 6.5 at a total flow rate of 12 ml min^{-1}, but the precision was poor, with injection-to-injection scatter of 3.4% for 10^{-5} M hydrogen peroxide. To maximize precision and to conserve reagents, with minimal loss of sensitivity, the preferred conditions for measurements are at pH 6, with a total flow rate of 4 ml min^{-1}. Under these conditions, the injection-to-injection RSD for 10^{-5} M peroxide was 0.3%.

Effects of METQ and buffer concentrations. Solutions of oxalate esters typically used for chemiluminescent reactions are prepared at their maximum solubilities of about 10^{-2} M in order to produce maximum emission. In flow systems, care must be taken to prevent precipitation. Because METQ is

quite soluble in acetonitrile, solubility limitations are less restrictive. The response to 10^{-5} M hydrogen peroxide with rhodamine-B as fluorophore (Fig. 4) increases dramatically for METQ concentrations between 1.5 and 5.5 mM. For concentrations above 5.5 mM, the emission appears to level off, possibly because further emission occurs when the sample zone is not in front of the detector.

High buffer concentrations can decrease the signal-to-noise ratio of peroxyoxalate chemiluminescence [8]. In order to evaluate this effect in the present system, the response to 10^{-5} M hydrogen peroxide was measured for 0.1 M and 1 mM phosphate buffer (pH 6) in each carrier stream. Increasing the buffer concentration increased the emissions of both the blank and the sample; the blank-corrected signal was relatively insensitive to buffer concentration.

Loop size. Increasing the loop size to 50 or 75 μl produced broader peaks of approximately the same height as those obtained with 27-μl loops. In order to maximize sampling rate, which is largely determined by peak width, 27-μl loops were used.

Response to hydrogen peroxide. Under the flow conditions recommended for the assay of glucose (see Experimental), the response to hydrogen peroxide standards was linear from 10^{-2} M down to the limit of detection of 7×10^{-8} M (defined as 3 SD of the blank). The responses to 10^{-7} M and 10^{-6} M peroxide are shown in Fig. 5. In the linear region, the injection-to-injection RSD ranged from 0 to 3%, with an average of 1.7%. The detectability of hydrogen peroxide is limited by the blank observed in the absence of injected peroxide (Fig. 5), which might be due to reagent impurities and/or the emission of light by a less efficient, peroxide-independent, reaction pathway [8, 16].

Effect of uric acid. Uric acid is known to interfere with the quantitation of glucose via the luminol reaction [3] but not with non-aqueous peroxyoxalate chemiluminescence [8]. In order to establish if uric acid would interfere with the quantitation of hydrogen peroxide under the proposed conditions,

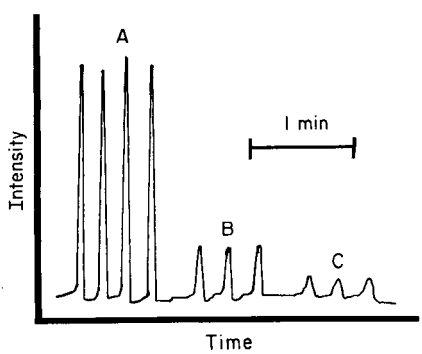

Fig. 5. Responses to hydrogen peroxide in flow system under the recommended conditions (see Experimental): (A) 10^{-6} M H_2O_2; (B) 10^{-7} M H_2O_2; (C) blank.

10^{-5} M peroxide samples were spiked to contain 0—1 mg dl^{-1} uric acid (concentrations analogous to a 1:200 dilution of urine). Uric acid did not affect the response to peroxide under the proposed conditions. This observation was supported by studies with urine samples. Urine samples (1 ml) were spiked with up to 100 μl of 2×10^{-2} M glucose. The slope of the standard additions plot was compared with that obtained by spiking 1-ml portions of distilled water. For the urine samples, the slope of the standard additions plot was 0.126 compared to a value of 0.124 for water samples. A *t*-test at the 95% confidence level showed no significant difference in the calculated slopes.

The authors thank A. Mohan and R. Schulze for assisting in the METQ synthesis, A. Weber and P. Snyder for providing the aminopyrene sulfonic acid, and A. Slowinski for assistance with the experiments. This work was presented in part at the 10th FACSS meeting, Philadelphia, 1983, and was funded in part with a grant from Control Equipment Corp., Lowell, MA.

REFERENCES

1 D. T. Bostick and D. M. Hercules, Anal. Lett., 7 (1974) 347.
2 J. P. Auses, S. L. Cook and J. T. Maloy, Anal. Chem., 47 (1975) 244.
3 D. T. Bostick and D. M. Hercules, Anal. Chem., 47 (1975) 447.
4 D. Pilosof and T. A. Nieman, Anal. Chem., 54 (1982) 1698.
5 C. Ridder, E. H. Hansen and J. Růžička, Anal. Lett., 15 (1982) 1751.
6 T. Kobayshi, K. Saga, S. Shimizu and T. Goto, Agric. Biol. Chem., 45 (1981) 1403.
7 J. E. Wampler, M. G. Mulkerrin and E. S. Rich, Jr., Clin. Chem., 25 (1979) 1628.
8 D. C. Williams III, G. F. Huff and W. R. Seitz, Anal. Chem., 48 (1976) 1003.
9 V. I. Rigin, Zh. Anal. Khim., 33 (1978) 1623.
10 V. I. Rigin, Zh. Anal. Khim., 34 (1979) 619.
11 G. Scott and W. R. Seitz, Anal. Chim. Acta, 115 (1980) 221.
12 W. R. Seitz, T. Cole and J. Mullin, Proceedings of the XI International Congress of Clinical Chemistry, Walter De Gruyter, Berlin, 1982, p. 1083.
13 F. McCapra, D. E. Tutt and R. M. Topping, British Patent 1,461,877 (1977).
14 W. L. Hinze, T. E. Riehl, H. N. Singh and Y. Baba, Anal. Chem., 56 (1984) 2180.
15 M. L. Grayeski and W. R. Seitz, Anal. Biochem., 136 (1984) 277.
16 P. Van Zoonen, D. A. Kamminga, C. Gooijer, N. H. Velthorst and R. W. Frei, Anal. Chim. Acta, 167 (1985) 249.
17 S. Tseng and M. M. Rauhut, U.S. Patent 4,282,357 (1981).
18 J. Arient, J. Dvorak and K. Brezina, Chem. Prumsyl, 11 (1961) 78.
19 A. Weber, Ph.D. Dissertation, Seton Hall University, 1985.
20 J. Růžička and E. H. Hansen, Flow Injection Analysis, Wiley, New York, 1981.
21 P. Lechtken and N. J. Turro, Mol. Photochem., 6 (1974) 95.
22 K. W. Sigvardson, J. M. Kennish and J. W. Birks, Anal. Chem., 56 (1984) 1096.

Analytica Chimica Acta, 183 (1986) 217—223
Elsevier Science Publishers B.V., Amsterdam — Printed in The Netherlands

DETERMINATION OF TRACES OF RUTHENIUM BY ADDITION OF CERIUM(IV) AND ATOMIC ABSORPTION SPECTROMETRY

KENJI MOTOJIMA* and KATSUYOSHI TATENUMA
Kaken Co. Ltd., 1044 Hori-cho, Mito, Ibaraki 310 (Japan)
ZENKO YOSHIDA, HIDEYO TAKEISHI and EIKO AKATSU
Japan Atomic Energy Research Institute, Tokai-mura, Ibaraki 319-11 (Japan)
(Received 10 July 1985)

SUMMARY

The sensitivity of the determination of ruthenium by flame atomic absorption spectrometry is increased 60 times by adding 1×10^{-2} M cerium(IV). Calibration is linear over the range of 0.05—5 μg ml^{-1} ruthenium. A method applicable to nitrosylruthenium complexes is described. The increased sensitivity results from formation of ruthenium tetroxide.

On account of the great variety of its oxidation states and chemical forms, ruthenium is one of the most interesting but sometimes most troublesome elements, and therefore many studies have been made, in the fields of chemistry and nuclear technology. To assist these studies, sensitive and simple methods for the determination of ruthenium are needed. There is only a little information on the determination of ruthenium by atomic absorption spectrometry (a.a.s.), but it is known that the sensitivity for ruthenium is extremely poor. Several attempts have been made empirically to improve the sensitivity of a.a.s. for ruthenium, by the addition of uranium ions [1, 2], copper sulfate, cadmium sulfate [3] or potassium cyanide [4]. Nevertheless, little improvement was obtained and the lower detection limit with these methods ranged from 1 to 10 μg ml^{-1}.

In the present paper, it is shown that the addition of cerium(IV) to the sample solution converts ruthenium(III) quantitatively to volatile ruthenium tetroxide. The sensitivity obtained by a.a.s. is greatly increased and the lower detection limit is only 0.05 μg ml^{-1}. Pretreatment of the sample solution with hydrogen peroxide is also investigated in order to decompose such stable complexes as tetranitronitrosylruthenate into ruthenium ions which can be oxidized to ruthenium tetroxide by cerium(IV).

0003-2670/86/$03.50

EXPERIMENTAL

Chemicals and apparatus

A stock solution of ruthenium(III) (ca. 1.00 mg Ru ml^{-1}) was prepared by dissolution of reagent-grade ruthenium trichloride hydrate in 5 M nitric acid and standardization by gravimetry [5]. This solution was diluted to give 1—20 μg Ru ml^{-1} standards in 0.2 M nitric acid. Sodium hydroxotetranitronitrosylruthenate(III), $Na_2[Ru(NO)(NO_2)_4(OH)]\cdot 2H_2O$, was synthesized as reported previously [6]. A stock solution (1.00 mg Ru ml^{-1}) of this compound was prepared by dissolution in water, and then diluted with water to give 1—20 μg Ru ml^{-1} standards. Reagent-grade ammonium cerium(IV) nitrate was dissolved in water to give a 0.5 M cerium(IV) solution. All other chemicals used were of reagent grade. Distilled water was used throughout.

The atomic absorption spectrometer (Shimadzu Model AA-646) used was equipped with a burner of 100-mm slot length and a hollow-cathode lamp (Hamamatsu). The optimum conditions to obtain maximum stable absorbance readings were as follows: burner height usually 3 mm; wavelength 349.9 nm; slit-width 19 nm; lamp current 15 mA; acetylene 2.5 l min^{-1}; air 10 l min^{-1}.

Recommended procedure

Place a known volume, usually 15—20 ml, of sample solution containing 0.25—125 μg of ruthenium and 0.5—1 M of nitric acid in a 25-ml Pyrex volumetric flask and add 0.5 ml of 0.5 M cerium(IV) solution. Measure the absorbance of this solution and determine the ruthenium content with the aid of the calibration graph prepared from the results obtained from standards treated in the same way.

For the tetranitronitrosylruthenium species, decompose the complex first by adding 0.5 ml of 30% hydrogen peroxide to the sample solution and heating in a boiling water bath for 1 h. If an appreciable quantity of hydrogen peroxide remains in the solution after the decomposition of the complex, add 2—3 mg of iron(III) nitrate and continue to heat in the boiling water bath for 30 min. Cool the solution before preceding with the addition of cerium(IV) as described above.

RESULTS AND DISCUSSION

It was found that the sensitivity for the determination of ruthenium by a.a.s. could be increased by the oxidation of ruthenium(III) ions to ruthenium tetroxide. Of various oxidizing ions tested (peroxodisulfate, periodate, chromate, permanganate and cerium(IV)), cerium (IV) was found to be the most effective for enhancing the sensitivity. The following investigations, therefore, were made to establish the optimum conditions for the determination of ruthenium after addition of cerium(IV). Nitric acid was used as the

medium, because this is widely encountered in the samples obtained from nuclear technology.

Study of optimum conditions

Effect of the concentrations of cerium(IV) and nitric acid. When 25 ml of 0.5 M nitric acid solution containing 2 μg ml^{-1} ruthenium(III) and >5 × 10^{-3} M cerium(IV) was used, a constant absorbance was obtained that was 60 times higher than in the absence of cerium(IV) (Fig. 1). Similar results were obtained with 0.1 or 5 μg ml^{-1} solutions of ruthenium. The effect of nitric acid concentration is shown in Fig. 2. At >2 M nitric acid, the absorbance decreased. On the basis of these results, the conditions for greatest sensitivity were 1 × 10^{-2} M cerium(IV) and 0.1—1.5 M nitric acid.

Effect of time after addition of cerium(IV). Figure 2 also shows the effect of acid concentration on the absorbance obtained 24 h after mixing the ruthenium solution with cerium(IV) in a Pyrex glass-stoppered flask. Absorbances of solutions >0.2 M in nitric acid were almost identical with those measured immediately after the addition of cerium(IV). This shows that the oxidation of ruthenium(III) to ruthenium textroxide reaches equilibrium rapidly after addition of cerium(IV) and that the ruthenium tetroxide is stable for at least 24 h. In <0.2 M nitric acid, the decrease in absorbance with time indicates that ruthenium tetroxide is less stable in solution of lower acidity.

When the same kinetic experiment was done in a flask made of polyethylene or polypropylene instead of Pyrex glass, a black deposit of a

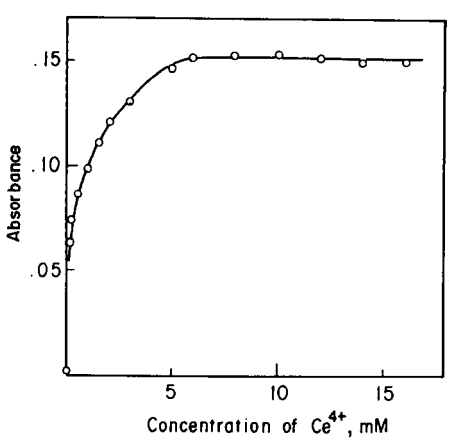

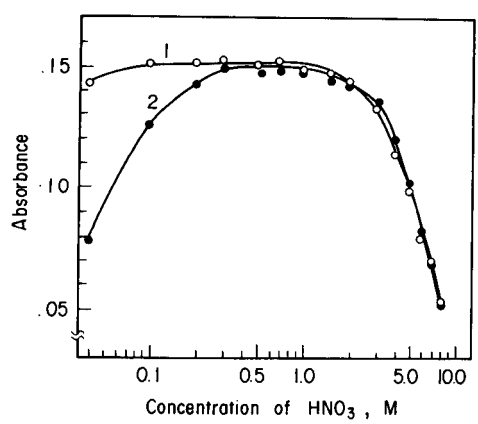

Fig. 1. Effect of cerium(IV) concentration on the absorbance of ruthenium (2 μg ml^{-1}) in 0.5 M nitric acid.

Fig. 2. Effect of nitric acid concentration on the absorbance of ruthenium (2 μg ml^{-1}): (1) immediately after addition of 1 × 10^{-2} M cerium(IV); (2) 24 h after addition of the cerium(IV).

ruthenium compound, possibly ruthenium dioxide [7, 8], was formed on the surface of the vessel, and ruthenium was lost from the solution.

Calibration

Atomic absorption measurements were made on 25 ml of 0.5 M nitric acid solutions which contained various amounts of ruthenium(III) and were 1×10^{-2} M in cerium(IV). As shown in Fig. 3, the calibration graph was linear over the range 0.05—5 μg Ru ml^{-1}. The relative standard deviations for ten measurements of 1.0 and 2.0 μg Ru ml^{-1} were 3.5 and 3.0%, respectively. Figure 3 also shows the calibration graph obtained without the addition of cerium(IV), as well as the calibration graph obtained by adding potassium cyanide to the ruthenium solution according to the procedure proposed by El-Defrawy et al. [4], which was previously considered to be the most sensitive flame a.a.s. method for ruthenium. Although the addition of cyanide also resulted in an increase of absorbance, and the calibration graph was linear up to at least 10 μg ml^{-1}, the absorbance strongly depended on the composition of the sample solution, especially on the concentration of sulfuric acid.

Effect of diverse ions

The effects of other ions on the absorbances of 0.5 M nitric acid solutions containing 2 μg Ru(III) ml^{-1} are listed in Table 1. Ions such as manganese(II), chromium(III), bromide, iodide, sulfite, nitrite, reducing

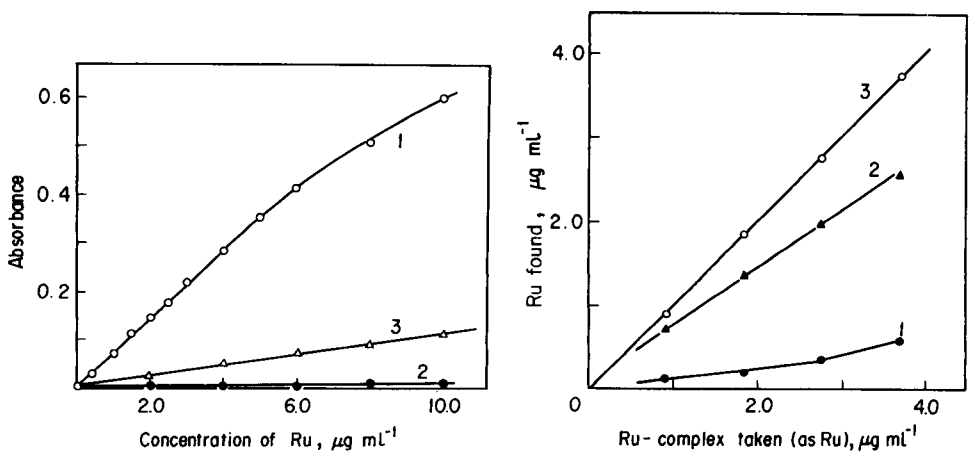

Fig. 3. Calibration graphs for ruthenium: (1) in 0.5 M nitric acid with 1×10^{-2} M cerium(IV); (2) as (1) but without cerium(IV); (3) in 2 M hydrochloric acid/8×10^{-2} M sulfuric acid/2×10^{-2} M potassium cyanide [4].

Fig. 4. Results for ruthenium present initially as tetranitronitrosylruthenate(III) (1 M nitric acid, 1×10^{-2} M cerium(IV)): (1) without pretreatment; (2) in boiling water bath for 1 h before addition of cerium(IV); (3) as (2) but in the initial presence of 0.5 ml of 30% hydrogen peroxide.

TABLE 1

Effect of diverse ions on the determination of 2 μg ml^{-1} ruthenium in 0.5 M nitric acid

Ion	Conc. (M)	Ru recovery (%)	Ion	Conc. (M)	Ru recovery (%)
Na^+	0.5	98.7	Cl^-	0.5	98.2
K^+	0.5	100	Br^-	0.5	18.9
NH_4^+	0.5	101	I^-	0.5	16.5
Cr^{3+}	0.002	99.7	SO_4^{2-}	0.05	96.9[a]
	0.08	59.0	NO_2^-	0.05	105[b]
Mn^{2+}	0.002	101	SO_3^{2-}	0.05	101[b]
	0.08	23.0	H_2O_2	0.05	103[b]
$Cr_2O_7^{2-}$	0.05	101	Formate	0.5	97.5
MnO_4^-	0.05	104	Acetate	0.5	98.4
Fe^{3+}	0.05	101	Oxalate	0.05	17.6
Co^{2+}	0.05	101	Citrate	0.05	13.8
Ni^{2+}	0.05	99.5	Tartrate	0.05	20.1
Cu^{2+}	0.05	101			

[a]Measured in supernatant liquid. [b]Measured after 1 h in boiling water bath.

organic cations, and hydrogen peroxide, which consume cerium(IV) by reduction, interfere, but their effect can be eliminated by the use of more cerium(IV). Sulfite, nitrite and hydrogen peroxide can also be decomposed readily by keeping the solution in a boiling water bath for 1 h before addition of cerium(IV). The a.a.s. results in the presence of nitrite show that ruthenium as a nitrosylruthenium complex, which may be formed in the solution containing nitrite, can also be oxidized by cerium(IV). However, tetranitronitrosylruthenate is an exception, as is described later.

Sulfate forms a precipitate with cerium(IV) which affects the reproducibility of the a.a.s. measurements. When the concentration of sulfate was $<5 \times 10^{-2}$ M, however, ruthenium could be determined by using the supernatant liquid as the sample solution for a.a.s. Filtration of the precipitate with a filter composed of organic material should be avoided, because ruthenium tetroxide may be reduced at the surface of the filter.

Noble metals, except iridium, did not interfere, nor did silver, as shown in Table 2. However, as little as 1.2 μg ml^{-1} iridium(IV) interfered. It is presumed that iridium(IV) is oxidized by cerium(IV), possibly to $Ir^{4.5+}$ [9], and this iridium species oxidizes chloride to chlorine or water to oxygen, thus, regenerating iridium(IV). This cyclic reaction between cerium(IV) and iridium(IV) would consume cerium(IV). For the determination of ruthenium in the presence of 2 and 4 μg ml^{-1} iridium(IV), it is necessary to add $>2 \times 10^{-2}$ and $>4 \times 10^{-2}$ M cerium(IV), respectively. It was also found that the recovery of ruthenium in the presence of iridium(IV) strongly depended on the time elapsed after the addition of cerium(IV), because the concentration of cerium(IV) decreased with time as a result of the cyclic

TABLE 2

Effect of noble metal and silver ions on the determination of 2 μg ml^{-1} ruthenium in 0.5 M nitric acid

Ion	Conc. (mg ml^{-1})	Ru recovery (%)	Ion	Conc. (mg ml^{-1})	Ru recovery (%)
Rh^{3+}	0.04	104	Ir^{4+}	0.8×10^{-3}	101
Pd^{2+}	0.04	96.7		1.2×10^{-3}	85
Ag^{+}	0.4	104		2.0×10^{-3}	104[a]
OsO_4	0.4 (as Os)	101		2.8×10^{-3}	52[a]
Pt^{4+}	0.04	102		4.0×10^{-3}	101[b]
Au^{3+}	0.4	101			

[a]In the presence of 2×10^{-2} M cerium(IV). [b]In the presence of 4×10^{-2} M cerium(IV).

reaction discussed above. Any a.a.s. measurement in the presence of iridium(IV) should be done within 30 min of adding the oxidant.

Decomposition of tetranitronitrosylruthenate(III)

As is well known, under certain conditions nitrosylruthenium, $Ru(NO)^{3+}$, forms tetranitronitrosylruthenate(III), which is considered to be the most stable inorganic ruthenium complex [10]. This complex was too stable to be oxidized quantitatively to ruthenium tetroxide in a dilute sodium hydroxide solution [11]. Figure 4 shows calibration graphs for tetranitronitrosylruthenate. When absorbances were measured immediately after adding 0.5 ml of 0.5 M cerium(IV), they were considerably lower than those given by other ruthenium solutions (Fig. 3). Even when the solution was kept in a boiling water bath for 1 h before the addition of cerium(IV), results were still low, although greater than without this treatment. A procedure to decompose the complex was therefore sought.

When the sample solution containing the complex was placed in a boiling water bath for 1 h in the presence of 0.5 ml of 30% hydrogen peroxide and was then mixed with cerium(IV), the ruthenium content found by a.a.s. was found to be accurate. This suggests that the complex was decomposed by hydrogen peroxide, thus allowing the ruthenium to be oxidized to ruthenium tetroxide by cerium(IV). Ruthenium was not lost from the solution during this decomposition procedure. This is consistent with the fact that hydrochloric acid containing hydrogen peroxide has been used as an absorbent for ruthenium tetroxide [12]. Because appreciable amounts of hydrogen peroxide affect the a.a.s. measurement, the amount of hydrogen peroxide in the solution after the decomposition of the complex should be minimized. The solution was kept in the boiling water bath, therefore, until the bubbles arising from decomposition of hydrogen peroxide were not observed on stirring the solution. The decomposition of hydrogen peroxide was accelerated by ruthenium ions and hydrogen peroxide could be decomposed within 1 h when the solution contained more than about

0.5 μg Ru ml^{-1}. If the ruthenium concentration was much smaller than this, the decomposition of hydrogen peroxide was time-consuming. In this case, a few milligrams of iron(III) nitrate should be added to the solution and the solution was kept in the boiling water bath for 30 min. Iron(III) is well known as an effective catalyst for decomposing hydrogen peroxide [13].

Conclusions

The pronounced increase of the atomic absorbance of ruthenium achieved in this method may not be caused entirely by the increased evaporation rate of ruthenium resulting from the high volatility of ruthenium tetroxide. It is likely that the atomization of ruthenium tetroxide in the flame is also more effective than that of ruthenium(III). The lower detection limit obtained by this procedure is similar to that obtained for nickel, cobalt or iron by a.a.s. The results for hydroxotetranitronitrosylruthenate(III) ions, believed to be the most stable inorganic complex of ruthenium, demonstrate that the a.a.s. method with pretreatment by hydrogen peroxide can be applied to the precise determination of total ruthenium in nitric acid solutions.

The authors are grateful to Mr. F. Morikawa, head of the Numadzu Factory, Nippon Engelhard, and his staff for preparing the ruthenium standard solution and also the iridium solution.

REFERENCES

1 J. M. Scarborough, Anal. Chem., 41 (1969) 250.
2 B. Montford and S. C. Cribbs, Anal. Chim. Acta, 53 (1971) 101.
3 W. B. Rowston and J. M. Ottaway, Anal. Lett., 3 (1970) 411.
4 M. M. M. El-Defrawy, J. Posta and M. T. Beck, Anal. Chim. Acta, 102 (1978) 185.
5 C. V. Banks and J. W. O'Laughlin, Anal. Chem., 29 (1957) 1412.
6 E. Akatsu, C. Yonezawa and K. Motojima, Ann. Nucl. Energy, 6 (1979) 399.
7 Y. Koda, J. Radioanal. Chem., 6 (1970) 345.
8 T. J. Walsh and E. A. Hausman, Treatise on Analytical Chemistry, Part II, Vol. 8, Interscience, New York, 1963, p. 379.
9 A. D. Maynes and W. A. E. McBryde, Analyst (London), 79 (1954) 230.
10 A. A. Siczek and M. J. Steindler, At. Energy Rev., 164 (1978) 575.
11 E. Akatsu, JAERI-M9159 (1980).
12 H. Zachariasen and F. E. Beamish, Talanta, 4 (1960) 44.
13 Gmelins Handbuch der Anorganishen Chemie, Sauerstoff, Lieferung 7, Wasserstoff-peroxid, 8. Aufl., Verlag Chemie, Weinheim, 1966, p. 2289.

Analytica Chimica Acta, 183 (1986) 225—230
Elsevier Science Publishers B.V., Amsterdam — Printed in The Netherlands

ATOMIC ABSORPTION SPECTROMETRIC DETERMINATION OF THE ISOTOPIC COMPOSITION OF LITHIUM BY AN ULTIMATE ABSORBANCE-RATIO TECHNIQUE

KOUHEI KUSHITA

Department of Radioisotopes, Japan Atomic Energy Research Institute, Tokai-mura, Naka-gun, Ibaraki-ken 319-11 (Japan)

(Received 16th July 1985)

SUMMARY

The conventional absorbance-ratio technique for determining the isotopic composition of lithium by atomic absorption spectrometry is improved by the use of "ultimate absorbance ratios" of sample solutions. These ratios are obtained by extrapolating the linear portion of lithium content/absorbance-ratio plots to the intercept at 0 mol m^{-3} lithium. These graphs are obtained measuring the absorbances of solutions of known ^6Li abundance and of various lithium contents with natural and ^6Li-enriched lithium hollow-cathode lamps. Linear calibration is attained over the range 0.0—99.3% ^6Li, and the lithium isotopic abundance can be determined with an absolute error of ±0.7% ^6Li for >0.01 mol m^{-3} lithium solutions. The method requires neither prior measurement of the total lithium content in sample solutions nor adjustment of the content to match that in the standard solutions.

Determination of lithium isotopic abundance is needed in studies of tritium production for nuclear fusion technology [1] because the abundance in a neutron-irradiated lithium target corresponds to the burnup rate of lithium-6, which is used to estimate an amount of tritium produced by the $^6Li(n, \alpha)T$ reaction. Atomic absorption spectrometry (a.a.s.) has some advantages for the isotopic analysis of lithium, compared with mass spectrometry and other methods [2—4]. It is easy to prepare samples, measurements are quick, there is no isotopic fractionation, and the apparatus is inexpensive.

Lithium isotopic analysis by a.a.s., proposed by Walsh [5], was first achieved by Zaidel' and Korennoi [6]. The absorbance measured with a ^7Li lamp was calibrated by lithium isotope standards. An absorbance-ratio technique, reported by Manning and Slavin [7], was applied by Goleb and Yokoyama [8], who used hollow cathodes for both the emission and the absorption source of free lithium atoms to obtain a linear calibration graph in the range 2.5—10% ^6Li. The absorbance-ratio technique was further developed by Wheat [9] and applied by Birch et al. [10]. These techniques, however, relied on the total lithium concentration and gave slight calibration curvature especially above 70% ^6Li. Chapman and co-workers [11, 12] constructed a dual-beam instrument and a ratio amplifier for direct measurement

0003-2670/86/$03.50

of the absorbance ratio. Stable and rapid determinations at natural abundance levels were obtained with this apparatus. However, the requirement of specially designed apparatus and the restriction on the lithium concentration that can be used are not desirable.

This paper reports an "ultimate absorbance-ratio technique" which improves the conventional absorbance-ratio method. The technique does not rely on the total lithium concentration in the sample solutions and gives linear calibration.

THEORY

The lithium 670.8-nm line is a doublet, the spacing of which is 0.015 nm for both ^{6}Li and ^{7}Li. The isotopic shift between ^{6}Li and ^{7}Li is 0.015 nm. Hence, the spectral line of a mixture of ^{6}Li and ^{7}Li appears as a triplet. The theoretical absorbances obtainable by using ^{6}Li and ^{7}Li hollow-cathode emission sources are given by Zaidel' and Korennoi [6] as

$$-A_6 = \log (I_6'/I_6) = \log \{[2 \exp (-\alpha) + 1]/3\} - 0.434\alpha C_6 \quad (1)$$

$$-A_7 = \log (I_7'/I_7) = \log \langle \{2 \exp [-\alpha(1 + 3C_6)] + 1\} \exp [-\alpha(1 + C_6)]/3 \rangle \quad (2)$$

respectively, where A is the absorbance, and I and I' are the intensities of the incident and transmitted light; $\alpha = k(n_6 + n_7)$ is the absorption coefficient, k the experimental coefficient; n_6 and n_7 are the concentrations of ^{6}Li and ^{7}Li in the sample solutions, and $C_6 = n_6/(n_6 + n_7)$ is the isotopic abundance of ^{6}Li in the solution.

The calculated absorbance ratio (A_6/A_7) as a function of C_6 for various values of α is represented in Fig. 1. The line shows curvature beyond $C_6 = 0.7$ for relatively large values of α. Figure 1 also shows that the calibration curve becomes essentially a straight line when $\alpha = k(n_1 + n_2)$ becomes small and the lithium concentration in the solution approaches zero.

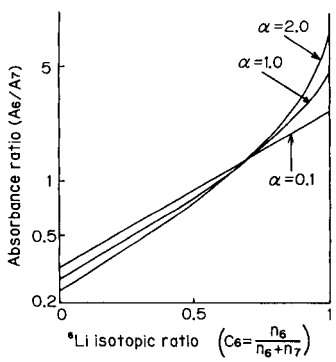

Fig. 1. Dependence of absorbance ratio on ^{6}Li isotopic ratio as calculated for various values of the absorption coefficient α.

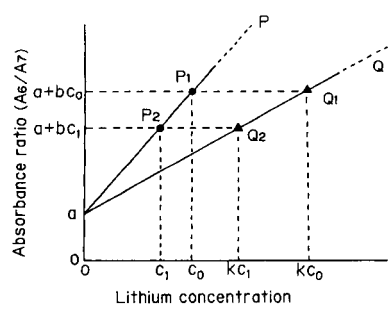

Fig. 2. Method of obtaining the ultimate absorbance ratio of a sample solution.

It is expected that if the absorbance ratios obtained by extrapolating lithium concentration/absorbance ratio curves to the axis are used, a virtually linear calibration graph will be obtained. Furthermore, if "ultimate absorbance ratios" obtained in the manner mentioned above are used for calibration, adjustment of the lithium concentration in sample solutions is not necessarily required to determine the isotopic ratio. The reason is as follows. The curve P in Fig. 2 can be obtained by measuring the atomic absorbance ratios R of sample solutions of various lithium concentrations. The relationship $R = a + bc$, where c is the total lithium concentration, is obtained from the plots of the linear region of the curve. The ultimate absorbance ratio for the sample becomes a. Even if the lithium concentration in the sample solution is not known, the assumed concentration $c(Q_1)$ at point Q_1 in the linear region which corresponds to P_1 $(c_0, a + bc_0)$ might be adopted as kc_0; $k = c(Q_1)/c_0$ is the constant. The concentration of Q_2 which corresponds to P_2 $(c_1, a + bc_1)$ can be expressed as $(c_1/c_0)kc_0 = kc_1$. The straight line drawn through the points Q_1 and Q_2 can be expressed as:

$$[R - (a + bc_0)]/(c - kc_0) = [(a + bc_0) - (a + bc_1)]/(kc_0 - kc_1)$$

Finally one can obtain the relation $R = a + (b/k)c$. Hence, the ultimate absorbance ratio, even for the assumptive curve Q, falls on a. As described above, the isotopic ratio of lithium in a sample solution can be determined by using the ultimate absorbance-ratio technique, regardless of the real lithium concentration in the samples.

EXPERIMENTAL

Atomic absorption spectra were measured with a Nippon Jarrell-Ash model AA-855 spectrometer. An air/acetylene flame was used at flow rates of 7 dm^3 min^{-1} for air and 2 dm^3 min^{-1} for acetylene. The emission sources used were a neon-filled natural lithium hollow-cathode lamp (Hamamatsu Photonics) and a neon-filled enriched ^6Li hollow-cathode lamp (Westinghouse). The lamps were operated at 10 mA. The spectral slit-width was set at 0.17 nm for the 670.8-nm lithium line to avoid interference from the neon 671.7-nm line.

Lithium carbonates (99.29% ^6Li and 99.99% ^7Li) used for the isotopic standards were obtained from the Oak Ridge National Laboratory. Mass spectrometric measurements of the isotopic composition of lithium were carried out at Analytical Chemistry Laboratory of the Japan Atomic Energy Research Institute. Stock solutions (100 mol m^{-3} lithium) of the isotopic standards were prepared by dissolving the ^6Li-enriched and ^7Li-enriched lithium carbonates in dilute hydrochloric acid, the final pH of the solution being adjusted to 1—3. Isotopic standards were prepared by diluting mixtures of these stock solutions quantitatively to 0.01—1.00 mol m^{-3} lithium. Sample solutions for isotopic analysis were prepared from an analytical-grade lithium carbonate and from ^6Li-enriched lithium metal by dissolving them in

the same manner as described for the standard solution. Because lithium easily takes up moisture from the air, the ^{6}Li-enriched lithium metal sample was only roughly weighed and an estimated lithium concentration (ca. 30 mol m^{-3}) in the mother solution of the sample was used. This solution was diluted quantitatively to obtain the ultimate absorbance ratio which would be used for the isotopic determination.

Calibration was achieved by plotting the ultimate absorbance ratio of each isotopic standard against the ^{6}Li abundance (0.0—99.3% ^{6}Li). These ratios were obtained by extrapolating the linear portion of the total lithium content/absorbance ratio curves for each standard to the axis at 0 mol m^{-3} lithium. The isotopic determination was made by comparing the ultimate absorbance ratios of the sample solutions with those of the isotopic standards.

RESULTS AND DISCUSSION

The absorbance ratio (A_6/A_7) should be affected by the total lithium concentration especially at the extreme isotopic composition range (^{6}Li > 70%), as described above. This was confirmed experimentally by measuring the absorbance ratios of solutions of various lithium concentrations and various isotopic ratios, as shown in Fig. 3. The relationship between the ratio and the concentration was linear for 0.01—1.00 mol m^{-3} lithium. The slopes of the lines were different for samples with different lithium isotopic composition.

Chapman et al. [12] reported that their method was independent of the lithium concentration. However, they studied the concentration effect only for solutions of 50% ^{6}Li. Figure 3 shows that solutions of 50—70% ^{6}Li were the least dependent on the lithium concentration. Hence, their method

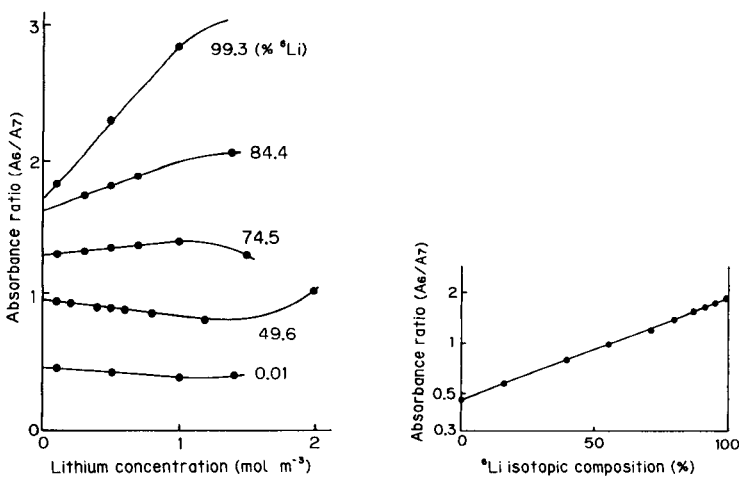

Fig. 3. Dependence of absorbance ratio on lithium concentration for various ^{6}Li contents.

Fig. 4. Typical calibration graph obtained from the ultimate absorbance-ratio technique.

should be concentration-dependent, especially at higher ^{6}Li abundances. A plot of log (absorbance ratio), which was obtained by extrapolating the linear portion of the curves in Fig. 3 to the axis at zero lithium concentration, against ^{6}Li isotopic composition was a straight line. Figure 4 shows a typical calibration graph obtained in the manner mentioned above over the range 0.0—99.3% ^{6}Li. The graph agrees well with the expression $\log (A_6/A_7) = a + bc_6$, where a and b are the constants; the correlation coefficient is 0.9998. The calculations of A_6/A_7 from Eqns. 1 and 2 do not suggest any abrupt change in the linearity of the calibration graph. This method, therefore, can be considered to give linear calibration up to 100% ^{6}Li. When this calibration graph was used, adjustment of the lithium concentration in the sample solution was not essential to determine the ^{6}Li abundances, for the reason described in the theoretical section.

Table 1 shows the isotopic abundances obtained for the natural and ^{6}Li-enriched lithium samples by applying this technique, together with the values obtained by mass spectrometry. The results show that the ultimate absorbance-ratio technique is reliable for determining the isotopic composition even for samples with extreme isotopic ratios.

The uncertainty in the absorbance measurements for the hollow-cathode lamps was ca. ±0.7%; the uncertainty in the isotopic ratio therefore was ±1.0%. From this value and a typical calibration graph, the absolute uncertainty of this method is estimated to be ±0.7% ^{6}Li.

Wheat [9] measured ^{6}Li abundances of 26—65% ^{6}Li solutions and estimated the uncertainty of the absorbance-ratio technique to be ±0.5% ^{6}Li, which is comparable with that of the ultimate absorbance technique. The conventional absorbance-ratio method, however, is concentration-dependent, as seen in Fig. 3, especially in the higher range of ^{6}Li abundance. Therefore, intimate matching of the lithium concentration in a sample solution with that in the standards is required when isotopic analyses are made for samples of higher ^{6}Li abundances. For this purpose, some procedure such as flame emission spectrometry should be applied before the atomic absorption measurements [2]. This procedure, in practice, will be time-consuming and also bring another uncertainty to the final ^{6}Li abundance data. As mentioned above, the ultimate absorbance-ratio technique requires no prior measurement of total lithium content. It can be said, therefore, that the technique

TABLE 1

Lithium-6 isotopic abundances found for natural and enriched lithium samples

^{6}Li isotopic abundance (%)	
This work	Mass spectrometry
7.1 ± 0.4	7.51 ± 0.03
95.5 ± 0.7	95.41 ± 0.01

described here is more efficient, and gives better precision especially for samples of higher ^{6}Li abundance.

The author is indebted to Mr. S. Tamura and Mrs. K. Tamura for obtaining the mass spectrometric data. He also thanks Mr. K. Hoizumi for his useful suggestions and encouragement through this work.

REFERENCES

1 T. Abe, K. Yamaguchi, H. Kudo, M. Tanase, E. Shikata, H. Umei, K. Tachikawa and K. Tanaka, Proc. Tritium Technology in Fission, Fusion and Isotopic Applications, Dayton, OH, CONF-800427 (1980) 367.
2 L. Brown, R. S. Rajan, R. B. Roberts, F. Tera and D. J. Whitford, Nucl. Instrum. Methods, 156 (1978) 541.
3 J. Asher and M. T. Swinhoe, Nucl. Instrum. Methods, 213 (1983) 503.
4 H. Fukushima, Bunko Kenkyu, 21 (1972) 416.
5 A. Walsh, Spectrochim. Acta, 7 (1955) 108.
6 A. N. Zaidel' and E. P. Korennoi, Opt. Spectrosc., 10 (1961) 299.
7 D. C. Manning and W. Slavin, At. Absorpt. Newsl., 1 (1962) 1.
8 J. A. Goleb and Y. Yokoyama, Anal. Chim. Acta, 30 (1964) 213.
9 J. A. Wheat, Appl. Spectrosc., 25 (1971) 328.
10 N. J. Birch, D. Robinson, R. A. Inie and R. P. Hullin, J. Pharmacol., 30 (1978) 683.
11 J. F. Chapman and L. S. Dale, Anal. Chim. Acta, 87 (1976) 91.
12 J. F. Chapman, L. S. Dale and H. J. Fraser, Anal. Chim. Acta, 116 (1980) 427.

Analytica Chimica Acta, 183 (1986) 231—238
Elsevier Science Publishers B.V., Amsterdam — Printed in The Netherlands

AN ACID DISSOLUTION PROCEDURE FOR THE DETERMINATION OF BORON IN COAL ASH AND SILICATES BY INDUCTIVELY-COUPLED PLASMA EMISSION SPECTROMETRY WITH CONVENTIONAL GLASS NEBULIZERS

JOHN C. MILLS

The Broken Hill Proprietary Company Ltd., Central Research Laboratories, P.O. Box 188, Wallsend 2287, New South Wales (Australia)

(Received 10th September 1985)

SUMMARY

Coal ash and silicate samples are completely resolved by dissolution in nitric and hydrofluoric acids. Boron is retained during a volume-reduction step while most of the silicon is volatilized. Excess of fluoride is complexed by addition of aluminium chloride solution. After dilution, the sample solution does not attack the borosilicate glassware of conventional nebulizers. Boron is determined at the 249.678-nm emission line by inductively-coupled plasma emission spectrometry, with correction for iron interference. The preparation is also useful for determination of some other trace elements, and results are presented for twelve elements in certified reference materials.

A high-voltage spark optical emission spectrometric procedure for the determination of boron and other elements in coal ash and geological materials was reported recently [1]. However, low results were obtained for ashes which had fused at very high temperature (e.g., 1500°C) because of particle size and mineralogical effects. It was necessary to use an alternative procedure such as inductively-coupled plasma emission spectrometry (i.c.p.e.s.) for which the sample had been taken completely into solution. Several i.c.p.e.s. methods for boron have been published [2—6]. Low boron recoveries were obtained with: (i) aqua regia attack on 750°C ashes in a teflon-lined bomb [2]; (ii) combustion of coal in a pressurized oxygen bomb [3]; (iii) alkaline oxidation of soils with sodium hydroxide and sodium hypobromite [4]; and (iv) digestion of soils in nitric acid, mannitol solution and hydrofluoric acid, the mannitol having been added to prevent loss of boron during volatilization of silica [4].

A sodium carbonate fusion procedure [5] with a detection limit of 5 $\mu g\,g^{-1}$ boron for rock and ash, was not successful in this laboratory. Boron yields were often low, probably because of the variable quantities of insoluble residues obtained on leaching the carbonate melt, and a technique for dealing with this problem was not found. The carbonate fusion procedure was also found to be ineffective for boron determination, because of incomplete iron

0003-2670/86/$03.50

removal and precipitation of sulphates, by Din [6] who prepared iron-free solutions from geological materials by successive fusions with potassium dihydrogenphosphate and potassium hydroxide followed by an aqueous leach and acidification. Accurate boron results were reported for reference materials; however, the two-fusion method is lengthy, with many manipulative steps.

The procedure described here achieves complete dissolution of silicate samples including ash in a single step, with complete retention of boron. Hydrofluoric acid is necessary in the acid mixture to ensure complete dissolution [7]. Nebulizer and torch assemblies for i.c.p.e.s. which are resistant to hydrofluoric acid are expensive. The conventional borosilicate glass nebulizer and spray chamber and quartz torch are attacked by such acid mixtures, but may be used after treatment of the solution, which classically is done either by fuming with perchloric acid to volatilize hydrogen fluoride and hexafluorosilicic acid, or by adding boric acid to complex excess of fluoride. Investigation of the fuming treatment showed that boron was volatilized along with the silicon. The complexation treatment with boric acid is clearly not appropriate when traces of boron in the sample are being determined. However, complexation of fluoride with a large excess of aluminium ions was suggested recently in another context [8] and this approach was adopted successfully. The dissolution procedure involves the volatilization of most of the silicon-fluoride species under conditions which permit retention of boron-fluoride species in solution. Consequently, a relatively small quantity of aluminium chloride is required to complex fluoride and the sample dilution factor is more favourable for trace analysis. The preparation is suitable for the determination of other trace elements, and results are given below for analysis of reference materials.

In order to assess the volatility behaviour of boron during ashing of coal [9], a variation of the procedure was developed to enable boron to be determined after combustion of whole coal samples in an oxygen bomb.

EXPERIMENTAL

Reagents and apparatus

Reagents of analytical-reagent and spectrographically-pure grades were used. Water was distilled and deionized. Merck extra-pure crystalline $AlCl_3 \cdot 6H_2O$ was used. The i.c.p.e.s. measurements were made with an ARL 35000-C sequential vacuum spectrometer. Alternative nebulizer systems were used: (i) a Meinhard concentric glass with conical spray chamber and pneumatic solution uptake; (ii) a GMK-Labtam modified Babington-type fed by a peristaltic pump. Detection limits were the same for the two nebulizers for boron, but the GMK nebulizer was preferred for other elements because generally superior detection limits were achieved. It was necessary to reserve a separate plasma torch for this work. Boron contamination at the top of the torch capillary could not be removed easily when the torch was used in

routine analysis of solutions containing dissolved borate fusions. Nebulizer and spray chamber glassware was easily cleaned by nitric acid rinsing before trace-boron determinations. Polyethylene bottles for solution storage were also reserved solely for trace-boron work, and care was taken to clean all other apparatus thoroughly to avoid contamination from borates.

Sample preparation for coal ash and silicates

Coal ash was prepared at 815°C in accordance with Australian Standard AS 1038 [10], cooled rapidly in a desiccator to minimize errors resulting from absorption of moisture and carbon dioxide, and weighed within 30 min of removal from the furnace. Mineral matter in coal prepared by low-temperature (ca. 150°C) radiofrequency (r.f.) oxygen plasma ashing was equilibrated with the laboratory atmosphere and a concurrent moisture determination was done as specified in AS 1038 to allow calculation of the results to a dry basis. Mineral and geological samples were crushed to 76 μm and dried at 105°C for 2 h before weighing. Certified reference materials (CRM) were pretreated according to certificate instructions.

The dissolution procedure is as follows. Weigh 0.200 g of ash or other sample into a 50-ml PTFE beaker and cover with a PTFE lid. Add 10 ml of nitric acid (d. 1.21) and 1.5 ml of hydrofluoric acid (d. 1.18). Place on a mat at 130°C (±10°) on a hotplate, with the lid slightly open. Evaporate to a volume of 1—1.5 ml. Visual estimation of the volume is adequate and is done by comparison with 1 ml of water in a similar beaker. This digestion and volume reduction step takes about 1.5 h. Remove from the hotplate, add 10 ml of nitric acid (d. 1.1), and add from a dispensing bottle [11] 5.00 g (±0.02 g) of 20% (w/w) $AlCl_3 \cdot 6H_2O$ solution (top loading balance). Warm on the hotplate for ca. 10 min if necessary to dissolve fluorides. Cool for 10 min, transfer to a tared 100-ml polyethylene bottle with cap, and dilute to a solution mass of 50 g with water. Unburnt carbon, if any, in the ash is not dissolved; separate by filtering or decanting if desired.

Sample preparation for whole coal

Coal samples (1 g) were combusted in the oxygen bomb used for determination of specific energy, the residue and absorbing solution being transferred to a PTFE beaker and processed as above for ash. Details of the procedure are as follows. Set up the bomb apparatus as in Australian Standard AS 1038, Part 5 [12]. Weigh 1.00 g (±0.01 g) of coal into the crucible and level the surface. Add 2.0 ml of water into the bomb vessel. Close, pressurize, check and fire the bomb in the usual way. Wait for 10 min before releasing the pressure and dismantling. Brush the ash from the crucible into a 50-ml PTFE beaker, ensuring quantitative transfer. Transfer the solution into the same beaker. Rinse and wash the internal bomb surfaces into the beaker using a fine jet of water. Reduce the volume to <10 ml by heating on a mat on the hotplate without boiling. Cool for ca. 30 min. Add 10 ml of nitric acid (d. 1.21) and 1.5 ml of hydrofluoric acid (d. 1.18) and proceed as for the ash method.

This bomb method is not recommended for general use because the transfer and volume reduction steps are slow and painstaking.

Calibration and line selection

Calibration solutions were prepared on a mass basis from mixtures of laboratory standard solutions, plus matching quantities of aluminium chloride and nitric acid (but without hydrofluoric acid, to avoid attack on the glassware). In addition to the analytes, interfering elements were included in the calibration solution series to allow concurrent correction for spectral interference (e.g., iron and titanium), although concentrations of interfering elements were not reported by this procedure.

The 249.678-nm boron line was used and corrected for spectral-overlap interference from iron; the correction was calculated as $-(0.1388 \times 10^{-3}\ [Fe] + 0.367 \times 10^{-7}\ [Fe]^2)$. The criteria for boron line selection in the presence of high iron concentration have been reported [13]. The 249.773-nm line suffers higher iron interference than the 249.678-nm line. In this work, the boron 208.959-nm line was rejected because of high background from aluminium, and the boron 182.640-nm line was rejected because of overlap with the sulphur 182.625-nm line and the tendency of the sequential spectrometer to find the incorrect peak at low boron concentration. However, at high iron concentration (>ca. 20% Fe), the relatively small iron interference on the 182.64-nm line [13] provided more accurate results. For other analyte elements, a sensitive i.c.p.e.s. line was chosen, as listed in Table 5. Corrections (factor in brackets) were required for titanium (3.16×10^{-5}) on beryllium and for iron on chromium (2.0×10^{-5}), nickel (9×10^{-5}), and vanadium (4.9×10^{-5}). Lines of suitably low sensitivity were chosen for interfering elements: Fe 273.955 nm, Ti 334.941 nm.

RESULTS AND DISCUSSION

Texts on decomposition methods [14, 15] describe how readily boron may be lost wholly or partly in procedures based on hydrofluoric acid attack. However, for retention of boron, the texts suggest only the mannitol addition method, which was recently reported as unsuccessful [4]. The method described here uses conditions which allow complete retention of boron without addition of mannitol or any other substance.

Dissolution and retention were examined with a synthetic ash composed of spectrographically pure oxides, and the ash of an in-house standard coal. Various combinations of acids (nitric, hydrochloric, perchloric, hydrofluoric and aqua regia) were tested without evaporating to dryness. The nitric/hydrofluoric acid mixture was the simplest combination giving complete dissolution and boron retention. Use of perchloric acid always resulted in some loss of boron. Dissolution was not quite complete for all samples within about 2 h unless a small volume reduction (up to 20% relative) was effected. Attack on the borosilicate nebulizer glassware was observed when replicate

sprays showed increasing silicon and boron intensities; in these cases, a following water sample produced decreasing silicon and boron intensities over several minutes until the baseline was reached. It was found that even large additions of aluminium chloride solution (20 g) failed to prevent attack on the glassware unless the proportion of silicon retained was reduced to <25%. The effect of the final volume to which the digestion was reduced on the retention of boron and silicon is shown in Table 1. None of these volumes led to attack on the glassware. Clearly, evaporation to dryness (which can be difficult to judge) could lead to boron loss, and was unnecessary for adequate silicon removal. The 1—1.5 ml range was reached in reasonable time (about 1.5 h) and the method remained effective both above and below this volume so that measurement of the volume was not necessary. The temperature of the surface of the mat on the hotplate was chosen to produce slow evaporation from the partly-covered PTFE vessels, and was measured with a contact thermometer. A minimum quantity of 2.5 g of aluminium chloride solution was necessary to prevent glassware attack by retained fluoride. The chosen quality, 5 g, allowed larger than recommended final volumes to be still useful, and caused no deterioration in detection limit for boron.

The detection limit for boron (Table 2) in solution was marginally inferior to that obtained by other workers. However, this translates to a superior detection limit in this work on the ash/rock basis, ca. 2 $\mu g\ g^{-1}$, because of the purity of the reagents; the alkali salts used as fluxes in the fusion methods [5, 6] contained boron impurities. This limit is adequate for accurate analysis of coal ash and most silicates; lower limits with i.c.p.e.s. could be obtained only after separation and concentration procedures, e.g., distillation and solvent extraction [16] or methyl ester formation [8].

TABLE 1

Effect of volume reduction of nitric/hydrofluoric acid preparations on retention of boron and silicon

Final volume (ml)	2.5—3	1—1.5	0.5	dryness
B retained (%)	100	100	98	84—96
Si retained (%)	10	0.2—0.8	0.1	<0.1

TABLE 2

Detection limits for boron by i.c.p.e.s.

Reference	B in solution ($mg\ l^{-1}$)	B in ash or rock ($\mu g\ g^{-1}$)
This work	0.007	1.8
[2]	0.005	—
[5]	0.005	5
[6]	0.005	5

Results of the study of boron volatility during ashing of Australian and U.S.A. coals are given in Table 3; a complete discussion has been given elsewhere [17]. This work confirmed that oxidative ashing at ca. 815°C, as used in the Australian and ISO standards, allows retention of boron and provides the pathway to a rapid and accurate method for the determination of boron in coal. Ashing at other temperatures may cause boron loss for some coals. The sample preparation method for whole coal using combustion in the oxygen bomb, described earlier, provided accurate boron results for the NBS coal SRMs.

TABLE 3

Volatility of boron during ashing of coal

Sample	Ashing temp. (°C)	Boron content ($\mu g\ g^{-1}$) on dry coal basis[a]			
		BHP-SC147 bituminous	BHP-SC143B bituminous	NBS 1632a bituminous	NBS 1635 sub-bitum.
Raw coal[b]		13	37	52	104
Ash	ca. 150[c]	—	40	51	26
	370	9	37	30	69
	815	12	36	53	110
	1500	12	38	49	8
				51—55[d]	105—135[d]

[a]BHP coals are from Australia, NBS coals are from U.S.A. [b]Method using bomb combustion. [c]Low-temperature r.f. oxygen plasma ashing. [d]Range of literature values, from Gladney et al. [18].

TABLE 4

Boron results ($\mu g\ g^{-1}$ dry basis) in certified reference materials

Sample	This work	Precision (1σ)	Literature values	Ref.
Coal[a]				
NBS 1632a	53	0.6[b]	53	18
NBS 1635	110		115	18
Ash				
NBS 1633a	40		39.7	18
BHP-SC143	127	2.2[c]	133	1
Silicates				
CCRMP-SY2	86		86	19
NBS 278	24	1.1[b]	25	cert.[d]
NBS 688	<2		1	18
NBS 91	294		302	18
USGS-GSP1	3		1	20

[a]Analysed as 815°C ash, results calculated to dry coal basis. [b]11 replicates, same solution. [c]9 replicate preparations. [d]Certificate of analysis.

TABLE 5

Other trace elements in ash and silicates by this method ($\mu g\ g^{-1}$)

	λ (nm)	NBS 1633a fly ash		CCRMP-SY2 syenite		NBS 688 basalt		SARM 18 coal[c]	
		Cert.[a]	I.c.p.e.s.	Lit.[b]	I.c.p.e.s.	Cert.[a]	I.c.p.e.s.	Cert.[a]	I.c.p.e.s.
Ba	455.403	(1500)	1400	460	460	(200)	180	78	84
Be	313.107	(12)	12.4	23	23.2	(0.2)[d]	0.1	4.1	4.1
Cr	267.716	196	188	12	13	332	338	16	17
Cu	324.754	118	113	7	7.8	(96)	87	5.9	6.2
Li	670.784	(192)[e]	190	86	85	(7)[d]	8	(11)	nd[f]
Mn	257.610	(190)	182	2500	2465	1290	1210	22	23
Ni	231.604	127	140	11	15	(150)	160	10.8	12
Pb	220.353	72	90	83	40	3.3	<30	(5)	7
Sr	407.771	830	838	270	280	169	170	44	47
V	290.882	(300)	280	46	47	(250)	242	23	23
Zn	213.856	220	230	250	256	(79)[d]	82	5.5	6.1

[a]Certificate of analysis; values in brackets are uncertified. [b]Literature values [19, 21]. [c]Analysed as 815°C ash, results calculated to dry coal basis. [d]Ref. 22. [e]Ref. 23. [f]Not determined.

The results for determination of boron in a range of certified reference materials (CRMs) are shown in Table 4. The accuracy of the method is confirmed by the good agreement between the concentrations found by i.c.p.e.s. and the values recommended in the literature; the mean ratio of found/recommended values is 0.98 with a standard deviation of 0.02, for concentrations >5 $\mu g\ g^{-1}$ boron. The precision of replicate determinations of the same solution was found to be equal to the detection limit. The relative standard deviation for replicate preparations of an ash was 2%.

Although the method was developed for boron, it was useful to investigate whether the same solution was suitable also for the determination of various other trace elements of interest in coal, ash and silicates. Some results of analyses of CRMs are presented in Table 5. Only lead was not determined satisfactorily; an elevated sloping background caused by the added aluminium chloride (Al 220.462-nm line) interferes with the sensitive Pb 220.353-nm line, resulting in an unfavourable detection limit of 30 $\mu g\ g^{-1}$ lead in ash. Ten other elements show useful results.

The author thanks S. Gill, who did the experimental work, and K. J. Doolan and B. A. Zarcinas for helpful discussions. Appreciation is expressed to the Broken Hill Proprietary Company Ltd. for permission to publish this work. This paper was presented in part at the 8th Australian Symposium on Analytical Chemistry, Melbourne, April, 1985.

REFERENCES

1 J. C. Mills, Anal. Chim. Acta, 154 (1983) 227.
2 R. A. Nadkarni, Anal. Chem., 52 (1980) 929.
3 R. A. Nadkarni, Int. Lab., 11 (1981) 26.
4 M. W. Pritchard and J. Lee, Anal. Chim. Acta, 157 (1984) 313.
5 J. W. Owens, E. S. Gladney and D. Knab, Anal. Chim. Acta, 135 (1982) 169.
6 V. K. Din, Anal. Chim. Acta, 159 (1984) 387.
7 J. C. Mills and C. B. Belcher, Prog. Anal. At. Spectrosc., 4 (1981) 49.
8 D. D. Siemer, Anal. Chem., 54 (1982) 1321.
9 K. J. Doolan, K. E. Turner, J. C. Mills, A. C. Knott and R. R. Ruch, Part 6, Final Rep. NERDDP Grant 80-0220, July, 1983.
10 Standards Association of Australia, AS 1038, Part 3: Proximate Analysis of Hard Coal, SAA, Sydney, 1979.
11 T. D. Rice, Anal. Chim. Acta, 97 (1978) 213.
12 Standards Association of Australia, AS 1038, Part 5: Gross Specific Energy of Coal and Coke, SAA, Sydney, 1979.
13 G. F. Wallace, At. Spectrosc., 2 (1981) 61.
14 Z. Sulcek, P. Povondra and J. Dolezal, Crit. Rev. Anal. Chem., 6 (1977) 255.
15 R. Bock, A Handbook of Decomposition Methods in Analytical Chemistry, International Textbook Co., Glasgow, 1979.
16 E. Grallath, P. Tschöpel, G. Kölblin, U. Stix and G. Tölg, Fresenius' Z. Anal. Chem., 302 (1980) 40.
17 K. J. Doolan, K. E. Turner, J. C. Mills, A. C. Knott and R. R. Ruch, Prepr. Pap. Natl. Meet., Div. Fuel Chem. Am. Chem. Soc., 29 (1984) 127.
18 E. S. Gladney, C. E. Burns, D. R. Perrin, I. Roelandts and T. E. Gills, NBS Spec. Publ., 260-88, U.S.A. National Bureau of Standards, March, 1984.
19 S. Abbey, Geol. Surv. Can., Paper 77-34; X-ray Spectrom., 7 (1978) 99.
20 E. S. Gladney, D. B. Curtis and D. R. Perrin, Geostand. Newsl., 8 (1984) 43.
21 S. Abbey, A. H. Gillieson and G. Perrault, Rep. MRP/MSL 75-132, CANMET, Ottawa, 1975.
22 J. G. Crock, F. E. Lichte and P. H. Briggs, Geostand. Newsl., 7 (1983) 335.
23 T. D. Rice, N.S.W. Dept Miner. Resour., Chem. Lab. Rep. 85/5, Sydney, March, 1985.

Analytica Chimica Acta, 183 (1986) 239—249
Elsevier Science Publishers B.V., Amsterdam — Printed in The Netherlands

SIMULTANEOUS DETERMINATION OF 14 LANTHANIDES AND YTTRIUM IN RARE EARTH ORES BY INDUCTIVELY-COUPLED PLASMA ATOMIC EMISSION SPECTROMETRY

KIYOSHI IWASAKI[a], KEIICHIRO FUWA and HIROKI HARAGUCHI*

Department of Chemistry, Faculty of Science, University of Tokyo, Bunkyo-ku, Tokyo 113 (Japan)

(Received 6th June 1985)

SUMMARY

A method is described for simultaneous determination of 14 lanthanides and yttrium in monazites and xenotimes by inductively-coupled plasma atomic emission spectrometry. The ore samples were decomposed by heating with nitric acid/perchloric acid or hydrofluoric/nitric/perchloric acids, or sulfuric acid, or by fusion with sodium carbonate. Among these methods, treatment of the samples with sulfuric acid, by evaporation to dryness followed by dissolution of the residue with hydrochloric acid is recommended; it provided complete decomposition for the five monazites and xenotimes examined. The accuracy and precision of the results were significantly influenced by spectral interferences of the rare earth elements themselves; correction methods and factors are given. The chondrite-normalized rare-earth patterns were examined to characterize the monazite and xenotime samples.

Accurate and convenient methods of determining rare earth elements (REE) are important for the development of geochemical knowledge and industrial applications [1, 2]. Several instrumental methods have been successfully applied. Neutron activation [3—6] and isotope-dilution mass spectrometry [7, 8] provide suitable sensitivity, but are inconvenient because of complicated and sometimes prolonged experimental procedures. Neutron activation requires chemical group separation of the elements of interest from interfering elements [3, 5]. Isotope-dilution mass spectrometry usually provides precise results, but it has an essential disadvantage in that four lanthanides (Pr, Tb, Ho and Tm) cannot be determined because they have no plural isotopes. In contrast, atomic absorption spectrometry [9—12] is easily applied for determining all REEs, but the sensitivities tend to be poor.

Inductively-coupled plasma atomic emission spectrometry (i.c.p./a.e.s.) has been applied to the determination of REEs in ores and minerals [13], rare earth concentrates [14, 15] and various geochemical materials [16—19]. There are several advantages, i.e., wide dynamic ranges, freedom from chemi-

[a]On leave from Industrial Research Institute of Kanagawa Prefecture, Showa-machi, Kanazawa-ku, Yokohama 236, Japan.

0003-2670/86/$03.50

cal and ionization interferences, and capability of simultaneous or sequential multielement determination. In addition, i.c.p./a.e.s. provides much higher sensitivities for REEs than atomic absorption spectrometry [20]. The method, however, often suffers from spectral and physical interferences because of complicated sample matrices. In such cases, the method has been used in combination with ion-exchange [16—19] or high-performance liquid chromatography [21, 22] for the separation of REEs from interfering matrices.

In the present work, i.c.p./a.e.s. is utilized for the simple and rapid determination of REEs (14 lanthanides and yttrium) in the rare earth ores, monazite and xenotime. Rare earth elements which are present at the major-to-trace levels in these ores are simultaneously determined by using the digested sample solution without any separation for REEs. Decomposition methods and the correction of spectral interferences are examined in detail in order to evaluate the accuracy and precision of the results.

EXPERIMENTAL

Chemicals

The standard stock solutions of REEs (5.00 mg ml^{-1}) were prepared by dissolving their pure oxides (99.9—99.99%) in hot concentrated hydrochloric acid. For cerium, the oxide was dissolved by heating with nitric acid and 2—3 ml of 30% hydrogen peroxide, the excess of hydrogen peroxide being decomposed by boiling the solution. All oxides of REEs were used after heating at about 900°C for 3 h. Five groups of working standard solutions, in which each REE was 10.0 μg ml^{-1} in 1.2 M HCl, were prepared by mixing and diluting the stock solutions. The combinations of elements in the groups were as follows; (1) Sm; (2) Gd, Tb; (3) La, Ce, Tm, Yb; (4) Pr, Eu, Dy, Y; (5) Nd, Ho, Er, Lu. These combinations were selected after studying the spectral interference data given in Table 3; consequently, the mutual spectral interferences were negligibly small.

Acids of analytical grade and distilled-deionized water were used for all preparations of the standard and sample solutions.

Instrumentation

The emission measurements were made with a Jarrell-Ash Plasma Atomcomp Model MK II. The operating conditions of the i.c.p. instrument were as shown in Table 1. The emission signals of all REEs were almost maximal at an observation height of 16 mm above load coil; the signal-to-background ratios increased at the higher observation position between 12 and 18 mm. The signal-to-background ratio also increased as the carrier argon pressure was increased in the range 17—20 psi, but the larger pressure caused significant decrease of the emission intensity.

The analytical wavelengths given in Table 2 were chosen for minimal spectral interferences, as discussed by Crock and Lichte [17].

TABLE 1

Operating conditions

I.c.p. source and sample introduction system	
Forward r.f. power	1.1 kW
Reflected r.f. power	<5 W
Coolant argon flow	19 l min^{-1}
Auxiliary argon flow	0.2 l min^{-1}
Carrier argon flow	0.52 l min^{-1} at 19 psi
Observation height	16 mm above load coil
Nebulizer	Cross-flow type
Solution uptake rate	1.6 ml min^{-1}
Spectrometer	
Type	Paschen-Runge
Focal length	75 cm
Grating	2400 grooves mm^{-1}
Slit widths	Entrance 25 μm, exit 50 μm
Integration time	10 s

Sample preparation for rare-earth ores

Several techniques have been applied for the decomposition of rare-earth ores and minerals with satisfactory results. The following treatments with single or mixed acids or alkali fusion were examined as described below.

Decomposition with concentrated sulfuric acid. Powdered sample (0.2 g) in a covered 100-ml beaker was heated with 5 ml of concentrated sulfuric acid on a hot plate at 250—300°C for 3 h. Excess of the acid was evaporated to dryness by removing the watch glass. After cooling, the residue was dissolved by heating with 25 ml of concentrated hydrochloric acid. The solution was diluted with water, passed through a filter paper to remove any residue and then diluted to 100 ml with water. For the emission measurements, the solution was further diluted to an appropriate volume (a 4-ml aliquot to 25 ml for monazite and a 2-ml aliquot to 25 ml for xenotime) with 1.2 M HCl. At this stage, 10 μg ml^{-1} cadmium was added as an internal standard.

Decomposition with nitric/perchloric acid or hydrofluoric/nitric/perchloric acid. The ore sample (0.2 g) was treated with 30 ml of nitric/perchloric acid mixture (4:1, v/v) in a covered 100-ml beaker at about 120°C for 6 h. The watch glass was removed and the mixture was evaporated to dryness at about 150°C. Another mixed acid, $HF/HNO_3/HClO_4$ (2:2:1, v/v), was also tested for the decomposition of monazite and xenotime in a similar manner by using a teflon beaker. The subsequent procedures were similar to those described for the sulfuric acid decomposition.

Fusion with sodium carbonate. The ore sample (0.2 g) was mixed well with 2 g of sodium carbonate in a platinum crucible, and fused by heating on a Meker burner. After cooling, the cake was transferred carefully with 30—40 ml of 3 M HCl to a beaker and then completely dissolved by heating with

20 ml of concentrated hydrochloric acid. The refractory residue was removed by filtration. To separate the REEs from the large amount of sodium salt in the sample solution, in order to reduce the salt effect on physical interferences, coprecipitation with hydrated iron(III) oxide was adopted. To a 1/10 aliquot of the above solution, 20 mg of Fe(III) (as a chloride solution) was added, and diluted ammonia liquor was added. The solution was boiled for a few minutes, and the precipitate was filtered, washed with water, and then dissolved again in 30 ml of 6 M HCl. The iron carrier was removed by liquid-liquid extraction using methyl isobutyl ketone. The aqueous phase containing the REEs was evaporated to near dryness twice with addition of nitric acid, and finally diluted with 1.2 M HCl to the appropriate concentrations of REEs.

RESULTS AND DISCUSSION

Analytical figures of merit for the determination of rare earth elements and correction of spectral interferences

The wavelengths, signal-to-background ratios for 1 μg ml^{-1}, and detection limits are summarized in Table 2. The detection limit is defined as the concentration corresponding to the emission intensity equivalent to twice the standard deviation of the background intensity. The values obtained were similar to those reported by Crock and Lichte [17] except for that of thulium.

TABLE 2

Analytical wavelengths, signal-to-background ratios (S/B) and detection limits for rare earth elements

Metal	Wavelength (nm)	S/B[a]	Detection limit (μg l^{-1})	
			Present work	Published[b]
La	398.852	4.3	2.1	4.3
Ce	418.660	0.77	12	31
Pr	422.293	0.98	16	64
Nd	430.358	1.0	8.6	22
Sm	442.434	0.49	92	30
Eu	381.967	22	0.9	0.9
Gd	303.284	1.1	17	18
Tb	367.635	1.1	9.2	58
Dy	340.780	1.4	15	25
Ho	345.600	4.6	2.4	3.6
Er	369.265	3.6	3.1	8.0
Tm	313.126	0.46	69	5.1
Yb	328.937	31	0.4	2.2
Lu	261.542	39	0.8	1.0
Y	377.433	16	0.7	—

[a]The S/B values were estimated by measuring the emission intensities of 1 μg ml^{-1} solutions for all REEs. [b]Cited from Crock and Lichte [17].

Spectral interferences were corrected on the basis of the equation, $C_i = A_i - \Sigma_j k_{ij} C_j$, where C_i is the concentration of the analyte i, A_i the apparent concentration of the analyte i, C_j the concentration of interfering element j, and k_{ij} the interference coefficient of the element j for the element i.

The k_{ij} values were determined for 14 REEs and Y by measuring the emission intensities at the specified 15 wavelengths by using the single element solutions. The k_{ij} values found are shown in Table 3; values are also given for thorium interference which cannot be neglected in analyses of monazite.

The accuracy and precision in the correction of spectral interferences were checked by analyzing two artificial solutions which were prepared by mixing single element solution of the REEs; one was similar to monazite composition and the other to xenotime composition. For the monazite-type solution, trace constituents such as Eu, Tm and Lu were added in much larger amounts than the abundance in real rare-earth ores. The correction was made by using all k_{ij} values larger than 0.5 given in Table 3. As shown in Table 4, the results obtained after correction were in good agreement with the prepared composition within an error of 0.6% for the major elements at 15 μg ml^{-1} or more, and 4% for most of the minor and trace elements. The large error found for thulium is probably due to insufficient correction of spectral interferences. It can be concluded that the accuracy and precision of the present corrections were satisfactory for practical analysis of rare-earth ores.

TABLE 3

Interelement spectral interferences of rare earth elements

Element	Interfering element and interference coefficient k_{ij} (ng ml^{-1} analyte/μg ml^{-1} interferent)
La	Ce 0.7, Pr 3.7, Nd 3.1, Sm 1.9, Eu 2.5, Yb 5.8, (Th 2.8).
Ce	La 0.9, Pr 11, Nd 14, Sm 6.8, Eu 1.8, Gd 2.4, Tb 11, Dy 187, Er 15, Y 0.7, (Th 1.6).
Pr	Ce 18, Nd 27, Sm 12, Gd 13, Tb 12, Dy 2.5, (Th 2.0).
Nd	Ce 1.0, Pr 94, Sm 2.9, Eu 2.0, Gd 6.0, Tb 3.1, Dy 3.8, Er 14.
Sm	La 1.9, Ce 10, Pr 29, Nd 5.7, Gd 3.8, Tb 4.9, Ho 2.7, Er 2.6.
Eu	Pr 0.7, Nd 3.7, Sm 0.5, Gd 0.5.
Gd	Ce 1.5, Pr 5.7, Nd 4.1, Sm 8.2, Eu 1.7, Tb 28, Dy 11, Ho 18, Er 8.4, Tm 33, Yb 12, Y 0.6, (Th 172).
Tb	La 0.8, Ce 5.9, Pr 11, Nd 8.1, Sm 11, Eu 1.4, Gd 1.9, Dy 102, Ho 3.9, Er 34, (Th 3.4).
Dy	Ce 1.6, Pr 3.9, Nd 3.9, Sm 19, Gd 49, Tb 16, Ho 24, Er 13, Tm 4.6, (Th 6.0).
Ho	Pr 2.7, Nd 2.0, Sm 3.4, Gd 5.4, Tb 7.4, Dy 11, Tm 8.1.
Er	Pr 3.3, Nd 3.7, Sm 10, Eu 2.6, Gd 1.2, Tb 4.9, Dy 2.2, Yb 60, Y 1.2.
Tm	Pr 2.7, Nd 13, Sm 17, Eu 3.9, Gd 114, Tb 50, Dy 14, Ho 18, Er 13, Yb 36, (Th 28).
Yb	Nd 0.5, Sm 0.6, Tb 0.5, Dy 0.9, Ho 1.3, Tm 1.5.
Lu	Yb 0.5.
Y	Pr 1.2, Nd 0.7, Sm 4.9, Gd 3.8, Ho 1.2.

TABLE 4

Accuracy and precision of the correction for spectral interference for artificial solutions of rare-earth ore compositions

Composition ($\mu g\ ml^{-1}$)		Found ($\mu g\ ml^{-1}$)[a]	
		Without correction	With correction
Monazite type solution			
La	30.0	30.2 ± 0.2	30.0 ± 0.2
Ce	80.0	80.2 ± 1.1	79.6 ± 1.1
Pr	8.00	10.3 ± 0.2	8.16 ± 0.12
Nd	30.0	30.8 ± 1.0	29.9 ± 1.0
Sm	6.00	7.16 ± 0.08	5.88 ± 0.07
Eu	0.50	0.64 ± 0.01	0.50 ± 0.01
Gd	5.00	5.15 ± 0.06	4.80 ± 0.05
Tb	0.50	1.48 ± 0.03	0.49 ± 0.02
Dy	1.00	1.69 ± 0.03	0.98 ± 0.03
Ho	0.50	0.69 ± 0.02	0.49 ± 0.02
Er	0.50	0.76 ± 0.02	0.48 ± 0.02
Tm	0.10	1.30 ± 0.04	0.07 ± 0.06
Yb	0.30	0.34 ± 0.00	0.30 ± 0.00
Lu	0.10	0.10 ± 0.02	0.10 ± 0.02
Y	5.00	5.11 ± 0.05	5.01 ± 0.05
Xenotime type solution			
La	2.00	2.21 ± 0.02	2.08 ± 0.02
Ce	5.00	8.16 ± 0.05	4.95 ± 0.03
Pr	1.00	1.45 ± 0.04	1.07 ± 0.04
Nd	5.00	5.29 ± 0.05	4.87 ± 0.04
Sm	2.00	2.31 ± 0.03	2.07 ± 0.02
Eu	0.10	0.14 ± 0.00	0.11 ± 0.00
Gd	5.00	5.68 ± 0.06	4.95 ± 0.06
Tb	2.00	4.28 ± 0.04	2.08 ± 0.03
Dy	15.0	15.5 ± 0.1	14.9 ± 0.1
Ho	2.00	2.33 ± 0.02	2.02 ± 0.01
Er	15.0	16.0 ± 0.1	14.9 ± 0.1
Tm	2.00	3.74 ± 0.09	1.99 ± 0.08
Yb	15.0	15.3 ± 0.1	15.2 ± 0.1
Lu	2.00	2.08 ± 0.06	2.08 ± 0.06
Y	90.0	89.8 ± 0.5	89.8 ± 0.5

[a]Mean of 5 determinations with standard deviation.

Evaluation of sample decomposition methods

The results obtained for REEs in three monazites and two xenotimes are given in Table 5, where the four kinds of the decomposition method examined here are compared. The insoluble residues were also analyzed qualitatively by x-ray fluorescence spectrometry to check if they contained REEs. The results gave detailed information about the effectiveness of decomposition for the rare-earth ores.

TABLE 5

Results obtained for rare earth elements in rare earth ores treated by various decomposition methods (wt. %)

Metal	Acid decomposition			Na_2CO_3 fusion	Acid decomposition			Na_2CO_3 fusion
	HNO_3/ $HClO_4$	HF/HNO_3/ $HClO_4$	H_2SO_4[a]		HNO_3/ $HClO_4$	HF/HNO_3/ $HClO_4$	H_2SO_4[a]	
Monazite I					*Monazite II (yellow monazite)*			
La	—[b]	8.19	8.13 ± 0.03	8.18	9.02	9.46	9.26 ± 0.07	9.44
Ce	—[b]	21.8	21.5 ± 0.1	21.9	23.2	23.0	23.1 ± 0.2	23.0
Pr	—[b]	2.54	2.49 ± 0.01	2.59	2.57	2.64	2.59 ± 0.03	2.52
Nd	—[b]	9.16	8.57 ± 0.02	8.94	9.14	9.85	9.20 ± 0.12	8.89
Sm	—[b]	1.79	1.77 ± 0.14	1.74	1.84	1.71	1.72 ± 0.09	1.65
Eu	—[b]	0.015	0.015 ± 0.003	0.015	0.071	0.068	0.070 ± 0.002	0.066
Gd	—[b]	1.04	1.12 ± 0.04	1.11	1.04	1.06	1.09 ± 0.04	1.01
Tb	—[b]	0.14	0.14 ± 0.01	0.14	0.15	0.12	0.12 ± 0.01	0.11
Dy	—[b]	0.45	0.54 ± 0.02	0.54	0.40	0.35	0.39 ± 0.02	0.34
Ho	—[b]	0.070	0.077 ± 0.01	0.081	0.043	0.049	0.047 ± 0.004	0.045
Er	—[b]	0.13	0.18 ± 0.01	0.17	0.074	0.080	0.088 ± 0.005	0.078
Tm	—[b]	—[c]	—[c]	—[c]	—[c]	—[c]	—[c]	—[c]
Yb	—[b]	0.055	0.11 ± 0.01	0.11	0.023	0.022	0.029 ± 0.001	0.027
Lu	—[b]	—[d]	—[d]	—[d]	—[d]	—[d]	—[d]	—[d]
Y	—[b]	1.43	1.86 ± 0.02	1.86	1.01	1.06	1.11 ± 0.02	1.08
Monazite III (black monazite)					*Xenotime I*			
La	6.58	6.53	6.49 ± 0.06	6.69	0.65	0.66	0.63 ± 0.02	0.66
Ce	19.6	19.8	19.0 ± 0.2	16.6	1.77	1.85	1.88 ± 0.05	1.86
Pr	2.24	2.33	2.29 ± 0.01	2.28	0.24	0.22	0.23 ± 0.01	0.22
Nd	8.16	8.48	8.43 ± 0.03	8.46	0.81	0.79	0.93 ± 0.01	0.91
Sm	1.74	1.71	1.57 ± 0.09	1.66	0.29	0.40	0.58 ± 0.02	0.54
Eu	0.24	0.24	0.25 ± 0.01	0.23	0.006	0.003	0.008 ± 0.002	0.009
Gd	0.77	0.78	0.73 ± 0.01	0.76	0.57	0.73	1.60 ± 0.01	1.52
Tb	0.10	0.056	0.064 ± 0.008	0.049	0.14	0.18	0.41 ± 0.01	0.47
Dy	0.21	0.18	0.20 ± 0.02	0.18	0.87	1.44	3.66 ± 0.05	3.68
Ho	0.018	0.016	0.019 ± 0.003	0.015	0.18	0.34	0.85 ± 0.05	0.86
Er	0.030	0.015	0.020 ± 0.007	0.015	0.69	1.13	2.97 ± 0.04	2.86
Tm	—[c]	—[c]	—[c]	—[c]	0.19	0.22	0.56 ± 0.02	0.52
Yb	0.004	0.003	0.005 ± 0.002	0.006	0.76	1.25	3.22 ± 0.01	3.25
Lu	—[d]	—[d]	—[d]	—[d]	0.16	0.22	0.47 ± 0.02	0.45
Y	0.36	0.36	0.37 ± 0.01	0.36	5.89	9.69	25.2 ± 0.2	25.2
Xenotime II								
La	0.38	0.43	0.42 ± 0.01	0.41				
Ce	0.93	1.15	1.15 ± 0.05	1.15				
Pr	0.14	0.14	0.18 ± 0.02	0.15				
Nd	0.48	0.60	0.74 ± 0.02	0.72				
Sm	0.17	0.34	0.50 ± 0.04	0.54				
Eu	0.003	0.006	0.012 ± 0.001	0.012				
Gd	0.49	0.75	1.89 ± 0.04	1.79				
Tb	0.09	0.18	0.49 ± 0.02	0.45				
Dy	0.51	1.26	3.87 ± 0.03	3.82				
Ho	0.11	0.32	0.85 ± 0.08	0.96				
Er	0.41	1.07	3.15 ± 0.05	3.19				
Tm	0.071	0.18	0.58 ± 0.02	0.55				
Yb	0.45	1.14	3.52 ± 0.04	3.52				
Lu	0.10	0.20	0.58 ± 0.02	0.52				
Y	3.60	8.79	28.2 ± 0.2	27.8				

[a]Determined 3 times separately. [b]Not analyzed because of shortage of sample. [c]Not evaluated because of large spectral interferences. [d]Not evaluated because of poor reproducibility.

For the decomposition with the mixed nitric and perchloric acids, the x-ray fluorescence spectra indicated that the amount of REEs remaining in the insoluble residues of the monazite samples were negligibly small, i.e., the monazites were almost completely decomposed. In contrast, decomposition of the xenotimes was difficult; about 60—80% of Y and heavy REEs remained in the insoluble residues, while La, Ce and Pr were dissolved almost completely.

The mixed hydrofluoric, nitric and perchloric acids provided similar results to the nitric/perchloric acid mixture. The addition of hydrofluoric acid did not improve the decomposition although it might help to digest minerals such as niobate-tantalate or silicate present in the samples. There was little possibility of the existence of REEs as difficultly soluble fluorides because the fluorides were easily decomposed on heating with perchloric acid. Monazites, which mainly consists of orthophosphates of the cerium group members with thorium silicate, could be decomposed with the mixed acid including perchloric acid as reported by Ooghe and Verbeek [9]. In contrast, xenotimes were hardly decomposed with the triple acid mixture even on prolonged heating treatment although they also contain the orthophosphates.

Concentrated sulfuric acid was very effective for the decomposition of both monazites and xenotimes. All 14 lanthanides and yttrium in the samples were dissolved quantitatively by heating with sulfuric acid to dryness and subsequently dissolving the residues with hydrochloric acid. The insoluble materials were also analyzed for their major constituents. The results are shown in Table 6. The REEs remaining in the insoluble materials were only trace levels of Ce and Nd for monazites and traces of Y, Dy, Er and Yb for xenotimes.

Fusion of the ore samples with sodium carbonate followed by dissolution with hydrochloric acid was also effective for the dissolution of REEs in these monazites and xenotimes. The alkali fusion method, however, is time-consuming when further chemical separation of REEs is required in the analyses.

It is concluded from the results described above that the heating of the sample to dryness with concentrated sulfuric acid and subsequent dissolution of the residue in hydrochloric acid is to be recommended for dissolution of monazites and xenotimes in REE determinations.

TABLE 6

Constituents in insoluble residues of rare-earth ores after decomposition with concentrated sulfuric acid

Rare earth ore	Residue (%)	Major constituents
Monazite I	4.4 ± 0.2	Zr, Nb, Ta, Sn, Si.
Monazite II	2.6 ± 0.1	Zr, Si.
Monazite III	21 ± 1	Zr, Si.
Xenotime I	7.6 ± 0.3	Zr, Nb, Ta, Fe, Ti, Si.
Xenotime II	4.7 ± 0.4	Zr, Nb, Ta, Si.

Evaluation of results for the REEs in monazite and xenotime

The results obtained by the recommended procedure were very reproducible, as can be seen in Table 5. It was difficult to determine simultaneously very small amounts of thulium and lutetium in the monazite samples together with the other REEs. In particular, the determination of thulium was nearly impossible because of serious spectral interferences from the other REEs.

Besides the mutual spectral interferences of REEs, interferences caused by other constituents in the ore samples must be taken into consideration. Qualitative analysis by x-ray fluorescence spectrometry indicated that the monazite and xenotime samples contained Th, U, Zr, Nb, Ta, Sn, Ti, Fe, Si and P as major or minor constituents. In the recommended decomposition with concentrated sulfuric acid, most of the Zr, Nb and Ta were left in the insoluble residues, and they were not found in the sample solutions except for about 0.3% of niobium in xenotime II. The partly dissolved iron (0.4—2.0%) and titanium (0—0.9%) did not interfere with the REE determination. Small amounts of uranium, which provided poor emission sensitivity, also caused negligible interferences. Only the interference of thorium was found in the analysis of the monazite samples. As can be seen in Table 3, 1 μg ml^{-1} thorium gave a signal equivalent to 0.172 μg ml^{-1} gadolinium. When this value was used along with the concentration of thorium in the sample solutions, it was estimated that thorium caused ca. 90, 70 and 9% positive errors for gadolinium in monazites I, II and III, respectively. For xenotimes, however, the errors caused by thorium were not significant because the contents of thorium in xenotimes are much lower than those in monazites.

Characterization of rare-earth ores based on distribution pattern of rare earth elements

An attempt was made to characterize the rare-earth ores by normalizing their rare earth abundances with those of chondrite, as has been proposed by Masuda [23] and Coryell et al. [24]. The normalized rare-earth patterns for the three monazite samples analyzed here are shown in Fig. 1 along with those for the monazite 71aG (England) and a Taiwan black monazite. The absolute rare earth contents for the latter two were reported by Ooghe et al. [9] and Hwang et al. [25], respectively. The rare earth abundance of Leedey chondrite used for the present normalization was taken from the values reported by Masuda et al. [8, 26]. For the monazite samples, the normalized abundances generally decreased with increasing atomic number, and the rare earth patterns obtained were composed of some rectilinear segments with europium anomaly. The rare earth pattern of monazite III (a black monazite of unknown origin, M III in Fig. 1) was nearly identical to that of the Taiwan black monazite (R I). The rare earth patterns of monazite II (M II) and 71aG (R II) were also similar to each other. In the rare earth pattern of monazite I (M I), the linear line was broken at the holmium position. Such simple and rectilinear relationships as those seen for monazites were not obtained for xenotimes.

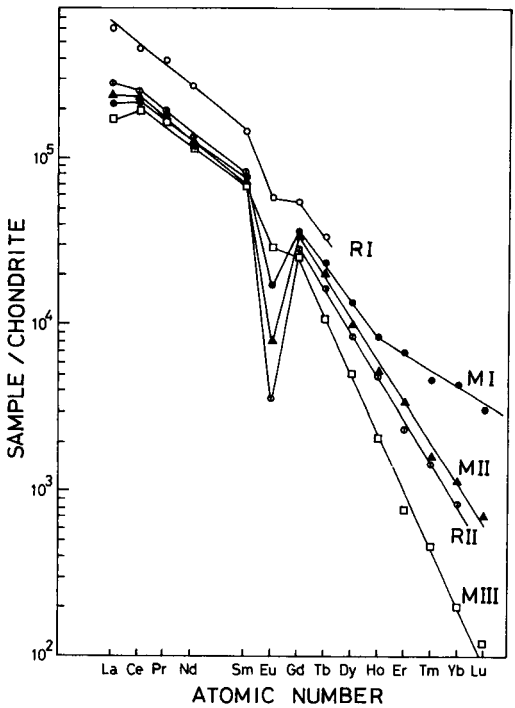

Fig. 1. Chondrite-normalized rare-earth patterns for monazites. M I, monazite I; M II, monazite II (yellow monazite); M III, monazite III (black monazite); R I, Taiwan black monazite [25]; R II, 71 aG from the Bureau of Analysed Samples, England [9]. Thulium and lutetium in monazites I, II and III were determined separately by using a higher-resolution spectrometer during the present work.

Conclusion

In spite of the difference of three orders of magnitude in concentration between the major and trace REE constituents of rare-earth ores, the REEs could be determined accurately, easily, and rapidly without any separation and preconcentration of the elements of interest. Only thulium and lutetium in monazites were subject to large errors because of their low contents as well as severe spectral interferences. When the analytical wavelengths selected here were used, thorium interfered with the determination of gadolinium. The results for 14 lanthanides can be used to illustrate simple and rectilinear rare earth patterns for monazites by normalization with the rare earth contents in chondrite.

This research was supported by a Grant-in-Aid of Scientific Research (No. 59470024) from the Ministry of Education, Culture and Science, Japan.

REFERENCES

1 N. E. Topp, The Chemistry of Rare Earth Elements, Elsevier, New York, 1965.
2 T. Kanoh and H. Yanagida (Eds.), Rare Earths: Properties and Applications, Gihodo, Tokyo, 1980.
3 K. Tomura, H. Higuchi, N. Miyaji, N. Onuma and H. Hamaguchi, Anal. Chim. Acta, 41 (1968) 217.
4 P. Henderson and C. T. Williams, J. Radioanal. Chem., 67 (1981) 445.
5 R. Zilliacus, M. Kaistila and R. J. Rosenberg, J. Radioanal. Chem., 71 (1982) 323.
6 P. Vukotic, J. Radioanal. Chem., 78 (1983) 105.
7 C. C. Schnetzler, H. H. Thomas and J. A. Philpotts, Anal. Chem., 39 (1967) 1888.
8 A. Masuda, N. Nakamura and T. Tanaka, Geochim. Cosmochim. Acta, 37 (1973) 239.
9 W. Ooghe and F. Verbeek, Anal. Chim. Acta, 73 (1974) 87.
10 J. G. Sen Gupta, Talanta, 23 (1976) 343.
11 J. G. Sen Gupta, Talanta, 28 (1981) 31.
12 P. Sicinska and M. Michalewska, Fresenius' Z. Anal. Chem., 312 (1982) 530.
13 T. Fries, P. J. Lamothe and J. J. Pesek, Anal. Chim. Acta, 159 (1984) 329.
14 T. Tanaka, T. Yamada, T. Johnokuchi, J. Yamada, K. Kumamoto and K. Hattori, Bunseki Kagaku, 31 (1982) 385.
15 H. Ishii and K. Satoh, Talanta, 30 (1983) 111.
16 J. N. Walsh, F. Buckly and J. Barker, Chem. Geol., 33 (1981) 141.
17 J. G. Crock and F. E. Lichte, Anal. Chem., 54 (1982) 1329.
18 A. Balton, J. Hwang and A. V. Voet, Spectrochim. Acta, Part B: 38 (1983) 165.
19 K. Toyoda and H. Haraguchi, Chem. Lett., (1985) 981.
20 V. A. Fassel and R. N. Knisely, Anal. Chem., 46 (1974) 1110A.
21 K. Yoshida, K. Fuwa and H. Haraguchi, Chem. Lett., (1983) 1879.
22 K. Yoshida and H. Haraguchi, Anal. Chem., 56 (1984) 2580.
23 A. Masuda, J. Earth Sci., Nagoya Univ., 10 (1962) 173.
24 C. D. Coryell, J. W. Chase and J. W. Winchester, J. Geophys. Res., 68 (1963) 559.
25 J. Hwang, J. Shih, Y. Yeh and S. Wu, Analyst (London), 106 (1981) 869.
26 A. Masuda, Geochem. J., 9 (1975) 183.

Analytica Chimica Acta, 183 (1986) 251—256
Elsevier Science Publishers B.V., Amsterdam — Printed in The Netherlands

Short Communication

TRACE DETERMINATION OF SOME AROMATIC MOLECULES BY LASER TWO-PHOTON IONIZATION

SUNAO YAMADA* and TEIICHIRO OGAWA

Department of Molecular Science and Technology, Kyushu University, Kasuga-shi, Fukuoka 816 (Japan)

PEIHUAN ZHANG

Changchun Institute of Applied Chemistry, Academia Sinica, Changchun 130021 (China)

(Received 1st July 1985)

Summary. A simplified yet sensitive system is described for the detection of the two-photon ionization signal in solution. The photo-ionization cell consists of a quartz cuvette and a pair of stainless steel electrodes. Several aromatic compounds, including quinones, can be detected in the ng l^{-1}—mg l^{-1} range both in hexane and in methanol; detection limits of pyrene in hexane and in methanol are 0.02 $\mu g\ l^{-1}$ and 4 $\mu g\ l^{-1}$, respectively. The detectability in hexane is much better than that in methanol. The detection limits and the molar absorptivities at the excitation wavelength are shown to be correlated.

Laser two-photon ionization provides a sensitive [1—3], instrumentally simple [4—6], and widely applicable technique for the determination of small amounts of molecules that absorb photons. Its application as a liquid chromatographic detector has been successful [7—9]. A detection limit of 6 ng l^{-1} has been reported for pyrene and 2-aminoanthracene in hexane with a windowless flow cell [3]; for highly sensitive detection in polar solvents, the background noise is excessive because of high leakage currents [2, 9]. There is still considerable room for improvement of the photoionization detection system in terms of breadth of application and practical convenience.

In the present report, the system is improved by introduction of a new photo-ionization cell consisting of a quartz cuvette and stainless steel electrodes, and by modifying the signal-processing circuits. Aromatic molecules and quinones are measured in hexane and methanol; the detection limits correlate with their molar absorptivities in both solvents.

Experimental

Instrumentation. The experimental arrangement was similar to those described previously [3, 4], thus only major features and new modifications are described here. The Molectron UV-12 nitrogen laser (pulse duration 10 ns, pulse energy 2.5 mJ) was operated at a repetition rate of 5—10 Hz; its pulse energy was varied with the use of a comb and was monitored by a Molectron P1-13H pyroelectric detector, which was calibrated with a Scientech 36-0001

0003-2670/86/$03.50

surface absorbing disc calorimeter. The transient current induced by the laser irradiation was converted to voltage by appropriate current-to-voltage (I/V) converters (10^8 I/V for hexane and 10^7 I/V for methanol). The output signal from the 10^8 I/V converter was averaged by a boxcar integrator; its gate width was optimized to synchronize with the signal. The output signal from the 10^7 I/V converter was amplified by an NF P-61 (input impedance 10^8 ohm, frequency response DC-100 kHz, gain 1—1000) or an NF P-62 (input impedance 10^6 ohm, frequency response DC-100 kHz, gain 1—1000) amplifier. Low-frequency noise, which was especially intense for methanol solution, was suppressed by use of an NF E-3201 multifunction decade filter; the cutoff frequency was set at 300 Hz [9]. The voltage output was then averaged by the boxcar integrator.

The photo-ionization cell with a quartz cuvette (4 × 1 × 1 cm) is outlined in Fig. 1A. Two stainless steel electrodes (5 mm × 6 mm) are supported in the cell. The laser beam is focused by a quartz lens (focal length 30 cm) at the central point between the electrodes. When the solution was unstirred, the signal fluctuated greatly, probably because of sample decomposition and/or physical heterogeneity (e.g., thermal lensing) of the solution. Bubbling the solution with nitrogen decreased the fluctuation notably, but signals were measured within 1 min to avoid any decomposition.

For hexane with very low leakage current, the signal was detected by the circuit shown in Fig. 1B; the high d.c. voltage was applied to one electrode while the other collected the signal. The optimum electrode spacing and voltage gradient were 1.5 mm and 1 kV, respectively. A solvent with high leakage current would saturate the converter output in this circuit, and so the leakage current must be shunted to ground while the desired pulsed signal

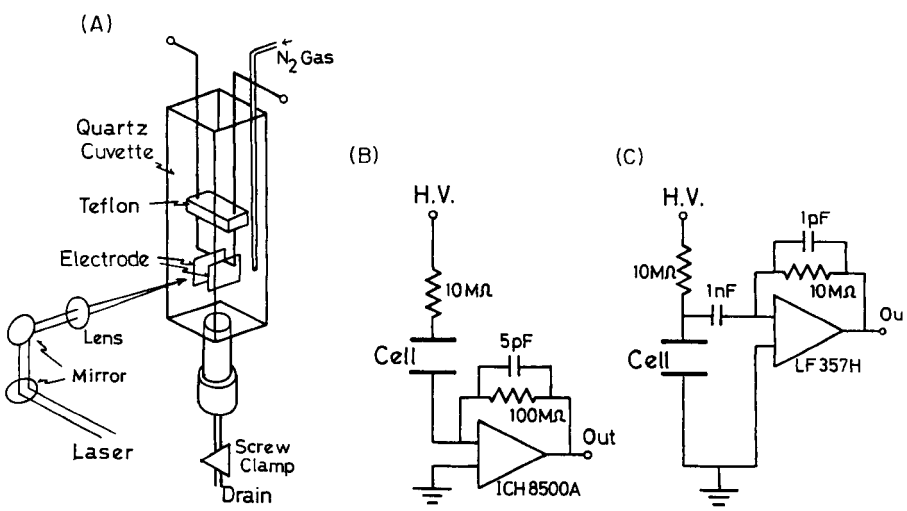

Fig. 1. (A) The photoionization cell. (B, C) Basic circuits for signal pickup with hexane (B) and methanol (C) as solvent.

is passed prior to its amplification [2]. The circuit shown in Fig. 1C was used for methanol with high leakage current; the high d.c. voltage applied was blocked with a capacitor (3 kV, 1 nF) prior to signal conversion, and the other electrode was electrically grounded. This method is instrumentally simple and showed satisfactory signal-to-noise (*S/N*) ratios. The optimum electrode spacing and voltage gradient were 3 mm and 0.5 kV, respectively.

Chemicals. Pyrene (Nakarai Chemicals) was purified [4]. Hexane and methanol (liquid chromatographic grade, Kishida Chemicals) and other chemicals (reagent grade) were used as received. Sample solutions were prepared just before use from freshly prepared stock solutions (10^{-2}—10^{-3} M) in hexane or methanol.

Procedures. The solutions were added to a depth of 3 cm in the cell and removed via the drain (Fig. 1A) after measurements. All measurements were made at room temperature. The observed photo-ionization signal (i_s) was obtained by integration over eight laser pulses, and eight runs measured under identical conditions were averaged. The blank signal (i_b) was measured for 16 runs under the same conditions. The signal from the sample (i_c) was obtained from $i_c = i_s - i_b$. The calibration graphs were logarithmic plots of i_c vs. the analyte concentration; the measured log-log slopes were near unity with correlation coefficients of 0.97 or better. The detection limit is defined as the concentration giving a signal (i_c) twice the standard deviation of i_b.

Results and discussion

Many aromatic molecules such as naphthalenes [3, 5] anthracenes [1, 3, 5, 7, 8, 10], pyrene [1, 3—9, 11, 12], and perylene [1, 6] photo-ionize when u.v. lasers (308—351 nm) are used. In the present study, the photo-ionization signal of pyrene in hexane or methanol showed quadratic behaviour for the low-energy region of the laser pulse ($\leqslant$200 μJ), indicating a two-photon process. However, the signals from 2-methyl- and 2-hydroxy-1,4-naphthoquinone in methanol showed one-photon behaviour; the relationships between the photo-ionization signals and the laser pulse energy were roughly linear. Reduction of the excited quinone with methanol or water impurity may produce a charged intermediate such as a quinone anionic radical [13, 14] which causes the signal.

In the windowless flow cell reported previously [3], it was necessary to use a flowing solution to avoid the signal degradation caused by deflection of the laser beam at the solution surface (solvent volatilization). The modified cell has an entrance window so that beam deflection is negligible. The photo-ionization signal in hexane is lower for this cell because the irradiation volume and applied voltage are smaller than those used previously [3]. However, the collection of the signal per unit area of the electrode is more efficient because of the smaller electrode area, so that the *S/N* ratios are similar for the two cells (cf. detection limits in Table 1).

Electron mobility in non-polar solvents such as hexane is much higher than that in polar solvents such as ethanol [15] whereas the apparent quantum

TABLE 1

Photo-ionization detection limits and molar absorptivities of aromatic molecules at 337.1 nm

No.	Compound	Solvent	Molar absorptivity (l mol^{-1} cm^{-1})	Detection limit (μg l^{-1})
1	Pyrene	Hexane	15 000	0.02 (0.006)[a] (0.02)[j]
		Methanol	16 000	4
2	Triphenylene	Hexane	160	0.3
3	Perylene	Hexane	1200	0.1 (0.1)[b]
4	Acenaphthene	Hexane	2	50
5	1-Aminonaphthalene	Hexane	3000	0.2
6	1-Bromonaphthalene	Hexane	0.6	7×10^5
7	4,4'''-bis(2-butyloctyl)oxy-*p*-quaterphenyl	Hexane	(2900)[a]	0.2 (0.3)[a]
8	Phenanthrene	Methanol	250	90
9	1,5-Diaminonaphthalene	Methanol	9900	4
10	2-Hydroxynaphthalene	Methanol	980	50
11	2-Hydroxy-1,4-naphthoquinone	Methanol	3000	300
12	2-Methyl-1,4-naphthoquinone	Methanol	2400	80
13	2-Chloro-9,10-anthraquinone	Methanol	4400	50
14	Benzophenone		150	2000

[a] Data from Ref. 3. [b] Data from Ref. 6.

efficiency of photo-ionization is much higher in polar solvents [12]. These factors tend to cancel each other out in considering signal intensities in non-polar and polar solvents. Because the observed photo-ionization signal is a convolution of the slow time response function of the *I/V* converter with the much faster photoionization signal, which will be discussed elsewhere, the observed signal does not reflect directly the change in the true photo-ionization signal for different solvents. These aspects are compatible with the result that the actual photo-ionization signals for pyrene did not vary very significantly between hexane and methanol.

In the measurements with hexane solutions, the *I/V* converter with slow time response (RC time constant of ca. 0.5 ms and 10^8 *I/V*) was normally used to process the signal (Fig. 1B). Methanolic solutions produced much noise at frequencies of less than several hundred hertz with this converter and so a converter with a faster time response (time constant of ca. 10 μs and 10^7 *I/V*) was used to remove the unwanted noise while the photo-ionization signal was put through a high-pass filter (Fig. 1C). The detection limit for pyrene in hexane was about an order of magnitude lower with the circuit shown in Fig. 1A (0.02 μg l^{-1}) than that with the circuit in Fig. 1C (0.5 μg l^{-1}), presumably because of the different methods for signal pickup and processing. The detection limit for pyrene in methanol (4 μg l^{-1}) was worse than that in hexane under identical conditions with the circuit of Fig. 1C, mainly because of the larger fluctuation of the blank signal.

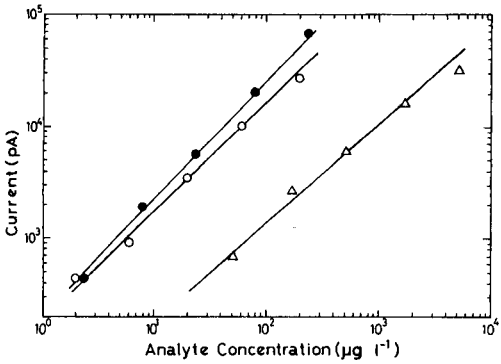

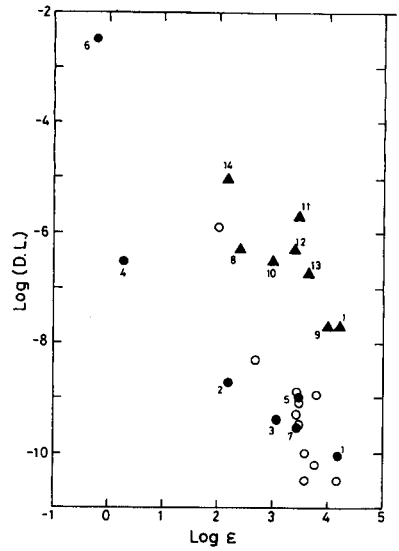

Fig. 2. Log-log calibration plots for methanolic solutions: (○) pyrene; (●) 1,5-diaminonaphthalene; (▲) 2-methyl-1,4-naphthoquinone.

Fig. 3. Correlation between detection limits and molar absorptivities at 337.1 nm: (●) in hexane, (▲) in methanol, (○) in hexane with the windowless flow cell [3]. The numbers correspond to the compounds listed in Table 1.

All compounds showed satisfactory linear log-log calibration plots; examples are given in Fig. 2. Detection limits (S/N = 2) are summarized in Table 1, together with the molar absorptivities of the samples at 337.1 nm. The lowest and the highest detection limits are 0.02 $\mu g\ l^{-1}$ for pyrene and 700 mg l^{-1} for 1-bromonaphthalene in hexane. The present system with hexane is as sensitive as earlier similar systems [3, 6] though it is less sensitive than fluorimetry for the polynuclear hydrocarbons.

Previously, it was shown that the photo-ionization detection limit in hexane tended to decrease as the molar absorptivity of the substance at the excitation wavelength (337.1 nm) increased [3]. The present results in hexane show some correlation between the detection limit and the molar absorptivity for a larger number of molecules than before (Fig. 3); a similar correlation was also obtained with methanol as solvent. Thus the use of a tunable dye laser would improve the sensitivity of photo-ionization detection; the wavelength of the laser could be tuned to the absorption maximum of the molecule.

The authors thank C. Sakane and N. Sato for their assistance in the measurements. The present work was partly supported by Asahi Glass Foundation for Industrial Technology.

REFERENCES

1 E. Voigtman, A. Jurgensen and J. D. Winefordner, Anal. Chem., 53 (1981) 1921.
2 E. Voigtman and J. D. Winefordner, Anal. Chem., 54 (1982) 1834.
3 S. Yamada, A. Hino, K. Kano and T. Ogawa, Anal. Chem., 55 (1983) 1914.
4 S. Yamada, K. Kano and T. Ogawa, Bunseki Kagaku, 31 (1982) E247.
5 E. Voigtman and J. D. Winefordner, Talanta, 30 (1983) 75.
6 K. Fujiwara, E. Voigtman and J. D. Winefordner, Spectrosc. Lett., 17 (1984) 9.
7 E. Voigtman and J. D. Winefordner, J. Liq. Chromatogr., 5 (1982) 2113; 6 (1983) 1275.
8 S. Yamada, A. Hino and T. Ogawa, Anal. Chim. Acta, 156 (1984) 273; Bunseki Kagaku, 33 (1984) E37.
9 A. Hino, S. Yamada, T. Nagamura and T. Ogawa, Bunseki Kagaku, 33 (1984) E393.
10 C. L. Braun and T. W. Scott, J. Phys. Chem., 87 (1983) 4776.
11 J. L. Metzger and H. Labhart, Chem. Phys., 11 (1975) 441.
12 P. L. Picuo and J. K. Thomas, J. Chem. Phys., 68 (1978) 3260.
13 J. M. Bruce, in S. Patai (Ed.), The Chemistry of Quinonoid Compounds, Part 1, Wiley, New York, 1974, p. 466.
14 N. J. Turro, Modern Molecular Photochemistry, Benjamin/Cumming, California, 1978, p. 362.
15 G. Beck and J. K. Thomas, Chem. Phys. Lett., 13 (1972) 295.

Analytica Chimica Acta, 183 (1986) 257—262
Elsevier Science Publishers B.V., Amsterdam — Printed in The Netherlands

Short Communication

APPLICATIONS OF LABORATORY ROBOTICS IN SPECTROPHOTOMETRIC SAMPLE PREPARATION AND EXPERIMENTAL OPTIMIZATION

C. H. LOCHMÜLLER* and K. R. LUNG

Department of Chemistry, Paul M. Gross Chemical Laboratory, Duke University, Durham, NC 27706 (U.S.A.)

(Received 7th October 1985)

Summary. Optimal experimental conditions for spectrophotometric solution-preparation procedures for determinations of iron(III) and phosphate were determined by a completely robotic application of the SIMPLEX algorithm, factorial design methods, and response surface fitting. The overall reliability of the approach, the precision observed and its significance are discussed.

Laboratory robotics is a relatively new area in analytical instrumentation. Although several reviews of the application of robotics in the laboratory have appeared [1—3], with one notable exception [4], these applications involve the robot in routine sample preparation procedures. A likely area for future development in laboratory automation will be the integration of artificial intelligence software and statistical optimization methods with robot technology. One can conceive of a computer-based "expert system" linked to less-intelligent laboratory robots, with the integrated system dedicated to the development of laboratory procedures. This paper describes additional attempts to involve a robot, interfaced to an exernal decision-making computer, in the total process of sample preparation, measurement, evaluation of results and optimization of experimental conditions.

Under current conditions, questions of robot reliability and adaptation remain unsettled. As the degree of complexity of the chemical task is increased, the best models for testing may be complex, but well understood, chemical reactions. By selecting such reactions, the robotic approach can be tested uncluttered by chemical complications. Here, two examples of a completely robotic approach to "research" are presented: (1) a 2^3 factorial design and (2) a 2-factor optimization of reaction parameters.

The spectrophotometric determination of iron as its 1,10-phenanthroline complex after reduction of iron(III) to iron(II) with hydroxylamine was chosen to evaluate a robotics-based factorial design scheme. This procedure is routinely used in the determination of iron [5] and is a good model system for testing the robot. The reduction of Fe(III) to Fe(II) is pH-dependent

0003-2670/86/$03.50

and zinc(II) is expected to interfere by competing for the chelating agent to form a colorless tris(1,10-phenanthroline)zinc(II) complex. A scheme was devised to examine the effects of zinc ions, acidity and temperature, using a factorial design program to control the sample-processing sequence of the robot. A permutation of three "flags" (1 or 0) is transmitted to the robot controller. Depending on the state of the first two flags, the robot will include/exclude the addition of Zn(II) or HCl. The third flag controls the inclusion of a 5-min heating period at 65 ± 2°C during the color development.

The second application involved the determination of phosphate. The use of simplex optimization [6] in robotics-based method development for spectrophotometric analysis was previously demonstrated [7]. To investigate the competence of the robot system further, a study of the more complex polymeric molybdenum-blue system was assigned to the robot. The molybdenum blue reaction is used for the routine determination of phosphate in different sample matrices. In this spectrophotometric method, phosphate reacts with molybdate ($Mo_7O_{24}^{6+}$) to form an ammonium molybdophosphate complex [8, 9]. Reduction of this complex at precisely-controlled acid and reducing-agent concentration produces the polymeric species commonly known as molybdenum blue. The final molar absorptivity and the spectral properties of molybdenum blue depend on the type of reducing agent used, concentration of the reagents, and on the temperature and duration of reaction. Such a reaction presents an interesting challenge for the robotic approach because the timing of mixing, heating and measurement can all be precisely controlled. Elimination of these timing variables would enhance precision and thus the mapping of the response surface with respect to the effect of acid and reducing agent concentration.

Experimental

Configuration of the robot. The Zymate robot is manufactured by Zymark Corporation (Hopkinton, MA 01748). In the configuration used, the system consisted of a servo-motor-driven robot arm, a general-purpose hand, a syringe hand, a "Master Laboratory Station", a "Power and Event Controller" and a vortex mixing station. All elements were centrally controlled by a microcomputer called the "Zymark Controller" programmed in a FORTH-like language, EASYLAB. EASYLAB is designed primarily to control the movement of the robot system and is less suitable for computation and data analysis. Decisions involving the directions for each subsequent experiment were made for the robot by BASIC programs located in an external Apple-IIc microcomputer. Communication between the Zymark computer and the Apple-IIc computer was channeled through the Zymark Z840 computer (RS-423) interface and the serial (RS-232) interface of the Apple-IIc computer. Details of the interfacing procedures are elsewhere [10—12].

Robotic sequence. (1) The robot receives the initial experimental condition from the Apple-II computer. (2) A spectrophotometric blank is prepared

and the transmittance of the blank solution is read. (3) The chromogenic reagent, analyte solution and any other solutions are delivered by the Master Laboratory Station into a 13 × 100-mm test tube. (4) The test tube is transported to the vortex station, mixed, (then heated if required) and inserted into the sample compartment of a Bausch and Lomb Spectronic-20 spectrophotometer by the robot gripper hand. (5) The transmittance of the solution is read by the analog-to-digital converter of the robotic station and transmitted to the Apple-II computer for evaluation. (6) The SIMPLEX program or the factorial-analysis program in the Apple-II computer evaluates the result and sends a new set of experimental conditions to the robot. The robot routinely processed up to 50 samples unattended.

Reagents. All solutions were prepared from reagent-grade chemicals and deionized water. All sample preparation, measurement, decision-making and data-reporting operations were executed by the robot system with no human intervention.

Results and discussion

Factorial design study of the iron(1,10-phenanthroline) procedure. The absorbance of the dark orange $[Fe(phen)_3]^{2+}$ was measured at 508 nm. The result of a typical duplicate factorial analysis is shown in Table 1 and Fig. 1. Interaction computation is shown in Table 2.

The addition of 0.026 M zinc ions, corresponding to a 1:1 Zn(II) to 1,10-phenanthroline mole ratio, reduces the absorbance by 0.22. Similarly, the addition of 0.033 M HCl reduces the absorbance by 0.198. Both Zn(II) and H^+ ions are expected to compete for 1,10-phenanthroline and lower the equilibrium concentration of $[Fe(1,10\text{-phen})_3]^{2+}$. Heating was found to cause a relatively insignificant increase of 0.095 in the absorbance, indicating that the chelation of Fe(II) is kinetically fast relative to the time scale of the

TABLE 1

Typical factorial-design results for the Fe(II) studies[a]

Zn	Heating	Acid	Absorbance, *A*
1	1	1	0.185
1	1	0	0.454
1	0	1	0.003
1	0	0	0.293
0	1	1	0.423
0	1	0	0.504
0	0	1	0.369
0	0	0	0.522

[a]Zn effect = $(0.185A + 0.454A + 0.003A + 0.293A)/4 - (0.423A + 0.504A + 0.369A + 0.522A)/4 = -0.220A$. Heating effect = $(0.185A + 0.454A + 0.423A + 0.504A)/4 - (0.003A + 0.293A + 0.369A + 0.522A)/4 = 0.95A$. Acid Effect = $(0.185A + 0.003A + 0.423A + 0.309A)/4 - (0.454A + 0.293A + 0.504A + 0.522A)/4 = -0.198A$.

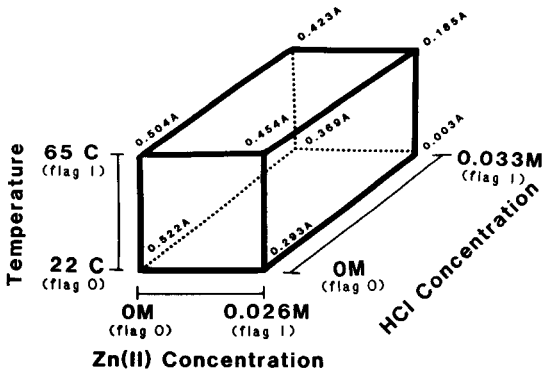

Fig. 1. Factorial design results for a typical Fe(II)/1,10-phenanthroline determination.

TABLE 2

Computation of interactions[a]

Zn	Heating	Acid	Zn * Heating	Zn * Acid	Heating * Acid	Zn * H * A	Absorbance
1(+)	1(+)	1(+)	+	+	+	+	0.185
1(+)	1(+)	0(—)	+	—	—	—	0.454
1(+)	0(—)	1(+)	—	+	—	—	0.003
1(+)	0(—)	0(—)	—	—	+	+	0.293
0(—)	1(+)	1(+)	—	—	+	—	0.423
0(—)	1(+)	0(—)	—	+	—	+	0.504
0(—)	0(—)	1(+)	+	—	—	+	0.369
0(—)	0(—)	0(—)	+	+	+	—	0.522

[a]Zn* Heating = $((+0.185A + 0.454A - 0.003A - 0.293A - 0.423A - 0.504A + 0.369A + 0.522A)/4 = 0.0768A$. Zn * Acid = $(+0.185A - 0.454A + 0.003A - 0.293A - 0.423A + 0.504A - 0.369A + 0.522A)/4 = -0.0813A$. Heating * Acid = $(0.185A - 0.454A - 0.003A + 0.293A + 0.423A - 0.504A - 0.369A + 0.522A)/4 = 0.0233A$. Zn * Heating * Acid = $(+0.185A - 0.454A - 0.003A + 0.293A - 0.423A + 0.504A + 0.369A - 0.522A)/4 = 0.0824A$.

robotic experiment. Previous study of this experiment showed an overall absorbance reproducibility of ±0.05 [12].

Examination of the interaction calculations showed that the three parameters, Zn(II), heating and acidity, do not interact with each other significantly. This is consistent with the known rapid kinetics of chelation and the fact that Zn(II) does not react with H^+.

Phosphate determination. Solutions containing 0.056 M hydrazine sulfate, 0.50 M sulfuric acid, 0.0059 M ammonium molybdate and 1 mg l^{-1} phosphate were used. The same grid search and SIMPLEX program as described earlier [7] were used. The response surface of the molybdenum blue method, based on 100 robot-performed measurements on the same phosphate sample, is presented in Fig. 2. The paths of the fixed and variable-size SIMPLEX, using

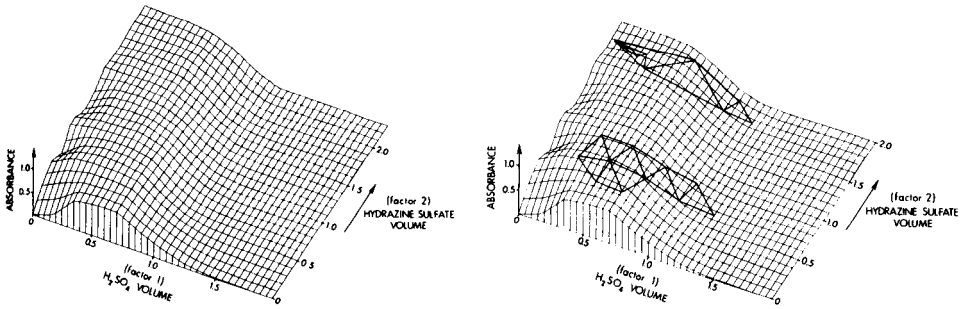

Fig. 2. The response surface of the phosphate spectrophotometric procedure plotted as a function of reducing agent and acid concentration.

Fig. 3. Progress of the fixed-size and variable-size SIMPLEX superimposed on the response surface generated from a systematic grid-search.

maximum absorbance as the optimum, are superimposed onto the response surface transect plot as shown in Fig. 3. As expected, both the fixed and variable-sized SIMPLEX algorithms located the "plateau region" of the absorbance response surface.

The simplex optimization of the phosphate procedure required 3—5 h. All of the actual experimental data were performed by the unattended robot during the evening hours. Such procedures, at best tedious for a human operator, can be very effectively done by a robot during its "spare time". The results indicate that even with the help of a relatively unsophisticated microcomputer, complex reaction sequences can be studied reliably by a robot. Coupled with a more powerful computer (and possibly a more dexterous robot arm), completely robotic execution of more complicated tasks in method development should be possible.

An obvious extension of this project is the adaptation of more sophisticated chemometric algorithms, expert system and artificial intelligence software to laboratory robotics. This combination may prove to be the method of choice in the future generations of automated laboratories [3].

REFERENCES

1 C. H. Lochmüller, M. R. Cushman and K. R. Lung, Nachr. Chem. Tech. Lab., 33 (1985) 482; J. Chromatogr. Sci., 23 (1985) 429.
2 C. H. Lochmüller, ACS Symp. Ser., 265 (1984) 11.
3 T. L. Isenhour, J. Chem. Inf. Comput. Sci., 25 (1985) 292.
4 A. R. Frisbee, M. H. Nantz, G. W. Kramer and P. L. Fuchs, J. Am. Chem. Soc., 106 (1984) 7143.
5 E. B. Sandell, Colorimetric Determination of Traces of Metals, 3rd edn., Interscience, New York, 1959.
6 S. N. Deming and S. L. Morgan, Anal. Chem., 45 (1973) 278A.
7 C. H. Lochmüller, K. R. Lung and K. R. Cousins, Anal. Lett., 18(A4) (1985) 467.
8 J. T. Woods and M. G. Mellon, Ind. Eng. Chem. Anal. Ed., 13 (1941) 760.

9 D. F. Boltz and M. G. Mellon, Ind. Eng. Chem. Anal. Ed., 19 (1947) 873.
10 C. H. Lochmüller, A. Colborn and K. Cousins, Zymate Laboratory Automation Newsletter, 1(1) (1984).
11 C. H. Lochmüller and K. R. Lung, Zymate Laboratory Automation Newsletter, 1(4) (1984).
12 C. H. Lochmüller and K. R. Lung, Zymate Laboratory Automation Newsletter, 2(3) (1985) 7.

Analytica Chimica Acta, 183 (1986) 263—267
Elsevier Science Publishers B.V., Amsterdam — Printed in The Netherlands

Short Communication

FLUORIMETRIC DETERMINATION OF CHROMIUM AT LOW LEVELS WITH 3-HYDROXYFLAVONE AND APPLICATION OF THE METHOD TO STEELS

A. CABRERA-MARTÍN*[a], J. S. DURAND[b] and S. RUBIO-BARROSO

Departamento de Química Analítica, C.S.I.C. and Facultad de Ciencias Químicas, Universidad Complutense de Madrid, 28040 Madrid (Spain)

(Received 27th July 1985)

Summary. The method is based on a 1:1 Cr(VI)/3-hydroxyflavone complex which is extracted into benzene at $H_0 = -0.6$. The complex has a pK^* value of 7.8 ± 0.1. Chromium is determined in the range 10—650 ng ml^{-1} with excitation at 358 nm and emission measurement at 530 nm. The relative standard deviation is 6.1% for 332 ng ml^{-1} chromium ($n = 10$). The method is applied to the determination of chromium in steels.

Flavonols containing hydroxyl groups at positions 3 and/or 5 are useful for analytical purposes. The relations between the structures of hydroxyflavones, their metal reactivity and the fluorescence of the products have often been studied. Present knowledge indicates that metals (including Zr, Th, Ga, Al, Sc, Ge, Nb and Ta) are chelated by adjacent hydroxyl and carbonyl groups and hydroxyflavones not having this configuration are unreactive. In neutral or alkaline solution, the reactive group can be peri-hydroxycarbonyl or vicinal hydroxyl [1]; in acidic solution, metals react with a hydroxyl group and an adjacent carbonyl group [2]. The *o*-hydroxyl group is believed to be responsible for fluorescence, i.e., bonding of metal to oxygen attached to the carbon in the 3- and 4-positions produces fluorescence [3]. The ratio of metal to hydroxyflavone in the chelate species is often 1:1 or 1:2, but can be higher, and, for a particular metal, can vary with acidity. Some of the species are charged and can be extracted into oxygenated solvents. Even if uncharged, some chelates of polyhydroxyflavones cannot be extracted into solvents such as chloroform [4]. However, the gallium and indium complexes of kaempferol can be extracted into chloroform from perchlorate medium [5].

3-Hydroxyflavone has been used in acidic media for the fluorimetric determination of Al, Hf(IV), Sn(IV), W(VI) [3], Be [6], Sb(III) [7] and

[a]Present address: Departamento de Química II, E.T.S. de Ingenieros Industriales, Universidad Politécnica de Madrid, José Gutierrez Abascal 2, 28006 Madrid, Spain.
[b]Present address: Departamento de Química Analítica, Facultad de Ciencias Químicas, Universidad del País Vasco, 20017 San Sebastian, Guipuzcoa, Spain.

0003-2670/86/$03.50

boron [8]. It is shown here that chromium(VI) reacts with 3-hydroxyflavone in a 24% (v/v) ethanol/water medium giving a 1:2 non-fluorescent complex with a global dissociation constant (pK) of 10.6 ± 0.2. The related pK_a values in that medium are pK_{a2} = −2.4 ± 0.1 and pK_{a1} = 9.0 ± 0.1. The spectrofluorimetric behaviour of 3-hydroxyflavone in the ethanolic medium is studied as well as the reaction in benzene medium at H_o = −0.6. A fluorimetric method based on quenching of the reagent fluorescence is proposed to determine chromium in steels.

Experimental

Reagents. 3-Hydroxyflavone, 5 × 10^{-4} M, was prepared by dissolving 11.9 mg of the solid (Eastman-Kodak) in 100 ml of absolute ethanol. Standard solutions of Cr(VI), 5 × 10^{-4} M, were prepared by dissolving 18.38 mg of potassium dichromate (Merck p.a.) in 250 ml of distilled water. Solutions of cations and anions were prepared from appropriate soluble salts (Merck p.a.), generally nitrates or sodium salts, with initial concentration of 0.1 M.

Apparatus. Fluorescence intensities were measured with a Perkin-Elmer model MPF-44A spectrofluorimeter, with 1-cm quartz cells and a 150-W xenon-arc source. Standard fluorescent samples no. 1 and no. 2 (Perkin-Elmer) were used to standardize the source intensity daily. The pH values were measured with a Metrohm E-516 meter provided with a combined glass/calomel electrode (EA-120).

Procedure. In an extraction tube, 8 μl of 5 × 10^{-4} M 3-hydroxyflavone and the appropriate volume of 5 × 10^{-4} M chromium(VI) were mixed with enough perchloric acid to reach H_o = −0.6 in the final volume of 4 ml. For calibration, 0.8 ml of 60% perchloric acid was added. Then, the chromium complex was extracted into 4 ml of benzene, after shaking during 1 min. The fluorescence intensity at λ_{ex} = 358 nm and λ_{em} = 530 nm, with both slits at 4 nm and the sensitivity at S × 10, was measured against a blank. The measurements are stable during 72 h if no irradiation occurs.

Results and discussion

Acid-base characteristics of 3-hydroxyflavone in the excited state. In a preliminary study, the fluorescence intensity of the reagent (in 24% ethanol/water) was found to increase swiftly as the concentration was increased from 10^{-6} to 10^{-4} M. At concentrations exceeding 5 × 10^{-4} M, the reagent precipitated, therefore the concentration chosen for the recommended procedure was 10^{-5} M.

Absorption and emission spectra were recorded at several pH values. In acidic media, the wavelength excitation maximum occurs at 354 nm (HL species) but in alkaline media, this is shifted to 410 nm because of dissociation of the hydroxyl group to give the unprotonated ligand. The emission maximum occurs at 525 nm in acidic media with excitation at 354 nm, and at 516 nm in alkaline media with excitation at 410 nm. In strongly acidic media, maximum emission occurs at 435 nm with excitation at 383 nm because the H_2L^+ species is formed.

Quenching of the fluorescence intensity with time was observed in all media, the decrease being 11.6% after 60 min of irradiation. The temperature has a great influence; above 25°C the intensity decreases, below 15°C it increases. The intensity remains constant in the range 15—25°C. Ionic strength did not affect the fluorescence intensity up to 0.5 M in sodium perchlorate or nitrate.

Determination of the apparent pK_a *of 3-hydroxyflavone.* The related acidity constants were calculated from plots of the variation of fluorescence intensity vs. the concentration of proton in the medium [9]. The fluorescence intensities were measured at λ_{ex} = 354, 410 and 383 nm (characteristic of HL, L^- and H_2L^+ species, respectively) and λ_{em} = 520 nm for pH 1—13 and 435 nm for the Hammett acidity zone (Fig. 1).

For the equilibria $H_2L^+ \rightleftharpoons HL + H^+$ (K^*_{a2}) and $HL \rightleftharpoons L^- + H^+$ (K^*_{a1}), the values obtained were $pK^*_{a2} = -3.45 \pm 0.05$ and $pK^*_{a1} = 8.85 \pm 0.05$ at 20°C and ionic strength 0.1 M. These pK^*_a values in the excited state are different from those found for the ground state, which were $pK_{a2} = -2.40 \pm 0.10$ and $pK_{a1} = 9.00 \pm 0.10$ because the acid-base properties of HL are different in the excited and ground states, particularly in strongly acidic media.

Spectrofluorimetric study of the chromium(IV) system in benzene medium. In a 24% (v/v) ethanol/water medium, chromium(VI) did not affect the fluorescence of the neutral species of 3-hydroxyflavone. Less polar media were therefore tested and benzene proved to be the most suitable. The efficiency of extraction of 3-hydroxyflavone and its Cr(VI) complex was studied by determining the ligand and Cr(VI) concentrations remaining in the aqueous layer. The extraction efficiency was found to be almost 100% at

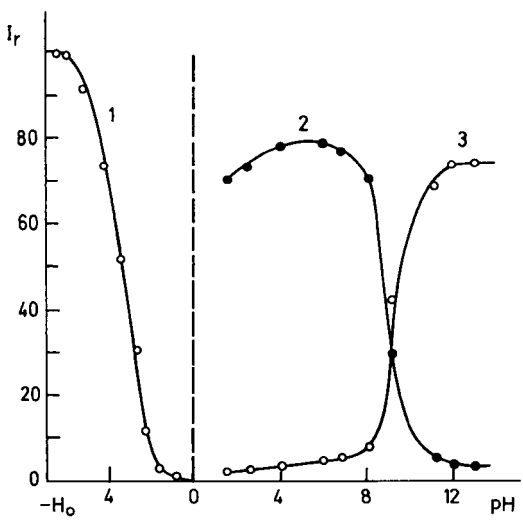

Fig. 1. Variation of the fluorescence intensity of 3-hydroxyflavone (HL) as a function of $[H^+]$. [HL] = 1.0×10^{-5} M. Medium: 24% ethanol/water (v/v). Curves: (1) λ_{ex} = 383 nm, λ_{em} = 435 nm; (2) λ_{ex} = 354 nm, λ_{em} = 520 nm; (3) λ_{ex} = 410 nm, λ_{em} = 520 nm.

pH <9 for the ligand; at pH >9 the extraction decreased because of ionization of the ligand. The extraction efficiency for the chromium(VI) complex was found to be near 100% when $H_o = -0.6$. A shaking time of 1 min sufficed to reach equilibrium between the aqueous and organic layers.

The fluorescence emission of the complex in the benzene layer was measured at 530 nm with excitation at 358 nm (4-nm slit-widths) after extraction from solution at $H_o = -0.6$ (in perchloric acid). The fluorescence intensities after 60 min of irradiation were stable for <5 min. The fluorescence quenching observed was 5% after 5 and 12% after 30 min. The recorded spectra of the complex at different acidities were similar to those for the ligand itself in the same media; they differed only in the intensities measured, the fluorescence being quenched when the complex was formed. The most suitable acidity was $H_o = -0.6$ in perchloric acid. At lower acidities, the complex seemed not to be formed.

Stoichiometry and stability constant. The stoichiometry of the Cr(VI) complex was established by the mole ratio and continuous variations methods, under the experimental conditions giving maximum emission. The composition of the complex was 1:1. The apparent dissociation constant in the excited state was calculated as $pK^* = 7.8 \pm 0.1$, at 20°C and $\mu = 0.1$. In other work, it was found that the complex in the ground state had a stoichiometry (1:2 Cr(VI)/L) and infrared spectroscopy indicated that the uncharged ligand present in the ground state becomes a zwitterion in the excited state. This is in agreement with reported data on 4-methyl-7-hydroxycoumarin [10]. It seems likely that the zwitterionic species reacts with $HCrO_4^-$ to form a seven-membered ring complex.

Calibration graph. A linear relationship between the fluorescence intensity and the Cr(VI) concentration was found for the range 10—650 nm ml^{-1}; the correlation coefficient was 0.991. The detection limit for a signal/noise ratio of 3 [11] was 10 ng ml^{-1} Cr(VI).

To examine the statistics of the method, a 325 ng ml^{-1} Cr(VI) solution was taken through the procedure 10 times; the mean result was 332 ± 45.6 ng ml^{-1} at the 95% probability level, the relative error being 4.4%, and the relative standard deviation 6.1%.

Interferences. The interferences of foreign substances were studied by mixing 335 ng l^{-1} Cr(VI), the foreign substance and enough perchloric acid or sodium hydroxide to give $H_o = -0.6$ before the benzene extraction. Ions which did not interfere at 100-fold molar concentrations compared to Cr(VI) were BO_2^-, SO_4^{2-}, SO_3^{2-}, SCN^-, PO_4^{3-}, F^-, ClO_4^-, ClO_3^-, Cl^-, NO_3^-, tartrate, Li, Na, K, NH_4^+, Al, As(V), Pb(II), Cd, Zn, W(VI), Th(IV), Os(VIII), Se(VI) or Te(VI). There was no interference at 10-fold molar levels from Cu(II), Be, Sr, Ni(II), Co(II), Ga, Mn(II), Ce(III), U(VI), Tl(I) or oxalate. Equimolar concentrations of Zr, Mo(VI), La, Bi, Fe(III) and Pd(II) were tolerated. Excess of fluoride masked the interference of 100-fold molar amounts of Fe(III), Sn(IV), Zr, U(VI) and Ga. Iron(III) could also be masked by 15% phosphoric acid. Interference was defined as any variation in the fluorescence

TABLE 1

Determination of chromium in steels

Sample	Chromium content (%)		Error
	Certified	Found[a]	
1[b]	2.72	2.60 ± 0.3	−0.12
2[c]	0.70	0.62 ± 0.2	−0.08
3[d]	1.18	1.15 ± 0.1	−0.03

[a]Average of five determinations with standard deviation. [b]Chromium-nickel steel (Hoepfner Gebr., Hamburg) containing 0.29% Mo and 0.66% Ni. [c]Steel F-154 (CENIM, Madrid) containing 0.11% C, 0.415% Mn, 0.108% Si, 0.0141% P, 0.0129% S and 2.889% Ni. [d]Steel F-122 (CENIM, Madrid) containing 0.33% C, 0.57% Mn, 0.26% Si, 0.015% P, 0.012% S and 4.18% Ni.

intensity measured exceeding 2.5 times the standard deviation obtained for the measurement of Cr(VI) alone.

Application to the determination of chromium in steels. The proposed method was applied to the determination of chromium in various steels (Table 1). The samples (0.5—1.0 g) were dissolved in 50 ml of acid mixture (3:1 HCL/HNO_3 for sample 1 and 4:3:1 HNO_3/$HClO_4$/HCl for samples 2 and 3). The solutions obtained were diluted to exactly 250 ml and aliquots were treated with 0.1 N permanganate in 50% phosphoric acid in order to oxidize chromium to Cr(VI) and to mask iron. The excess of permanganate was then reduced by addition of 1% sodium azide. These solutions were suitable for application of the method proposed above. The results for chromium are shown in Table 1.

REFERENCES

1 M. Katyal, Talanta, 15 (1968) 95.
2 T. Kanno, Japan Analyst (London), 10 (1961) 8.
3 M. Katyal and S. Prakash, Talanta, 24 (1977) 367.
4 E. B. Sandell and H. Onishi, Photometric Determination of Traces of Metals, Part 1, 4th edn., Interscience-Wiley, New York, 1978, p. 325.
5 B. S. Garg and R. P. Singh, Talanta, 18 (1971) 761.
6 T. Hayashi, K. Hara, S. Kawai and T. Ohno, Chem. Pharm. Bull., 18 (1970) 1112.
7 A. Mukara, E. Omae and T. Suzuki, Bunseki Kagaku, 29 (1980) 780; Chem. Abs., 94 (1981) 95139t.
8 W. Tkacz and L. Pszonicki, Chem. Anal., 22 (1977) 1013.
9 T. Förster, Z. Elektrochem., 54 (1950) 42.
10 G. Takatan, R. J. Juneau and S. G. Schulman, Anal. Chim. Acta, 64 (1972) 1044.
11 J. D. Winefordner, W. J. McCarthy and P. A. St. John, J. Chem. Educ., 44 (1967) 80.

Analytica Chimica Acta, 183 (1986) 269—274
Elsevier Science Publishers B.V., Amsterdam — Printed in The Netherlands

Short Communication

FLOW-INJECTION SPECTROPHOTOMETRIC DETERMINATION OF TRACE VANADIUM BASED ON CATALYSIS OF THE GALLIC ACID BROMATE REACTION

TSUTOMU FUKASAWA*, SUSUMU KAWAKUBO and AKIHIRO UNNO

Department of Applied Chemistry, Faculty of Engineering, Yamanashi University, Takeda-4, Kofu-shi 400 (Japan)

(Received 31st January 1985)

Summary. High sensitivity is obtained by using high concentrations of gallic acid and bromate, although the uncatalyzed reaction is significant. Various reactant concentrations, reaction temperature, pH and residence times can be used to alter the linear calibration ranges and sensitivity for vanadium. With reagent streams of 1.76 M bromate and 0.06 M gallic acid at pH 3.8 (each at 1 ml min^{-1}), 0.2—20 ng of vanadium (20-μl injections) can be determined at 30°C. Oxidized gallic acid is detected at 380 nm. When the bromate concentration is decreased to 0.5 M and the temperature is 65°C, 0.05—4 ng of vanadium can be determined; the relative standard deviation is ca. 5% for 0.6 ng of vanadium. The tolerances for Al(III), Fe(III), Mo(VI) and iodide are 10 ng, 10 ng, 50 ng and 200 ng, respectively, for the determination of 1 ng of vanadium. About 12 samples can be injected per hour.

Spectrophotometric kinetic methods based on catalytic reactions are very sensitive, but require rigid control of reaction time and temperature for accurate determinations. Flow injection analysis (f.i.a.) can provide these requirements and are useful for the analysis of microlitre samples. Combinations of catalytic-kinetic methods with f.i.a. have been shown to be useful [1—5]. Recently, a spectrophotometric kinetic method based on a vanadium-catalyzed gallic acid/bromate redox reaction has been studied for the determination of traces of vanadium [6, 7]. The reaction was later studied by using reactants at concentrations as high as possible [8] to find a practical limit for increased sensitivity and to obtain experimental information on its possible application in f.i.a. In this communication, conditions for the most sensitive practical determination of nanogram levels of vanadium are reported; the improved catalytic reaction [8] is combined with flow-injection techniques and some general information is given on the conversion of a catalytic kinetic method to flow analysis. The proposed method is suitable for determining as little as 0.05 ng of vanadium in 20 μl of sample and wide ranges of vanadium can be quantified by changing the reactant concentrations, temperature, pH, etc.

0003-2670/86/$03.50

Experimental

Reagents. All reagents were of analytical grade. Deionized and distilled water was used throughout. A standard aqueous vanadium solution (400 μg ml^{-1}) was prepared from ammonium metavanadate, and diluted appropriately before use. Bromate solutions were prepared by dissolving sodium bromate in water and mixed with acetate buffer so that the medium was 0.1 M sodium acetate/0.44 M acetic acid (pH 3.8). Gallic acid solutions were prepared in water. Both these solutions were used within two days. The pH of reacting solutions was adjusted as required by adding 10 M acetic acid or 10 M sodium hydroxide to the bromate solution. Interfering ion solutions were prepared by dissolving aluminum potassium sulfate, ammonium iron(III) sulfate (both dodecahydrates), ammonium heptamolybdate(VI) tetrahydrate and potassium iodide in water.

Apparatus. The flow-injection system is shown in Fig. 1. The two-channel peristaltic pump (Atto, Model SJ-1220, 100 V, 20 W) was fitted with two silicone rubber tubes (2.0 mm i.d., 1 m length). A Dyflon Y-type mixing joint, a Dyflon injection part with silicone rubber septum (as for liquid chromatography), and a quartz glass flow cell (1.5 mm i.d., 10 mm light path) were used. Teflon tubing of 1 mm i.d. was used for the mixing coil and for connections. The thermostated bath was kept at a given temperature within ±0.5°C. The flow cell was set in the thermostated cell chamber of a Hitachi Model 100-10 single-beam spectrophotometer. The linear-scale absorbance at 380 nm was recorded on a strip-chart recorder (Yokogawa, Model 3056-11) with a full-scale absorbance of 2.0 or 0.5 (chart speed, 0.1 or 0.33 cm min^{-1}). Samples (20 or 100 μl) were injected with a Terumo Model MS-50 gas-tight syringe. A Hitachi-Horiba model M-5 pH meter was used.

Recommended procedure. Bromate (Fig. 1, R_1) and 0.06 M gallic acid (R_2) solutions, previously thermostated at the appropriate temperature, are each pumped at 0.5 ml min^{-1}. The redox reaction begins at joint M. The concentration of the bromate solution and reaction temperature are selected depending on the sensitivity and lower limit of determination required; reaction at 30°C with 1.76 M bromate is recommended for general purposes, and

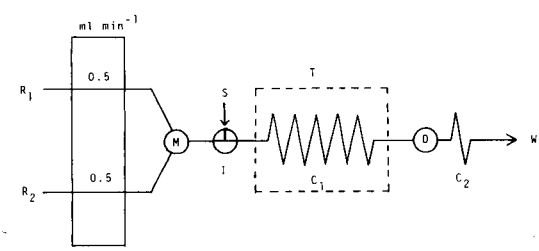

Fig. 1. Schematic diagram of the flow-injection system. (R_1) sodium bromate containing buffer solution; (R_2) gallic acid; (M) mixing joint; (I) injection port; (C_1) 50-m teflon reaction tube coiled to 8-cm diameter; (T) thermostated bath; (D) flow cell; (C_2) 20-cm teflon (0.25 mm i.d.) back-pressure tube coiled to 3-cm diameter; (W) waste.

reaction at 65°C with 0.5 M bromate for low nanogram to subnanogram amounts of vanadium (see below). A 20-μl sample containing upto 20 ng or 4 ng of vanadium is injected. The absorbance of the yellow oxidized product of gallic acid is measured against water at 380 nm and recorded (see Table 1). In the case of reaction at 65°C, an absorption filter (0.5 absorbance) is used as reference instead of water, to compensate for the baseline absorbance caused by the uncatalyzed reaction. Peak heights are measured. The calibration curve is prepared by using aliquots of the standard vanadium solution.

Results and discussion

Effect of pH. As shown previously [8], both the catalyzed and uncatalyzed reaction were affected by pH. The effect in the flow-injection method with 1.76 M bromate was very similar to that in the batch method; at pH 3.1—3.2, the baseline absorbance was high (ca. 0.7) but much lower (ca. 0.2) at the recommended pH of 3.8. The relative standard deviations for the peak height were about 4% (n = 8) for 10 ng of vanadium at 30°C at both pH 3.1 and 3.8, whereas those in the batch method [8] were 63% for pH 3.1 and 8.3% for pH 3.8. These lower values, especially for pH 3.1, are due to the well-established repeatability of the reaction by using flow-injection systems.

Effect of reagent concentrations. Previous results [8] suggested that the reactants should be as concentrated as possible for any application to f.i.a. Therefore, sodium bromate was used instead of the potassium salt because of its greater solubility [8]. The effects of the reactant concentrations on the catalyzed and uncatalyzed reactions were studied by using upto 2.0 M

TABLE 1

Experimental conditions, sensitivities and precisions

Experiment no.[a]	1		2		3
Temperature (°C)	30		65		30
Bromate (M)	1.76		0.5		0.054
Gallic acid (M)	0.06		0.06		0.022
Full scale (abs.)	2.0	0.5	2.0	0.5[c]	2.0
Max. abs.[b]	0.94	0.5	1.5	0.5[c]	—
Baseline abs.	0.18	0.15	0.65	0.15[c]	0.01
Linear range of calibration curve (ng)	0—20	0—10[d]	0—4	0—2[d]	—
Δ Abs.[e]	0.01	0.0025	0.01	0.0025	0.01
Sensitivity (ng/Δ Abs.)	0.32	0.080	0.060	0.015	2.6
Precision					
V determined (ng)	10	2	1	0.6	40
S.d. (n = 5) (ng)	0.39	0.15	0.060	0.027	1.1

[a]20-μl sample; pH 3.8; 5-m reaction coil; flow rate 0.5 ml min^{-1}. [b]The maximum absorbance measured including baseline absorbance. [c]Against the absorption filter with 0.5 absorbance. [d]Limited by the full-scale absorbance. [e]Lowest detectable absorbance change.

bromate and upto 0.060 M (almost saturated) gallic acid. The initial concentrations of the reactants in the mixing coil are, of course, half these concentrations.

Figure 2 shows that both the uncatalyzed and catalyzed reactions increased with increasing bromate concentration, as expected from the chemical kinetics [8]. However, there are clear differences between the two reactions, i.e., the uncatalyzed reaction proceeded as a pseudo-first-order reaction at both temperatures, whereas the catalyzed reaction increased only gently at bromate concentrations above 0.25 M. At 65°C, the catalyzed reaction was very sensitive but the uncatalyzed reaction was excessive (Fig. 2B). At 30°C, 0.5 M bromate had little effect on the reaction rate; 1.76 M bromate was selected to provide the best sensitivity under these conditions. At 65°C, the choice of 0.5 M bromate provides a compromise between high sensitivity and excessive baseline absorbance.

The effect of gallic acid concentration was studied for 1.76 M bromate at 30°C and 0.5 M bromate at 65°C (Fig. 3). At 30°C with 1.76 M bromate, the effect of gallic acid concentration was very much as expected [8]. Despite the increased extent of the uncatalyzed reaction at 65°C, 0.06 M gallic acid was preferred at both temperatures to provide a compromise between sensitivity and possible range of determination.

Reaction temperature. The effect of temperature on the rates of the catalyzed and uncatalyzed reactions has been discussed [8]. In the flow systems, the uncatalyzed reaction increased greatly with temperature whether 1.76 or 0.5 M bromate was used. Use of 1.76 M bromate at 65°C was impossible because the uncatalyzed reaction produced a (baseline) absorbance of >1.5. At 50°C, the useful range of determination was very narrow. In the case of the 0.5 M bromate/0.06 M gallic acid reaction at 65°C, a useful range was obtained upto the maximum absorbance of about 2 (Table 1).

Flow rate of reactants and length of reaction tube. In the application of any catalytic kinetic reaction, the absorbance change obviously depends on

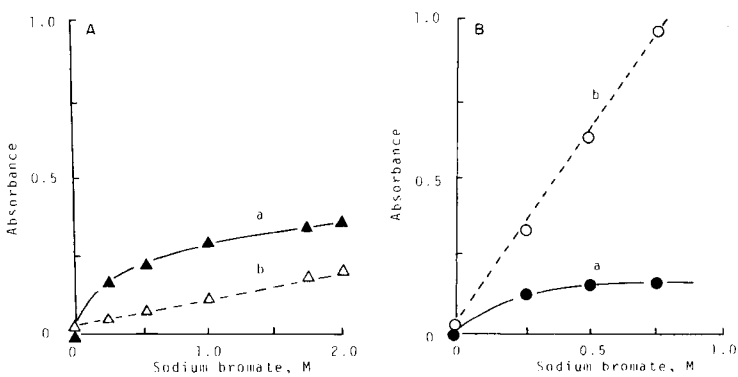

Fig. 2. Effect of concentration of bromate: (A) on reaction of 10 ng V at 30°C; (B) on reaction of 1 ng V at 66°C. Curves: (a) peak height; (b) baseline. (0.06 M gallic acid; other conditions as in the recommended procedure.)

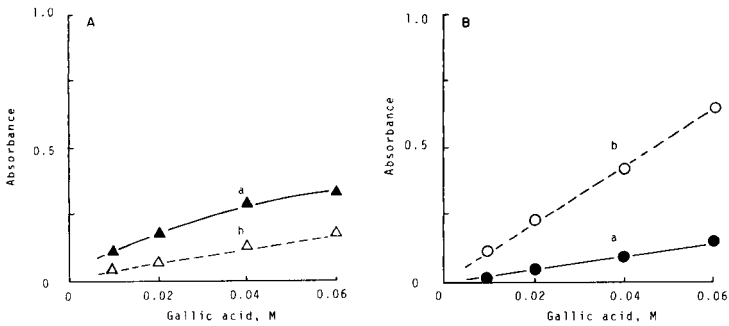

Fig. 3. Effect of concentration of gallic acid: (A) for 10 ng V at 30°C with 1.76 M bromate; (B) for 1 ng at 65°C with 0.5 M bromate. Curves: (a) peak height; (b) baseline. (Other conditions as in the recommended procedure.)

the residence time of the sample zone in the system, i.e., on the flow rate and the tube length. The effect of flow rate was checked for the range 0.3—2.0 ml min^{-1} in each stream for both the 30°C (1.76 M bromate) or 65°C (0.5 M bromate) reactions. The lower flow rates gave higher peaks for both the reactions, but at 0.3 ml min^{-1} the peak-height reproducibility was poor, and the peaks broadened leading to lower sample throughput. The loss of sensitivity was great at flow rates $\geqslant$1.0 ml min^{-1}, thus a flow rate of 0.5 ml min^{-1} was selected as the best compromise between the conflicting demands of reproducibility, sensitivity and throughput.

Reaction coils of 1—7 m were tested. For the 30°C reaction, there was little increase in peak height when a 7-m coil was used instead of a 5-m coil, but decreased sensitivity with 1—3 m coils. For the 65°C reaction, the extent of the uncatalyzed reaction increased rapidly with longer coils. The coil length of 5 m was adopted as the best compromise for both sets of conditions. With the 5-m reaction coil and the flow rate of 0.5 ml min^{-1}, the reaction time was about 5.6 min, comparable to that used in the batch method [8]. About twelve samples per hour were injected.

Sample volume. For the 65°C (0.5 M bromate) reaction, sample volumes of 10—100 μl gave constant peak heights. For the 30°C (1.76 M bromate) reaction, sample volumes of 50—100 μl gave a proportional increase in sensitivity of 20—40%, compared to 20-μl volumes. However, the larger volumes increased the size of the negative blank peak (see Fig. 4) and so 20 μl was preferred.

Determination of vanadium. Table 1 summarizes the experimental conditions and results. The sensitivity is given as nanogram of vanadium providing the lowest detectable absorbance change equivalent to 0.5% of the full-scale absorbance. Figure 4 shows typical recordings for the determination of vanadium. Table 1 shows that the 30°C reaction with a high bromate concentration (experiment 1) is suitable for the determination of wide ranges of vanadium, whereas the 65°C reaction (experiment 2) can be used for narrower

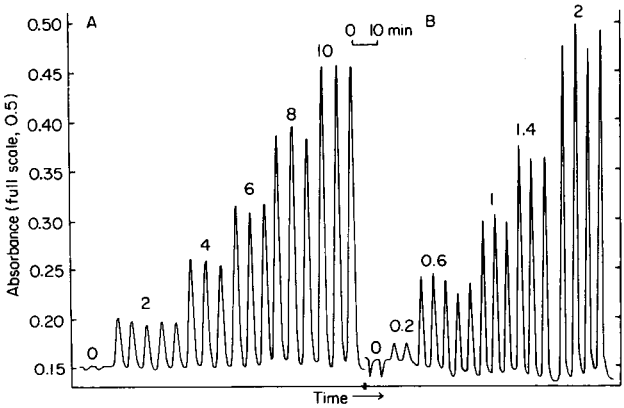

Fig. 4. Typical recordings for the determination of vanadium. The numbers on the peaks are nanograms of vanadium injected. Experimental conditions are listed in Table 1; A corresponds to experiment 1 and B to experiment 2.

ranges with much better sensitivity. Scale expansion improved both sensitivity and precision in the determination of small amounts of vanadium. Experiment 3 shows that the low reactant concentrations, such as those used in a batch method [6], provided very low sensitivity.

The results obtained above show that this catalytic reaction can be applied in flow injection analysis to provide various sensitivities and ranges of determination depending on the conditions selected. Thus 0.05—4 ng of vanadium was determined at 65° C with 0.5 M bromate/0.06 M gallic acid, and 0.2—20 ng at 30° C with 1.76 M bromate/0.06 M gallic acid.

Effect of foreign elements. In previous work [6, 8] four elements caused significant interferences. Their effects on the flow-injection method were tested for determinations of 10 or 1 ng of vanadium under the conditions of experiment 1 or 2 (Table 1), respectively. The tolerable amounts of aluminum-(III), iron(III), molybdenum(VI) and iodide were 2000, 200, 500 and 500 ng in the 30° reaction, and 10, 10, 50 and 200 ng in the 65° C reaction, respectively.

REFERENCES

1 S. M. Ramasamy, A. Iob and H. A. Mottola, Anal. Chem., 51 (1979) 1637.
2 J. L. Burguera and A. Townshend, Anal. Chim. Acta, 114 (1980) 209.
3 T. Yamane and T. Fukasawa, Anal. Chim. Acta, 119 (1980) 389.
4 K. Hirayama and N. Unohara, J. Chem. Soc. Jpn., 1981 (1981) 98.
5 J. L. Burguera and M. Burguera, Anal. Chim. Acta, 127 (1981) 199.
6 T. Yamane and T. Fukasawa, Bunseki Kagaku, 25 (1976) 454.
7 T. Fukasawa and T. Yamane, Anal. Chim. Acta, 88 (1977) 147; Bunseki Kagaku, 26 (1977) 692; Anal. Chim. Acta, 113 (1980) 123.
8 T. Fukasawa, S. Kawakubo and T. Yamanouchi, Anal. Chim. Acta, 171 (1985) 325.

Analytica Chimica Acta, 183 (1986) 275—280
Elsevier Science Publishers B.V., Amsterdam — Printed in The Netherlands

Short Communication

QUANTITATION OF TRACE AQUEOUS HALIDES BY VOLATILIZATION INTO A MICROWAVE-INDUCED HELIUM PLASMA

KEVIN G. MICHLEWICZ and JON W. CARNAHAN*
Department of Chemistry, Northern Illinois University, DeKalb, IL 60115 (U.S.A.)
(Received 2nd October 1985)

Summary. Chloride and bromide in aqueous solutions are determined using chemical vaporization coupled with a 500-W helium microwave-induced plasma emission system. The halide is converted to the corresponding hydrogen halide by mixing with concentrated sulfuric acid in a continuously flowing cell. The observed linear ranges cover 2—3 orders of magnitude. Detection limits for chloride and bromide are 0.2 and 0.3 mg l^{-1}, respectively. The sample throughput is 6—10 h^{-1}. Matrix matching is needed for real samples.

The determination of halides in aqueous solution by atomic spectrometry is difficult, primarily because the resonance transitions of the halide (except astatine) atoms are all of energies greater than 6.9 eV [1]. Consequently, the halogen atom resonance lines are in the vacuum ultraviolet (v.u.v.) region of the spectrum, at <178 nm. The same situation occurs for resonance halogen ion (X^+) lines. Because of the practical difficulties of operation in the v.u.v. region, techniques have been developed to monitor nonmetals by observing nonresonance transitions. Several comprehensive tabulations of nonmetal emission lines have been prepared for plasma emission sources [2—5]. The inductively-coupled argon plasma (i.c.a.p.) produces intense nonmetal emission in both the v.u.v. [6] and near-infrared (n.i.r.) [2—5] regions. Using direct solution nebulization, monitoring halogen emission in the v.u.v. region, an argon-purged optical path, and nonabsorbing optics, Nygaard et al. [6] obtained detection limits of 10, 3, and 1 mg l^{-1} for Cl, Br and I, respectively. Detection limits in the n.i.r. region were considerably greater, at 2000, 100 and 500 mg l^{-1} for F, Cl, and Br.

With ≤200-W helium microwave-induced plasma (He-m.i.p.) systems, intense nonmetal emission has been noted in the visible [7] and n.i.r. [8] regions of the spectrum. However, because of the low tolerance of these systems to sample loading [9, 10], the He-m.i.p. has been used primarily as an element-selective detector for gaseous samples [10—20]. With the development of systems of greater power input, solutions have been nebulized directly into helium [21, 22], argon [22—24], air [22, 25] and nitrogen [26, 27] m.i.p. sources. Recently, chloride has been determined directly from nebulized

0003-2670/86/$03.50

aqueous solutions in the visible region [21]. The detection limit for chloride (signal equivalent to 2 times the standard deviation of the background noise) was 7 mg l^{-1} and the linear range was greater than 2.5 orders of magnitude, which are the best values so far reported for this type of determination.

Alder et al. [18, 19] determined chloride by adding discrete aqueous samples to a sulfuric acid solution. The resultant hydrogen chloride was swept into a 110-W He-m.i.p. with helium. The chloride detection limit was 0.12 mg l^{-1}. This concept is extended to bromide with operation in a continuous sampling mode in this communication.

In terms of volatility, HCl, HBr and HI should behave similarly; their boiling points are −85° C, −67° C and −35° C, respectively. (Because the boiling point of HF is 19.5° C, this extension was not considered.) Reduction/oxidation may also occur, e.g., it is well known that sulfuric acid may oxidize bromide and iodide to Br_2 and I_2, which boil at 59° C and 184° C, respectively. It should be noted that phosphoric acid can be used to produce hydrogen halides from halide without oxidation.

Experimental

Reagents. Aqueous solutions were prepared in deionized/distilled water. Potassium halides were A.C.S. reagent grade. The 98% sulfuric acid and 85% phosphoric acid were A.C.S. reagent grade (Fisher Scientific).

Instrumentation. The spectrometer/plasma system has been described recently [22]. The spectrometers were a 0.35 m GCA/McPherson EU-700 scanning spectrometer with a 1200 groove/mm holographic grating and a 0.75-m Echelle Spectrospan III. The plasma system consisted of a 500-W Micro-Now (Chicago) Model 420-B microwave generator (2.45 GHz) and a cavity/torch system [22]. The pyrex coolant jacket was replaced with one of quartz [21].

Reaction system (Fig. 1). The cell (30 mm tall) was constructed from a 12-mm i.d. pyrex tube with a ground-glass cap. Two solution inlets (1-mm i.d.) located 3 mm from the base were used to introduce stock acid and aqueous analyte-containing solutions. Helium inlet and outlets (3-mm i.d.) were located 28 mm from the cell base. An outlet (7-mm i.d.) located 15 mm from the cell base was used to route the waste solution to a beaker; the outlet tube was immersed in solution to route the sample gas to the plasma. The analyte transfer line was heated to 90° C with resistively heated nichrome wire controlled by a Variac, to prevent water condensation in the sampling tube.

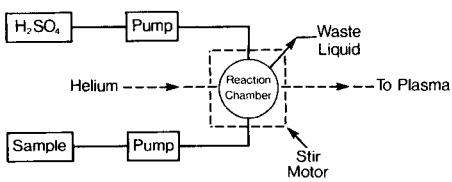

Fig. 1. Schematic diagram of acid halide generation apparatus.

Solutions were pumped into the cell with two Rainen Rabbit (Rainin Instrument Co., Wolburn, MA) peristaltic pumps. Tubing was poly(vinyl chloride) for the aqueous solutions and viton for sulfuric and phosphoric acids. Viton tubing is strongly recommended for acid introduction. All connections to the cell were made with teflon fittings and tubing.

Results and discussion

Acid halide formation was considered for chloride, bromide and iodide. Equal flows (1 ml min^{-1}) of aqueous 100 mg l^{-1} halide solution and 98% sulfuric acid produced significant amounts of hydrogen bromide and chloride and intense emission was detected at the 479.5-nm and 478.6-nm ion lines, respectively. These lines were used for all subsequent investigations. Although the 470.5-nm bromine line is generally more intense in the He-m.i.p., intense molecular emission from C_2 (bandheads at 471.5 and 473.7 nm), N_2^+ (bandhead at 470.9 nm) and N_2 (bandhead at 472.3 nm) precluded its use.

Sulfuric acid oxidized a significant portion of the iodide to iodine, producing a brownish/purple precipitate. Iodine emission was detected at the 206.2-nm atomic line, indicating that some iodide was converted to HI or that I_2 was carried to the plasma as a mist. The signal was not intense enough for quantitative purposes and residual elemental emission from the iodine precipitate caused excessive sample clean-out time. In an attempt to avoid the oxidizing properties of sulfuric acid, 85% phosphoric acid was tested; oxidation of iodide was not then visible but significant concentrations of hydrogen iodide were not produced. Studies of HI formation were abandoned.

Optimization. For bromide and chloride determinations, parameters were varied to maximize the signal/background ratio (s./b.). Parameters considered include sample gas flow rate, plasma gas flow rate, power applied, and rates of introduction of analyte and sulfuric acid. After optimum conditions had been established, each parameter was varied to indicate the trends with respect to s./b. For both chloride and bromide, the s./b. increased as the sample gas flow rate decreased from 1.00 to 0.30 l min^{-1}. With flows of 300—100 ml min^{-1}, the signal did not vary significantly. At flow rates of less than 100 ml min^{-1}, the signal decreased. Therefore, the sample gas flow was maintained at 250 ml min^{-1}.

Trends of s./b. vs. power and plasma gas flow were similar for both chloride and bromide (Fig. 2). Decreasing the flow to the minimum rate (approximately 7.5 l min^{-1}) produced the maximum signal, regardless of the power applied. At these lower flow rates, the chloride signal is virtually independent of power and the bromide signal is almost independent of power from 440 to 500 W. At higher flow rates (ca. 15 l min^{-1}), higher powers generally produce more intense signals (Fig. 2). Obviously, the residence time of the analyte in the plasma is very important. At higher plasma-gas flow rates this factor becomes even more apparent. For quantitative work, the power and flow rates were maintained at 450 W and 7.5 l min^{-1}, respectively. It is noteworthy that the sample-introduction system was not compatible

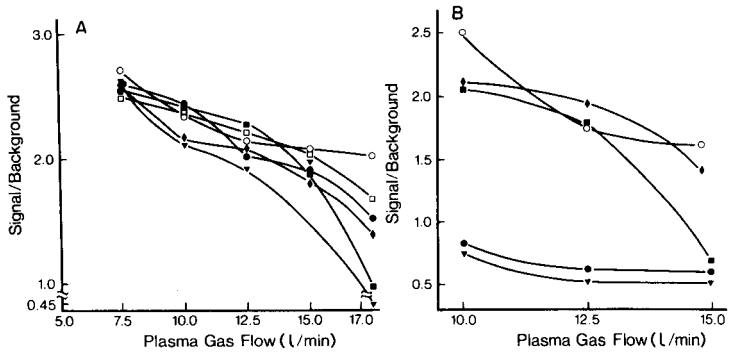

Fig. 2. Correlation of plasma gas flow rate (l min^{-1}) and generator forward power (W). (A) HCl: (▾) 390, (▪) 405, (•) 420, (▫) 435, (○) 450, (◇) 480 W. (B) HBr: (▾) 380, (•) 420, (▪) 440, (○) 480, (◇) 500 W.

with a 100-W plasma maintained in a 6-mm o.d., 2-mm i.d. quartz tube, as the plasma was extinguished on sample introduction.

Factors governing the optimum values for acid and aqueous solution flow rates include the acidity in the cell and analyte through-put. The possible oxidation of bromide to bromine must also be considered. Trends are easily explainable for hydrogen chloride formation. At a given aqueous solution flow rate, increasing the flow rate of sulfuric acid increases the concentration of hydrogen chloride (Fig. 3A). The signal generally increases with the flow rate of aqueous solution at a given flow rate of sulfuric acid, because of the greater availability of chloride ion. For the subsequent studies with chloride, the pump rates were 0.9 ml min^{-1} for the aqueous solution and 1.8 ml min^{-1} for the sulfuric acid.

Again, with formation of hydrogen bromide, increasing the sulfuric acid flow at a given aqueous solution flow increases the signal (Fig. 3B). However, at higher sulfuric acid flow rates, decreasing the aqueous sample flow rate increases the signal. This trend is opposite to that of the HCl reaction. A notable difference from the chloride experiment is that bromine formation is observed during the reaction through discoloration of the solution. It has not been possible to explain these trends using calculated equilibrium constants from reduction potentials. Possible reasons for this failure could be that incomplete mixing does not allow the reaction to reach equilibrium or that kinetic effects were not included in the calculations. Pump rates used for subsequent work with hydrogen bromide were 0.6 ml min^{-1} of aqueous solution and 1.5 ml min^{-1} of 98% sulfuric acid.

Linear ranges and detection limits. The reaction at optimum conditions with chloride produced a linear range from 0.5 to 500 mg l^{-1}. The linear regression equation was: relative signal intensity = $(0.063 \pm 0.009)x + (1.41 \pm 0.54)$, where x is the concentration in mg l^{-1}. The correlation coefficient was 0.998. For bromide, the linear range was from 1.0 to 250 mg l^{-1}. The linear regression equation was: relative signal intensity = $(0.110 \pm 0.016)x +$

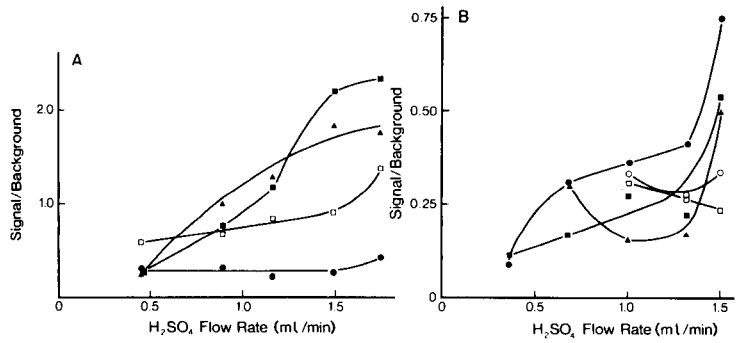

Fig. 3. Correlation of sulfuric acid flow rate (ml min^{-1}) and analyte flow rate (ml min^{-1}). (A) HCl: (•) 0.23, (□) 0.45, (▲) 0.68, (■) 0.90 ml min^{-1}. (B) HBr: (•) 0.60, (■) 1.4, (▲) 2.2, (□) 3.0, (○) 3.8 ml min^{-1}.

(−0.079 ± 0.201) and the correlation coefficient was 0.9995. The detection limits were evaluated at concentrations approximately 10 times greater than the detection limit and found to be 0.21 and 0.27 mg l^{-1} for chlorine and bromine, respectively. For chloride, this value is similar to that obtained by Alder et al. (0.12 mg l^{-1}) [19] and is a factor of 33 better than the solution nebulization detection limit (7 mg l^{-1}) with this plasma [21].

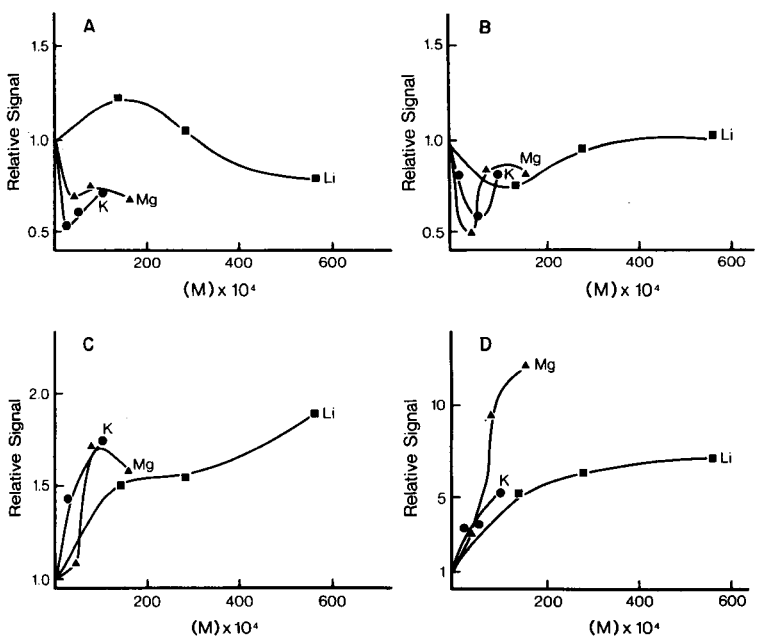

Fig. 4. The effects of various added metals on halide emission: (A) chloride, uncorrected; (B) chloride, background-corrected; (C) bromide, uncorrected; (D) bromide, background-corrected.

Sample composition effects. With 1000-mg l^{-1} solutions of bromide and chloride, the effects of added aqueous Li^+, K^+ and Mg^{2+} were determined. The solution composition was varied and the halide signal was observed in two modes. In one mode (Fig. 4A, C) the spectrometer was adjusted to the analytical wavelength of interest; in the second mode (Fig. 4B, D) scanning was done across the wavelength of interest so that background shifts could be studied. From these results, it is clear that matrix matching of the samples and calibration standards will be necessary for the application of this technique to real samples.

Sample clean-out time. When changing from analyte to distilled water for formation of both HCl and HBr, about 4 min was required for the signal to decay to 10% of the sample signal. The signal vs. time plot approximated the exponential signal decay expected such systems. This factor restricted sampling times to 7—10 min. Alternative cell designs are being studied to improve this aspect.

Synthetic samples. Four aqueous samples (400—600 mg l^{-1}) were prepared from Thorn Smith soluble chloride samples. The range of error was +18 to —24 mg l^{-1} or +3.3 to —4.2% relative. The average relative error and the standard deviation of this error was 0.4 ± 3.4%. Thus, for this set of samples, the errors were random and no consistent trend was indicated toward high or low values.

REFERENCES

1 R. Mavrodineanu and H. Boiteux, Flame Spectroscopy, Wiley, New York, 1965.
2 S. J. Northway and R. C. Fry, Appl. Spectrosc., 34 (1980) 332.
3 S. J. Northway, R. M. Brown and R. C. Fry, Appl. Spectrosc., 34 (1980) 338.
4 R. C. Fry, S. J. Northway, R. M. Brown and S. K. Hughes, Anal. Chem., 52 (1980) 1716.
5 S. K. Hughes and R. C. Fry, Anal. Chem., 53 (1980) 1111.
6 D. D. Nygaard, R. G. Schleicher and D. A. Leighty, Am. Lab., 17(6) (1985) 59.
7 K. Tanabe, H. Hariguchi and K. Fuwa, Spectrochim. Acta, Part B: 36 (1981) 119.
8 J. E. Freeman and G. M. Hieftje, Appl. Spectrosc., 39 (1985) 211; Spectrochim. Acta, Part B: 40 (1985) 475.
9 S. R. Koirtyohann, Anal. Chem., 55 (1983) 376.
10 S. A. Estes, P. C. Uden and R. M. Barnes, Anal. Chem., 53 (1981) 1829.
11 A. J. McCormack, S. C. Tong and W. D. Cooke, Anal. Chem., 37 (1965) 1470.
12 C. I. M. Beenakker, Spectrochim. Acta, Part B: 32 (1977) 173.
13 J. W. Carnahan, K. J. Mulligan and J. A. Caruso, Anal. Chim. Acta, 130 (1981) 227.
14 T. H. Risby and Y. Talmi, CRC Crit. Rev. Anal. Chem., 14 (1984) 231.
15 C. I. M. Beenakker, Philips Tech. Rev., 39 (1980) 65.
16 D. G. Mitchell, K. M. Aldous and E. Canelli, Anal. Chem., 49 (1977) 1235.
17 J. W. Carnahan and J. A. Caruso, Anal. Chim. Acta, 136 (1982) 261.
18 J. F. Alder, Q. Jin and R. D. Snook, Anal. Chim. Acta, 120 (1981) 147.
19 J. F. Alder, Q. Jin and R. D. Snook, Anal. Chim. Acta, 123 (1981) 329.
20 A. T. Zander and G. M. Hieftje, Appl. Spectrosc., 35 (1981) 357.
21 K. G. Michlewicz and J. W. Carnahan, Anal. Chem., 57 (1985) 1092.
22 K. G. Michlewicz, J. J. Urh and J. W. Carnahan, Spectrochim. Acta, Part B: 40 (1985) 493.
23 D. L. Haas, J. W. Carnahan and J. A. Caruso, Appl. Spectrosc., 37 (1983) 82.
24 D. L. Haas and J. A. Caruso, Anal. Chem., 56 (1984) 2014.
25 J. J. Urh and J. W. Carnahan, Anal. Chem., 57 (1985) 1253.
26 J. Burman and K. Bostrom, Anal. Chem., 51 (1979) 516.
27 R. D. Deutsch and G. M. Hieftje, Appl. Spectrosc., 39 (1985) 214.

Analytica Chimica Acta, 183 (1986) 281—286
Elsevier Science Publishers B.V., Amsterdam — Printed in The Netherlands

Short Communication

DETERMINATION OF POLYCYCLIC AROMATIC HYDROCARBONS BY ELECTRON SPIN RESONANCE SPECTROMETRY

D. THORBURN BURNS, MOHAMED A. SALEM, R. IVAN BAXTER and BRIAN D. FLOCKHART*

Department of Pure and Applied Chemistry, The Queen's University, Belfast BT9 5AG (Northern Ireland)

(Received 19th December 1985)

Summary. The use of electron spin resonance spectrometry with a modern instrument is described for the determination of polynuclear aromatic hydrocarbons (PAHs) down to nanogram levels, after adsorption on calcined silica/alumina. A single PAH or the total number of moles of PAHs can be determined. Implications for liquid chromatography are discussed.

Polycyclic aromatic hydrocarbons (PAHs) are probably the most widespread of all chemical environmental pollutants with the potential for carcinogenicity and mutagenicity in humans. Because these compounds are produced in virtually all combustion processes and in degradation processes of organic materials, they are often present in environmental samples as extremely complex mixtures and in almost every type of sample matrix. The identification and determination of PAHs are therefore of fundamental importance to those engaged in environmental assessment. Modern analytical methods for PAHs have been reviewed in detail recently [1—3], but no reference was made to the use of electron spin resonance (e.s.r.) spectrometry in this area.

The application of e.s.r. for the detection and estimation of a number of hydrocarbons (anthracene, 9,10-dimethylanthracene, perylene, naphthacene) was reported [4] as early as 1962. These compounds are quantitatively converted to the cation-radical form on the surface of a strongly calcined silica/alumina adsorbent of the type normally used as a catalyst in the cracking of hydrocarbons. The resulting radical species are stable in the adsorbed state. The PAH concentration in an unknown solution can, therefore, be determined by direct comparison of the signal for the unknown with that obtained from a standard solution of the same compound. Unfortunately, because of the overlap of spectra from individual PAHs, the e.s.r. method is not specific. Hitherto, therefore, the technique was not generally applicable to mixtures of these compounds, nor was it widely adopted. Recent advances in separation techniques, particularly capillary column gas chromatography [5] and high-performance liquid chromatography (h.p.l.c.) [6] have transformed the situation.

0003-2670/86/$03.50

This communication explores the feasibility of a h.p.l.c./e.s.r. method for the identification and determination of PAHs present at low concentrations in mixtures. Nanogram quantities of individual compounds can be determined by the method described.

Experimental

Apparatus. The e.s.r. measurements were made with a Varian E-109 spectrometer operated at ca. 9.5 GHz with a magnetic field modulation of 100 kHz.

The optimum size of sample tube for present purposes was established by putting the same amount of 1,1-diphenyl-2-picrylhydrazyl (DPPH), dissolved in toluene, into quartz tubes with internal diameters ranging from 1 to 6 mm (wall thickness 0.8—1.2 mm), and measuring the signal amplitude (peak-to-peak height on the first derivative curve). The results are summarized in Fig. 1. Clearly, quartz tubes of 4-mm bore are the most suitable, and this size of tube was used for the remainder of the work.

Reagents. The commercial sample of silica/alumina (wt. %, dry basis: Al_2O_3, 13; Fe, 0.04; Na_2O, 0.02; SO_4, 0.04) was supplied by Joseph Crosfield and Sons, Ltd. The adsorbent was washed in distilled water, dried at 120° C, activated by heating in air for 2 h at 800° C in an electric muffle furnace, and cooled to room temperature under vacuum (10^{-2} mm Hg) over phosphorus-(V) oxide. Samples of adsorbent activated at lower temperatures may also be used; although their saturation adsorptive capacity is less than that of the 800°C activated adsorbent, this is not a serious problem. Samples activated for more than 2 h do not show a noticeable increase in electron-accepting ability over that of samples heated for 2 h.

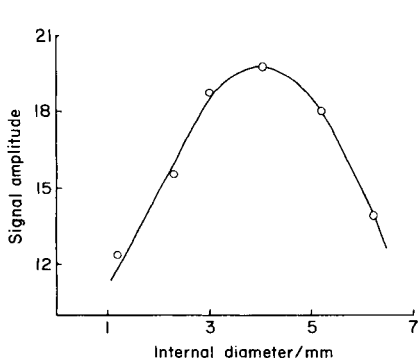

Fig. 1. Signal amplitude (peak-to-peak height on the first derivative curve in arbitrary units) as a function of the internal diameter of the quartz sample tube.

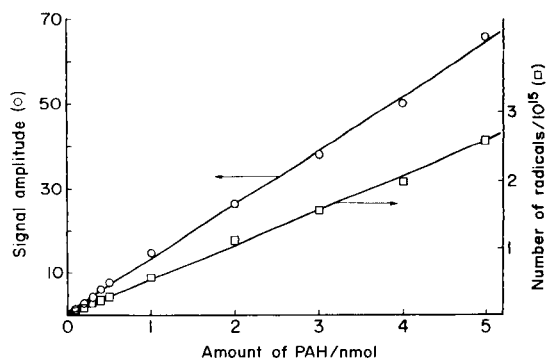

Fig. 2. Signal amplitude (○) and number of radicals (□) as a function of the amount of PAH initially present. Each point on the graph up to 0.5 nmol represents the addition of another PAH, and this pattern is repeated from 1 to 5 nmol. The hydrocarbons used were perylene, anthracene, chrysene, pyrene and 3,4-benzopyrene, added in that order.

Perylene (Aldrich Chemical Co.) and anthracene (microanalytical standard, BDH Chemicals) were used as received. Chrysene (BDH) was further purified by recrystallization from toluene. Pyrene and 3,4-benzopyrene (Koch-Light Laboratories) were recrystallized from ethanol/water. Toluene (AnalaR) and hexane (Spectrosol grade, Aldrich) were used as solvents.

Procedure. Appropriate volumes of PAH solution were measured with an Agla micrometer syringe into separate sample tubes. Additional solvent was added to bring the level of liquid in each tube to about the same height (see below). Activated adsorbent was added via a small funnel until the depth of solid sample was ca. 22 mm, the contents of the tube were stirred carefully, and the tube was stoppered. This depth of adsorbent ensured maximum magnetic absorption. The level of liquid in the tube is not important, provided that it is sufficient to cover the solid and thus prevent deactivation by water adsorbed directly from the atmosphere.

The stability of the adsorbed ion-radical for analytical purposes was assessed for initial PAH amounts of 1 μg and 40 μg. The results for the percentage change in signal amplitude with time are summarized in Table 1; however, measurement of integrated intensities gave similar values (±5%) in all cases. Of the five PAHs examined, perylene yielded the most stable adsorbed radical, and chrysene the least stable. Measurements of signal amplitude and integrated intensity reported below were made 1 h after preparation of the sample.

Results

Treatment of certain PAHs at low concentrations in a non-polar solvent with an active silica/alumina cracking catalyst leads to quantitative conversion of the PAH into its cation-radical form. An earlier study [4] showed that a linear relationship exists between the amplitude of the e.s.r. signal and the amount of PAH present, the calibration line passing through the origin. With the equipment available at that time, the lower limit for quantitative measurement was ca. 3 μg of PAH. As a result of instrumental improvements in recent years, it seemed likely that currently available commercial instru-

TABLE 1

Decrease (%) in signal amplitude with time (1—24 h) relative to the value at 20 min

Compound	Decrease (%) in signal amplitude with time (h)									
	1 μg PAH					40 μg PAH				
	1	3	5	9	24	1	3	5	9	24
Perylene	0	0	0	1	1	0	0	1	1	1
Anthracene	3	7	11	16	30	1	—	0	7	13
Chrysene	17	35	48	61	74	4	9	12	20	29
Pyrene	4	9	12	15	25	0	2	2	2	2
3,4-Benzopyrene	2	4	4	6	10	0	0	1	1	5

ments would permit much lower limits of determination. A re-evaluation of the e.s.r. method was, therefore, undertaken using a modern spectrometer.

The plots of signal amplitude vs. amount of PAH for perylene and anthracene were found to be linear up to 50 μg and 30 μg, respectively. The sensitivities can be seen in the calibration equations. The least-squares fit equation for the perylene results was: $x = (0.77 \pm 0.24) + (63.45 \pm 0.55)y$. For anthracene, the equation was $x = (0.57 \pm 0.20) + (40.94 \pm 0.50)y$. In both equations, x is the signal amplitude in arbitrary units and y is the amount of PAH in μg. Quantitative measurements were possible down to 10 ng of PAH. For six replicate measurements of 5 μg of perylene, the relative standard deviation was 4.8%.

Complete chromatographic separation of the complex mixtures of PAHs frequently found in environmental samples may not be achieved. Instead, separation of the mixture into fractions that each contain a few components may be the practical limit. In order to evaluate the e.s.r. method in such a situation, synthetic mixtures containing up to five PAHs were prepared as described in the legend to Fig. 2; this figure shows the linear plot obtained for the number of adsorbed radicals vs. the total amount of PAH in these samples. The radical concentrations were evaluated by comparing the integrated intensities (obtained by double integration of the first derivative curves) of the PAH spectra with that for a standard solution of DPPH in toluene. With appropriate settings of the spectrometer, the spectra for these PAH mixtures could be partially resolved. The modulation amplitude was therefore increased just enough to remove the resolution and the signal amplitudes were recorded. Over-modulation of the spectrum is clearly necessary for work with mixtures if peak-to-peak height is to be taken as a measure of the total PAH content. The peak-to-peak values so obtained are plotted in Fig. 2 against the total amount of PAH. Again, a straight line is obtained. Six replicate measurements at the 0.6-μg level gave a relative standard deviation of 2.3%. The quantitative nature of the conversion was verified by comparison of the integrated intensity of the spectrum obtained for an equimolar mixture of the five PAHs with that for a standard solution of DPPH. The PAH solution contained 1.20×10^{15} molecules of hydrocarbon; the number of adsorbed radicals was $1.10 \pm 0.06 \times 10^{15}$.

Discussion

Qualitative and quantitative analyses for PAHs are complicated by the great number of species, often isomeric, that have to be identified and determined. Nevertheless, the significant advances in separation and analytical techniques achieved in recent years have made it possible to determine PAHs in samples of environmental interest. In particular, h.p.l.c. has proved to be very useful for the isolation of these compounds for subsequent determination by other methods. This technique was not available when the e.s.r. method for determining PAHs was first described [4], and a difficulty with the e.s.r. method has been that of obtaining authentic compounds for the

preparation of standard solutions. A combination of h.p.l.c. separation and e.s.r. detection should therefore provide a useful method for the estimation of a single PAH or the total number of moles of PAHs.

The present investigation shows that PAHs can be determined down to the nanogram level when a modern e.s.r. spectrometer is used. With the adsorbent used in this study, the plot of signal amplitude vs. amount of PAH was linear up to 50 μg of perylene. The corresponding plot obtained with the catalyst used earlier [4] was linear up to 140 μg, but detection limits were also higher. A catalyst can of course be used outside the linear range if curved calibration is acceptable, and in this way >250 μg of perylene can be determined with the present sample of silica/alumina. Even if complete separation of a mixture of PAHs has not been achieved, the e.s.r. method can still be used for their quantitation, provided that all the components of a fraction generate radicals on the catalyst surface. The signal amplitude and the integrated intensity are equally useful for this determination (Fig. 2).

A noteworthy point is the surprising stability of many PAHs when converted into the free-radical form on the surface of a silica/alumina cracking catalyst. In the present investigation, spectral measurements were made 1 h after preparation of the sample. For some PAHs, however, this interval may be greatly extended (Table 1), but with an increase in error not exceeding a few per cent. This advantage of the e.s.r. method over other methods may be emphasized by reference to one investigation [7] in which the concentrations of PAHs in some environmental samples decreased by 40—60% when the analysis was delayed. This necessitated storage of the samples in the dark at −4°C and analysis as soon as possible after the extraction of the PAHs from the samples.

Anthracene, chrysene, perylene, pyrene and 3,4-benzopyrene have ionization potentials of 7.43, 7.81, 7.07, 7.53 and 7.21 eV, respectively [8]. Because the ionization potentials of molecules provide a convenient index of electron-donor ability, any PAH with an ionization potential < ca. 7.8 eV is potentially suitable for determination by e.s.r. spectrometry. Many PAHs are in this category [8—10].

M. Salem thanks the Egyptian Government and the ORS Award Scheme for financial support.

REFERENCES

1 P. W. Jones and R. I. Freudenthal (Eds.), Polynuclear Aromatic Hydrocarbons: Second International Symposium on Analysis, Chemistry, and Biology, in Carcinogenesis — A Comprehensive Survey, Vol. 3, Raven Press, New York, 1978.
2 M. L. Lee, M. V. Novotny and K. D. Bartle, Analytical Chemistry of Polycyclic Aromatic Compounds, Academic Press, London, 1981.
3 K. D. Bartle, M. L. Lee and S. A. Wise, Chem. Soc. Rev., 10 (1981) 113.
4 B. D. Flockhart and R. C. Pink, Talanta, 9 (1962) 931.
5 Y. Hirata and M. Novotny, J. Chromatogr., 186 (1980) 521.

6 P. A. Peaden, M. L. Lee, Y. Hirata and M. Novotny, Anal. Chem., 52 (1980) 2268.
7 A. M. Krstulovic, D. M. Rosie and P. R. Brown, Int. Lab., Sept./Oct. (1977) 11.
8 E. S. Pysh and N. C. Yang, J. Am. Chem. Soc., 85 (1963) 2124.
9 G. Briegleb, Angew. Chem. Int. Ed., 3 (1964) 617.
10 V. I. Vedeneyev, L. V. Gurvich, V. N. Kondrat'yev, V. A. Medvedev and Ye L. Frankevich, Bond Energies, Ionization Potentials and Electron Affinities, Edward Arnold, London, 1965, Table 8.

Analytica Chimica Acta, 183 (1986) 287—292
Elsevier Science Publishers B.V., Amsterdam — Printed in The Netherlands

Short Communication

A FLOW-INJECTION SYSTEM FOR ASSAY OF THE ACTIVITY OF AN IMMOBILIZED ENZYME CHEMICALLY-MODIFIED ELECTRODE

JAMES A. OSBORN[a] and ALEXANDER M. YACYNYCH*

Department of Chemistry, Rutgers, The State University of New Jersey, New Brunswick, NJ 08903 (U.S.A.)

DAVID C. ROBERTS

Mitre Corporation, 1820 Dolly Madison Blvd., McLean, VA 22102 (U.S.A.)

(Received 25th July 1985)

Summary. Chymotrypsin, covalently immobilized to the surface of an IrO_2-coated titanium electrode, responds potentiometrically to various substrates. A flow-injection system is described for assay of the activity of the immobilized enzyme with *N*-benzoyl-L-tyrosine ethyl ester as substrate and an ultraviolet detector. Least-squares fits of peak height vs. time typically yield correlation coefficients of 0.999 and standard errors of estimate of 0.0043 absorbance for a total absorbance change of about 0.130. Slopes of such plots vary linearly with enzyme activity.

The use of immobilized enzymes in analytical chemistry has been a fertile area of research in recent years [1]. Much attention has been paid to the development of quantitative methods based on electrodes that involve immobilized enzymes. Less effort has been spent on the characterization of such electrodes, with respect to parameters such as enzymatic activity [2, 3].

Several enzyme immobilization techniques have been implemented with varying degrees of control over the amount of enzyme immobilized [4, 5]. In any case, some degrees of enzyme activity is usually lost upon immobilization [1]. It is important, then, to have reliable methods for the determination of enzyme activity of electrochemical-based sensors, as enzyme activity [6] can play a significant role in determining electrode response. It is frequently necessary to modify standard procedures used for homogeneous solutions to determine activities of immobilized enzymes. In the present case, the small amount of enzyme immobilized on the electrode precluded the possibility of a fixed-time, two-point difference approach. The difference technique resulted in a small signal, similar to the noise level. A means of replenishing the supply of substrate to the surface on which the enzyme is immobilized is another necessity of a heterogeneous system. This is usually done by stirring.

[a]Present address: ICI Americas, Inc., Stewart Analytical Development, Wilmington, DE 19897, U.S.A.

0003-2670/86/$03.50

Unsegmented, continuous-flow procedures [7—9] are now well known. For enzyme reactions, a redox dye, coupled to the enzyme-catalyzed reaction, is often used to monitor the extent of the reaction over a fixed time. Similar types of automated enzyme assays have been described with air-segmented flow [10]. More recently, the use of enzymes, both free and immobilized, in flowing systems has largely been aimed at the determination of substrates [11—13]. There are some notable exceptions: Stewart et al. [14] described an unsegmented flow procedure for determining trypsin activity. Olsen et al. [15] demonstrated the use of gradient techniques adapted to the quantitation of lactate dehydrogenase activity.

This communication concerns the development of a flow-injection system for the sensitive assay of chymotrypsin immobilized on metal-oxide electrodes. These electrodes respond potentiometrically to certain ester substrates [16]. Assay methods have been developed which depend on the change in absorption of the substrate upon hydrolysis. It was desirable to assay the immobilized enzymes with the same substrates to which they responded potentiometrically. The amount of enzyme present did not allow for a simple two-point, fixed-time assay as the associated absorbance change was too close to background. The proposed method takes advantage of the sensitivity of an ultraviolet (u.v.) detector to monitor small changes in absorbance between a substrate solution which has been in contact with the immobilized enzyme electrode and that in the flowing stream.

Experimental

Apparatus. The flow injection system (Fig. 1) consisted of a Model 6000A chromatography pump (Waters Associates), a syringe loading sample injector (Model 7125, Rheodyne) equipped with a 20-μl sample loop, a variable-wavelength u.v. detector (Model SP769, Kratos, Westwood, NJ), an Omnigraphic 2000 X-Y recorder (Houston Instruments) and a water bath thermostatted with a Lauda constant-temperature immersion circulator (Model MT, Fisher Scientific). A diode-array spectrophotometer (Model 8450, Hewlett-Packard) was used for additional homogeneous enzyme assays.

Materials. Metal-oxide electrodes were constructed using segments of a piece of stock titanium (5-mm diameter, 15 cm long; Alpha Ventron, Danvers,

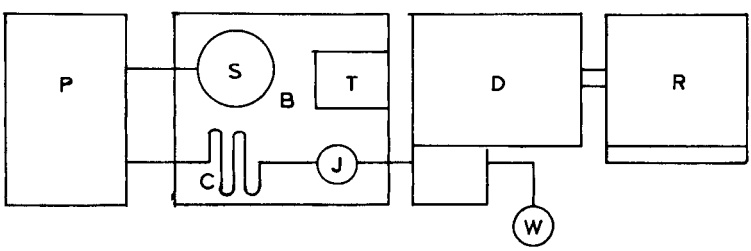

Fig. 1. Schematic diagram of the flow system: S, substrate solution; P, LC pump; C, coiled tubing; B, water bath; T, constant-temperature immersion circulator; J, injection port; D, variable-wavelength u.v. detector; W, waste; R, recorder. For details, see text.

MA). A high-temperature oven was used in the preparation of the metal oxide electrodes (Model 4601, Hydor Therme Corporation, Pennsauken, NJ). Metal-chloride solutions were aspirated in the preparation of the metal-oxide electrodes with a Jet-Pak spray atomizer (100 ml; Spray On Products, Cleveland, OH) operated with high-purity nitrogen.

Chymotrypsin (Type II, 50 IU mg^{-1}; E.C. 3.4.21.1) and *N*-benzoyl-L-tyrosine ethyl ester (BTEE) were obtained from Sigma Chemical Company. Iridium(III) chloride trihydrate (99.9%) and ruthenium(III) chloride trihydrate were obtained from Aldrich Chemical Company. Purum-grade cyanuric chloride was used as received from Tridom Chemical Company. Acetone was distilled and stored over 4-Å molecular sieves. Tris-HCl buffer (0.05 M) containing 0.1 M calcium chloride was prepared from reagent-grade materials. Methanol, used for the dissolution of substrates, was of spectroscopic grade. All solutions were prepared from distilled-deionized water.

Construction of immobilized enzyme electrodes. The metal-oxide electrodes were prepared as described elsewhere [16]. A metal chloride solution in isopropanol was aspirated onto a titanium disk and thermally decomposed to the corresponding pH-sensitive metal oxide. The resulting metal-oxide electrodes were fitted with a copper wire for electrical contact, and the entire assembly, except for the sensing surface, was dipped into a plastic coating solution for electrical insulation.

The metal-oxide electrode was equilibrated in 2.0 M sodium hydroxide to increase the reactivity of the hydroxyl groups to cyanuric chloride. A saturated solution of cyanuric chloride is used to activate the surface for subsequent enzyme linking through lysine residues. The electrode was stirred in a solution containing the enzyme at 10 mg ml^{-1}.

Operation of the flow-injection system. The system was arranged as shown in Fig. 1. The appropriate substrate solution was pumped through the system at a rate of 2 ml min^{-1} unless otherwise stated. The substrate reservoir was thermostatted in the water bath set at 25.0 ± 0.1°C, and the substrate solution flowed through about 3 m of coiled tubing (ca. 25 ml) in the bath before reaching the partially thermostatted injector. The solution continued flowing through the u.v. detector (8 μl, 1.0-cm path length).

The assay was a modified version of Hummel's assay of chymotrypsin [17]. The change in absorbance of BTEE on hydrolysis by chymotrypsin was monitored at 256 nm. The concentration of substrate used was 0.5 mM. The substrate solution also contained 0.05 M Tris (pH 7.8), 0.1 M calcium chloride and 20% (v/v) methanol.

Homogeneous enzyme assay was done as follows: a 2-ml sample of substrate solution in a small tube was thermostatted at 25°C. The flow system was activated and operated at a flow rate of 2 ml min^{-1}. A 10-μl sample of enzyme solution in the same buffer was added to the tube, the tube contents were mixed and the timer was started. Part of the contents of the tube was drawn into a 1.0-ml syringe, and 100-μl portions were flushed through the 20-μl injection loop. At precise time intervals, 20 μl of the sample was

injected into the flowing stream. The syringe was thermostatted during the course of the injections. Changes in the absorbance of the sample, relative to the stream, were recorded as positive peaks. As the enzyme reaction proceeded in the syringe, the aliquots injected resulted in an increase in peak height with time, and provided a rate of increase associated with the activity of the sample. The linear portion of the absorbance vs. time plot was fitted to a linear model with an Apple II+ microcomputer.

The assays of immobilized enzyme activity were done in a similar manner. The electrode was immersed in 2 ml of a well stirred substrate solution and a timer was started. Aliquots (50 μl) were taken at fixed-time periods, flushed through the 20-μl injection loop and injected into the flowing stream. In this case, the critical timing occurred in removing the sample.

Batch-type assays were done identically to those of Hummel [17] to obtain specific activities for the conditions used here. From this information, a calibration plot was prepared to relate flow data for homogeneous samples to activities obtained by the batch-type procedure. The activity of immobilized enzyme on the electrodes could then be obtained from such a calibration curve.

Results and discussion

A typical standard run over a range of 2.91—29.1 $\times$ 10^{-3} IU of chymotrypsin provided a rate of absorbance change of 0.0393 min^{-1} per IU, with a standard error of estimate of S_{yx} = 0.81 $\times$ 10^{-4} min^{-1} and a correlation coefficient (r) of 0.983. For higher enzyme concentrations, aliquots were typically injected at 1-min intervals for a period of 5 min. The linearity of the peak height vs. time relationship is indicated by the typical values of r = 0.999 and S_{yx} = 4.3 $\times$ 10^{-4} absorbance over an absorbance range of ca. 130 $\times$ 10^{-4}. At lower enzyme concentrations, longer times were needed to provide a change in peak height large enough to ensure reliable measurements. The reproducibility of individual assays was found to be better than 5% RSD in most cases.

A homogeneous assay done with the diode-array spectrophotometer provided an activity for the chymotrypsin of 58.3 $\pm$ 0.4 IU mg^{-1}. An assay of this type typically involved 10 times the amount of enzyme used in the calibration stock solution (ca. 50 mg l^{-1}).

The peak height vs. time relationship for longer times is illustrated in Fig. 2 and resembles a typical trend exhibited by enzymes following pseudo-Michaelis-Menten kinetics. The time required to reach the plateau increases with decreasing enzyme concentration. In this case (0.03 IU of enzyme), the peak height vs. time plot levels off in approximately 48 min.

The rate for a given assay was found to vary only slightly over the range 1—4 ml min^{-1} (i.e., 7.1%). The rate decreased slightly at higher flow rates. The flow rate of 2 ml min^{-1} was chosen because it conserved reagent while providing an acceptable peak width. At 1 ml min^{-1}, the baseline peak width was about 1 min and interfered with the homogeneous assays. The volume between the injector and the detector was measured to be 0.385 $\pm$ 0.15 ml.

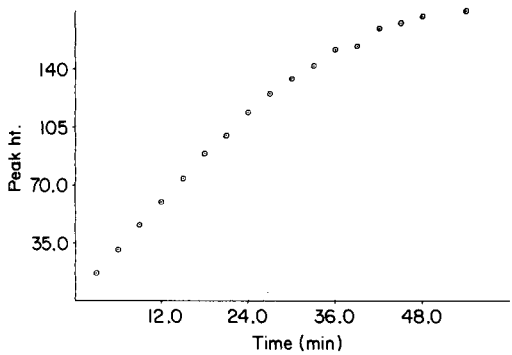

Fig. 2. Peak height (given as 10^{-4} absorbance) vs. time for a homogeneous chymotrypsin assay. Conditions: 0.5 mM BTEE, pH 7.8, 0.1 M $CaCl_2$, 20% methanol, 0.03 IU of enzyme.

TABLE 1

Activity of Chymotrypsin-modified IrO_2 electrodes[a]

Electrode	1	2	3	4
Activity[b] (10^{-3} μmol min^{-1})	5.4 ± 0.8	4.4 ± 1.2	1.3 ± 0.7	0.45 ± 0.09

[a]Conditions: 5 × 10^{-4} M BTEE, 25.0°C, pH 7.8. [b]Average of 2—3 results.

At a flow rate of 2 ml min^{-1}, the time required to clear this volume is 11.5 ± 0.4 s. As expected, the peak width increased with decreasing flow rate.

The activities of several immobilized enzyme electrodes were quantified, and found to be related to the response of the potentiometric sensor [16]. The activities found for four different electrodes are shown in Table 1. Electrodes 1 and 2 exhibited a normal potentiometric response whereas the responses of electrodes 3 and 4 were degraded. The activity was greatest for the electrodes demonstrating best responses.

N-Benzoyl-L-tyrosine ethyl ester was used as substrate because it was among the substrates used to study the potentiometric response of the electrode [16]. Its chief problem arose from trying to observe an absorbance change on top of a substantial background. The absorptivity associated with the difference in absorbance between the substrate and its hydrolysis products is 0.964 cm^2 μmol [18]. The use of a substrate such as a *p*-nitroanilide derivative would be expected to provide approximately a 10-fold increase in sensitivity with a substantially reduced background [18].

The authors thank the National Institute of Health (GM-33732) for research support.

REFERENCES

1 P. W. Carr and L. D. Bowers, Immobilized Enzymes in Analytical and Clinical Chemistry, Wiley, New York, 1980.
2 C. R. Bradley and G. A. Rechnitz, Anal. Chem., 56 (1984) 664.
3 M. A. Arnold and G. A. Rechnitz, Anal. Chem., 54 (1982) 2315.
4 O. R. Zaborsky, Immobilized Enzymes, CRC Press, Cleveland, OH, 1973.
5 A. Wiseman, Handbook of Enzyme Biotechnology, Wiley, New York, 1975.
6 A. L. Lehninger, Biochemistry, Worth, New York, 1975, Chap. 8.
7 J. Růžička and E. H. Hansen, Anal. Chim. Acta, 78 (1975) 145.
8 W. J. Blaedel and G. P. Hicks, Anal. Chem., 34 (1962) 388.
9 G. P. Hicks and W. J. Blaedel, Anal. Chem., 37 (1965) 354.
10 W. H. Marsh, B. Fingerhut and E. Kirsch, Clin. Chem., 2 (1959) 119.
11 B. Rocks and C. Riley, Clin. Chem., 28 (1982) 409.
12 K. Stewart, Anal. Chem., 55 (1983) 931A.
13 H. A. Mottola, Anal. Chim. Acta, 145 (1983) 27.
14 K. K. Stewart, G. R. Beecher and P. E. Hare, Anal. Biochem., 70 (1976) 167.
15 S. Olsen, J. Růžička and E. H. Hansen, Anal. Chim. Acta, 136 (1982) 101.
16 D. C. Roberts, J. A. Osborn and A. M. Yacynych, Anal. Chem., 58 (1986) 140.
17 B. C. Hummel, Can. J. Biochem. Physiol., 37 (1959) 1393.
18 H. U. Bergmeyer, Methods of Enzymatic Analysis, Vol. II, Academic Press, New York, 1974, pp. 516, 1011.

Analytica Chimica Acta, 183 (1986) 293—299
Elsevier Science Publishers B.V., Amsterdam — Printed in The Netherlands

Short Communication

PNEUMATOPOTENTIOMETRIC DETERMINATION OF NANOGRAM AMOUNTS OF CYANIDE

FRANTIŠEK OPEKAR

The UNESCO Laboratory of Environmental Electrochemistry, J. Heyrovský Institute of Physical Chemistry and Electrochemistry, Czechoslovak Academy of Sciences, Jilská 16, 110 00 Prague 1 (Czechoslovakia)

(Received 25th September 1984)

Summary. Hydrogen cyanide is liberated from aqueous samples by reaction with sulphuric acid and transferred by a stream of nitrogen to a silver porous membrane electrode. Some HCN passes through the membrane into an alkaline dicyanoargentate solution; the cyanide ion produced causes a decrease in the equilibrium Ag^+ concentration and the change of potential is related to the amount of cyanide in the sample. The detection limit is 3.0 ng ml^{-1} cyanide in the injected solution; the relative standard deviation is 0.82% for 17 ng of cyanide. Sulphide interferes (as H_2S) but can be removed on a lead acetate column.

Cyanide ions can be determined indirectly with a silver(I)-selective electrode placed in a solution of the dicyanoargentate complex [1]. The determination is based on the change caused by cyanide in the equilibrium concentration of Ag^+ ions in a solution of potassium dicyanoargentate. This principle has been used in the determination of cyanide with a silver(I)-selective electrode [2—4] or a silver wire electrode [5]. The same principle is utilized here; cyanide is determined indirectly with a silver porous membrane electrode (AgPME) used potentiometrically. The method may be named pneumatopotentiometry, as it is experimentally analogous to the pneumatoamperometric method introduced recently [6, 7] for the determination of various substances which can be converted in solution to an equivalent amount of a volatile electroactive compound. The volatile compound is swept with a carrier gas to an amperometric membrane electrode. In the potentiometric modification, some of the volatile compound passes through the membrane and causes a change in the ambient solution that is sensed by the membrane electrode.

In the determination of cyanide (Fig. 1), the AgPME is immersed in an alkaline buffered solution of potassium dicyanoargentate. From the test solution containing cyanide, hydrogen cyanide is liberated by reaction with an acid and swept from solution with a nitrogen stream. When the gas reaches the AgPME, part of the hydrogen cyanide diffuses through the membrane pores into the dicyanoargentate solution where it dissociates to cyanide ions. The corresponding decrease in concentration of silver ions is indicated by a change in the electrode potential.

0003-2760/86/$03.50

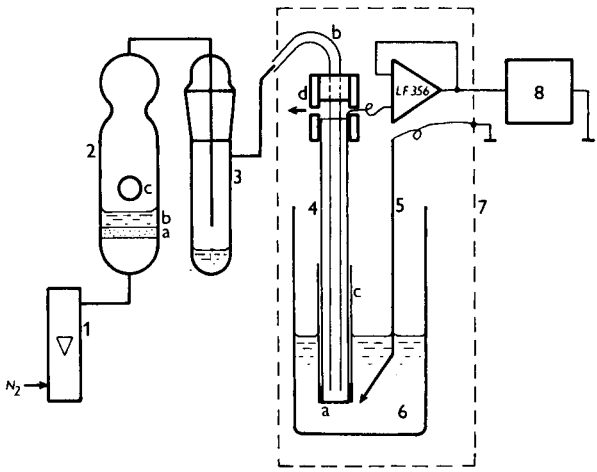

Fig. 1. Schematic diagram of the pneumatopotentiometric apparatus: (1) flow meter; (2) reaction vessel with (a) glass frit, (b) 6 M sulphuric acid and (c) rubber septum; (3) separation trap with 18 M sulphuric acid; (4) AgPME with (a) silver-plated membrane, (b) polyethylene inlet tube, (c) teflon tape and (d) silicone rubber tubing with holes for the gas outlet; (5) reference electrode; (6) working cell with $KAg(CN)_2$ solution; (7) Faraday cage; (8) recorder connected with a LF-356 voltage follower.

In contrast to the determinations described previously [1—5], the silver ion concentration is not changed in the bulk solution in pneumatopotentiometry, but only in the immediate vicinity of the electrode. Diffusional transport processes act against this change and restore within a certain time the original state, i.e., the initial equilibrium concentration of the Ag^+ ions. Therefore, the pneumatopotentiometric response has the shape of a peak. As the amount of hydrogen cyanide that passes through the membrane is proportional to the amount of cyanide in the test solution [8], the maximum potential change corresponding to the peak height, E_p, is also proportional to the initial amount of cyanide in the test solution.

Because of the various transport processes in the system, the potentials are measured under non-equilibrium conditions, and the dependence of E_p on the logarithm of the initial cyanide concentration must be established empirically.

Experimental

Apparatus. The apparatus was very similar to that used for pneumatoamperometry (Fig. 1). The reaction vessel was filled with 2 ml of 6 M sulphuric acid. The nitrogen carrier gas was dried by passage through a trap (1 cm i.d.) containing 2 ml of concentrated sulphuric acid; the flow rate was 5.5 ml s^{-1}.

The AgPME was made by placing a porous teflon membrane (Gore-Tex No. S-10363; W. L. Gore and Assoc., Elkton, U.S.A.), vacuum-plated with

silver, over the end of a glass tube (4 mm i.d.). The metal layer was on the side in contact with the dicyanoargentate solution. A platinum wire was placed down the side of the tube to act as contact and fixed to the silver layer with teflon tape. Thick-walled silicone rubber tubing was attached to the upper part of the tube, with holes for escape of gas from inside the electrode. Polyethylene tubing was used to introduce the carrier gas to a position about 3 mm above the porous membrane. Each day, before the measurements, the AgPME was reduced for 5 min at −2.5 V in 0.5 M sulphuric acid, rinsed thoroughly with twice-distilled water and transferred to the working cell. After the measurements, the electrode was stored in the air.

The AgPME potential was measured against a saturated calomel electrode connected to the solution in the working cell by a bridge filled with the buffer used. The potential was measured by a voltage follower and recorded. A Faraday cage was used as shown.

Chemicals. A 0.5 M stock solution of potassium dicyanoargentate (Safina, Vestec, Czechoslovakia) was prepared in a 0.01 M solution of borate buffer pH 9.5. Working solutions were prepared by dilution of the stock with the same buffer. The working cell was filled with 50 ml of dicyanoargentate solution at concentrations ranging from 5×10^{-2} to 4×10^{-4} M. Argentometric titration showed that the dicyanoargentate used contained 0.15% of free potassium cyanide. This excess of cyanide prevents the formation of AgCN (this is why a 1% excess of cyanide is recommended in determinations with ion-selective electrodes [2, 4]) and further ensures that changes in the cyanide ion concentration (and so in the Ag^+ concentration) caused by samples are negligible in the bulk solution in the working cell, given the very small amounts of hydrogen cyanide involved (see below).

A 10^{-2} M stock solution of potassium cyanide was prepared in 10^{-2} M sodium hydroxide. The solution was standardized argentometrically and working solutions were prepared by suitable dilution with 10^{-2} M sodium hydroxide. Cyanide samples were injected into the reaction vessel from a microlitre syringe through the rubber septum.

All the chemicals used were of p.a. purity and water was twice-distilled in a quartz apparatus. All measurements were made at room temperature (ca. 22°C).

Procedure. The AgPME, pretreated by reduction in sulphuric acid, was immersed in the dicyanoargentate solution (50 ml) in the working cell. The reaction vessel was charged with 2 ml of 6 M sulphuric acid and the nitrogen flow rate was adjusted to 5.5 ml s^{-1}. After 30—40 min, the AgPME potential became constant and a potassium cyanide sample (100 μl) was injected into the reaction vessel. The next sample was injected after the response to the previous sample had decayed. The dicyanoargentate solution in the working cell was replaced daily. For 0—200 ng of cyanide, 2×10^{-3} M dicyanoargentate is recommended.

Results and discussion

Concentration dependence. The dependence of the height of the response peak, E_p, on the amount of cyanide injected was studied in the range 0—200 ng of cyanide for dicyanoargentate solutions at pH 9.5. A pH of 11—11.5 is normally recommended for ion-selective electrodes because hydrogen cyanide is then present mostly (99%) as cyanide ion whereas at pH 9.5 only 61% is present as cyanide ion [2, 4]. However, the AgPME response to the same amount of cyanide was found to be similar at pH 9.5 and 11.5. At pH 11.5, the potential after immersion of the AgPME stabilized more slowly, possibly because of formation of $Ag(OH)(CN)^-$. Therefore, all subsequent measurements were made at pH 9.5, which was recommended by Fligier et al. [5].

The calibration curves for various concentrations of dicyanoargentate in the working cell are given in Fig. 2 (curves 1—4). It can be seen that the response to a given amount of cyanide in the sample increases as the dicyanoargentate concentration is decreased in the working solution, i.e., as the concentration of Ag^+ ions decreases. Diffusional transport processes act against the changes in Ag^+ concentration at the electrode surface; thus the initial equilibrium concentration of Ag^+ ions is restored more quickly with higher concentrations of these ions in the bulk solution.

The character of the calibration dependence of E_p on log (ng CN^-) is governed by the ratio of the amount of cyanide in the sample to the concentration of Ag^+ ions in the working solution. If this ratio is less than a critical value, the change in the Ag^+ concentration at the electrode surface is eliminated rapidly by transport processes. The peaks are narrow, but the potential change is much lower than expected from theory. Measurements are made under conditions very different from those of equilibrium potentiometry (Fig. 2, curve 4). If this ratio is larger than the critical value, the region in which Ag^+ ions are depleted extends well into the bulk solution and the potential measurement is unaffected by transport processes for some time. For a given amount of cyanide, sensitivity improves as the Ag^+ concentration in the working solution decreases (Fig. 2, curve 1). Under these conditions, the dependence of E_p on log (ng CN^-) is a straight line with a slope of 124 mV, which is close to the theoretical value of 118 mV. The amounts of cyanide in samples for which the E_p vs. log (ng CN^-) plots become linear in solutions with various concentrations of dicyanoargentate can be obtained from curves 1—3 (Fig. 2). For a given dicyanoargentate concentration and solution pH, the concentration of Ag^+ ions can be estimated from the relationship, $[Ag^+] = \{[KAg(CN)_2](K_a + [H^+])^2/4\beta_2 K_a^2\}^{1/3}$, where $K_a = 4.8 \times 10^{-10}$ is the dissociation constant of HCN. From these data, the critical value of the (ng CN^-)/$[Ag^+]$ ratio under the given experimental conditions was found to be ca. 5.5×10^9.

For 0—200 ng of cyanide, a 2×10^{-3} M dicyanoargentate solution provided a good compromise between sensitivity and sufficiently rapid decay of the potential change. The potential changes corresponding to 1.2 ng and 120 ng of cyanide in this solution decayed within ca. 300 s and 800 s, respectively.

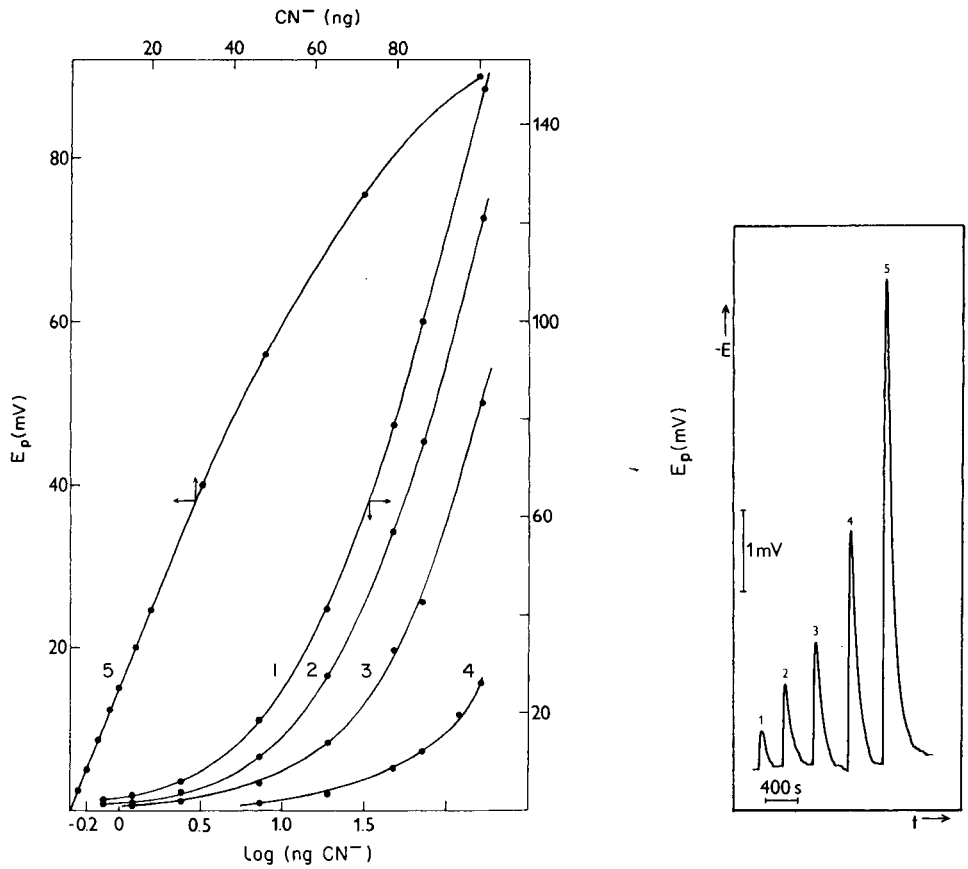

Fig. 2. Concentration dependence of E_p vs. log (ng CN^-) (curves 1—4) and E_p vs. ng CN^- (curve 5). Dicyanoargentate concentration in borate buffer pH 9.5: (1) 4×10^{-4} M; (2 and 5) 2×10^{-3} M; (3) 10^{-2} M; (4) 5×10^{-2} M.

Fig. 3. Recording of the pneumatopotentiometric responses of the AgPME in a solution of 2×10^{-3} M dicyanoargentate, pH 9.5. Amount of cyanide: (1) 0.4; (2) 0.8; (3) 1.2; (4) 2.4; (5) 4.8 ng.

The plot of E_p vs. ng of cyanide for 2×10^{-3} M dicyanoargentate (Fig. 2, curve 5) is linear from 0 to ca. 40 ng. For this interval, linear regression (n = 10) gave the equation E_p (mV) = (1.24 ± 0.02) (ng CN^-) + (0.08 ± 0.11), with a standard deviation of 0.11 mV and a correlation coefficient of 0.9998. From the values of the slope and the standard deviation, the detection limit was 0.3 ng of cyanide in 100 μl of injected sample solution, i.e., 0.15 ng l^{-1} in reaction vessel solution. The relative standard deviation for ten measurements of 17 ng of cyanide was 0.82%. Figure 3 shows the pneumatopotentiometric response of the AgPME for 0.4—4.8 ng of cyanide.

The E_p value was independent of the carrier gas flow rate from 2.33 to

10.67 ml s^{-1}. This demonstrates that the process governing the concentration of Ag^+ ions at the AgPME surface is the rate of the transport processes in the dicyanoargentate solution and not the rate at which the hydrogen cyanide is transported from the liquid phase into the gas stream.

Interferences. The transfer of cyanide from the sample into the gaseous phase ensures separation of cyanide from many substances; the sulphuric acid also decomposes many labile cyanide complexes of heavy metals. Of the commoner substances that yield gaseous products on acidification (CO_3^{2-}, Cl^-, Br^-, I^-, SO_3^{2-}, NO_2^- and S^{2-}), only sulphite and sulphide gave a response. The response to SO_2 was small (reduction of Ag^+ ions); for $SO_3^{2-}/CN^- = 5$, the ratio $E_p(SO_2)/E_p(HCN)$ was 0.03 when 48 ng of cyanide was used. The response for H_2S is similar to that for HCN; for $S^{2-}/CN^- = 1$, the ratio $E_p(H_2S)/E_p(HCN)$ was 1.1. The effect of sulphide on the determination of cyanide was eliminated by placing a glass column (100 mm long, 5 mm i.d.) packed with crystals of lead(II) acetate between the reaction vessel and the AgPME. The column caused no change in the response to cyanide, but trapped most of the H_2S; e.g., when this column was used, the ratio $E_p(H_2S)/E_p(HCN)$ was 0.06 for $S^{2-}/CN^- = 5$ with 48 ng of cyanide.

Conclusion

The possibility of using metallized membrane electrodes for potentiometric determination of gaseous substances after their production in solution was tested for the determination of small amounts of cyanide with a silver porous membrane electrode. A comparison of the features of the cyanide determina-

TABLE 1

Comparison of the features of the cyanide determination by the pneumatoamperometric and pneumatopotentiometric methods

Feature	Pneumatoamperometry		Pneumatopotentiometry
	Indirect [9][a]	Direct [10]	
Detection limit (ng ml^{-1})	1.25	2.5	0.15
R.s.d.	3.1% (300 ng CN^-) 14% (40 ng CN^-)	1.27% (52 ng CN^-)	0.82% (17 ng CN^-)
Calibration (Interval)	Linear (10—500 ng CN^-)	Linear (13—1560 ng CN^-)	Nonlinear (0.4—200 ng CN^-)
Time needed (min)	⩽40	3	10—20
Flow-rate dependence	Yes	Yes	No
S^{2-} interference	No	Yes[b]	Yes[c]

[a]Cyanide is converted to ICN and the equivalent amount of iodine liberated by the decomposition of ICN by a strong acid is measured. [b]Sulphide and cyanide were separated on a chromatographic column and determined sequentially. [c]Sulphide was removed on lead(II) acetate.

tion by the pneumatopotentiometric and pneumatoamperometric methods is shown in Table 1. Pneumatopotentiometry is especially suitable for small amounts of cyanide and has the advantage of independence of the response from changes in flow rate. A drawback is the non-linearity of the calibration curves over wide ranges. The only serious interference in the pneumatopotentiometric determination of cyanide is sulphide, which was readily eliminated by placing a column packed with lead(II) acetate before the indicator electrode.

REFERENCES

1 B. Fleet and H. von Storp, Anal. Lett., 4 (1971) 425.
2 M. S. Frant, J. W. Ross and J. H. Riseman, Anal. Chem., 44 (1972) 2227.
3 J. H. Riseman, Am. Lab., 4 (1972) 63.
4 R. A. Durst, Anal. Lett., 10 (1977) 961.
5 J. Fligier, P. Czichon and Z. Gregorowicz, Anal. Chim. Acta, 118 (1980) 145.
6 P. R. Gifford and S. Bruckenstein, Anal. Chem., 52 (1980) 1024.
7 D. D. Nygaard, Anal. Chem., 52 (1980) 358.
8 P. Beran and S. Bruckenstein, Anal. Chem., 52 (1980) 2207.
9 P. Beran and S. Bruckenstein, Anal. Chem., 52 (1980) 1183.
10 F. Opekar and S. Bruckenstein, Anal. Chim. Acta, 169 (1985) 407.

Analytica Chimica Acta, 183 (1986) 301—305
Elsevier Science Publishers B.V., Amsterdam — Printed in The Netherlands

Short Communication

BEHAVIOUR IN SOLUTION OF PIEZOELECTRIC QUARTZ CRYSTALS COATED WITH POLY(VINYLPYRIDINES). APPLICATION TO THE DETERMINATION OF COPPER(II)

T. NOMURA* and M. SAKAI

Department of Chemistry, Faculty of Science, Shinshu University, Asahi, Matsumoto 390 (Japan)

(Received 2nd October 1985)

Summary. Poly(2-vinylpyridine) or poly(4-vinylpyridine) coated on a piezoelectric quartz crystal adsorbed copper, thus decreasing the oscillation frequency. The bound copper could be removed by EDTA solution. Poly(4-vinylpyridine) is recommended to determine copper (5—35 μM) in a maleate buffer at pH 6.6 flowing over the coated crystal for 5 min. Iron(III) and cadmium interfered.

The oscillation frequency of a piezoelectric quartz crystal immersed in a solution decreases in proportion to the increasing weight of the electrode on the crystal if the properties of the solution are held constant with a buffer solution [1]. Therefore, materials in solution which react with the electrodes to form soluble or insoluble compounds can be determined from the frequency change resulting from the change in weight of the electrode [1]. As the electrodes in this method are consumed in the chemical reaction involved, they must be restored by replating. Organic reagents coated on the crystal, which are insoluble in the solution, but react with metal ions to form insoluble compounds on the electrode, have been used for the determination of lead [2]. Copper(II) oleate was the reagent used but the selectivity was poor.

It has been reported that poly(4-vinylpyridine) reacts specifically with chromium(VI), which is bound to the resin [3]. In this paper, the behaviour of a crystal coated with poly(2-vinylpyridine) or poly(4-vinylpyridine) is studied in solutions containing metal ions. Chromium(VI) did not react with these resins to form compounds that resulted in any frequency change. Copper(II) reacted with both resins; the change in frequency was proportional to the copper concentration. Results with poly(2-vinylpyridine) were less reproducible and sensitive. Thus poly(4-vinylpyridine) was applied to the determination of copper.

Experimental

Apparatus and reagents. The piezoelectric quartz crystal used was an AT-cut, 9-MHz crystal (Toyo Craft) having a gold electrode (5-mm diameter)

0003-2670/86/$03.50

on each side. The crystal was coated by immersion in a 0.5% (w/v) solution of the poly(vinylpyridine) (General Science Corporation) in chloroform and air dried. The amount of coating corresponded to a 3—6 kHz frequency decrease in air. The crystal was placed in a flow cell [4] and directly connected to an integrated circuit (i.c.) oscillator supplied with 5 V from a power unit (Metronix 521C). The same apparatus as in a preceding paper [1] was used to measure the frequency change of the crystal.

Metal ions adhering to the resins were removed by passing 1 mM disodium-EDTA solution through the cell until the frequency of the crystal was constant, followed by the 0.01 M buffer solution (reagent blank) to be used in the next experiment. When experiments gave poor reproducibility, usually after about 100 runs, the coating was removed by dissolution in chloroform for several seconds after removal from the cell. The crystal was washed with ethanol followed by acetone, air-dried and recoated with the relevant poly(vinylpyridine) as described above.

The buffer solutions (0.01 M) used were sodium acetate/acetic acid (pH 3.5—6.0), sodium hydroxide/maleic acid (pH 6.0—7.0) and sodium borate/boric acid (pH 7.0—9.0).

Procedure. Transfer the sample or standard solution in 0.01 M buffer and the reagent blank solution to their respective containers. Pass the reagent blank solution through the cell at 6.1 ml min^{-1}. When the crystal frequency has become constant (F_1), pass the sample solution for exactly 5 min and then the reagent blank solution until the frequency is constant (F_2). Plot the frequency change, $\Delta F = F_1 - F_2$, vs. the concentration of copper(II) (the calibration graph is linear). After each run, pass 1 mM EDTA through the cell for ca. 5 min to remove the metal ions in preparation for the next run.

Results and discussion

Behaviour of poly(vinylpyridines) on the crystal and reaction with metal ions. The frequency of the crystal coated with poly(2-vinylpyridine) gradually increased in acetate buffer (pH 5.0) solution but became constant after 90 min; the coating dissolved gradually in alkaline solutions. The frequency increased with increasing concentration of salts in the order of increasing specific conductivity of the solutions, whereas the frequency of an uncoated crystal decreased with increasing specific conductivity [1]. The behaviour of the coated crystal in solutions of pH 5.0, 6.1 or 8.7, containing Al, Cd, Co(II), Cu(II), Mg, Mn(II), Ni, Pb and Zn ions was investigated. Of these metal ions, copper(II) greatly changed the frequency over some of the pH range discussed. As shown in Fig. 1A, the frequency in acidic copper(II) solution slightly decreased. This decreased value was the same as that achieved just before copper(II) was introduced and after the EDTA and then the reagent blank solutions had passed through the cell. In nearly neutral solutions, the frequency increased initially and then decreased on passing copper(II) solution. The copper(II) which adhered to the crystal, so decreasing the frequency, at pH 7.08 slowly dissolved when the reagent blank

solution was subsequently passed. In alkaline solutions, the frequency increased on passing copper(II) solution. When EDTA and reagent blank solutions were then passed, the frequency returned to a higher value than at the outset, indicating that the substrate was gradually dissolved by the reagent blank solution. Aluminium at pH 6.1 and 8.7 and manganese(II) at pH 8.7 caused a slight frequency change, with a similar profile to copper at each pH. The other metal ions at all pH values increased the frequency with increasing specific conductivity, and almost the same frequency was obtained just before passing the metal ions and after passing the reagent blank solutions.

Poly(4-vinylpyridine) coated on the crystal gave a constant frequency after about 60 min in flowing buffer solution at pH 6.6—7.3 but dissolved gradually at pH 6.0, giving a continually increasing frequency. The frequency also increased with increasing salt concentration, i.e., increasing specific conductivity, as for poly(2-vinylpyridine), but decreased at pH 3.92. The frequency in copper(II) solution at pH 5.80 (Fig. 1B) was changed by adsorption of copper but it increased gradually as the reagent blank solution was passed. The frequency after the EDTA and reagent blank solutions had been passed was higher than that just before introduction of the copper-(II) solution. The frequency at pH 6.14 or 6.40 was almost the same as at pH 5.80, but the frequency changes caused by copper(II) were much higher and the dissolution of adsorbed copper(II) and substrate was less, at the higher pH values. In nearly neutral solutions, the frequency in the presence of copper ions first increased and then decreased, as at the other pH values, but the sorbed copper was not dissolved by the reagent blank solution, only by the EDTA solution. The initial increase in frequency caused by copper(II) increased with increasing pH. The other metal ions, except iron-

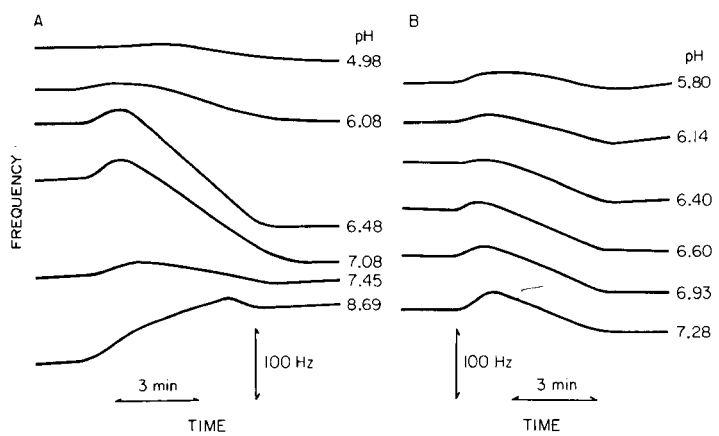

Fig. 1. Frequency change of coated crystals on adsorption of copper(II) at the pH values stated on the curves: (A) poly(2-vinylpyridine); (B) poly(4-vinylpyridine). Copper(II) solution: (A) 0.1 mM; (B) 20 μM. Flow rate, 6.1 ml min^{-1} for 5 min; readings begin at left-hand side.

(III) at pH 6.0, did not adsorb on the substrate at pH 3.92 or 6.0. Iron(III) adsorbed in a similar way to copper(II).

The initial increase in frequency for copper(II) depended on the concentration of copper(II) and increased with increasing pH for both substrates. The frequency of a crystal coated with poly(4-vinylpyridine) at pH 3.92, however, was decreased by any other metal ion in solution and copper(II) and manganese (II) enhanced this phenomenon. Possibly, copper(II) reacts with the substrate to form a compound which initially affects the crystal as if it were surrounded by a solution with low specific conductivity and then forms a second compound which increases the weight of the crystal and therefore decreases the frequency. This could explain the increasing frequency in any metal ion solution. Cations first react with the substrate to form positively-charged compounds (as a barrier layer), which affects the crystal as if it were surrounded by a solution with a low specific conductivity. These compounds release the cations into the reagent blank solution except for copper(II) and iron(III); these ions form more stable compounds which are not dissolved by the reagent blank solutions. The compounds formed between aluminium or manganese(II) and poly(2-vinylpyridine) at pH 8.7 only slowly dissolve in the reagent blank solution.

As poly(4-vinylpyridine) gave better reproducibility than the 2-isomer, and gave reasonable sensitivity, it was chosen for further investigation as a coating for the determination of copper.

Determination of copper(II). Below pH 6.0, the frequency of a crystal coated with poly(4-vinylpyridine) was not stable because the substrate dissolved in the reagent blank solution. In addition, as the binding of the substrate to copper was weak, bound copper(II) was released into the reagent blank solution. The dependence of the frequency change on pH between pH 5.8 and pH 6.9 is shown in Fig. 2. The frequency change was constant between pH 6.4 and 6.8. Iron(III) also sorbed and changed the frequency over almost the same pH range as copper but with less sensitivity (Fig. 2). A maleic acid/sodium hydroxide buffer, pH 6.6, is therefore recommended for copper determination.

The frequency change resulting from the sorption of copper was linearly proportional to the flow rate of the copper solution up to 8 ml min^{-1}, above which it slightly decreased. The flow rate used subsequently was 6.1 ml min^{-1}.

The frequency change was also linearly proportional to the volume of copper solution that passed over the crystal (i.e., the time for which the sample solution passed through the cell) over the range 1—7 min. Below 1 min, the frequency change was negative because initially the copper sample solution interacted with the substrate and increased the frequency, as described above. After 7 min, no further frequency change was obtained, indicating saturation of the substrate with copper. Thus a 5-min reaction time is recommended.

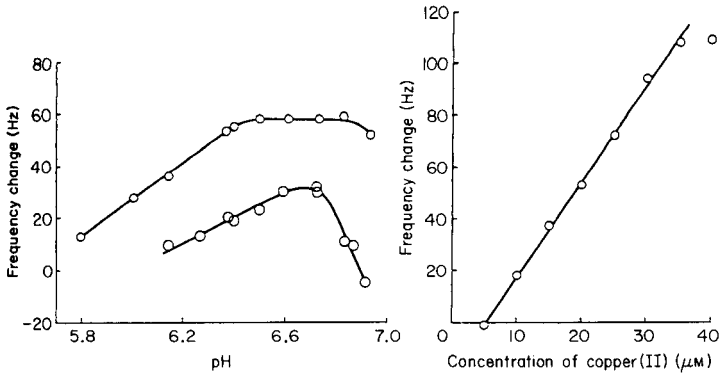

Fig. 2. Dependence of frequency change on pH: (a) for 20 μM copper(II); (b) for 20 μM iron(III). Flow rate, 6.1 ml min^{-1} for 5 min.

Fig. 3. Calibration graph for copper(II) determination at pH 6.57, in a solution flowing at 6.1 ml min^{-1} for 5 min.

Calibration, reproducibility and interferences. The calibration graph of frequency change against copper(II) concentration was linear over the range 5–35 μM, as shown in Fig. 3. The frequency change produced by <5 μM copper was negative, but could also be used for copper determination. No further decrease in frequency was obtained above 35 μM, because of the saturation of the substrate with copper. The standard deviation was 1.72 Hz (2.9%) for 6 determinations of 30 μM copper(II).

The effect of various ions on the determination of 30 μM copper(II) was investigated. Changes in frequency of more than ±5% were considered to result from interferences. Ten-fold molar amounts of aluminium, cobalt(II), lead, magnesium, manganese(II), nickel and zinc did not interfere, but cadmium and equal molar concentrations of iron(III) gave positive errors by sorption in the same way as copper. Anions which formed stable complexes or precipitates with copper(II) interfered; ten-fold amounts of cyanide, thiosulfate and thiocyanate gave negative errors, and sulfide gave positive errors perhaps because the precipitate adheres to the crystal. Ten-fold amounts of bromide, carbonate, chloride, chromate, iodide, nitrate, perchlorate, phosphate or sulfate could be tolerated.

The authors gratefully acknowledge the financial support of research grants from the Education Ministry of Japan.

REFERENCES

1 T. Nomura, M. Watanabe and T. S. West, Anal. Chim. Acta, 175 (1985) 107.
2 T. Nomura, T. Okuhara and T. Hasegawa, Anal. Chim. Acta, 182 (1986) 261.
3 J. A. Cox and P. J. Kulesza, Anal. Chim. Acta, 154 (1983) 71.
4 T. Nomura and K. Tsuge, Anal. Chim. Acta, 169 (1985) 257.

Analytica Chimica Acta, 183 (1986) 307—311
Elsevier Science Publishers B.V., Amsterdam — Printed in The Netherlands

Short Communication

SEPARATION OF TRACES AND MINOR AMOUNTS OF LEAD FROM LARGE AMOUNTS OF ZINC, INDIUM, GALLIUM AND OTHER ELEMENTS ON A LOW CROSS-LINKED ANION-EXCHANGE RESIN

F. W. E. STRELOW

National Chemical Research Laboratory, P.O. Box 395, Pretoria 0001 (South Africa)

(Received 9th September 1985)

Summary. Lead is separated from gram amounts of Zn, In, Ga, Fe(III), Cu(II), Co(II), Mn(II), U(VI), Ca and Ba on a short column of AG1-X4 anion-exchange resin in the bromide form. Lead is retained from 0.2 M hydrobromic acid while the other elements are eluted completely with this reagent. Lead is then eluted with 2 M nitric acid. Separations are sharp and quantitative and, especially for gram amounts of zinc, much better than those obtained with an 8% cross-linked resin; up to 10 mg of lead can be separated from 2 g of zinc. Results are given for synthetic mixtures and lead is determined in several analytical grade chemicals.

Traces of lead can be separated quantitatively from gram amounts of bismuth, tin, cadmium, indium and other elements forming more stable chloride complexes than lead, by eluting these elements with 1 M hydrochloric acid/methanol (1:1) from a column containing only 1 g of a macroporous cation-exchange resin [1]. No comparable method seems to have been described for separating traces of lead from gram amounts of zinc and elements such as iron(II), gallium, etc., which form less stable chloride or bromide complexes than lead. The widely applied and very selective anion-exchange separation of lead in hydrochloric acid [2] is less suitable when zinc has to be separated, because zinc is still retained when lead is eluted at high concentrations of hydrochloric acid; large columns would be required for large amounts of zinc, particularly as lead is only relatively weakly adsorbed ($D \approx 27$). Lead is considerably more strongly adsorbed by anion-exchange resins from dilute hydrobromic acid than from dilute hydrochloric acid solutions [3]. This enables lead to be separated from many other elements (including zinc) by eluting them with 0.1 M hydrobromic acid from an 8% cross-linked cation-exchange resin [4]. Applications include the determination of lead in water [5], in uranium oxide and yellow cake [6] and in geological materials [7]. Leclerq and Duyckaerts [8] separated traces of lead from larger amounts of zinc sulphate by using hydrochloric acid eluents, but both cation- and an anion-exchange columns were needed because the zinc was also retained. Uny et al. [9] determined lead in high-purity cobalt by atomic absorption spectrometry (a.a.s.) after eluting cobalt and other elements from Dowex AG1-X8 resin with 0.3 M hydrobromic acid. However,

0003-2670/86/$03.50

when this method was tested here to separate small amounts of lead from 2-g amounts of zinc on 2 g of the resin (200—400 mesh), serious tailing of zinc was observed; the tailing decreased at lower acidities but was still evident with 0.1 M hydrobromic acid. Elution with 0.3 M HBr/0.3 M HNO_3 reduced the tailing considerably, but slight heading of lead occurred. By use of a resin of lower (4%) cross-linkage, these problems could be avoided. The quantitative aspects of this separation of traces or small amounts of lead from large amounts of zinc and other elements were therefore investigated and the separation was applied to the determination of traces of lead in analytical-grade chemicals.

Experimental

Reagents. The resins were AG1-X4 and AG1-X8 microporous anion exchangers (200—400 mesh; Bio-Rad, Richmond, CA). Distilled-deionized water was used. Metal bromides (analytical-reagent grade) were purified from lead by passing the solutions containing 0.5 M free hydrobromic acid through a 20-g resin column. The stock solutions contained ca. 40 mg ml^{-1} metal ion in 0.4 M hydrobromic acid. The lead nitrate solution contained 1.000 mg ml^{-1} lead in water. Suitable dilutions were prepared as required.

Columns and apparatus. Borosilicate glass tubes (11-mm i.d., 140 mm long) fitted with a No. 1 porosity glass sinter and a tap served as columns; the top end was widened to take a separatory funnel as reservoir in the usual manner. The columns were filled with resin slurry until the settled resin reached a 5.8-ml mark (AG1-X4) or a 4.6-ml mark (AG1-X8). The resin columns were 60 and 48 mm long, respectively, when the resin was in the chloride form and contained 2 g of resin (dry chloride form). The columns were rinsed with 100 ml of 2 M nitric acid and 10 ml of deionized water, and converted to the bromide form and equilibrated by passing 50 ml of 0.5 M and 20 ml of 0.20 M hydrobromic acid.

For a.a.s., a Varian-Techtron AA-5 spectrometer was used with an air/acetylene or the nitrous oxide/acetylene flame.

Elution curves. When the 8% cross-linked resin was tested, 2 g of zinc (as ZnO) was dissolved in a measured amount of 5 M hydrobromic acid and about 50 ml of water; 10 ml of 1 mg ml^{-1} lead solution was added and the mixture was diluted to about 100 ml (0.3 M in hydrobromic acid). The solution was passed through the 2-g column of AG1-X8 resin, zinc was eluted with 500 ml of 0.30 M hydrobromic acid and lead with 2.0 M nitric acid, both at 2.0 ± 0.3 ml min^{-1}. Fractions (10 ml) were taken from the start of the ion-exchange. Zinc and lead in the fractions were determined by a.a.s. with the air/acetylene flame. Suitable dilutions were appplied as required. The elution curve is shown in Fig. 1.

When 0.2 M hydrobromic acid solutions were used throughout, the zinc tailing was reduced, but even fraction 40 contained 2.6 mg l^{-1} zinc.

The 4% cross-linked resin (AG1-X4) was examined under the same conditions as above by using adsorption from the elution with 0.20 M hydro-

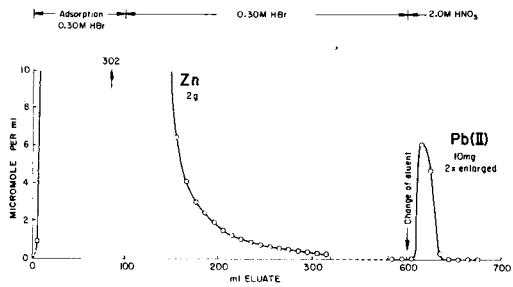

Fig. 1. Elution curve for Zn/Pb(II) with 0.30 M HBr on AG1-X8 resin (200—400 mesh).

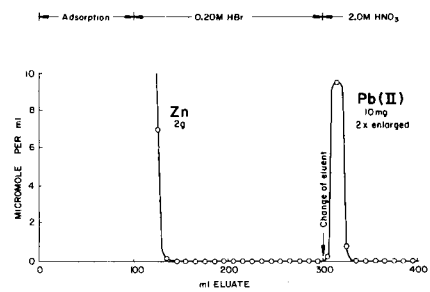

Fig. 2. Elution curve for Zn/Pb(II) with 0.20 M HBr on AG1-X4 resin (200—400 mesh).

bromic acid. Elution of zinc was extremely sharp; fraction 16 contained only 0.5 mg l^{-1} zinc. The first traces of lead (ca. 0.2 mg l^{-1}) appeared in fraction 30 (about 0.2 ppm). The elution curve is shown in Fig. 2. No lead (<0.02 mg l^{-1}) was eluted up to 600 ml when the column contained 3 g of this resin, whereas the elution of zinc was similar to that shown in Fig. 2. Elution of In, Ga, Fe(III) and Cu(II) with 0.2 M hydrobromic acid was even sharper than the elution of zinc.

Quantitative separations. Appropriate amounts of standard solutions of lead and one other element (50 ml for gram amounts) were diluted to 100 ml with a final acidity of 0.2 M hydrobromic acid. The mixed solutions were passed onto the 2-g columns of AG1-X4 resin, as described above. Zinc and the other ions were washed in and eluted with 0.20 M hydrobromic acid at 2.0 ± 0.3 ml min^{-1} (about 120 ml for zinc and 100 ml for the other ions), before elution of lead with 2.0 M nitric acid as above (about 100 ml for 10 mg of lead and 60 ml for less). Experiments were done in triplicate; duplicate blanks were run simultaneously. After suitable evaporation or dilution of the fractions, the metals were determined by suitable procedures [10]. Lead was determined by a.a.s. (air/acetylene flame) at 217.0 nm; samples and standards were 0.5 M in nitric acid. The results corrected for blanks are presented in Table 1.

Determination of lead in analytical-grade reagents. Zinc (10 g), iron wire (10 g) or zinc oxide (15 g) was dissolved by heating with a calculated amount of hydrobromic acid (enough to form the bromides and to give 500 ml of 0.20 M hydrobromic acid). The solutions were diluted to 500 ml and 100-ml portions were passed through the 2-g columns of AG1-X4 resin. Zinc and the other elements were eluted as described for the above quantitative separations. The other chemicals (listed in Table 2) were dissolved in water plus a calculated amount of 5.0 M hydrobromic acid (enough to be equivalent to the cation present and to give 100 ml of 0.2 M hydrobromic acid or 200 ml in the cases of $MnCl_2$ and $FeCl_3$). The nitrate, sulphate or chloride concentrations were kept below about 0.35 M. The total bromide concentration therefore remained below 0.55 M during the adsorption step. Adsorption

TABLE 1

Quantitative separations of synthetic mixtures

Lead (mg)		Other element (mg)		Lead (mg)		Other element (mg)	
Taken	Found[a]	Taken	Found[a]	Taken	Found[a]	Taken	Found[a]
10.00	10.01 ± 0.03	Zn 100.7	100.7 ± 0.06	0.1000	0.1001 ± 0.0003	Fe(II) 1401	1402 ±
10.00	10.00 ± 0.03	Zn 2014	2014 ± 1	0.1000	0.0999 ± 0.0002	Cu(II) 2001	2001 ±
0.1000	0.0999 ± 0.0003	Zn 2014	2015 ± 1	0.1000	0.1000 ± 0.0003	Co(II) 1997	1998 ±
0.0100	0.0100 ± 0.0001	Zn 2014	2014 ± 1	0.1000	0.1000 ± 0.0002	Mn(II) 2012	2012 ±
0.1000	0.1000 ± 0.0002	In 2011	2010 ± 2	0.1000	0.1001 ± 0.0003	U(VI) 2017	2017 ±
10.00	9.99 ± 0.02	In 2011	2011 ± 1	0.1000	0.0999 ± 0.0003	Ca 1613	1613 ±
0.1000	0.1000 ± 0.0003	Ga 2004	2005 ± 1	0.1000	0.1000 ± 0.0003	Ba 2008	2009 ±

[a] Average of at least triplicate runs.

TABLE 2

Determination of lead in analytical-grade chemicals

Chemical	Source	Amount taken (g)	Lead content (mg kg^{-1})		Residual major elem (μg)
			Certified	Found[a]	
Zinc metal	Merck	2.014	<50	10.3 ± 0.1	2.4—4.2
Zinc oxide	Merck	3.000	<50	7.5 ± 0.1	2.0—2.8
$ZnSO_4 \cdot 7H_2O$	BDH	5.000	<10	4.01 ± 0.04	1.3—1.5
$ZnCl_2$ (pure)	BDH	1.000	<700	127 ± 1	1.1—2.4
Iron wire	Baker	2.000	—	3.43 ± 0.07	0.7—3.3
$Cu(NO_3)_2 \cdot 3H_2O$	Merck	4.000	<10	0.32 ± 0.03	5.1—13.3
$Co(NO_3)_2 \cdot 6H_2O$	Merck	4.000	<10	0.19 ± 0.03	<0.5
$MnCl_2 \cdot 4H_2O$	Merck	5.000	<10	0.06 ± 0.03	0.2—0.5
$FeCl_3 \cdot 6H_2O$	Merck	5.000	<20	0.03 ± 0.02	2.7—3.3
$InCl_3 \cdot 4H_2O$	Fluka pururm	3.000	—	22.4 ± 0.1	1.4—7.4

[a] Average of quadruplicate runs.

took place from the above volumes. When zinc chloride was tested, 150 ml of solution was used and the chloride concentration was limited to 0.1 M to avoid excessive competition for exchange sites. After the other elements had been eluted, lead was eluted with 60 ml of 2.0 M nitric acid and determined as described above. Duplicate blanks were run and the results were corrected accordingly. Traces of the major elements remaining in the lead fraction were determined by standard a.a.s. procedures. The results are presented in Table 2.

Discussion

The relevant distribution coefficients [11] indicated that for the elution of zinc, the most critical element, the hydrobromic acid concentration should not be much greater than 0.3 M. The method described, with 0.2 M hydro-

bromic acid, provides a clean separation of traces or small amounts of lead from gram amounts of Zn, In, Ga, Fe(III), Cu(II), Co(II), Mn(II), U(VI), Ca and Ba. Many other elements (alkali metals, Be, Sr, Mg, Sc, Y and the lanthanides, Al, Ti(IV), Zr, Hf and Th) should pose no problems, because they have negligible tendencies to bromide complex formation. The use of the 4% cross-linked resin instead of the 8% or 10% cross-linked resins used previously [2–9] improves the separations very markedly, apparently because of improved exchange rates. The improvement for zinc is particularly noteworthy (cf. Figs. 1 and 2).

Separation and determination of lead, ranging from 10 μg to 10 mg, was excellent in all cases. A limiting factor for larger amounts would be the solubility of lead in the solution from which adsorption takes place. If major amounts of zinc were absent, adsorption could be done from 1–2 M hydrobromic acid so that larger amounts of lead could be accommodated. A 5-g resin column could handle up to 10 g of zinc.

Up to about 0.35 M nitrate or 0.175 M sulphate can be present in solution during the adsorption step without detrimental effect, but should be compensated by the presence of an equivalent concentration of bromide. Chloride can be present in similar amounts except when zinc is the major element. Zinc chloride is adsorbed more strongly at low concentration than bromide and therefore competes more strongly with lead bromide for exchange sites. Up to about 0.1 M chloride has no observable effect but larger concentrations cause premature breakthrough. When zinc and indium are not among the major elements, adsorption is possible from about 1 M hydrobromic acid and then even 0.6 M chloride, nitrate or sulphate can be present.

Duplicate blank runs were around 0.5 μg of lead and differences between duplicates never exceeded 0.1 μg. The detection limit obviously depended on sample size and was about 0.1 $\mu g\ g^{-1}$ lead for a 2-g sample and 0.04 $\mu g\ g^{-1}$ for a 5-g sample. The lead contents of the manganese and iron(III) chloride samples in Table 2 were near the limit of detection.

REFERENCES

1 F. W. E. Strelow, Anal. Chem., 57 (1985) 2268.
2 F. Nelson and K. A. Kraus, J. Am. Chem. Soc., 76 (1954) 5916.
3 T. Anderson and A. B. Knutsen, Acta Chem. Scand., 16 (1962) 849.
4 F. W. E. Strelow and F. Von S. Toerien, Anal. Chem., 38 (1966) 545.
5 J. Korkisch and A. Sorio, Talanta, 22 (1975) 273.
6 J. Korkisch and H. Gross, Mikrochim. Acta, II (1975) 413.
7 J. Korkisch and H. Gross, Talanta, 21 (1974) 1025.
8 M. Leclerq and G. Duyckaerts, Anal. Chim. Acta, 29 (1963) 139.
9 G. Uny, C. Mathieu, J. P. Tardif and Tran Van Danh, Anal. Chim. Acta, 55 (1971) 109.
10 See, e.g., F. W. E. Strelow, Anal. Chim. Acta, 127 (1981) 63.
11 F. W. E. Strelow, Anal. Chem., 50 (1978) 1359.

Analytica Chimica Acta, 183 (1986) 313—318
Elsevier Science Publishers B.V., Amsterdam — Printed in The Netherlands

Short Communication

LIMITATIONS OF SOME ESTERIFICATION TECHNIQUES IN STRUCTURAL STUDIES OF KEROGEN-DERIVED ACIDS

K. G. McLAREN

Division of Energy Chemistry, CSIRO, Private Mail Bag 7, Sutherland, N.S.W. 2232 (Australia)

(Received 5th November 1985)

Summary. Oxidative degradation techniques for characterizing kerogens in oil shales often lead to major yields of precipitated acids (PA), which are less amenable than soluble acid products to analysis by gas chromatography/mass spectrometry (g.c./m.s.). A PA complex produced by oxidation of a Julia Creek (Queensland) kerogen was studied by applying four different esterification techniques before g.c./m.s. Methods based on reaction with diazomethane or boron trifluoride/methanol were of limited effectiveness. Reaction with dimethyl sulphate in acetone with potassium carbonate catalyst led to the detection of by far the widest range of components in the PA complex. This method is recommended for esterifying acid products derived from kerogen, especially in comparative characterization studies of kerogens.

Kerogens are complex macromolecular materials that are not amenable to the usual methods of structural elucidation. Controlled oxidative degradation is a useful way of converting kerogens into structurally significant fragments which can be separated by chromatographic techniques and subsequently identified. The major oxidation products consist of a wide variety of carboxylic acids which can range from aliphatic straight- and branched-chain mono- and di-acids, through isoprenoid, cycloparaffinic and heterocyclic acids, to aromatic mono- and poly-carboxylic acids. The main analytical method used for such complex mixtures is g.c./m.s. Because of difficulties encountered with the free acids, the usual practice is to convert them to more volatile, less polar methyl esters before g.c./m.s.

Examination of the literature (e.g., Darbre [1] and references therein) shows that no single method of esterification can be expected to work quantitatively and universally with all components of complex mixtures such as those mentioned above. Thus the types and relative proportions of kerogen-derived acids detected, and any conclusions drawn about their contribution to the parent kerogen structure, could show a significant bias, depending on the choice of esterification procedure. This would be more likely to be a problem with acids of high molecular weight and those not readily soluble in the esterification media. The "regenerated humic acid" [2, 3] or "precipitated acid" [4—8] fractions, which often represent the

0003-2670/86/$03.50

major component in kerogen oxidation products, come into the latter category.

This communication presents results obtained with a precipitated acid complex (PA) obtained by oxidation of kerogen from Julia Creek (Queensland) shale with alkaline permanganate solution. Of four typical esterification procedures used, one based on reaction with dimethyl sulphate gave much more information about the composition of the acid complex than the others. It is suggested as a preferred method for kerogen structure studies of the oxidative degradation type.

Experimental

Kerogen concentrate. The oil shale was from the Julia Creek deposit which is part of the Toolebuc Formation in Northern Australia. A kerogen concentrate was prepared by exhaustive Soxhlet extraction of the shale with azeotropic benzene/methanol mixture, followed by a relatively mild acid attack (1 M HCl, 1 h at 65 ± 5°C; 46% HF/5 M HCl (2:1); 5 h at 65 ± 5°C) to remove most of the mineral matter (mainly calcite and quartz) with minimal degradation of the kerogen. The kerogen concentrate was washed free of soluble material and dried in air at 70°C. The ash content was 12.1%. Before elemental analysis, the small pyrites content was removed by treating the kerogen with zinc and hydrochloric acid. The resulting kerogen concentrate gave the following results (dry, ash-free basis): 67.1% C, 6.55% H, 2.0% N, 9.35% S, 15.1% O (difference). The low H/C atomic ratio (1.17) indicates a high aromaticity; ^{13}C-n.m.r. measurements [9] indicated an aromaticity of 45%.

Alkaline permanganate oxidation. A stepwise technique based on that recommended by Vitorovic et al. [6] for maximizing soluble acid yields, was used. In each step, the kerogen was treated at 75°C with 200 ml of solution containing 1.6 g of potassium hydroxide and 0.286 g of potassium permanganate. The initial weight of kerogen concentrate was 2 g, and a total of 25 steps was used. After extraction of neutral compounds with ether, the alkaline solution of oxidation products was acidified to pH 1. The acids which precipitated were recovered by centrifugation, washed and dried at 70°C in air. Elemental analysis gave 62.0% C, 6.8% H, 1.7% N, 4.5% S, 25.1% O (difference). Soluble acid fractions were recovered by extraction of the acidic aqueous solution before and after evaporation to dryness. The product distribution was: neutrals 1.9%; soluble acids 59.6%; precipitated acids 38.5%. Only the precipitated acids were studied in this work.

Esterification procedures. The four procedures are outlined below.

In Method A, based on the procedure of Metcalfe and Schmitz [10], a 30-mg sample was refluxed with 7 ml of methanol containing 14% boron trifluoride for 2 h. A black resinous residue was produced. The reaction mixture was diluted with water and made alkaline; then the esters were extracted with petroleum spirit (60—80°C), and then with dichloromethane.

In Method B, after Schlenk and Gellerman [11], diazomethane was generated by reacting *N*-methyl-*N*-nitroso-*p*-toluenesulphonamide with potassium hydroxide in diethylene glycol monoethyl ether, and passed into a tube containing 33 mg of sample and 4 ml of methanol at room temperature. When the reaction was complete (1 h), the mixture was diluted with water and made alkaline, and then the esters were extracted with diethyl ether.

In Method C, after Clinton and Laskowski [12], a 34-mg sample was refluxed for a total time of 15 h with a mixture consisting of 10 ml of methanol, 25 ml of 1,2-dichloroethane and 3 ml of 18 M sulphuric acid. A black resinous residue was produced. The dichloroethane extract was washed with water and sodium hydrogen carbonate solution, and the esters were recovered by evaporation of the solvent.

In Method D, after Rao et al. [13], a 99-mg sample was refluxed with a mixture of 1 ml of dimethyl sulphate, 20 ml of acetone and 2.07 g of anhydrous potassium carbonate, for a total of 17.5 h. The acetone was evaporated off, and water was added. The esters were extracted with diethyl ether from the resultant alkaline solution.

Analysis by g.c./m.s. A JEOL JMS-DX300 instrument was coupled with the JEOL JMA-DA5000 mass data system. The g.c. column was a 25-m bonded-phase silica capillary column (BP-1; S.G.E. Scientific, Australia), and the oven was programmed at 4°C min^{-1} from 10°C to 320°C. Peaks were identified on the basis of their mass spectra and retention times, and where possible, by comparison with reference materials. Peaks with intensities as low as 0.1% of the major peak were examined to ensure detection of esters, even at low concentrations. Estimates of abundances are semi-quantitative, and are expressed relative to the n-C_{16} alkanoic acid, which was the major component in the mixture. "Small" is used to denote abundances of the order 1—10%, and "minor" less than 1%.

Results

Components found in the "precipitated acid" (PA) complex are summarised by class below.

1. Alkanoic acids. The straight-chain group contained the largest number of acids detected, comprising 66% (by number) of the total. In all, there were twenty acids ranging from C_9 to C_{29}, and the major group was (C_{12}—C_{18}) with a maximum at C_{16}. Most of the (C_9—C_{20}) group were revealed by each of the esterification methods, but acids above C_{20} were found only by Methods C and D.

α-Methyl-branched alkanoic acids numbered 20% of the total and consisted of fourteen acids in the range C_{11}—C_{26}; the major group was C_{13}—C_{17}, with a maximum at C_{17}. All of these acids were revealed by Method D, whereas Method B showed smaller amounts of only five acids (C_{15}—C_{19}). Method C showed only a trace of C_{19}, and Method A revealed none of these acids.

In the isoprenoid group, four acids were detected, in the range C_{14}—C_{19}.

Method D revealed all four acids (small amounts of C_{14}—C_{16} and a minor amount of C_{19}). Method A showed three acids (minor amounts of C_{14}—C_{16}), and Method C showed minor amounts of two acids (C_{16} and C_{19}). No acids were detected by Method B.

Eleven acids having other branched chains were detected, in small to minor amounts. Most were in the C_{12}—C_{16} range, with minor amounts of one C_{19} and one C_{25} acid. Method C revealed eight acids (two C_{12}, three C_{15}, two C_{16} and one C_{25}), but Method D showed only four acids (C_{14}—C_{16}, C_{19}). Four acids (one C_{14} and three C_{15}) were detected by Method A, but none was found by Method B.

2. Alkane dioic acids. Thirteen straight-chain acids were detected, representing 8% of the total found. Most were present in small amounts, with C_{14} and C_{22} as the major components. The range was C_{12}, C_{14}—C_{19}, C_{21}—C_{26}. All thirteen acids were detected by Methods C and D, with the latter method indicating generally higher proportions of the acids than Method C. Only a few lower-molecular-weight acids were revealed by the other two methods (Method A: C_{14}—C_{16}; Method B: C_{12} and C_{14}).

Only Method D revealed branched-chain acids. There were 9 acids (C_{15}—C_{18}; C_{22}—C_{24}), in small to minor amounts.

3. Aromatic acids and acids containing sulphur or nitrogen. The H/C ratios and ^{13}C-n.m.r. data [9] indicate that Julia Creek kerogen is highly aromatic in character. Significant amounts of a wide variety of aromatic acids were found in soluble acids obtained by electro-oxidation of this kerogen [14], but none was detected in the PA complex studied here. Although the PA complex contains sulphur (4.5%) and nitrogen (1.67%), no acids containing these elements were detected in the PA complex.

Comparison of esterification methods

Results for the three main groups of acid products are detailed in Table 1. They show that the boron trifluoride/methanol and diazomethane esterification procedures were of limited effectiveness with this PA complex. Method C gave considerably more information, but Method D, based on reaction with dimethyl sulphate, led to the detection of by far the widest range of components in the PA complex. Not surprisingly, the relative proportions of the major components detected in the mixture show marked variations from method to method.

Some of the discrepancies in the detection of esters by the different methods could possibly be explained on the basis of experimental factors such as losses by evaporation during recovery and handling of the more volatile esters (e.g., C_9—C_{11}), and fractionation and losses of high-boiling esters in the g.c. injection system. However, it is considered that such possibilities have little significance in the clear overall picture shown here, that esterification Method D is far superior to the others in this particular application.

From the viewpoint of intercomparison of results with different oil shales

TABLE 1

Acids detected in the precipitated acid complex from oxidation of Julia Creek kerogen after the four esterification procedures

Carbon no. of acid	Detection after 4 esterification procedures[a]			
	Method A	Method B	Method C	Method D
Straight-chain alkanoic acids				
C_9	No	Yes	No	No
C_{10}—C_{11}	No	Yes	Yes	Yes
C_{12}—C_{18}	Yes	Yes	Yes	Yes
C_{19}—C_{20}	Yes	No	Yes	Yes
C_{21}	No	No	Yes	Yes
C_{22}	No	No	No	Yes
C_{23}—C_{28}	No	No	Yes	Yes
C_{29}	No	No	No	Yes
Maximum	C_{16}(100)	C_{16}(100)	C_{16}(100)	C_{16}(100)
2nd largest peak	C_{14}(35)	C_{14}(44)	C_{18}(49)	C_{12}(88)
3rd largest peak	C_{18}(29)	C_{12}(34)	C_{15}(26)	C_{14}(64)
4th largest peak	C_{12}(25)	C_{13}(28)	C_{14}(19)	C_{15}(42)
5th largest peak	C_{15}(21)	C_{15}(25)	C_{17}(16)	C_{18}(40)
α-Methyl-branched alkanoic acids				
C_{11}—C_{14}	No	No	No	Yes
C_{15}—C_{18}	No	Yes	No	Yes
C_{19}	No	Yes	Yes	Yes
C_{22}—C_{26}	No	No	No	Yes
Maximum	—	C_{17}(165)	C_{19}(0.4)	C_{17}(40)
2nd largest peak	—	C_{15}(51)	—	C_{13}(34)
3rd largest peak	—	C_{19}(48)	—	C_{15}(21)
4th largest peak	—	C_{16}(42)	—	C_{16}(11)
5th largest peak	—	C_{18}(9)	—	C_{19}(11)
Isoprenoid				
C_{14}—C_{15}	Yes	No	No	Yes
C_{16}	Yes	No	Yes	Yes
C_{19}	No	No	Yes	Yes
Maximum	C_{15}(2)	—	C_{16}(1.3)	C_{15}(6)

[a]Relative concentrations (n-C_{16} = 100) are shown in parentheses.

and from different workers, it seems highly desirable to standardize analytical procedures as far as possible. The dimethyl sulphate method recommended here is suggested as a promising candidate for the method of choice for use with all types of kerogen oxidation product acids. It works with a wide range of aromatic acids, as shown in a study of the soluble acids referred to earlier [14].

The author expresses his thanks to Mr I. Liepa for running the g.c./m.s. and for guidance in using the mass data system, also to Dr A. L. Chaffee for

helpful discussions and guidance in the interpretation of the g.c./m.s. data. Thanks are also due to C.S.R. Ltd., who provided a bulk sample of Julia Creek shale, and to Dr M. A. Wilson (CSIRO Division of Fossil Fuels, North Ryde, NSW) for the ^{13}C-n.m.r. measurements.

REFERENCES

1 A. Darbre, Esterification, in K. Blau and G. King (Eds.), Handbook of Derivatives for Chromatography, Heyden & Son, London, 1978, p. 39.
2 T. E. Dancy and V. Giedroyc, J. Inst. Pet., London, 36 (1950) 607.
3 W. E. Robinson, H. H. Heady and A. B. Hubbard, Ind. Eng. Chem., 45 (1953) 788.
4 M. Djuricic, R. C. Murphy, D. Vitorovic and K. Biemann, Geochim. Cosmochim. Acta, 35 (1971) 1201.
5 M. V. Djuricic, D. Vitorovic, B. D. Andresen, H. S. Hertz, R. C. Murphy, G. Preti and K. Biemann, in H. R. Von Gaertner and H. Wehner (Eds.), Advances in Organic Geochemistry, Pergamon, Oxford, 1972, p. 305.
6 D. Vitorovic, V. D. Krsmanovic and P. A. Pfendt, in A. G. Douglas and J. R. Maxwell (Eds.), Advances in Organic Geochemistry (Physics and Chemistry of the Earth), Vol. 12, Pergamon, Oxford, 1979, p. 585.
7 D. Vitorovic, M. Djordevic, A. Ambles and J. C. Jacquesy, Org. Geochem., 5 (1984) 289.
8 D. K. Young and T. F. Yen, Geochim. Cosmochim. Acta, 41 (1977) 1411.
9 M. A. Wilson, private communication.
10 L. D. Metcalfe and A. A. Schmitz, Anal. Chem., 33 (1961) 363.
11 H. Schlenk and J. L. Gellerman, Anal. Chem., 32 (1960) 1412.
12 R. O. Clinton and S. C. Laskowski, J. Am. Chem. Soc., 70 (1948) 3135.
13 A. V. Rao, M. N. Deshmukh and L. Sivadasan, Chem. Ind. (London), 5 (1981) 164.
14 K. G. McLaren and A. L. Chaffee, unpublished work.

Analytica Chimica Acta, 183 (1986) 319—329
Elsevier Science Publishers B.V., Amsterdam — Printed in The Netherlands

Book Reviews

R. L. Grob and M. A. Kaiser, *Environmental Problem Solving using Gas and Liquid Chromatography*. Elsevier, Amsterdam, 1982 (ISBN 0-444-42065-7), pp. xiv + 240. Price $59.00.

This volume is the twenty-first in the Elsevier series on chromatography and comprehensively covers all aspects of environmental analysis using gas and liquid chromatography. There is an introductory chapter followed by three chapters dealing with sampling and sample treatment, two chapters on applications of gas chromatography and liquid chromatography, and chapters on laboratory safety and regulatory matters. The book is well written and clearly presented and would serve as an interesting and easily readable text for the general reader wishing to learn about environmental analysis in general and chromatographic applications in particular. However, there are also a number of useful tables and a comprehensive set of references which make the book suitable for practising analytical chemists and environmental chemists in industrial laboratories and in public and academic institutions.

The authors have quite rightly placed considerable emphasis on sampling and sample treatment procedures. The requirements, problems and regulations affecting sampling are outlined and an international list of suppliers of standards is given. Sampling theory and practical sampling methods from a variety of sample matrices are covered, as are physical and chemical means of sample treatment. The final chapter covers the legislation of several national and international agencies with respect to environmental problems requiring the use of chromatographic techniques for analysis. Information from the U.K., however, is noticeably absent.

This book provides a comprehensive coverage of environmental problem solving using chromatographic techniques and at the same time is interesting and easy to read throughout. It is, therefore, to be recommended, both as a general text and as a useful reference for practising environmental chemists.

P. J. Worsfold

F. Vögtle (Ed.), *Host Guest Complex Chemistry I: Vol. 98* in the series, F. L. Boschke (Managing Ed.), *Topics in Current Chemistry*. Springer-Verlag, Berlin, Heidelberg, New York and Tokyo, 1981 (ISBN 0-387-10793-2) pp. x + 197. Price $32.40.

F. Vögtle and E. Webber, *Host Guest Complex Chemistry: Vol. 121* in the series, F. L. Boschke (Managing Ed.), *Topics in Current Chemistry*. Springer-Verlag, Berlin, Heidelberg, New York and Tokyo, 1984 (ISBN 0-387-12821-2) pp. xiv + 224. Price $38.10.

These are not analytical chemistry books, yet the contents are of considerable interest to analytical chemists concerned with chemical sensors, chromogenic reagents, solvent extraction, chromatography, electroanalysis, etc.

Volume 98 lays down an introduction to crown-type compounds in the introductory review by Edwin Webber and Fritz Vögtle. This is most useful for it types these materials as well as discussing their main properties and consequences of these properties. This is a helpful background to the other articles on "Concept, Structure and Binding in Complexation" (D. J. Cram and K. N. Trueblood), "Complexation of Uncharged Molecules and Anions by Crown-Type Host Molecules" (F. Vögtle, H. Sieger and W. M. Muller), and "Analytical Applications" (E. Blasium and K.-P. Janzen). The bulk is, therefore, concerned with the structural recognition between the crown compounds and guest-type partners and the methods of studying the matched partners. This is interesting and the results permit predictions to be made in the applications field of analytical interest. Against this, the chapter on analytical applications is extremely disappointing in being far too brief to be of any real value.

Interspersed between the two volumes discussed here is "Host Guest Complex Chemistry II" which, although not under review, for the record has articles concerned with structure of the ionophores and their complexes with cations, membrane transport phenomena, reactions with chiral neutral ligands and phase-transfer catalyzed reactions. The first of these has considerable repercussions in the field of electrochemical cation sensors.

The first two articles in the third member of this group, that is Volume 121, are of direct interest to analytical chemists. The first on "Solvent Extraction of Metal Ions by Crown Compounds" (Takeda) is in an area which has an increasingly important impact in analytical chemistry, although the treatment here is more from the standpoint of the use of solvent extraction for studying complexing ability of crown ethers. Therein, however, lie clues of use to analytical chemists, as also in the second article by Takagi and Ueno on "Crown Compounds as Alkali and Alkaline Earth Metal Ion Selective Chromogenic Reagents". The modification of crown ethers by the incorporation of chromophoric groups by these authors has led to an interesting range of photometric reagents which are selective for alkali and alkaline earth metals. The reviewer recalls with delight the fascinating lecture on crown ether dyes given to him in his home as an audience of one, when Professor Takagi visited Cardiff in 1979. This was a truly privileged preview of what is in this book. That the authors still regard the crown ether dyes as being in the early stage of development as chromogenic reagents must be so, since photometric reagents are especially suited for the rapidly developing automatic flow analysis.

The remaining four articles, namely, "Photocontrol of Ion Extraction and Ion Transport by Photofunctional Crown Ethers" (Shinkai and Manabe), "Macroheterocyclic Ligands on Polymers" (Smid and Sinta), "Synthesis and Metal Complexes of Aza-Macrocycles with Pendant Arms having Additional

Ligating Groups" (Kaden), and "Bridged, Capped and Fenced Porphyrins" (Baldwin and Perlmutter) also have their connotations in the developing field of analytical chemistry. They add to the commendation that these are books that ought to be on the shelves of those who are involved in analytical research and development.

J. D. R. Thomas

David J. Malcolme-Lawes, *Microcomputers and Laboratory Instrumentation.* Plenum Press, Northvale, NJ, 1984 (ISBN 0-306-41668-9). pp. 246. Price $35.00.

This book is concerned with the use of microcomputers to measure and control in the science laboratory. Its aim is to provide an understanding of the principles on which the interfaces operate that connect the microcomputer to the laboratory apparatus, and to get the reader to appreciate the capabilities and limitations of these interfaces. It should then be possible to design experiments using microcomputers in the reader's field of interest.

Such an understanding can only come about with "hands-on" experience and the author's students were able to have this, as well as the benefit of the written material that has become the basis of this book. A number of interface circuits are discussed in some detail, and are for use with the PET, Apple, BBC and Spectrum computers.

There is a continuing flood of books on this topic and the present one must be judged in the light of the others that are available (and known to the reviewer). For the beginner other books that are one-machine orientated, and that start very simply and build up from there, are probably a better start; this book would be too much for a beginner. It is intended for the serious student and discusses very lucidly the basics of laboratory signals such as transducers, sensitivity, noise and interference, analog signal handling with operational amplifiers, digital signal handling with logic gates, the workings of the microcomputer, the various interfacing techniques and standard interfaces. The final chapter is a case study on the design of a liquid chromatography data-collection system. This is a particularly useful chapter as it takes the reader step by step through the various stages that are necessary to convert a vague idea into a working system.

The book has been produced directly from the author's word-processed copy and having just the one typeface (one size and one style) it has a rather monotonous appearance. I would certainly have liked to have seen the figure and table legends and the section headings in a different style and size. The careful reader will also find a few spelling mistakes. These are, however, minor criticisms of a fine book; any laboratory that uses microcomputers for measurement and control should certainly have a copy.

D. E. Webster

J. Keith Grime, *Analytical Solution Calorimetry*. Wiley, New York, 1985, pp. 401. Price £69.40.

This book gives a comprehensive account of the present applications of solution calorimetry in analysis. It is written by seven contributors from American universities and industrial companies but this has led to only a small amount of repetition. The various sections are concerned with the construction and operation of present day analytical calorimeters in both batch and flow modes and with a very well indexed range of applications. The text contains a wealth of typical experimental results and care is taken to compare techniques in terms of sensitivity and reproducibility. This should provide a valuable reference book both for those who are contemplating the use of calorimetric methods in analysis and for comparison with results being obtained by those already in the field.

The references extend generally to 1981—2, with occasional mention up to 1984. The text is best regarded as describing the state of the art up to that time; it will inevitably be short-lived in such a rapidly developing field so that its cost might be regarded as rather high. The introductory parts, giving general principles, are the weakest since they are superficial and contain errors (equations 1.4 and 1.15); however the rest of the text is operational and does not depend on these parts.

P. G. Francis

J. R. Chapman, *Practical Organic Mass Spectrometry*. Wiley-Interscience, Chichester, 1985, pp. ix + 198. Price £19.50.

This volume provides a well written and produced review of some aspects of practical mass spectrometry in less than 200 pages. The material covered deals with: Instrumentation (Chap. 1), Sample Introduction (Chap. 2), Chemical Ionisation (Chap. 3), Negative Ion Chemical Ionisation (Chap. 4), Ionisation of Labile Molecules (Chap. 5), Metastable Ions (Chap. 6) and Quantitative Analysis (Chap. 7). Theory is kept to a minimum and an extensive listing of references is provided, although this is not completely current.

The author claims he has produced the text with three aims in mind; first to give the reader an understanding of the principles of the techniques described, second, to enable the reader to assess the potential of these techniques as an analytical tool and thirdly, to provide the reader with sufficient information about each technique to use it in practice. I believe he has succeeded in the first two aims to a large extent but has not adequately been able to fulfil the third owing to the limitations of scope and space in a book of this type when compared to the literature specific to a particular system provided by manufacturers.

Although the title of the book is *Practical Organic Mass Spectrometry*, it is only in the first two chapters that dedicated practical procedures are de-

scribed. Later chapters are written in less specific terms and provide a broader overall view of the techniques with practical details relegated to the references. It is perhaps unfortunate that electron impact (EI), still the most popular method of ionisation in commercial spectrometers, is dismissed in only a few lines under the heading of source design. The author makes no attempt to demonstrate the use of EI fragmentation in analysis and structure determination.

The volume will undoubtedly be of interest to those who are about to enter, or those who have just entered, the field of practical mass spectrometry and will provide a useful source of reference and comparison between techniques at a reasonable price. Students pursuing a theoretical interest or requiring a descriptive text will also find this book a useful addition to their libraries. Experienced mass spectroscopists may find less to interest them than the two former groups; nevertheless I am sure there is valuable information for everyone with a working interest in mass spectrometry within this volume.

A. D. Roberts

F. K. Zimmerman and R. E. Taylor-Mayer (Eds.), *Mutagenicity Testing in Environmental Pollution Control.* Horwood, Chichester, U.K., 1985, pp. 195. Price £27.50.

The mutagenic effect of compounds is currently of great interest, mainly because of the close link between mutagenicity and carcinogenicity. Consequently, considerable efforts have been made to devise screening tests for mutagenic effects that will ultimately replace long-term animal testing. Of the numerous tests that have been proposed none, including the celebrated Ames test, give results that always correlate with mutagenetic and carcinogenic effects on mammalian and, especially, human species. Nevertheless, a combination of such tests does provide an economic and reasonable indication of potential harmful effects.

The occurrence of mutagenic compounds in the environment is widespread and, therefore, a matter of concern. This book deals with the methods and results of tesing for such compounds in food and drink, river water, marine organisms, effluents from paper mills, airborne particulates and pesticide residues. It includes useful introductions to human genetics, mutation mechanisms and selection of tests, excellently done within just 33 pages. There are also chapters on direct testing on TLC plates after separation of compounds, genetic assays of maize for environmental pollution control and the induction of mitotic aneuploidy in yeast. The book concludes with a brief history of the evaluation of risk from ionizing radiations.

The text is extremely useful, timely and compact. It gives a wide-ranging, informative discussion of a subject that can be considered as being at one of the limits of analytical science, and which is of great importance to the well-being of all.

A. Townshend

S. G. Schulman (Ed.), *Molecular Luminescence Spectroscopy.* Methods and Applications: Part I. Wiley, New York, 1985 (ISBN 0-471-86848-5). pp. x + 826. Price £98.25.

This monograph is Volume 77 in the Wiley series on Analytical Chemistry and its Applications, and, together with its companion volume, covers several applications of luminescence spectroscopy. This particular volume focuses on the application of fluorescence, phosphorescence and chemiluminescence spectra to the analysis of organic and inorganic compounds. There is a brief overview of luminescence spectroscopy, followed by applications chapters on pharmaceuticals, organic natural products, inorganic substances and bioinorganic compounds and chapters discussing excited-state optical activity, fluorescence detection in chromatography and luminescence immunoassay. Each chapter is written by authors who are active researchers in the areas discussed and they are generally very readable and comprehensive accounts. Some of the techniques discussed, such as bioinorganic luminescence spectroscopy and excited-state optical activity, are new areas of application for analytical chemists and demonstrate the advances made in molecular luminescence over the past decade. The attractions of luminescence detection are also well illustrated in the chapters on fluorescence detection in chromatography and luminescence immunoassay.

The breadth of material covered in the first volume certainly supports the editor's view that there is something of interest for all analytical chemists. However, the field that this title attempts to cover, even in two volumes, is vast, and the reader with a specific area of personal interest within the field may be disappointed. One hopes that a more detailed discussion of, e.g., instrumentation and experimental procedure, chemiluminescence and bioluminescence processes, micellar enhanced fluorescence and certain industrial applications will be included in the second volume.

Nonetheless, it is a well written book which has been diligently researched and will provide a useful, although expensive, reference (in conjunction with its companion volume) for all analytical chemists working within the area of molecular luminescence spectroscopy.

P. J. Worsfold

Bernhard Welz, *Atomabsorptionsspektrometrie, 3rd edn.* Verlag Chemie, Weinheim, 1983, pp. xiii + 527. Price DM 128.00.

This is the third, rewritten edition of one of the most popular German-language texts on atomic absorption spectrometry. It contains chapters on basic theory, light sources, atomizers, (including information on pyrolytic graphite atomizers, the L'vov platform and furnace probes, and hydride generation), optical matters, data acquisition and handling, practical information, and interferences (including background correction in some detail).

There are separate chapters on atomization processes in flames and furnaces and their impact on analytical measurements, and similar considerations of hydride and cold-vapour mercury generation. There is a brief diversion into atomic emission spectrometry in flames, the ICP and the graphite furnace, and a mention of atomic fluorescence. The remaining, almost half, of the book is concerned with details of the determination of each element, arranged alphabetically, and of the analysis of various types of sample, and 2491 references.

The coverage of the subject is comprehensive. It is clearly presented, with ample illustrations, and, although written in German, it will not provide too many difficulties to those of us who have only a modicum of elementary German. It gives an up-to-date picture of an area of analytical chemistry that is still developing rapidly, and is probably the best available text on the subject. An English translation would be most worthwhile.

A. Townshend

E. Scholz, *Karl Fischer Titration.* Springer-Verlag, Berlin-Heidelberg, 1984. x + 138 pp. Price DM 98.

During recent years the Karl Fischer method for water determinations has undergone important development through the advent of new microprocessor-controlled titration equipment as well as new and more efficient reagents. Moreover, and not least thanks to the fundamental studies of the author himself, the chemistry of the Karl Fischer titration is now, for the first time since its introduction in 1935, relatively well understood.

This book is unique, the only guide of its kind to methods based on the Karl Fischer reaction. It is concise and comprehensive and covers the most important theoretical and practical aspects. Of special importance for the analyst is the second half of the book dealing with applications and sources of errors. This part is a very nice piece of work constituting a critical review of methods proposed in the literature for water determinations in a variety of organic and inorganic compounds as well as in materials like foodstuffs, technical products and natural products.

This book can be strongly recommended to all people coming into contact with the problem of determining water by means of the Karl Fischer reagent.

A. Cedergren

D. T. Sawyer, W. R. Heineman and J. M. Beebe, *Chemistry Experiments for Instrumental Methods.* Wiley, New York, 1984 (ISBN0-431-89303-X). xv + 427 pp. Price £18.35 (paperback).

The title of the book has been carefully chosen. The contents are not a compendium of instrumental analysis experiments, but of experiments in

broader areas of chemistry which, mostly, involve instrumental measurements. This does not mean that the analytical aspect is neglected; on the contrary, much of the material relates to analytical procedures (e.g., determination of mercury in fish by cold-vapour a.a.s., determination of glucose with an enzyme electrode). But the perspective is broader, covering topics as diverse as a study of the electrode mechanism of acetaminophen oxidation by cyclic voltammetry, spectrophotometric measurement of stability constants and a study of the dehydration of butanol by g.l.c. The book derives from an earlier manual by the much-loved C. N. Reilley, and D. T. Sawyer, and was planned before Reilley's death in 1981. It reflects his belief (and mine) in giving students a thorough knowledge of the basic concepts underlying any analytical technique, and this aspect is emphasized throughout.

The manual covers a wide range of electrochemical techniques, u.v.-visible absorption and fluorescence spectrometry of molecules and atoms, n.m.r. and e.s.r. spectroscopy, gas, liquid and ion-exchange chromatography and, curiously, t.l.c. and electrophoresis, neither of which involves any instrumentation. In each case, there are full experimental details, references, safety details and questions given, as well as the theoretical information. In addition, there are appendices giving information on project experiments published in *Journal of Chemical Education*, tables of data such as stability and activity constants, electrode potentials and atomic emission wavelengths.

The book fulfils its aims admirably. It provides a compendium of experiments that work, which show the student chemist the value of instrumental measurements of the type commonly employed by the analytical chemist and in chemistry generally. It would be less successful if it had intended to illustrate the power of modern instrumental analysis, but as a means of introducing analytical technology to all chemists, it is highly recommended.

A. Townshend

S. B. Pal (Ed.), *Immunoassay Technology, Vol. 1*. W. de Gruyter, Berlin, 1985 (ISBN 3-11-010062-2). viii + 192 pp. Price DM 118.

This publication is intended to be the first of a regular series of review volumes covering nonisotopic immunoassay techniques. The aim of the series is to provide a primary literature source for those who are actively engaged in immunoassay work in order to avoid time-consuming literature searches. This volume contains six papers that cover a variety of techniques and applications, generally from a practical viewpoint. There are technique papers on isoelectric focusing (J. H. Jackson) and luminescence immunoassays (W. G. Wood); applications papers on urinary constituents (T. R. Trinick and M. F. Laker) and steroid hormones (U. M. Joshi); and specific applications papers on pancreatic glucagen determination in plasma by enzyme immunoassay (S. Iwasa) and biopterin and neopterin determination in urine by fluoroimmunoassay (M. Sawada et al.). Contributors to this

volume are based in Japan, U.S.A., India, U.K. and F.R.G. The presentation is in the form of direct copy of typewritten material, and although the text is uniform and clear, some of the figures are difficult to read.

For the non-expert, the variety of nonisotopic immunoassay techniques available can be confusing, and although the article on luminescence immunoassays gives a comprehensive account of the terminology used in such procedures, this volume is clearly of more interest to the current user than to the general reader. The future success of the series will, therefore, depend to a large extent on whether it becomes established as a primary source of publication and reference for those working in the area.

Paul Worsfold

G. R. Aiken, D. M. McNight, R. L. Wershaw and P. MacCarthy (Eds.), *Humic Substances in Soil, Sediment and Water: Geochemistry, Isolation and Characterisation.* Wiley, New York, 1985. 692 pp. Price £61.35.

This book is a major review of the nature and roles of humic substances in the environment covering the years 1786 to 1984. It is divided into three main sections, dealing in sequence with the geochemistry, isolation and fractionation, and characterisation of humic material, each main section then being subdivided into chapters covering soils, peat, groundwater, lakes, lake sediments, streams, estuaries, marine waters and sediments.

In the editor's words, the purpose of the book is "to bring together what we know, what we don't known and what we think we know concerning the geochemistry of humic substances in natural environments". Whilst this is a daunting task in such a broad-ranging and contentious subject area, this goal has been largely achieved. What is more, despite its bringing together such a wealth of information, the book remains, unlike many similar works, extremely readable.

It is a comprehensive critical review combining, in a lucid and stimulating manner, the results of some 200 years of research. The standard of presentation of the work is particularly high; the text is well laid out and essentially free of typographical errors. It is commendable that the editors have recognised that their work is likely to attract readers from a variety of disciplines and have included an extensive glossary of terms.

In conclusion, this work is comprehensive in its coverage, well written and clearly presented, and should be required reading for both experienced researchers in the field and for those contemplating entering the area.

A. G. Howard

Lothar Sachs, *Angewandte Statistik — Anwendung statistischer Methoden Sechste Auflage.* Springer Verlag, Berlin, Heidelberg, 1984. xxiv + 552 pp.

This thorough text on statistical methods has now reached its sixth edition (and carries the new title since the fourth). It is aimed at a wide-ranging

readership including medics, economists, scientists and engineers. An introductory chapter contains basic mathematics, necessary to understand the rest. Chaper 1 (Statistical Decision Techniques) runs to more than 120 pages and contains all the essential statistics, followed by a chapter (2) on applications. Separate chapters are devoted to comparison of independent samples (3), further tests (4), correlation and regression (5), multivariate statistics (6) and analysis of variance (7). An interesting page describes the outstanding historical events in the development of statistics. A sixty-page long selected and classified list of pertinent statistical literature is followed by numerical problems and their solutions, a short German-English statistical dictionary, author and subject indices and a few explanatory notes to certain parts of the text.

Undoubtedly, this is a fine and comprehensive book and is recommended to anybody who wishes to get involved more deeply in statistics (an English translation of the 5th edition is also available). It contains far more than the analytical chemist needs in his everyday work. The clear presentation of material, detailed statistical tables, well-chosen numerical problems and the comprehensive bibliography are commendable.

Gyula Svehla

John C. Macdonald (Ed.), *Inorganic Chromatographic Analysis.* Wiley-Interscience, New York, 1985 (ISBN 0-471-86283-0). 450 pp. Price £67.00.

My first thoughts on seeing the title was how welcome such a book was going to be on my bookshelf. A quick look at the chapter titles suggested that the book would consist of a series of "state of the art" reviews. Unfortunately I was to be very disappointed. The chapter on the theory of chromatography (134 pp.) is excessively long (about 40% of the entire book) and consists largely of a standard treatise on the physical chemistry of separation science. Most of the material is available in many other texts. Disappointing chapters on instrumentation followed. Fundamental principles and simple diagrams are dealt with in a manner which relates little to the practical side of chromatographic hardware. The chapter on the HPLC of inorganic and organometallic compounds is incomplete and very short.

I then turned to a large chapter (58 pp.) on ion chromatography. Previously I had read on the dust cover of this book a brief review of another book entitled "The Practice of Ion Chromatography" which referred to "this rapidly growing field". After reading the chapter on ion chromatography I was left with the impression that the subject was the sole property of one commercial organisation and relied excessively on special columns and equipment for success to be achieved. Indirect photometric detection receives only a very brief mention as does indirect refractive index detection. The important work of Schill and of Cassidy and Elchuk is scarcely even noted.

Finally a far too brief chapter on computer literature searching gives a taste of what this book might have been.

In summary, therefore, this book is very limited in scope and pedestrian in concept. It is a great pity that the editor has not taken this opportunity to compile a really worthwhile contribution to the literature.

M. Cooke

Robert A. A. Maes, Michael Oellerich and Peter W. Enders, *Theophylline Profile, Report V of the Senate Commission for Clinical-Toxicological Analysis.* VCH Verlagsgesellschaft, Weinheim, 1985, viii + 39 pp.

This booklet is the first of a series of reports by this West German Senate Commission covering the determination of individual drugs in blood. It deals with theophylline under the headings of physicochemical and pharmacokinetic properties, methods for prediction of dosage, recommended doses, serum levels and concentration/response relationships, therapeutic actions in case of toxic response, methods of determination (g.c., h.p.l.c., immunoassay), formulations, references, and a list of members of the Commission. The series recognizes the close relations between clinical and toxicological analyses for drugs, and in this case provides concise but comprehensive information on those current aspects of theophylline monitoring that are necessary for those involved in such work.

Analytica Chimica Acta, 183 (1986) 331
Elsevier Science Publishers B.V., Amsterdam — Printed in The Netherlands

Erratum

A. M. Abdallah, M. M. El-Defrawy, M. A. Mostafa and A. B. Sakla, Characterization of Interfering Effects in the Determination of Molybdenum by Atomic Absorption Spectrometry.

Anal. Chim. Acta, 174 (1985) 347—352.

The legends to Figs. 3 and 7 should read:

Fig. 3. Effect of potassium cyanide on the absorbance from 100 μg Mo ml^{-1} in presence of 4×10^{-3} M: (1) DCTA; (2) NTA; (3) EDTA; (4) sulphosalicylic acid; (5) glycine. (Absorbance of 100 μg ml^{-1} molybdenum alone was 100.)

Fig. 7. Effect of boric acid on absorbance of: (1) Mg; (2) Ca; (3) Sr (all at 1×10^{-3} M).

In Table 1 the stoichiometries obtained (Mo:M) for manganese and magnesium are: Mn, 1:3; Mg, 1:2.

ANALYTICA CHIMICA ACTA, VOL. 183 (1986)

AUTHOR INDEX

d from outside back cover)

CONTENTS

(Abstracted, Indexed in: Anal. Abstr.; Biol. Abstr.; Chem. Abstr.; Curr. Contents Phys. Chem. Earth Sci.; Life Sci.; Index Med.; Mass Spectrom. Bull.; Sci. Citation Index; Excerpta Med.)

(continued on inside ba